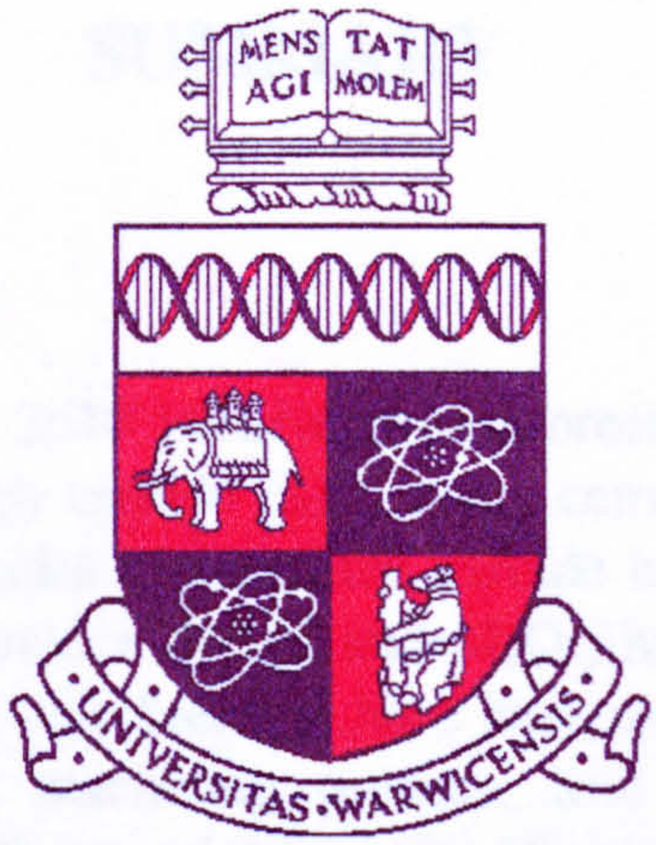

MACHINING OF ALUMINIUM BASED METAL MATRIX COMPOSITE (MMC)

By

ABU ABDULLAH
BSc (Birmingham), MSc (Warwick)

A Thesis Submitted For The Degree Of
Doctor Of Philosophy

Department Of Engineering
University Of Warwick
United Kingdom

June 1996

SUMMARY

The machining of aluminium 2618 particulate reinforced Metal Matrix Composite (MMC) with 18 vol. % silicon carbide (SiC) using cemented carbide cutting tools has been undertaken. Two grades of cemented carbide inserts, uncoated K68 grade and coated KC910 grade (coated with TiC and Al_2O_3) having negative and positive rake angles (with and without chip breaker) have been used to machine this material in order to understand the machining process, tool failure modes and wear mechanisms. Turning tests in the speed range 15 - 10 m/min have been carried out at 0.2, 0.4 and 0.6 mm/rev feed rates and 2 mm and 4 mm depths of cut.

Both cemented carbide tools have been shown to be capable of machining the MMC and give reasonable tool lives. Low speed and high feed rate are found to be a good combination in order to machine this material effectively. Coated KC910 grade inserts with negative rake angle gave the best performance. The use of a chip breaker has no significant effect on the machining process of the MMC because the material is one which inherently short chips due to ductility limitations caused by the particles.

Tool failure mode studies showed that the tools failed by flank wear. Tool wear mechanism analysis indicated that abrasion wear was the tool life controlling factor under all cutting conditions. The tool wear is related to the direct contact between the abrasive hard SiC particles and the cutting edge and their relative motion to the rake and clearance face. Hence, the hardness of the SiC particles is a dominant factor for the tool wear. Two separate models of abrasion have been suggested. Built-up edge (BUE) which has a distinct shape was more pronounced at lower cutting speeds, high feed rates and greater depth of cut. The presence of BUE has been found to increase tool life and reduce tool wear but at the expense of surface finish. The increase in tool life or reduction in tool wear is likely due to the protective layer that the BUE formed on the tool surface preventing a direct contact between the tool and chip. Linear regression analysis showed that the value of Taylor exponent n is high (0.8-1.0) compared to the values of n (0.2-0.3) obtained when machining steel. This indicates that the tool life is less sensitive to cutting speed for MMC than it is for steel.

ACKNOWLEDGEMENTS

The author would like to express his sincere gratitude to Professor S K Bhattacharrya, Professor of Manufacturing, Warwick Manufacturing Group, University of Warwick, for the provision of research facilities and to the DTI and the consortium of companies - BAe, Kennemetal, Cincinatti-Milacron, Rolls-Royce, Rover and Aerostructures for supporting the work. Sincere thanks and gratitude to Dr I R Pashby, Senior Lecturer, Department of Engineering, University of Warwick for his magnificent supervision, guidance, continuous encouragement and many valuable discussions which led to the successful completion of this work. The author is also grateful to Dr S Barnes for his valuable help, contribution and discussions throughout the development of this work.

Additional thanks should go to the technical staff that have contributed to this work in term of help and time spent on the practical work, particularly Mr M A Robinson, Mr S Fox, Mr G Booth and Mrs V Kading for her assistance on the SEM and Mr G C Canham for the photographic aspect of this project.

The author wishes to express his thanks and appreciation to The Public Service Department, Government of MALAYSIA and International Islamic University MALAYSIA (IIUM), for their financial supports through out the period of this work.

Finally, the author would like express his appreciation and sincere thanks to his beloved parents Haji Abdullah Kadir and Hajjah Esah Hitam and his beloved wife Suraya Ahmad and three daughters, Nadiah, Nasiha and Nabilah for their patience, encouragement, belief and trust. The author will forever remain grateful for their sacrifices.

DECLARATION

This thesis is presented according to the regulation of the degree of Doctor of Philosophy. The work described in this thesis is the result of my own investigation except where references are made to the work of others. It has not been submitted in any previous application for any degree.

TABLE OF CONTENTS

LIST OF TABLES

LIST OF FIGURES

LIST OF ABBREVIATION

SYMBOL	DESCRIPTION
Al	Aluminium
Al_2O_3	Aluminium Oxide
B_4C	Boron Carbide
BUE	Built-up Edge
CBN	Cubic Boron Nitride
CNC	Computer Numerical Control
Co	Cobalt
CVD	Chemical Vapour Deposition
DOC	Depth of Cut
ECM	Electro-Chemical Machining
EDM	Eleectro-Discharge Machining
F_c	Cutting Force
F_f	Feed Force
F_r	Radial Force
f	Feed Rate (mm/rev)
HSS	High Speed Steel
K68	Uncoated Cemented Carbide Tool
KC910	Coated Cemented Carbide Tool
MMC	Metal Matrix Composite
MRR	Material Removal Rate
PCBN	Polycrystalline Cubic Boron Nitride (PCBN)
PCD	Polycrystalline diamond (PCD) Tool
PM	Powder Metallurgy
PVD	Physical Vapour Deposition
Ra	Surface Roughness
SEM	Scanning Electron Microscope
SiC	Silicon Carbide
SiCp	Silicon Carbide Particulate
TEM	Transmission Electron Microscope
TaC	Tantalum Carbide
TiC	Titanium Carbide
TiN	Titanium Nitride
Ti(C,N)	Titanium Carbonitride
v	Cutting Speed
Vb	Average Flank Wear
Vb_{max}	Maximum Flank Wear
WC	Tungsten Carbide
α	Rake Angle
ϕ	Shear Plane Angle

Chapter 1

1.0 INTRODUCTION

Since the beginning of civilisation, the production and application of materials have been fundamental to industrial activity. The successive breakthroughs in materials technology have been characterised by the Stone, Bronze and Iron Ages, and more recently the plastics and composites industries have largely set the pace for the integration of technical progress in the economy.

In general, composite materials may be defined as material systems combining two or more dispersed material phases, each of which maintains its own distinct volumetric region and properties. The class of materials known as metal matrix composites (MMC) encompass a broad range of materials, each offering its own unique set of properties and advantages. MMC consist of high performance reinforcements such as silicon carbide (SiC) and aluminium oxide (Al_2O_3) in a metallic matrix, for example an aluminium alloy. Of particular interest are those that consist of any combination of fibres, whiskers, and particles in a common matrix.

The main thrust of research in MMC has been on their production, properties and physical metallurgy [1][2][3][4][5]. Focus on the machinability of MMC has been somewhat limited, there is a relatively small quantity of published data on the machinability of these materials. Workers involved in the machining of MMC agree that they are extremely difficult to machine and have suggested that "the more widespread usage of particulate aluminium matrix composites is significantly impeded by their poor machinability" [4].

The industrial revolution may be regarded as the beginning of modern machining technology. The fundamental mechanics of the metal cutting process have been well established throughout this century. However, it is essential for every researcher in the field of metal cutting to understand the basic activities and changes that occur at the tool-work interface, and to understand both failure modes and wear mechanisms. Among major factors that should be considered in the metal cutting process are optimising cutting speed, feed rate and depth of cut. All these will lead to an ultimate goal of higher productivity and lower production cost.

The objective in metal cutting is to maximise metal removal rates, while maintaining the surface finish quality, and dimensional accuracy of the machined materials. However, machining at higher cutting speeds may create chip disposal problems as well as high tool wear, which will decrease the tool life.

Workers in the metal cutting field have attempted to develop an analysis of the cutting process that gives a clear understanding of the mechanisms involved. The findings have further enabled them to predict the important parameters in machining. The development of metal cutting theory was reviewed in detail by Finnie [6]. Finnie reported that the earliest documented research in metal cutting was done by Cocquilhat in 1851. The research was mainly directed towards measuring the work required to remove a given volume of metal in drilling. Finnie further reported that the first attempts to explain chip formations were made by Time and by Tresca [6]. Taylor [7], in his pioneering work on metal cutting, investigated the effect of tool material and cutting conditions on tool life during roughing cuts. His discovery of the empirical law governing the relationship between cutting speed and tool life is still used and has been employed as the basis for much research in machining. Many researchers have published their work in explaining the complex behaviour at the tool-workpiece interface [8] [9] [10].

The discovery of exotic and advanced materials with improved mechanical properties has posed a great challenge in the field of machining. A new set of cutting parameters, cutting tool materials and improved manufacturing processes are needed before full scale production of engineering components can start. Metal matrix composites (MMC), an advanced class of materials, are one such example which are currently experiencing intense research and development in the USA, Japan and Europe.

One of the most maligned and least understood fabrication technologies for MMC is machining. Almost every potential MMC component is machined to some degree - even if only for fastener holes. The cost of using aluminium composites includes the cost of machining final parts, this cost has not yet been fully established. However, a few individuals and organisations have devoted considerable resources over the past ten years to develop an understanding of how to economically machine MMC [11].

At present, there are manufacturing techniques with which it is possible to produce high quality MMC components to near-net shape. Unfortunately, for reasons such as component design and dimensional tolerance requirements, the need for machining cannot be completely eliminated. A high percentage of the cost involved in producing a finished component for a high performance application results from machining. Therefore, in order to reduce the final cost of components produced from MMC, it is important that their machinability is fully understood and optimised.

To date, aluminium and its alloys are the major category of matrix for use in MMC. Their popularity as a matrix materials is a result of their low cost, relative to the other light structural metals such as magnesium and titanium, their current dominance in aerospace and automotive markets, and their versatility in terms of physical and mechanical properties and ease of production.

Earlier workers involved in machining of MMC have indicated that MMC are difficult to machine because of the presence of a hard ceramic phase within a softer

metallic matrix. The main problem for the conventional machining of MMC is the rapid tool wear which is caused by hard and abrasive reinforcements. Machinability trials show that uncoated and coated cemented carbide, and polycrystalline diamond (PCD) tools are suitable for the machining of MMC [12].

The objective of this project is to investigate the use of uncoated and coated cemented carbide tools for machining aluminium 2618 particulate reinforced MMC, and the research has been focused into two main areas:

1) To understand the machining process in term of chip/tool interface conditions, tool failure modes and wear mechanisms when machining aluminium 2618 MMC with uncoated and coated cemented carbide tools.

2) To quantify the effect of cutting conditions (cutting speeds, feed rates, depth of cut), tool geometries, tool materials etc., for machining aluminium 2618 MMC reinforced with SiC particles such that industrially relevant cutting conditions may be specified.

Objective (1) will help to understand what goes on during the process of machining. While objective (2) will help the introduction of uncoated and coated cemented carbide tools on production lines.

Chapter 2

MACHINING PROCESSES

2.1 Introduction

There are several ways of cutting metals, and the most widely used in manufacturing industry is machining. Machining, a basic manufacturing process, is the removal of certain selected areas for obtaining a desired shape or finish, often to great precision. It is a complex process because it involves an entire system consisting of a machine, a variety of inputs, outputs, and internal considerations.

The term *"metal cutting"* is often used to refer to the machining of a specific group of materials, always metals. It is an operation in which a thin layer of metal, the chip or swarf, is removed by a wedge-shaped tool from a larger body [13]. This chip formation machining is sometimes called traditional machining whereas machining operations such as electrodischarge machining or laser machining , where no chip is formed, is called non-traditional machining. There are different techniques employed within the traditional method which can be performed by various machine tools. Each machine tool and/or machining technique has its own features - the workpiece

may be stationary or rotating and the tool may rotate, tools may be single point, multipoint or abrasive wheels.

Turning, milling and drilling are the three most commonly used machining processes in industry. Turning is probably the most used of all the machining processes and about one third of the machines in production are employed in turning.

Research into machining has been carried out for more than 100 years and there is a vast amount of literature on the topic. Reviews which, taken together, cover the work from the early period up to the 1950s have been given by Finnie [6], Zorev [14] and Shaw [15].

2.2 Turning Process

Turning is a process where a rough cylindrical workpiece revolves about a central axis and a single point tool penetrates beneath its surface and travels parallel to the centre of rotation, removing unwanted material to produce a surface of revolution [16][17] . Figures 2.1 (a) and (b) show the main components of an engine lathe and component parts involved in a turning operation.

Turning has been the main machining process for generating machinability data. Further, turning lends itself to test work in that it is a continuous cutting operation,

the range of practical tool geometries is limited and simple, chip flow patterns are predictable, and the tool used is relatively cheap [18].

2.2.1 Terms and Definitions

Figure 2.2 shows the general terms and tool elements used for a single-point cutting tool. BS 1296 Part 2 [19] has defined the cutting geometry employed in a turning operation, a complex series of angles and planes are described. Summarised below are definitions of the most important tool parts and angles.

Rake face ($A\gamma$)	the surface over which the chip flows
Flank face ($A\alpha$)	the surface or surfaces over which the surface produced on the workpiece passes.
Cutting edge (S)	that edge of the surface intended to perform cutting.
Corner	the junction between major and minor cutting edges, commonly known as the nose

With reference to Figure 2.3

Tool cutting edge angle(K_r)	the angle between the cutting edge and a line parallel to the work surface
Tool approach angle (ψ_r)	the angle between cutting edge and a line normal to the work surface
Tool included angle (ε_r)	the angle between the major cutting edge and minor

	cutting edge.
Tool normal rake (γ_n)	the angle between the rake face and a plane measured from the major cutting edge.
Tool normal wedge angle (β_n)	the included angle between rake and flank face.
Tool normal clearance angle (α_n)	the angle between the flank and the cutting edge measured normal to the cutting edge

Other important cutting parameters associated with the turning process which have been defined in BS5623: 1979 [20] include the following:

Cutting Speed (**v**)	the rate at which the workpiece is passing over the cutting edge.
Feed Rate (**f**)	the distance travelled by the tool for one revolution of the workpiece
Depth of Cut (DOC)($\mathbf{a_p}$)	the distance the tool penetrates radially into the workpiece.

2.2.2 Orthogonal Cutting

Orthogonal cutting and oblique cutting are based on the angular relationship between the cutting velocity vector and the cutting edge of the tool. In orthogonal cutting, the cutting edge of the tool is perpendicular to the cutting speed direction, i.e. rake and approach angle are 0° . In oblique cutting, the angle between the cutting edge and cutting velocity is different from 90°. Figure 2.4 illustrates the two cases [17].

Since orthogonal cutting represents a two-dimensional situation and eliminates many independent variables, it is widely used in theoretical and experimental work.

To allow an experimental analysis of machining to be developed, some assumptions must be made [6]:

a) The tool is perfectly sharp and there is no contact along the flank or clearance face.
b) The shear surface is a plane extending upward from the cutting edge
c) The cutting edge is a straight line extending perpendicular to the direction of motion and generates a plane surface as the work moves past it.
d) The chip does not flow to either side
e) The depth of cut is constant
f) The width of the cutting edge is greater than that of the workpiece
g) The work moves relative to the tool with uniform velocity
h) A continuous chip is formed without built-up edge (BUE)
i) The shear and normal stresses along the shear plane and the tool are uniform.

Planing and the turning of a tube are two examples of ideal orthogonal cutting operations.

2.3 Chip Formation and Classification

Early work suggested that the chip was produced by a 'splitting action' in the workpiece material ahead of the cutting edge as the tool passed through it. This theory was dismissed in favour of a shear plane theory which explained that the chip is formed by deformation along the shear plane, elastically and then plastically, as it passes through a point of stress concentration, this is presented diagrammatically in Figure 2.5, Piispanen's [21] 'card model' analogy idealised the situation of how the shearing action occurs. Merchant [22] , Lee and Shaffer [23] have quantified this model. In reality, the deformation occurs over a zone of finite width, described as the primary deformation or shear zone, not a single plane.

An enormous variety of shapes and sizes of chips are produced in industrial machining operations. Ernst [24], who used high speed motion pictures in addition to photomicrographs, pointed out that there are actually three basic type of chip, namely; continuous, discontinuous and continuous with build up edge, as shown in Figure 2.6. A fairly complete mathematical analysis of the geometry, mechanics and the plasticity conditions governing the formation of the continuous chips has been made by Merchant [25]. Field and Merchant [26] have produced a similar formulation for the discontinuous chip.

The type of chips formed depends upon variables such as the cutting speed, the feed rate, the depth of cut, the material being cut and the tool rigidity.

2.3.1 Chip Types And Chip Forms

2.3.1.1 Discontinuous or Type I Chips

Discontinuous or Type I chip formation involves periodic rupture which causes the chips to break into segments (Figure 2.6 (a)). Fracture is a dominant mechanism in forming discontinuous chips. The fracture occurs because the workpiece material is inherently non-ductile, or because it produces little work-hardening during machining. In this situation, cutting begins at a relatively high shear angle which decreases as the cutting proceeds. When the strain in the chip reaches a critical value, the chip fractures and the process begins over again [26] [27].

Discontinuous chips are produced when cutting inherently brittle materials such as grey cast iron or when turning ductile materials at low cutting speeds. The latter case being due to the presence of substantial friction between tool and chip [28] . The shape and size of discontinuous chips can vary considerably, ranging from needle-like swarf to rather longer segments. Pashby [29] has obtained varieties of discontinuous chips when machining austempered ductile iron (ADI), but the size of individual pieces varied with cutting speed, tool material, heat treatment condition and tool wear.

Generally, discontinuous chips have a practical advantage in the sense that the swarf can be removed easily from the cutting area and little room is needed within the machine itself.

2.3.1.2 Continuous or Type II Chips

Continuous or ribbon-like chips are produced when machining ductile materials such as low alloy steels, ductile aluminium alloys, brass and copper (Fig. 2.6 (b)). The mechanism for the chip formation is almost entirely plastic deformation [30]. The metal shears off from the parent material along the shear plane, remaining in a homogeneous form without fragmenting. It behaves as if it was a rigid plastic material. Higher values of rake angle will produce continuous chips as has been pointed out by Cook *et al.* [27].

Quasi-continuous chips with secondary deformation is an important practical subset of continuous chips. They have a serrated appearance, indicating the metal has been sheared in discrete segments, but the ductility of the chip prevents the metal from fragmenting into Type I chips [30].

Continuous chips may be straight, tangled or curled, and can cause problems in clearing from the machine. Different techniques have been used to control the chips, these include the use of tools with a chip breaker, moulding geometric features onto the rake face of cutting tool inserts and using a high pressure coolant jet to promote breakages [13].

2.3.1.3 Continuous Chips with Built-Up Edge (BUE) or Type III Chips

Continuous chips with built up edge occur when certain conditions exist on the rake face between cutting tool and chip, and this is explained in detail in section 2.4.3.

The chip material welds to the rake face of the tool forming a built-up edge (BUE) (Fig. 2.6 c). BUE increases friction which causes layer upon layer of chip material to build up until it becomes unstable and breaks off, often taking a small amount of the cutting edge with it and gouging the workpiece surface in the process. The entire process is then repeated. Type III chips should be avoided as that can cause both the wear of the cutting edge and a roughened workpiece surface.

Low carbon and free machining steels, stainless steel, high temperatures alloys, aluminium and titanium are materials which tend to form BUE. Low cutting speeds and negative rake geometry are the usual promoting factors for BUE [26].

2.3.2 Deformation Zone

Plastic deformation is particularly important for continuous and continuous with built-up edge chips. A model of the deformation zone is required before forces or temperature may be predicted.

Thin zone or shear *plane* models (Fig. 2.7 a) proposed by Piispanen [21], Merchant [22] and Ernst [24] claimed that the chips are formed by simple shear on a plane running from the tool point to a point on the free work surface. No plastic flow takes place on either side of this shear plane.

Thick zone or shear *zone* models suggested by Trent [13] , Oxley [31] , Okushima and Hitomi [32] there is a deformation zone somewhat like that shown in Figure

2.7(b). The assumption is that shear is the main mechanism for chip formation taking place in a three dimensions volume, or region, ahead of the cutting edge. This is probably the way that all deformation occurs. As the speed increases, the included angle between these two planes tends to decrease so that it appears that this volume collapses to a single plane. At low cutting speeds, particularly when cutting metals which are in the annealed conditions, the *thick zone* model is usually more realistic.

2.3.3 Chips Classification

A comprehensive chip form classification based on sizes and shapes of the chips that are generally obtained in metal cutting are given by the ISO 3685:1977 as shown in Figure 2.8 [33] . This consists of eight descriptive shape groups, with each of these groups being subdivided into further subgroups defining the size (e.g. long, short, etc.) and the physical conditions (e.g. connected, loose, snarled, etc.). This classification system also includes a third digit numerical identification for certain types of the chips, description of the direction of chip flow, and the mode of chip breaking. A more recent work by Nakayama *et al.* [34] is based on the cutting mechanism. This work includes a geometric analysis of the origin of chip forms for three different situations: (a) chip flow with no side curling, (b) chip flow with side-curling in the normal direction, and (c) chip flow with side curling in the opposite direction.

2.4 The Tool/Chip Interface

It has already been mentioned that the shearing action at the shear plane or primary shear zone causes chip formation. The movement of the chip and of the work material across the faces and around the edge of the cutting tool can strongly influence the performance of the tools. It was believed that once formed, the chip crosses over the rake face of the tool by sliding. The classical concept of friction based on Amonton's and Coulomb's law stated that:

1. The friction force is independent of the apparent area of contact and proportional to the normal load between the two surfaces ($F = \mu N$, frictional force is proportional to the normal force N, where μ is the coefficient of friction).
2. The friction force is independent of the speed of sliding.

$F = \mu N$ does not apply because, in most sliding, the real areas of contact is very small (as surfaces are rough). In metal cutting there is much more contact owing to the high value of N (up to 3.5 GN/m^2 when machining steel) [17]. The condition at the chip-tool interface is one of the most important area of study in metal cutting.

2.4.1 Friction In Metal Cutting

On a microscopic scale, when two finished surfaces are placed together, contact is established at the peak of only a few irregularities in each surface (hills and valleys). The real areas of contact (A_R) is much less than the apparent area of contact (A), often by a factor of 10^3. If a normal load is applied, the points of contact are

plastically deformed and the real areas of contact (A_R) increases until it is capable of supporting the applied load. Three different regions of solid friction have been identified by Shaw [35] (Figure 2.9)

1. $A_R << A$ (μ is constant) - where Amonton's Law holds.
2. $A_R < A$ (transition region) - where μ decreases with increase in N
3. $A_R = A$ (no free surface) - where solid bonding exist, F and N are independent.

Wallace and Boothroyd [36] supported the change from Regime I to Regime III without taking account of Regime II, and believed that the coefficient of friction remains constant under high normal pressures up to the yield pressure of the softer material, represented by line CD in Figure 2.9. Zorev [37] emphasised that Regime I and Region III are correlated, i.e. most of the factors directly influencing the processes of plastic deformation in the chip formation zone and in the zone of contact between the chip and tool face are correlated. He represented a model of stress distribution on the rake face of a cutting tool by dividing the contact length into two regions: the *sliding region*, where Regime I conditions hold, and the *sticking region,* where Regime III hold (see Figure 2.10). Therefore, the tangential force on the tool face is given by the sum of the tangential force components in the sliding and sticking regions.

2.4.2 The Seizure Conditions

After analysing various photomicrographs of quick-stop sections of several work materials machined with high speed steel and cemented carbide tools, Trent [13]

concluded that 'contact between tool and work surface is so nearly complete over a large part of the total area of the interface, that sliding at the interface is impossible under most cutting conditions'. This rejects the classical theory of friction and the existence of boundary lubrication. This condition was called *"seizure conditions"*. In reality Regime III (A_R=A) occurred at the interface. Apart from seizure, another region of intermittent contact exists under the majority of machining conditions (Figure 2.11). Under conditions of seizure, movement over the work surface takes place by shear in the work material. A zone of extremely intense shear is formed near to, but not necessarily at, the interface; this has been termed the *"flow zone"* , Figure 2.12 [38]. A steep velocity gradient exists within this flow zone near the tool surface. Frictional force becomes the force necessary to shear the work material over the area of contact at extremely high rates of strain, high temperature, and under compressive stress [38].

In a three part paper, Trent [39][40][41] emphasised that the seizure condition is unavoidable at the interface of the work material and the tool. Factors like high compressive stress, high rates of strain and the cleanliness of the work material in contact with the tool are responsible for interlocking and atomic bonding between tool and work material [39]. However, sliding and seizure may occur simultaneously, sliding most commonly in peripheral regions of the contact area [40]. The intense localised shear strain under the seizure condition and associated fracture take place by two different modes [40]:

(1) at low speed and feed, with the formation of built-up edge (BUE) by dislocation movement resulting in strain hardening. (2) At higher metal removal rates, the intense shear strain concentrated in a flow zone because, at a critical condition, strain hardening ceases and yield stress is reduced by dynamic recovery which occurs as temperature increases. The plastic deformation is thought to involve grain boundary sliding. Temperature is an important factor in the seizure zone, not only dictating the conditions of deformation but also having great influence on the tool wear mechanisms [41].

As mentioned earlier, sliding conditions were observed at the periphery of the contact area when machining many materials using high speed steel and cemented carbide tools [39]. The zone of intense flow is absent under this condition because the interfacial bond is weaker than either workpiece or tool material and relative motion takes place at the interface. The strength of the tool-work material bond is the main factor in determining whether sliding or seizure conditions predominate.

Wright [42] machined commercially pure lead, aluminium, copper, iron and nickel using steel, cemented carbide, and sapphire cutting tools. He pointed out that both sliding and seizure occurred at different cutting conditions with different cutting tools materials. Sliding occurs when machining soft materials for short times using sapphire tools, as suggested by Doyle *et al* [43] . This indicates that the tools were coated with a few organic contaminants, the bond is weak and sliding takes place.

His results agreed with Trent's [39] [40] when cutting at other conditions using high speed steel and cemented carbide tools.

Wright *et al.* [44] proposed that the interface should be viewed as a network of micro-regions which at any instant may be either fully seized or sliding. A general equation for relating the seized area A_S to real area of contact A_R is given as $A_S = kA_R$. The constant k depends on the factors such as material purity, tool material and preparation, the cutting time, the cutting speed, engagement time of cut, lubrication and machine stability. Wright demonstrated that when machining without the presence of surface oxide on the workpiece, full seizure takes place [44].

Wright *et al.* [45] have suggested that there are five different wear mechanisms operating under conditions of seizure between tool and work material i.e. (a) superficial plastic deformation, (b) plastic deformation, (c) diffusion, (d) attrition, and (e) abrasion, when machining steels, cast iron and a nickel-based alloy with high speed steel tool. The first three are dependent on temperature, and temperature distribution in the tool is of major importance. Rake face wear can be caused by (a) or (c), the former being rapid and the latter relatively slow. Flank wear may be caused by (c) , (d) or (e). Even though the contribution of abrasion to tool wear appeared to be small the evidence of abrasion (e) by Ti(C,N) particles in austenitic steel is conclusive. Detailed discussion on tool wear mechanisms will be presented in Chapter 4.

2.4.3 Built-Up Edge (BUE)

Built-up edge (BUE) is the accumulation of work hardened material attached to the rake face of a cutting tool. It occurs when cutting many alloys at relatively low speeds and feeds. The built-up edge has been the subject of many investigations, and it is well known that it has a large effect on surface roughness. If cutting at conditions which produce BUE, increasing either speed or feed tends to reduce it's occurance and eventually no built-up edge forms. The workpiece is still 'bonded' to the rake face and shear is now confined to a narrow zone known as the secondary shear zone [46]. This condition is often termed seizure at the tool workpiece interface. Figure 2.13 shows a schematic representation of BUE.

BUE is a dynamic structure greatly hardened under extreme strain conditions. It is not considered as a separate body of hardened work material but is seen to be continuous with the work material [13]. During cutting, under high compressive stress, bonding at the interface is strong enough to prevent sliding. The chip moves over the tool by plastic deformation between A and B and by fracture at A and at B (Figure 2.14).

Trent [40] explained that : *"the first material to bond to the tool surface is strain hardened and its yield stress greatly increased but the shear stress is insufficient to break the bond to the tool. Strain then continues in the adjacent metal further from the tool surface until this also becomes intensely strain hardened. By repetition of this process a succession of layers forms the BUE"*.

The BUE process is not a continuous process. As BUE grows, it becomes unstable and parts of it are torn off and carried away by the flowing chip, this leads to the formation of a scale like appearance on the machined surface .

Four different types of BUE, based on their shape, have been classified by Heginbotham and Gogia [47] :

1) Positive wedge - occurs at the lowest speed by a nucleation process which involves the removal of the oxide layer and bonding of the two surfaces.
2) Rectangular wedge - occurs at higher speed than (1) and results from an increased temperature at the nose of the build up which causes softening. It is a more stable type of BUE and causes more damage to the chip surface than the workpiece.
3) Negative wedge - occurs at higher speed than (2) and is the result of the same heating and collapse of the softened nose of the build up.
4) Flow layer wedge - a layer is formed on the tool face which is very stable and gives a 'good clean' surface.

The form and structure of BUE depends on the cutting conditions. Increases in cutting speed, and hence the temperature, were found to cause BUE to change from type 1 to type 4 (i.e. a decrease in BUE size), Figure 2.15.

Through investigations using the quick-stop, Hoshi and Hoshi [48] obtained samples of the built-up edge formed on a carbide tool by a 0.25% carbon steel. They pointed out that the secondary plastic flow in chip formation was the direct source of the work-hardened metal which forms the BUE.

Nakajima *et al.* [49] have combined the techniques of X-ray, electron microscopy and electron probe X-ray microanalysis (EPMA) to clarify the formation of BUE and the structural changes in the cutting tool during cutting. They concluded that the formation of BUE is strongly related to plastic flow in the surface layer of a chip in contact with a cutting tool. Segregation of alloying elements due to dynamic interaction with dislocations influenced the characteristics of the interface because of the effect of the solute on the mechanical properties of metals.

Takeyama and Ono [50] investigated the nucleation mechanism of the built-up edge and stated that mechanical bonding was caused by the physico-chemical adhesion on an atomic or molecular scale. The causes of adhesion and growth of adhered metal were therefore thought to occur from one or more of four causes:

a) Metallic bonding

b) Diffusion across the interface

c) Production of alloy at the interface

d) Metallic compound produced at the interface.

Williams and Rollason [51] investigated the metallurgical parameters governing the formation of the built-up edge. A wide range of materials, feeds and speeds were used and a systematic analysis on the effect of the microstructure was attempted. They concluded that BUE only forms when machining workpiece material containing more than one phase, and that BUE can occur when cutting materials other than steel. The effect of increasing feed was shown to be similar to that of increasing speed, i.e. causing a decrease in build up edge size. Increasing the rake angle also caused a reduction of the BUE and it's eventual disappearance.

In using a 0.2% carbon steel as a workpiece, Ramaswami [52] has measured the microhardness of the built-up edge to be 585 kgm/mm^2. This was stated to be as hard as material quenched from the austenitic state. He discovered that the maximum hardness of the built up edge decreased as the type of build up changed with increasing speeds, tempering occured due to an increase in temperature. Using Heginbotham's classification, he described the structure as:

a) Positive wedge - alternate layers of ferrite and pearlite

b) Rectangular wedge - streaks of drawn out pearlite and partially dispersed carbides

c) Negative wedge - very fine particles dispersed in a matrix of lower hardness

d) Flow layer - recrystallined ferrite

In reviewing the knowledge on the formation of BUE by other workers, Pekelharing [53] presented some of his own ideas with regards to BUE. He pointed out that there is no stable built-up edge, and thus divided the phenomenon into three classes:

a) A stable body which remains temporarily

b) An unstable top which was intermittently rubbed off, and

c) A delayed layer which causes the rubbing

According to Pekelhering, class (a) is a phenomenon which consists of metals being delayed and compressed whilst flowing towards workpiece or chip. This is called retarded or delayed zone. Class (b) is seen as a zone subjected to a high-frequency cyclic strain, fluctuating between the speed of the delayed layer and the stable layer. This cycle however was visualised as being a stochastic process. Some of the build-up remains with the tools when stopped suddenly, and several workers have tried to relate the size of this to the stable body of the build up but with little success [49][51]. Therefore, he suggested that the quick-stop device is the only way of observing the phenomenon.

Using a transmission electron microscope (TEM) technique, Wallbank [54] studied the formation of BUE when cutting steel. The presence of elongated ferrite cells were presented as evidence that the material of the BUE has been very severely strain hardened, but the temperature had not increased enough for recrystallisation to take place. He has also suggested that the temperature of the BUE during machining

does not exceed 400°C because of the drop in hardness which would be seen caused by annealing at this temperature. Microcracks detected in the shear zone around the BUE were said to be responsible for BUE formation. He then defined the BUE as *"one that occurs when the material fractures before passing the cutting edge, thus forming a new workpiece surface away from the surface of the tool"*.

Wallbank [55] identified four types of BUE when machining low carbon free cutting steel with high speed steel tools, namely (a) positive wedge, (b) rectangular wedge, (c) negative wedge, and (d) layer type wedge, these are shown in Figure 2.16. Transition from one type to another depends on the amount of deformation in microcrack formation and the temperature generated. It has been reported [56] that the formation of BUE can be prevented by preheating the cutting tool above the re-crystallisation temperature. This shows the important role played by the temperature in controlling the chip-tool interface conditions.

The presence of BUE can be advantageous or disadvantageous. Machining with the presence of BUE will completely alter the tool's geometry, causing a poor surface finish [57]. Values of cutting forces are reported to be low [58] when a BUE is present due to the large effective rake angle associated with the BUE. It also affects the tool wear mechanism and can accelerate wear of the cutting tools [52][59]. BUE may prevent tool wear by moving the cutting action away from the tool edge and is thus advantageous when making roughing cuts. Yaguchi [46] [60] has thoroughly

reviewed the metallurgical factors such as inclusion density and type, and other factors which effect BUE formation.

Conventionally, the way of eliminating the built-up edge is to increase cutting speed and feed, thus increasing tool face temperature. In cutting hardened steel, Oishi [61] has concluded there is the possibility of producing a good surface finish and the elimination of BUE are as follows:

1) An increase in the workpiece hardness can improve surface finish
2) There exists a 'critical hardness' for the workpiece in terms of BUE formation. When the workpiece exceeds this critical hardness, the BUE disappears - no matter what the cutting conditions.

2.5 Forces And Stresses in Metal Cutting

2.5.1 Cutting Forces

In machining, the magnitude of the cutting forces has a direct influence on the generation of heat, tool wear, quality of machined surface and dimensional stability of the work piece. In production, the magnitude of cutting forces are needed for the design and application of machine tools, cutting tools and fixtures. Cutting forces can be regarded as one of the machinability indices [58].

In oblique cutting, forces generated can be resolved into 3 major components acting on a cutting tool. Figure 2.17 shows the 2 components forces, the cutting force (F_c)

acts on the rake face of the tool and the feed force (F_f) which resists the feed of the tool. The radial force tends to push the tool away from the work in the direction of Z-axis. Cutting force, F_c, is the largest force, radial force is small compared to the other two and normally ignored in most analyses. Dynamometers based on the elastic deflection of the tool have been used in cutting force measurements, and for a greater accuracy, either strain gauges or piezo electric transducers have been employed.

The cutting force originates from two sources. Firstly, it is due to the resistance to elastic and plastic deformation of the metal layer being cut, the chip and the machined surface layer. Secondly, it is due to the frictional forces between the cutting tool and chip, and between the cutting tool and machined surface.

Conditions at the tool/workpiece interface and in the region of the contact area at the rake face of the cutting tool have great influence on the cutting force generated during machining. Quantitatively, Trent [13] [40] and other workers [62] [63] [64] have shown that the shear plane angle (ϕ), the chip thickness and the contact area (length) (Figure 2.15) have a direct influence on cutting force (F_c) and feed force (F_f).

2.5.2 Stress

Knowledge of stresses operating on the tool is an important basis for tool design. The normal stress acting on the rake face of the tool varies from compressive,

exerted by the cutting force (F_c), for tools with a small rake angle to shearing stress imposed by the feed force (F_f). The average compressive stress can be determined by dividing the cutting force (F_c) by the contact area, and the shear stress is obtained by dividing the feed force (F_f) by the same contact area. Both compressive and shear stresses act on the clearance face of the tool when a worn surface is generated.

Zorev [37] proposed a model for analysis of the stress distribution on the tool face and showed that the compressive stress has a parabolic distribution with the maximum at the cutting edge, falling to zero where the chip breaks contact with the tool (see Figure 2.10). Again, the complex situation existing at the tool/work interface limits reliable experimental data and accurate modelling. Several techniques have been employed to analyse experimentally the stress distribution on the rake face of the cutting tool. These include the use of a photo-elastic technique using polymer tools [65] [66] [67] and a split-tool dynamometer technique [68] [69] [70] . In general, these experimental results suggest that the compressive stress is a maximum at, or very near to, the tool edge, which agrees with Zorev [37], but sometimes stress distributions are found which do not obeying a parabolic relationship with increasing distance from the cutting edge [65].

2.6 Temperatures in Metal Cutting

In machining operations, about 99% of the mechanical energy used to form the chip is converted into heat. Taylor [7] realised that the cutting heat is one of the

important phenomena arising from the work done in the cutting of metals and one which has a direct influence on tool wear and tool life.

Figure 2.18 shows three major zones of heat generation [16] [17][71] [72] :

a) Primary deformation zone, AB

b) Secondary deformation zone, BC

c) On the clearance face, BD

The temperature distribution generated by shearing and friction processes depends on several factors, with cutting speed and nature of work piece being the most important. About 80% of the energy is consumed in the primary and secondary deformation zones, 18% at the rake face and about 2% at the flank face. Only a small fraction of the total energy is stored in the chip and the rest is converted into heat [73].

2.6.1 Heat In Primary And Secondary Shear Zone

The shear zone is where much of the mechanical energy supplied to the cutting process is converted into heat. The heat generated either flows into the workpiece or is carried away by the chip. Boothroyd [17] has shown that the proportion of heat conducted into the workpiece is 10-15% for higher metal removal rates, and up to 50% at very low cutting speed. The temperature rise in the body of the chip is influenced by the cutting speed. However, the chip body temperature becomes independent of speed [13]. The normal range of chip body temperature is 200°C - 350°C when cutting low or medium carbon steel but it can be as high as 650°C when

machining fully hardened steel, or nickel based alloys, at high speed [13]. The temperature in the chip will only effect the tool performance when the two are in contact and has no influence after the chip breaks from the work material.

The second heat source is the rake face, where friction heat is generated as the chip moves along the cutting edge or heat results from secondary shear. The heat at the secondary shear zone is greatly responsible for the rise of temperature in the tool and is of major importance in relation to tool performance. When machining soft and low melting point material like aluminium and magnesium, the tool temperature is not a problem but it is an important factor limiting the rate of metal removal when cutting the higher melting point metals such as cast iron, steel, nickel and titanium based alloys. Wright *et al.* [45] used hardened steel tools to cut steels, cast iron and nickel based alloy and discovered that the temperature near the cutting edge is high enough to change the structure and hardness of the tool material. Smart *et al* [74] furthered the work of Wright *et al* [45] by machining iron, nickel and titanium. The minimum temperature to cause structural changes was approximately 650°C - 850°C, and temperature could be measured with an accuracy of ± 25°C.

Measurement of temperature distribution and temperature gradient at the tool/work interface is very difficult. Bickel [75] , Arndt *et al.* [76] and Dearnley [77] have given a brief analysis of the method employed to assess temperature in machining.

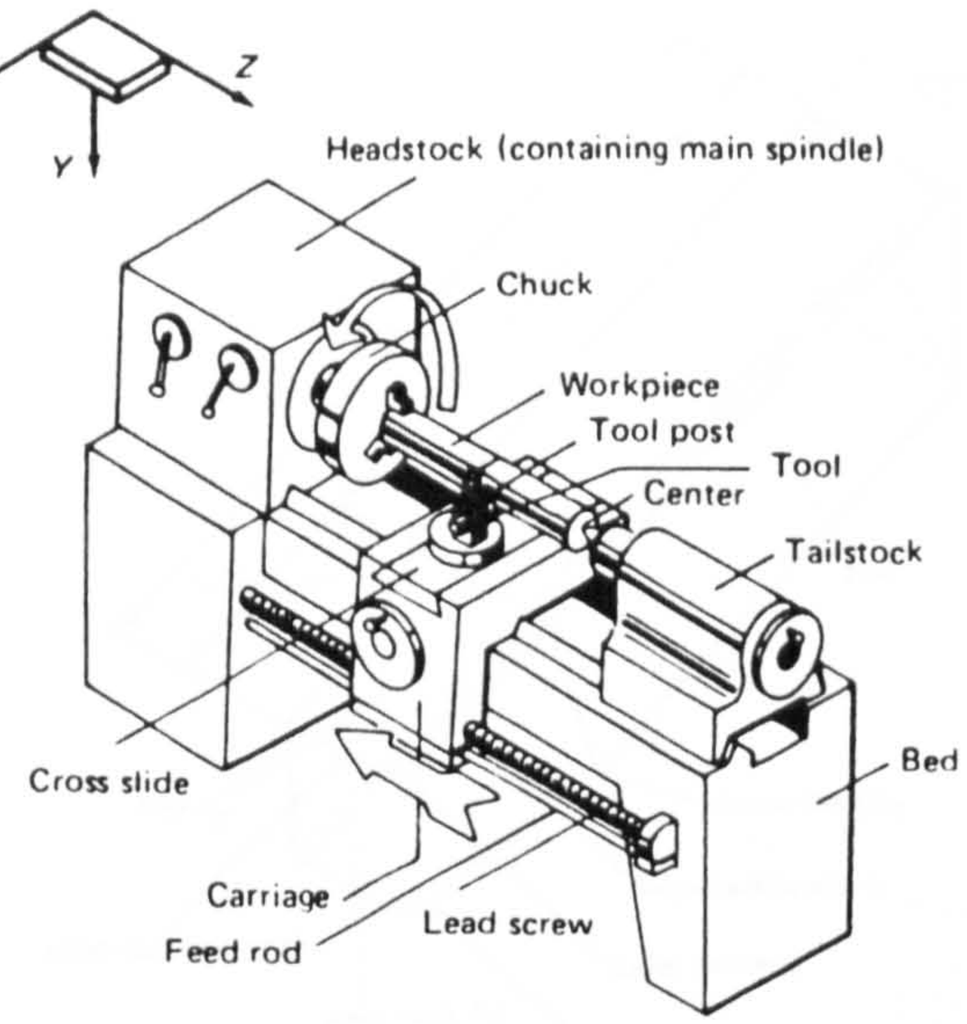

Figure 2.1 (a) An Engine Lathe [17]

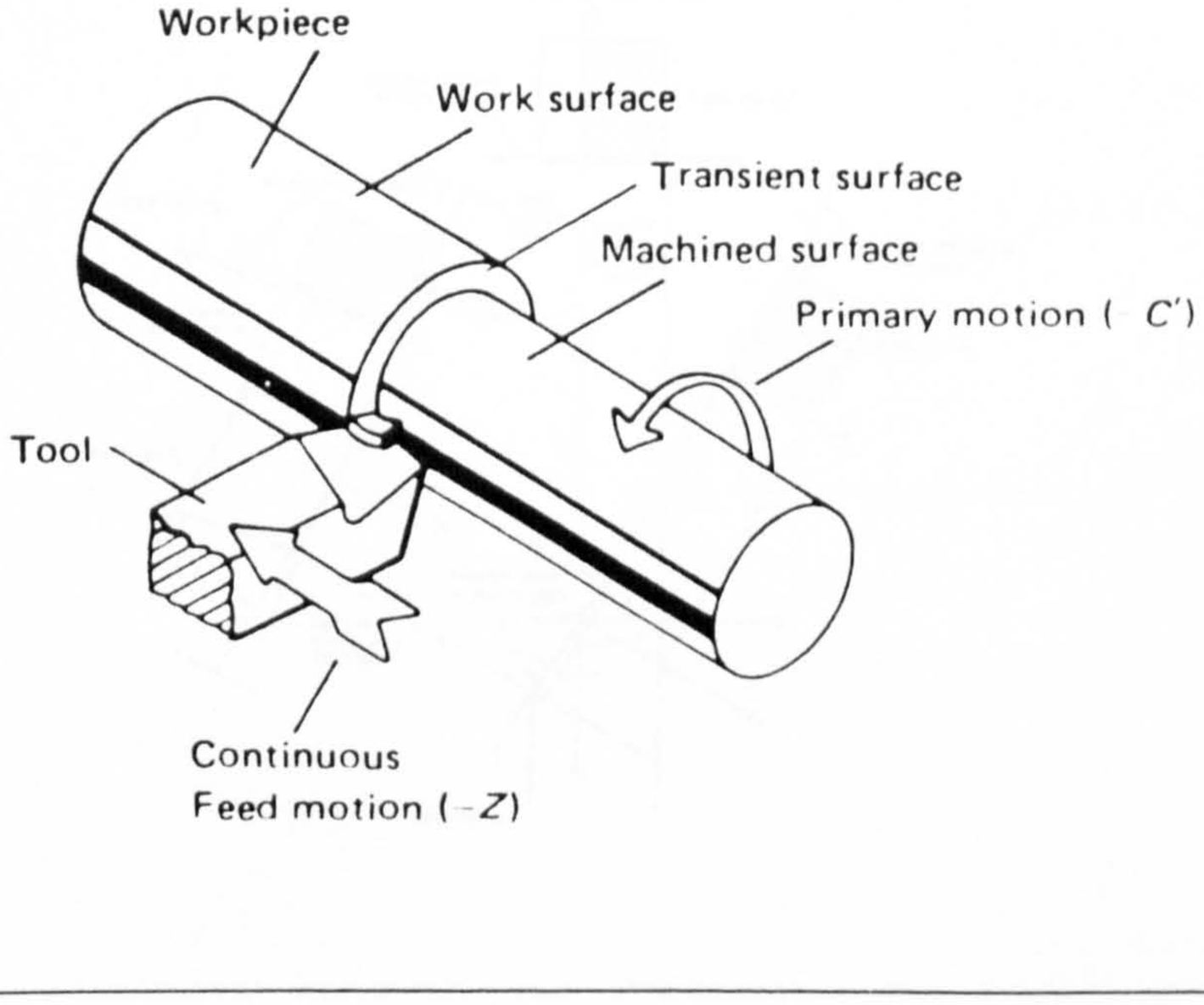

Figure 2.1 (b) Cylindrical Turning On An Engine Lathe [17]

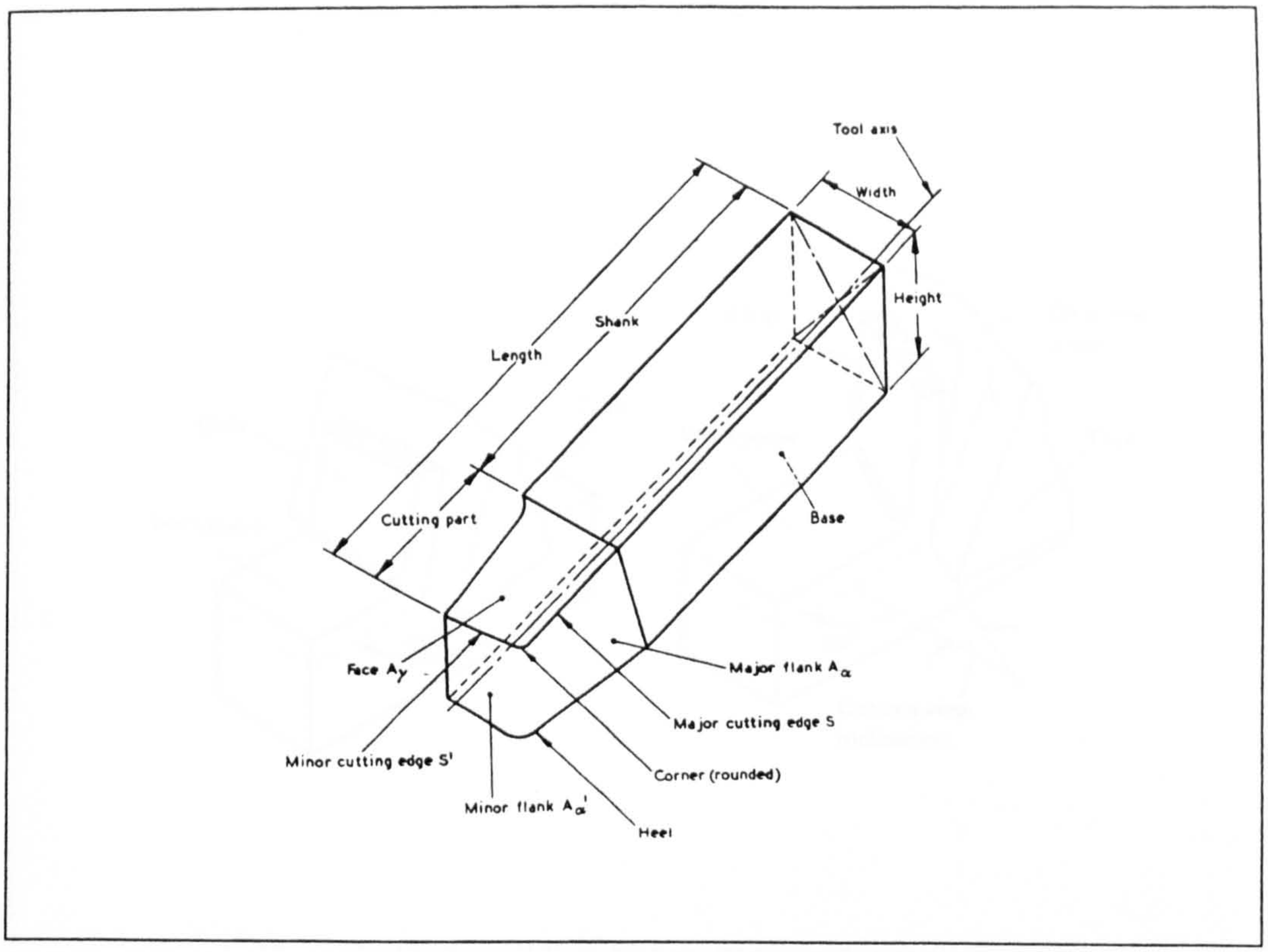

Figure 2.2 General Terms And Tool Element [19]

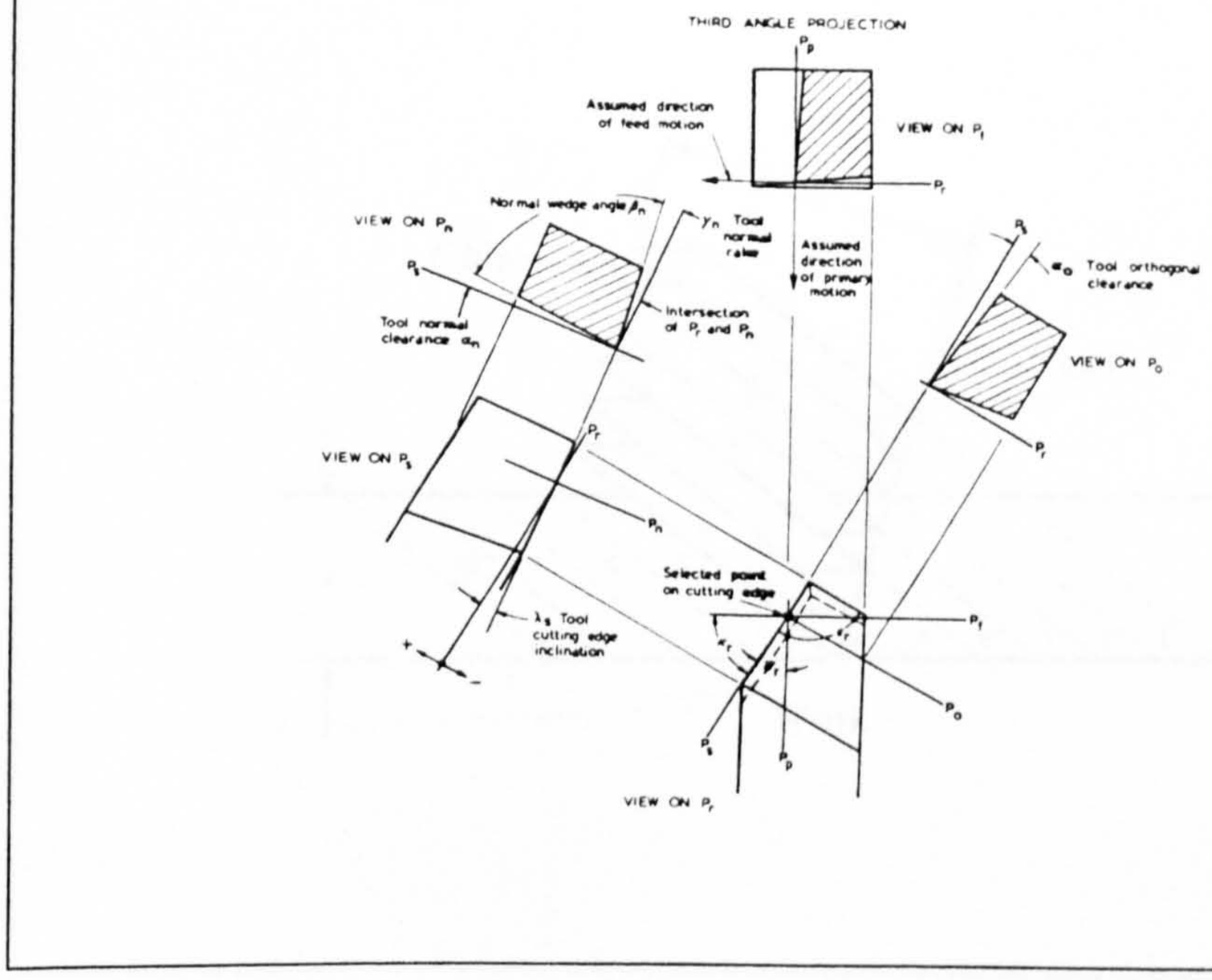

Figure 2.3 Tool Angles - Normal Rake System For A Straight Tool [19]

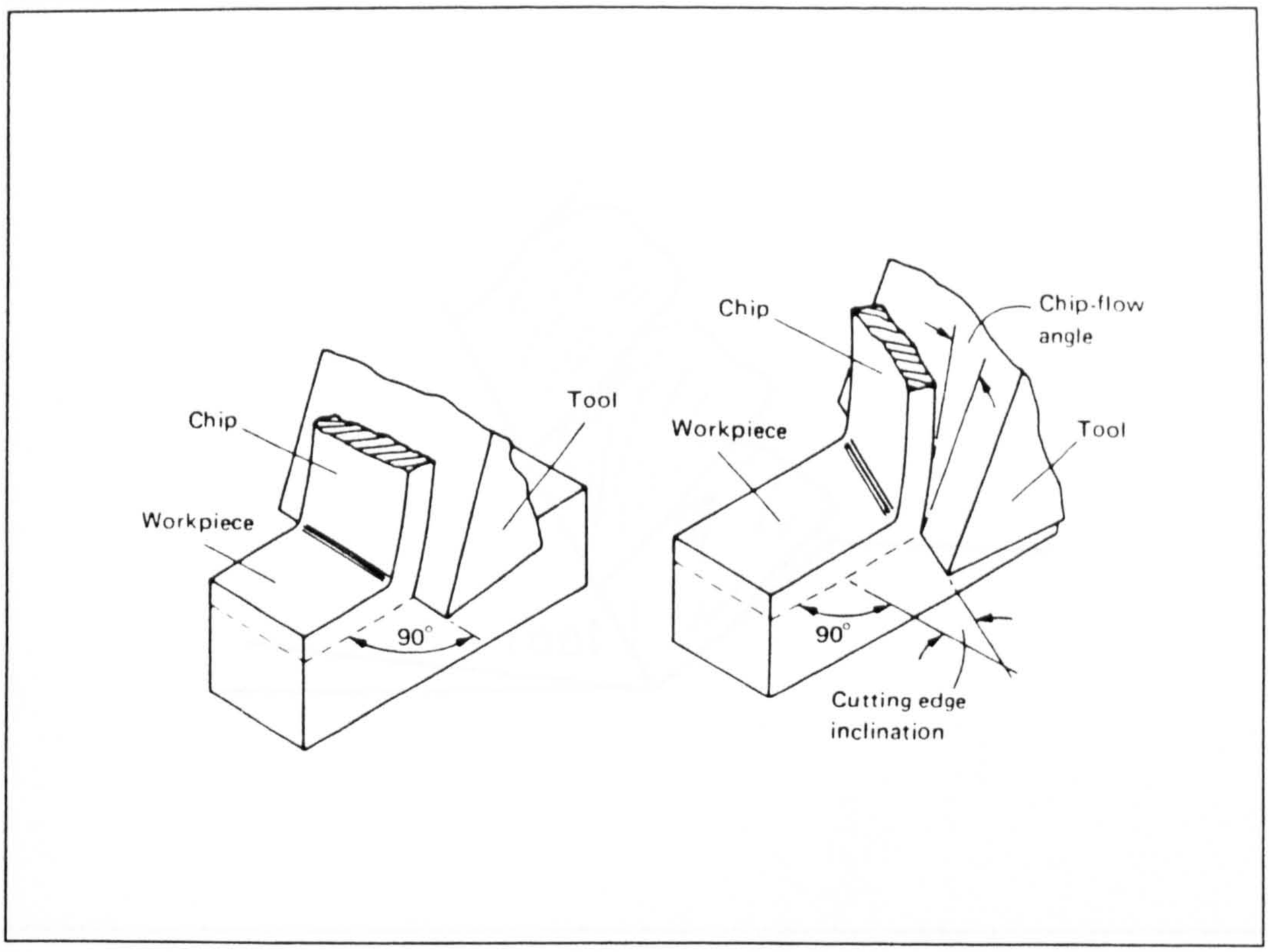

Figure 2.4 Orthogonal And Oblique Cutting [17]

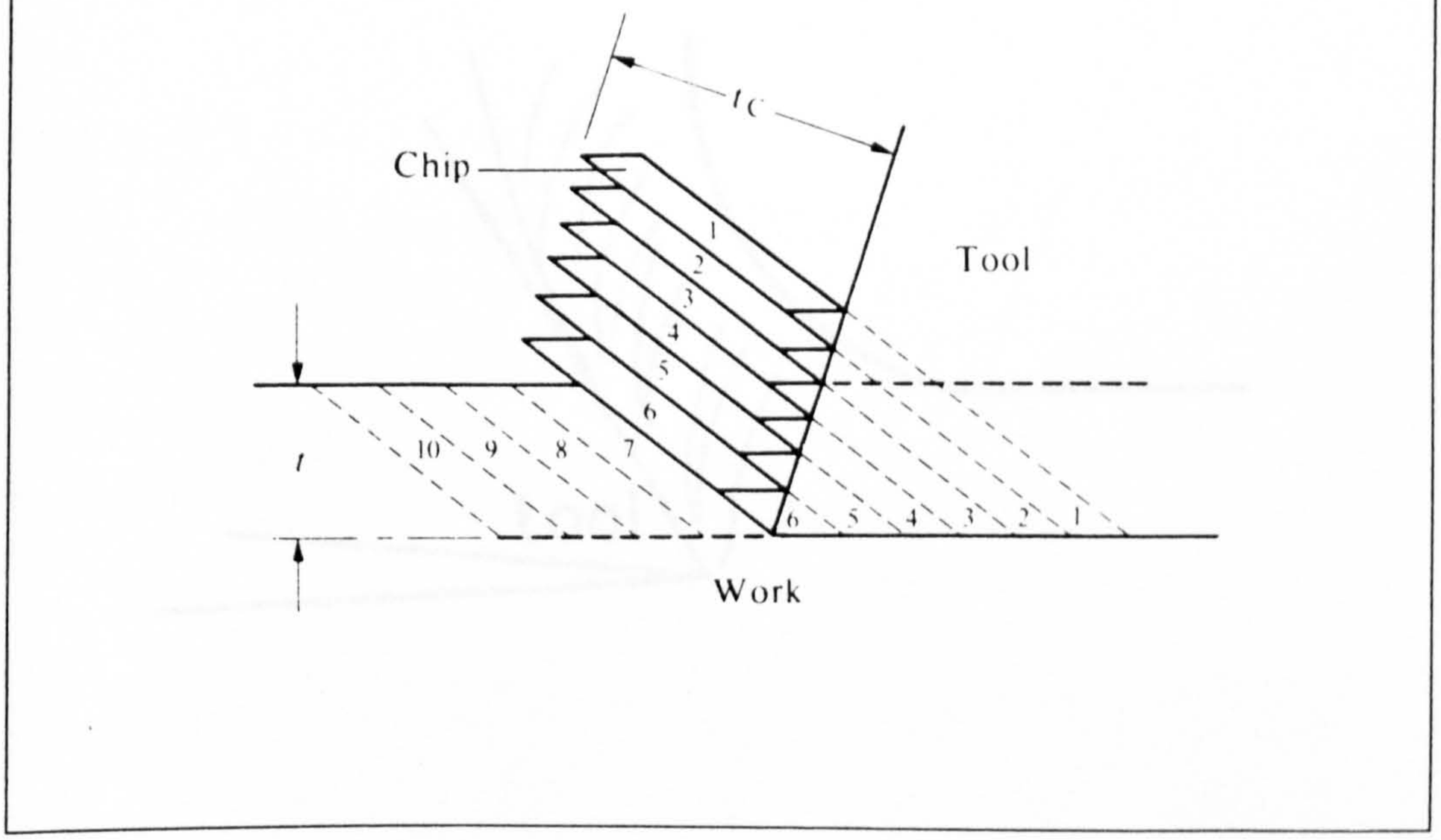

Figure 2.5 Piispanen's Idealized Model Of Cutting Process [16]

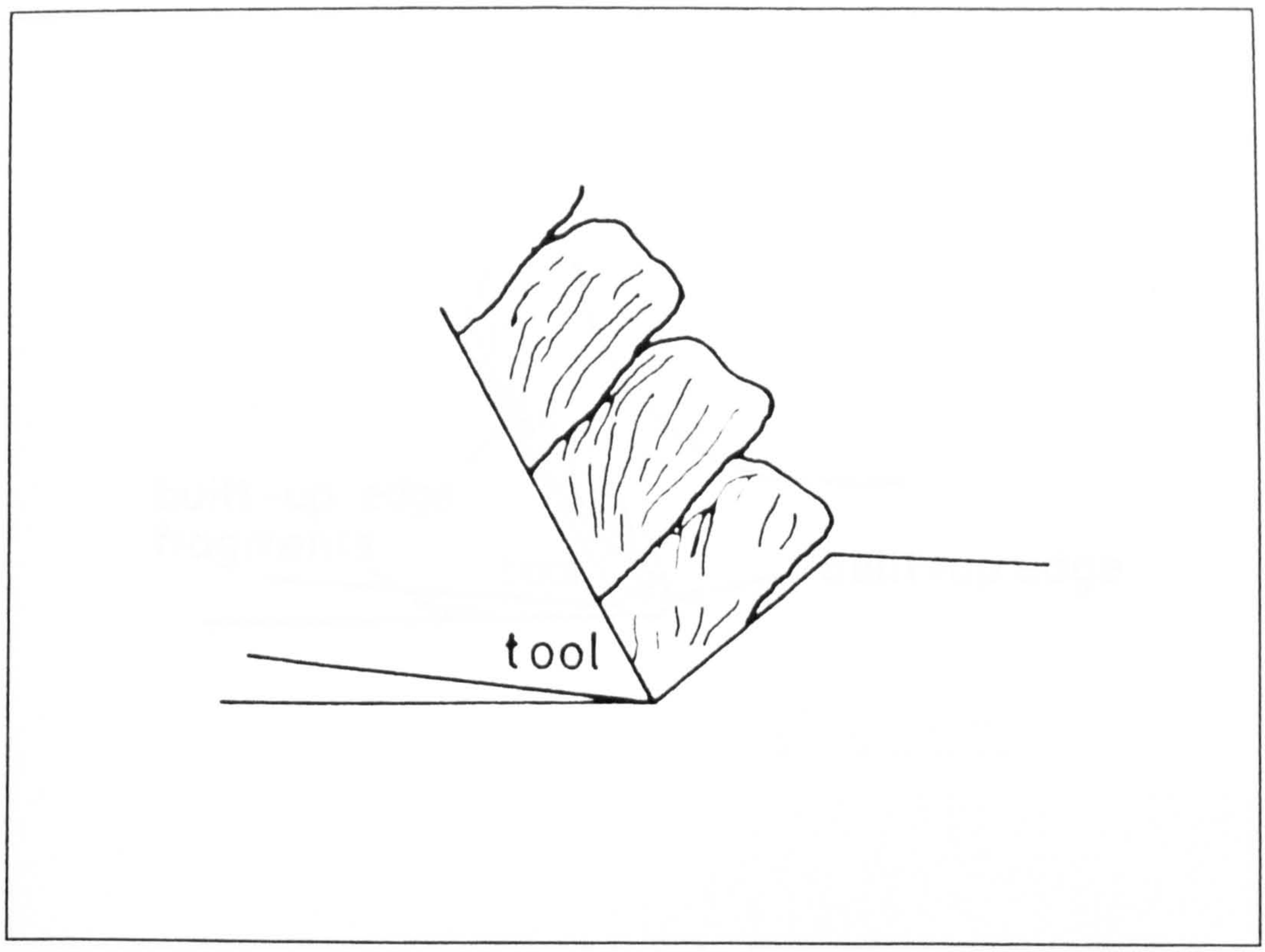

Figure 2.6 Sketches Of Different Types Of Chips [31]
(a) Discontinuous Chip

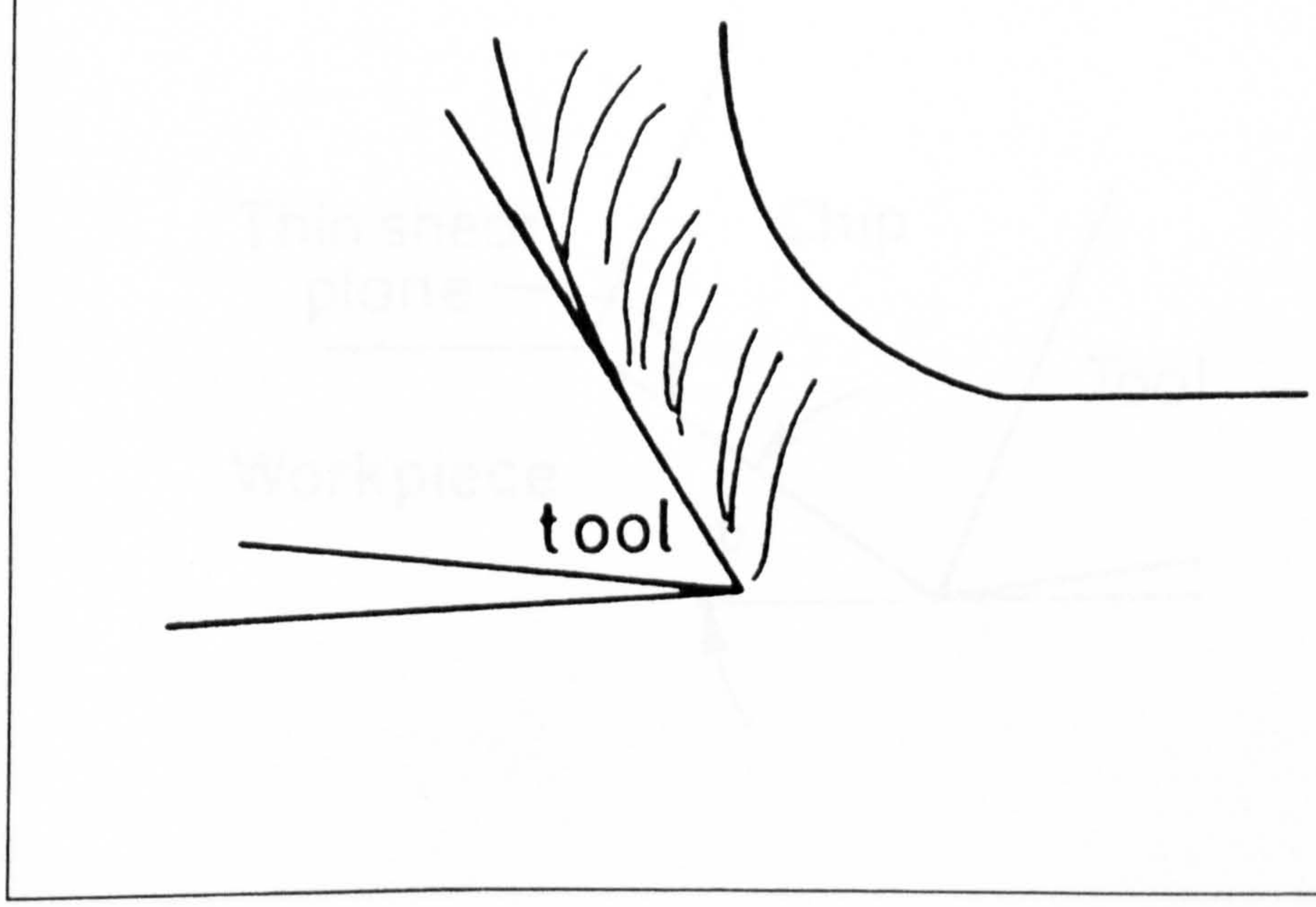

Figure 2.6 Sketches Of Different Types Of Chips [31]
(b) Continuous Chip

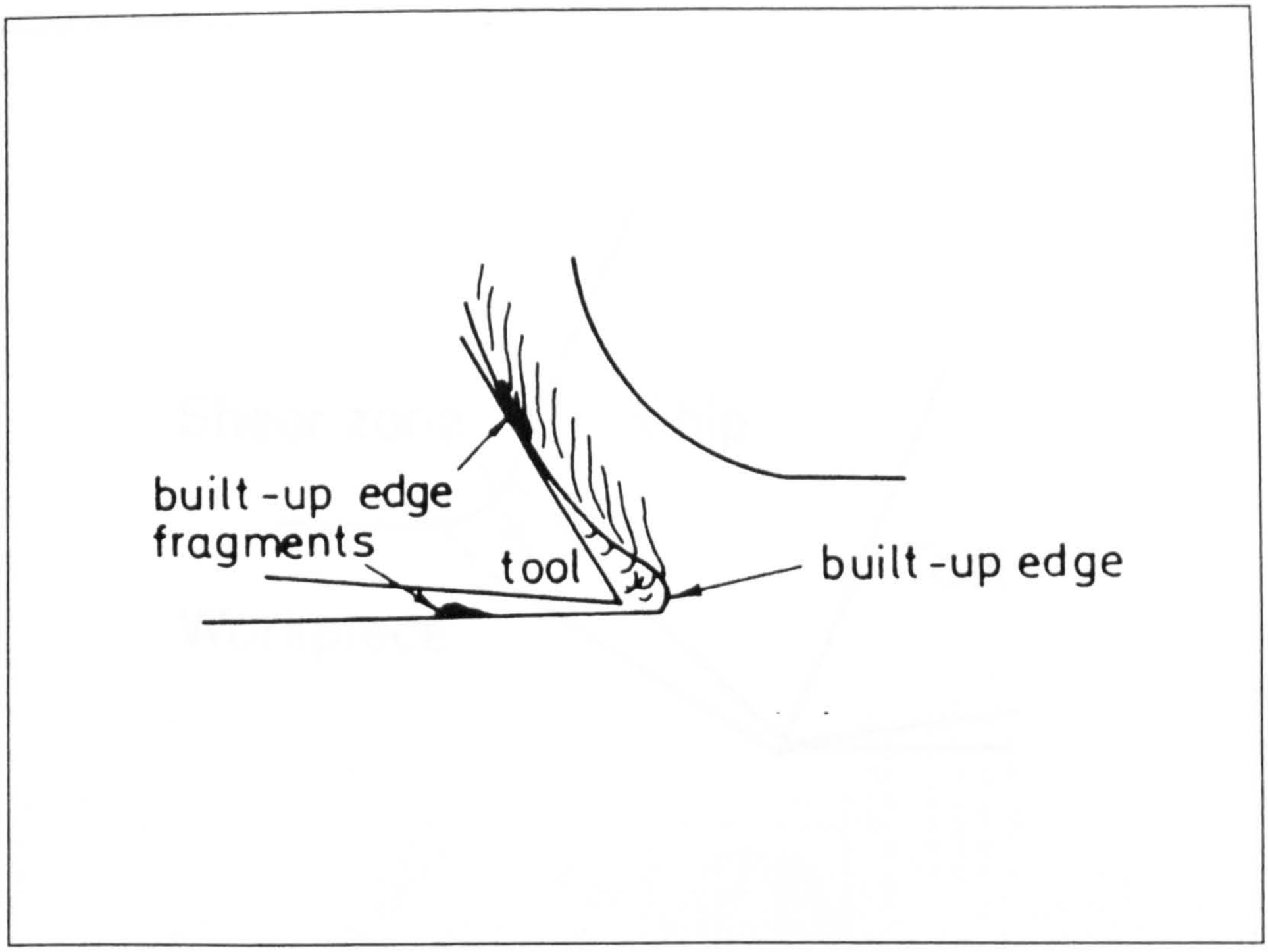

Figure 2.6 *Sketches Of Different Types Of Chips* [31]
(c) Continuous Chip With Built Up Edge

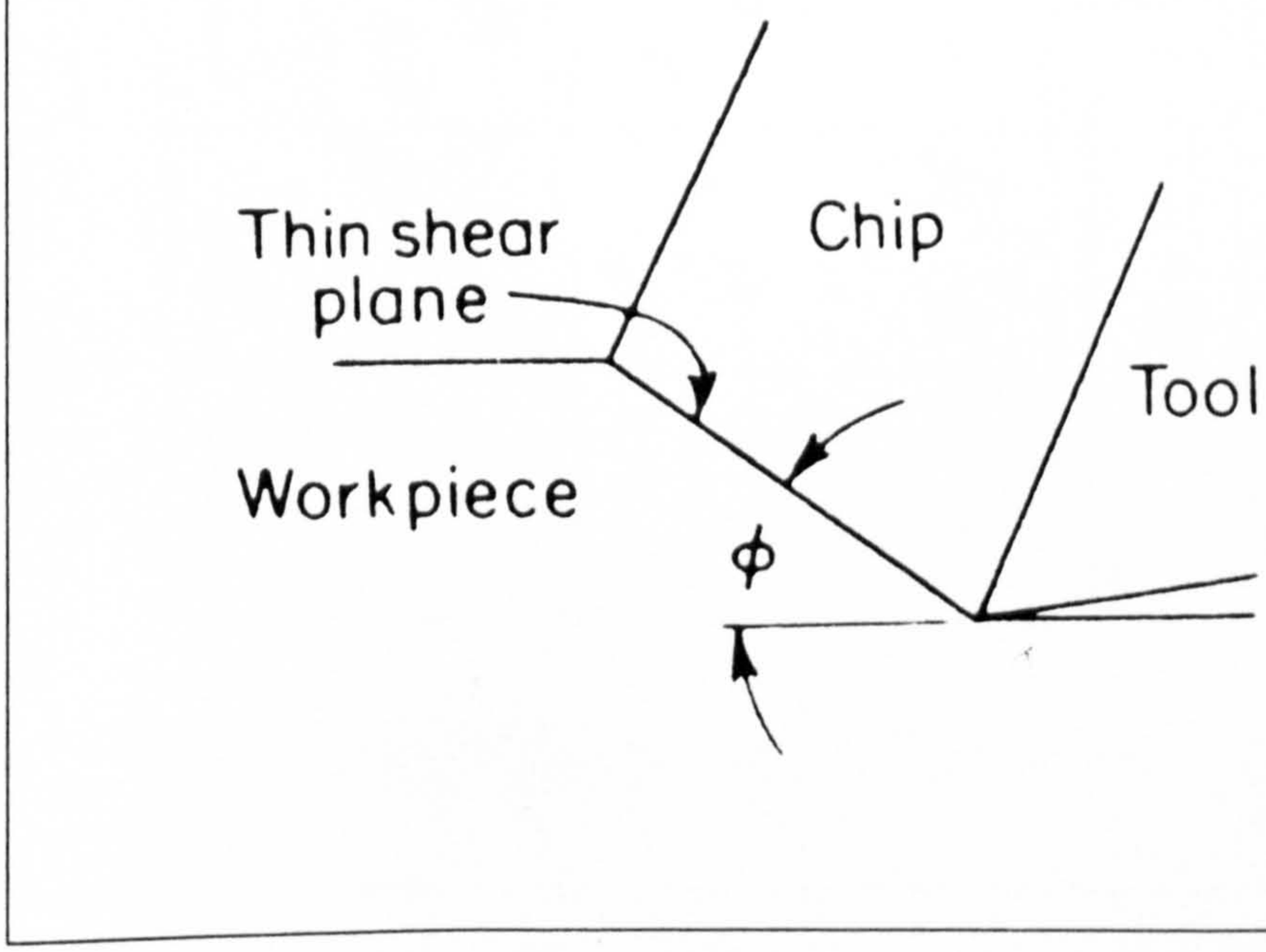

Figure 2.7 *Assumed Shape Of Deformation Zone In Cutting* [21]
(a) Thin Shear Plane Model (ϕ is the shear angle)

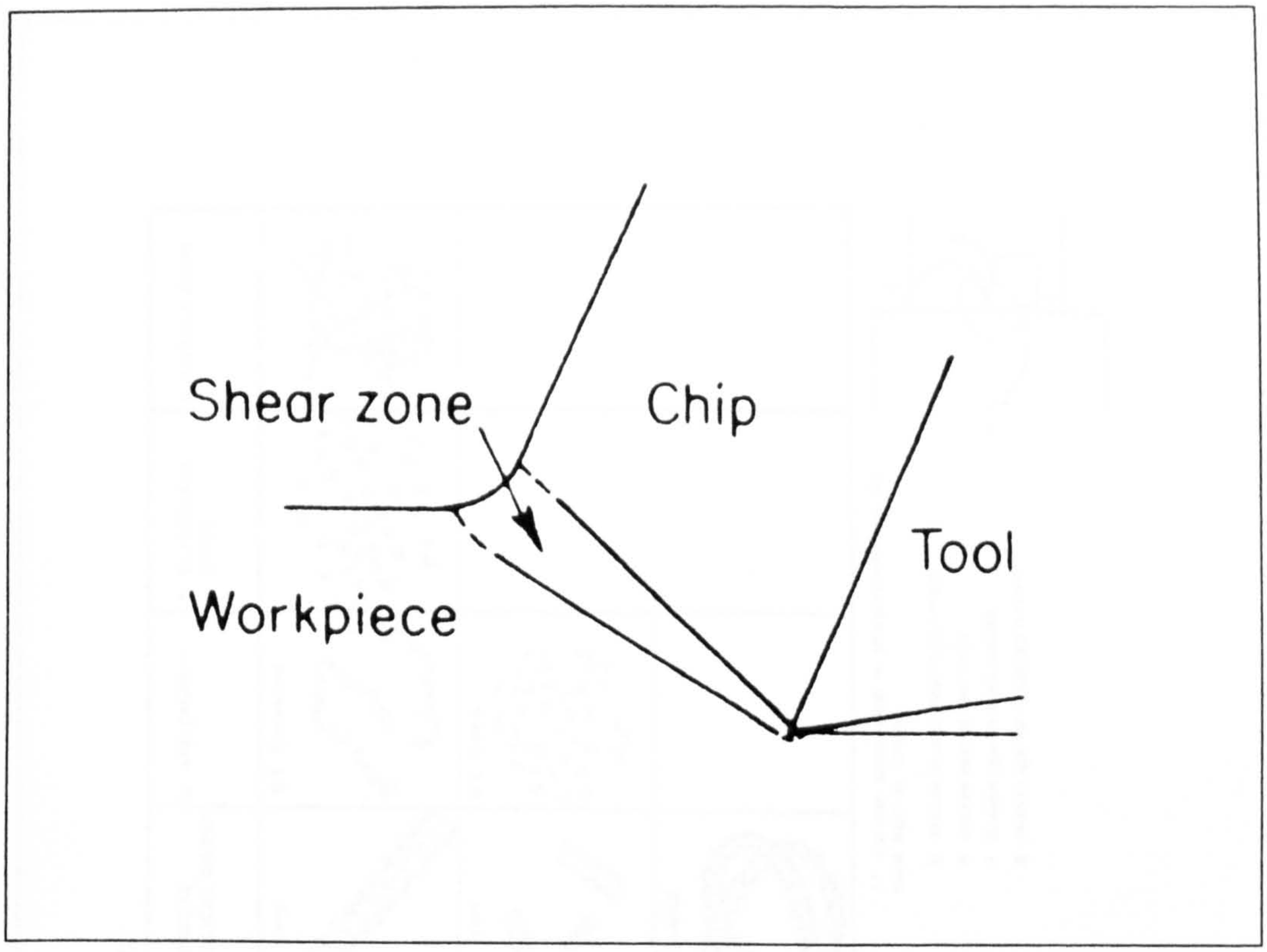

Figure 2.7 Assumed Shape Of Deformation Zone In Cutting [21]
(b) Thick Shear Zone Model

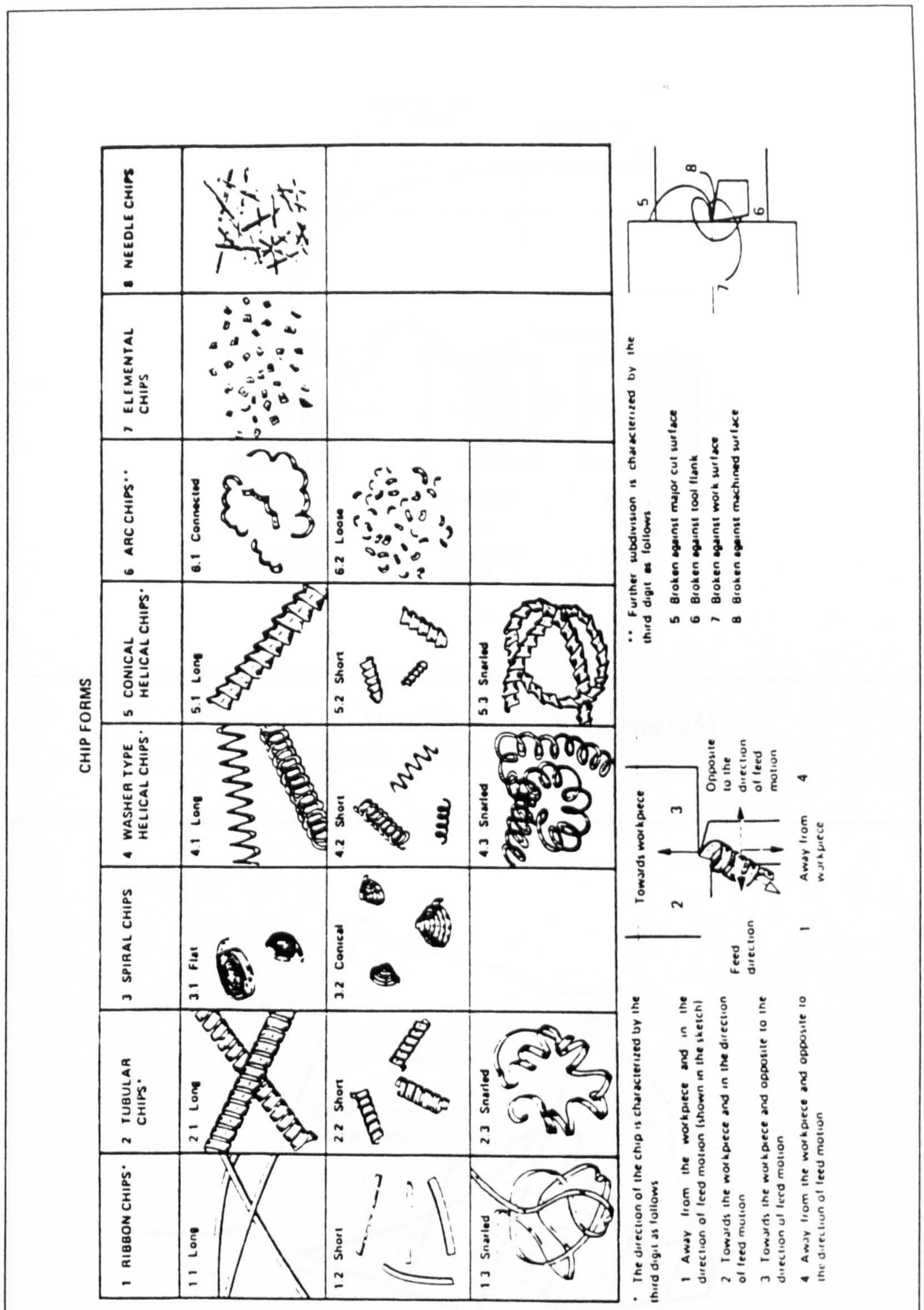

Figure 2.8 The ISO Chips Form Classification [33]

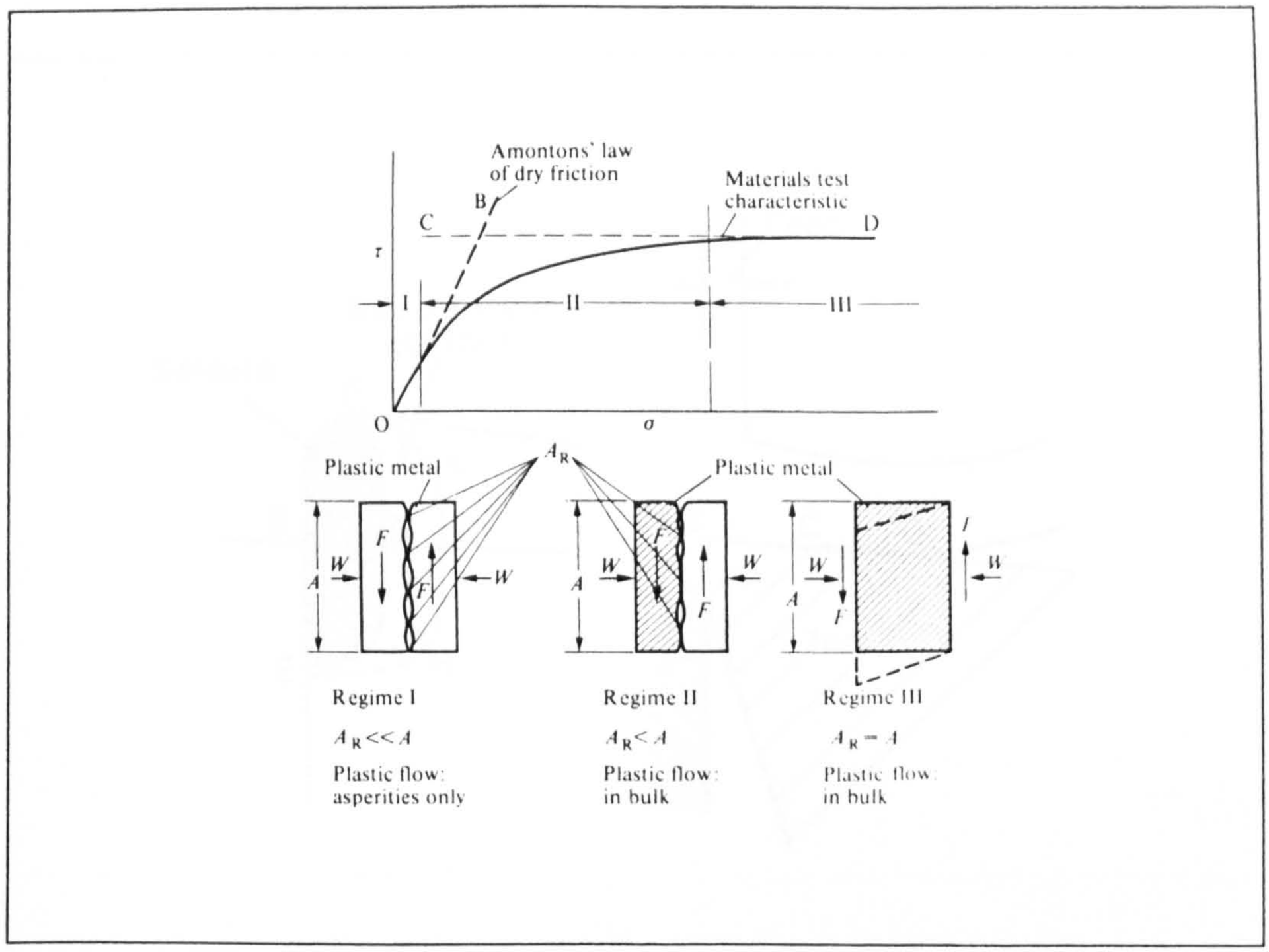

Figure 2.9 Three Regimes Of Friction [35]

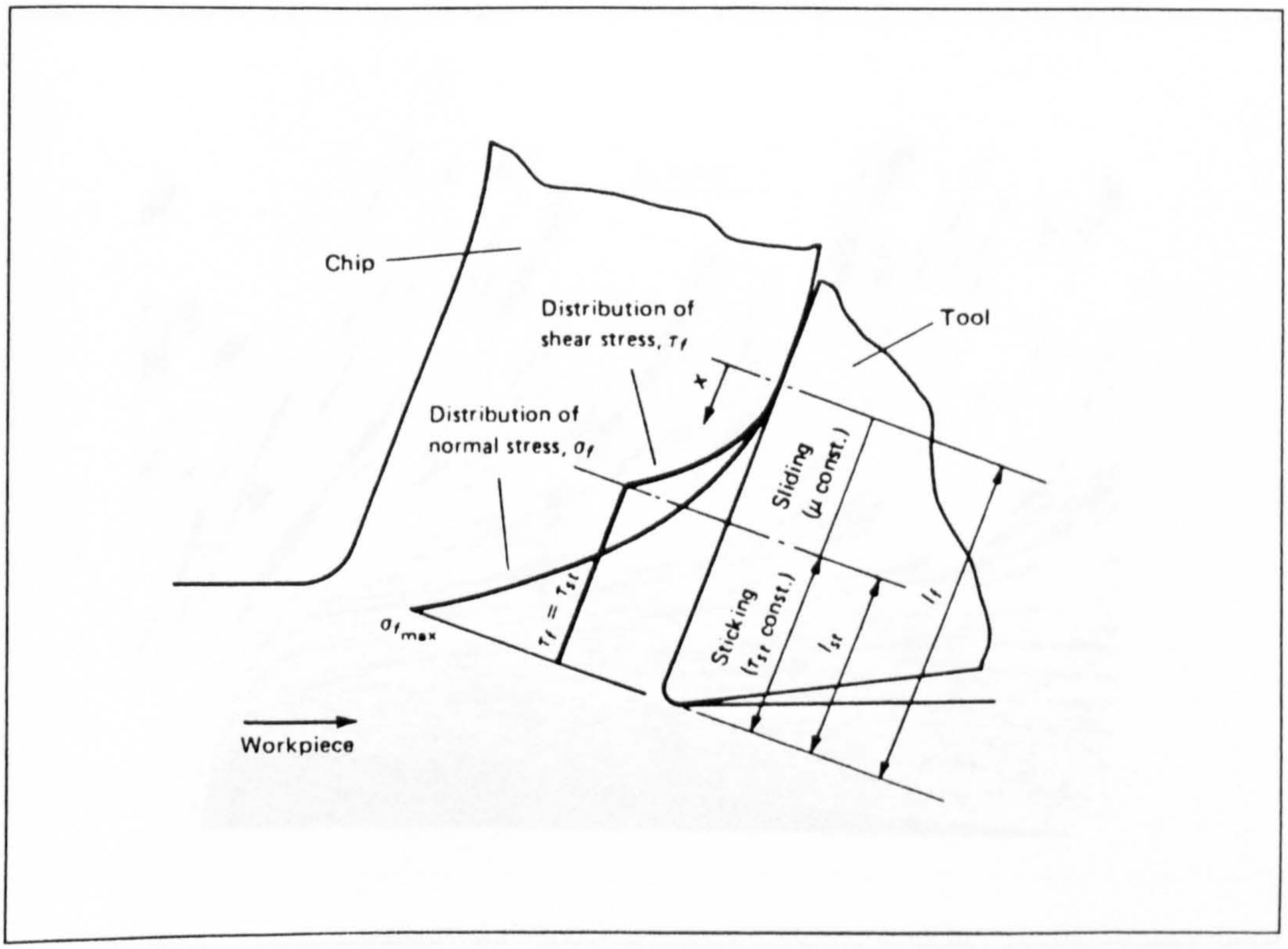

Figure 2.10 A Model Of Chip-Tool Friction In Orthogonal Cutting [35]

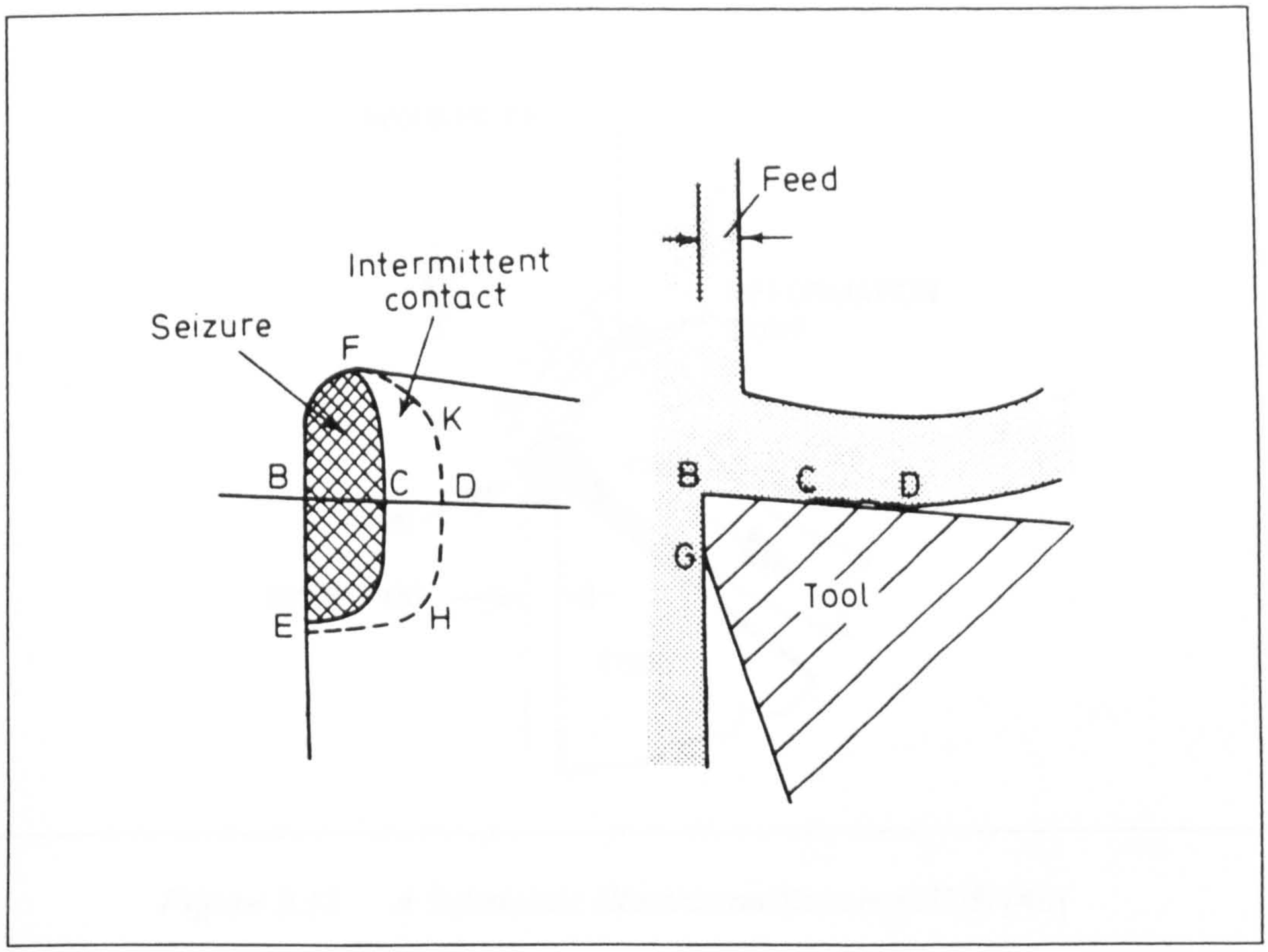

Figure 2.11 Areas Of Seizure On A Cutting Tool [13]

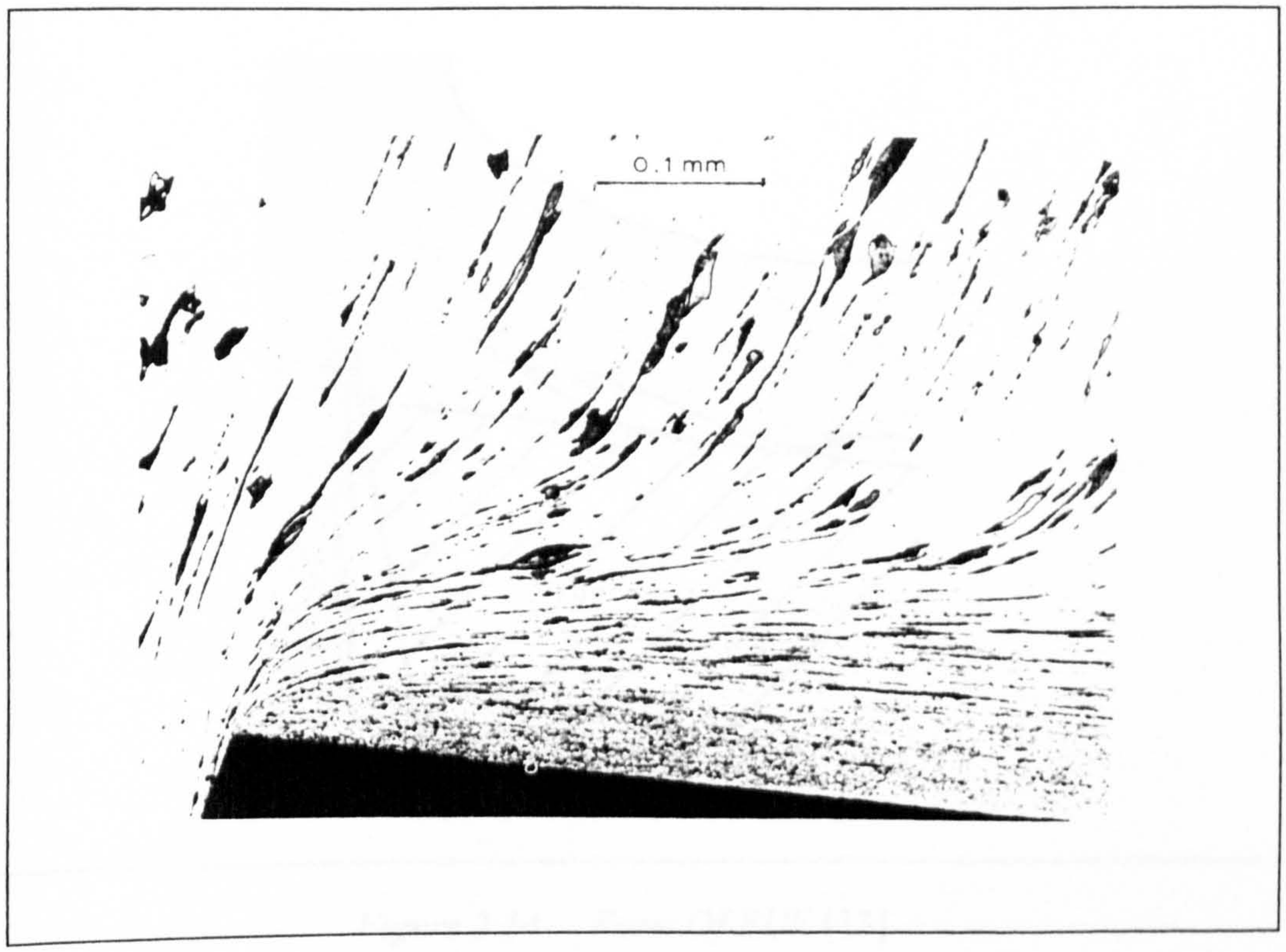

Figure 2.12 A Cross Section Through Quick Stop Showing Flow Zone [13]

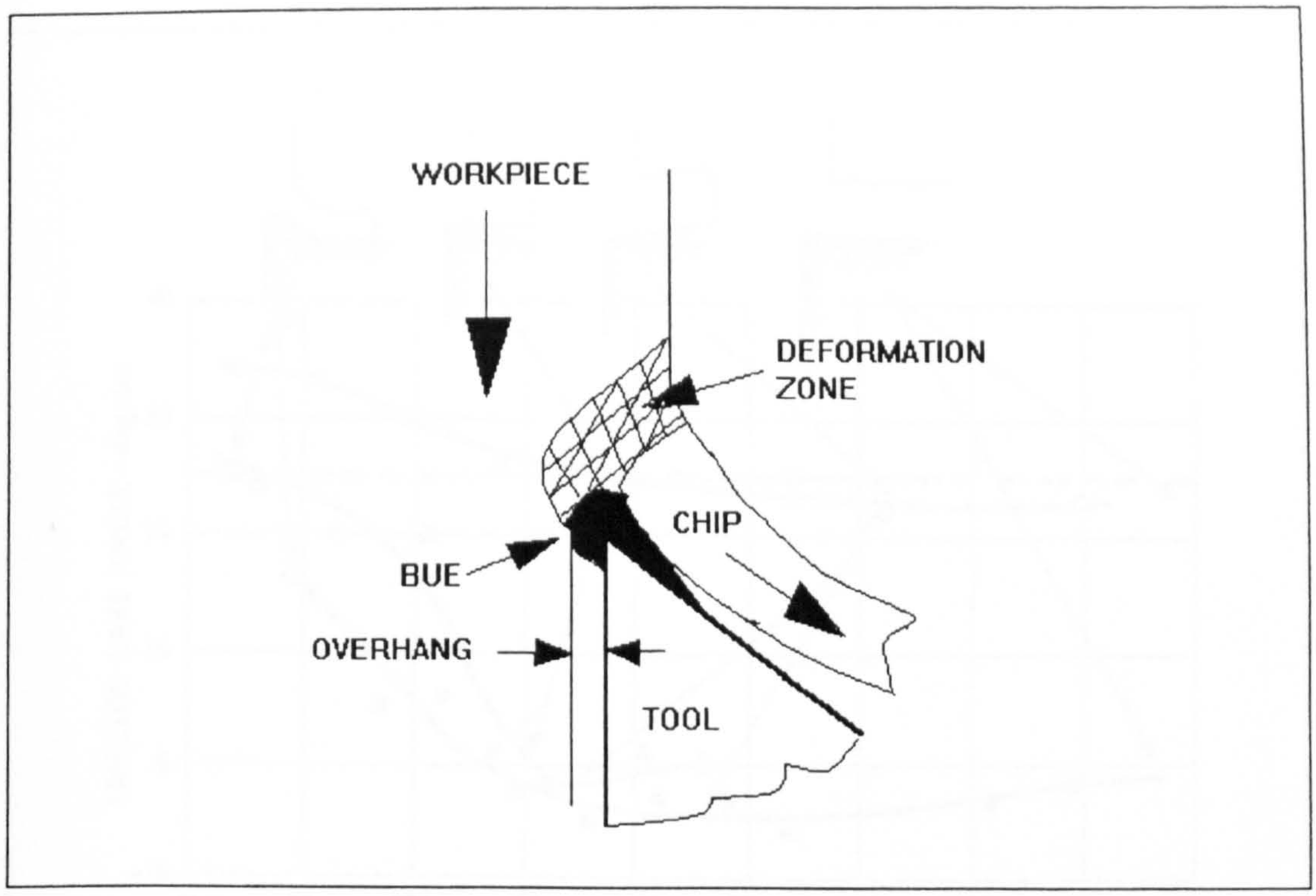

Figure 2.13 A Schematic Illustration Showing BUE [46]

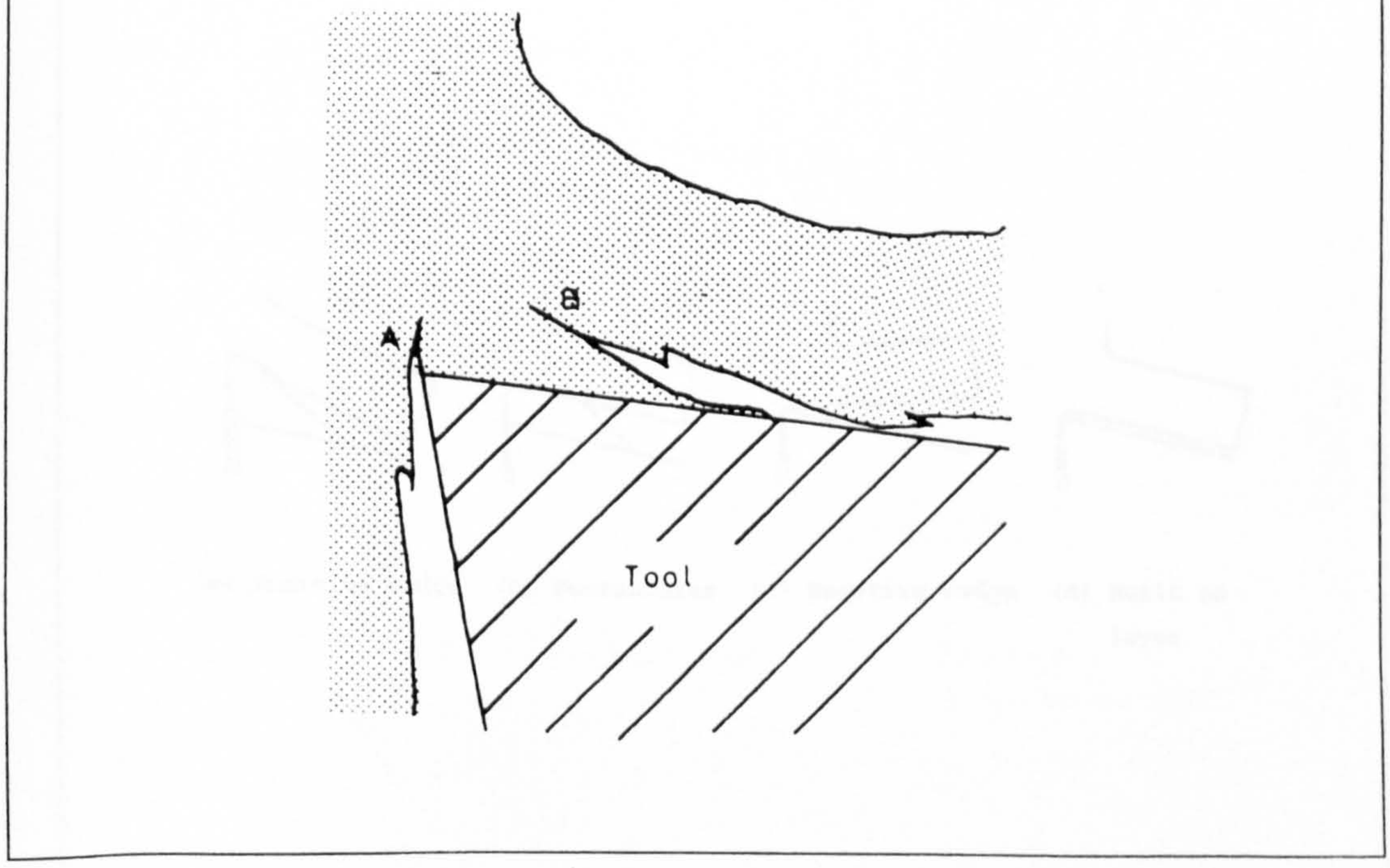

Figure 2.14 Form Of BUE [13]

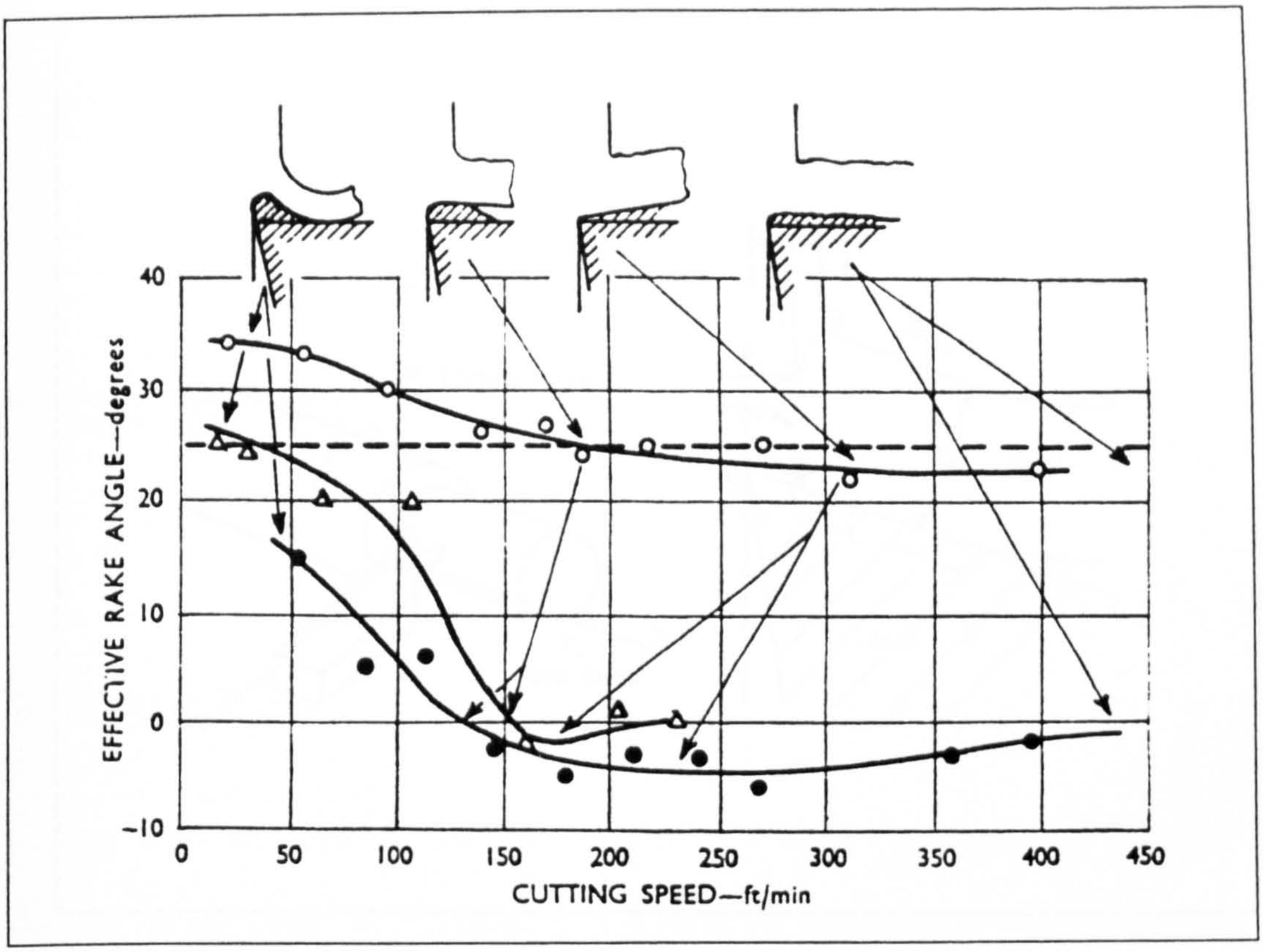

Figure 2.15 Effect Of The Various Classes Of BUE On Cutting Geometry [47]

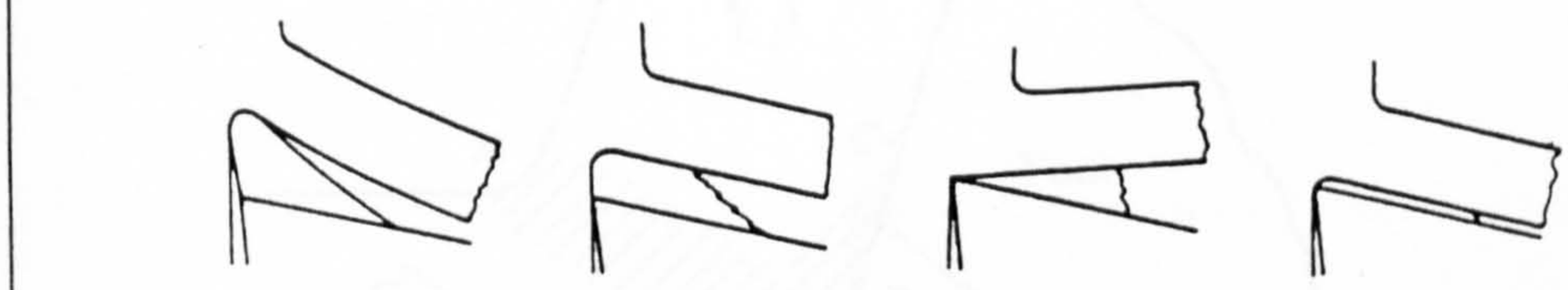

Figure 2.16 Four Types Of BUE [54]

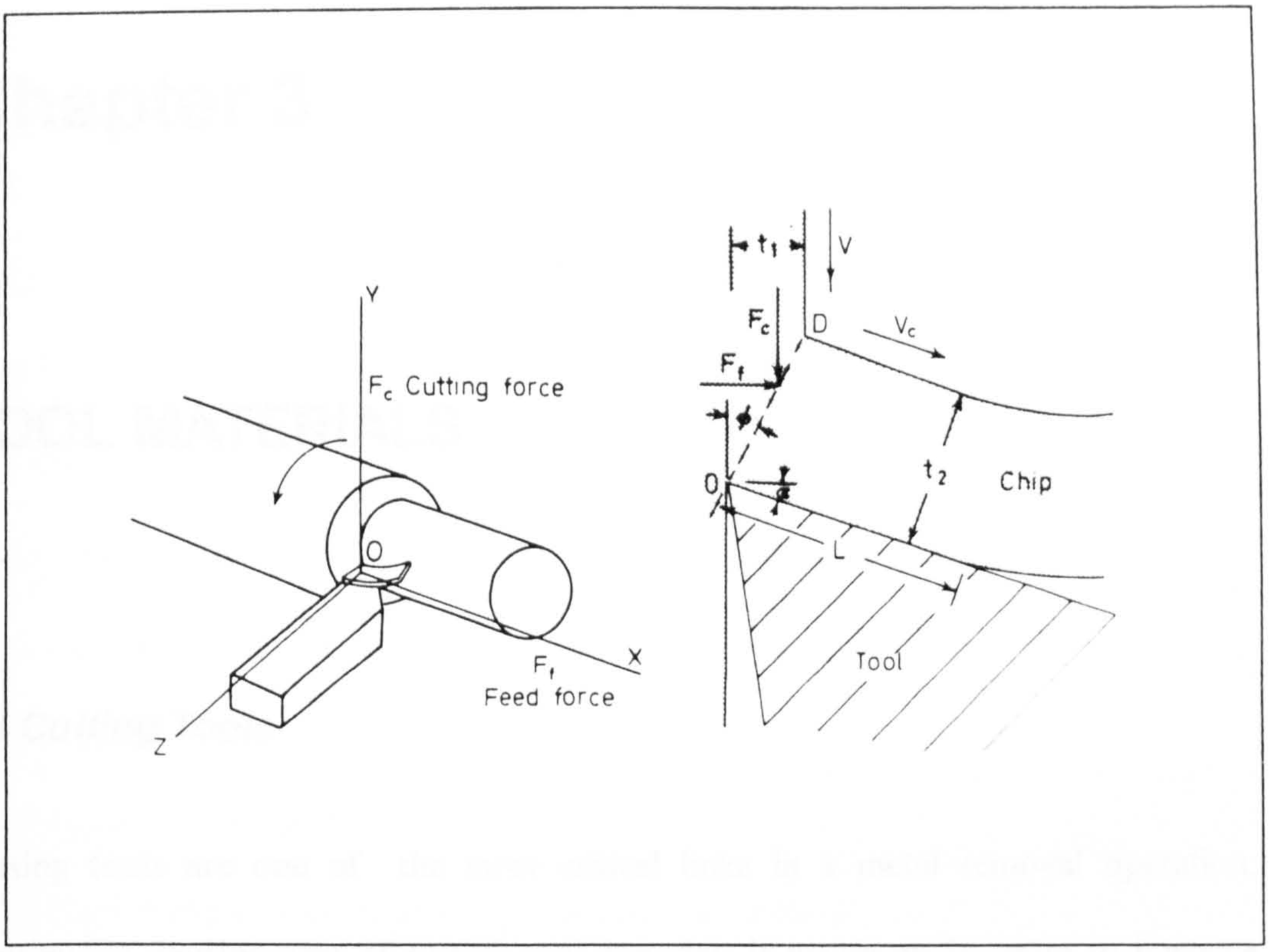

Figure 2.17 Forces Acting On Cutting Tool [13]

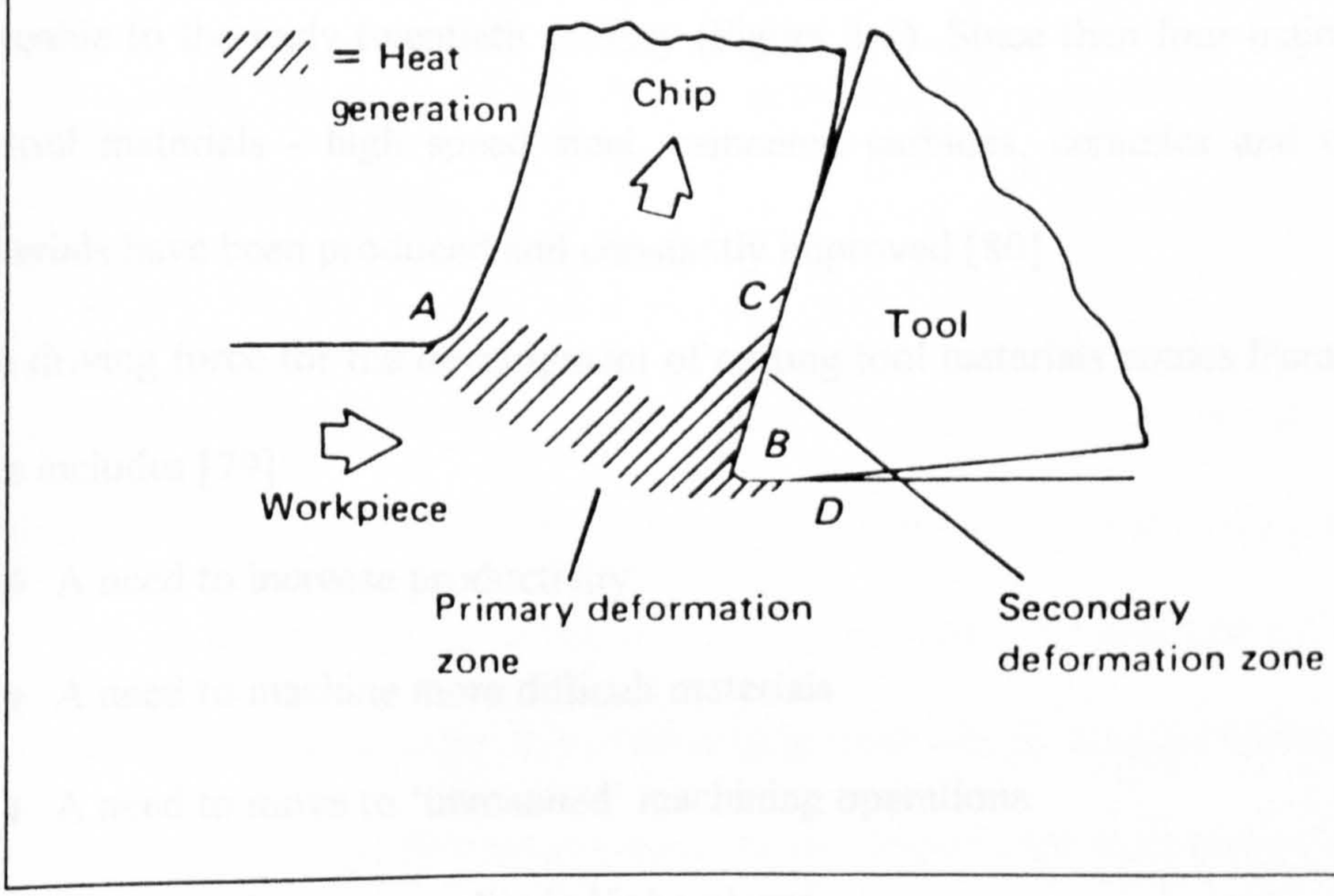

Figure 2.18 Generation Of Heat In Orthogonal Cutting [17]

Chapter 3

TOOL MATERIALS

3.1 Cutting Tools

Cutting tools are one of the most critical links in a metal removal operation. Continuous development of cutting tool materials is necessary in order to improve productivity and reliability. Technological advancements have contributed significantly in the development of cutting tool materials [78] [79]. Modern materials classified as suitable for use in metal cutting are relatively recent, the earliest traceable to the early twentieth century (Figure 3.1). Since then four major families of tool materials - high speed steel, cemented carbides, ceramics and ultra hard materials have been produced and constantly improved [80].

The driving force for the development of cutting tool materials comes from industry. This includes [79]:

- A need to increase productivity
- A need to machine more difficult materials
- A need to move to 'unmanned' machining operations
- A need to improve quality in high volume

3.2 Tool Material Requirements

A cutting tool material is exposed to an extremely hostile operating environment. Trent [81] has reviewed these conditions and the properties needed to withstand them are shown in Table 3.1. The properties required are very difficult to specify but they are a compromise which depends upon the application. However, they may be summarised as follows [81]:

a) High yield strength at cutting temperature

b) High fracture toughness

c) High wear resistance

d) High thermal capacity and high thermal conductivity

e) High resistance to thermal shock

f) Low solubility in the workpiece material

g) Chemical stability

The above properties are from the perspective of a 'producer's requirements list' but not the user. The user will view their requirements in term of function rather than properties of the tools [82].

Consequently, the best tool material will not necessarily be the one that offers the longest tool life but other factors such as tool material cost, the cutting speed and feeds play an important role in the selection of the best tool material for a specific operation. With the increased use of numerically controlled machine tools, reliability and predictability of performance are of greater importance than before and these

factors should be given more emphasis in selecting tool materials for such applications.

3.3 Major Tool Material Types

A wide range of cutting tool materials of different properties and performance capabilities is available today for the broad spectrum of machining applications. These include High Speed Steels, Stellite, Cemented Carbides (coated and uncoated), Cermets, Ceramics, Cubic Boron Nitride (CBN) and Diamond (synthetic & natural) [83]. Because of their high hardness, CBN and diamond are also referred as super or ultrahard materials. Shaw [16] has listed the major classes of cutting tool materials in order of increasing hot hardness (Figure 3.2). Increase in hardness will normally reduce the toughness and materials in the higher hardness region of the list may fail by fracture if used for heavy cuts.

Figure 3.3 shows the effect of temperature on the hardness of some of the major tool materials [84]. Recent development in tool materials have included the coating of these basic materials with thin, high wear resistance layers to improve performance, particularly for high speed steel and tungsten carbide tools. The main classes of tool materials will now be discussed in more detail.

3.4 High Speed Steel (HSS)

High speed steel (HSS) was invented by Taylor and White [7] using improved heat treatment techniques which resulted in an increase in metal removal rates and cutting speeds by up to 3-5 times that possible with carbon steel. The initial development of HSS was essentially in two steps. Firstly, the discovery of combinations of alloying element such as tungsten, molybdenum, vanadium and chromium which produced secondary hardening, these sustain the strength up to 600-650°C. Secondly, the discovery of elevated temperature austenitising to produce a greater volume of dissolved carbides for precipitation. HSS are broadly classified as T type and M type, which are based on tungsten and molybdenum (Mo) respectively as the prime alloying element [85] [86]. Kirk [87] has classified HSS into three groups based on their applications - a) normal duty, b) higher speeds, and c) harder materials. The choice of HSS within these three groupings should take account of hardness, toughness, hardness retention at cutting temperature, grindability, machinability, wear resistance, and specific application, as well as price.

Conventionally, HSS is produced through cast/wrought techniques and powder metallurgy techniques [88]. Various processes such as ion nitriding [89] , ion implantation [90] and carburising [91], are used to improve HSS properties.

Generally HSS are restricted to comparatively low cutting speed operations. Main areas of application includes drilling, end mills, solid milling cutters, slot drills, taps, reamers, broaches and hobs.

3.5 Cemented Carbides

Internationally these materials are known as *'hard metals'*. Cemented carbides are probably the most popular and most common high production tool materials available today. They were first introduced around 1920 in Germany for dies which were used for drawing tungsten wire [92]. Fabricated by powder metallurgy technology involving the bonding of fine carbide particles (56-96% tungsten carbides, WC) in a metal binder (usually cobalt, Co) which is liquid at the sintering temperature (~ 2000°C). Cemented carbides are superior in hardness at elevated temperatures and are chemically more stable than high speed steels. Early work with these materials was hampered by [93]:

1. Their brittleness and tendency to chip
2. Brazing difficulties
3. Grinding difficulties
4. Machine tool rigidity, power and speed problems
5. Cratering on the tool face at high cutting speeds, especially when machining low alloy steels.

Gradually the above mentioned problems were solved. Cratering was reduced by additions of titanium and tantalum carbides [94] .

Generally, cemented carbides can be classified into three main grades. There are:

1. Straight tungsten carbides (WC-Co) grade
2. Mixed cemented carbides (WC/TiC/TaC/Ta(Nb)C/Co) grade
3. Coated cemented carbides

Sintered WC-Co was introduced in 1920, the WC/TiC/Co and the WC/TiC/TaC/Ta(Nb)C/Co between 1931-1937, and coated cemented carbide in the 1960's.

3.5.1 Straight Tungsten Carbides (WC -Co) Grade

This is the simplest cemented carbide produced in commercial quantities, consisting of fine angular particles of tungsten carbide (WC) bonded with metallic cobalt (Co) [95]. Carbides of tantalum, chromium, vanadium, titanium and hafnium, (0.5-3 wt. %) are sometimes added to maintain a fine structure. Figures 3.4 and 3 5 show the structure of a 6% Co 94% WC straight cemented carbide with micrograin (less than 1 μm) and fine grain (between 1 - 5 μm) respectively [95]. Considering their hardness, WC-Co grades are used primarily for machining cast iron, austenitic steel, non-ferrous and non-metallic materials. WC has hardness in excess of 2000 HV whilst Co has a hardness of only 10% that of WC. A combination of brittle WC and tough Co results in a compromise between wear resistance and shock resistance which can be varied by controlling the relative proportions [96]. Two factors affect the cutting properties of straight tungsten carbides, these are [83] [97] [98]:

1) the cobalt content

2) the grain size of WC

The properties of cemented carbide tools, such as hardness and toughness, are greatly determined by the ratio of WC to Co. Increased Co content increases the toughness but reduces the hardness and therefore wear resistance. Coarser grain WC gives better shock resistance, and for a given Co content, reduces the hardness of an

alloy compared with finer grains. Figure 3.6 shows the typical hardness of commercial grade WC/Co with variation in Co content. Higher values relate to lower cobalt and finer grain size.

The practical range of Co content for cutting purposes (in weight percent) is 5 - 12 % with 0.5 - 5 μm WC grain size. The hardness of these alloys ranges from 1250 - 1800 HV. To attain optimal properties, the porosity should be kept low, regular grain size maintained and the carbon content of the tungsten carbide phase kept close to the stoichiometric value of 6.12% [94]. WC-Co grades are not recommended for the machining of steel because deep craters are formed immediately behind the cutting edge, this leads to an early tool failure.

3.5.2 Mixed Cemented Carbides (WC/TiC/Ta(Nb)C/Co) Grade

Mixed cemented carbide grades are called complex grades, multigrades or steel-cutting grades. Additions of tantalum carbide (TaC), titanium carbide (TiC) and niobium carbide (Nb)C increase the hot hardness of the alloy and help prevent plastic deformation of the cutting edge, they also generally lower strength. Figure 3.7 shows the structure of a mixed cemented carbide grade with a composition of 8.5% Co, 71.5% WC, 9% TiC and 11% Ta(Nb)C. This has a hardness of 1575 HV. The best sintered carbide of this class is able to cut at high speeds on all types of steels, including autenitic stainless varieties, ductile cast iron and nickel-base superalloys, where great heat and high pressures are generated at the cutting edge.

In particular, the addition of TaC, TiC and Ta(Nb)C reduce the diffusion rates on the rake face of the cutting tool and higher cutting speeds than those possible with straight carbide are permissible. Trent [81] has demonstrated experimentally the influence of TiC and TaC on reducing cratering of alloyed cemented carbides. Increasing the amounts of TiC and TaC also reduces the strength of the alloyed cemented carbides.

3.6 Coated Cemented Carbides

WC-Co grades suffer from cratering and chemical interaction when machining steels. Additions of triple carbides (TiC, TaC and NbC) largely overcome the crater problem, but simultaneously decrease the toughness of the tools. Efforts to achieve optimum chemical wear resistance and toughness led to the development of coated carbide tools in the 1960's.

The introduction of "throw away" indexable inserts in the 1960's initiated the development of coated carbide tools. The first coated carbide tools were laminated tips consisting of a thin layer, about 0.25 mm thick, of TiC with a base of WC-Co alloy.

Although metal cutting productivity improved with the use of laminated tools, the thermal expansion mismatch between the substrate and the surface layer caused thermal stress during machining and the flaking off of the surface layer. In the late 1960's the work on laminated tools was superseded by the application of a thin layer (~ 5 - 10μm) of TiC coating to cemented carbide tools by chemical vapour deposition (CVD).

Cemented carbide tools coated with a thin, hard, layer of refractory material became commercially available in the early 1970's. Coatings act as a diffusion barrier between the chip formed during machining and the cutting tool itself. The compounds which make up the coatings used are extremely hard (< 2000 HV) and very resistant to abrasion [83]. A CVD technique was normally used to coat thin layers (~ 5 - 10μm) on cemented carbides, with refractory materials such as titanium carbide (TiC), titanium nitride (TiN), titanium carbonitride (Ti(C,N)), hafnium nitride (HfN) or alumina (Al_2O_3) being compound used.

To be effective, the coatings should have the following properties: [99]

a) Hard, refractory and chemically stable

b) Chemically inert with respect to workpiece material

c) Binder-free and no porosity

d) Metallurgically bonded to the substrate with a graded interface

e) Good lubricity

f) Easy and inexpensive to deposit

The function of the coating is not only to improve the abrasion resistance, their action is more complicated than that. Other advantages of the coating includes [100][101]:

- Reduction of cutting forces
- Reduction of the cutting edge temperature
- Increase of abrasion resistance
- Act as a diffusion barrier.

There have been three different generations in the development of coated carbide tools i.e. the single layer coatings, the double and transitional layer coatings, and the multiple layer coatings. Each of the generations of the cemented carbide coatings has their own characteristic in terms of physical, chemical and mechanical properties, and their applications[102][103]. Figures 3.8, 3.9 and 3.10 show a photomicrograph of the double and transitional layer coatings, the multiple layer coatings, and multiple alternating coating layers respectively.

3.6.1 Coating Processes

Various coating processes such as nitriding, electroplating, chemical vapour deposition (CVD) and physical vapour deposition (PVD) are used for depositing coatings onto components [104] [105] [106]. CVD and PVD are the most widely used techniques for the coating of cemented carbide cutting tools [107] [108] [109]. Figures 3.11 and 3.12 show schematic diagrams of the CVD and PVD processes. CVD is by far the most used coating technology among tool manufacturers, with PVD usage no more than 5% industry wide, although it is used increasingly for

sharp-edge tools such as milling cutters [110] . The characteristics of each of these coating processes are highlighted in Table 3.3 [111].

3.6.2 Application of Cemented Carbide

Cemented carbide tools are being used widely in machining cast iron, steel and non-ferrous metals. The International Standards Organisation (ISO) has classified cemented carbides according to the material to be machined (Figure 3.12):

P Series - Triple carbide grades (WC- TiC- TaC / NbC -Co) tools used for machining of steel which produces long and continuous chip.

K Series - WC-Co grades used for machining cast iron and non-ferrous alloys that produce short and discontinuous chips.

M Series - This is an intermediate grade between P and K and is recommended for the machining of stainless steel.

More than 70% of cemented carbide tools used in industry today are coated. However, coated carbide are not suitable for all applications. They are used for rough and finish turning, facing, boring and grooving operations on steel, cast iron and aluminium alloys [112] [113].

3.7 Ceramic Tools

During the Second World War the scarcity of tungsten, the basic raw material for cemented carbides tools led to the introduction of ceramics in commercial quantities [114]. Ceramic cutting tools possess high hot hardness and wear resistance, high compressive strength, high resistance to plastic deformation and good chemical resistance; this allows them to operate at much higher cutting speeds than conventional cemented or coated carbides. However, ceramic tools are very brittle and any vibration and chatter will cause them to fracture [115]. Subsequent improvements in processing techniques have resulted in the production of higher strength, more uniform and better quality tools [115] [116] [117] [118].

There are two major groups of ceramic tools:

1. Alumina (Al_2O_3) Based Ceramic Tool
2. Silicon Nitride (Si_3N_4) Based Ceramic Tool

3.7.1 Alumina (Al_2O_3) Based Ceramic Tools

Traditionally, ceramic tool material has been aluminium oxide (Al_2O_3 - alumina), which is white in clolour and manufactured by cold pressing and sintering. Other oxides such as zirconium oxide (zirconia) are used as alloying constituents which act to significantly toughen the materials [113] [118]. The major drawback with alumina is that it has a low thermal conductivity which makes it very susceptible to thermal shock, this situation can be improved by the addition of titanium carbide. The resultant material, which is black, has to be hot-pressed or hot isostatically pressed.

An important innovation has been the introduction of reinforcement of the alumina matrix with up to 30% silicon carbide (SiC) single-crystal whiskers to improve the toughness of alumina based ceramics by mechanical rather than chemical means [79] [119] [120].

3.7.2 Silicon Nitride (Si_3N_4) Based Ceramic Tools

These were developed in the late 1970s. Joseph Lucas Industries Ltd. in the UK developed a ceramic tool of a complex compound under the tradename of syalon (representing SiAlON or silicon-aluminium oxynitride - Si_3N_4-Al_2O_3-Y_2O_3) [121]. The Si_3N_4 based ceramic tools posses high strength with hot hardness, good wear resistance, low coefficient of friction, shock resistance and toughness. At high temperatures (1200 - 1400^{o}C) they have many attractive characteristics such as good oxidation resistance, good mechanical strength, chemical inertness and high hardness.

Ceramic tools are successfully used for machining of cast irons, low and medium carbon steels, nickel based alloys and other superalloys [122] [123] [124].

3.8 Diamond, Polycrystalline Diamond (PCD) and Cubic Boron Nitride (CBN)

Diamond, polycrystalline diamond (PCD) and cubic boron nitride (CBN) are also known as *'Super or ultra-hard Materials'* Diamond is the hardest material with a hardness of 12,000 HV followed by PCD and CBN with hardnesses of 7000 -

10,000 HV and 3500 HV respectively [95]. Due to their extreme strength and hardness they are used in industrial processes for cutting and in a variety of other technological applications [125] [126]. Diamond tooling comes in two forms: natural, or single crystal diamonds, and synthetic, or polycrystalline diamond (PCD).

3.8.1 Natural or Single Crystal Diamonds

The complete crystal structure of the diamond lattice can be described as consisting of two interpenetrating face-centred cubic lattices where each carbon atom is attracted by covalent bonds. Diamond crystals are very anistropic. Their positive properties include [81] [118]:

a) High hardness.

b) Low thermal expansion coefficient and high thermal conductivity, which result in a very good resistance to thermal shock.

c) Very sharp cutting edges.

d) Low friction.

Diamonds are very expensive materials, they could be ideal material for metal cutting but have some drawbacks:

a) Extensive chemical interaction with most transition metals.

b) Extreme brittleness; single-crystal diamond cleaves easily.

c) Difficulty in shaping and resharpening after use.

These disadvantages coupled with limited supply and increasing demand for diamond tooling has initiated the search for an alternative and dependable source of diamond.

This search led to the ultra high pressure (~ 20 K bar), high temperature (1500°C) synthesis of diamond from graphite at the General Electric laboratories in the United States of America in the mid 1950's and the subsequent discovery of polycrystalline diamond (PCD) [126].

3.8.2 Polycrystalline diamond (PCD)

The introduction of polycrystalline diamond (PCD) tool blanks by the General Electric Company (GE) in 1973 began a new age in the machining of non-ferrous metals and abrasive non-metallic materials [127]. PCD tools are formed by sintering together a randomly orientated mass of fine diamond crystallites. Their advantages over single crystal diamond are uniform mechanical properties, higher shock resistance and larger tool size. The mechanical properties of single crystals vary for different crystal planes, while PCD has uniform hardness and wear resistance in all directions [128] [129].

PCDs are marketed under two major propriety names, General Electric's Compax© and the De Beers' Syndite©. The important properties of PCD tools are hardness, abrasion resistance, compressive strength, and thermal conductivity.

PCD tools are susceptible to temperature, like natural diamond, and this is the reason that their application is limited to non-ferrous/non-metallic materials [130] [131] [132] [133] . The other problems of PCD tools are price and grindability. The price is about 100 times higher than that of cemented carbides.

3.8.3 Cubic Boron Nitride (CBN)

Cubic boron nitride (CBN) is a manufactured tool material which is not a naturally occurring compound. CBN was developed in the late 1960's shortly after the development of synthetic diamond. Employing a similar technology, and having a hardness second to that of diamond. Normal boron nitride has a hexagonal crystal structure but, if subjected to high temperature (~ 1400°C) and high pressure (~ 60 Kbar), the hexagonal crystals are converted into a cubic structure which is the same as that of diamond.

Polycrystalline cubic boron nitride (PCBN) tool blanks and inserts are a combination of a layer of CBN bonded to a cemented carbide substrate. PCBN cutting tools posses properties such as hardness at high temperature, abrasion resistance, high strength, high impact resistance and thermal conductivity [134]. CBN tools have high thermal stability and no practical oxidation below 1000°C. They also have high thermal conductivity and a low coefficient of thermal expansion. However, they have a relatively low transverse rupture strength. Their high hot hardness property is used to offset their low impact strength [135].

The physical properties of a range of different tool materials including diamond and PCBN are given in Table 3.4.

The largest application of PCD tools is in cutting Al-Si alloys containing high Si level. Besides long tool life, a fine surface finish is obtained because of low tool wear and minimum welding of the workpiece to the tool [136] [137]. The major

application area for CBN tools is in the machining of nickel based superalloys and related cobalt and iron based materials, this is largely due to the retention of edge strength at high temperatures (~ 1200°C) and the lack of chemical reaction with the workpiece. Hardened tool and die steels together with chilled cast iron, are also suitable candidates for CBN tooling [138].

Table 3.1 Conditions Of Tool Environment And Tool Properties [80]

Conditions	Properties required in cutting tools	Comments
1. High compressive stress	Yield stress of tool material above that of work material (hardness gives good indication)	Major stresses near edge compressive
2. Tensile or shear stress	High breaking stress in tension	
3. Localised stress concentration	Toughness (ability to deform locally and absorb energy without cracking	Concentrated stress near cutting edge can cause fracture of tool
4. High temperature	Compression strength retained at elevated temperature	Important when machining strong materials
5. Temperture fluctuation / steep thermal gradients	Fatigue strength at temperature	Thermal expansion and thermal conductivity affect strength
6. Abrasion	Hardness	Due to abrasive inclusion of work materials
7. Diffusion	Compatibility between tool and work material	At high cutting speed, diffusion and reaction between tool and work material may control tool wear rate
8. Built-up edge (BUE)	Ability to withstand localised stresses caused by cutting in presence of BUE	

Table 3.2 Properties of Some Coating Materials [104]

Materials	Hardness (kg/mm^2)		Coefficient of Thermal Expansion ($\mu m/m.K$)
	at 25°C	at 1000°C	
Cemented Carbide Substate (WC-Co)	1500		7.3
Titanium Carbide (TiC)	3200	44	7.7
Titanium Carbonitride (TiCN)			8.0
Titanium Nitride (TiN)	2450	80	9.4
Aluminium Oxide (Al_2O_3)	2500	399	8.4

Table 3.3 Characteristics of CVD and PVD Processes [104]

Characteristics	CVD (Chemical Vapour Deposition)	PVD (Physical Vapour Deposition)
➔ Coating Temperatures	~ 1000°C	~ 500°C
➔ Tool Toughness	Reduced to certain extent	Unaffected
➔ Cutting edge	Honing required	Sharp or almost sharp
➔ Coating thickness	Up to 12 μm	Up to 4 μm
➔ Layers	Multi-layers TiC, TiC-TiCN-TiN, TiC-Al_2O_3	Single layer TiN, TiCN
➔ Main Applications	Turning Boring	Milling Threading Drilling
➔Advantages	High wear resistance High crater wear resistance Longer tool life	Replaced uncoated: Same toughness Same cutting edge configuration Same accuracy, Reduced Built-up Edges Longer Tool Life

Table 3.4 Physical Properties Of Selected Tool Materials [93] [118] [127]

Property/Tool Material	Conventional Ceramics	Tungsten Carbide (ISO K10)	Natural Diamond	PCD	PCBN
Density (g/cm^3)	3.2-4.3	14.7	3.52	3.43	3.1
Compressive Strength (GPa)	1.8	4.5	8.68	4.74	3.8
Toughness K_{IC} (Mpa $m^{1/2}$)	1.9-8.0	10.8	3.4	6.89	10
Hardness at 20°C (HV)	1500-2450	800-2400	8000-12000	6500-10000	3500-4500
Young's Modulus (GPa)	300-420	620	1141	925	680
Modulus of Rigidity (GPa)	-	258	553	426	280
Coefficient of Thermal Expansion ($x10^{-6}K^{-1}$)	3.2-8.5	5.4	1.5-4.8	3.8	4.9
Thermal Conductivity at 25^0C ($Wm^{-1}K^{-1}$)	8-23	80-120	500-2000	120	100

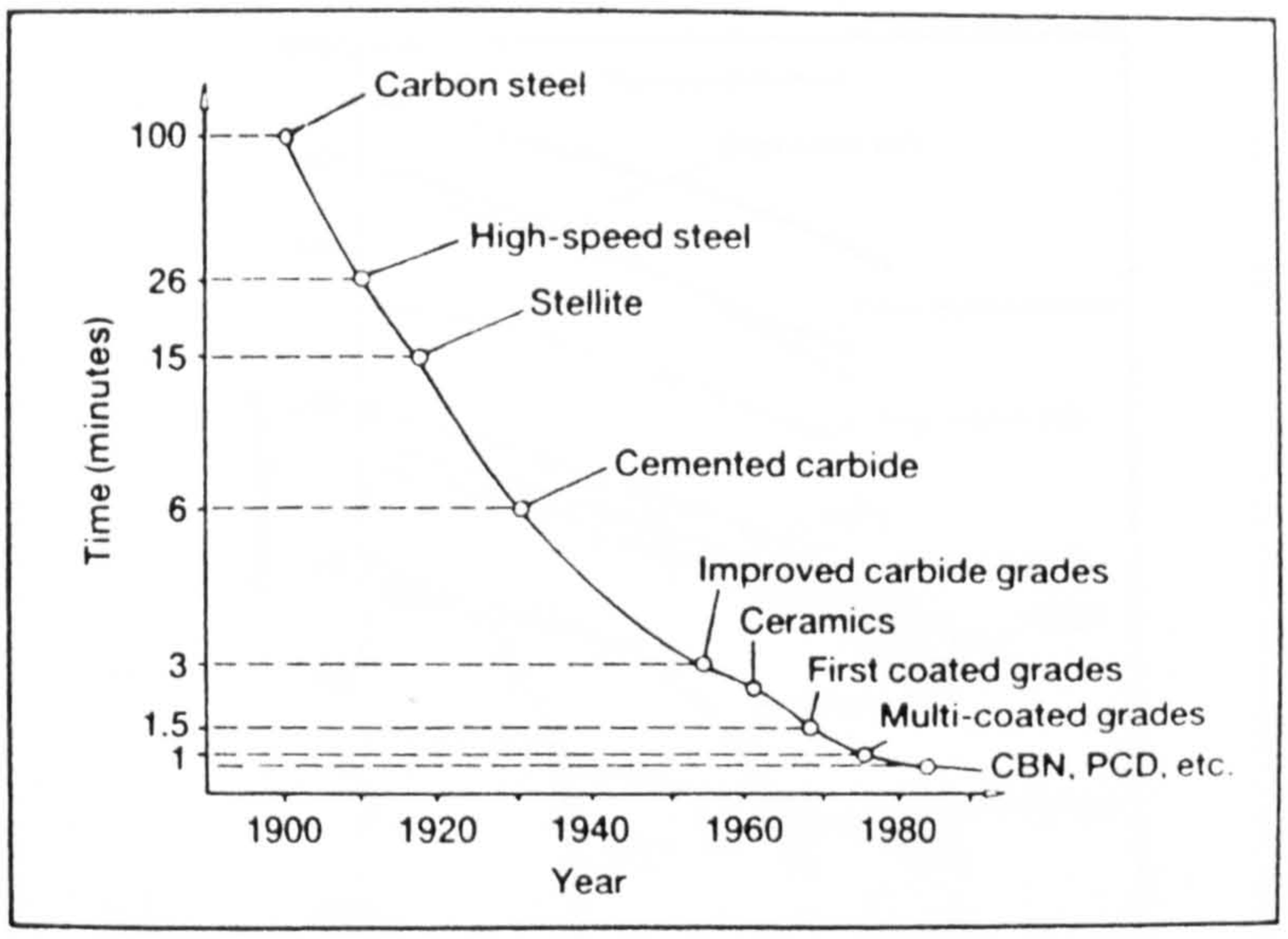

Figure 3.1 The Evolution Of Cutting Tool Material [57]

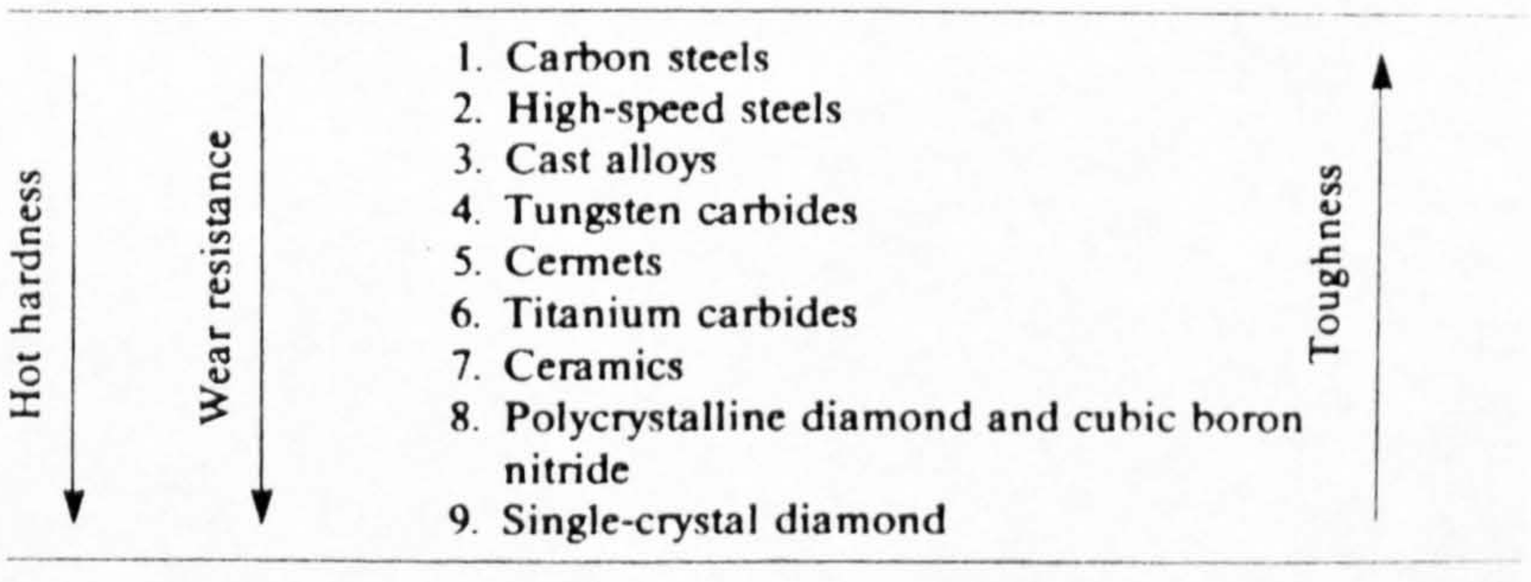

Figure 3.2 Principle Class Of Cutting Tool Material And Their Relative Toughness And Hardness At Elevated Temperature [16]

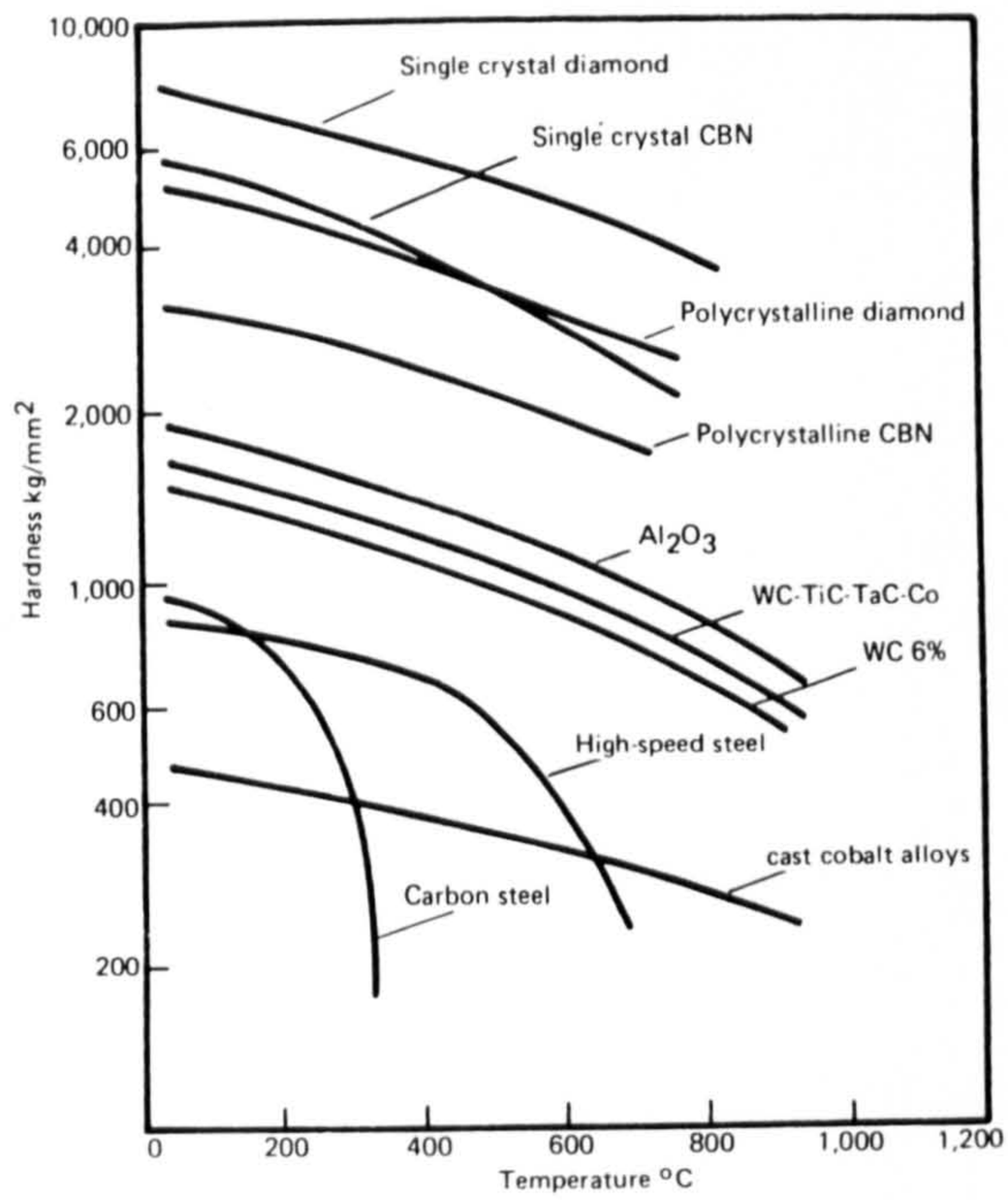

Figure 3.3 Variation Of Hardness With Temperature For Some Tool Material [13]

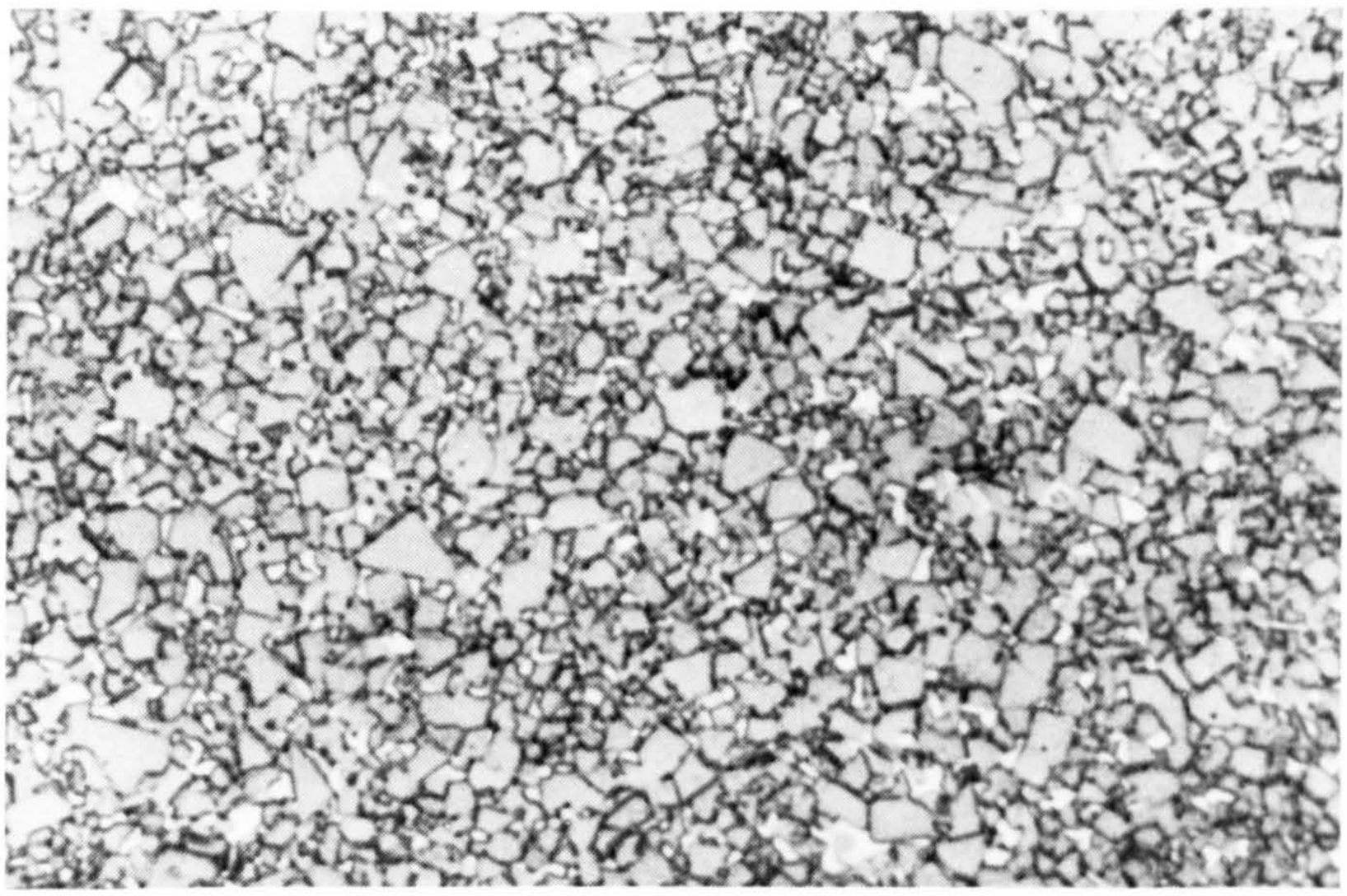

Figure 3.4 Microstructure Of Micrograin Grain 94WC/6Co Grade (X1500) [95]

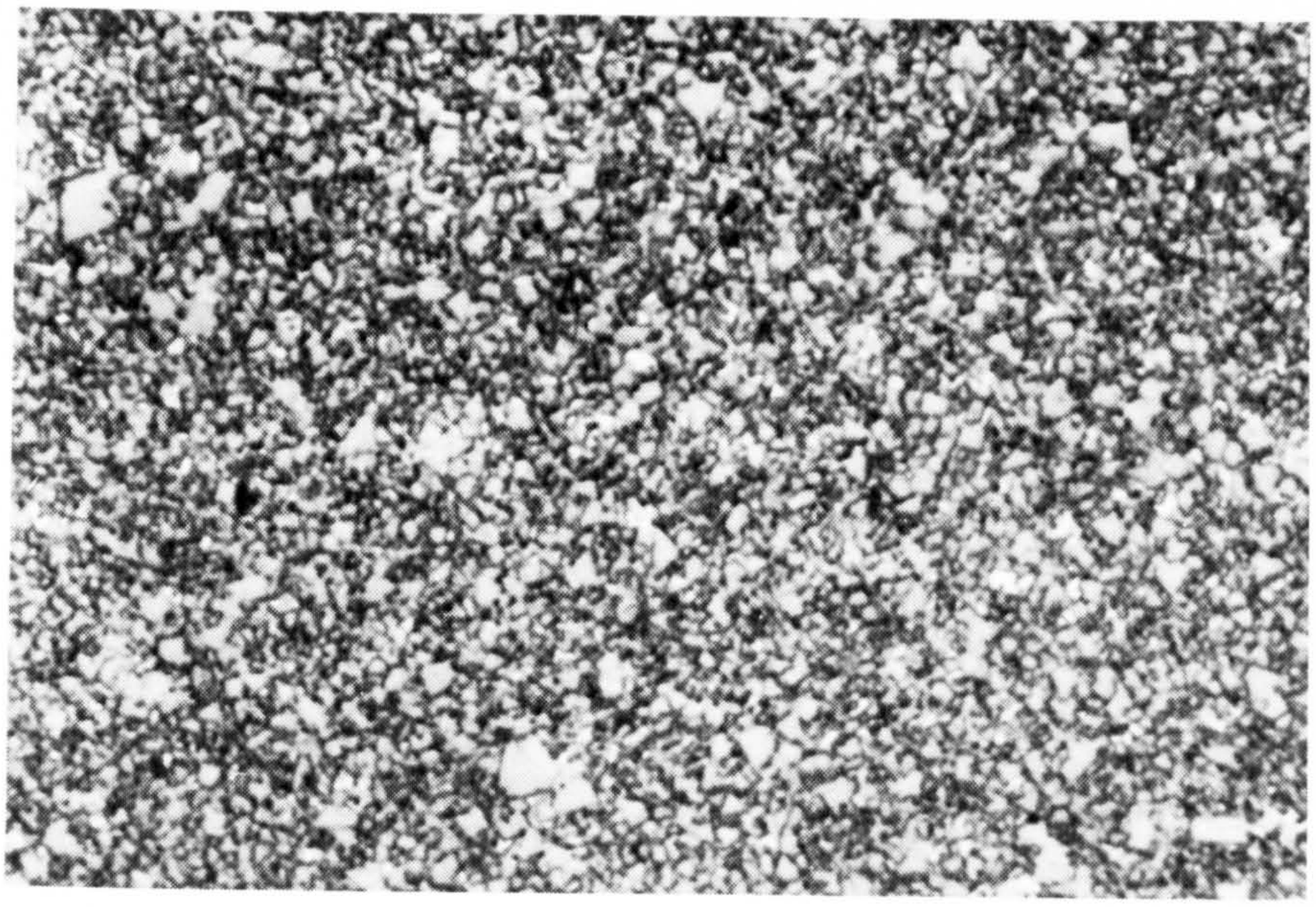

Figure 3.5 Microstructure Of Fine Grain 94WC/6Co Grade (X1500) [95]

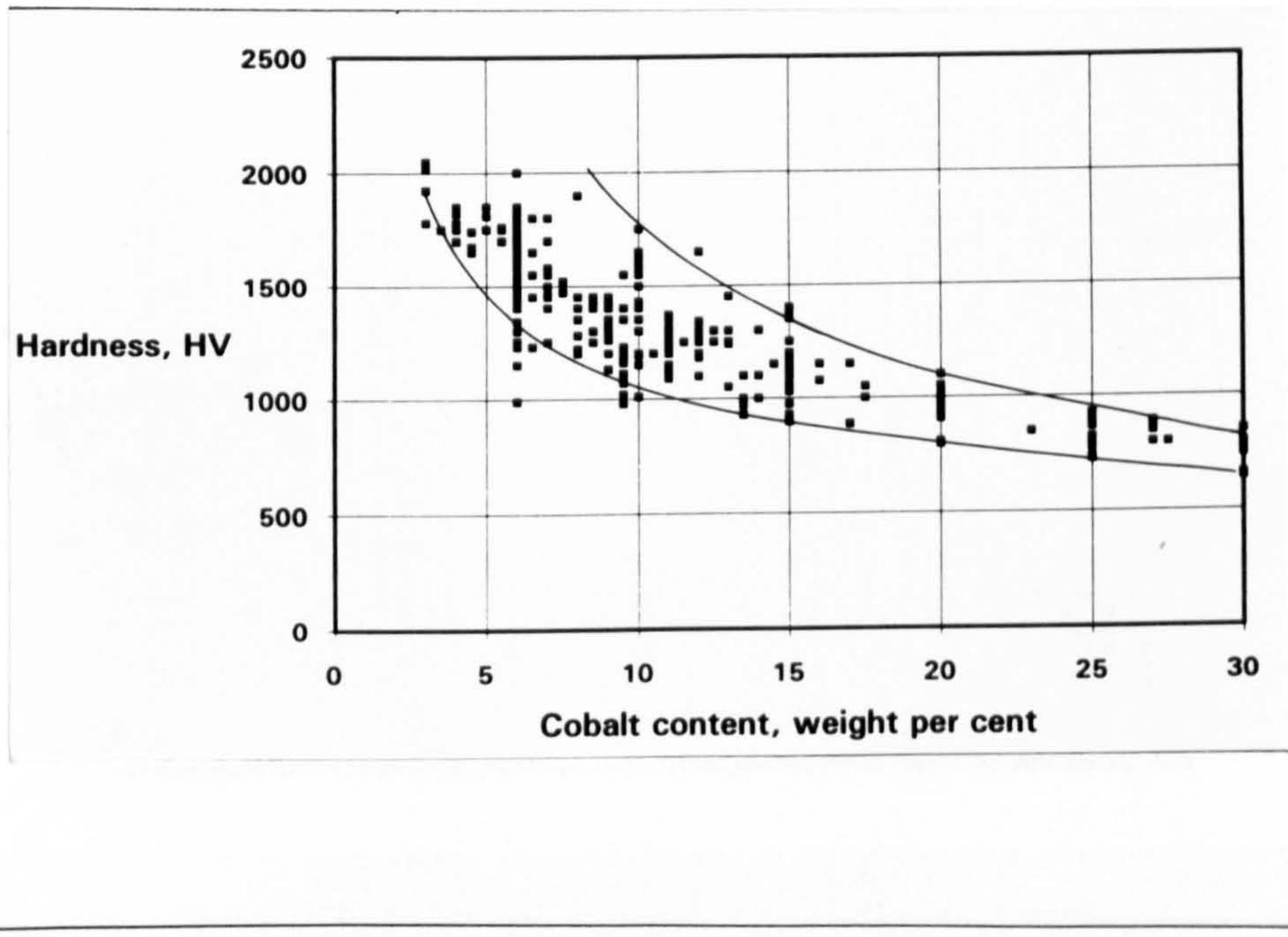

Figure 3.6 Variation Of Hardness With Co Content [95]

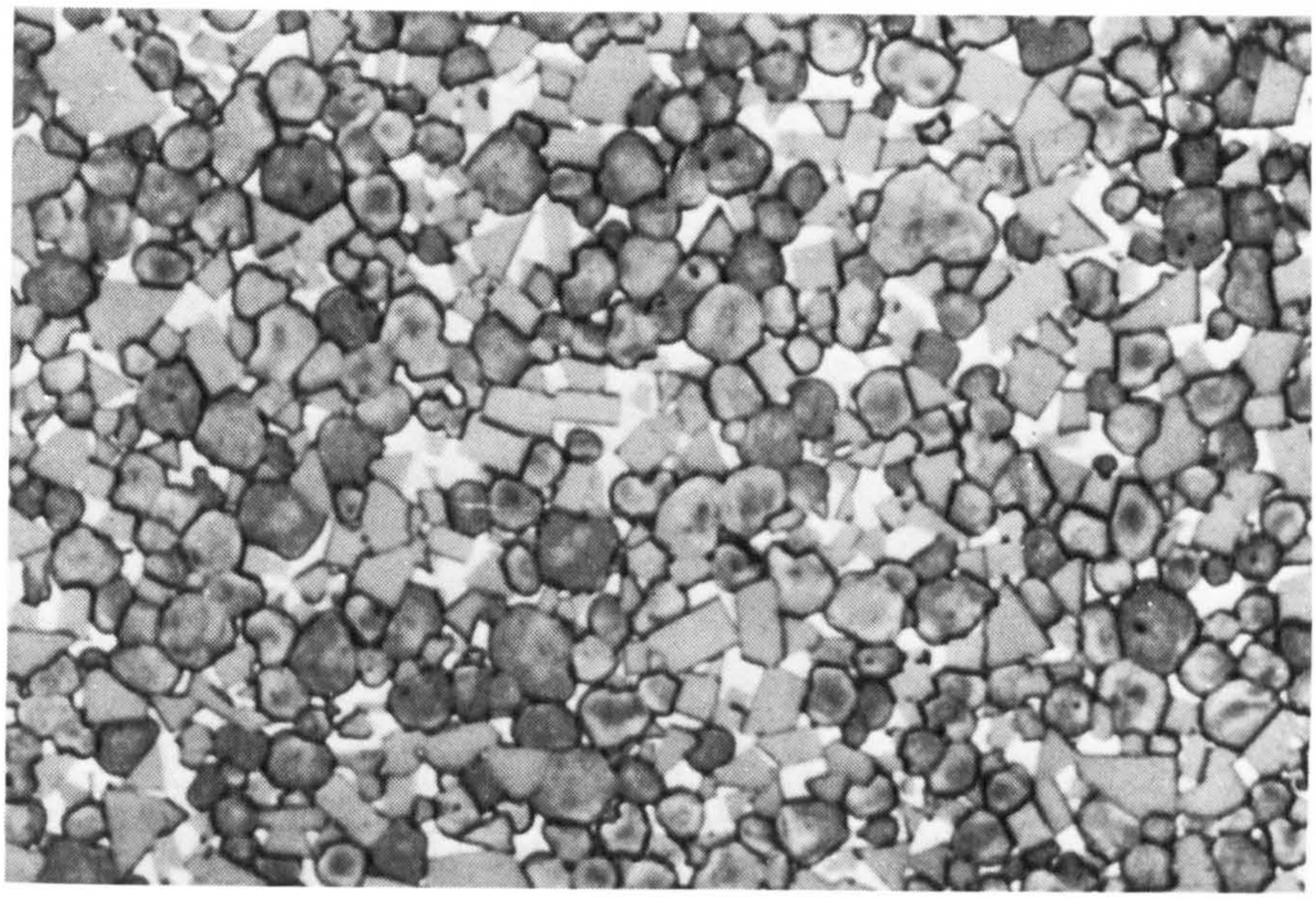

Figure 3.7 Microstructure Of 70WC/9TiC/12Ta(Nb)C/9Co Grade X1500 [95]

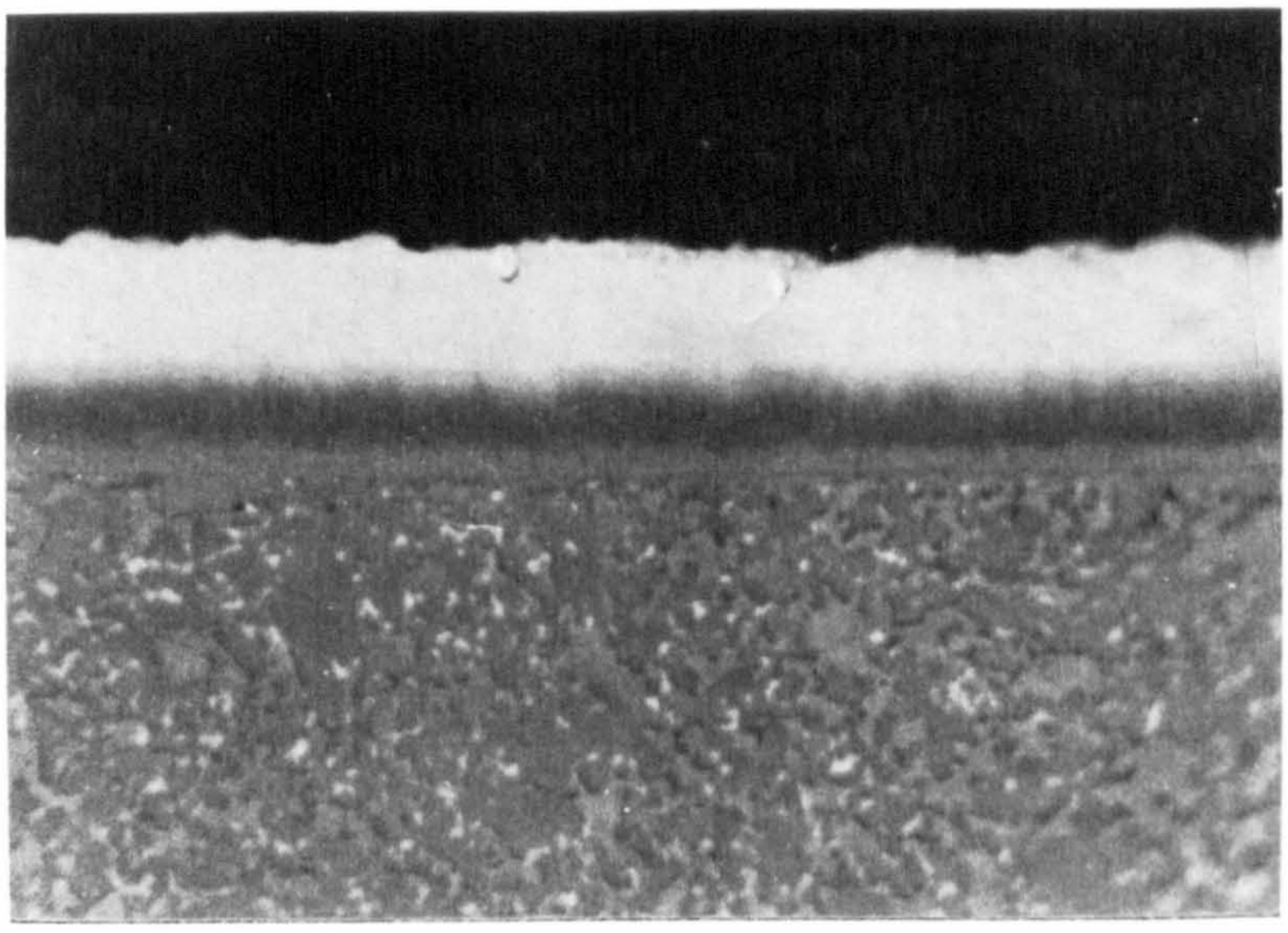

Figure 3.8 TiC/TiCN/TiN Coatings On Hardmetal (X1500) [83]

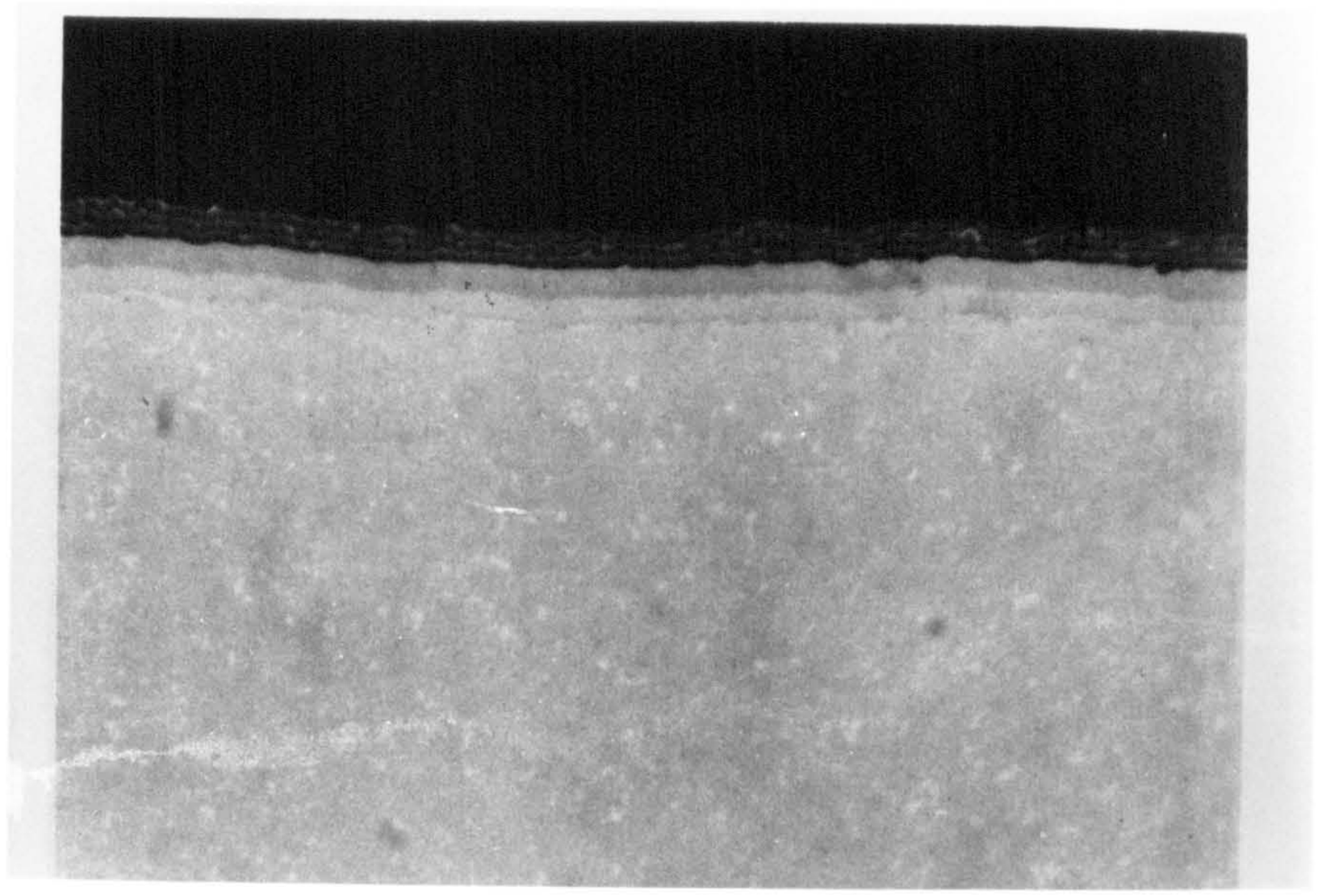

Figure 3.9 Multilayer Coating On Hardmetal (X1500) [83]

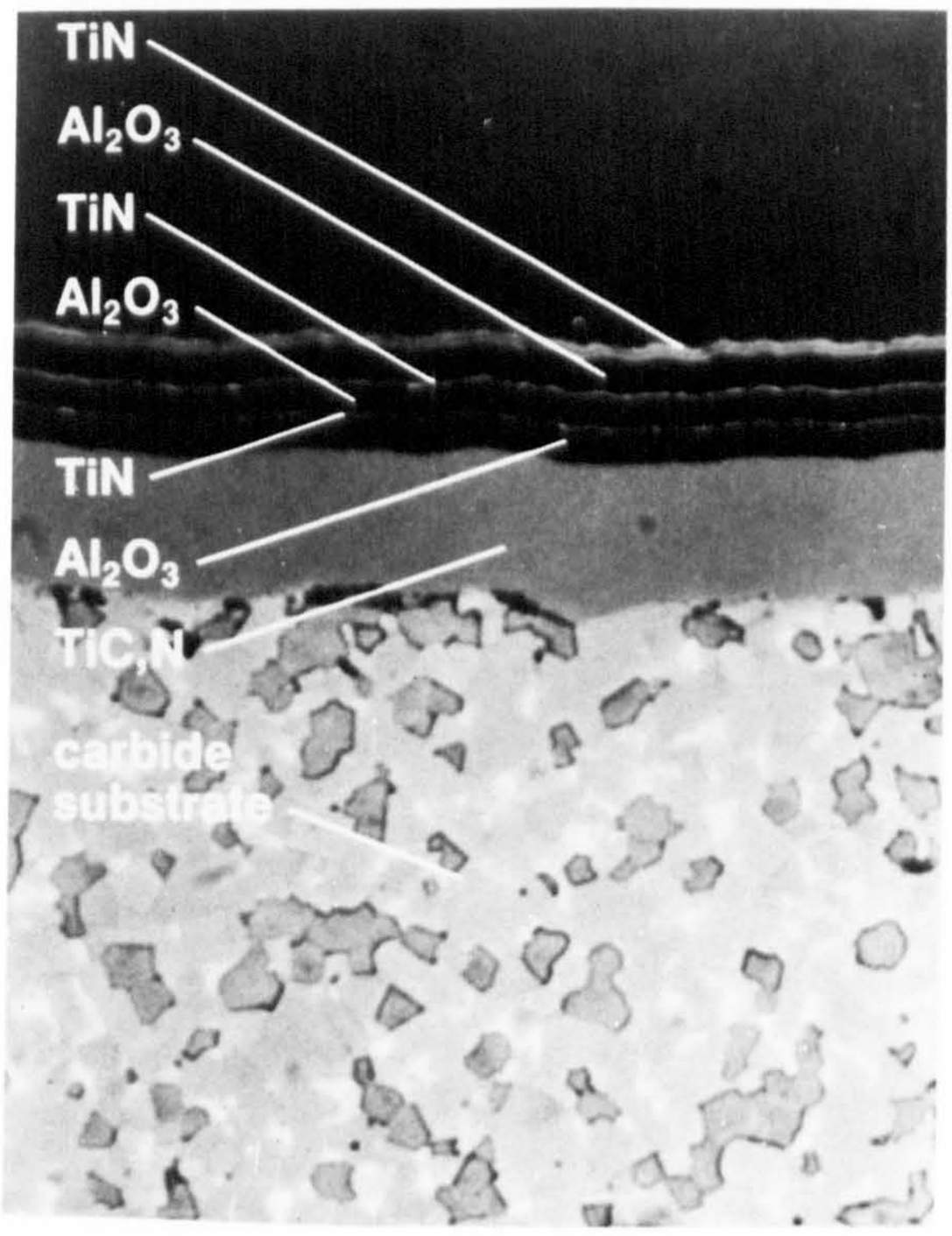

Figure 3.10 Multiple Alternating Coating Layers (X1500) [83]

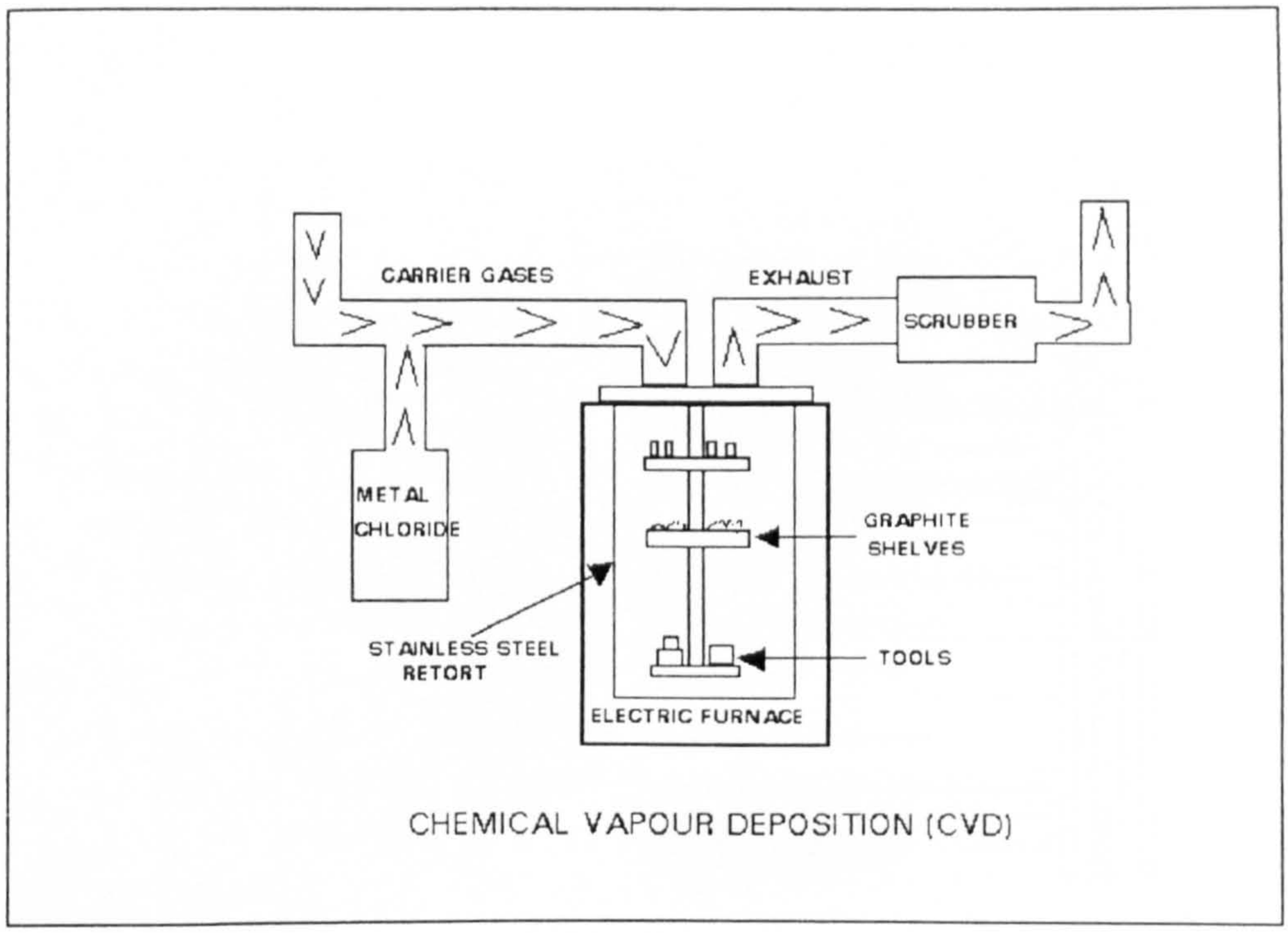

Figure 3.11 Schematic Diagram of Chemical Vapour Deposition (CVD) Process [109] [110]

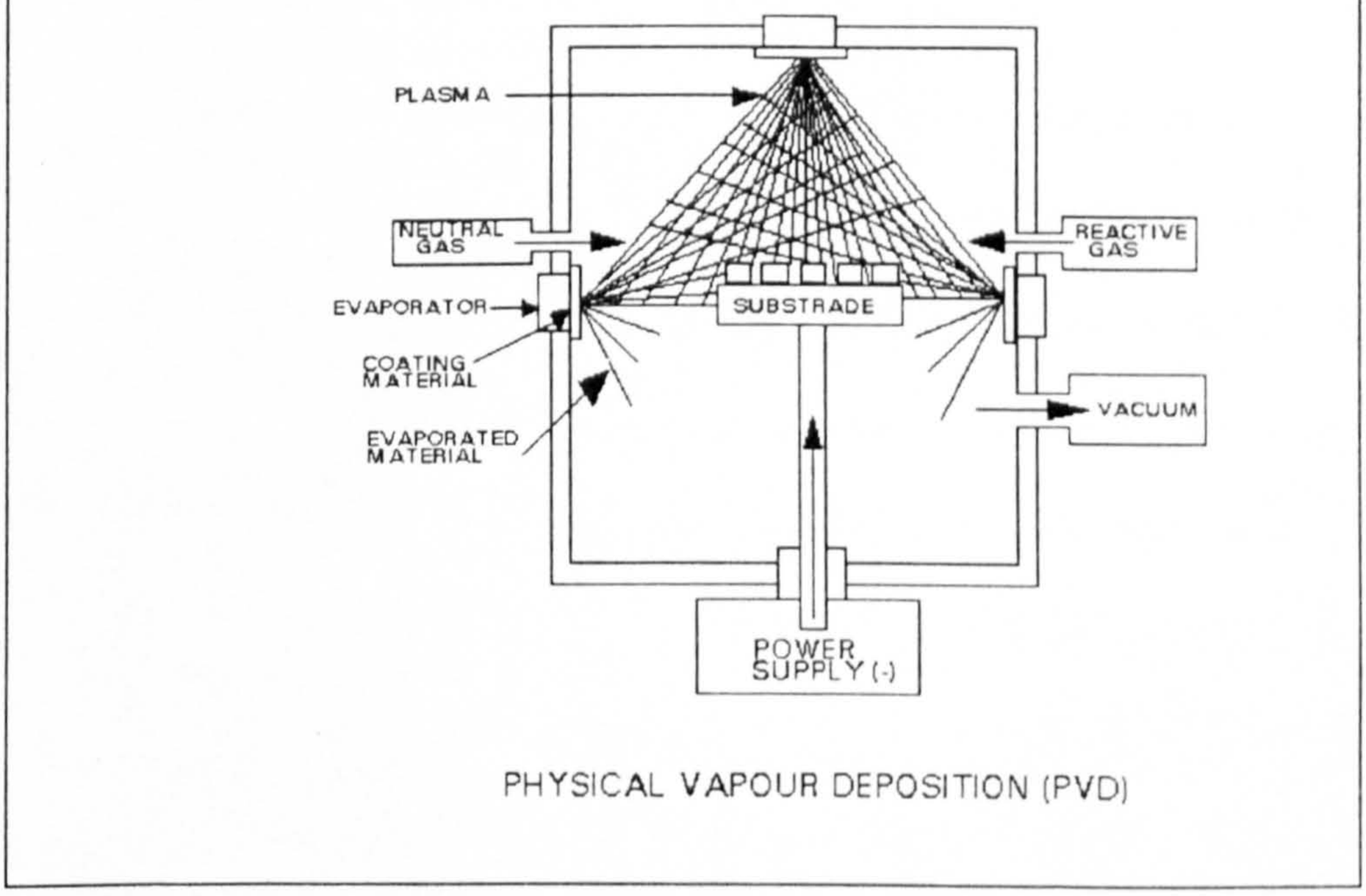

Figure 3.12 Schematic Diagram of Physical Vapour Deposition (PVD) Process [109] [110]

Main groups of chip removal			Groups of application			Direction of increase of characteristic	
Symbol	Broad categories of material to be machined	Distinguishing colours	Designation	Material to be machined	Use and working conditions	of cut	of carbide
P	Ferrous metals with long chips	BLUE	P01	Steel: steel castings	Finish turning and boring, high cutting speeds, small chip section, accuracy of dimensions and fine finish, vibration-free operation		
			P10	Steel: steel castings	Turning, copying, threading and milling, high cutting speeds, small or medium chip sections	↑ increasing speed ↓ increasing feed	↑ wear resistance ↓ toughness
			P20	Steel: steel castings Malleable cast iron with long chips	Turning, copying, milling, medium cutting speeds and chip sections, planing with small chip sections		
			P30	Steel: steel castings Malleable cast iron with long chips	Turning, milling, planing, medium or low cutting speeds, medium or large chip sections, and machining in unfavourable conditions'		
			P40	Steel Steel castings with sand inclusion and cavities	Turning, planing, slotting, low cutting speeds, large chip sections, with the possibility of large cutting angles for machining in unfavourable conditions' and work on automatic machines		
			P50	Steel Steel castings of medium or low tensile strength, with sand inclusion and cavities	For operations demanding very tough carbides: turning, planing, slotting, low cutting speeds, large chip sections, with the possibility of large cutting angles for machining in unfavourable conditions' and work on automatic machines		
M	Ferrous metals with long or short chips and non-ferrous metals	YELLOW	M10	Steel: steel castings, manganese steel Grey cast iron, alloy cast iron	Turning, medium or high cutting speeds. Small or medium chip sections	↑ increasing speed ↓ increasing feed	↑ wear resistance ↓ toughness
			M20	Steel: steel castings austenitic or manganese steel, grey cast iron	Turning, milling. Medium cutting speeds and chip sections		
			M30	Steel: steel castings, austenitic steel, grey cast iron, high temperature resistant alloys	Turning, milling, planing. Medium cutting speeds, medium or large chip sections		
			M40	Mild free-cutting steel, low-tensile steel Non-ferrous metals and light alloys	Turning, parting off, particularly on automatic machines		
K	Ferrous metals with short chips, non-ferrous metals and non-metallic materials	RED	K01	Very hard grey cast iron, chilled castings of over 85 Shore, high silicon aluminium alloys, hardened steel, highly abrasive plastics, hard cardboard, ceramics	Turning, finish turning, boring, miling, scraping	↑ increasing speed ↓ increasing feed	↑ wear resistance ↓ toughness
			K10	Grey cast iron over 220 Brinell, malleable cast iron with short chips, hardened steel, silicon aluminium alloys, copper alloys, plastics, glass, hard rubber, hard cardboard, porcelain, stone	Turning, milling, drilling, boring, broaching, scraping		
			K20	Grey cast iron up to 220 Brinell, non-ferrous metals, copper, brass, aluminium	Turning, milling, planing, boring, broaching, demanding very tough carbide		
			K30	Low hardness grey cast iron, low tensile steel, compressed wood	Turning, milling, planing, slotting, for machining in unfavourable conditions and with the possibility of large cutting angles		
			K40	Softwood or hard wood Non-ferrous metals	Turning, milling, planing, slotting, for machining in unfavourable conditions and with the possibility of large cutting angles		

Figure 3.13 ISO Classification Of Cemented Carbide Tools [57]

Chapter 4

TOOL FAILURE MODES AND WEAR MECHANISMS

4.1 Introduction

Cutting tools are in the position between machine and workpiece, and represent the interface of the manufacturing system in the process. Near net shape production and new materials are the challenges in metal cutting, especially in tooling. A useful service life of a cutting tool may be terminated by plastic deformation due to softening , fracture due to mechanical loads or thermal stress or by a process of gradual wear. Plastic deformation will change the tool geometry when the strength of the cutting edge cannot sustain the original tool shape under high temperature, high pressure situations. Excessive pressure and load or shocks may cause tool failure by brittle fracture. These failures can be prevented by a proper selection of tool materials, tool geometry and cutting conditions. Under such controlled conditions, cutting tools still continue to fail by a process of wear which is due to interaction between the chip and the tool or between the workpiece and the tool.

4.2 Tool Failure Modes

In the process of machining there are three regions on the cutting tool which are effected by wear as shown in Figure 4.1:

1. The Flank or the Clearance Face
2. The Rake or the Top Face
3. The End Clearance Face

The wear takes place progressively in two ways: [17] (a) wear on the tool face resulting from the action of the chip flowing along the face, and (b) wear on the flank due to interaction between major cutting edge and newly generated workpiece material, Figure 4.2. The modes of tool wear vary depending on factors such as cutting conditions, feed rates and cutting speeds, compatibility of tool and workpiece, tool geometry, lubricants, etc.

4.2.1 Flank Face Wear

Flank wear (region B in Figure 4.1) on the cutting tool is usually seen as a narrow band on the clearance face of the cutting tool parallel to the cutting edge. It is caused by friction between the newly cut workpiece surface and the contact area on the tool flank. On account of abrasion, adhesion, shear and plastic deformation, the wear land develops and grows in size with time or distance cut. Rather than developing at an even rate, the worn cutting edge develops in three 'S' stages as in Figure 4.3 [17]. A rapid and finite wear land is established during the break-in period, forming Zone A. In Zone B, where the wear progresses at a uniform rate and is predictable. Zone C

develops when the wear land grows to the point where heat and force exceed the tools capacity. It is advisable to replace the tool before Zone B wear ends in order to avoid catastrophic tool failure [77].

In industrial environments, flank wear is an important life limiting factor of a cutting tool, because the conditions used are such that rake face wear is not usually extensive. In order to optimise productivity and tool life, factors affecting flank wear such as depth of cut, feed rate and material removal rate should be balanced. At low cutting speed, the workpiece abrading the cutting edge causes flank wear while at high cutting speed, a chemical reaction between the tool and workpiece can cause diffusion wear.

From a research point of view, not enough work has been done on flank face wear. However, the appearance of the flank wear surfaces (rough, plucked and smooth, depending on cutting conditions) suggests that it has undergone a similar mechanism of wear as found on the rake face of the tool [38].

4.2.2 Rake Face Wear

On the rake face of turning tools a cavity or crater frequently forms a short distance from the cutting edge (region A in Figure 4.1). Welding and galling between the chip and rake face create a relatively smooth and regular depression, or crater, in the tool. Much of the tool wear research has been concentrated on rake face wear which has led to four basic types of wear mechanisms being postulated:

a) Abrasion wear

b) Attrition wear

c) Diffusion wear

d) Plastic deformation

The resulting crater can grow quickly until it breaks through the cutting edge. It is most commonly observed when machining steels and other high-melting point metals at high cutting speed with cemented carbide tools [139]. Cratering can be inhibited by using coated inserts or uncoated grades or by reducing temperature, e.g. using coolant or reducing the cutting speed [140].

4.2.3 Notching

Notch wear or grooving is often found at both extremities of the depth of cut (regions C and D in Figure 4.1). Notching may be caused by chemical reaction at the periphery of the tool/chip interface or by abrasion caused by work hardening of the workpiece material due to high pressure at the tool/workpiece interface, especially on high-temperature alloys and other work hardened materials. Much localised wear on the rake face and the flank at the depth of cut line was observed with this type of wear [140][141].

4.3 Tool Wear Mechanisms

The failure process of a cutting tool is multidimensional and thus a complex phenomenon. Major wear mechanisms observed with tools used for machining metals are abrasion, attrition, diffusion, and plastic deformation. In order to understand these mechanisms, three factors have been identified inherent to cutting processes [142]:

1. The surface against which the tool rubs is always newly cut from the workpiece material and there is little time for oxides or other films to form.
2. The surface on which the tool is rubbing becomes severely hardened owing to the strain developed to form the chip.
3. The pressure and temperatures at the tool-chip interface are high.

The above factors depend on the workpiece and cutting tools materials combination and may not always necessarily applicable in all situations.

4.3.1 Abrasion

Abrasion is a process by which material is gradually removed from a softer surface by harder inclusions, or particles, by mechanical action. There are several factors that influence the process of abrasion, these include [143]:

a) The hardness of the particles

b) The particle size

c) The shape and degree of angularity of the particles

d) The applied load

Traditionally, abrasive wear can be categorised by two body or three body wear [144][145], as shown in Figure 4.4. Two body abrasive wear is where a hard, rough surface slides against a softer surface, digs into it and ploughs a series of grooves. Three body abrasive wear is where hard abrasive particles are introduced between sliding surfaces and abrade material off each.

Abrasive wear occurs in a sliding situation. When surfaces of different materials are in sliding contact, the microscopic difference in hardness of wear surfaces should be large in order to produce true abrasive wear [146]. Archard [147] used an empirical model, as shown in Fig. 4.5, to describe abrasion. He modelled the volume of material removed (V) on the assumption that it depended on: the true area of contact (A), the sliding distance (l), and other effect such as temperature and material combination (k') : $V = k'Al$. Taking the time derivative of this expression, the wear rate is $V = k'Av$. This model is suited when describing things that affect the wear of a cutting tool; for example the normal load N, analogous to the cutting force Fc, and velocity v, both increase the wear rate. This model is probably correct to describe the wear of a cutting tool, but rather than all wear occurring on the softer material , wear occurs at much lower rate on the cutting tool.

The rake and flank faces are both being affected by abrasive wear simultaneously. The abrasive action tends to produce a uniform surface on the tool and causes such conditions as flank and notch wear, Figure 4.6. Typical appearance rresulting from

abrasion consists of long straight grooves or scratches, as when a surface is lapped and polished with a hard abrasive [148] [149].

It is believed that the surfaces to be abraded should be softer than the particles causing abrasion. In metal cutting, since the tool is usually harder than the material to be cut, little direct evidence of abrasion is published as a mechanism of tool wear. Tabor [150] states that abrasion wear is most likely to occur when machining work material containing hard inclusions. Hard inclusions having smooth, spherical edges and tend to groove the surface by plastic deformation, hard inclusions having sharp edges produce microcutting and give higher wear rates [151] .

Wright *et. al.* [44] state that the entrapment of hard particles being the cause of abrasion. It is possible to abrade the tool when machining rough castings with trapped sand-pockets or alloys which contain hard inclusions. He has also shown that hard particles of small size have little influence on the wear rate but large hard concentrated particles increase the rate of abrasion. It has been reported by Lardener [152] that abrasion is often confused with attrition wear, in which particles are plucked from the surface of the tool and dragged over it. In this process the hard particles lifted from the tool slide on the tool itself causing abrasion. Focke *et al.* [153] state that machining of superalloys causes adhesion of a work material layer on the rake and flank face of the tool yet abrasion is mostly responsible for the tool wear.

Ramalingham *et al.* [154] have discussed in detail the mechanism of abrasion, comparing the machining of two stainless steels of similar bulk properties but different inclusion content. One grade, AISI type 316, was titanium stabilized and contained hard abrasive particles whereas the other did not contain such particles. The abrasive particles clearly promote a higher wear rate for all cutting times, with more influence in the first few minutes. The evidence indicates that the abrasive particles are particularly active while the cutting edge is sharp, but as the tool is worn they are more likely to be embedded in the tool and remove less material.

Abrasion has been seen as one of the major wear mechanisms when machining aluminium-silicon alloys. Generally, alloys containing 10-13% Si are considered to be most difficult to machine. The high silicon content, together with the occasional presence of hard free silicon particles, causes them to be abrasive to high speed steel and cemented carbide tools, leading to rapid wear [155] [156] [157] [158] [159].

4.3.2 Attrition

Attrition, or adhesive wear, is a wear process in which the tool geometry is changed by the periodic mechanical detachment of microscopic size particles of the tool material. It is an important wear mechanism which controls the tool life under the condition of seizure at low cutting speeds [160] [13]. Many workers have observed that attrition occurs under any of the following conditions:

1) When the tool surface is rough or irregular

2) When the flow of material over the tool is uneven or turbulent

3) When the contact between the tool and work is intermittent.

Attrition wear is also associated with built-up edges. When unstable built-up edge detaches from the face it will carry with it small quantities of tool material if strong bonding occurs between the built-up edge and tool material [18][161]. Small fragments of the tool's edge are continually and progressively removed as the built-up edge breaks down. When this process continues over a long period of time, it appears as if the tool surface has been nibbled away and made uneven [13]. As the result, a surface subjected to attrition wear will have a characteristically rough appearance.

Attrition is not greatly influenced by high temperatures, and it is likely to disappear completely as the chip flow becomes more laminar. The grain size of the tool material plays an important part in controlling the attrition wear. The smaller the grain size (provided they are strongly bonded), the lower the rate of attrition wear [18].

4.3.3 Diffusion

Diffusion wear has been defined as a wear mechanism in which the tool shape is changed by diffusion into the work material of atoms from one or more phases in the tool material [160]. The movement of the atoms is in the direction from regions of

high atomic concentration to low atomic concentration with a tendency to reach homogeneity of the solution. Diffusion depends on atomic agitation and is highly temperature dependent. The diffusion rate is approximately double for an increment of the order of 20^0C. Three conditions for diffusion wear to take place are [160] :

1) Metallurgical bonding of the two surfaces so that atoms can move freely across the interface

2) High temperature

3) Some solubility of the tool material phases in the work material.

In metal cutting, the metal to metal contact which produces temperatures of 700^0C to 900^0C (depending on the materials being cut) are high enough for diffusion to take place. This wear mechanism is one of the major cause of cratering at high speeds and may also act at the flank face [13]. It has been shown theoretically that the role of diffusional metal transfer at the flank is less significant whereas the predominant rake face wear at high cutting speeds can be attributed to direct diffusion [162]. The crater formed on the rake face of tools is located at the region of highest temperature. A characteristic feature of diffusion wear is the smoothness of the worn surface.

Opitz and Konig [163] agree in general that diffusion plays a role in crater wear, especially with cemented carbide tools. They have shown that under the static conditions which occur in the seizure region on the face of a cutting tool, cobalt will diffuse into steel. With the binding element removed, a low shear strength layer exists on the surface of the tool which is transported from the tool by the underside

of the chip. Their theory suggested that the effect of diffusion is to form new complex carbides which result in the weakening of the microstructure of the tool. However, Trent [13] [164] did not agree with Optiz and Konig, and has shown that additions of titanium carbide (TiC) and tantalum carbide (TaC) reduce cratering wear by diffusion since they modify the structure of the tungsten carbide (WC) grains and this lowers their solubility in the workpiece. Thin coatings are applied to most carbides tools to interrupt the diffusion mechanism by adding an inert barrier at the interface between workpiece and the tool.

Trent [164] and Colding *et al.* [165] have suggested that wear by diffusion is probably responsible for the Taylor tool life equation $VT^n = C$ (where V = cutting speed, T = cutting time, C and n are constants) between tool life and cutting speeds which was based on flank wear rate. Tool lives are longer at lower cutting speed where diffusion becomes insignificant. If tool wear is entirely controlled by diffusion then the tool life should becomes infinite at low speeds. But these curves cannot be extrapolated back because other wear mechanisms may be operating which control tool lives.

Attrition and diffusion wear processes may occur simultaneously on the same worn surface or at different positions on the same tool. And, it may be difficult to distinguish which mechanism is controlling the life of the tool [166].

4.3.4 Plastic Deformation/Fracture/Chipping

Plastic deformation, brittle fracture and edge chipping are not considered to be true wear processes, but they do contribute to the actual wear of cutting tools. Plastic deformation may adversely change the tool geometry. This can result from high concentration of compressive stress and high temperature near the cutting edge. It is not strictly classified as a tool wear mechanism since tool material is not lost, but it may initiate the wear processes which lead to tool failure. However, the deformation may result in much accelerated wear on tool flank or nose with sudden collapse of the tool.

Taylor [7] has studied extensively the effect of heat which initiates the deformation of high speed steel and carbide tools when cutting hard workpiece materials. He stated that according to the role which heat has in producing wear, worn tools may be categorised into 3 classes: (i) wear of tools in which heat has been so slight as to have no softening effect upon the surface of the tool, (ii) wear of tools in which the heat has been so great as to soften the cutting edge of the tool beneath the chips instantly after commencing the cut, (iii) in which heat has played the principal part in the wear of the tool.

Many workers have concentrated on the deformation of the cutting tools as it takes place under conditions of high temperatures and stresses when machining at high speeds and feeds. Some of their findings can be summarised as follows: [167]

- The plastic deformation is more significant when machining a relatively hard workpiece.
- The bulging of the tool due to deformation can be observed on the flank and rake faces.
- Low cobalt contents in carbide tools and a finer grain size give better resistance to plastic deformation.
- Maximum deformation occurs predominantly at the nose of the cutting edge.

The inherent brittleness of cemented carbide and ceramic tooling renders them susceptible to severe damage by chipping or fracture if sudden loads or thermal gradients are applied to their cutting edge [168]. Such problems are normally associated with milling operations and other interrupted cuts. In turning tests, Tlusty and Massod [169] concluded that chipping is a ductile failure mechanism due to high shear stresses at the cutting edge and breakage is brittle fracture originating at the rake face at a local maximum of tensile stress.

4.4 Tool Failure Criteria

The shape and geometry of the cutting tool changes gradually due to the action of cutting during machining. The time for which a cutting edge can be usefully employed before regrinding or replacing is called *" the tool life"*. The use of the tool beyond its useful life will affect both dimensional accuracy and the surface finish of the machined surface, ultimately leading to the production of rejects. Continued use

of worn tool would cause catastropic failure or total loss of the tool and even damage to the component. Therefore certain tool failure criteria must then be used to determine the end of the tool life in order to maintain the machining process economically. Figure 4.7 shows a schematic diagram of tool wear measurement area used in the turning test. Normal criterion recommended by ISO [33] are:

a) Average flank wear, $VB = 0.3$ mm

b) Maximum flank wear, $VB\max = 0.6$ mm

c) Crater depth, $KT = 0.06 + 0.3\mathrm{f}$, where f is the feed rate

d) Catastropic failure.

It is common to use the notch wear, $VN = 1.0$ mm where notch wear prevails when machining materials like nickel alloys with cemented carbide or ceramic tools. In industrial application, these values may be varied because this will depend on many variables such as machine tool rigidity, component accuracy, workpiece materials etc. which are different for different companies. The criteria used for wear measurement in this project are based on industrial and workshop experience and are stated in Chapter 6.

4.5 Wear And Failure Of Different Tool Materials

4.5.1 High Speed Steel (HSS)

When cutting steel with HSS tools at low cutting speed, the temperature generated is relatively low ~ 700^0C, and the predominant wear mechanisms are adhesion (or

attrition) and abrasion. Attrition wear is more rapid during interrupted cuts or when chatter is present. At higher cutting speeds, especially when cutting steel and high melting point metals, the temperature rises above 700^{0}C, and the tools soften and deform plastically [170] . At higher temperatures, cratering becomes pronounced on account of diffusion [171]. Diffusion is a major wear process in HSS tools, being responsible for the flank wear in the higher speed range [13]. HSS tools coated with TiC have shown a reduction of flank wear and give a higher tool life than uncoated tools [172].

Trent [13] has classified 6 different types of wear mechanisms acting on HSS tools when cutting steels, cast iron and nickel based alloys (Figure 4.8), viz.:-

1. Plastic shear at high temperature
2. Deformation under compressive stress
3. Diffusion wear
4. Attrition wear
5. Abrasive wear
6. Sliding wear processes

Wear process 1, 2 and 3 are temperature dependent. Slow cratering is caused by process 1 and rapid cratering is caused by process 3. Flank wear is caused by diffusion or attrition [45].

4.5.2 Cemented Carbide

Trent [166], studying the worn straight tungsten carbide (WC-Co) and mixed cemented carbide used to cut cast iron and steel has shown the major types of wear and wear mechanisms includes:

1. Flank wear
2. Crater wear
3. Built-up edge and deterioration of rake face and cutting edge
4. Deformation due to high compressive stress and temperature
5. Cracking due to thermal stresses
6. Chipping or fracture due to mechanical impact.

The first four elements were affected by factors such as cutting speed, feed rate and the strength of materials being cut.

At low and medium cutting speeds, flank wear is caused by frequent shearing of welded material between carbide tools and steel by the formation of built-up edges. These occurred under one set of conditions with different types of built-up edge. In these condition the tool-life depends on the wear at the clearance face. It was established that temperature of the tool chip interface is a function of speed. As cutting speed increased, i.e. at higher temperature, the built-up edge disappeared [151] [165] [173] .

Ber [174] has investigated the effect of abrasion resistance and thermal properties of the cemented carbide cutting tool on the flank wear characteristics and discovered

that in the low range velocities (10 - 35 m/min), where temperatures are relatively low, one may expect an abrasive wear mechanism to exists. In the high range of velocities where interface temperatures reach the value of 900°C to 1150°C, a diffusion type wear takes place.

When cutting steel at high cutting speed, the chip-tool interface temperature exceeds 8500C. Apart from plastic deformation, the wear processes on carbide tools are based on diffusion or attrition [175] . Naerheim and Trent [176] have shown experimentally that the crater worn in the rake face at high speed is the result of diffusion rather than the mechanical detachment of fragments of tool material [177] . As a result of diffusion, abrasion, and plastic deformation, chip notches were also found on cemented carbide when cutting steel at high speeds [178] [179].

Chambers [180], in his study of wear of cemented carbide cutting tools when cutting steels, free cutting steel and nickel-based alloys discovered that there are three main failure modes:

1. Flank wear and nose grooving
2. Collapse of the cutting edge due to crater and flank wear
3. Deformation of the tool nose

Reduction in the contact length and the associated increases in temperatures and stresses gradually changed the failure mode from (1) to (2) to (3). Increasing the TiC content in the tool material resulted in reduction of rates of rake face and flank face wear.

Mari and Gonseth [181] presented a model of the mechanical behaviour of WC-Co cutting tools, divided into three temperature domains, based on Taylor's curve. Domain I - below 500°C, WC-Co fails by brittle fracture and the formation of built up edge is observed at low cutting speed. Domain II - between 500°C and 800°C, the tool starts to deform plastically. Domain III - above 800°C, plastic deformation of the tool occurred due to the dislocation motion in the cobalt phase and the tool life decreases rapidly. This model served as a new guideline for cutting tool manufacturers for designing binders, choosing grain size and determining optimum cutting conditions by monitoring the working temperature.

4.5.3 Coated Carbides

Suh [182] discussed the wear mechanisms of coated tungsten carbide inserts, including abrasive wear, diffusion wear , plastic deformation and fracture. The crater wear on coated cemented carbide is correlated with the chemical instability of the tool materials and not with the coating hardness. The coating acts as a barrier by preventing diffusion of either carbon or cobalt from the cutting tool into the iron-containing chip. Coatings also reduce the coefficient of friction between cutting tool and workpiece, this results in lower cutting temperatures than with uncoated inserts used under similar cutting conditions [183]. When machining mild steel with coated TiC and TiN cemented carbide tools, Venkatesh *et. al.* [184] reported that cratering in coated tools is due to plastic deformation, which in turn causes bulging and results in severe flank wear. Chip notching on the rake face and grooving wear on the clearance face were also observed, this resulted in the loss of the coating.

Chubb and Billingham [185] studied the wear of TiC coated inserts and reported that the initial flank wear is abrasive. Once the coating breaks, wear is accelerated since both diffusion and abrasive wear mechanisms act simultaneously. Small grained TiN coatings were found to be more effective in preventing crater wear than large columnar TiN grains [186] . The rate of flank and crater wear is reported to depend upon coating thickness and composition. Crater wear for Al_2O_3 coatings was less than for TiC or TiN coatings. The rate of flank wear for Al_2O_3 and TiC is reported to be independent of the coating thickness for films thicker than 5 μm [187].

Dearnley and Trent [77] reported experiments in which cemented carbides coated with TiC, TiN and Al_2O_3 were tested with different types of steel. They observed that wear is mainly on the rake and flank faces of the tools. Cratering of TiC coatings was by atomic diffusion and discrete plastic deformation while with TiN coatings atomic diffusion was solely responsible. Craters in Al_2O_3 coated tools were caused by discrete plastic deformation. Flank wear of the coated tools was principally by atomic diffusion [188].

Essential preconditions for a satisfactory cutting performance of coated carbide tools are good binding properties between the coating and the substrate. The coating is readily cracked under thermal shock because of the mismatch in the coefficients of thermal expansion of the coating and the substrate. When the effectiveness of the coating diminishes, the wear problem shifts to the substrate and the wear rate changes drastically at this junction [189] [190] [191] . Cemented carbide tools with

multilayer coatings have been reported to overcome the problem of microcracks under high cutting temperature conditions [192].

4.5.4 Ceramics

Due to their inherent brittleness, ceramic tools are subject to chipping, cracking, fracturing and gradual wear by abrasion, but retain more of their strength at high temperature [193]. Therefore, the main advantages of the ceramic materials over cemented carbide materials are at high cutting speeds, where the wear rates of carbides are high. When machining steel, Ham and Narutaki [194] have observed the following wear processes in ceramic tools: a) deep cratering; b) uniform flank wear c) cracks across flank, and d) diffusion.

The primary mechanism of ceramic tool failure is by flank wear and crater wear. Brandt [195] concluded that the flank wear is the result of a thermally activated process which depends on superficial plastic deformation but is predominantly an intergranular fracture mechanism, where crack initiation occurred by dislocation pile-ups. In the high speed machining of steels, the flank wear of alumina tools was mainly governed by thermomechanical/chemical wear [196]. When machining austempered ductile iron (ADI) with commercial ceramic cutting tools, flank wear was the most common cause of tool rejection although fracturing occurred at the highest cutting speed [197] [198] [199].

Sialon cutting tools have improved toughness compared to those of the alumina variety. Extensive research work has been carried out on the failure modes and wear mechanisms of sialon cutting tool when machining cast iron, nickel and titanium alloys [200], steel [201] and austempered ductile iron [29].

4.5.5 Diamond, Polycrystalline Diamond (PCD) and Polycrystalline Cubic Boron Nitride (PCBN)

Natural diamond tool wear can be divided into fracture and carbonization [126] . Due to their very high hardness diamond tools show a much lower rate of wear and longer tool life under abrasion conditions than carbides or oxides. In machining aluminium alloys, a smooth and flat wear land is observed on the rake face and the flank. Flank wear is caused by rubbing against the workpiece, and rake face wear by the metal swarf sliding over the surface. However, single crystal natural diamond tools are deficient in toughness and their sharp edges are easily chipped, fracture of the cutting edge is also a common feature [202] [203]. The wear behaviour of diamond tools depends strongly on workpiece materials, aluminium and copper are among the most common diamond machined materials. Tool wear caused by machining aluminium is characterised by the entire edge being rounded off [157] while machining copper causes little tool edge wear but severe cratering at the rake face can occur [204].

Like natural diamond, PCD is not recommended for machining materials such as low carbon steel, titanium, nickel or cobalt due to their high chemical reactivity. When

heated above 700°C PCD degrades rapidly due to (a) cobalt (the binder) has a higher coefficient of thermal expansion than diamond, and so forces the diamond grains apart, this causes cracking, and (b) cobalt acts as a catalyst for graphitisation [120] [205].

Flank wear, edge chipping and notching at the depth of cut are the main failure modes of PCBN tools when machining hardened cast irons and steels [13] [137]. Flank wear is influenced by both the inherent wear resistance of the compacts and the welding of the work materials on the cutting edge [206]. Notching was observed when machining nickel-base superalloys (Incoloy 901) due to chemical interaction between the tool and workpiece material in the presence of oxygen. Temperature has been identified as the major cause of notching at high speeds when machining Incoloy 901 with PCBN tooling [139].

Table 4.1 summarises tool materials compatibility, applications and wear mode.

Table 4.1 Tool Material Compatibility, Applications and Wear Modes [30]

Tool Material	Compatible Workpiece Material	Machining Processes and Speed Ranges	Typical Wear of Failure Modes	Special Remarks
High Carbon or Medium/Low Alloy Steels	Low strength & hardness material, non-ferrous alloys and plastics	Single point turning, drilling and tapping ($v < 0.5$ m/s)	Built-up, plastic deformation, abrasive wear, microchipping	
High Speed Steel (HSS)	All materials of low to medium strength and hardness	Single point turning, drilling , tapping, broaching and both face and end milling ($0.5 < v < 2.5$ m/s)	Flank and crater wear	Used in almost every machining application
Cemented Carbides	All materials of low to medium strength and hardness	Single point turning, drilling , tapping, broaching and both face and end milling ($0.5 < v < 2.5$ m/s)	Flank and crater wear	At low speeds, chips cold weld to carbide and micro chip
Coated Tools	Cast irons, alloys and stainless steel, superalloys (Ti is a notable exception)	Single point turning ($0.5 < v < 5$ m/s)	Flank and crater wear	At low speeds, chips cold weld to carbide and micro chip
Ceramic	Cast iron, Ni-based superalloys, non-ferrous alloys, plastics	Single point turning ($v > 2.5$ m/s)	Depth of cut notching, micro chipping and gross failure	Low thermo-mechanical fatigue strength means no interrupted cuts
Diamond	Pure Cu & Al, Si-Al alloys, cemented carbides, rock, cement, plastics, glass epoxy & fibrous composites, non-ferrous alloys	Single point turning, face milling ($v > 2.5$ m/s)	Chipping, oxidation, graphitization	Not for machining low carbon steels, Co, Ni Ti & Zr
Cubic Boron Nitride (CBN)	Hardened steel alloys and chilled cast iron, HSS, commercially pure Ni & Ni-based superalloys	Single point turning, face milling ($0.5 < v < 5$ m/s)	Depth of cut notching, chipping, oxidation, graphitization	Can handle most materials that diamond cannot

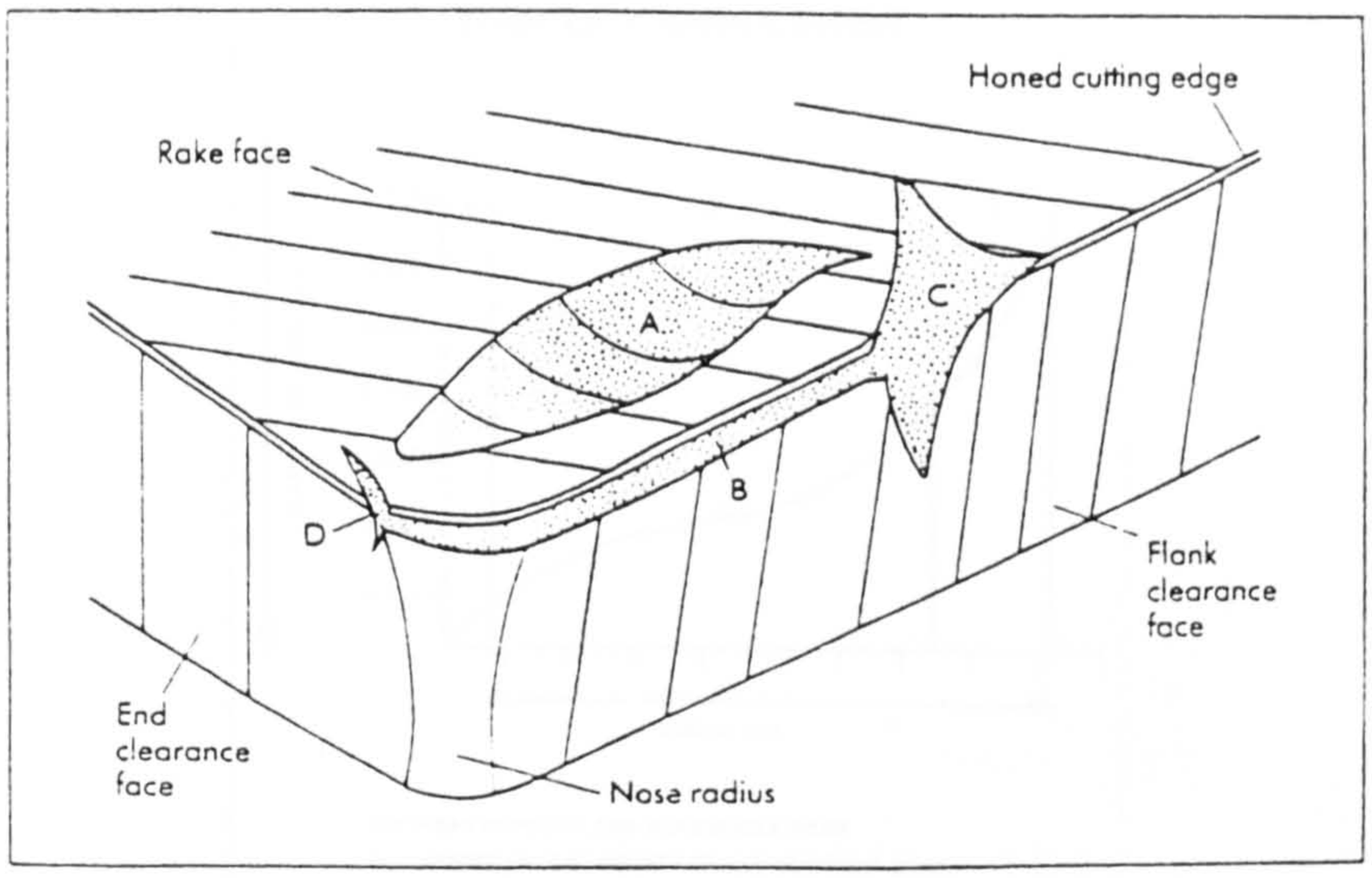

Figure 4.1 Principle Regions Of Tool Wear [77]

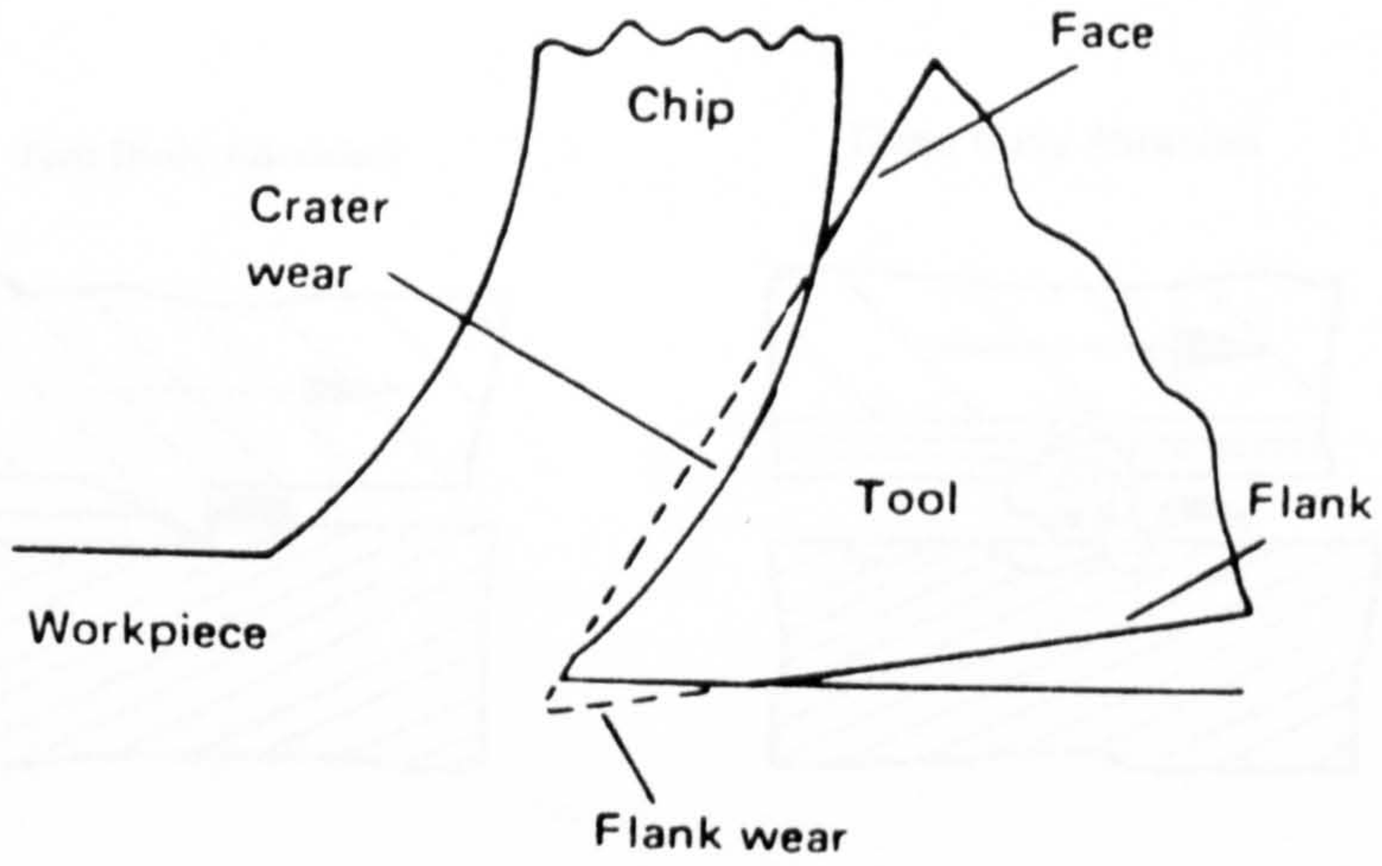

Figure 4.2 Regions Of Tool Wear In Single Point Cutting Tool [17]

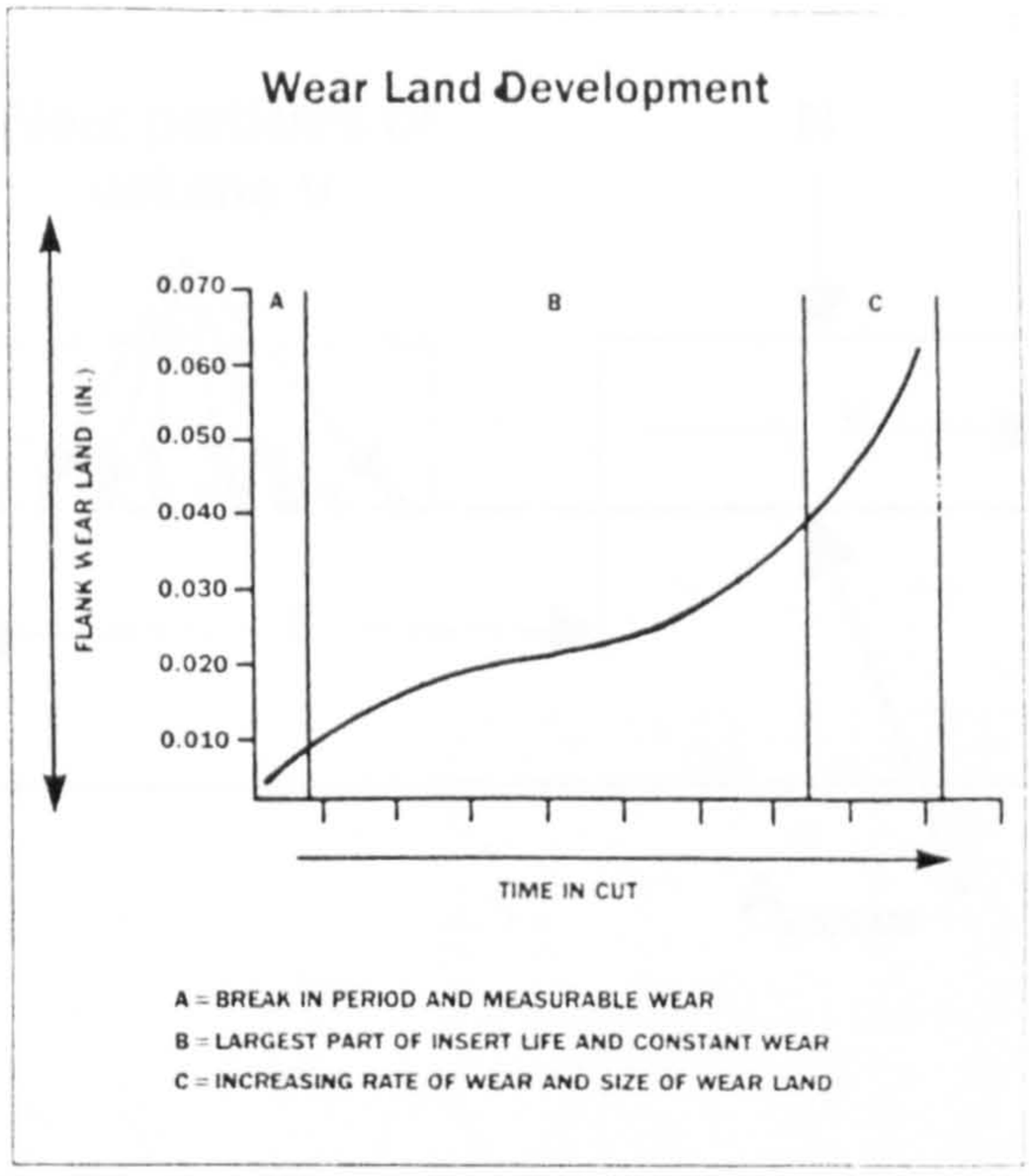

Figure 4.3 Wear Land Development For Cutting Tool [140]

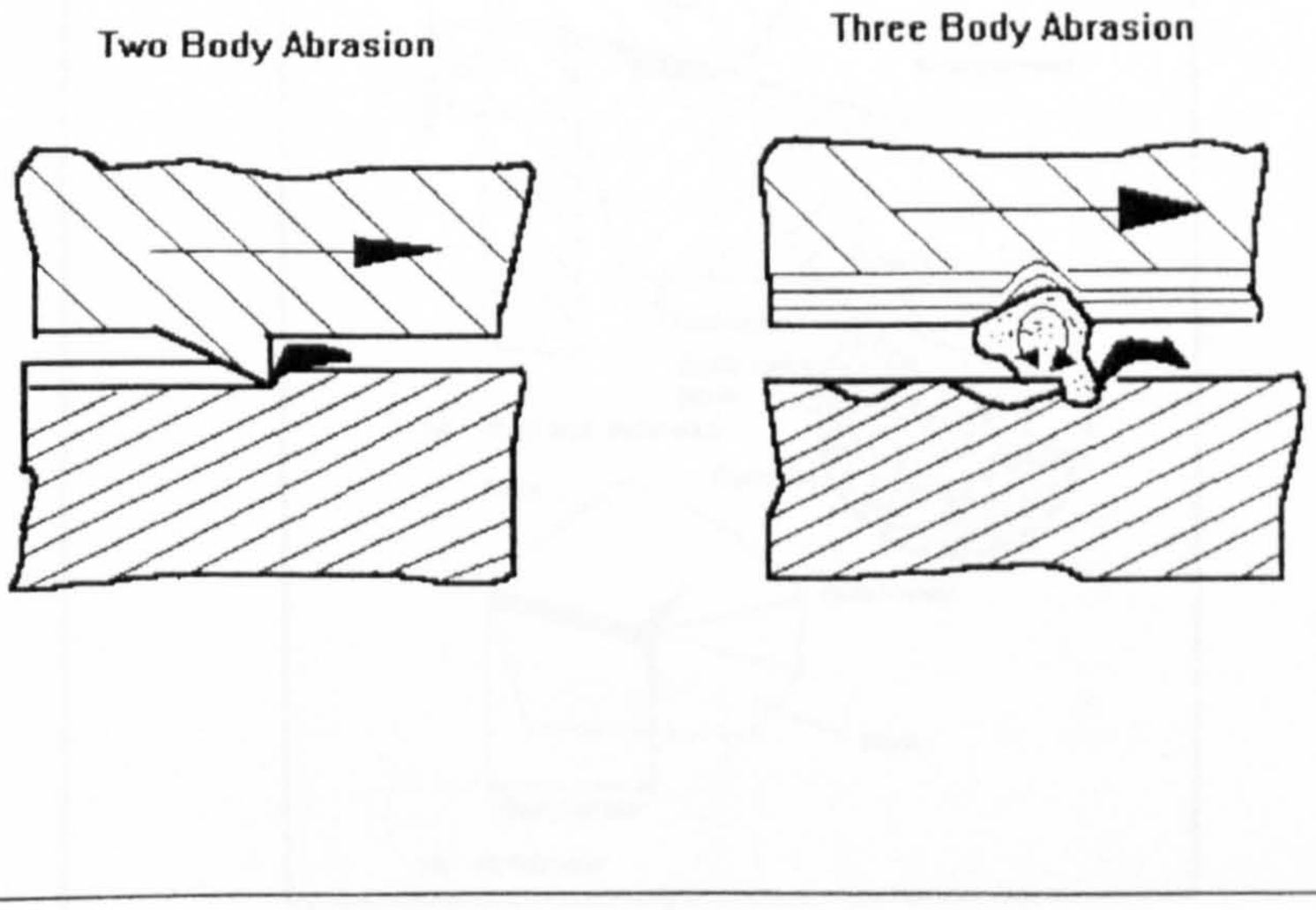

Figure 4.4 Two Body And Three Body Abrasion [145]

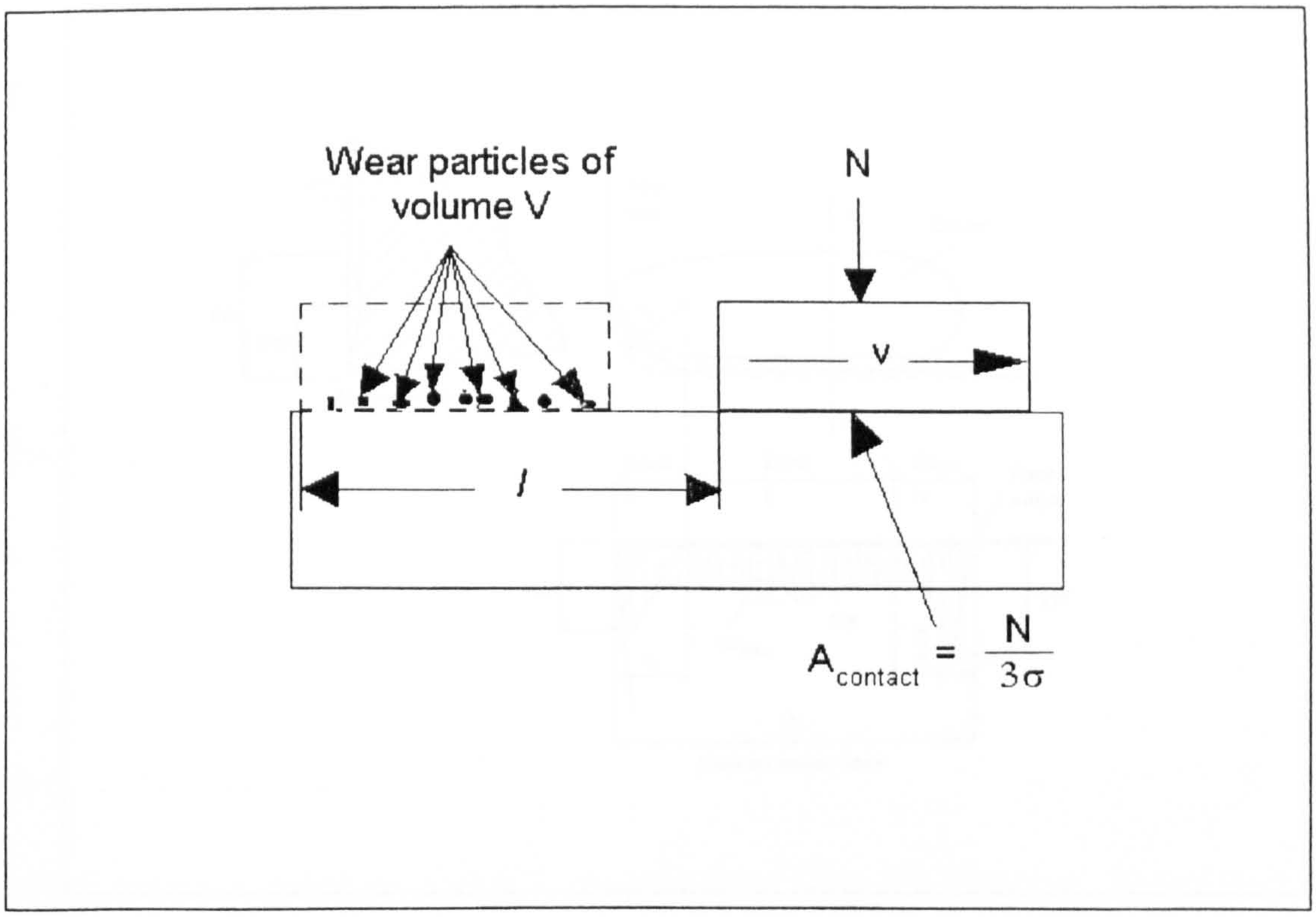

Figure 4.5 Archard Model of Slider Representation [147]

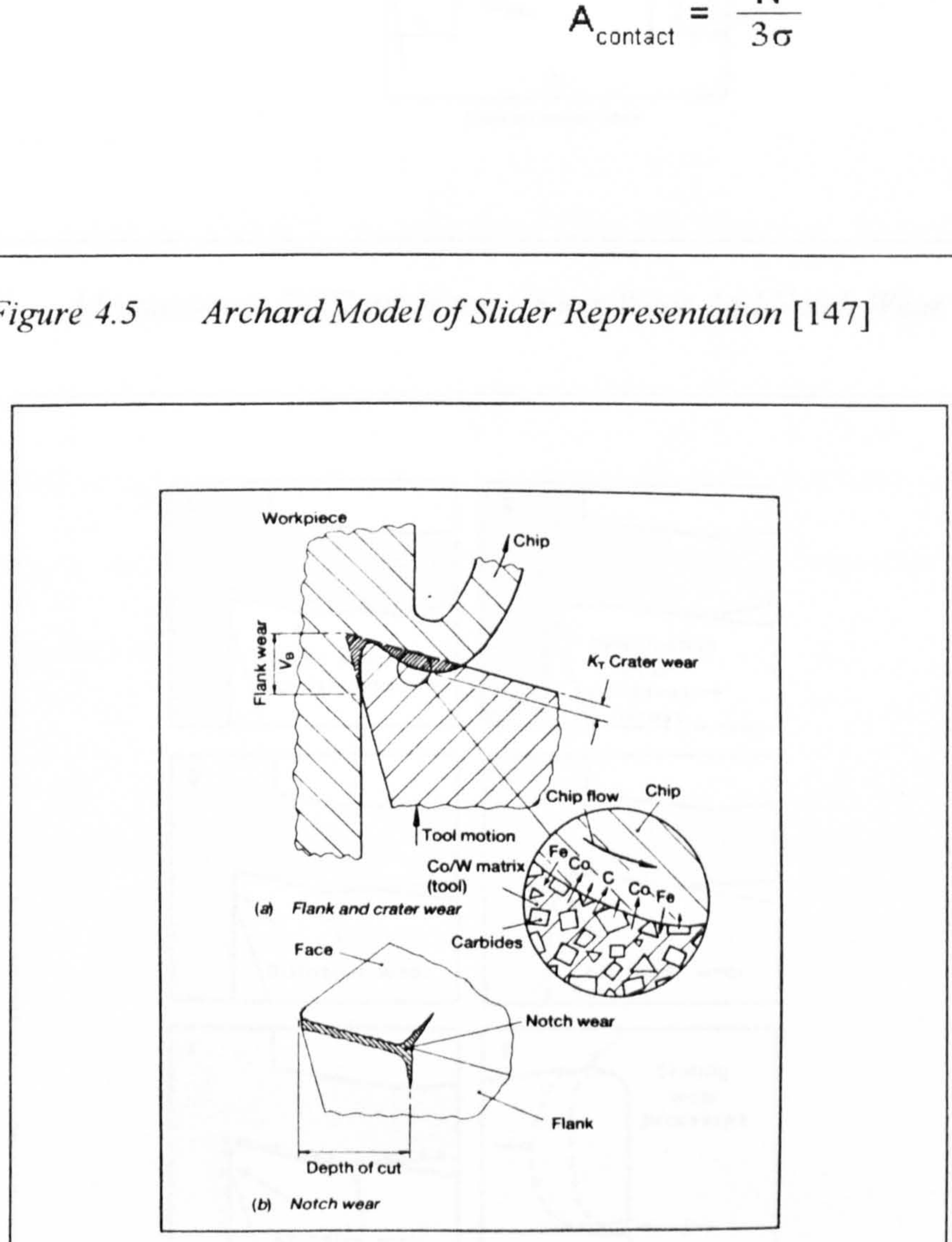

Figure 4.6 Flank Wear, Crater Wear And Notch Wear Location [57]

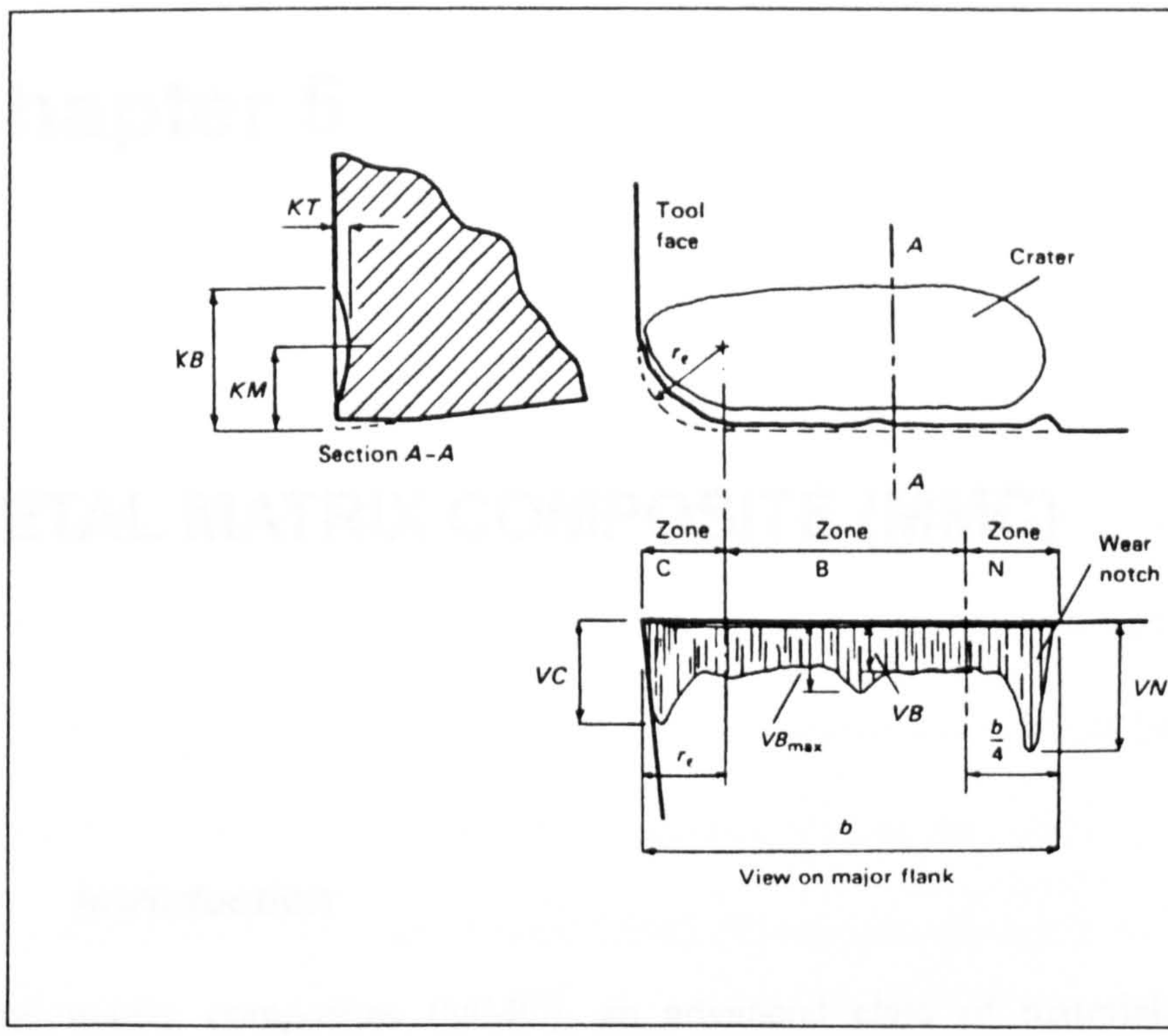

Figure 4.7 Measurement Of Flank Wear, Crater Wear And Notch Wear [20]

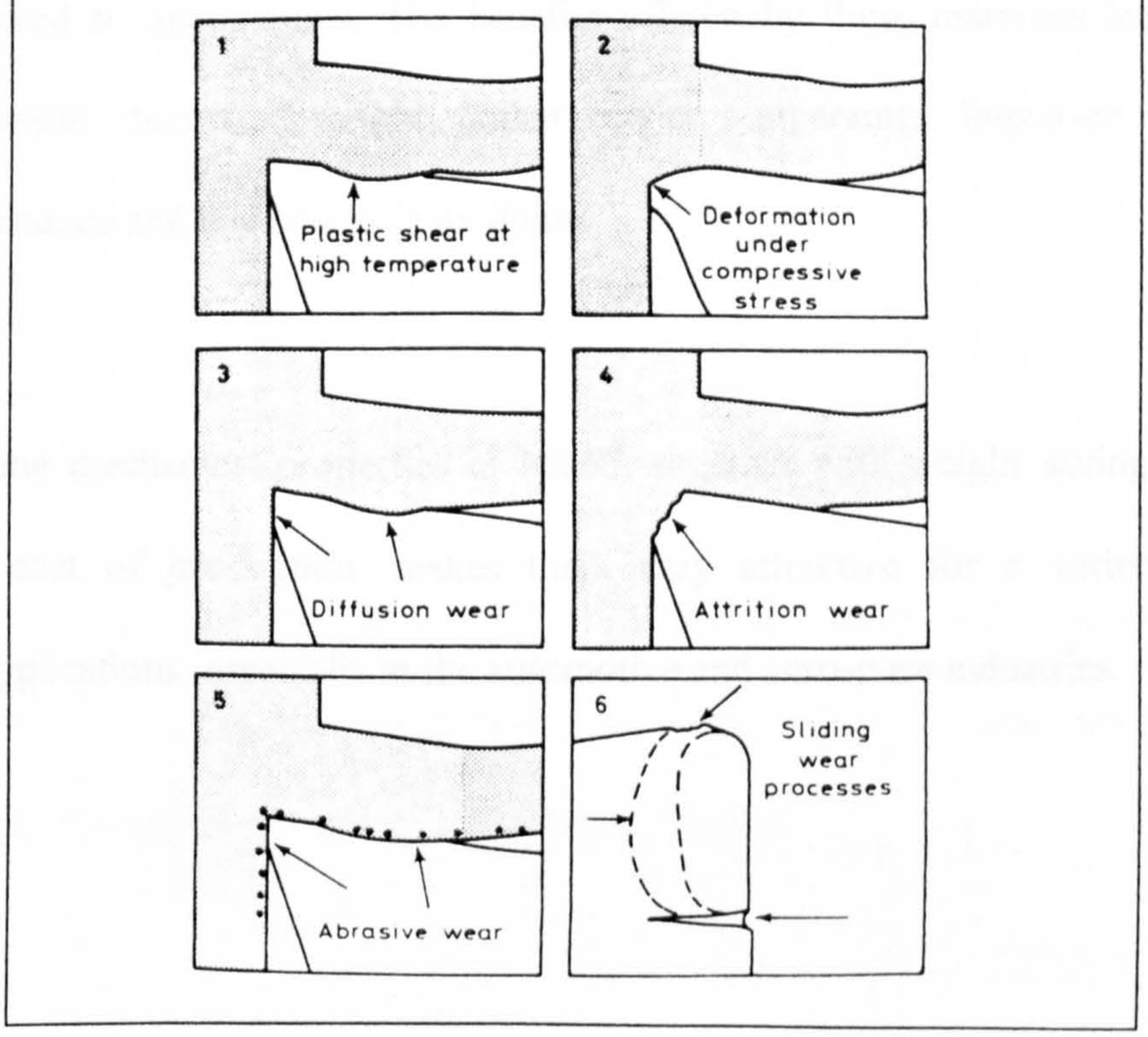

Figure 4.8 Six Different Types Of Wear Mechanisms [13]

Chapter 5

METAL MATRIX COMPOSITE (MMC)

5.1 Introduction

Metal matrix composites (MMC), an advanced class of materials, is currently experiencing intense research and development in the USA, Japan and Europe [207]. The single greatest advantage and future promise of MMC is their ability to 'create' materials tailored to applications. The benefits offered by these materials include improved strength, decreased weight, higher service temperature, improved wear and creep resistance and higher elastic modulus.

The outstanding mechanical properties of MMC, together with weight saving and relative low cost of production, makes them very attractive for a variety of engineering applications, especially in the automotive and aerospace industries.

5.2 MMC Concept

Generally, a composite material can be defined as a material that contains two or more chemically distinctive phases that are not in thermodynamic equilibrium. Steel reinforced concrete, for example, could be thought of as a composite material but it is not a composite in this sense. Therefore, there are certain criteria for a material to be a composite. It must be man-made, the constituents must be chemically distinct with a distinct interface, laminates of different materials are excluded such that the constituents must be combined three-dimensionally and the resulting properties must be different from each constituent [208]. These criteria result in three types of composites, i.e. dispersion strengthened, particle-reinforced and fibre (whisker or continuous) reinforced.

Dispersion Strengthened: Consisting of two or more phases where the second phase is a dispersion of fine particles, their diameter being between 0.01 - 0.1 μm and their volume percentage ranging from 1 to 15%.

Particle-reinforced: Same as dispersion strengthened composites although here the sizes of the particle are larger, their diameter greater than 1μm and volume fraction between 5 and 40%.

Fibre (whisker and continuous) reinforced: These depend on the reinforcement to carry all the load. The length of fibre ranges from 0.1 to 25μm to continuous fibres and volumes percentage may reach up to 70% [207] [208].

5.2.1 Matrix and Reinforcement

Composite material consists of matrix and reinforcement. Metal acts as the matrix, i.e. the bonding element. The matrix cements the reinforcement to the net shape and serves to transfer and distribute the load to the reinforcers, protects the reinforcer's surface and controls the fracture process via the interfacing [209]. Therefore, the selection of the matrix is important and can be based upon several properties [208]. Al, Ti, Mg, Ni, Cu, Pb, Fe, Ag, Zn, Sn and Si have been used as matrix materials, but Al, Ti and Mg are the most widely used [210][211]. Of these, aluminium is currently the most widely used because of its unique combination of good corrosion resistance, low density and excellent mechanical properties [212].

The development of the reinforcement materials that provide either improved properties or reduced cost (particulate is cheaper than continuous fibre) has become a major factor in stimulating the resurgence of MMC. Generally, the reinforcements used are ceramics, typically these ceramics being oxides, carbides and nitrides. Common reinforcement materials are silicon carbides (SiC), alumina (Al_2O_3) and boron carbide (B_4C) [213].

5.2.2 MMC Classification

MMC normally contain between 15% and 50% of reinforcement and are classified according to whether such reinforcement is continuous or discontinuous. Each of

the categories has their own characterisation, production, resultant physical and mechanical properties and corresponding applications.

At the bottom end of the cost scale come particulate-reinforced MMC and next come whisker or short fibre reinforced MMC, these are often found in the auto sectors. Top of the range MMC are reinforced with continuous fibres, and the cost of these generally limits them to aerospace niche markets.

5.2.2.1 Continuous Reinforced MMC

Continuous fibre-reinforced systems result in the highest strength and modulus improvements over the base alloys but they are highly anisotropic compared to most metals and alloys [214]. Primarily the degree of anisotropy depends on the degree of fibre orientation. The fibres acting as load bearers while the matrix serves to transfer and distribute the load to the fibres, to hold the fibres together and to align them in the desired stress direction. The efficiency of the matrix in transferring the load to the fibre will determine the mechanical properties of the composites, and is therefore related to the quality of the fibre/matrix bond [210]. The matrix also protects the fibres from any mechanical or environmental damage.

Low density non-metallic fibres of graphite, alumina, boron or silicon carbide with large diameter in the range of 100-200μm (monofilaments) or smaller diameter in the

range of 5-20μm (multifilaments) are the commonly used reinforcements [215] [216]. The high cost of continuous fibres can make them prohibitively expensive in some applications. Application of continuous fibre MMC are limited to specialist areas such as structural members of aerospace structures and military airplanes.

5.2.2.2 Discontinuous Reinforced MMC

Recently, this class of MMC has attracted considerable attention from the commercial world. Discontinuous reinforced MMC has emerged as new commercial material for aerospace, automotive and high-performance markets. In many stiffness, strength, and weight-critical applications, they offer higher performance than traditional aluminium alloys. For example, a 50% increase in modulus, achieved by substituting a discontinuous silicon carbide reinforced aluminium alloy for an unreinforced wrought counterpart, resulted in a 10% total weight reduction [217].

The reinforcement material for discontinuous reinforced MMC includes carbides (SiC, B_4C), nitrides (Si_3N_4, AlN), oxides (Al_2O_3, SiO_2) and elemental material (carbon and silicon) [218] [219]. Whisker, short fibres and particulate reinforcements are the family of discontinuously reinforced MMC [220][221].

Silicon carbide (SiC) is the most commonly used reinforcement material in the form of a particulate. Silicon carbide has excellent properties in terms of strength, stiffness and wear resistance. It is commercially available in sizes from ~ 0.5 micron to > 10

microns. Particulates are easily blended at higher volume percents with aluminium powders due to their matching particle size. MMC containing 40 vol. % particulate are common and MMC up to 55 vol. % particulate are being developed [210][220][222]. Some of the most common reinforcement materials and their properties are shown in Tables 5.1, 5.2 and 5.3.

5.2.3 Properties of MMC

The potential advantages of MMC materials are well documented. Several advantages that are very important for their use as structural materials include the combination of the following properties [208][212][213][215] [223] [224] [225]:

1. High strength
2. High modulus
3. High toughness and impact resistance
4. Low sensitivity to temperature changes or thermal shock
5. High electrical and thermal conductivity
6. Excellent resistance to severe environments
7. Improved elevated temperature properties
8. Improved thermal expansion
9. Improved wear resistance

However, the above properties depend on many factors such as the properties, size, shape and distribution, degree of bonding and amounts of reinforcement [209][211].

The advantages offered by MMC is best visualised by comparing it to different types of composites and unreinforced materials. Table 5.4 summarises these, together with the strengths and weakness of MMC.

5.3 MMC Applications

Presently, apart from the aerospace industry, MMC are used widely in the automotive industry, in leisure items, in sports goods and in structural design. From rigorous exploitation and development throughout the world, particulate reinforced MMC will find extensive markets in the future [207][223].

5.3.1 Automotive

Factors such as fuel economy, reducing vehicle emissions, increasing styling, enhanced performance, safety, durability and quality are the main driving forces for the commercial exploitation of MMC materials in the automotive industry [214] [226] [227]. Aluminium-based MMC are the major class of materials considered for use in the automotive industry. Table 5.5 lists some of the potential applications of MMC in automotive components and the attraction for their use.

5.3.2 Aerospace and Defence

Many developments in MMC have to date occurred in aerospace [228] [229] and defence industries where high performance materials were required in relatively low volumes, thus justifying costs. MMC, particularly SiC particulate in an aluminium

alloy matrix are viewed as a potential replacement of conventional Al and Al-Li alloys for aerospace components. Table 5.6 summarises some of the applications of MMC in the aerospace and defence industries.

5.3.3 Leisure and Sport Goods

Presently, MMC have already found application in various leisure and sporting goods. MMC with SiC particulate reinforcement are now used to make tennis rackets, the heads of golf clubs [223] and bicycle frames [207]. MMC with carbon fibre is used in reinforced fishing rods and squash rackets [212]. Other leisure and sport goods which employ MMC material include high performance ocean racing yachts and Grand Prix racing cars [215].

5.4 Aluminium Based MMC

In principle, any metallic material can be used as a matrix in an MMC. However, most of the work to date has been on lightweight alloys such as aluminium, magnesium and titanium. Aluminium and its alloys have been the most commonly used and widely investigated matrix for MMC. This popularity as a matrix material can be attributed to the following factors [230] :-

- its availability
- its low cost and ease of fabrication
- good corrosion resistance
- low density

- excellent mechanical properties.

Figures 5.1 shows comparative data for aluminium-based MMC and conventional aluminium-based alloys. Aluminium can accommodate a variety of reinforcements in the form of continuous fibres, whiskers, particulate and laminates. The melting point of aluminium (about 660^{0}C) is high enough to satisfy many application requirements, and aluminium alloys have made excellent MMC when reinforced with a variety of reinforcement materials including continuous boron, Al_2O_3, SiC, graphite, mica and talc [231] [232].

To date, aluminium-based MMC have used commercially available aluminium matrices, mainly of the 2XXX series (Al-Cu) alloys, 5XXX series (Al-Mg) alloys, 6XXX series (Al-Mg-Si) and 7XXX series (Al-Zn-Mg) alloys, and only recently have alloying elements been specifically evaluated which might aid fibre/matrix wettability or chemical compatibility. Adjustments in alloy chemistry and/or heat treatment may therefore be needed to compensate for the effects of the reinforcement - a factor which tends to be overlooked when processing aluminium MMC [233] [234].

Discontinuous reinforced aluminium MMC have been the most exploited [215] [224] [235]. They have the advantage that they can be generated by a wide range of well established primary processing routes (e.g. casting, powder processing, spray forming), and subsequently converted into product form by secondary processing such as forging, rolling, extrusion, machining, etc. [222] [236] [237]. Among the potential discontinuous reinforcements for aluminium alloys, SiC has been the most widely used in both particulate and whisker form.

5.5 Production and Processing of MMC

There are several fabrication techniques that have developed and reached the industrial level to manufacture MMC materials. The main factor determining the production route depends on the types of reinforcement and whether they are aimed at continuous or discontinuous MMC production. Basically there are three types of fabrication [238] :

(1) Solid-phase: diffusion bonding, hot rolling, extrusion, drawing, PM route etc.

(2) Liquid-phase: liquid-metal infiltration, squeeze casting, compocasting, pressure casting

(3) Deposition: spray codeposition.

Currently there are six manufacturing processes that have reached industrial status, i.e. diffusion bonding, powder metallurgy route, liquid metal infiltration, squeeze casting, spray co-deposition and compocasting [239] [240]. All of these

manufacturing processes are competing to produce the lowest cost material with the best mechanical properties [241]. Figures 5.2 and 5.3 summarise the multiplicity of the primary production route of the continuous and discontinuous reinforced composites.

The production method of MMC via co-spray deposition will be discussed in detail as the workpiece materials for this project were produced via this method. Details of the other production routes are widely reported [221][239][240][242] [243] [244] [245] [246] [247] .

5.5.1 Spray Deposition Process

This is one of the most economical methods of producing particulate reinforced MMC. A laboratory-scale deposition unit was installed by Alcan at it's Banbury Laboratories, which is now closed, to investigate the possibilities of manufacturing MMC's on an economic scale. This unit primarily focused on SiC as the reinforcing element [214][239][240].

This technique was commercially exploited by Alcan as a modification of the Osprey™ process. Figure 5.4 shows a schematic of the Alcan spray deposition process used for producing MMC reinforced with SiC particulate. Spray deposition is a combination of gas-atomising and compacting of particles, utilising the inherent kinetic energy and its heat content. The alloy to be sprayed is melted in a crucible by

induction heating. The crucible is pressurised and the metal is injected through a nozzle into the atomiser. At the same time the particles (reinforcement) are injected into the atomised metal and deposited on a pre-heated substrate placed in the line of flight. A solid deposit is built up on the collector. The deposited material, when cold, is moved from the substrate for subsequent processing. The shape of the final product depends on the atomising condition and the shape and the motion of the collector. The equipment can be simply modified to produce hollow tube, near-net shape forging stock, extrusion ingot or plate [214].

Some of the potential advantages of this technique includes:

- blending and degassing of powders involved in PM is eliminated.
- production of fine grain size is obtained due to rapid solidification (which will strengthen the matrix)
- minimisation of reactions between matrix and the reinforcement components

One of the possible disadvantages of the spray deposition process is the tendency for some porosity to be generated in the product [211].

5.6 Machining of MMC

The main thrust of research in MMC has been on its production, properties and physical metallurgy. Focus on machinability of MMC is somewhat limited. There is a relatively small quantity of published data concentrating on the machinability of these materials, these include [248][249][250][251][252]. All of the workers involved in the machining of MMC agree that they are extremely difficult to machine. Tomac

[252] suggests that *"the more widespread usage of particulate aluminium matrix composites is significantly impeded by their poor machinability"*.

There are manufacturing techniques which can produce high quality MMC components to near-net shape. Unfortunately, for reasons such as component design and dimensional tolerance requirements, the need for machining cannot be completely eliminated. A high percentage of the cost involved in producing a finished component for a high performance application results from machining. Therefore, in order to reduce the final cost of components produced from MMC, it is significant that their machinability is fully understood. Both traditional and non-traditional techniques have been used to machine MMC. Traditional machining processes, such as turning, milling and drilling offer the best possibility of higher material removal rates compared with non-traditional techniques such as electrical discharge machining (EDM), electrochemical machining (ECM), ultrasonic machining, laser machining, etc. [253]. The emphasis on the traditional method will be elaborated on in depth as this project is involved with the turning of MMC.

5.6.1 Turning of MMC

Turning operations have been used widely in the machining research carried out on MMC, milling and drilling have been used less often. This is due to the fact that, for turning, the machine tools required are inexpensive, the tooling is simple and easy to modify and the machining operation is easier to analyse. The majority of the MMC

materials under investigation had a matrix of aluminium alloy with reinforcement of SiC, B_4C or Al_2O_3 in the form of whiskers, short fibre or particles.

There is a consensus that the extremely abrasive nature of MMC make the choice of tool material and operating parameters crucial. Consequently, the key aspects of machining MMC are the size and morphology of the reinforcement, together with the volume percentage used [254] [255].

Cemented carbide and polycrystalline diamond (PCD) tools were the main cutting tools under investigation. Other cutting tools used include coated carbide, cubic boron nitride (CBN), Al_2O_3 and SIALON. The main objectives of the research concentrated on the comparison of the tool lives, wear mechanism, surface roughness, and tool/workpiece interactions. In most cases the tool geometry used, in terms of rake and approach angles was relatively standard. Coolant is not generally used in the turning operations as it was found to accelerate the tool wear [252] [254] [255].

When machining MMC reinforced with particulate SiC, Chambers and Stephens [249] report that cemented carbide tools could be used at low metal removal rates and show 'industrially acceptable tool lives if a low cutting speed, high feed rate combinations were used'. Tomac [252] also reported that cemented carbide tools are useful for "short-run" jobs if machining in the range of cutting speed of 20-50

m/min. They also reported that polycrystalline diamond (PCD) tools gave "significantly better performance".

Cronjager and Biermann [250] investigated the machining of fibre reinforced material. They discovered that Al_2O_3 fibre reinforced materials are less abrasive and hence easier to machine than particulate SiC reinforced materials due to the lower hardness of Al_2O_3 fibres compared to SiC particles. SiC particles have produced three times more wear than alumina fibres in identical matrices [251]. The cutting speeds used by the above authors were in the range of 20 to 30 m/min. Tool lives of 4.5 minutes at 20 m/min were obtained if 0.3 mm flank wear was used as the limiting factor [250].

Abrasion was the major wear mechanism involved when machining MMC with cemented carbide tools. This is due to the hardness of the reinforcement material compared to the tool material. Therefore the hardness of the reinforcements is a dominant factor for the tool wear. Knoop hardness value for cemented carbide is 13 - 16 GPa, silicon carbide is 19-27 GPa and Saffil™ fibre (Al_2O_3) is 7 - 8 GPa [256]. Silicon carbide is harder than cemented carbide and therefore expected to produce substantial abrasive wear.

The harder the cemented carbide tool the better its resistance to abrasive wear. Chambers and Stephens have shown that a K10 tool outperformed the softer K20.

Medium grain size cemented carbide tools performed better than a fine grain of equivalent hardness [249]. Other researchers have also shown that the grades of cemented carbide with larger grains size perform better than finer grain size of equal hardness [257][258]. However, a slight attrition has been observed by Cronjager and Biermann [250] when machining MMC using cemented carbide tools with fine grain size. With an increase in grain size, the flank wear rate decreases. This is because the larger cemented carbide grains can better withstand the wear attack of the hard particles, while fine grains are easier to separate from the binding of the cemented carbide [258]. The quantity of binder phase present will also effect the performance of the cemented carbide tools. Tools with the lowest binder content have shown the best performance [257].

Coated cemented carbide tools with TiC, Al_2O_3 and TiN coatings have been available for some time and have been successfully employed in machining steels where they prevent diffusion wear at higher cutting speed [77]. These coated carbide tools have also been investigated for machining MMC. Chambers and Stephens [249] reported that coated cemented carbide tools offer little additional protection. Examination of the cutting tools showed that the coating is rapidly lost through a combination of spalling and abrasion. Improvement with coated cemented carbide tools was obtained when low feed rates were used. This might be associated with differences in built-up formation and stability. Tomac [252] has machined particulate MMC with multiple coated cemented carbide tools at 60 m/min and observed that the coating was rapidly removed. To date, the hardness values of coating materials

investigated are not substantially higher than the harder grades of cemented carbide. Harder coatings called 'diamond-like coatings' are now becoming available which offer a surface hardness approaching that of diamond, and therefore are likely to improve the tool life under abrasive wear conditions.

The highest feed rate and depth of cut combination have been suggested by most workers in order to increase the amount of MMC that a carbide tool can remove during its life. It has been shown that these two factors have little or no effect on tool wear but will increase the metal removal rate (MRR) [249 - 254]. There is no corresponding consensus with regard to the most appropriate cutting speed. Some authors have suggested the use low cutting speed in order to prolong the tool life because they have observed the increase in flank wear rate as the cutting speed increased [249 - 252]. However, other workers have normalised such results to take account of the fact that the cut distance increases with cutting speed and concluded that cutting speed has very little effect on the flank wear [256]. Tomac [252] and Masounave *et al.*[259] have calculated a Taylor exponent value (n) of 0.6 and 0.5 respectively when machining MMC and suggested that the cutting speed has only a little effect on tool life.

The majority of the workers who have investigated the machining of metal matrix composite (MMC) have tested polycrystalline diamond (PCD) tools [238-244]. They have suggested that PCD tools were an obvious choice for machining metal matrix

composite (MMC). The general agreement is that PCD tools have a far longer tool life than cemented carbide tools, coated or uncoated, when machining particulate reinforced metal matrix composite (MMC). Chadwick and Heath [248] have reported that the tool life obtained when the machining metal matrix composite (MMC) reinforced with Safill fibres were not as expected. For example, the tool life increased by 50 - 200 fold when machining Al-20% Saffil™ as a result of changing from cemented carbide to PCD tools. The corresponding increase when machining a 20% Saffil™ Al-Mg5 alloy was only two fold. Crojanger and Biermann [250] have also indicated that the improvement in tool life associated with the use of PCD as opposed to cemented carbide is far less for Saffil than for SiC reinforced aluminium.

Weinert [258] [260] observed that the wear mechanism when cutting metal matrix composite (MMC) with PCD corresponds to the mechanism when cutting with cemented carbide. Larger grain sizes of the PCD improved the wear resistance and better withstood abrasion wear by microcutting.

5.6.1.1 *Formation of Built-Up Edge (BUE)*

The presence or absence of a BUE on the rake face of a cutting tool has important implications for all aspects of machining behaviour. Many workers have observed the presence of BUE when machining MMC with cemented carbide tools [249][250][252]. The existence of a protective BUE may have been responsible for the prolonged tool life observed when using cemented carbide tools at low cutting speed as suggested by Chambers and Stephens [249]. One of Tomac's [252] stated objectives was to identify the cutting conditions where a beneficial BUE could be formed. Unfortunately, the BUE that he observed protected the rake face but did not reduce the flank wear. Cronjager and Biermann [250] have noted that the tendency to form a BUE depended on the type of reinforcement as well as the cutting tool and the cutting conditions. Very large BUE's were found when machining materials reinforced with SiC particles at low cutting speed, These BUE's were stable and protected the tool. The detrimental effect that BUE's have on the surface roughness was also noted. There was no references made to the existence of BUE when machining MMC with PCD inserts. Some workers have suggested that it is not possible for a BUE to form on a PCD tool [242] [248] [252] [258].

5.6.1.2 *Chip Formation When Machining MMC*

Chip formation when machining MMC has been studied through the observation of the shape of the swarf and also using quick-stop techniques. The material which has been studied is predominantly aluminium with discontinuous reinforcement. The

swarf produced can be continuous or segmented according to the combination of cutting speed, feed and depth of cut used. Micrographs of quick-stop samples of aluminium AC8A+20vol% SiCw, show the chip being formed with a saw-blade tooth [261]. Similar swarf was observed when machining materials with a second rigid phase such as hypereutectic Al-Si alloys which contain silicon crystals dispersed in the matrix. In such materials it is believed that the accumulation of dislocation around the rigid phase during deformation creates a preferred path for crack propagation. This results in a very distinct shearing plane, which breaks periodically, producing the 'tooth' shape chips [157]. Another investigation of chip formation mechanisms was carried out by Monaghan [262] using quick-stop tests performed on a 25 vol.% fraction particulate SiC/Al MMC using cemented carbide tools. The chip produced was very fragmented and suggested that chip formation was due to a combined fracture/rupture/crumbling processes and was characterised by a high shear plane angle.

5.6.2 Milling of MMC

Milling research on MMC has not been carried out to the same extent as turning. The published work follows the same trend as that for turning where cemented carbide and PCD tools have been utilised for machining Saffil (Al_2O_3) and silicon carbide (SiC) reinforced materials.

Lane [263] discovered that double coated inserts (TiC/TiN) offered 1-5 times the tool life of the uncoated carbide when run at 91-183 m/min and feeds of 0.38-0.64

mm/rev. However, polycrystalline diamond (PCD) inserts were run 10 times faster and removed 100 times more material than the cemented carbide inserts at the same feed rate. When milling SiC particle reinforced MMC, at cutting speeds in the range of 20 - 80 m/min and feed rate of 0.1 and 0.2 mm/rev, Pashby *et al* [264] have reported that TiN coating offers no significant advantage in terms of tool life. They discovered that the tool material's hardness controlled tool life, and that the feed rate in the range studied had little effect on the rate of tool wear.

Chambers and Jarmakier [265] investigated the influence of volume fraction reinforcement when milling Aluminium-5% Mg/ Saffil materials using K10 cemented carbide tools. Coolant was not used in the trials, a constant feed and depth of cut were maintained and the cutting speed was varied between 20 and 100 m/min. They discovered that these materials can be effectively machined with cemented carbide cutting tools.

Cronjager and Meister [266] have investigated the milling of aluminium wrought alloys (AlMgSiCu, AlMg3) and casting alloys (AlSi7, AlSi12CuMgNi) reinforced with short fibres and particles. The cutting speed at which the PCD tools were operated was found to be an important factor. Speeds below 250 m/min caused fracture of the cutting edge whereas at higher cutting speeds fracture was not observed, although the flank wear was increased. At higher feed rates PCD tools with 25μm grain size exhibit less wear than 10μm grain size, however the use of

lower feed rates reversed this situation. Built-up edge (BUE) was only observed at the feed rates above 0.6 mm/tooth.

Lane [267] observed that increasing the volume fraction of SiC by 50% (from 20% to 30%) caused a reduction in the tool life of polycrystalline diamond (PCD) tools of 21%. A 500% increase in tool life was observed as the particle size of SiC was reduced by 27% (12.8μm to 9.3μm) indicating that particle size has a much stronger influence on tool life than volume fraction.

5.6.3 Drilling of MMC

Apart from cemented carbide and polycrystalline diamond (PCD) tools, high speed steel (HSS) tools have been used in drilling operations. As expected the coated and uncoated regular-twist HSS drills performed poorly [268]. McGinty and Preuss [255] conducted drilling tests on an aluminium-matrix material reinforced with "fibre-FP", Du Pont's alumina fibre, containing 50 - 55 vol.% alumina. It was found that when drilling with solid-carbide drills the tool wear varied as a function of feed rate but not with changes in the drill spindle speed. At an optimum feed rate of 0.3 mm/rev there was little difference in the magnitude of the tool wear over a range of cutting speeds. It was concluded from this result that a higher cutting speed, and therefore increased productivity, could be used without a significant change in the tool wear.

Jawaid *et al.* [269] have observed that the most evident mechanism of wear when drilling particulate reinforced MMC was that of abrasion. Chisel edge, margin, lip crater and lip flank wear were observed at most cutting conditions. Wear of the outer corner of the lip flank was found to have the most significant effect on performance. They concluded that the application of a coolant was found to be essential when drilling MMC in order to prevent seizure and drill breakage.

Short fibre and particulate reinforced materials have been drilled by Cronjager and Meister [270] using a range of solid carbide drills and polycrystalline diamond (PCD) drills. SiC-particle reinforced aluminium gave a higher tool wear rate than α-alumina short fibre material with solid carbide tools. It has been suggested that this difference was attributable to the differences in the type of built-up edge produced by each material. The shape of the wear for the two materials was different with a distinct rounding off at the cutting edge for the fibre material whereas the particles cause flank wear. PCD drills have shown that the wear produced was almost independent of cutting speed between 15 m/min and 300 m/min with harder B_4C producing substantially more wear. PCD tooling has shown an increased tool life of 1500 times over that of cemented carbide.

More recent work on MMC by Coelho *et al.* [271] has concentrated on the optimisation of drilling and reaming operations involving PCD tipped twist drills and both cemented carbide and PCD single blade reamer tools. They observed that the

PCD twist drills fabricated using spade-shaped "sandwich" style PCD blanks were able to make a minimum of 300 holes in AA2618+15 vol.% SiC particulate MMC. Some of the variation in performance of the drills resulted from slight differences in point geometry. These effects could be minimised by a standardisation of design and point geometry. They concluded that drilling MMC using PCD tipped twist drills showed moderate flank wear after 300 holes using a variety of cutting conditions.

5.6.4 Non-Traditional Machining of MMC

Non-traditional methods, such as electro-discharge (EDM), abrasive waterjet (AWJ) and laser machining are becoming increasingly popular for machining MMC [272]. Non-traditional methods have both advantages and disadvantages over the traditional methods. Ramulu and Taya [273], conducted experiments on MMC consisting of silicon carbide whiskers in an aluminium matrix (SiC/Al) with 15% and 25% volume fraction reinforcement respectively using EDM. The material removal rate (MRR) and the electrode wear rate (EWR) both increase with the average current. The EWR for brass is greater than for copper since the melting temperature of copper is higher. The machining rate is proportional to the volume fraction of the reinforcement.

Neailey and Bacon [274] compared the electrodischarge machining of a SiC particulate aluminium alloy with the behaviour of the unreinforced alloy. They observed that the material removal rates in the MMC are lower than in the base

material and the types of damage is different. There is migration of the reinforcement and various high temperature reactions between the aluminium, the silicon carbide and the environment, particularly at high currents or when arcing occurs.

Abrasive waterjet (AWJ) has been used on MMC in a turning operation. Machining rates to obtain the same surface quality are 38% lower for Mg/B_4 (15% B_4) than for unreinforced aluminium. With traditional turning methods, machining rates of Mg/B_4C and Al/SiC composites are about 15-20 times slower than those of aluminium [275] [276]. Removal rates, dimensional accuracy, and finish can all be limitations of AWJ depending on the material and its thickness. When cutting thick materials, the jet stream tends to angle away from the direction of cut, and the problem becomes more pronounced as the thickness and/or feed rate increases [277].

There are several types of lasers used for machining MMC . The major ones are gas (CO_2 and excimer) laser and solid-state (Nd:YAG and Nd:glass) lasers. Some of the benefits of laser machining include minimum material waste (kerf width), minimum set-up time, no tools (and thus no tool wear or replacement), smooth edge cuts, and low total heat input. A major disadvantage of laser machining is the heat-affected zone (HAZ), where high temperature imparted to the workpiece at, or near, the last cut can cause metallurgical changes. This can reduce the fatigue properties of the work material and the quality of holes in deep hole drilling [278].

5.7 Summary On Machining Of MMC

It has been shown that MMC can be machined using traditional techniques. Whether or not they can be machined economically depends to a great extent on the value of the component being produced and the potential cost savings arising from the use of MMC. Such decisions can only be realistically made on an individual basis. Machining problems can be reduced greatly if proper consideration in terms of reinforcement type, matrix material and appropriate cutting tools and conditions are given serious attention. Nevertheless, machining is an issue has to be addressed in more depth in order that these material can be exploited to their fullest potential.

The major problem in machining MMC using traditional methods is the rapid wear of the cutting tool. Major factors which govern the machinability of MMC are quite straight-forward, the more abrasive the material the greater will be the tool wear. The abrasiveness of MMC are determined by the following factors:

- Hardness of reinforcement
- Size of reinforcing phase
- Volume fraction of the reinforcement
- Matrix strength, and
- Regularities of the reinforcement

Abrasiveness increases as hardness, size, shape and volume fraction increases and matrix strength rises.

The literature suggests that there are primarily two groups of MMC being considered:

a) Alumina (Al_2O_3) reinforced in the form of fibre and particle

b) Silicon carbide (SiC) and boron carbide (B_4C) reinforced in the form of whiskers or particles

Group (a) can be machined with a certain degree of success using cemented carbide tools at low cutting speeds while group (b) are more difficult to machine owing to their more abrasive nature. Generally, PCD tools outperform cemented carbide tools in machining MMC because of their superior hardness. Other than selecting the hardest cutting tools available, less effort has been devoted into the investigation of different tool geometry, application of coolant and other variables.

The literature has indicated that research into further improving the mechanical and physical properties of MMC is continuing. As these properties improve, MMC are likely to become even harder to machine. In order to cope with greater challenges in the future, it is therefore important that the machining aspects of these materials are fully understood.

Table 5.1 Properties Of Selected Continuous Reinforcement Materials [220] [221]

Continuous Reinforcement	Aspect Ratio L X D (mm x μm)	Coeff. Of Thermal Exp. ($K^{-1}.10^{-6}$)	Density (g/cm^3)	UTS (GPa)	Young's Modulus (GPa)
Carbon	2.5 x 7.8	-	1.75	3.45	230
SiC	1-6 x 10-15	3.06	2.55	3	112-195
Al_2O_3	3-6 x 15-25	7.92	3.96	1.7	380
Al_2O_3 - Saffil™	0.1-1 x 1-5	-	3.3	2	300

Table 5.2 Properties Of Selected Whisker Reinforcement Materials [220] [221]

Discontinuous Reinforcement (Whiskers)	Aspect Ratio L X D (mm x μm)	Coeff. Of Thermal Exp. ($K^{-1}.10^{-6}$)	Density (g/cm^3)	UTS (GPa)	Young's Modulus (GPa)
SiC	50-200 x 0.1-1 cyl.	-	3.2	3-14	400-700
SiC	50 x 0.2-1 hex.	-	3.2	13	700
Al_2O_3	100 x 2	7.92	3.97	15	2275

Table 5.3 Properties Of Selected Particulate Reinforcement Materials [220] [221]

Discontinuous Reinforcement (particulate)	Average Diameter (μm)	Coeff. Of Thermal Exp. ($K^{-1}.10^{-6}$)	Density (g/cm^3)	UTS (GPa)	Young's Modulus (GPa)
Graphite	40-250	-	1.6-2.2	20	910
SiC	2-340	3.06	3.2	3	480
SiO_2	53	1.08	2.3	4.7	70
MgO	40	11.61	2.7-3.6	-	-
Si_3N_4	46	1.44	3.2	3-6	360
TiC	46	7.6	4.9	-	-
BN	46	-	2.25	0.8	100-500
Mica	180	-	-	-	170
ZrO_2	75-180	12.01	5.65-6.15	0.14	210
B_4C	40-130	6.08	2.5	6.5	480
TiO_2	20	-	3.9-4.3	-	-
Al_2O_3	40-340	7.92	3.97	8	460

Table 5.4 Comparisons Of Characteristics Of MMC With Other Materials. [210]

Strength/Weaknesses of MMC	MMC compared to other materials
A. Continuous Reinforced MMC *Advantages*: ultimate in terms of mechanical properties *Disadvantages*: expensive and difficult to produce; generally properties are anisotropy	**A. Compared to unreinforced metals** *Advantages*: higher specific strength; higher specific stiffness; improved high temperature creep resistance; improved wear resistance *Disadvantages*: lower toughness and ductility; production methods are more complicated and expensive.
B. Discontinuous Reinforced MMC *Advantages*: less expensive to produce; isotropic properties *Disadvantages*: inferior mechanical properties compared to continuous reinforced MMC; limited secondary formability.	**B. Compared to Polymer Matrix Composites (PMC)** *Advantages*: higher transverse strength; higher toughness; better damage tolerance; improved environmental resistance, higher thermal and electrical conductivity; higher temperature capability *Disadvantages*: less developed technology, limited data base properties, higher cost. **C. Compared to Ceramic Matrix Composites (CMC)** *Advantages*: higher toughness and ductility; ease of fabrication; lower cost. *Disadvantages*: inferior high temperature capability

Table 5.5 Potential Applications Of MMC In The Automotive Industry [211][212]

Components	Material	Attractions
Brake rotors (discs)	Silicon carbide particulate/aluminium	Weight saving and reduced fade
Connecting rod	Alumina fibre/aluminium	Weight saving, higher strength & stiffness
Cylinder liners	Silicon carbides particulate/aluminium	Improved wear resistance
Pistons	Alumina fibre/aluminium	Improved high temperature strength
Pistons	Silicon carbide particulate/aluminium	Improved wear resistance
Pulleys	Silicon carbide particulate/aluminium	Improved wear resistance and weight saving
Selector forks	Silicon carbide particulate/aluminium	Improved wear resistance and weight saving

Table 5.6 Application Of MMC In The Aerospace And Defence Industries [206][223]

COMPONENTS	ADVANTAGES
Defence	
Missile components	Increased stiffness and high temperature properties Improved performance
Tank components	Weight saving Improved wear resistance
Aerospace	
Space structure	Weight saving due to higher specific stiffness and lower density
Speed brake	Higher stiffness allows weight saving in military aircraft
Hydraulic components	Higher stiffness allows weight savings
Helicopter components	Weight saving Wear resistance

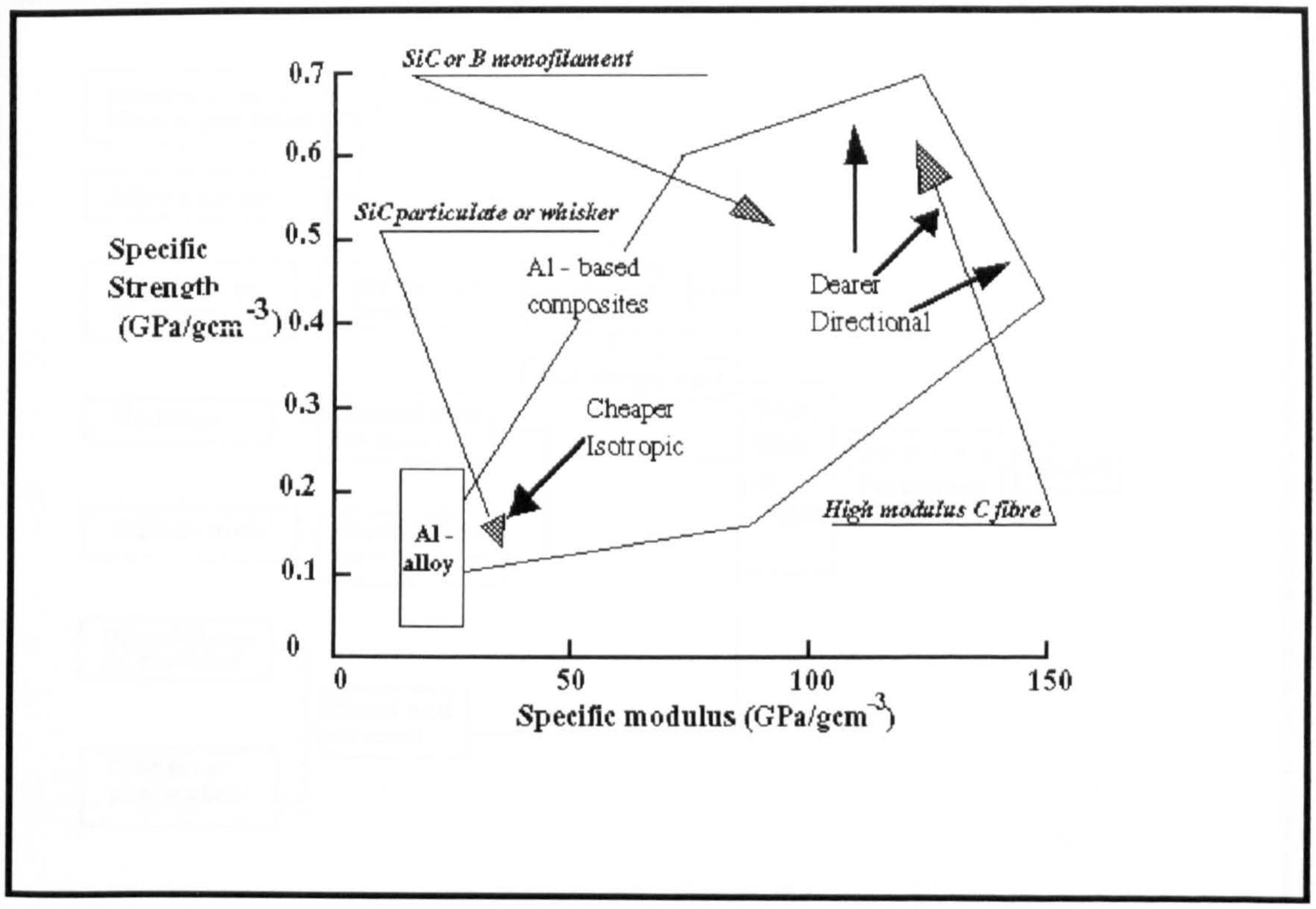

Figure 5.1 Stiffness And Strength Of Aluminium Composites [214]

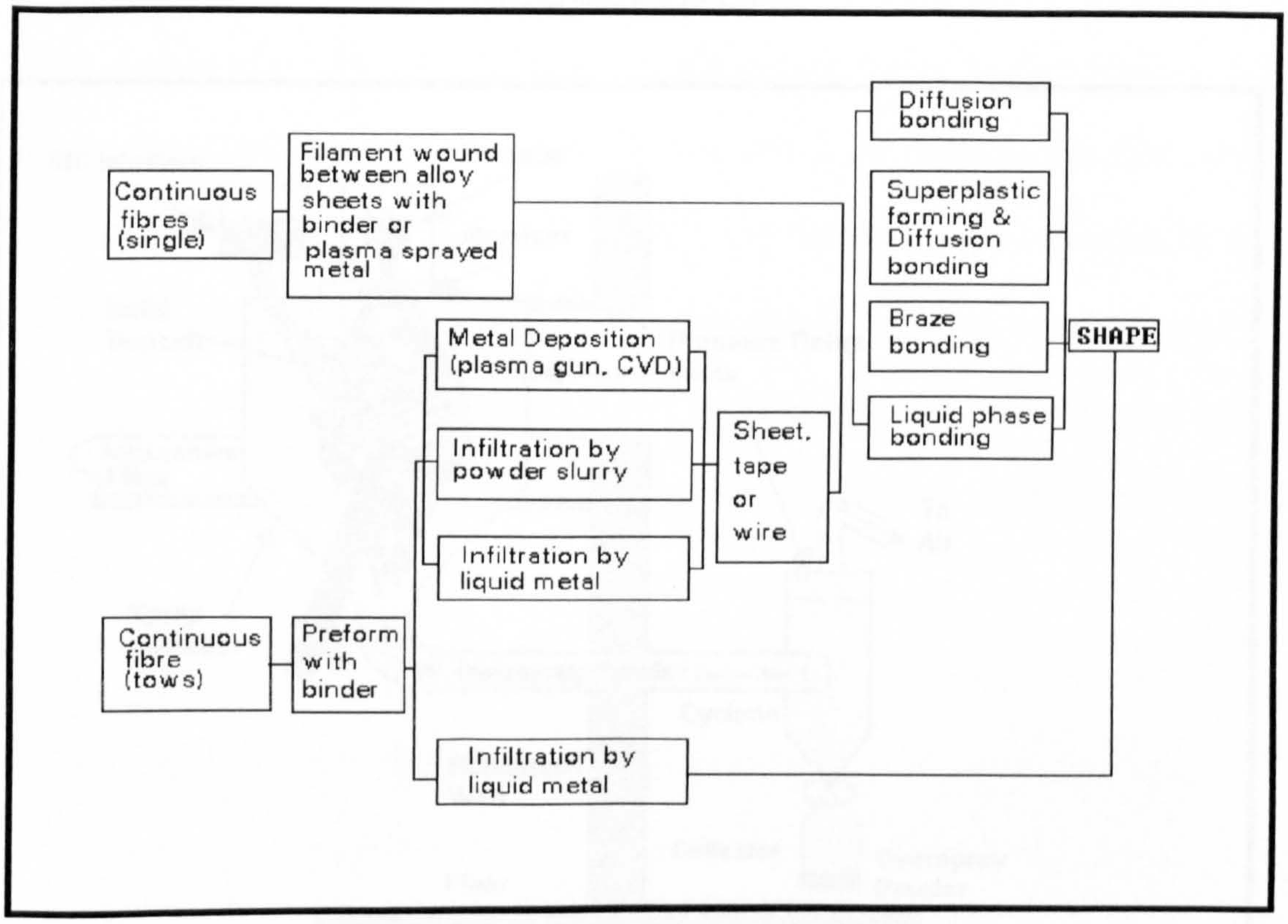

Figure 5.2 Primary Operations For Production Of Continuous Reinforced Composites [235] [236]

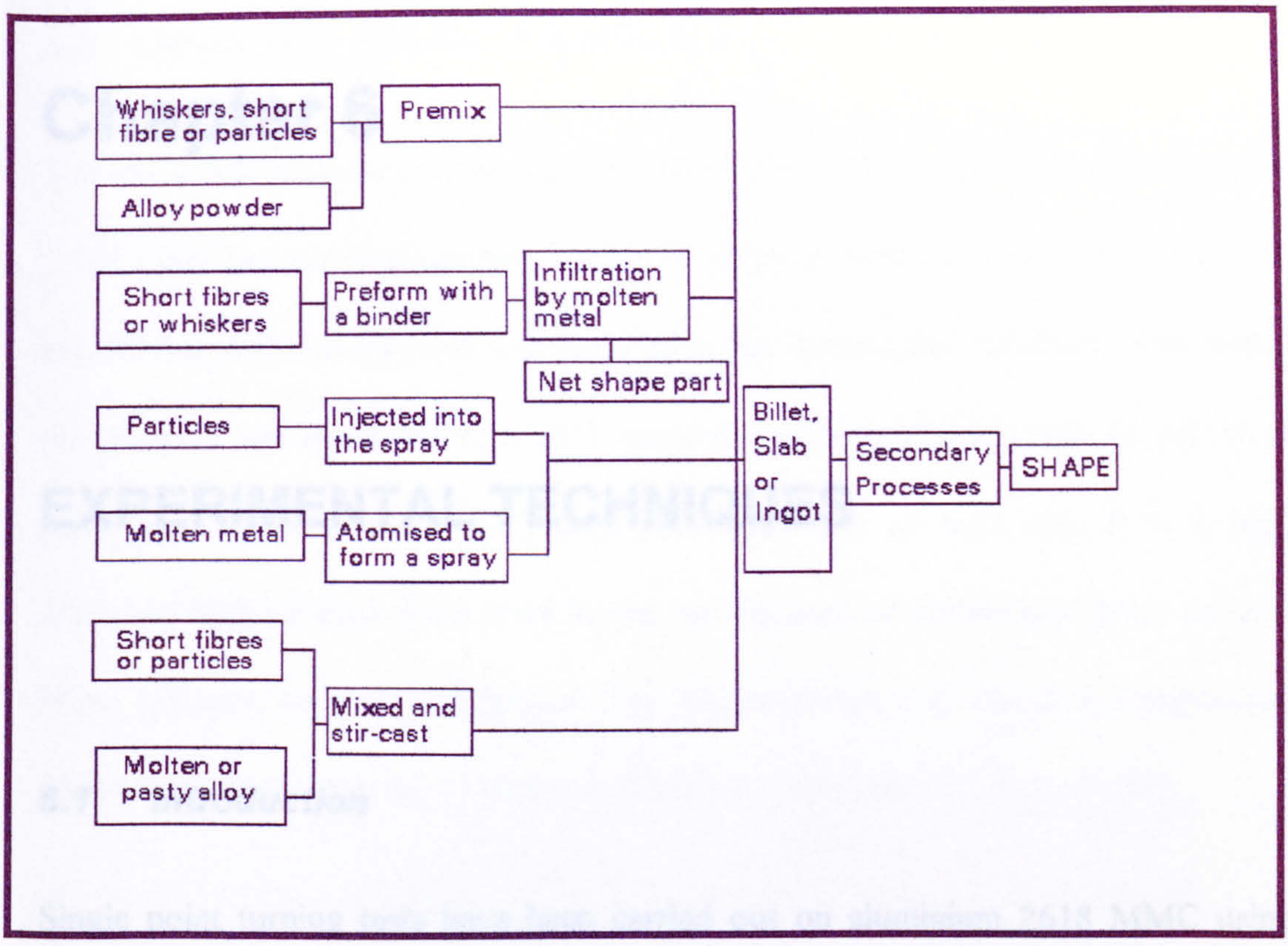

Figure 5.3 Primary Operations For Production Of Discontinuous Reinforced Composites [235]

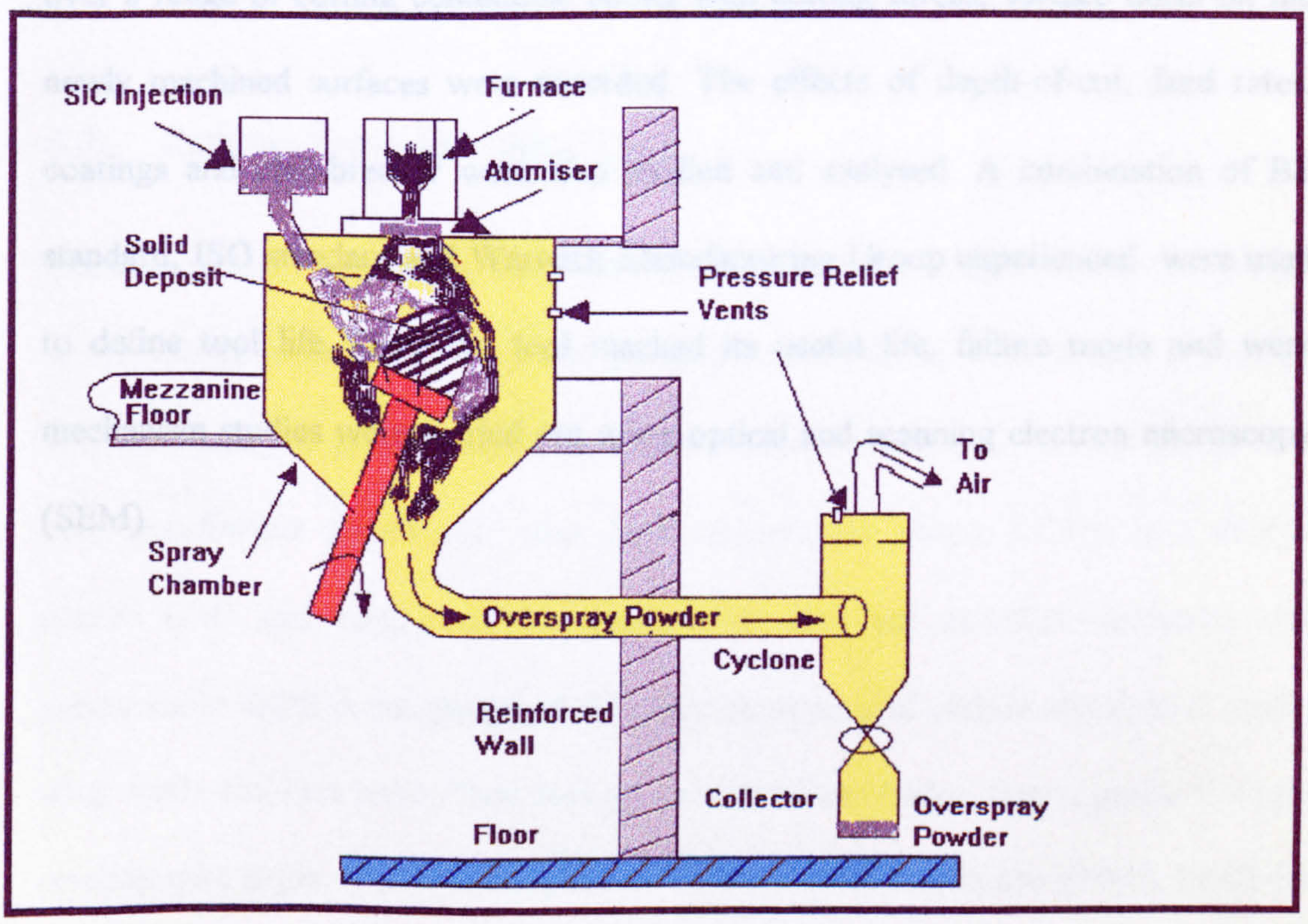

Figure 5.4 Schematic Of The Spray Deposition Technique [213]

Chapter 6

EXPERIMENTAL TECHNIQUES

6.1 Introduction

Single point turning tests have been carried out on aluminium 2618 MMC using cemented carbide cutting tools. The tool lives of the cutting tools were evaluated over a range of cutting conditions. Along with cutting forces, surface finish on the newly machined surfaces were recorded. The effects of depth-of-cut, feed rates, coatings and chip-breaker were also studied and analysed. A combination of BS standard, ISO standard and Warwick Manufacturing Group experienced were used to define tool life. Once the tool reached its useful life, failure mode and wear mechanism studies were carried out using optical and scanning electron microscopy (SEM).

6.2 Workpiece Material Specification

The workpiece material used throughout the course of this project was manufactured by ALCAN International Limited via the Co-spray deposition technique. It was then extruded to 220 mm diameter and supplied in the as-extruded condition. The matrix composition was equivalent to a 2618 aluminium alloy reinforced with 18 vol. % of particulate silicon carbide (SiC) with mean diameter of 6.25 μm. It is a high modulus, high strength alloy used in the manufacture of automotive parts such as brake callipers, conrods and pistons. The microstructure and chemical composition of the workpiece material are shown in Figure 6.1 and Table 6.1 respectively.

The physical and mechanical properties of the particulate reinforced 2618 aluminium metal matrix composite are shown in Table 6.2.

6.3 Cutting Tools Specification

The cutting tools used in the tests were produced by Kennametal® Inc. The grades of the carbide tools used throughout the tests were K68 and KC910. K68 is a tough WC-Co unalloyed grade which is generally used for machining stainless steels, cast iron, non-ferrous metals and other high temperature alloys. KC910 is a double coated (TiC and Al_2O_3) carbide grade with excellent abrasion resistance and resistance to BUE in roughing and finishing operations of carbon steels, tool steels, alloy steels and cast irons. Two tool geometries were chosen, one negative and one positive rake angle. The ISO designation for the carbide inserts are SNMA 12-04-08

and SPGN 12-03-08, these were clamped in MSDNN-2525M 12K and CSPDN-2525M 12 tool holders respectively. The tool holders used in the tests provided the geometry shown in Table 6.3. Basic data for the cutting materials used, i.e. K68 non-coated and KC910 coated cemented carbides are given in Table 6.4. Figures 6.2 and 6.3 show their microstructure.

6.4 Machine Tools

Continuous turning tests were carried out on a CNC Cincinnati Milacron 10CU lathe with a capacity to hold 10 inch diameter bars. The machine is driven with a variable speed, DC motor capable of 30 to 3,000 rpm and controlled with an Acramatic 900TC controller. The motor can supply 22 kW (30hp) over a 30 minute duty cycle. The programmable feed rate along each axis is 2.5 to 5080 mm/min and the rapid traverse rate along each axis is 7620 mm/min. Positioning accuracy is $\pm$ 0.025 mm in 600m, with a repeatability of $\pm$ 0.005 mm.

The force measurements and quick-stop tests were carried out on a CNC Torshalla S250 lathe. The machine is driven with a variable speed, DC motor with power of 38 kW, capable of 130-2800 rpm and is controlled by a GE Mark-Century 2000 controller.

6.5 Machining Operation

Bars of 2618 Aluminium Metal Matrix Composite 120 mm in diameter and 540 mm in length were used for the turning tests. The surface of each and every new MMC bar was removed to a depth of 1.5 mm prior to the start of tool life testing.

Table 6.5 shows the cutting conditions used in the tests. No cutting fluids were used, and the cutting speed, feed rate and depth of cut were varied as indicated in Table 6.5.

Before any machining, all cutting tools were examined under a 10X magnification to check for any defects or handling damage.

6.6 Tool Failure Mode Studies

6.6.1 Tool Life Criteria

A combination of the British Standards Institution publication [20], the ISO publication [33] and Warwick Manufacturing Group experienced were used to give a guide line for selecting the tool life criteria. The following criteria were adopted to determine the end of useful tool life.

The cutting edges were rejected when:

1. Average flank wear reached 0.4 mm
2. Maximum flank wear reached 0.7 mm
3. The crater depth reached 0.14 mm
4. Notching at the nose or depth of cut reached 1 mm

5. Fracture or premature failure of the insert occurred.

Machining was stopped and the wear on the tools measured at intervals appropriate to the tools and cutting conditions being used, this ranged from 1 minute when rapid wear was experienced, to 2 minutes when slow steady wear occurred.

6.6.2 Tool Wear Measurement

Both maximum and average flank wear land, and notch at the depth of cut were measured using a 10X magnification Olympus travelling microscope and a 2-axis moving table fitted with transducers linked to a Heidenhein digital-readout (DRO) equipment. The crater depth on the rake face was measured using a Talysurf-4.

6.6.3 Force Measurement

Force measurements were taken for each cutting speed during the first 20 seconds of cut using a Torshalla S250 turning centre, with the tool holder clamped into a Kistler 9263 piezo electric, 3 component force dynamometer. The construction of the equipment is discussed elsewhere [17]. This dynamometer is very stiff, it has a high resonant frequency, hence very rapid fluctuations in forces could be recorded satisfactorily. This set up would allow all three component forces to be measured, but in this project only two components of forces were recorded, the cutting force and the feed force. The dynamometer was calibrated with the help of static loads before and was frequently checked to maintain accuracy. The signal from the dynamometer was amplified with the help of charge amplifiers and recorded on to a portable personal computer (PC).

6.6.4 Surface Roughness Measurement

A reading of an average surface roughness value (Ra) of the newly generated machined surface on the workpiece was taken at right angle to the feed marks after every cut using a Rank-Taylor Hobson SURTRONIC 3, portable stylus instrument. An advantage of using this equipment is there is no need to remove the workpiece from the turning centre. A surface sample length of about 25 mm was used in all cases and an average of three readings taken. The equipment was calibrated at the beginning of the first reading.

6.6.5 Chip Thickness Measurement

Throughout the tests, representative chips at various cutting conditions were collected in order to measure their thickness. The chip thickness was measured using a pointed micrometer.

6.7 The Quick Stop Tests

In order to study and understand the metal cutting process, it is necessary to freeze the cutting action. This can be done by suddenly withdrawing the tool at high speed. A quick stop device using a humane killer gun positioned above a tool holder, which is supported by a notched shear pin of heat treated silver steel, was used for this purpose [62] . On firing, the bolt strikes the tool holder, breaking the shear pin, this suddenly accelerates the tool away from the cutting position, leaving a chip attached to the workpiece. Usually, the tool comes away more or less cleanly with the chip

attached to the bar. A segment of the bar, together with the chip attached, was cut out for further examination.

The cutting parameters used for the quick stop tests are given in Table 6.6.

6.8 Specimen Preparation

Three types of specimen were prepared, i.e. workpiece section, quick stop section and used inserts. A workpiece section was prepared in order to study its microstructure and the distribution of SiC particles, while the quick stop section is to study chip formation and chip/tool interface conditions, and used inserts were prepared in order to study and analyse the wear pattern and wear mechanisms.

Workpiece specimens from MMC bar were mounted in a Bakelite resin and ground on 40 μm grit size diamond at speed of 300 rpm and pressure of 4N in a Pedemax-2 grinding/polishing machine. Water was used as a lubricant. Then the samples were polished on diamond grit of 15, 6 and 1 μm respectively at a speed of 150 rpm and pressure of 3N for 2 minutes. In order to reveal the microstructure, samples were etched by immersion in Ramsays etch solution containing 25 ml of nitric acid (HNO_3), 2 ml hydrofluoric acid (HF) and 73 ml of water for approximately 7 seconds. Lastly, the sample was examined under an optical microscope at various magnifications.

The quick stop samples were first sectioned and mounted in transparent polyester resin (24 hours curing time), and were ground back halfway through their chip width

with 180, 360, 420, 600, 820 and 1200 μm silicon carbide papers. Next, the samples were polished to 6 and 1 μm finish using microcloth impregnated with diamond pastes for 2 minutes. Then the samples were examined under an optical microscope and photographs were taken at various magnifications. The quick stop samples were then etched with Ramseys solution for approximately 7 seconds and examined under an optical microscope.

Standard methods were used to prepare the tools for SEM inspection - ultrasonic cleaning in an acetone bath, attachment to aluminium stubs and sputter coating with a thin layer of gold to prevent charging of the specimen under the influence of the electron beam. Scanning Electron Microscopy (SEM) equipped with Energy Dispersive X-Ray Spectroscopy (EDS) was used extensively to analyse the cutting tools at various magnifications. A 5% hydrochloric acid (HCl) was used to dissolve the built-up layer on the inserts for further examination of the worn surfaces. Some of the worn inserts were mounted in Bakelite resin with the cutting edge vertical and the nose uppermost. These samples were ground on 40 μm grit diamond at a speed of 300 rpm and pressure of 4N until the cross-section was at a position one half the depth of cut. Then the sample was polished on diamond grit of 15, 6 and 1 μm respectively at a speed of 150 rpm and pressure of 3N for 2 minutes. Lastly, the samples were examined with an optical microscope at various magnifications.

Table 6.1 Chemical Composition (wt%) of 2618 Aluminium Metal Matrix Composite (MMC) Used In The Turning Tests.

ALLOY	Si	Fe	Cu	Mn	Mg	Ni	Zn	Ti	V	Al
2618Al MMC (18% SiC)	0.21	1.05	2.67	0.02	1.50	1.06	0.03	0.08	0.01	Rem

Table 6.2 Mechanical And Physical Properties Of 2618 Aluminium Metal Matrix Composite (MMC)

PROPERTIES	2618 Al MMC
Tensile Strength (MPa)	530
Tensile Yield Strength 0.2% PS (MPa)	460
Density (g/cm^3)	2.84
Coefficient Of Thermal Expansion (mm/K)	17.7×10^{-6}
Modulus Of Elasticity (GPa)	97
Hardness (HV_{10})	187

Table 6.3 Tool Holder Geometries

Tool Holder	MSDNN 2525M 12K	CSPDN 2525M 12
Approach angle (deg)	45	45
Front Rake angle (deg)	-7	+5
Side Rake angle (deg)	0	0
Clearance angle (deg)	7	6

Table 6.4 Properties Of Cutting Materials Used In The Machining Test

Cutting tool material	Type of coating	Binder wt. %	Grain size (μm)	Hardness (HRA)	Coating Thickness (μm)
K68	Uncoated K grade	5.7	1-4	92.7	-
KC910	$TiC + Al_2O_3$	6.0	1-6	91.8	9

Table 6.5 The Cutting Conditions Used In The Machining Tests

Feed Rate (mm/rev)	Depth Of Cut (mm)	Cutting Speed (m/min)							
		15	20	25	30	35	40	45	50
0.2	2 and 4	✓	✓	✓	✓	✓	✓	✓	✓
0.4	2 and 4	✓	✓	✓	✓	✓	✓	✓	✓
0.6	2 and 4	✓	✓	✓	✓				

Note: ✓ - test was carried out.

Table 6.6 Cutting Parameters For Quick Stop Tests

Cutting Speed (m/min)	Feed Rate (mm/rev)	Depth of Cut (mm)
15	0.4/0.6	2
20	0.4/0.6	2
25	0.4/0.6	2
30	0.4/0.6	2
35	0.4/0.6	2
40	0.4/0.6	2
15	0.4/0.6	4
20	0.4/0.6	4
25	0.4/0.6	4
30	0.4/0.6	4
35	0.4/0.6	4

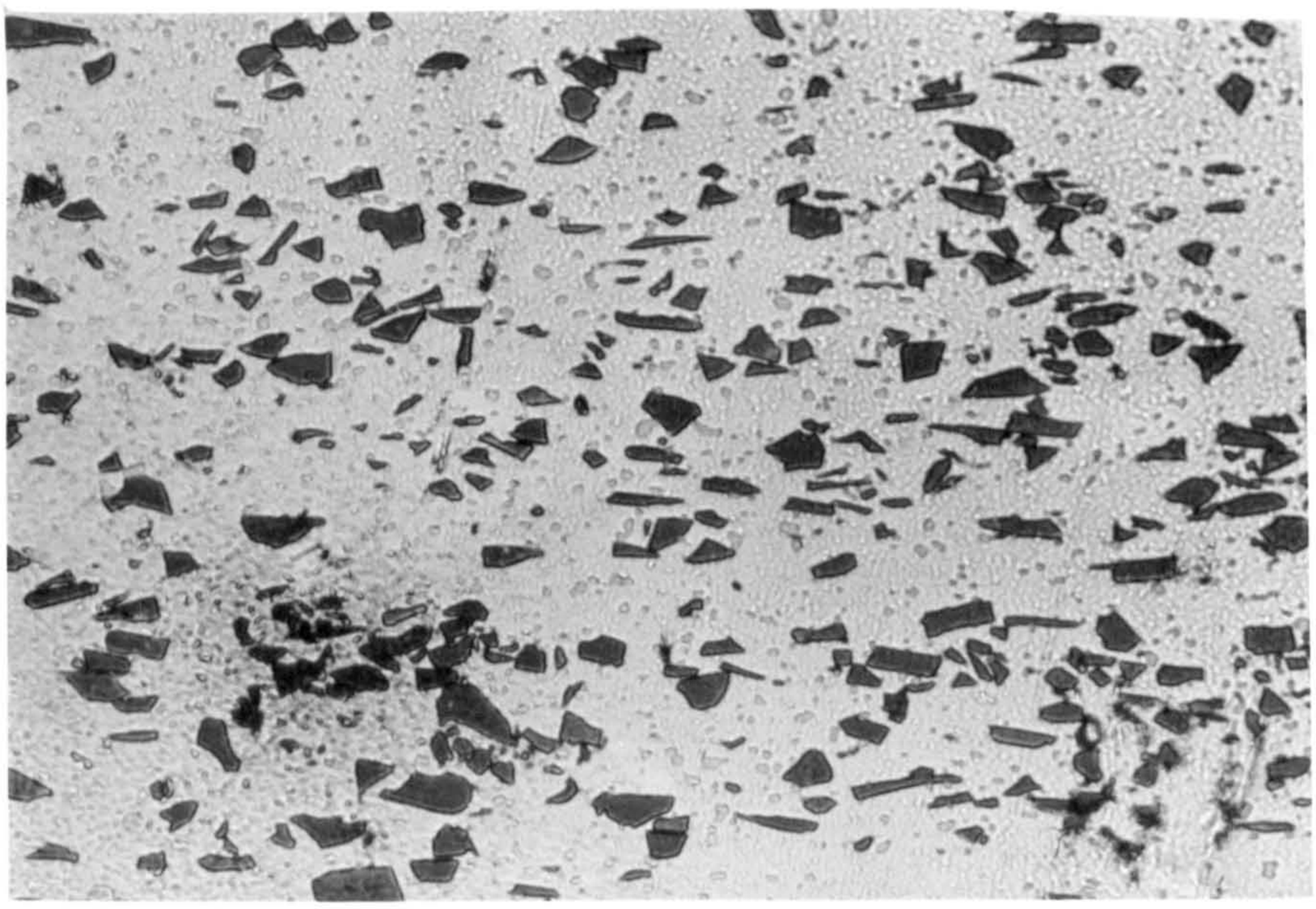

(a) Longitudinal Direction

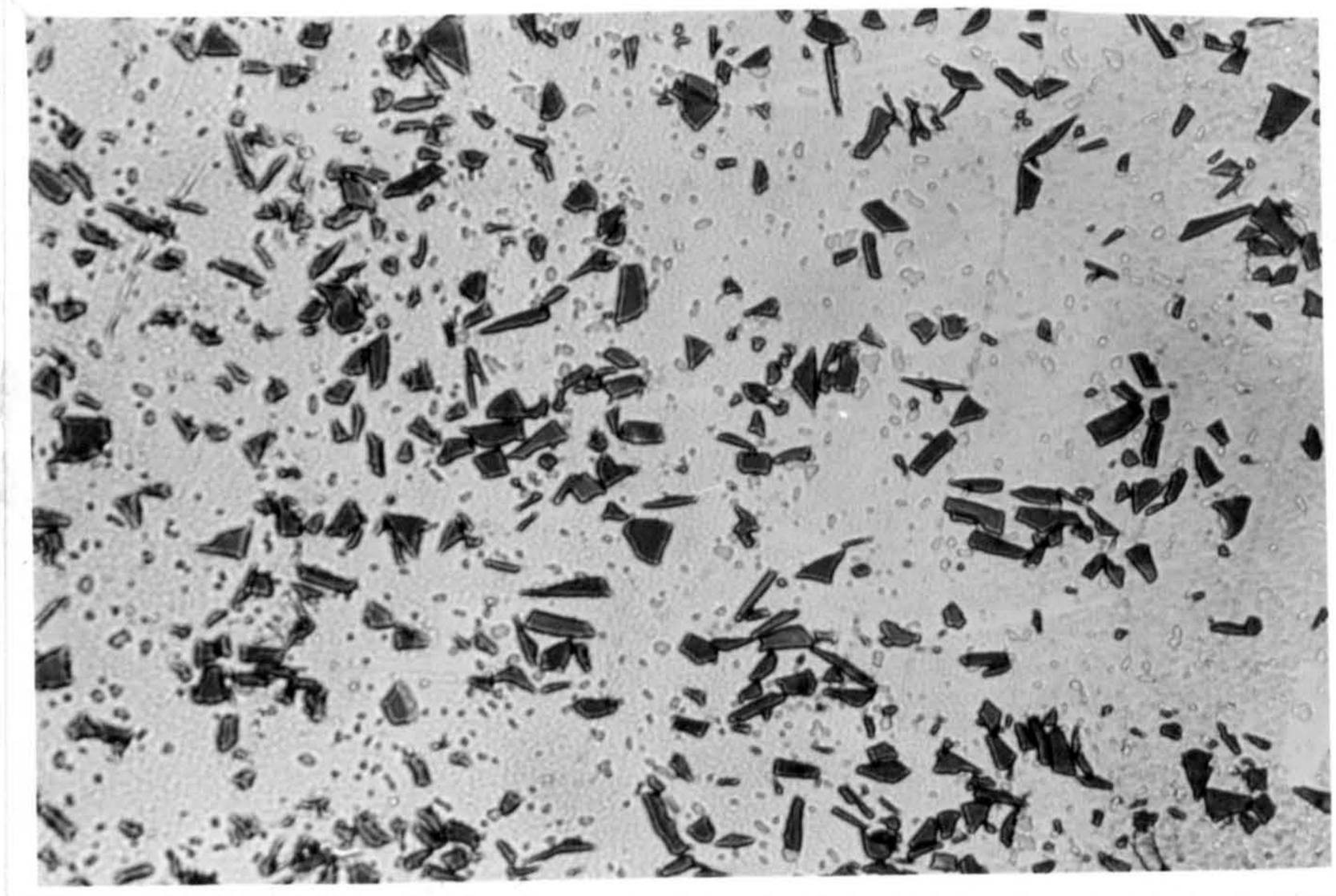

(b) Transverse Direction

Figure 6.1 *Typical Microstructure Of 2618 Aluminium MMC Reinforced With 18 vol. % SiCp* (450X)

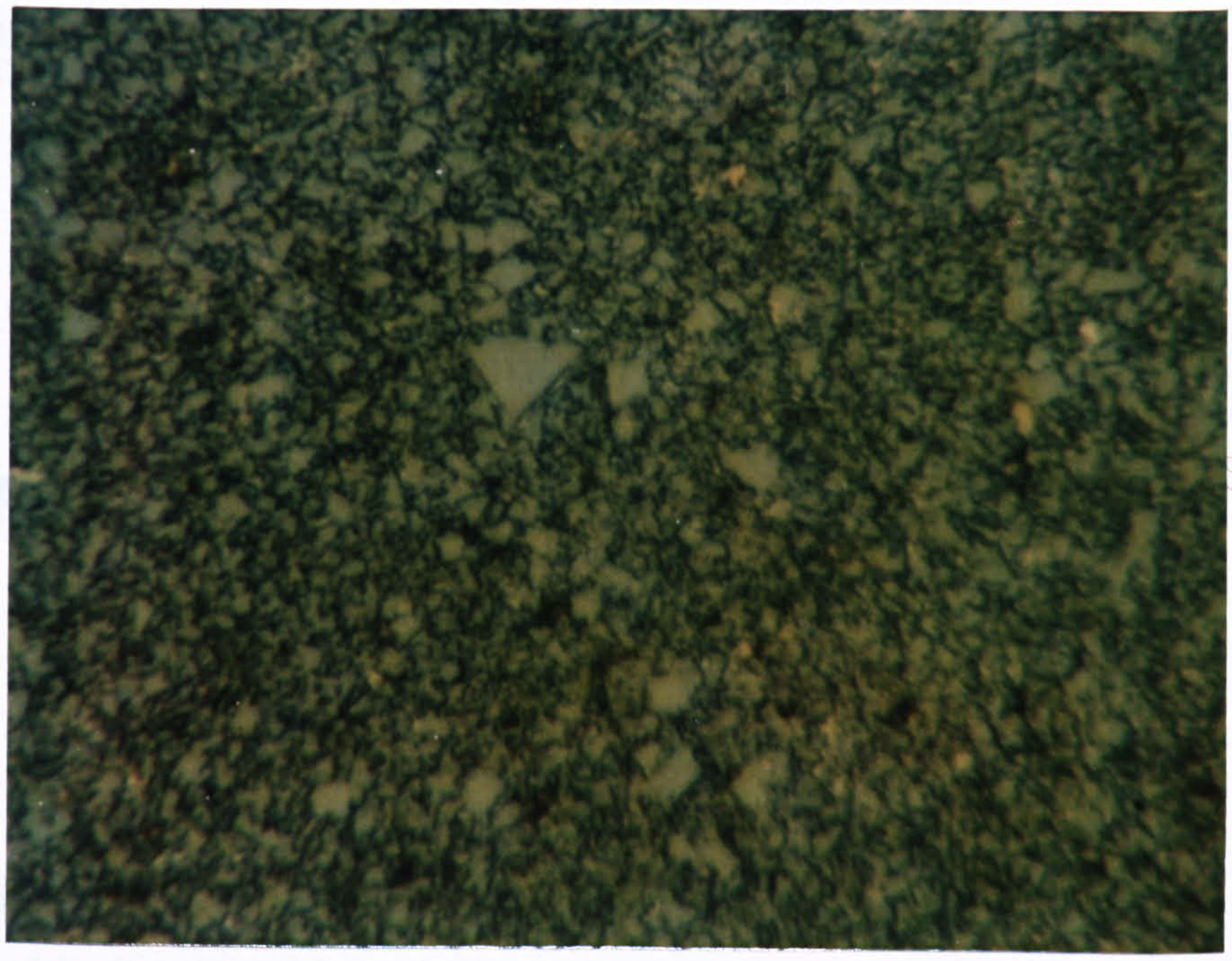

Figure 6.2 *Microstructure Of The K68 Insert* (1500X)

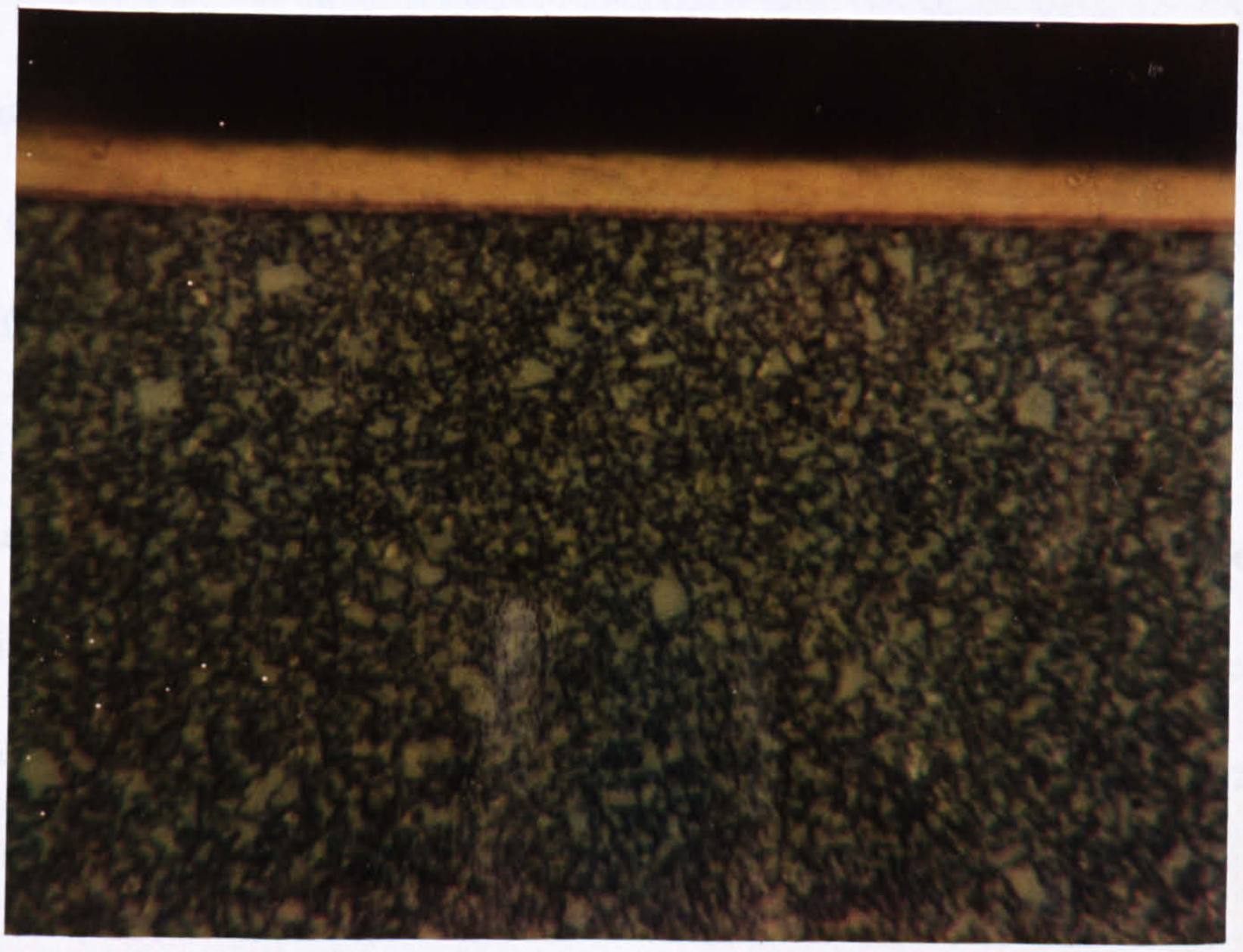

Figure 6.3 *Microstructure Of The KC910 Insert* (1500X)

Chapter 7

EXPERIMENTAL RESULTS

7.1 Description Of The Workpiece Material

Aluminium 2618 Metal Matrix Composite (MMC) reinforced with silicon carbide (SiC) particles produced by the spray deposition process and fully consolidated by extrusion has been used throughout the project. The hardness of the workpiece material as-received was 167 HV_{10}. It was manufactured and supplied by Cospray Ltd., part of ALCAN International Ltd. The chemical composition of the Aluminium 2618 MMC used has been described in Chapter 6.

Examination of the microstructure, using image analysis, revealed various shapes and sizes of SiC, nominally 6 - 8 μm in diameter and 5 - 18 μm in length (Figure 6.1). The hardness of the these particles, as stated by the manufacturer, ranges from 20 - 27 GPa.

7.2 Description of Tool Materials

Two grades of cemented carbide tools with positive and negative rake angle were used throughout the experiments, K68 and KC910. K68 is a WC-Co unalloyed grade which is generally used for the machining stainless steels, cast iron and non-ferrous metals. KC910 is a double coated grade with TiC and Al_2O_3 as coatings, these grades are normally used in roughing and finishing operations of carbon steels, tool steels and alloy steels. The composition and properties of K68 and KC910 are given in Table 6.4 while their microstructures are shown in Fig. 6.2 and 6.3 respectively. All of the cutting tools used in the tests were supplied by Kennametal ® Inc.

7.3 Machining Conditions

The cutting conditions used for machining aluminium 2618 MMC with cemented carbide (K68 grade) and coated cemented carbide (KC910 grade) tools are given below.

Feed Rate (mm/rev)	Depth Of Cut (mm)	Cutting Speed (m/min)							
		15	20	25	30	35	40	45	50
0.2	2 and 4	✓	✓	✓	✓	✓	✓	✓	✓
0.4	2 and 4	✓	✓	✓	✓	✓	✓	✓	✓
0.6	2 and 4	✓	✓	✓	✓				

Note: ✓ - test was carried out.

All experiments were carried out dry without the use of coolant.

7.4 Machining Of Aluminium 2618 MMC With Uncoated Carbide Tools (K68 Grade)

Detailed tool life tests using carbide inserts were conducted to evaluate their cutting performance under a range of cutting conditions as shown above. The independent variables investigated were cutting speed (V), feed rate (f) and depth of cut (DOC). The cutting speed, feed rate and depth of cut are of considerable importance since they control the tool failure modes, wear mechanisms, material removal rate and the production rate possible during the machining process. This machinability data was generated in order to quantify the effect of cutting conditions on these tools. Such an information is not available at present as MMC are a new class of material which are very expensive. The tools were discarded when any one of the defined criteria mentioned in Chapter 6 was reached. The effect of different tool geometry (negative and positive rake angle) and chip breakers were also investigated.

Examination of worn inserts, quick-stop samples, chip produced, forces and surface generated were carried out systematically and scientifically in order to understand the machining process of the MMC.

7.4.1 Machinability Results

The tool lives, the tool failure mode, the surface roughness and volume of material removed when machining aluminium 2618 MMC with K68 inserts in the speed range 15 - 50 m/min are tabulated in Table 7.1 and 7.2 in Appendix 1. Generally, the tool

life decreases as the cutting speed increases. At certain cutting conditions the tool life is unexpectedly high, for instance at cutting speeds of 20 m/min and 30 m/min. All of the cutting tools failed due to flank wear mode. The surface finish recorded shows that the Ra values increase as the feed rates increases. In some instances the reading of the surface finish was non measurable due to the very rough machined surface.

7.4.2 Tool Wear And Tool Life

The hardness of the reinforcement is a major factor in tool wear. In most condition, flank wear is the major life limiting factor when machining MMC with cemented carbide tools.

The development of flank wear against cutting time at various cutting conditions in the speed range 15 to 50 m/min is shown in Figures 7.1 - 7.10. It was observed that the flank wear was rapid at the initial stage of machining. In most cases, the flank wear increase progressively with time. As the cutting speed is increased, the time to reach the defined tool life criteria decreases.

Figures 7.11 to 7.15 show the tool life achieved at various cutting conditions in the speed range of 15 to 50 m/min. The general trend is for the tool life to decrease as the cutting speed increases.

7.4.2.1 Effect of Tool Geometry on Tool Wear

(a) Negative Rake Geometry.

The changes in tool flank wear with cutting speed for K68 with negative rake angled tools for feed rates of 0.2 mm/rev to 0.6 mm/rev with 2 mm and 4 mm depths of cut are shown in Figure 7.1 to 7.4. It can be seen that progressive increase in flank wear rate as the speed is increased. This happened under all cutting conditions. The tool wear was very rapid initially but became more uniform with time.

It can be seen in Figure 7.15 that the rate of wear is quite rapid when machining at a feed of 0.2 mm/rev with negative rake geometry. The flank wear rate increased as the cutting speed increased up to 30 m/min. The wear rate decreased slightly at a cutting speed of 40 m/min. A further increase in speed to 50 m/min resulted in a very rapid increase in the flank wear rate. However, a slower rate of flank wear was observed when machining with negative rake geometry at higher feed rates of 0.4 mm/rev and 0.6 mm/rev., Figures 7.2 and 7.4. Rapid flank wear was experienced when cutting speeds were increased i.e. above 35 m/min, and increasing the depth of cut from 2 mm to 4 mm had some influence on the cutting time at the feed rate 0.4 mm/rev and 0.6 mm/rev. However, there was no significant increase in cutting time as the DOC was increased from 2 mm to 4 mm at a feed rate of 0.2 mm/rev.

(b) Positive Rake Geometry

Figures 7.5 to 7.8 show the average tool wear against cutting time for K68 with a positive rake angle used at different cutting conditions. A positive rake angle has less

influence on the tool life and the wear rate is high. The rate of flank wear was similar at 0.2 mm/rev and 0.4 mm/rev with 2 mm or 4 mm depth of cut. Increases in feed rate had a more significant effect on flank wear rate than increases in the depth of cut.

In the case of negative and positive rake angled K68 inserts, plus negative rake angle K68 with chip breaker, the trend for life was to decrease as cutting speeds was increased. An increase in tool life was observed at certain cutting speeds when the feed rate was increased from 0.2 mm/rev to 0.4 mm/rev., Figures 7.11 to 7.13. For the negative rake angle inserts, Figure 7.11, a feed rate of 0.4 mm/rev gave a better tool life than 0.2 mm/rev feed rate in the range of speeds from 20 m/min to 35 m/min. A tool life of 18.5 minutes was recorded at a speed of 30 m/min and feed rate of 0.4 mm/rev, while a tool life of 3.8 minutes was recorded for the same speed with 0.2 mm/rev for negative rake tools. The tool life has been increased about 5 times when the feed rate is increased from 0.2 to 0.4 mm/rev.

(c) <u>Chip Breaker</u>

Figures 7.9 to 7.10 show the average flank wear against cutting time for K68 negative rake geometry tools (with chip breaker). Generally, the pattern of flank wear for negative rake geometry with chip breaker is similar to that without the chip breaker. The highest flank wear rate recorded is at a speed of 50 m/min and the lowest is at 15 m/min for 0.2 mm/rev feed. At 0.4 mm/rev. the slowest flank wear rate is at a speed of 20 m/min.

7.4.2.2 *Effect of Cutting Conditions On Tool Life*

(a) Effect of Cutting Speed

In general, as the cutting speed is increased from 15 m/min to 50 m/min the tool life recorded decreases for both positive and negative rake geometry inserts. However, for the negative rake geometry the tool life obtained was unexpectedly high in the cutting speed range 25 to 35 m/min, Figure 7.11. At 25 m/min, the recorded tool life is 11.2 min, then it was increased to 18.5 min at cutting speed of 30 m/min. At this particular conditions it was believed that the formation of a stable built-up edge might have protected the cutting tool, thus prolonging the tool life.

(b) Effect of Feed Rate

A significant increase in tool life was observed when the feed rate was increased from 0.2 to 0.4 mm/rev at cutting speeds of 25 to 35 m/min (2 mm depth of cut). Figures 7.11 to 7.13. For the negative rake angle tool, Figure 7.11, a feed rate of 0.4 mm/rev gave a better tool life than 0.2 mm/rev feed rate in the range of speeds from 20 m/min to 35 m/min. This shows that tool life has been increased about 5 times when the feed rate was increased from 0.2 mm/rev to 0.4 mm/rev. There was not much difference in tool life when the feed rate was increased to 0.6 mm/rev. As the speed was further increased the tool life dropped drastically.

(c) Effect of Depth of Cut (DOC)

Machining at DOC of 2 and 4 mm was carried out in the speed range 15 to 50 m/min and 15 to 30 m/min respectively. It was found that increasing the depth of cut from 2

mm to 4 mm at 0.2 mm/rev did not significantly change the life of the tools at any speed, as can be seen in Figures 7.11 and 7.14. However, the tool life recorded at 0.4 mm/rev feed with 4 mm DOC was longer than at 2 mm DOC, as shown in Figures 7.11 and 7.14.

Figure 7.12 shows the tool life achieved when machining with K68 inserts with chip breaker. There is no significant difference in tool life between the tool with and without chip breaker at 0.2 mm/rev feed for the cutting speed range 15 - 50 m/min. The highest tool life recorded for inserts with and without chip breaker is almost the same, 18.8 min and 18.5 min respectively at 0.4 mm/rev feed rate.

7.4.2.3 Taylor Tool Life Curve

A tool life equation is an empirical relationship between the tool life and one or more variables of cutting conditions such as cutting speed, feed rate and depth of cut. One famous tool life equation is due to Taylor. Based on his experimental work, Taylor showed that tool life (T) and cutting speed (V) are related in the following equation: $VT^n = C$ (where V = cutting speed in metres per minute, T is the tool life in minutes, n is the Taylor exponent and C is a constant). Therefore, on a log-log graph, the Taylor's tool life equation will represent a straight line.

Figures 7.6 - 7.8 show the relationship between the tool lives achieved against cutting speed when plotted on a log-log plot, as suggested by Taylor. Best fit straight lines were calculated using standard regression as described in ISO

publication [33], an example of which is given in Appendix 2. The values of n and C for negative geometry insert at 0.2 mm/rev and 0.4 feed rates and 2 mm depth of cut are 1.38 and 272.8, 1.07 and 223.45 respectively. Therefore, Taylor's tool life equation for negative geometry insert can be written as $VT^{1.38} = 272.2$ and $VT^{1.07} = 223.45$. For positive rake geometry the values of n and C at 0.2 mm/rev and 0.4 feed rates are 0.79 and 95.54, 0.75 and 95.49 respectively. As a result, Taylor's tool life equation for positive geometry can now be written as $VT^{0.79} = 95.54$ and $VT^{0.75} = 95.49$. Calculated values for Taylor exponent (n) and constant (C) for K68 inserts at different tool geometries, feed rates and depth of cut are recorded in Table 7.3 (Appendix 1), as are regression coefficients (r).

The regression coefficients (r) for positive rake geometry at 0.2 and 0.4 feeds with 2 mm depth of cut are 0.996 and 0.991. This values are close to unity, indicating that the experimental data plotted is a close approximation to a straight line. Inserts with negative rake geometry have r value of 0.691 and 0.533 which are not close to unity, and tend to show a non-linear Taylor curve. Inserts with chip breakers machining at 0.2 mm/rev feed show a linear Taylor curve, this is not so when machining at 0.4 mm/rev feed.

7.4.3 Volume of Material Removed

Volume of material removed during the life of the tool can be used in assessing tool performance. In order to establish whether a more acceptable tool life and material removal rate could be obtained, the effects of feed rate and depth of cut were

investigated for K68 inserts. Tables 7.1 and 7.2 in Appendix 1 show the appropriate values recorded and represented graphically in Figures 7.19 -7.22. At a feed rate of 0.2 mm/rev, the volume of material removed for negative and positive rake tools is about constant in the speed range tested, but once the feed rate is increased to 0.4 mm/rev., the volume of material removed is almost doubled for the same tool life. This proved so in tests with negative rake geometry K68 inserts at 30 m/min with feed rates of 0.2 mm/rev and 0.4 mm/rev. Increasing the depth of cut from 2 mm to 4 mm did not significantly affect the volume of material removed at any cutting speed (Figures 7.21 and 7.22). This condition can be employed in roughing cuts without experiencing additional wear problems. It has been observed that positive rake geometry K68 inserts are not sensitive to feed/DOC changes in the same way as negative rake geometry ones are with respect to tool life and hence material removal rate.

However, another way of looking at tool life can be represented by plotting flank wear against the distance cut. This method simply ignores the DOC, i.e. it is a function of speed and feed. This is shown in Figures 7.23 and 7.24, the numerical data from which is recorded in Tables 7.4 - 7.6 in Appendix 1. This plot allows for the fact that at higher cutting speeds, the tool cuts more material in the same unit of time than a tool used at slower cutting speeds. Figures 7.23 and 7.24 indicate that at speeds from 25 to 40 m/min there is an increase in the distance which could be cut before generating 0.4 mm flank wear, i.e. tool life increases, with a marked increase taking place between 35 and 40 m/min. Increasing the cutting speed beyond 40

m/min was then found to reduce the cut distance, with the maximum speed tested (50 m/min) producing the shortest distance.

7.4.4 Tool Failure Modes And Wear Appearance

A study of the failure modes of a cutting tool enables an understanding of the mechanisms of tool wear to be gained. The failure mode is generally controlled by the nature and composition of the work material, the tool material and the cutting conditions. When machining with K68 inserts, the tool life was limited by wear on the flank face of the insert. Slight rake face wear, chipping and notching were observed under certain cutting conditions but they were never the tool life limiting factor.

The general tool wear appearance for a negative and positive K68 inserts when machining aluminium 2618 MMC are shown in Figures 7.25(a) and 7.25 (b) respectively. Detailed results on the analysis of tool wear modes and wear mechanisms using SEM techniques and optical microscope are presented in the following section.

7.4.4.1 Flank Wear

At all cutting conditions, flank wear was responsible for limiting the tool life of K68 tools. The worn area of K68 tools was examined under the SEM once the tools reached one of the tool life limiting criterion. Typical flank wear generated during

the machining with uncoated K68 grade cemented carbide with positive and negative rake geometry insert is shown in Figure 7.26.

The unused flank face of a K68 insert which has not undergone the wear process is shown in Figure 7.27. When the worn flank faces were examined under the SEM, the surface was found to be covered wholly or partly by a thin smeared layer of the work material . With the help of a backscattered image it was possible to obtain sub-surface information. However, the layer of built up material on the inserts can be removed by treating the insert in 10% hydrochloric acid (HCl). There appears to be no attack by the acid on the carbide phases. This enables the finest details of the worn surfaces to be studied with SEM and much information about the insert can be gained in this way. Further examination of the wear surfaces on the flank face at different cutting speeds revealed a smoothly polished wear but with very fine scratches and sharp grooves, in which almost all the individual carbide grains are worn, this can be compared to the untouched flank face as seen in Figure 7.28(a), (b) and (c).

It can be seen clearly that grooves on the flank face are present parallel to the cutting direction, and scratches on the rake face of K68 inserts at various cutting speeds, Figures 7.29(a), (b) and (c). On the rake face, the wear has a similar appearance but was somewhat less severe. It is believed that the scratches and grooves were formed by the abrasion between the SiC particles in the workpiece and the tool.

To further investigate this, a number of worn inserts containing built-up material on the rake face were metallurgically sectioned, ground and polished for further examination. Figures 7.30 (a) and (b) show the cross-section of K68 tools with adhering MMC. The particle seen on the rake face is identified as SiC particle by using energy dispersive X-ray analysis. The X-ray analysis graph showing the composition of silicon (Si), aluminium (Al) and gold (Au) (from gold coating) is shown in Figure 7.31. These particles are believed to be responsible for producing scratches and grooves on the rake face as shown in Figures 7.29(a), (b) and (c). A similar wear process is believed to be responsible for the sharp grooves found on the worn flank face.

Close examination of the worn area on the flank face shows some of WC particles being pulled out, Figure 7.32(a). Further examination on the cross-section of the flank face of K68 insert shows that there was no sign of severe damage, Figure 7.32(b).

7.4.4.2 Rake Face Wear

Slight rake face wear was observed on the rake face of the K68 tools as shown in Figure 7.33 . As mentioned, light scratches were found on the rake face as shown in Figure 7.29(a), (b) and (c). Close examination of the worn tool shows a chipped off portion on the rake face, directly adjacent to the cutting edge, as seen in Figure 7.34.

7.4.4.3 Notching

Slight notching also appeared at the major and minor cutting flanks as shown in Figures 7.35, this was noticed only at slower cutting speeds with positive rake geometry inserts. Rounding of the tool at the tool nose was observed (Figure 7.36). Micro-chipping of the cutting edge was also observed for negative and positive geometry at certain cutting conditions (Figure 7.37(a) and (b)).

7.4.5 Cutting Forces

Both cutting and feed forces were recorded over the speed range 15 - 50 m/min when machining with K68 cemented carbide tools. As expected, the cutting force (F_c) was greater than the feed force (F_f) for K68 insert. The cutting forces and feed forces generated during machining at 0.2 and 0.4 mm/rev feed rates over the speed range 15 - 50 m/min are tabulated in Tables 7.7 - 7.8 (Appendix 1) and graphically presented in Figures 7.38 - 7.40. Negative rake geometry inserts produced higher forces than positive rake geometry inserts at all cutting conditions. At 0.2 mm/rev feed, both inserts, positive and negative rake geometry, experienced a steady increase in cutting force as the speed was raised from 15 to 30 m/min. Further increase in the cutting speed resulted in a gradual decrease in the cutting force. However, the opposite situation happened when the feed rate was increased to 0.4 mm/rev. Initially the cutting force was high, but as the speed was increased to 35 m/min, the cutting force dropped. When the cutting speed was increased above 35 m/min, the cutting force increased rapidly. As expected, the cutting force was more than doubled when the depth of cut was doubled (Table 7.15 in Appendix 1). These

effects may be explained by the fact that the tool/workpiece interface conditions altered, and hence the effective geometry of the cutting tool changes, leading to a rise in the cutting forces.

The positive and negative rake inserts behaved almost in the same manner at lower feed rate where forces are almost constant through the speed range tested. As the feed was increased, negative rake geometry tools generated a higher cutting force than positive rake geometry tools. The presence of a chip breaker has little effect in reducing the cutting force when machining with K68 cemented carbide inserts.

Figure 7.1 Average Flank Wear Against Cutting Time For K68 Inserts (Negative Geometry, Feed = 0.2 mm/rev, DOC = 2 mm)

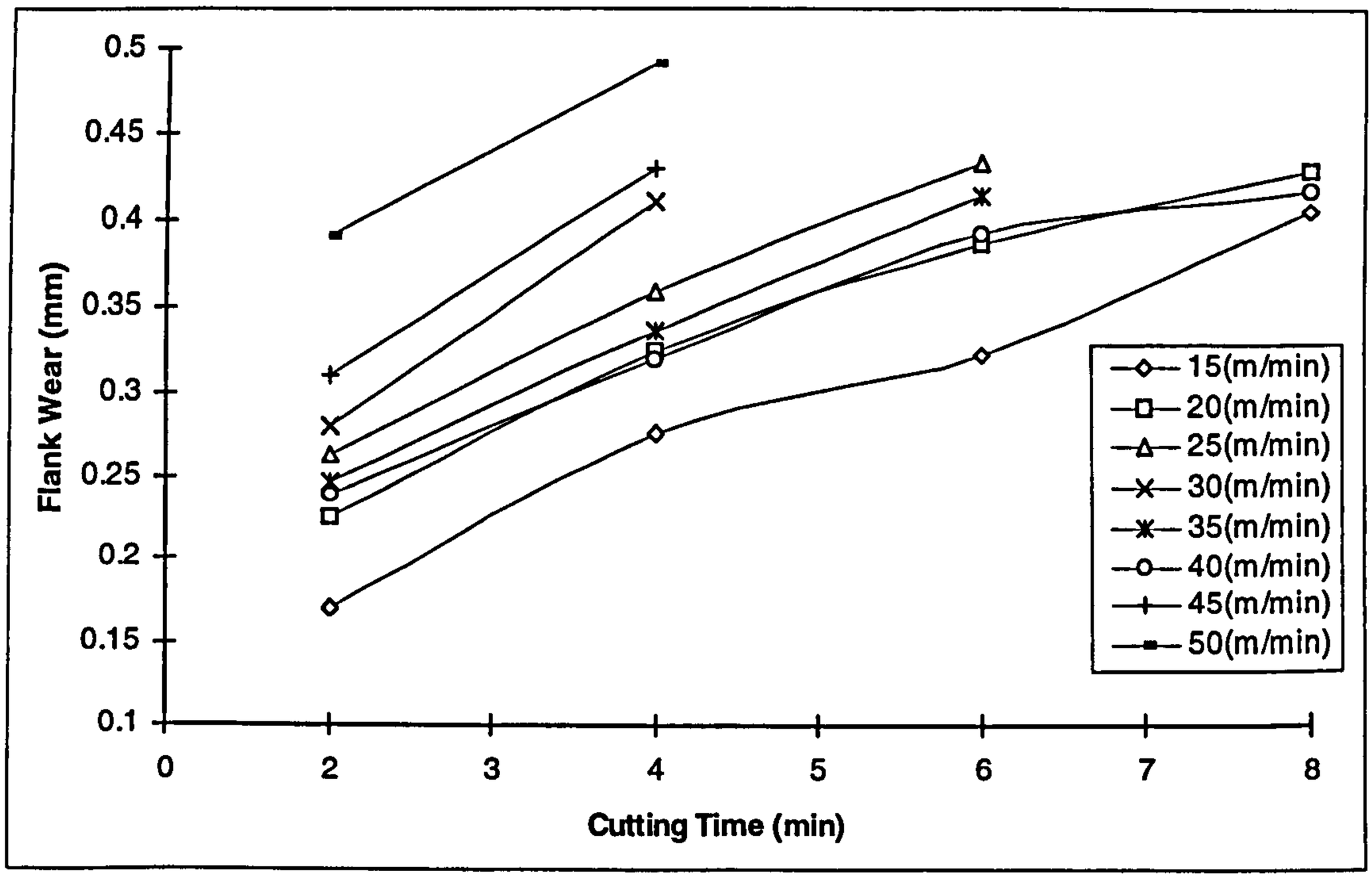

Figure 7.2 Average Flank Wear Against Cutting Time For K68 Inserts (Negative Geometry, Feed = 0.4 mm/rev, DOC = 2 mm)

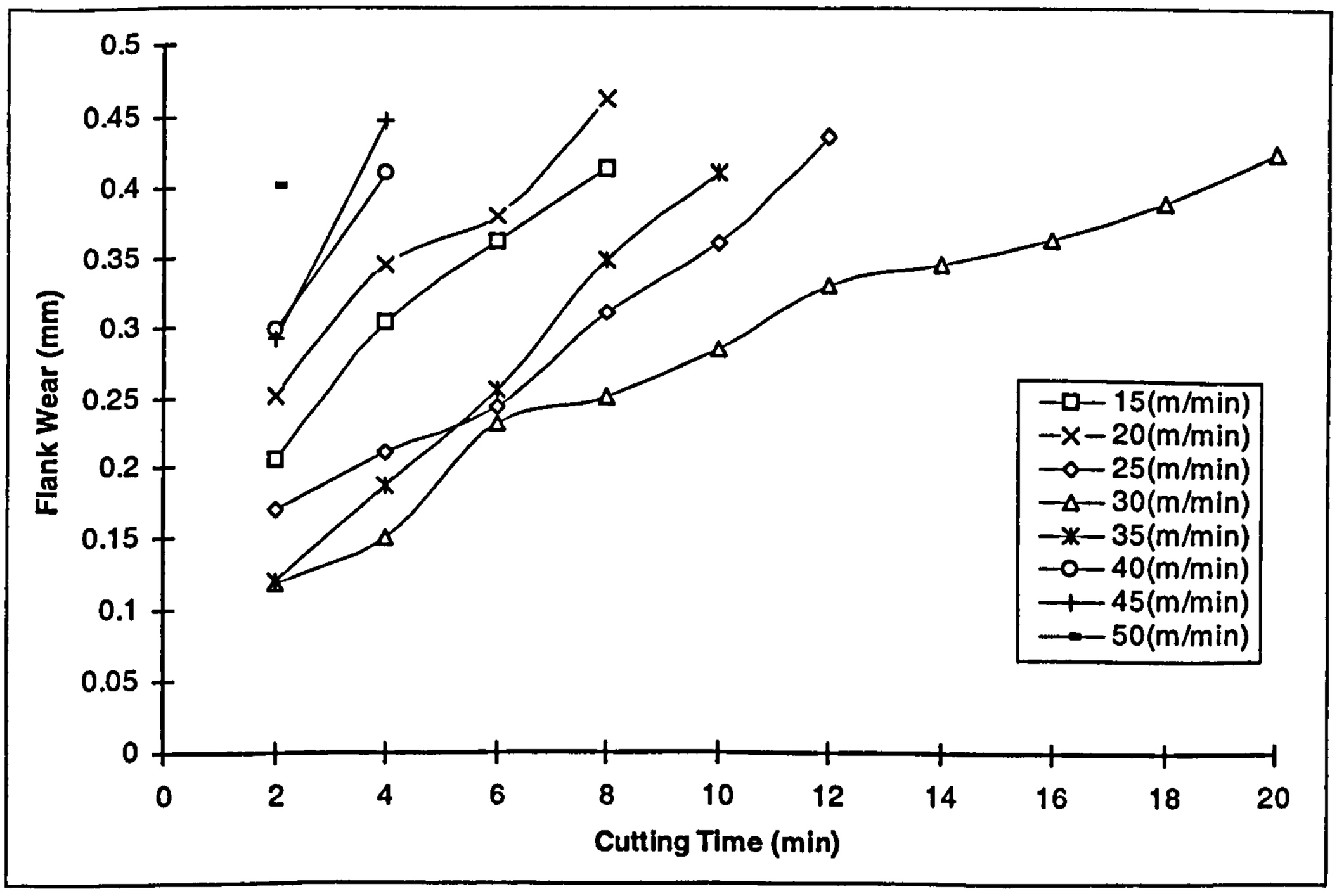

Figure 7.3 Average Flank Wear Against Cutting Time For K68 Inserts (Negative Geometry, Feed = 0.2 mm/rev, DOC = 4 mm)

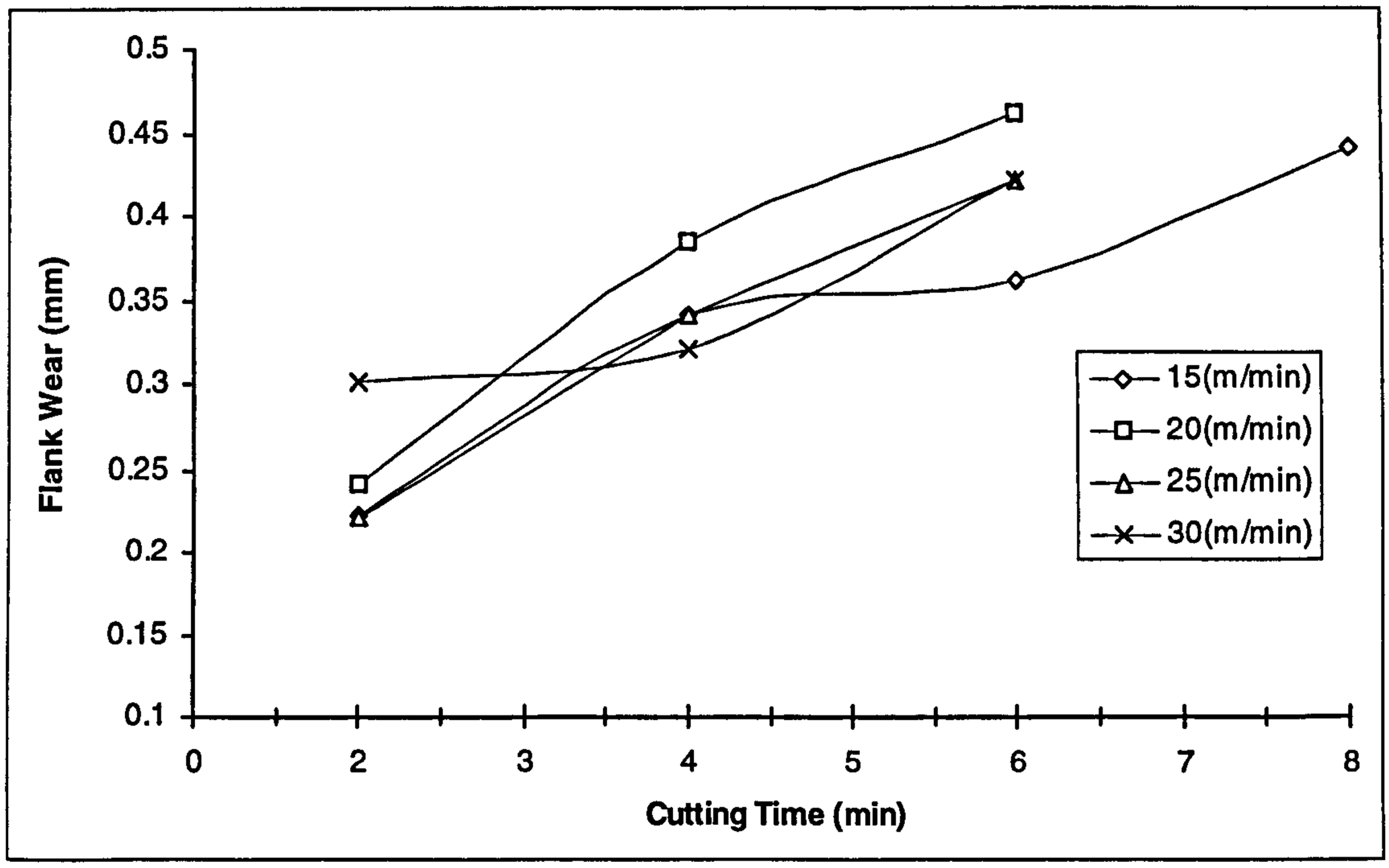

Figure 7.4 Average Flank Wear Against Cutting Time For K68 Inserts (Negative Geometry, Feed = 0.4 mm/rev, DOC = 4 mm)

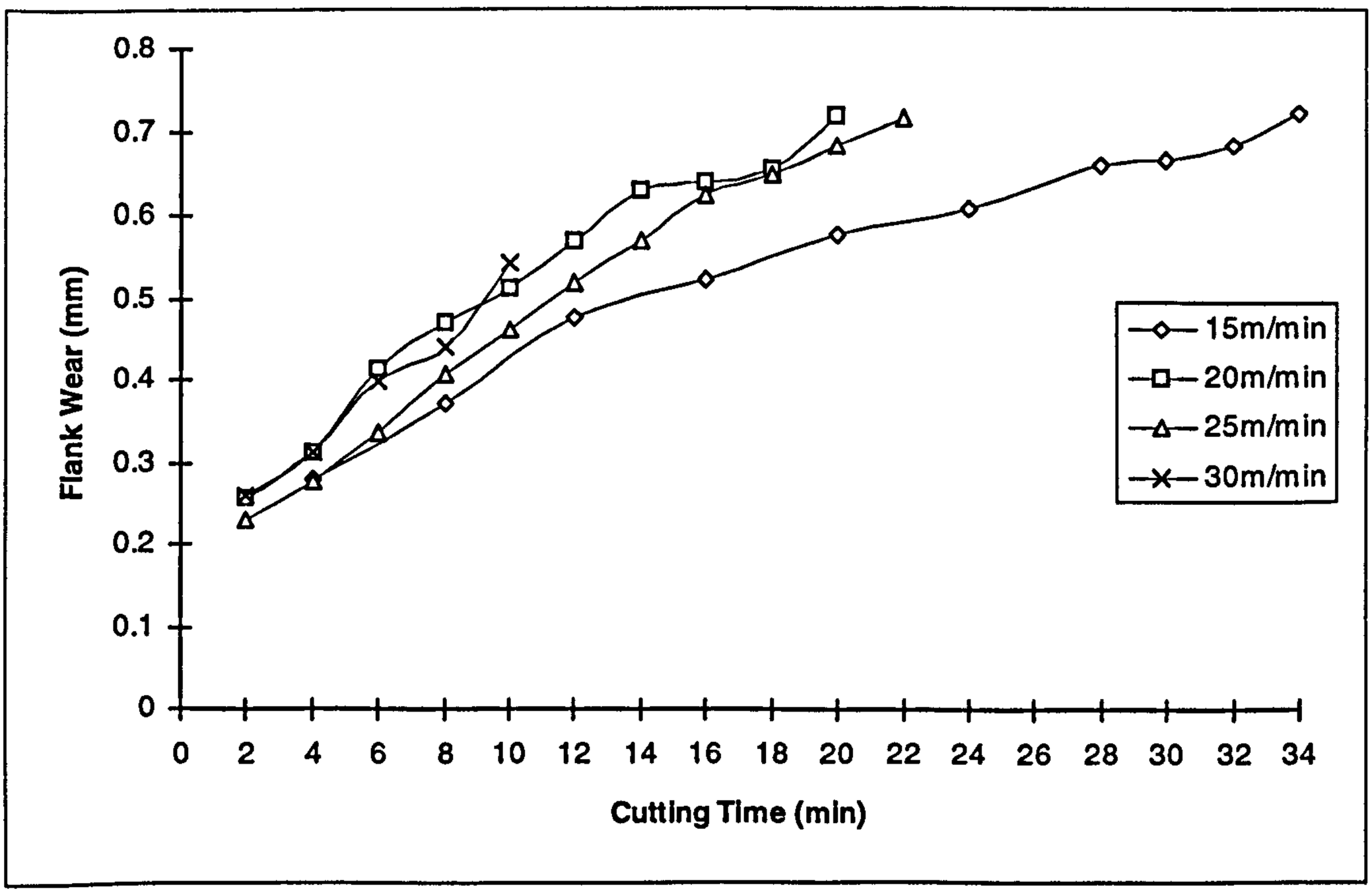

Figure 7.5 Average Flank Wear Against Cutting Time For K68 Inserts (Positive Geometry, Feed = 0.2 mm/rev, DOC = 2 mm)

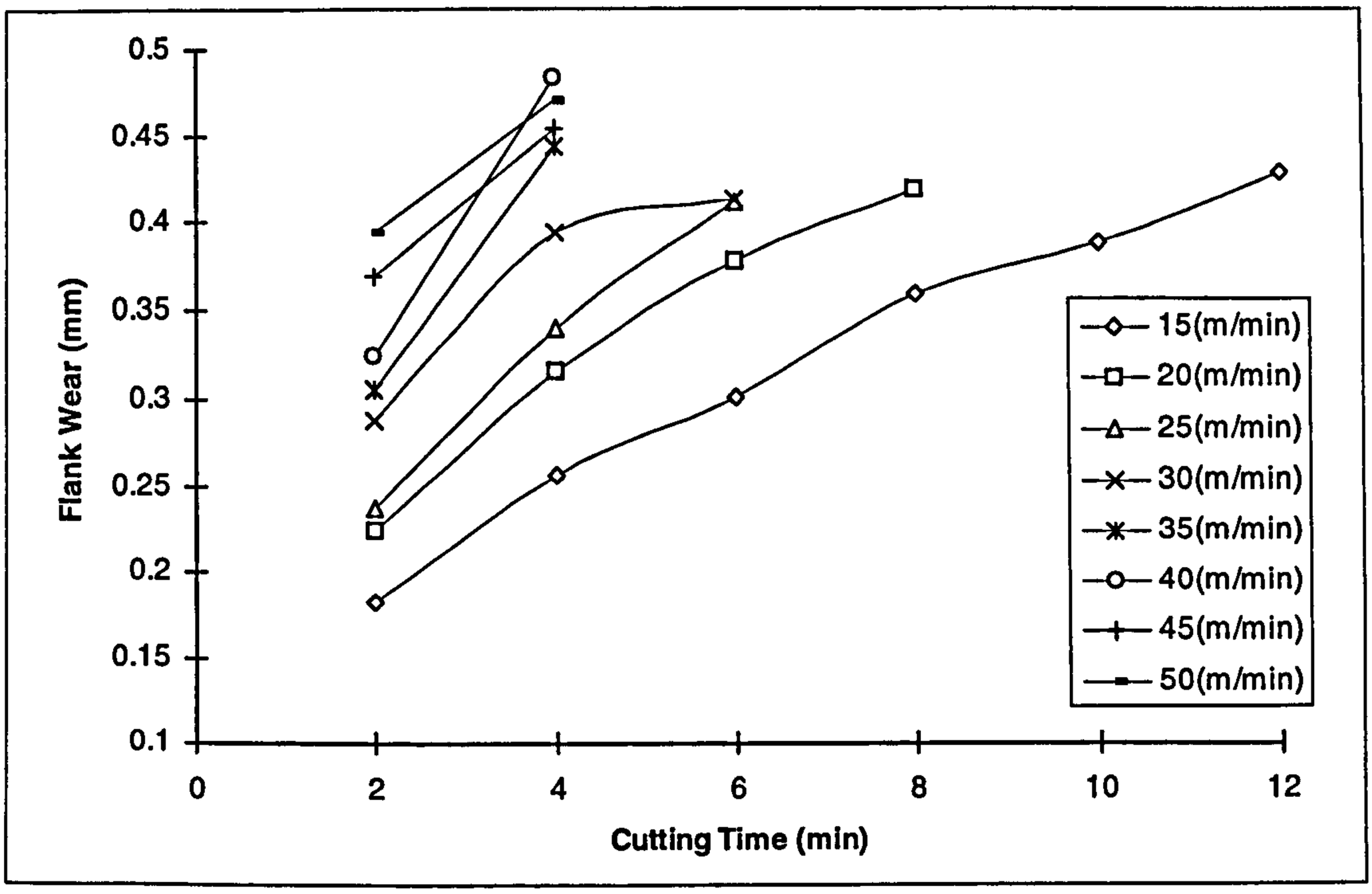

Figure 7.6 Average Flank Wear Against Cutting Time For K68 Inserts (Positive Geometry, Feed = 0.4 mm/rev, DOC = 2 mm)

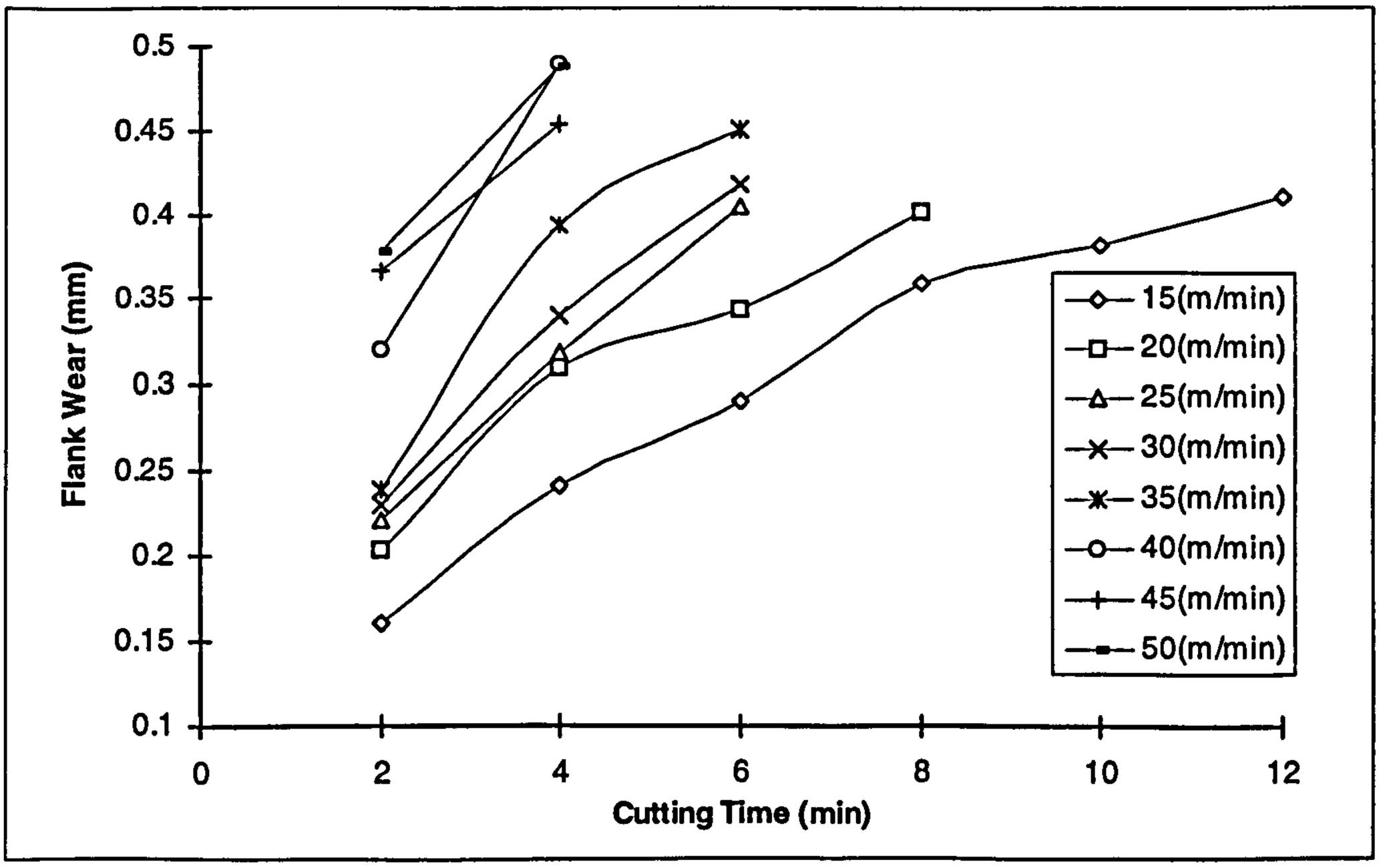

Figure 7.7 Average Flank Wear Against Cutting Time For K68 Inserts (Positive Geometry, Feed = 0.2 mm/rev, DOC = 4 mm)

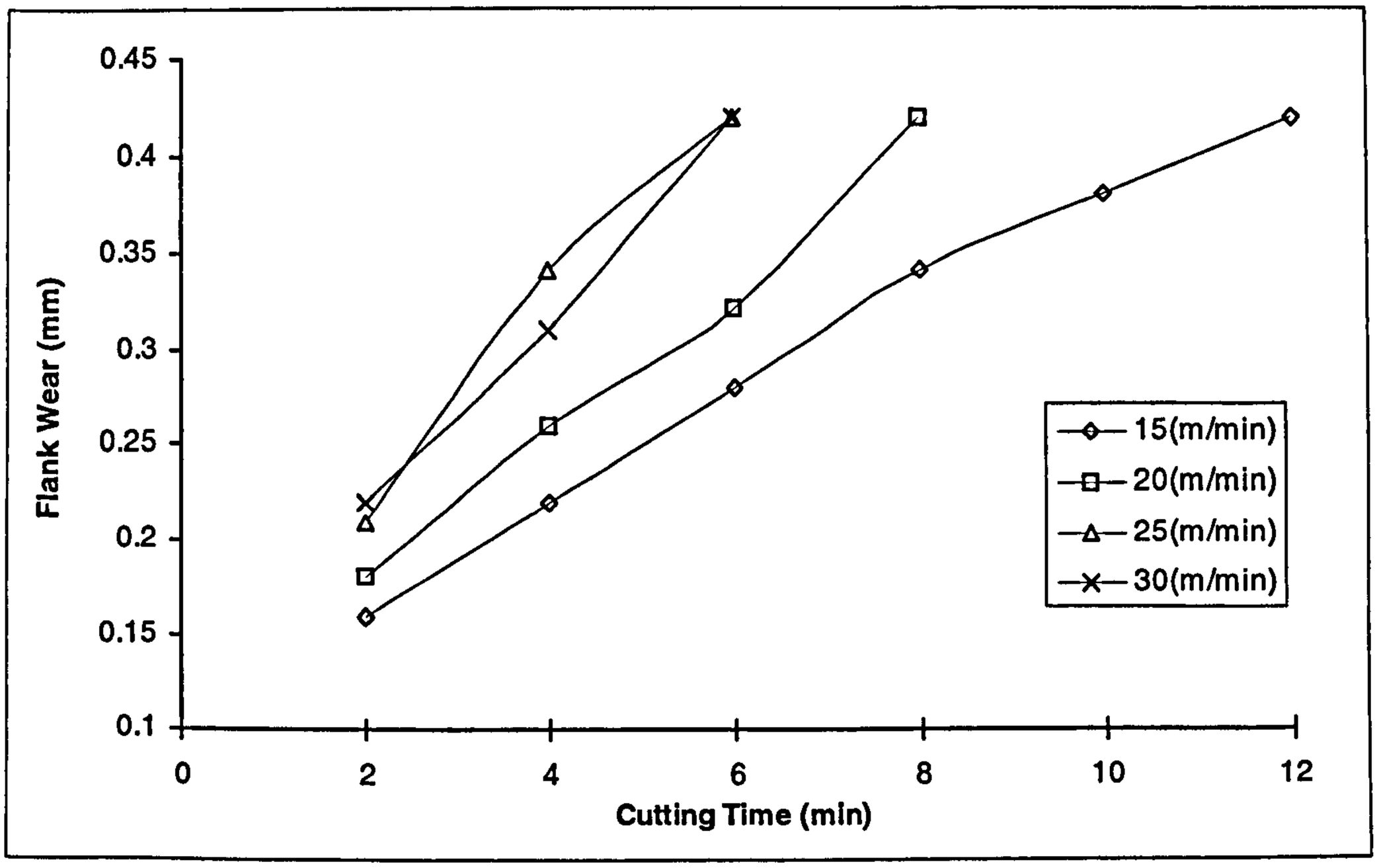

Figure 7.8 Average Flank Wear Against Cutting Time For K68 Inserts (Positive Geometry, Feed = 0.4 mm/rev, DOC = 4 mm)

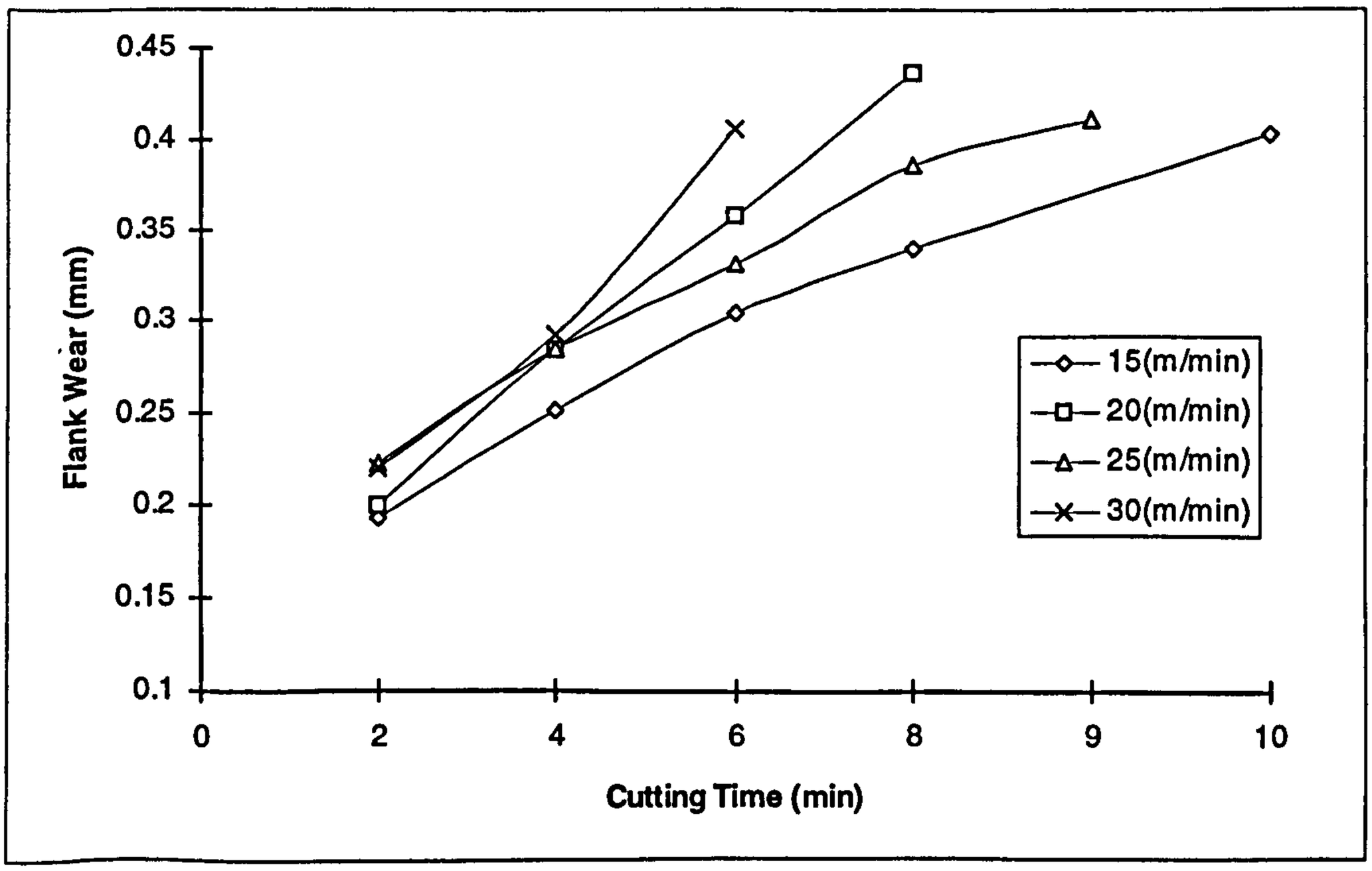

Figure 7.9 Average Flank Wear Against Cutting Time For K68 Inserts (Negative Geometry, WITH CHIP BREAKER, Feed = 0.2 mm/rev, DOC = 2 mm)

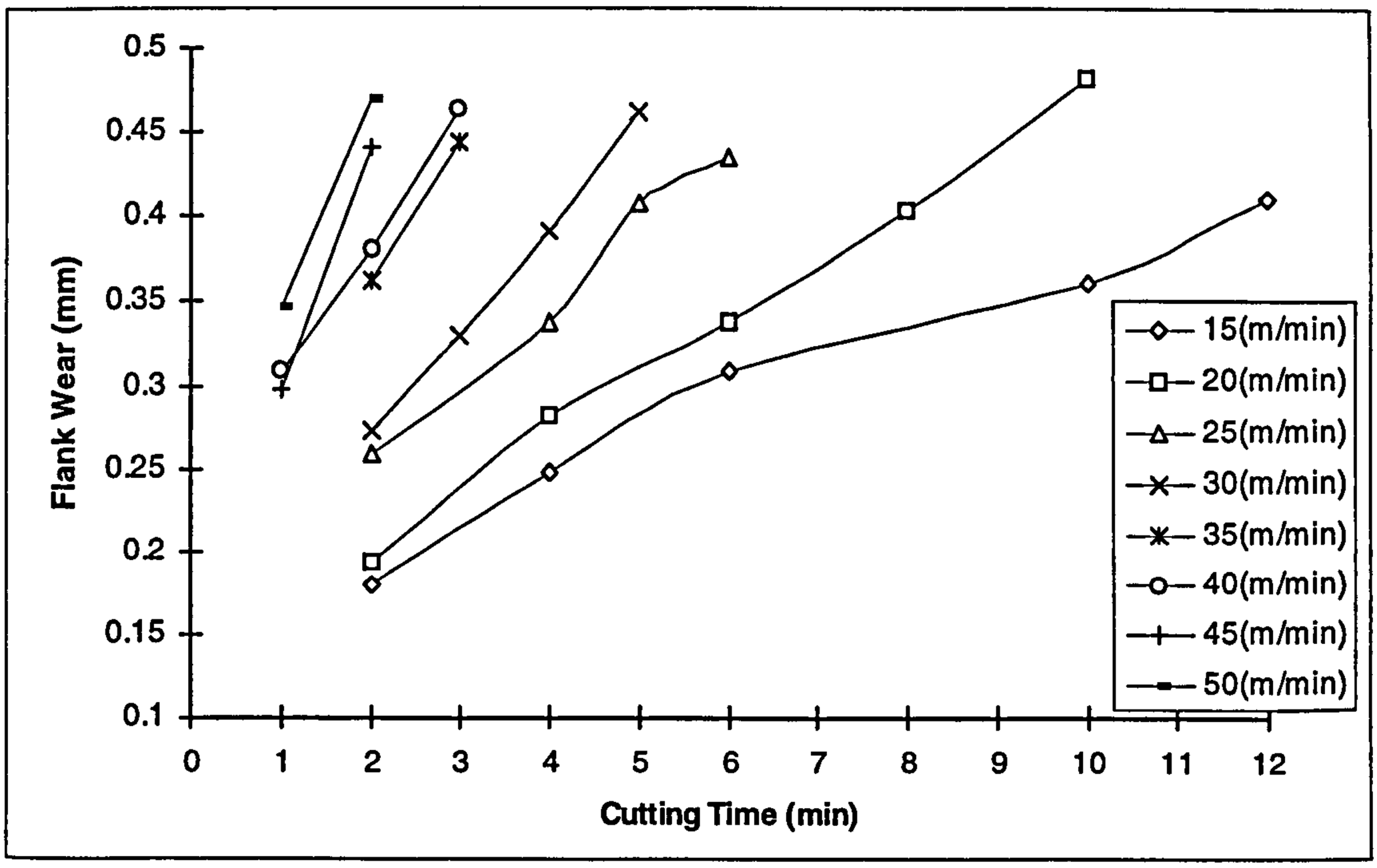

Figure 7.10 Average Flank Wear Against Cutting Time For K68 Inserts (Negative Geometry, WITH CHIP BREAKER, Feed = 0.4 mm/rev, DOC = 2 mm)

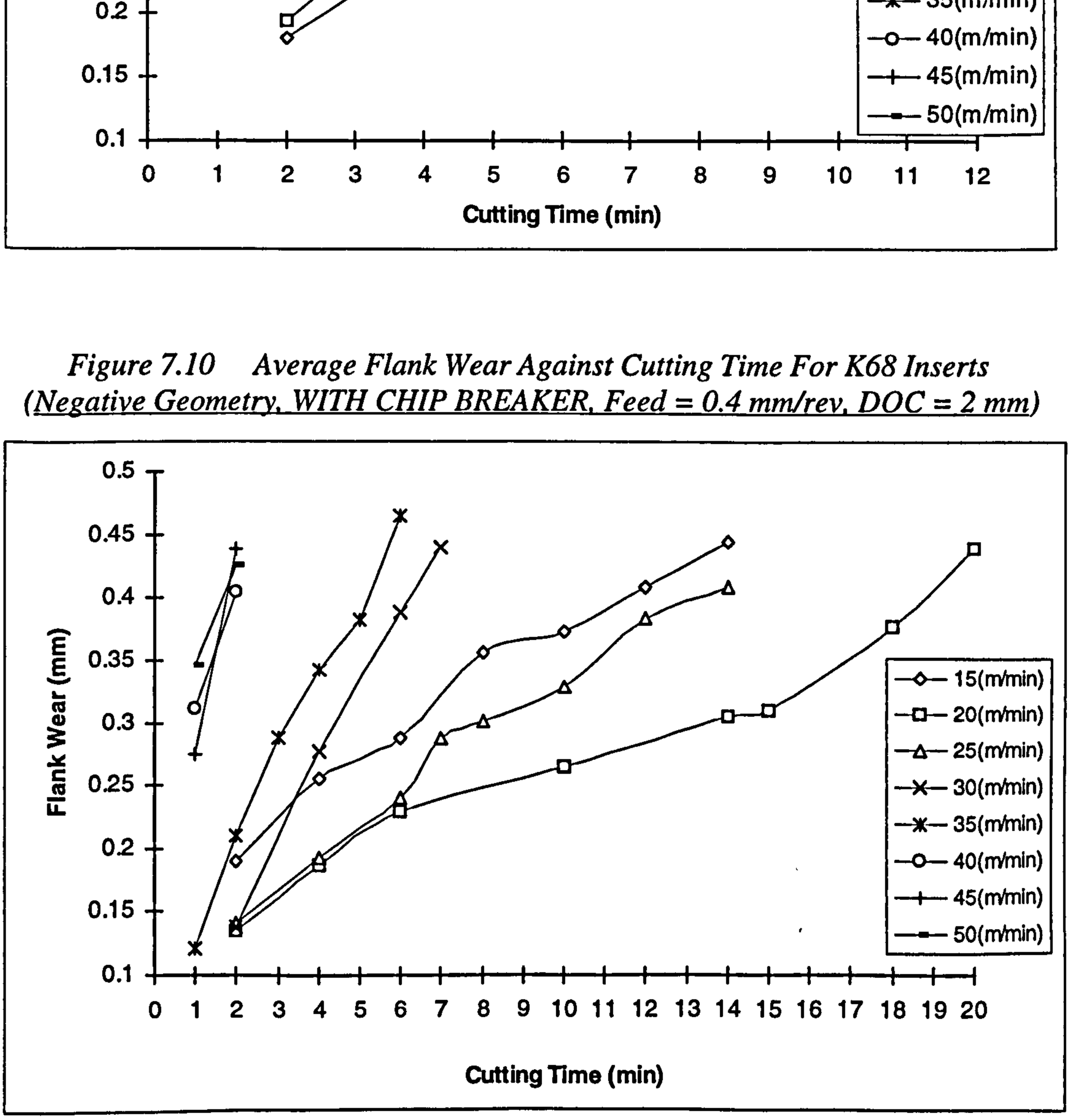

Figure 7.11 Tool Life Versus Cutting Speed For K68 Inserts At Different Feed Rates (Negative Geometry, DOC = 2 mm)

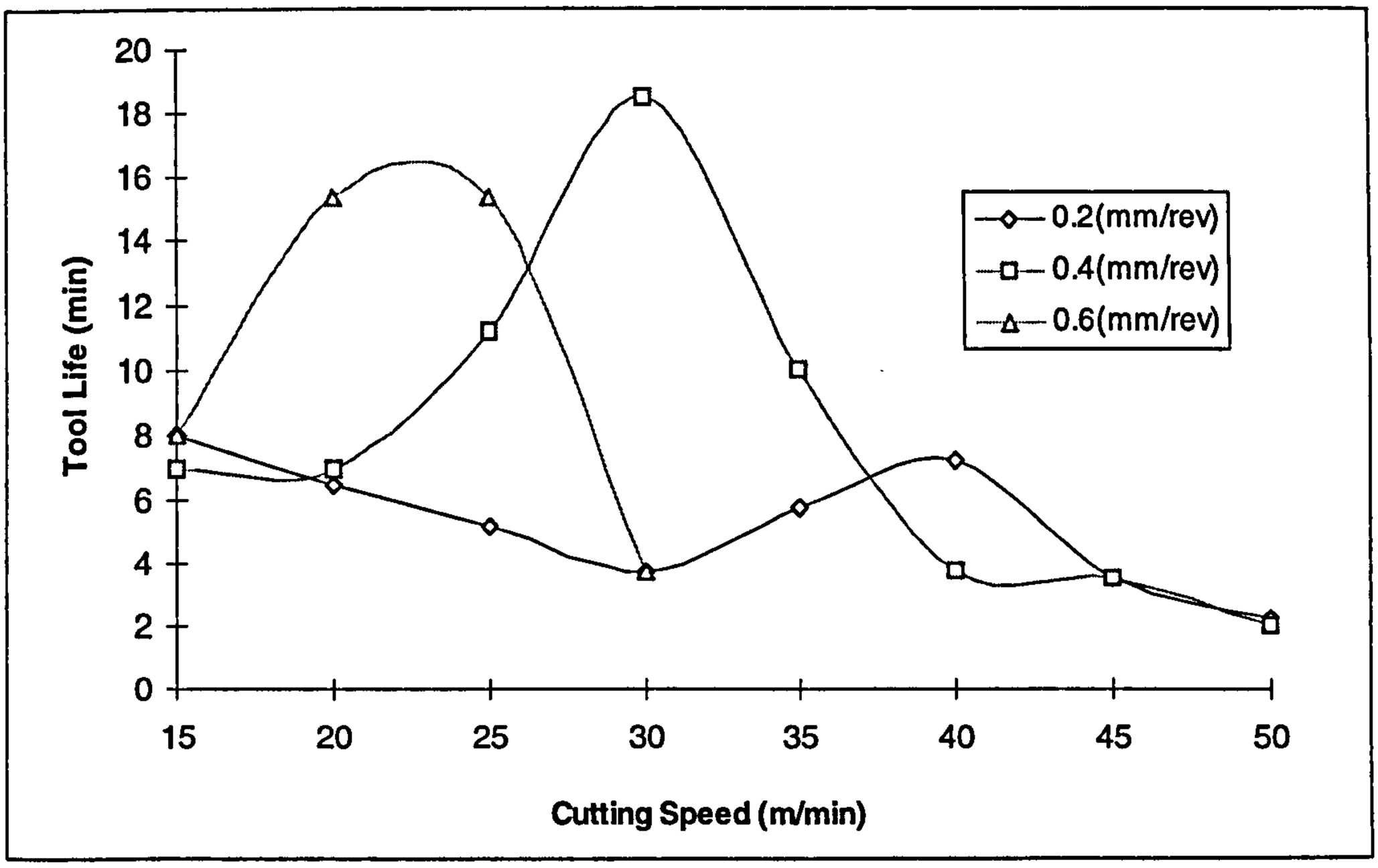

Figure 7.12 Tool Life Versus Cutting Speed For K68 Inserts At Different Feed Rates (Negative Geometry, WITH Chip Breaker, DOC = 2 mm)

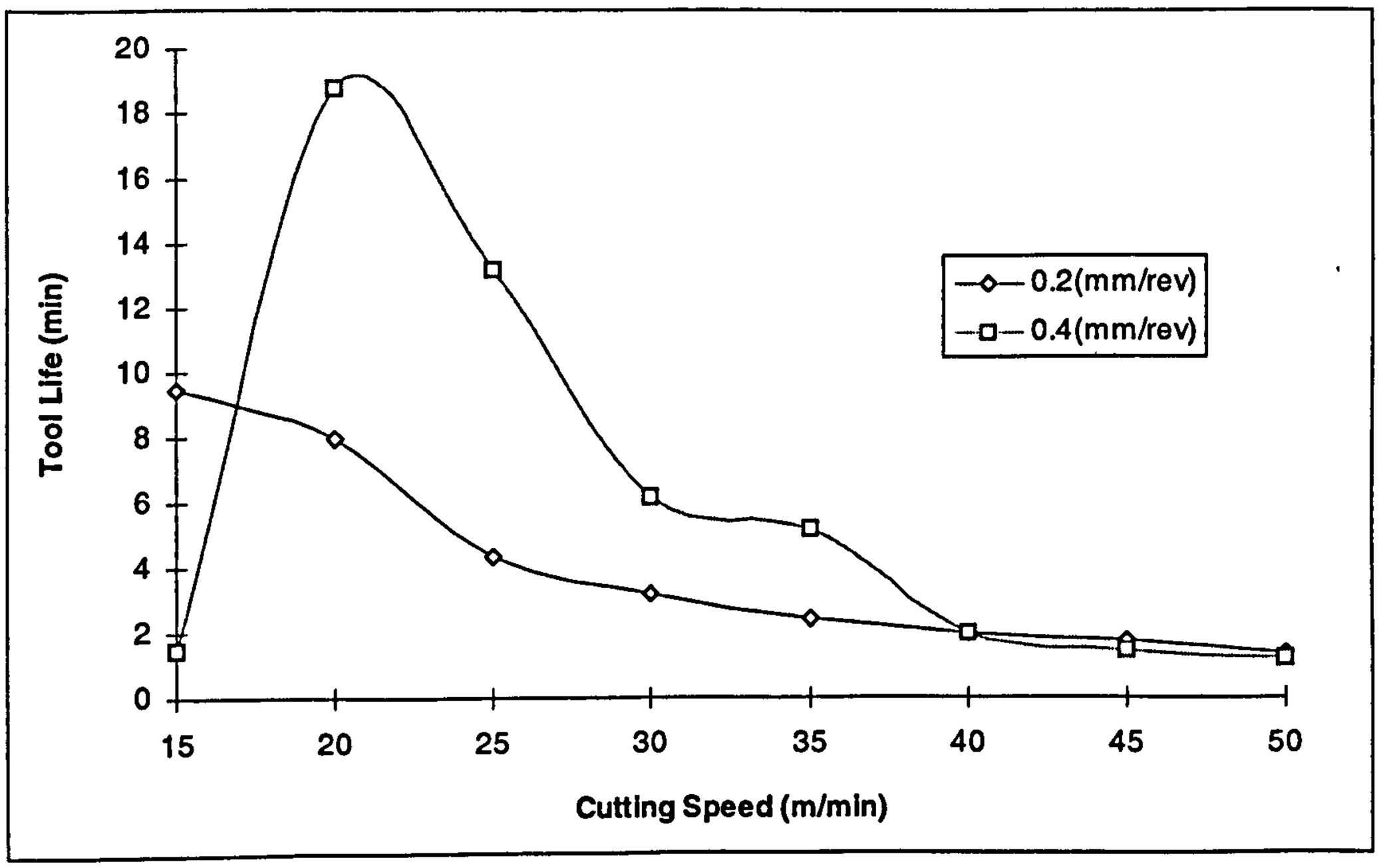

Figure 7.13 Tool Life Versus Cutting Speed For K68 Inserts At Different Feed Rates (Positive Geometry, DOC = 2 mm)

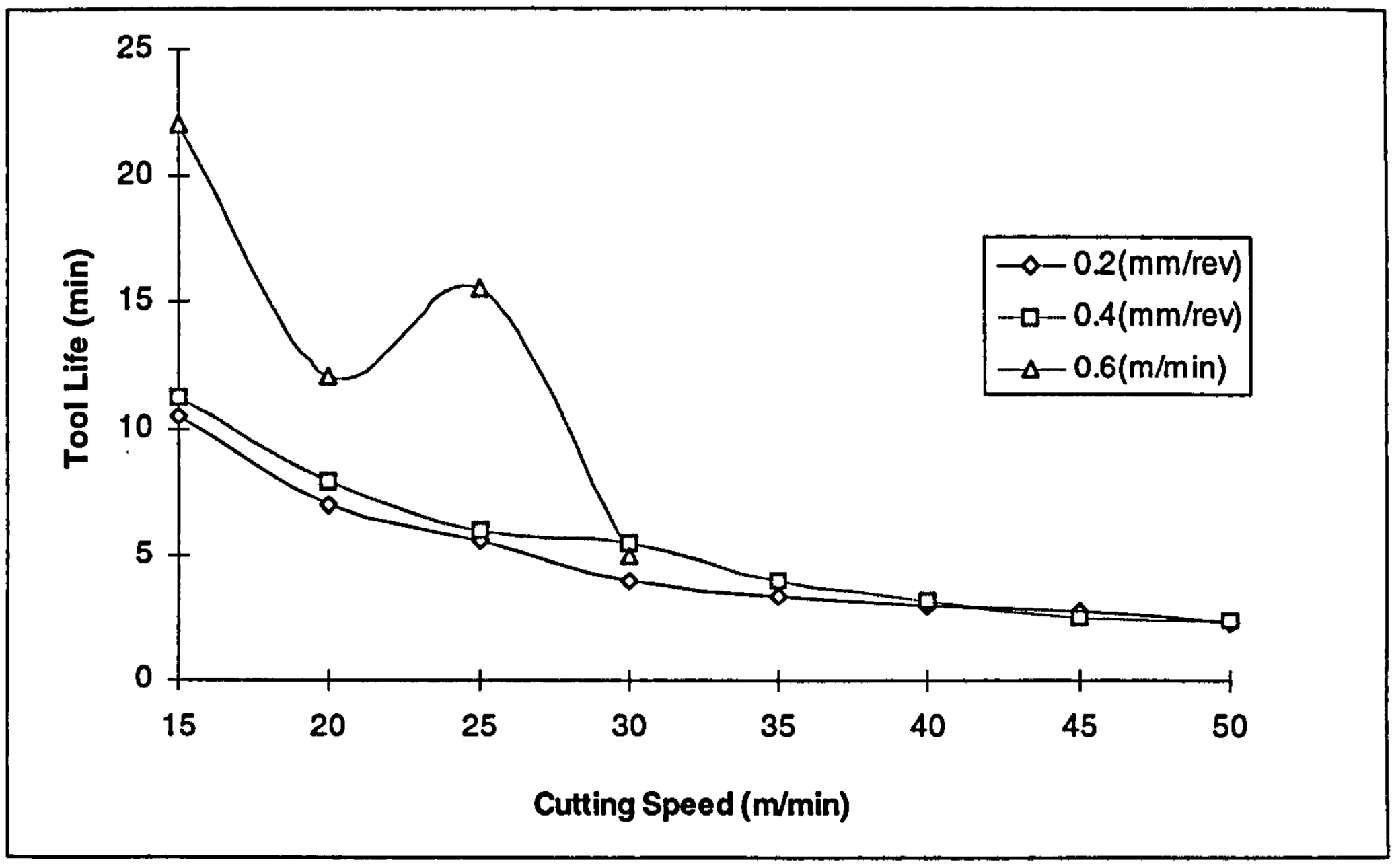

Figure 7.14 Tool Life Versus Cutting Speed For K68 Insers At Different Feed Rates (Negative Geometry, DOC = 4 mm)

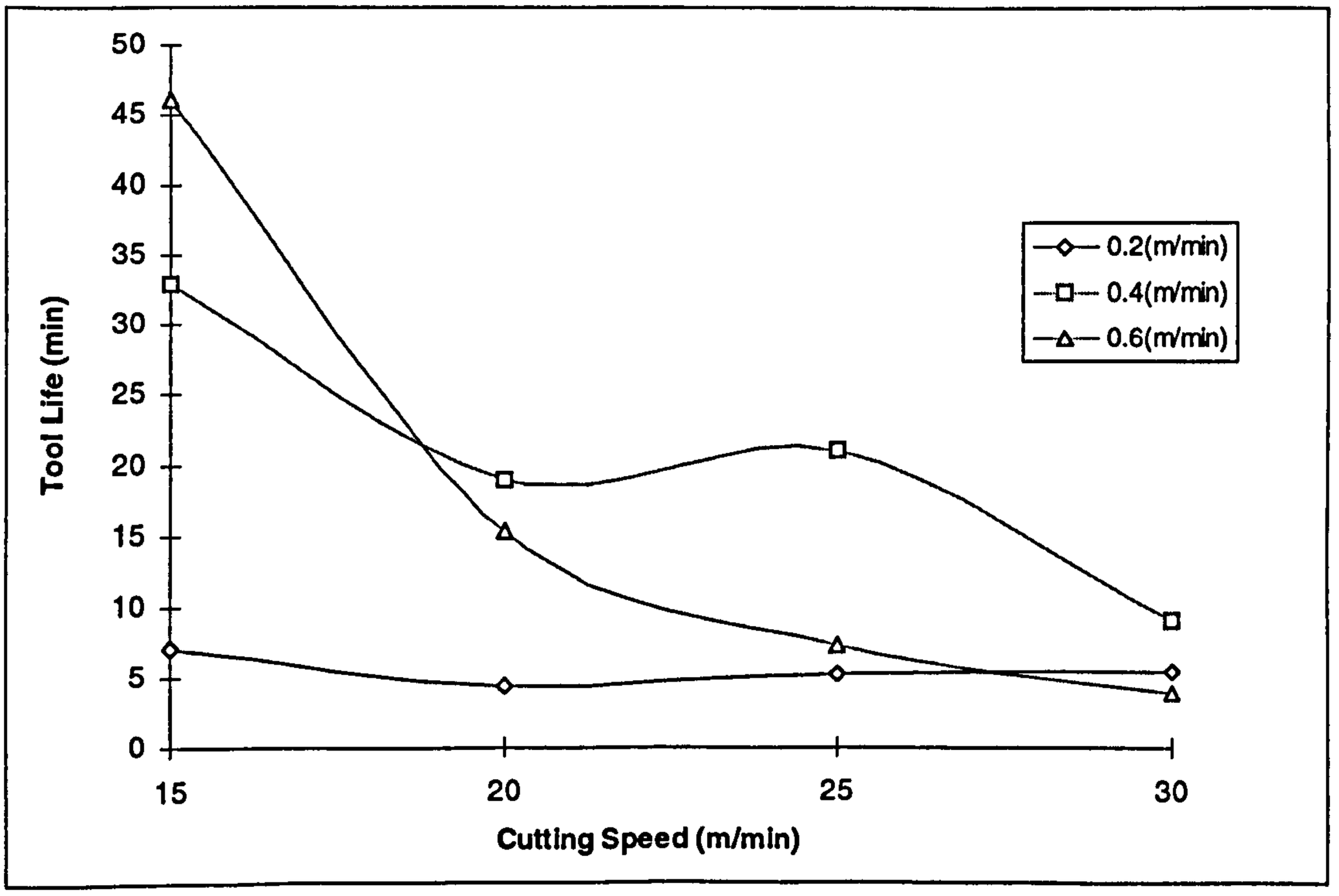

Figure 7.15 Tool Life Versus Cutting Speed For K68 Inserts At Different Feed Rates (Positive Geometry, DOC = 4 mm)

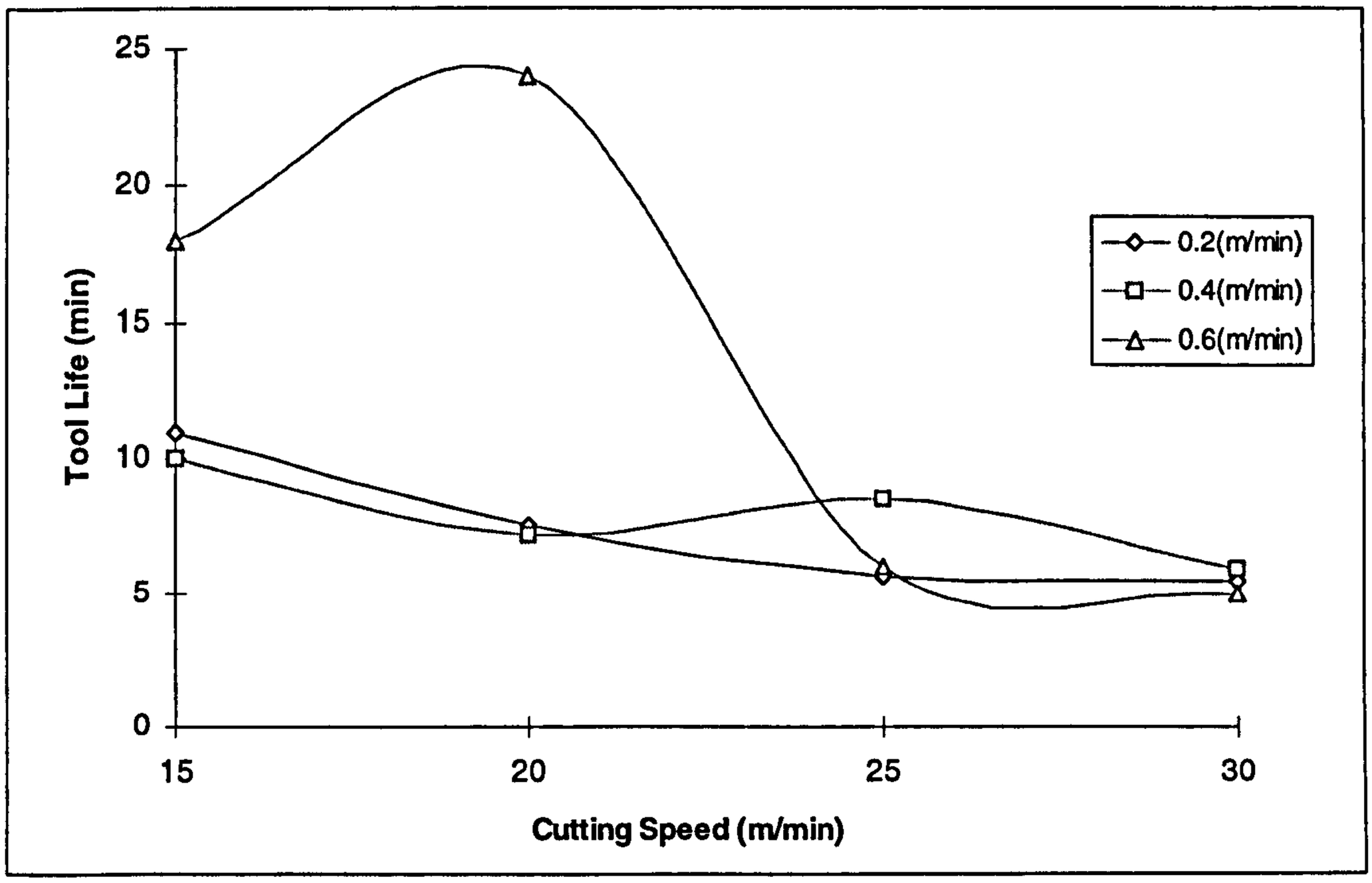

Figure 7.16 Taylor Tool Life Curve For K68 Inserts (Feed = 0.2 mm/rev, DOC = 2 mm)

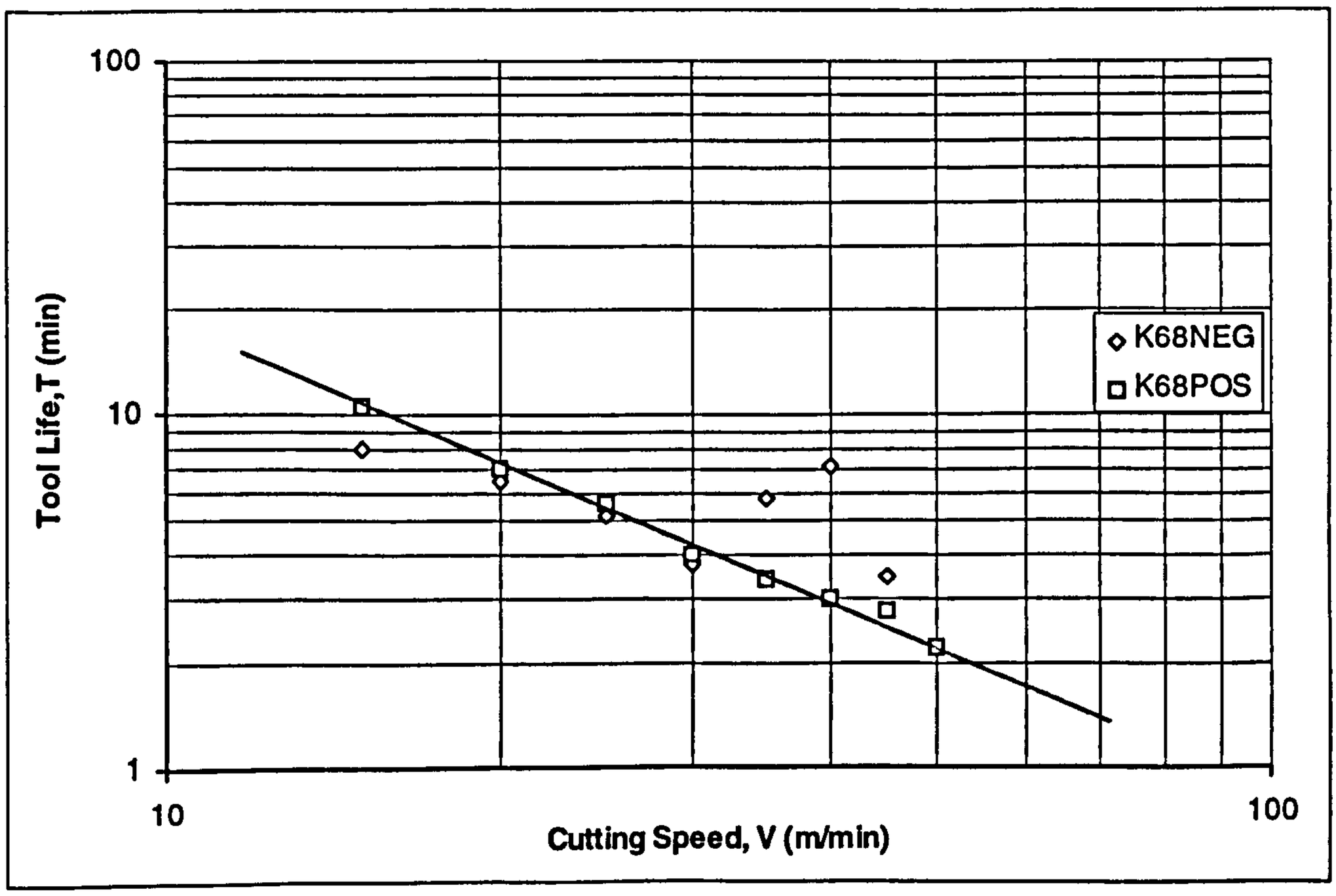

Figure 7.17 Taylor Tool Life Curve For K68 Inserts (Feed = 0.4 mm/rev , DOC = 2 mm)

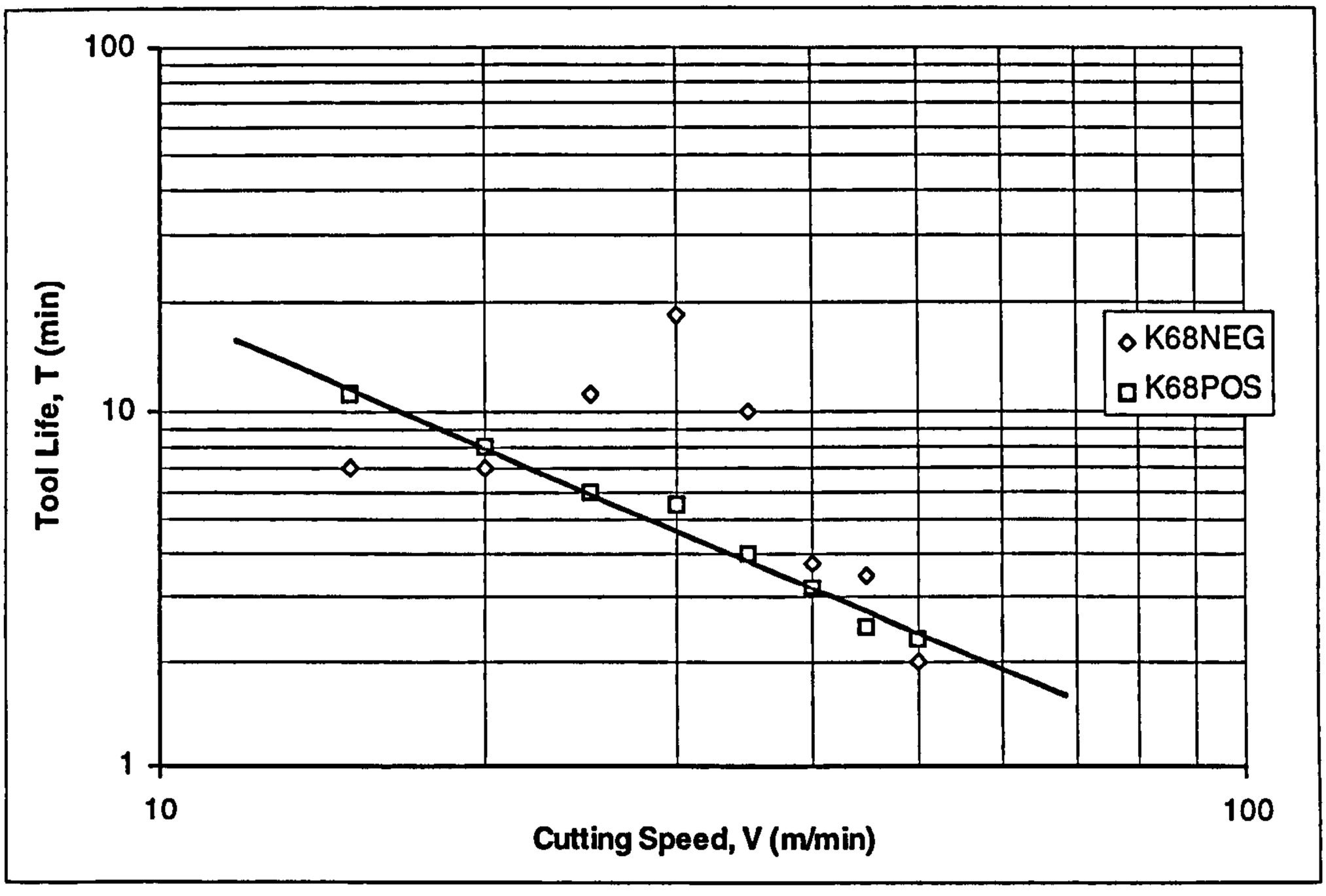

Figure 7.18 Taylor Tool Life Curve For K68 Inserts With 0.2 (mm/rev) And 0.4 (mm/rev) Feed (WITH Chip Breaker, DOC = 2 mm)

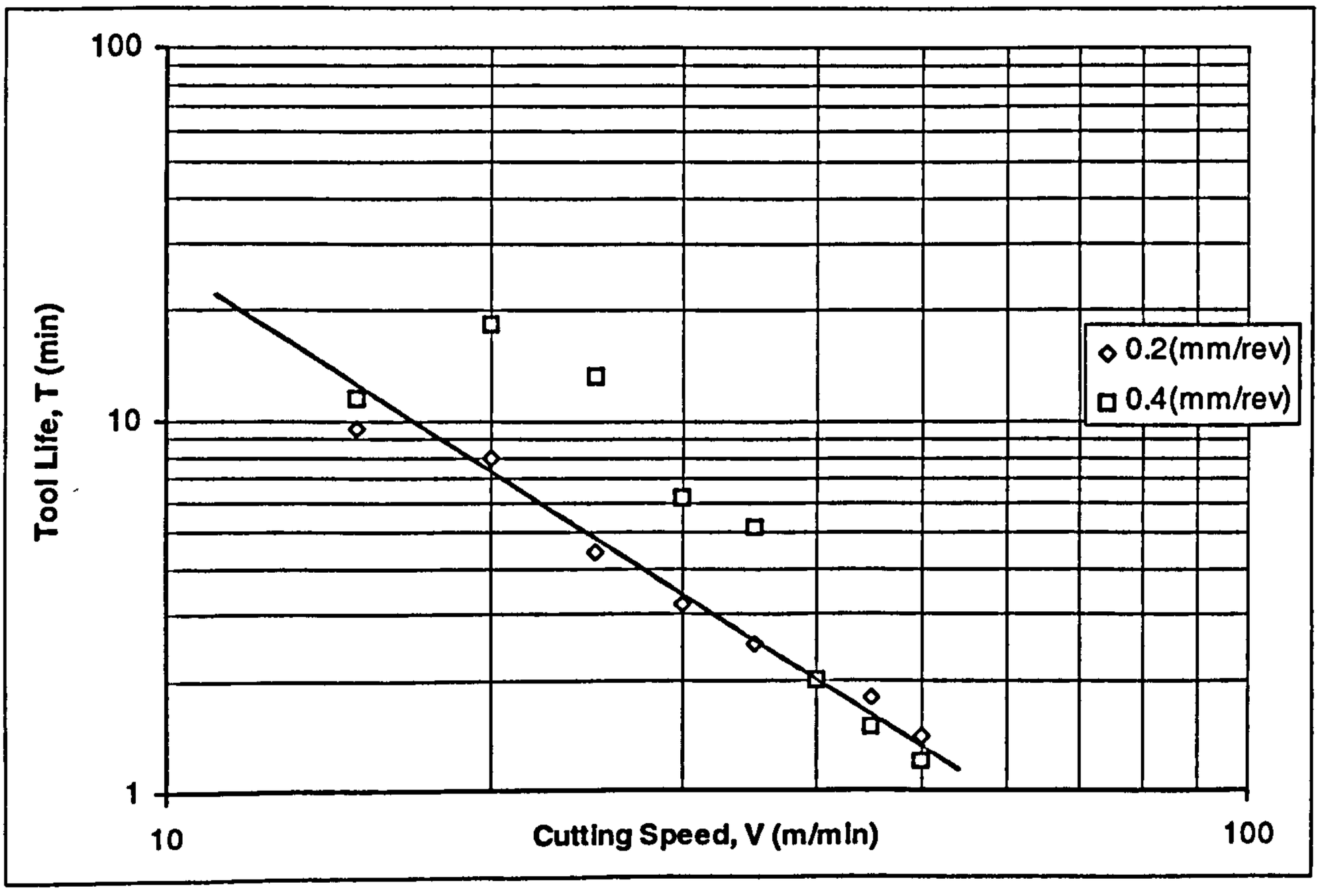

Figure 7.19 Volume Of Material Removed When Machining With K68 Inserts (Negative Geometry, DOC = 2 mm)

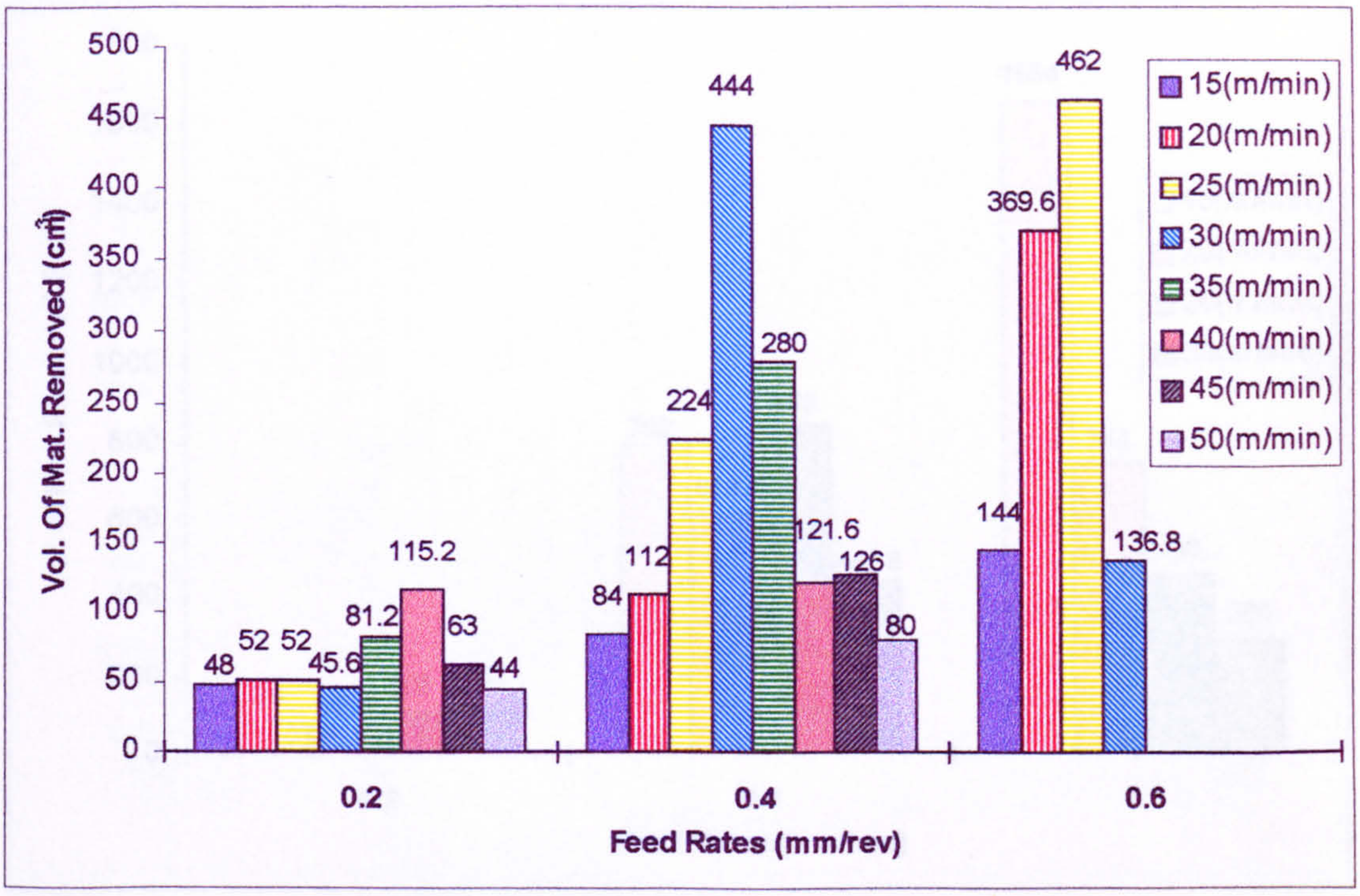

Figure 7.20 Volume Of Material Removed When Machining With K68 Inserts (Positive Geometry, DOC = 2 mm)

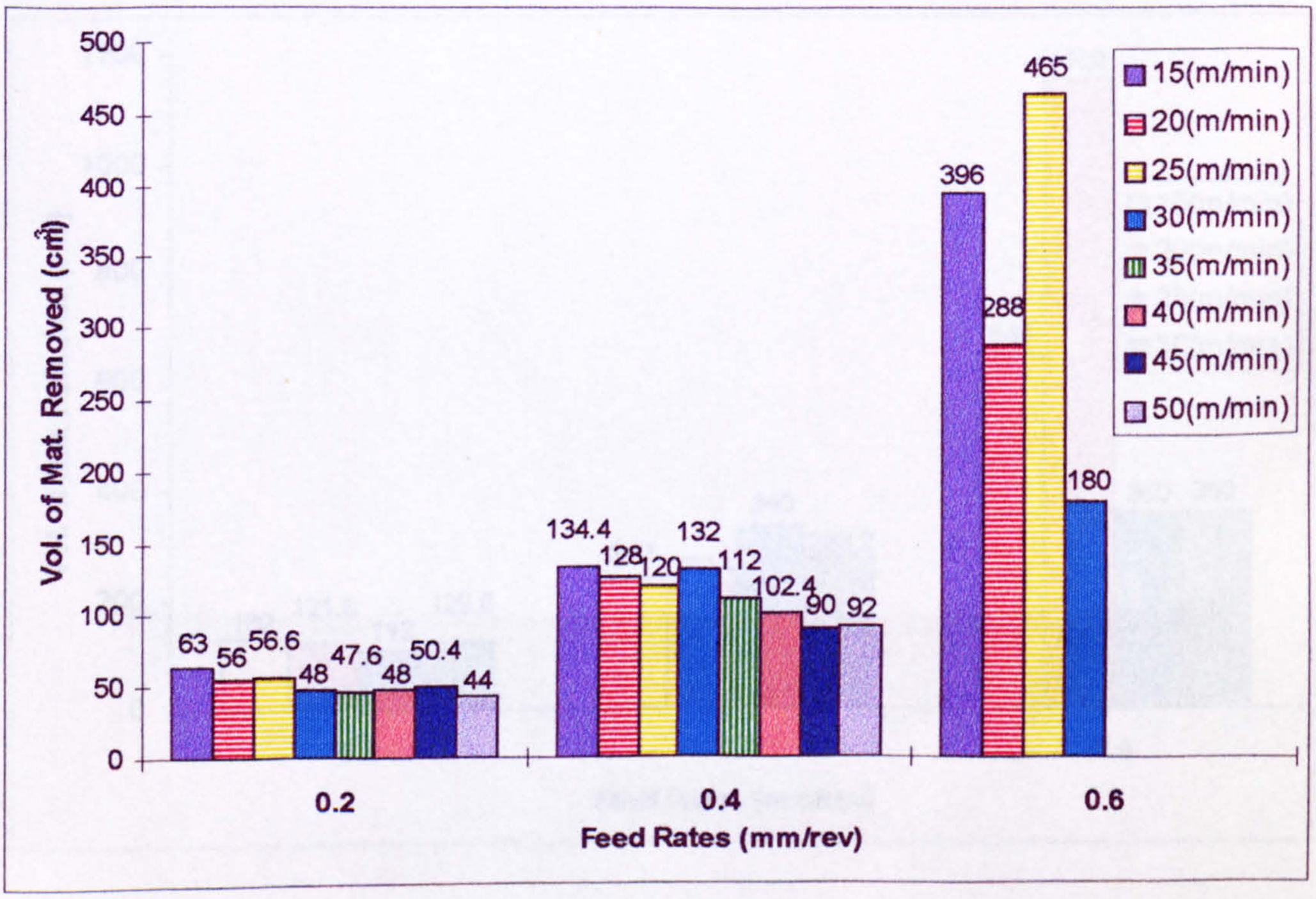

Figure 7.21 Volume Of Material Removed When Machining With K68 Inserts (Negative Geometry, DOC = 4 mm)

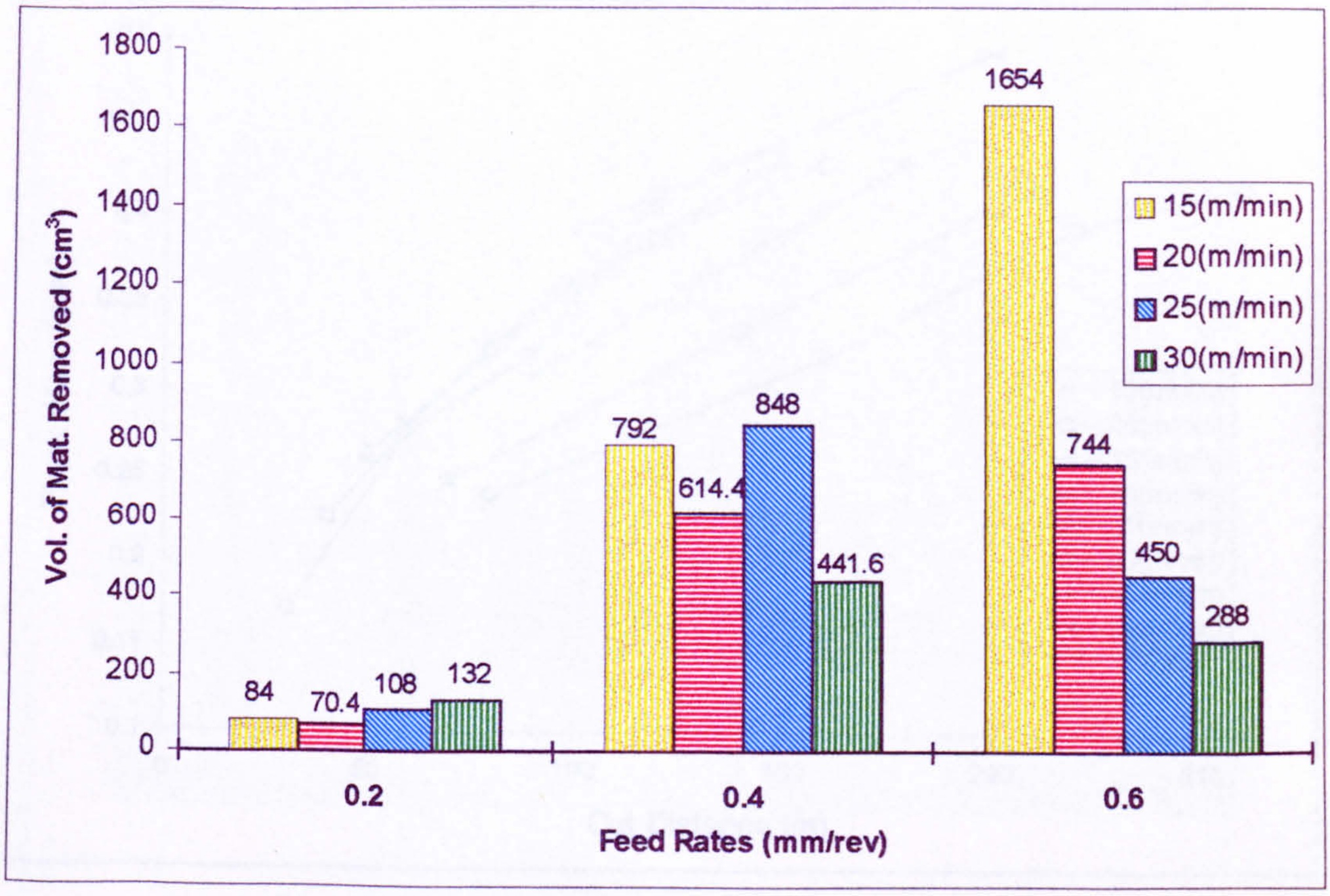

Figure 7.22 Volume Of Material Removed When K68 Inserts (Positive Geometry, DOC = 4 mm)

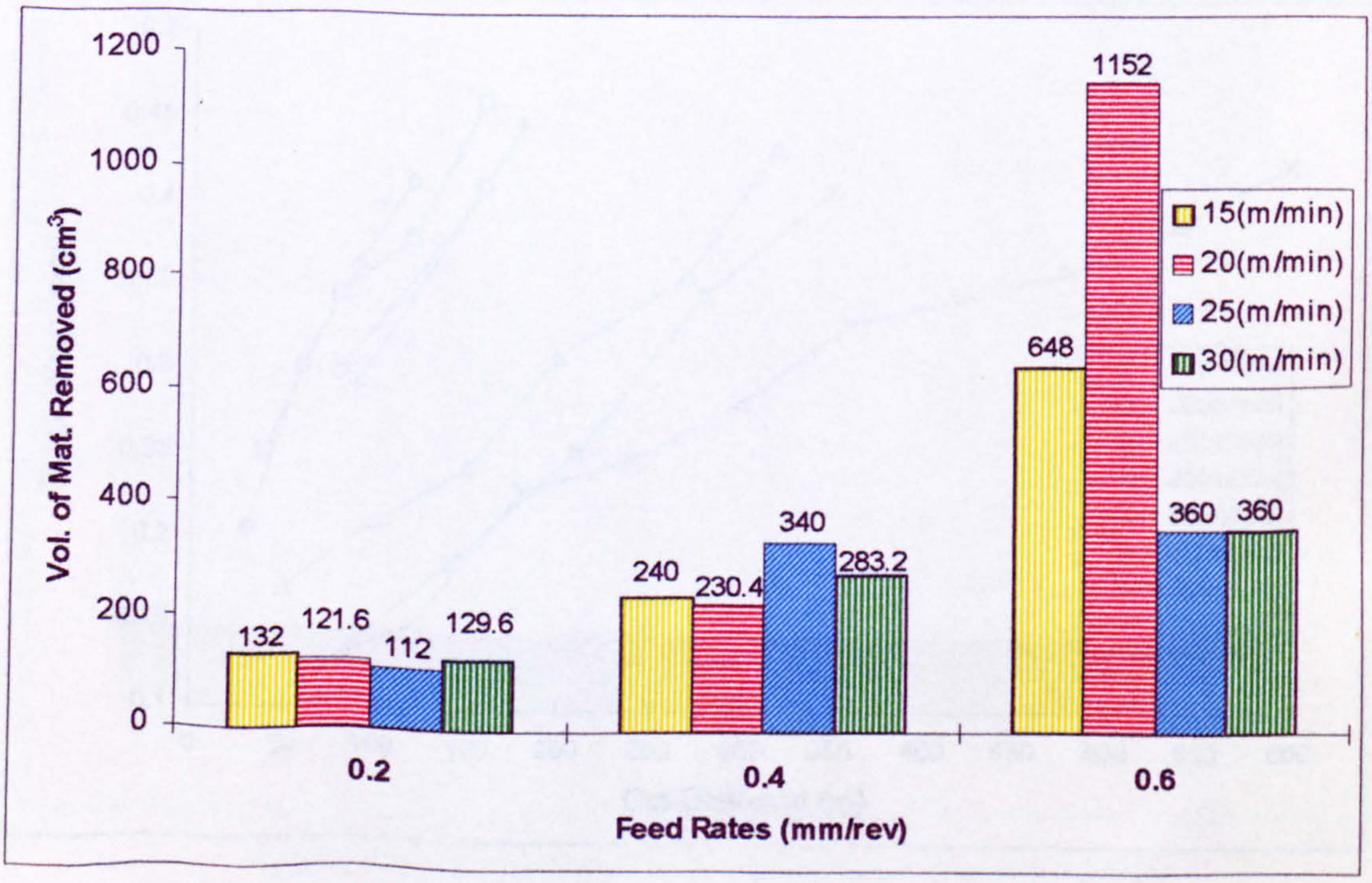

Figure 7.23 Variation of Flank Wear With Cut Distance For K68 Inserts (Negative Geometry, Feed = 0.2 mm/rev, DOC = 2 mm)

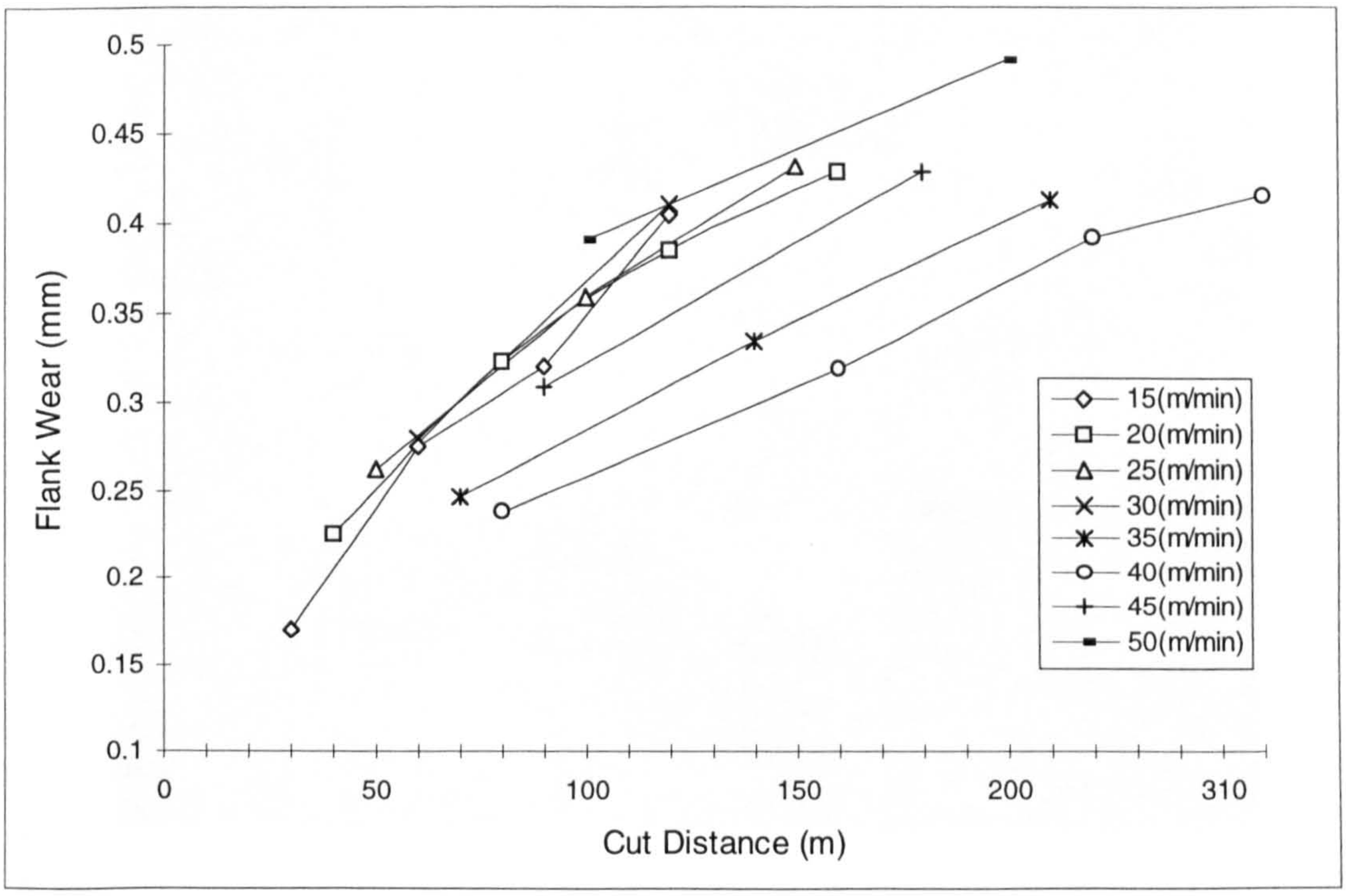

Figure 7.24 Variation of Flank Wear With Cut Distance For K68 Inserts (Negative Geometry, Feed = 0.4 mm/rev, DOC = 2 mm)

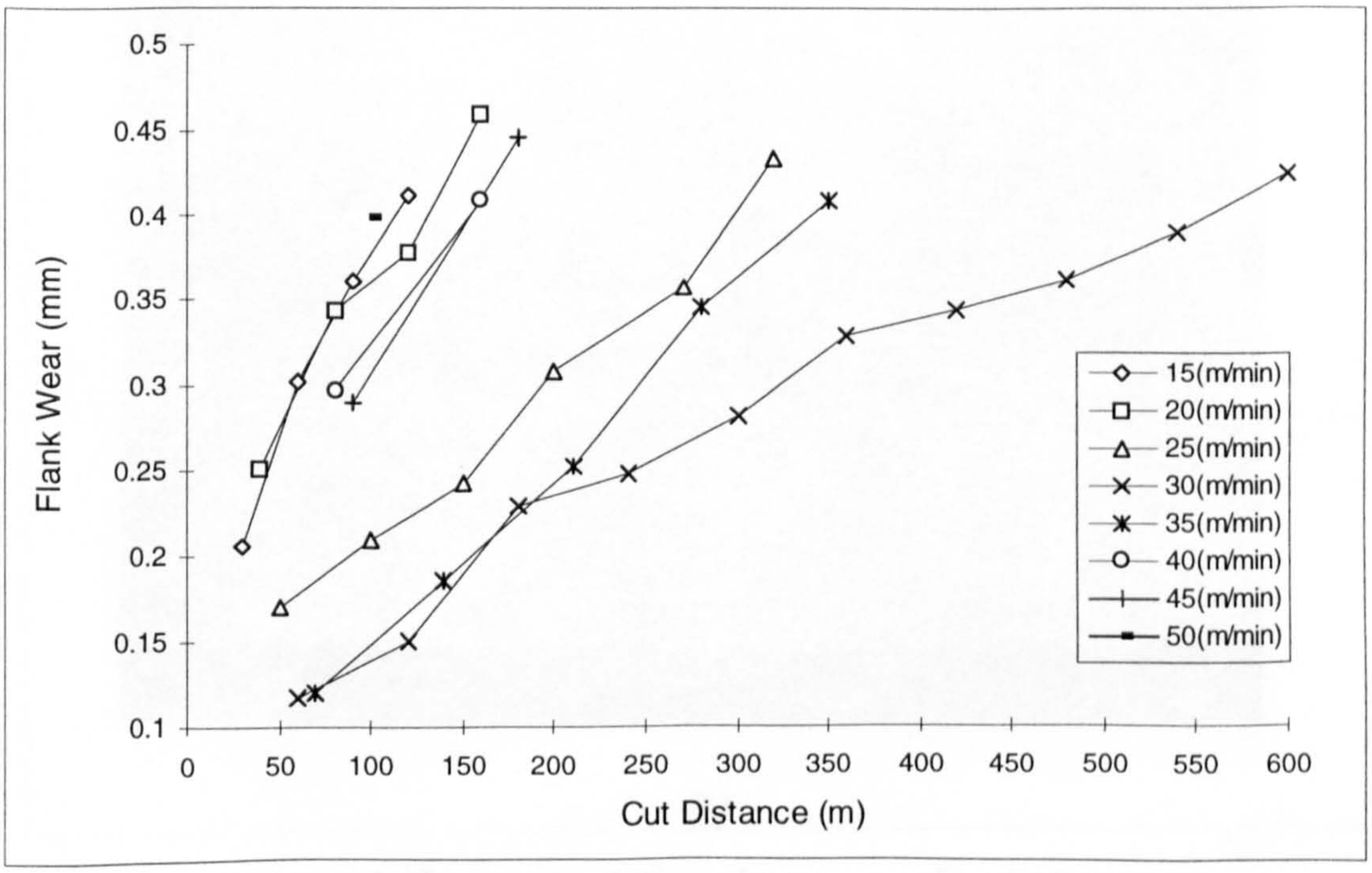

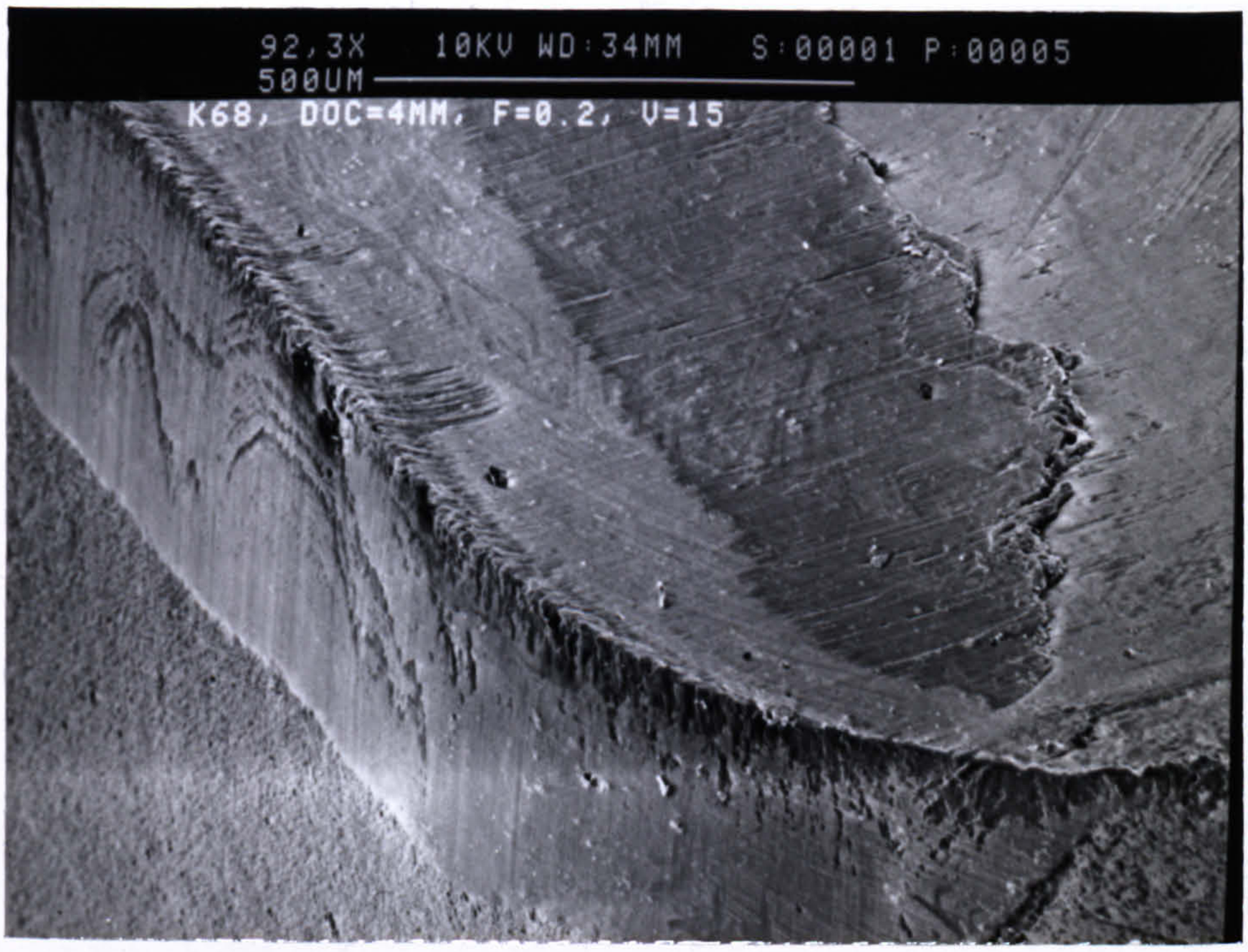

(a)

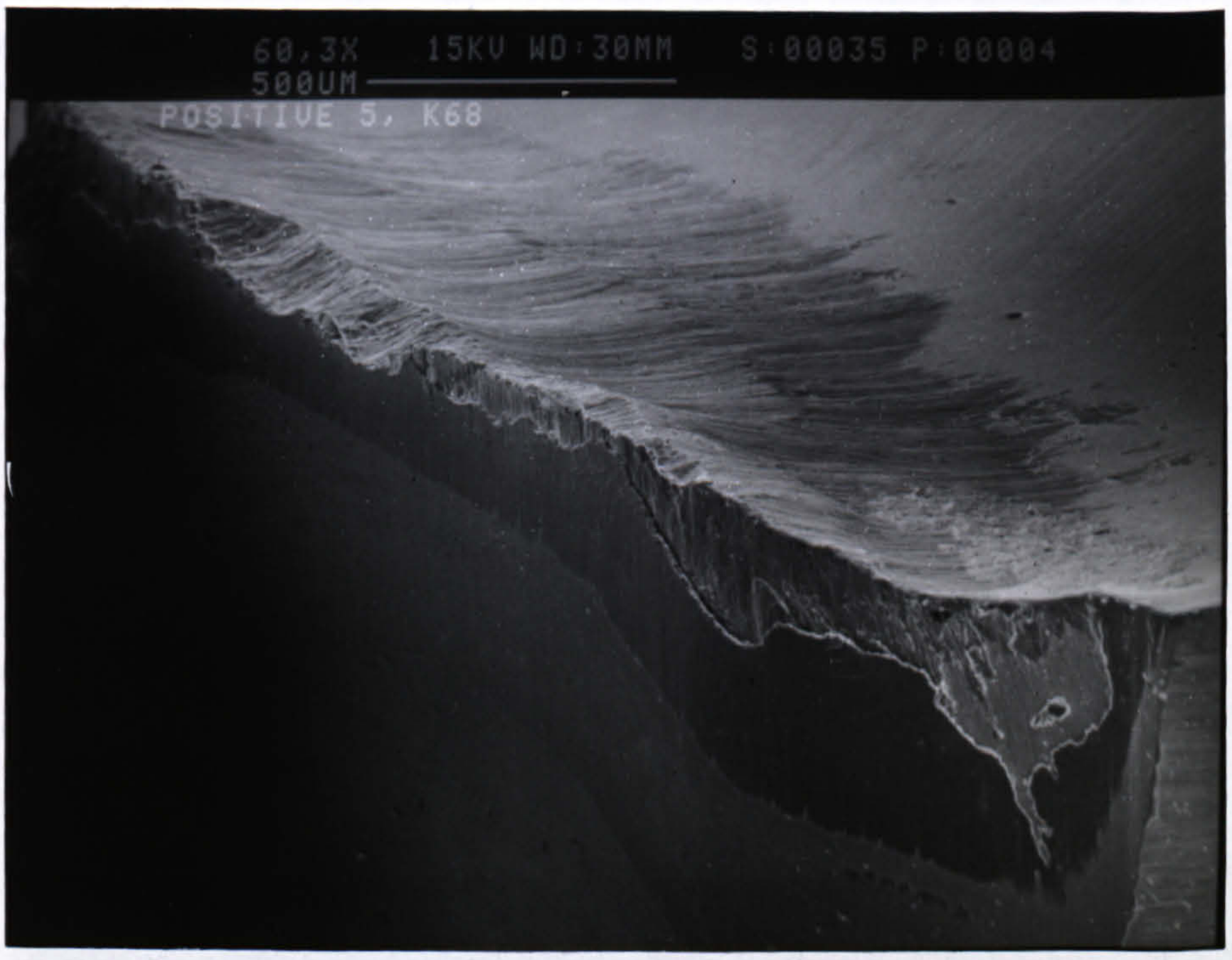

(b)

Figure 7.25 General Wear Appearance For K68 Insert
(a) Negative Geometry, and (b) Positive Geometry

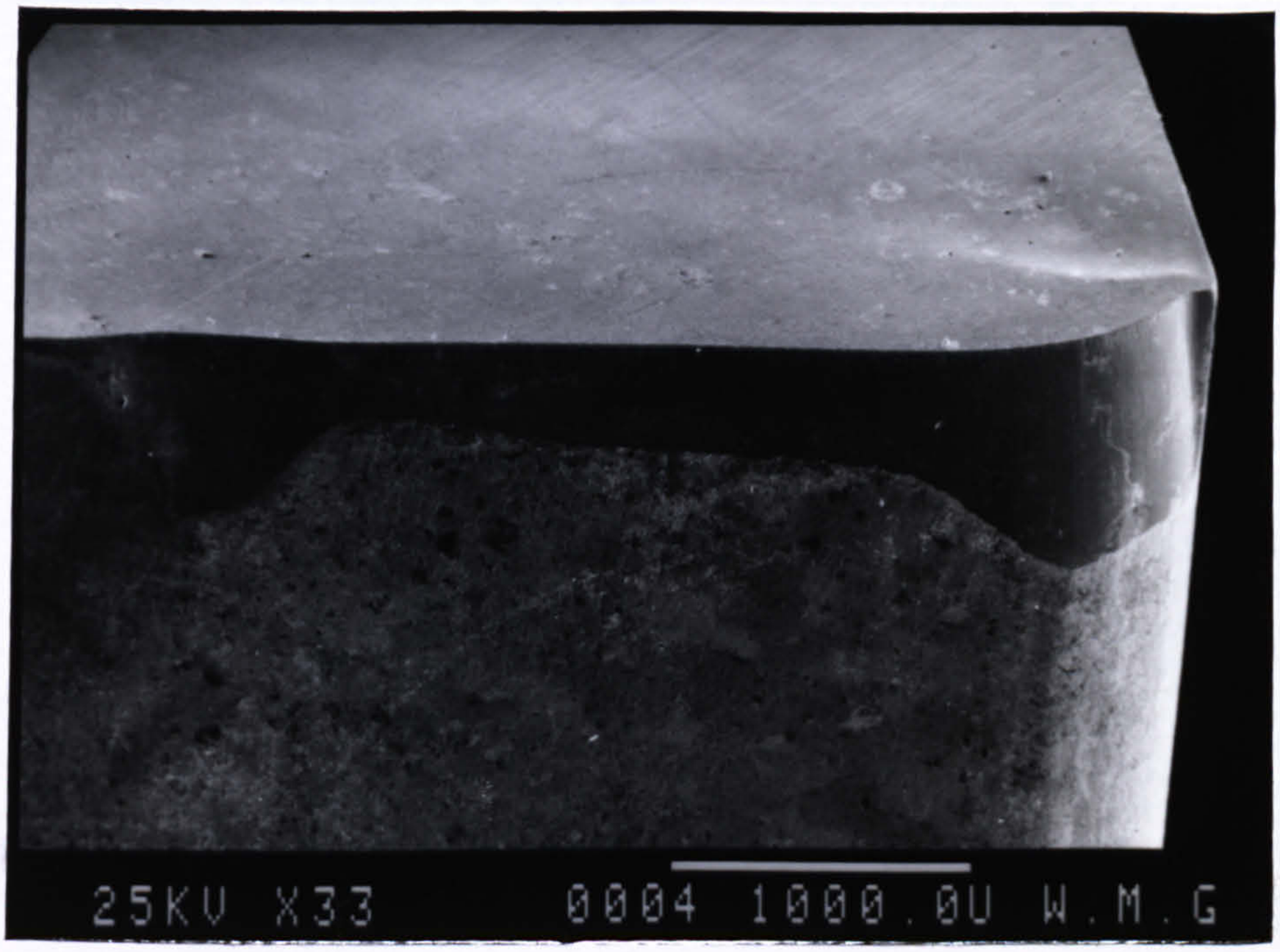

Figure 7.26 Typical Flank Wear On K68 Insert (V = 20 m/min, Feed = 0.4 mm/rev, DOC = 2mm)

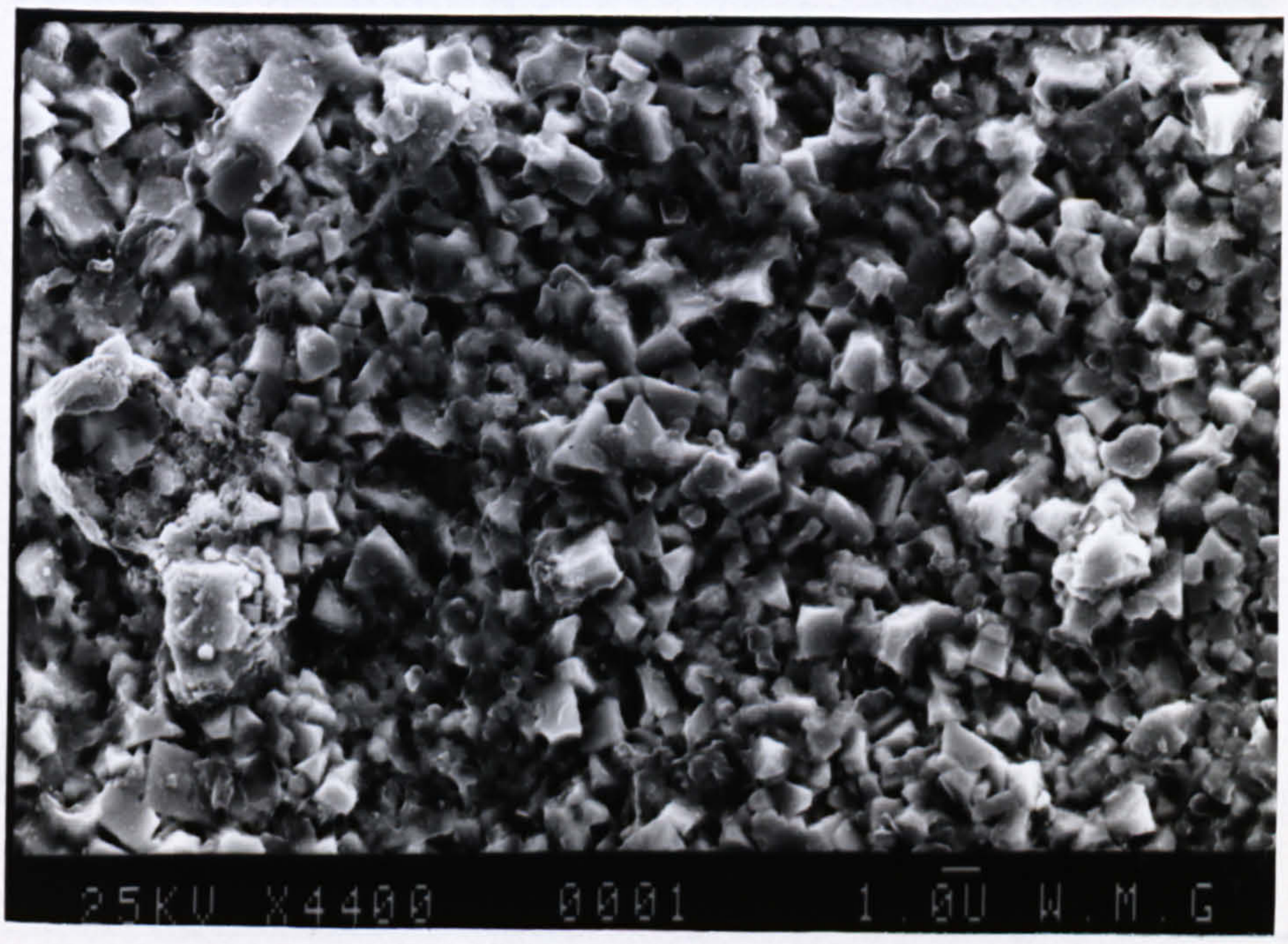

Figure 7.27 Untouched Flank Face of K68 Insert

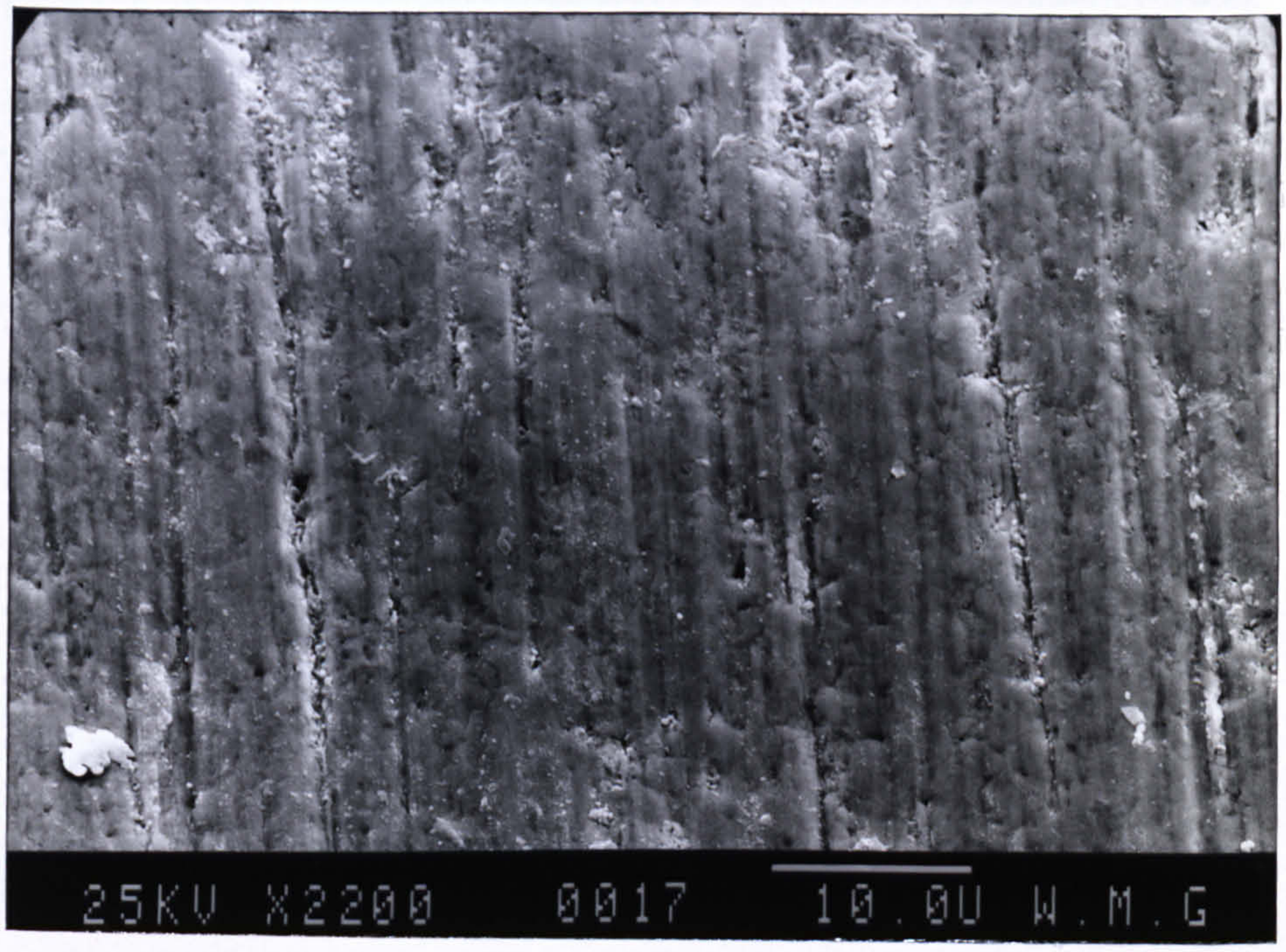

(a)

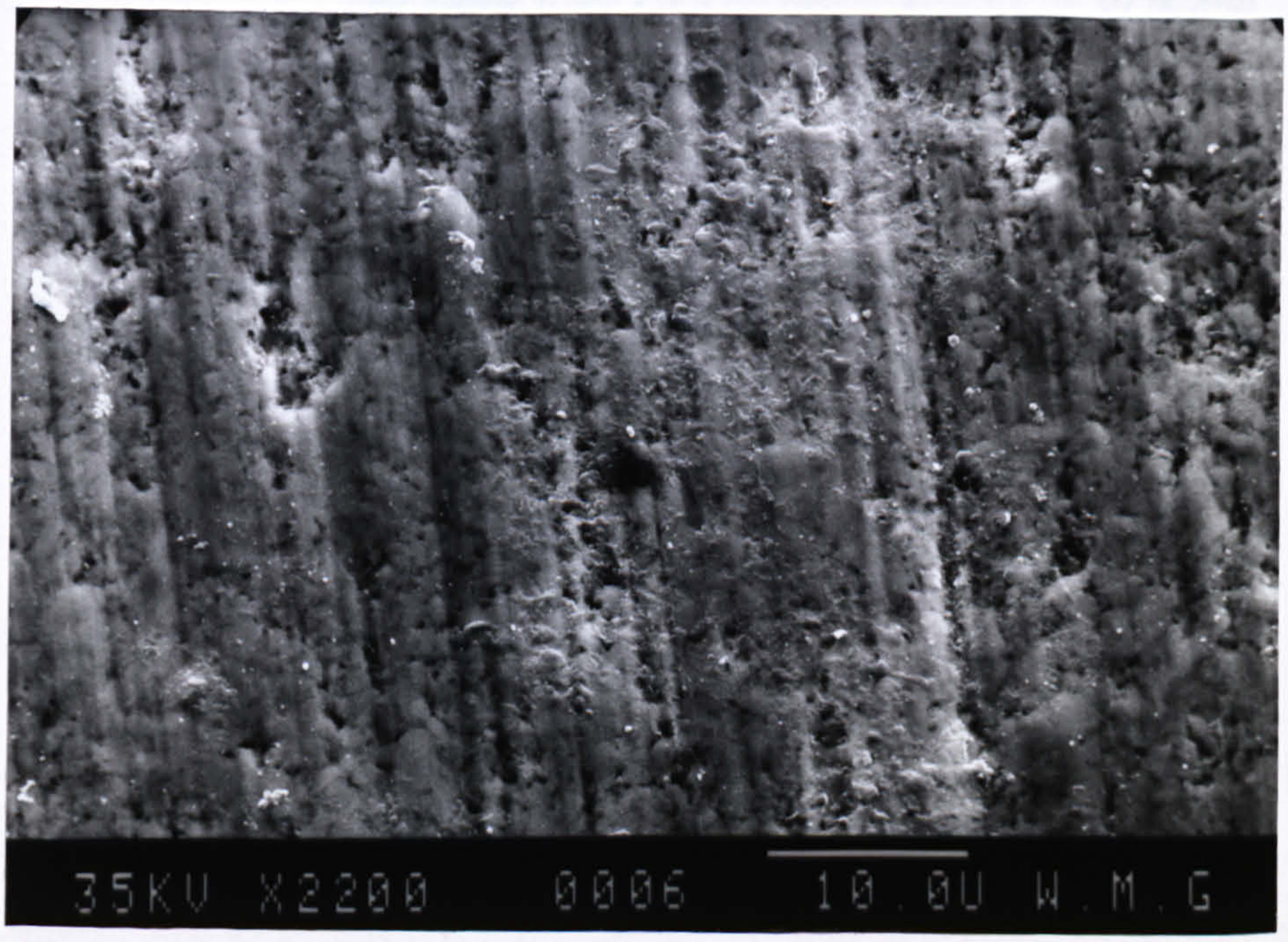

(b)

Figure 7.28 Smooth Wear Apperance Showing Scratches On The Flank Face Of K68 Insert At Various Cutting Speed (a) V = 15 m/min, (b) V = 25 m/min

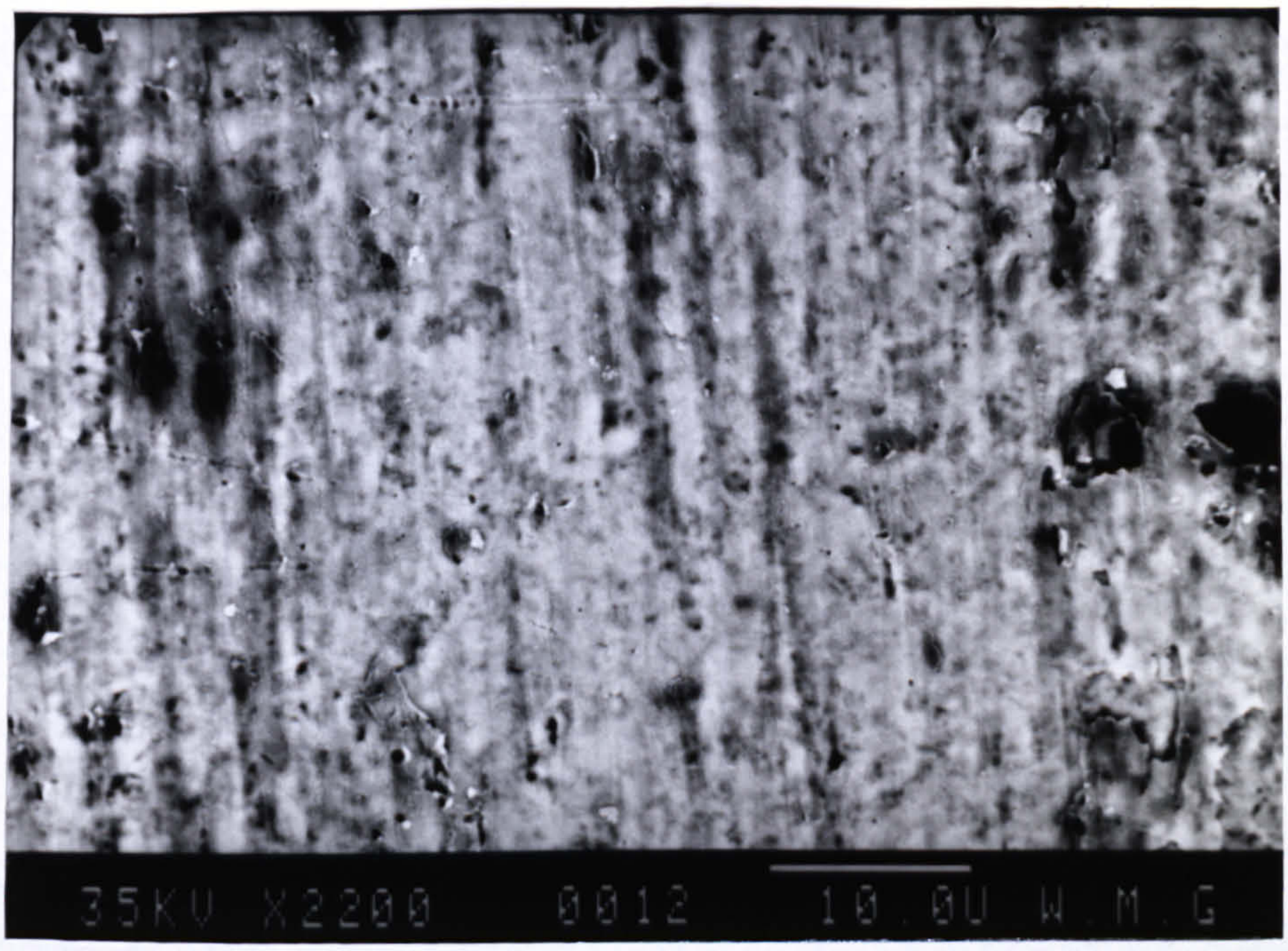

(c)

Figure 7.28 Smooth Wear Apperance Showing Scratches On The Flank Face Of K68 Insert At (c) V = 30 m/min

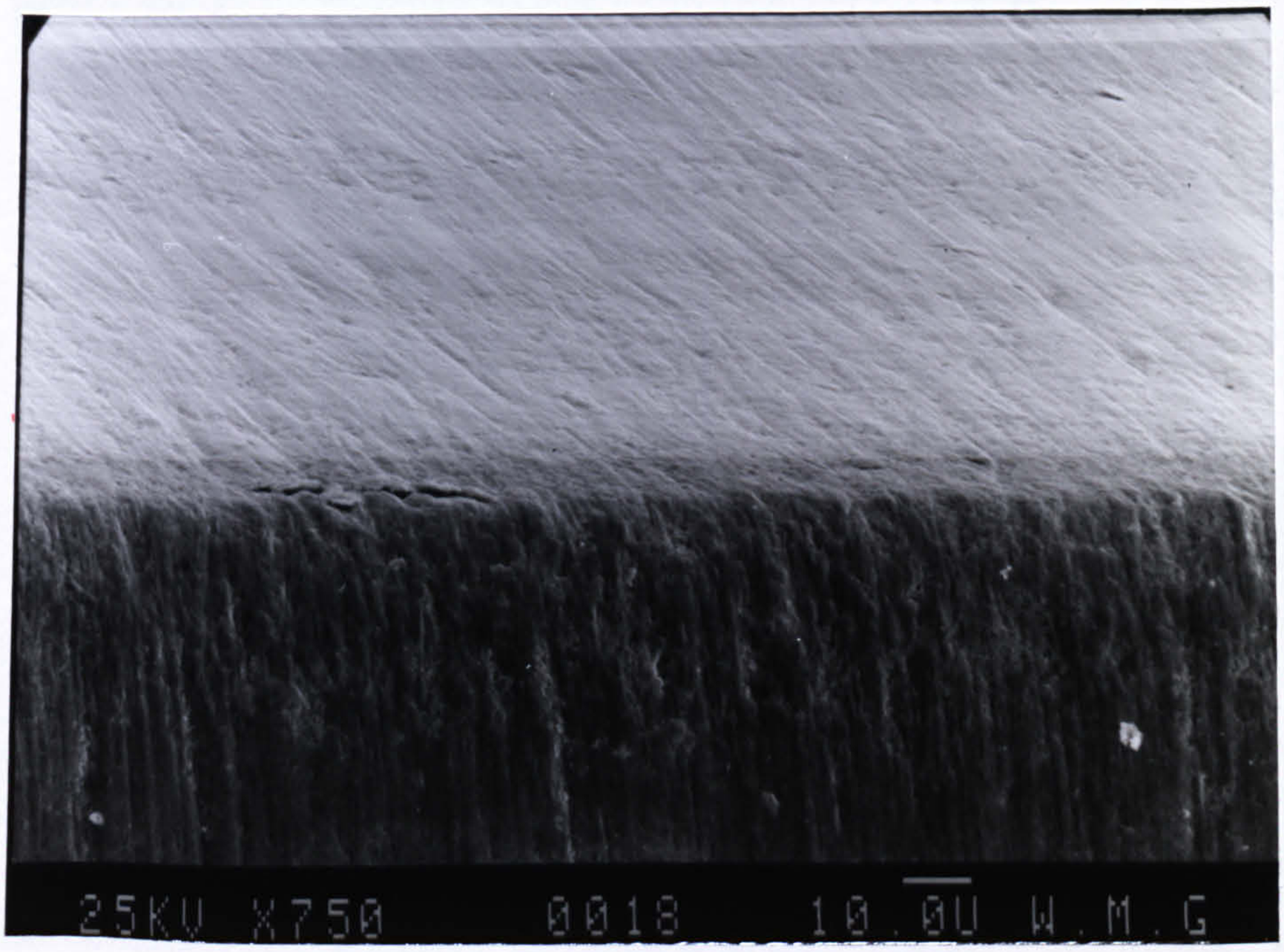

(a)

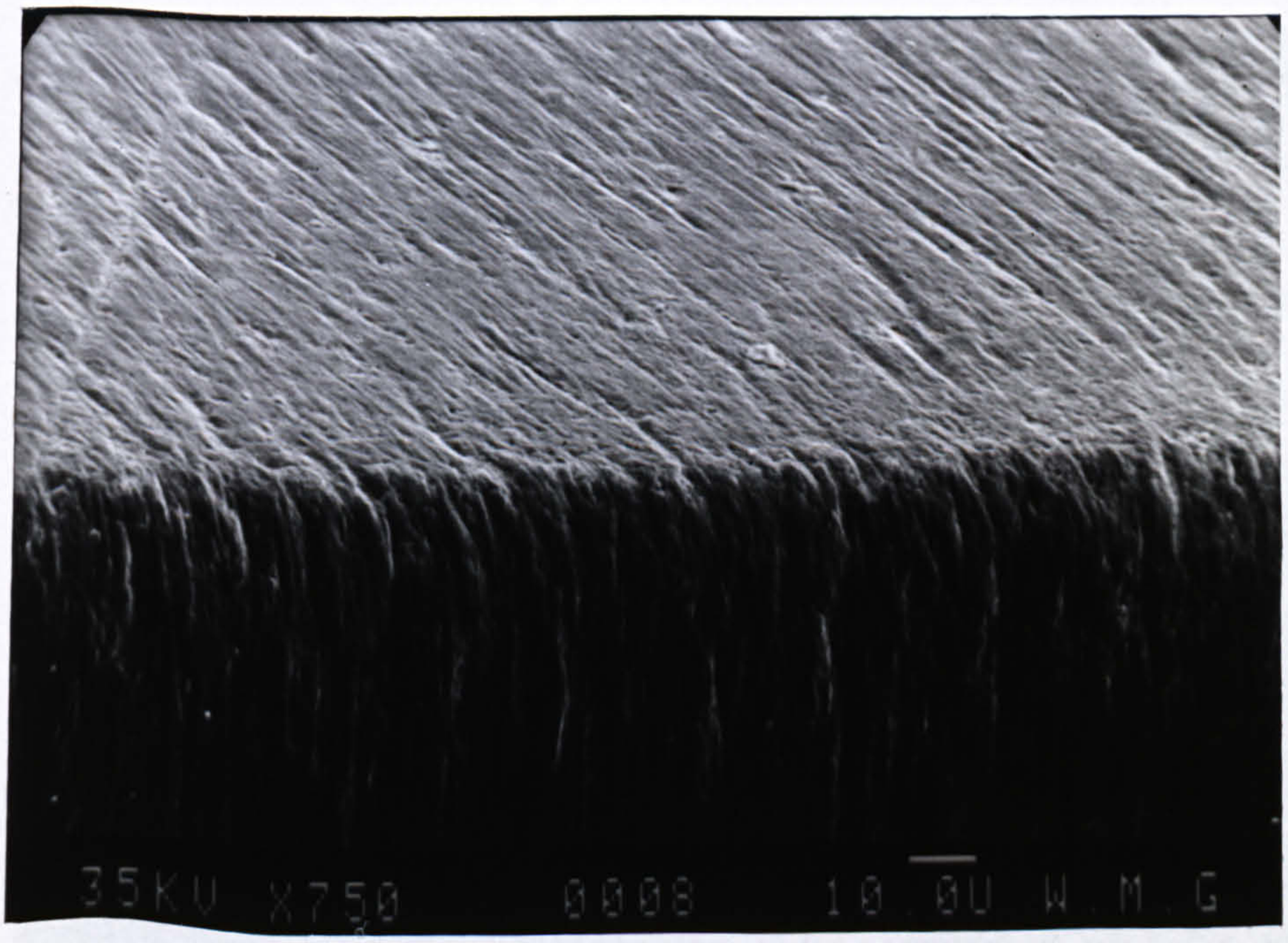

(b)

Figure 7.29 Grooves Parallel To Cutting Direction On The Flank Face And Scratches on The Rake Face Of K68 Insert At Various Cutting Speed (a) V = 15 m/min (b) V = 25 m/min

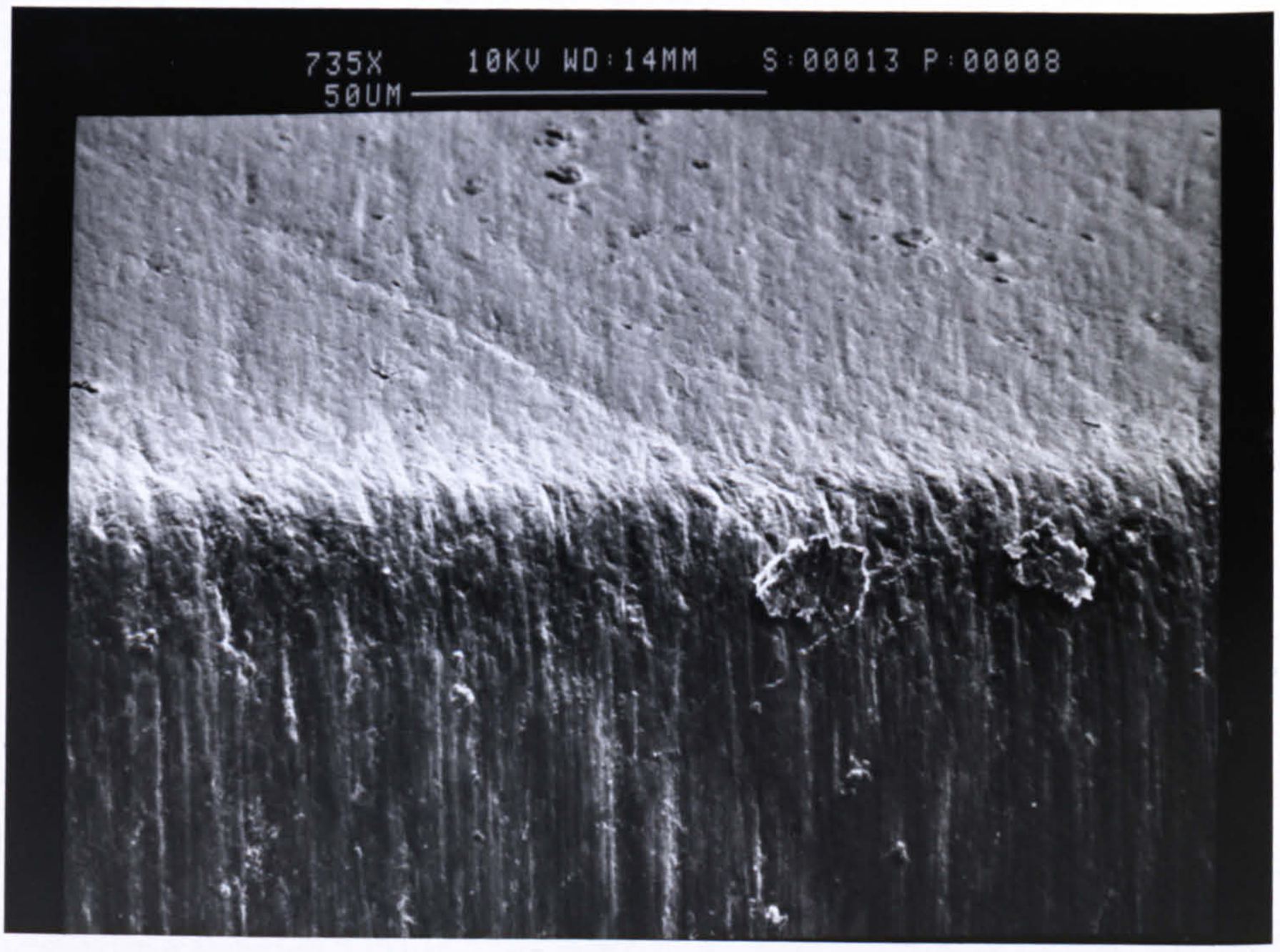

(c)

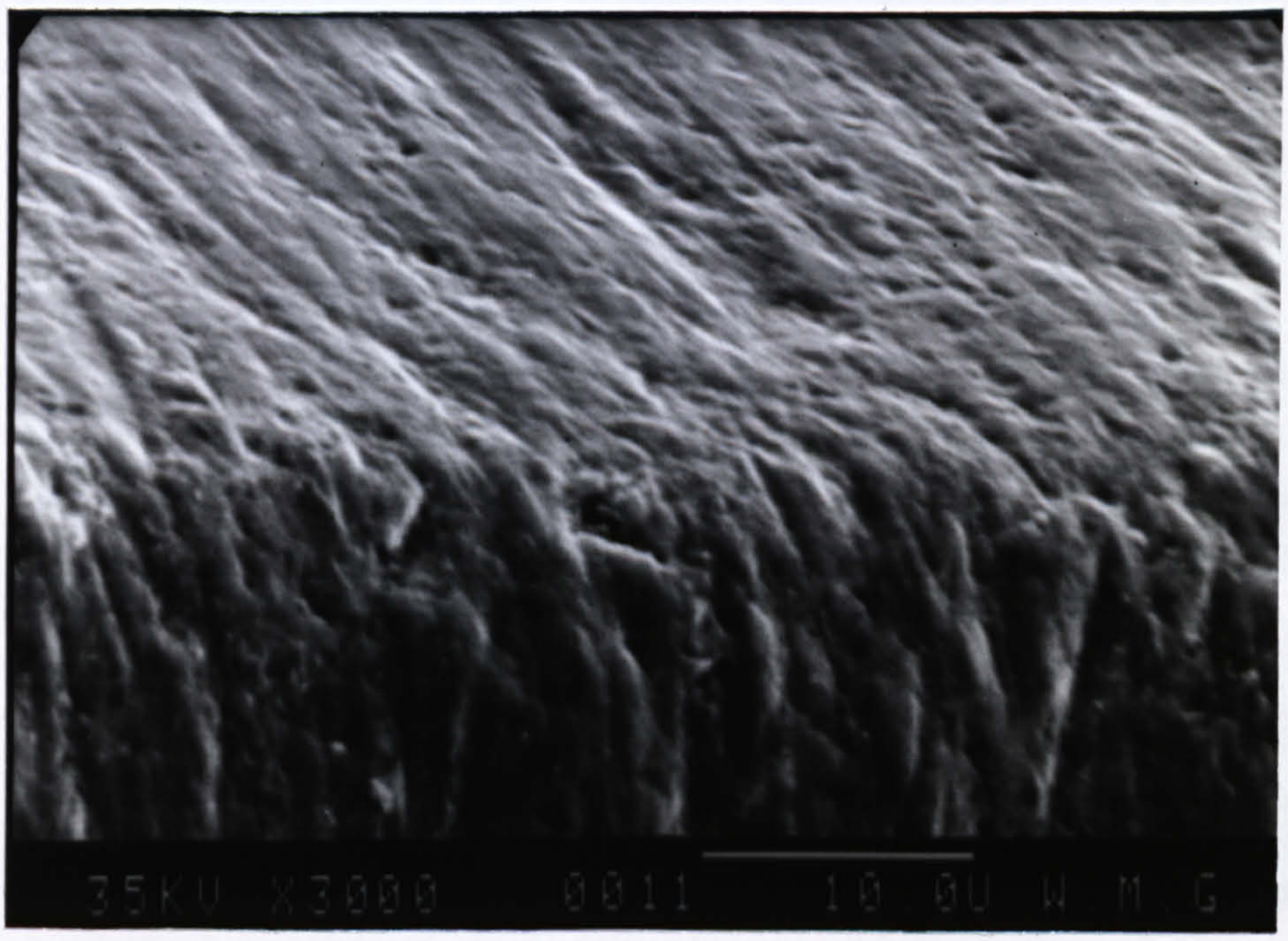

(d)

Figure 7.29 Grooves Parallel To Cutting Direction On The Flank Face And Scratches on The Rake Face Of K68 Insert At Cutting Speed, (c) V = 30 m/min, (d) Higher Magnification of Figure 7.29(b) above

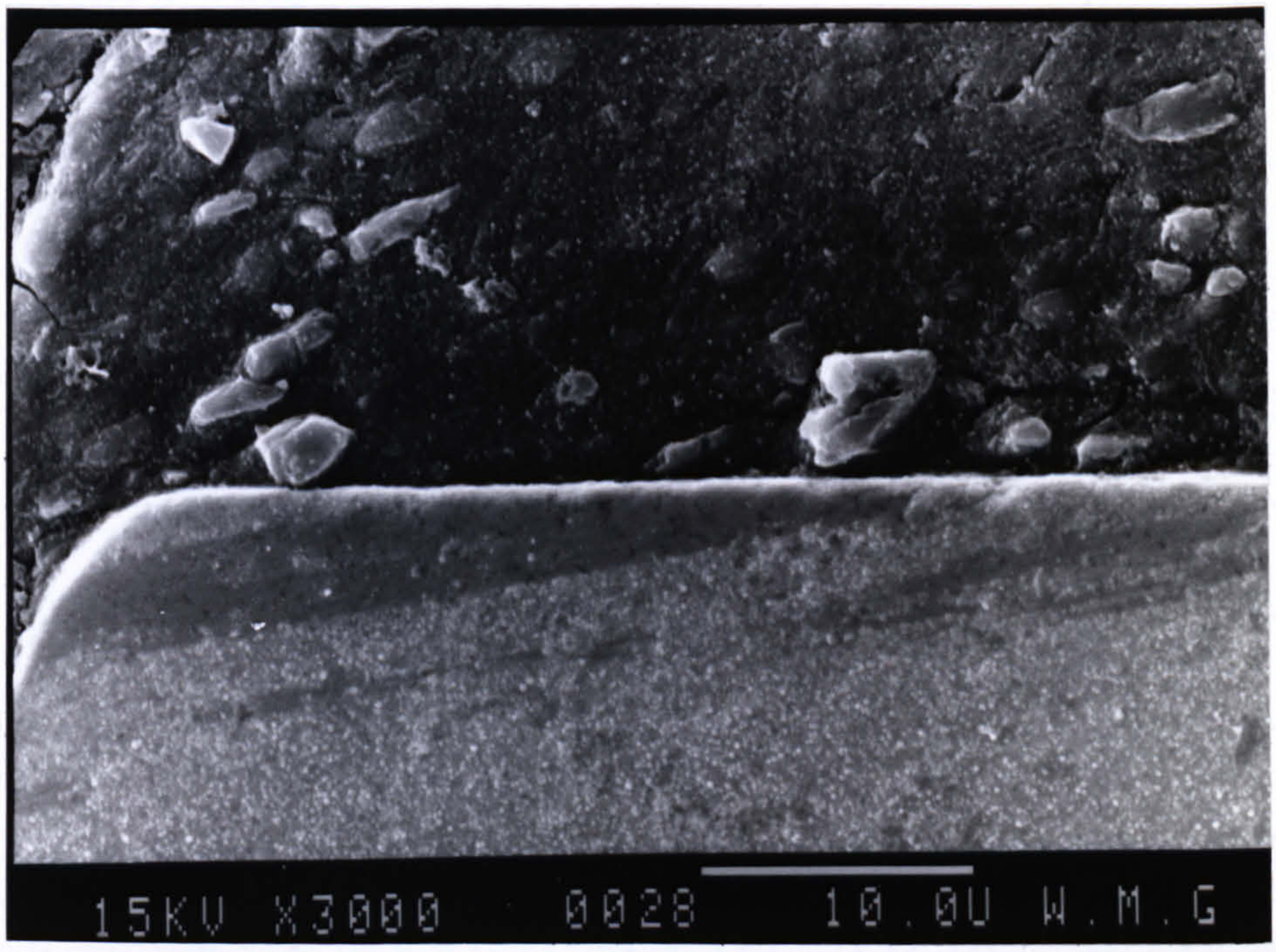

(a)

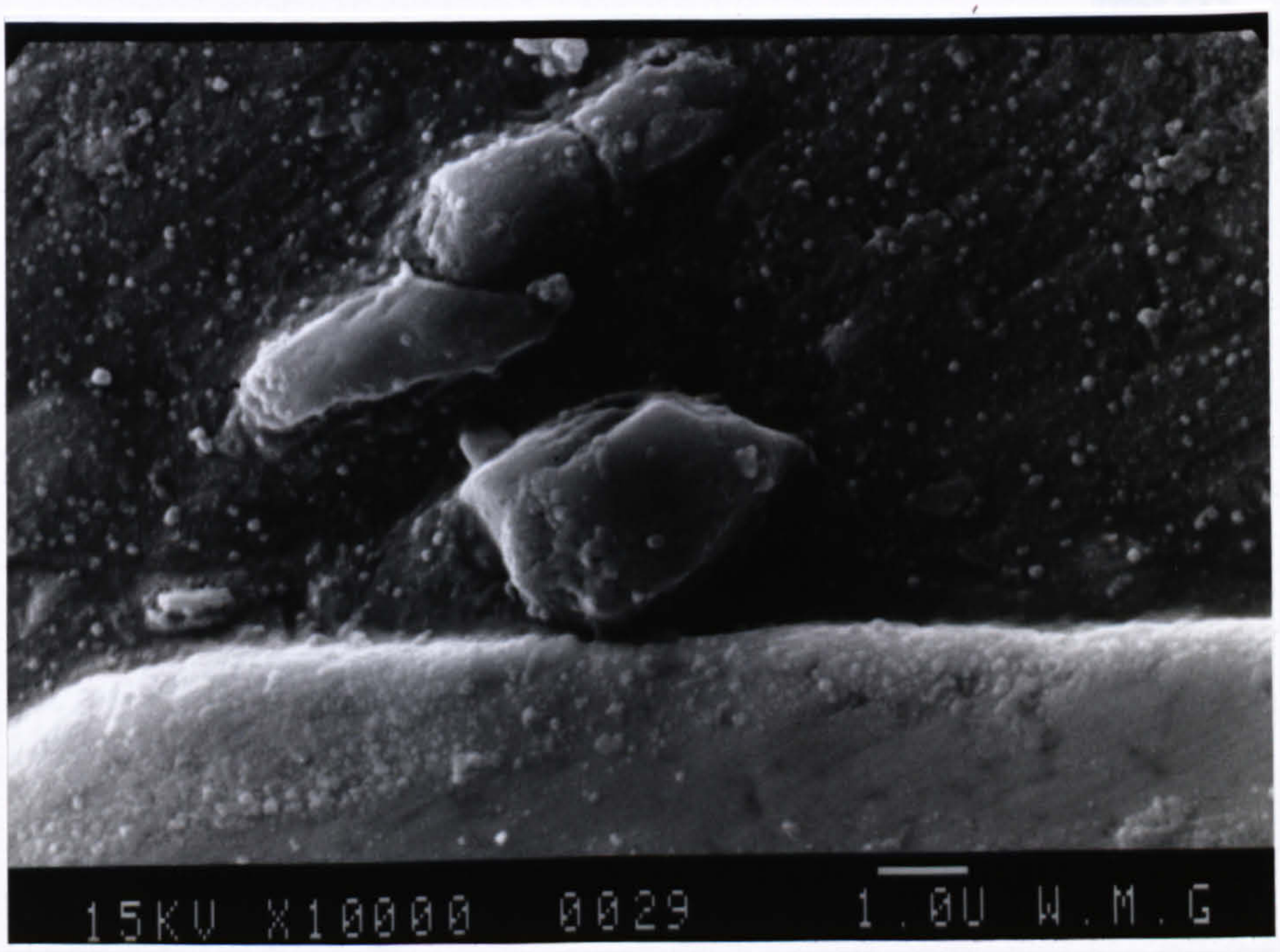

(b)

Figure 7.30 Cross-section of K68 Inserts Showing SiC Particles On The Rake Face (a) 3000X, and (b) 10000X (V = 25 m/min, Feed = 0.4 mm/rev)

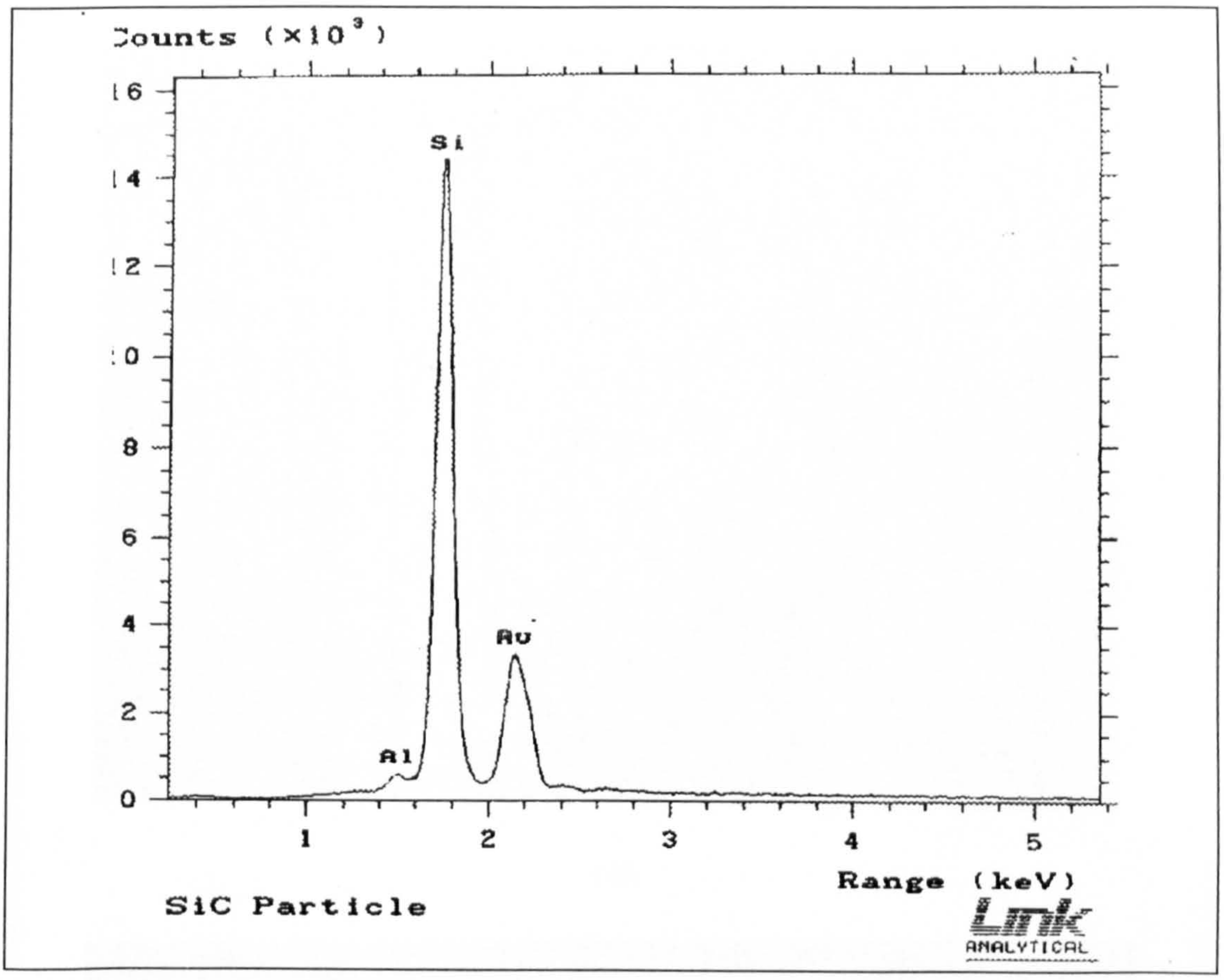

Figure 7. 31 Energy Dispersive X-Ray Analysis Graph Showing The Present of SiC Particle

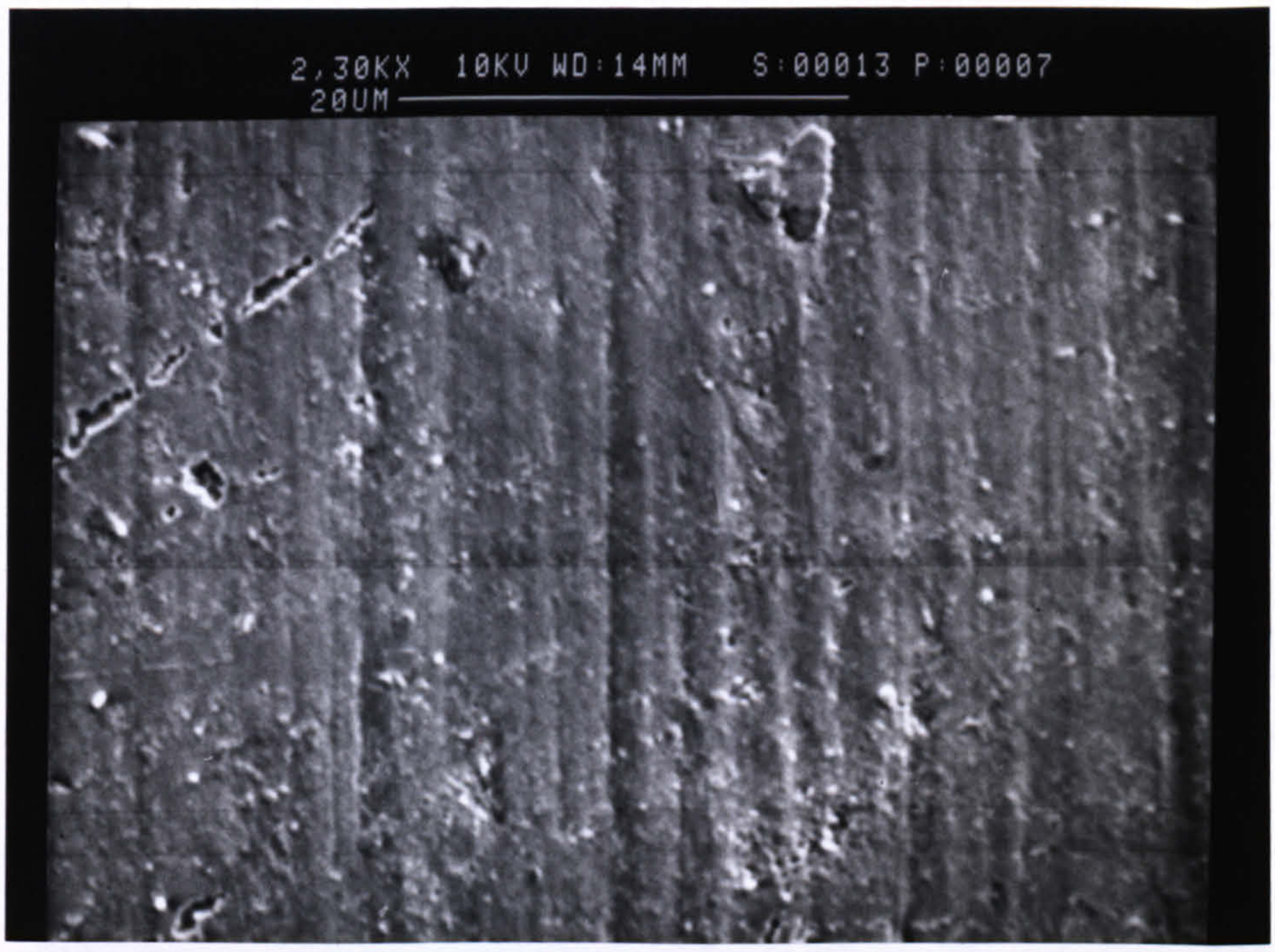

(a)

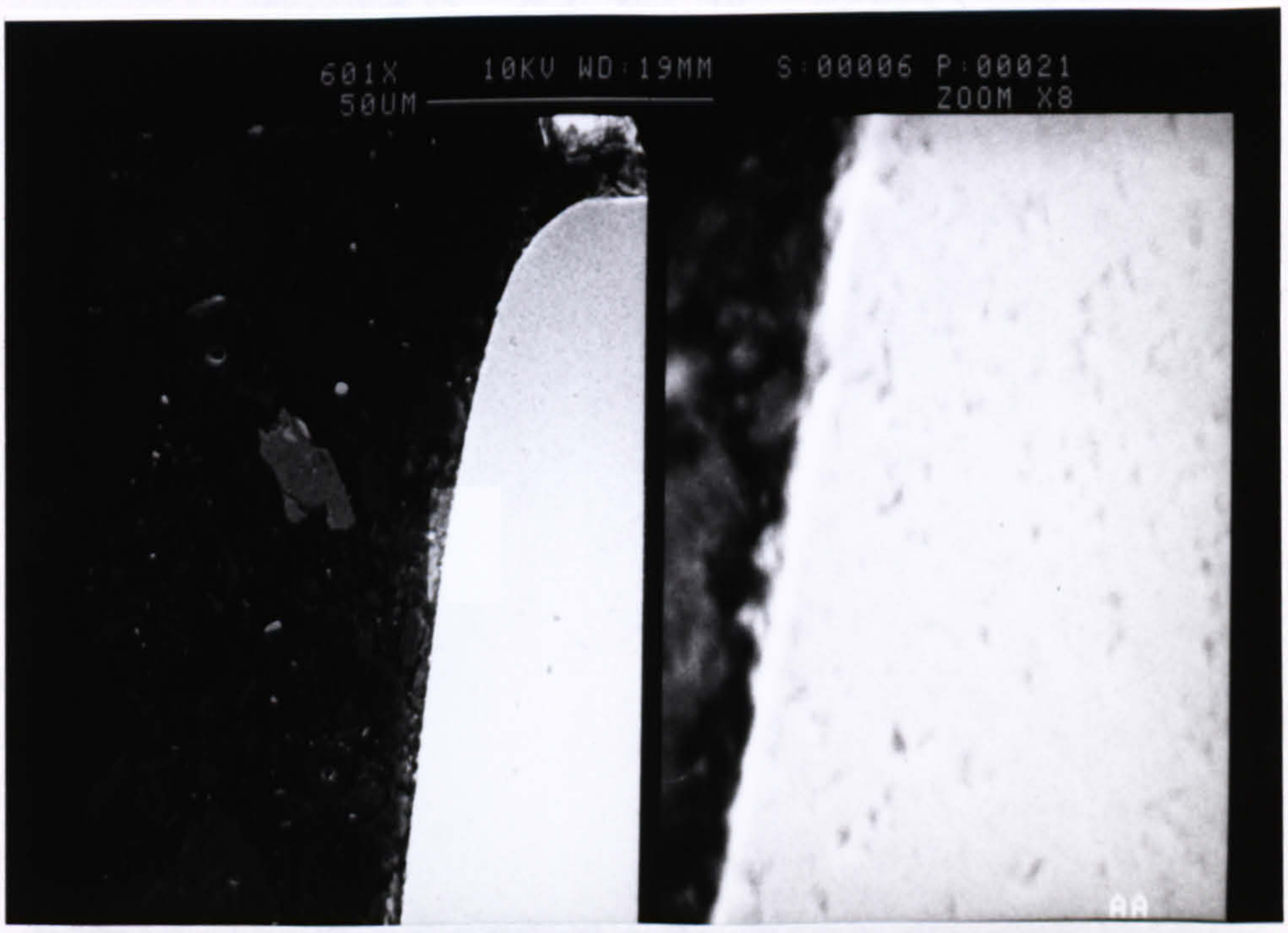

(b)

Figure 7. 32 (a) Flank Face of K68 Insert Showing Carbide Grains Were Pulled Out of The Surface, (b) Cross-Section of The Worn Flank Face of K68 Insert

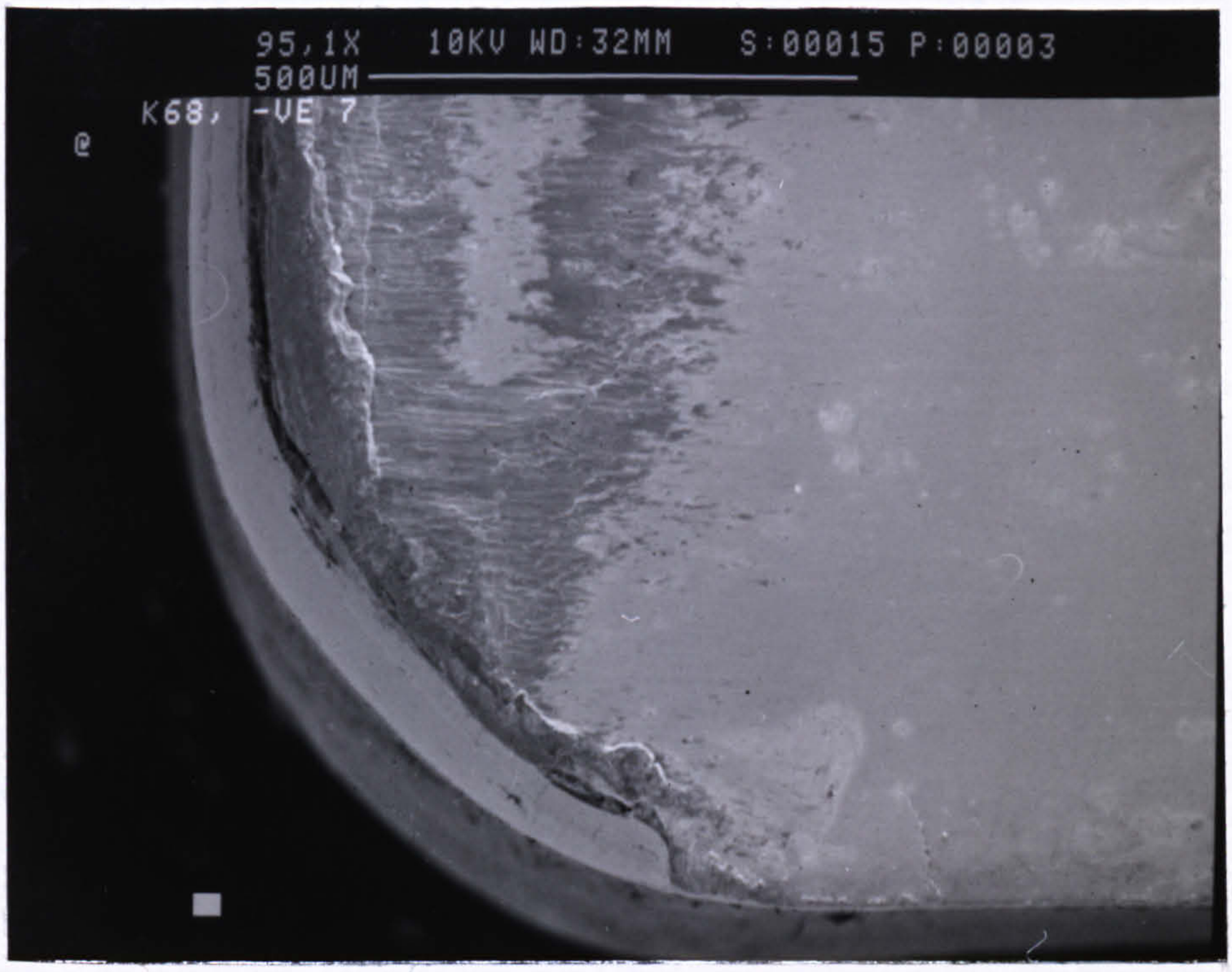

Figure 7.33 Rake Face Wear Of K68 Insert (V = 15 m/min, Feed = 0.4 mm/rev, DOC = 2 mm)

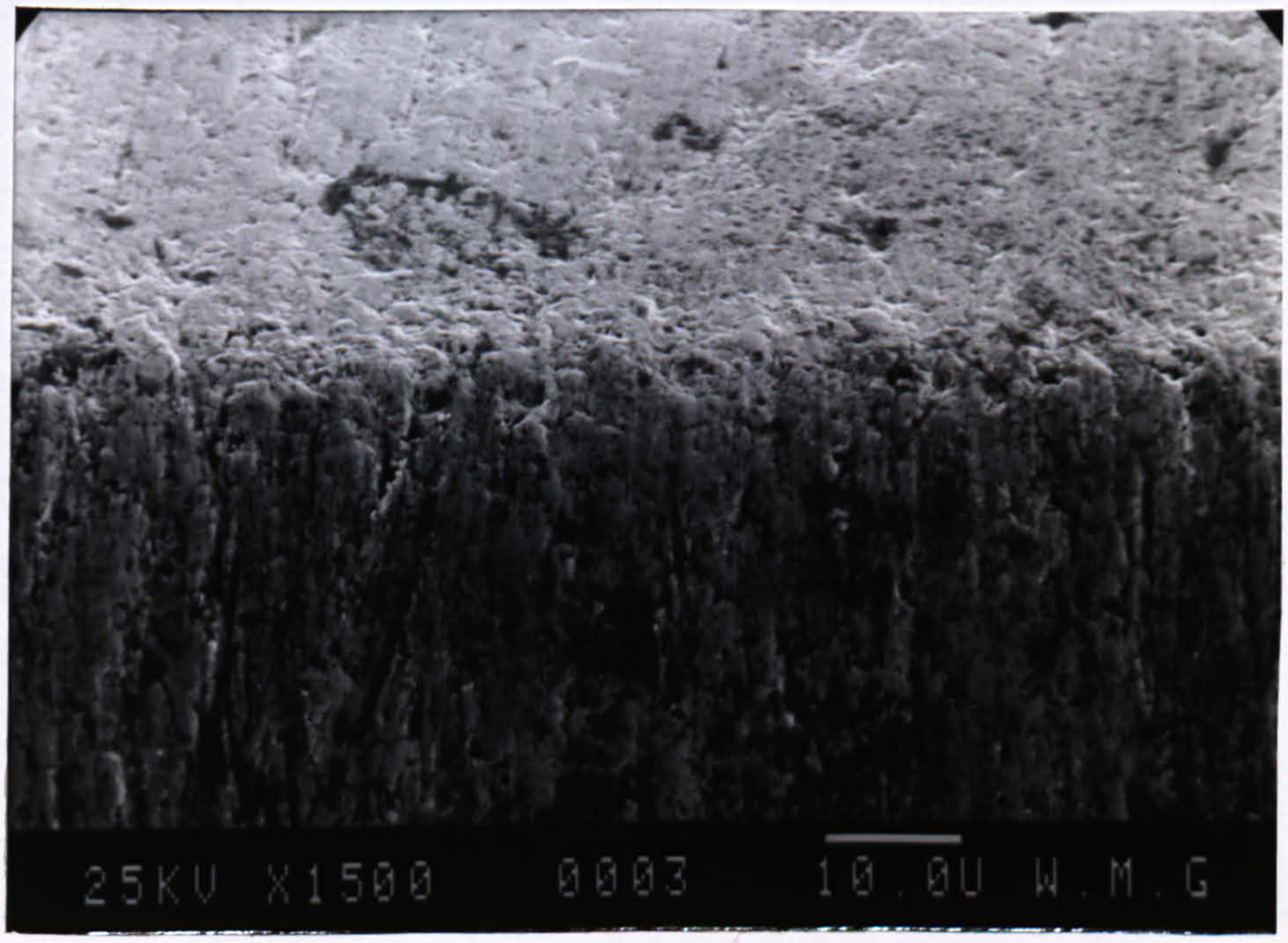

Figure 7.34 Chipped-Off Portion On The Rake Face Of K68 Insert (V = 20 m/min, Feed = 0.4 mm/rev, DOC = 2 mm)

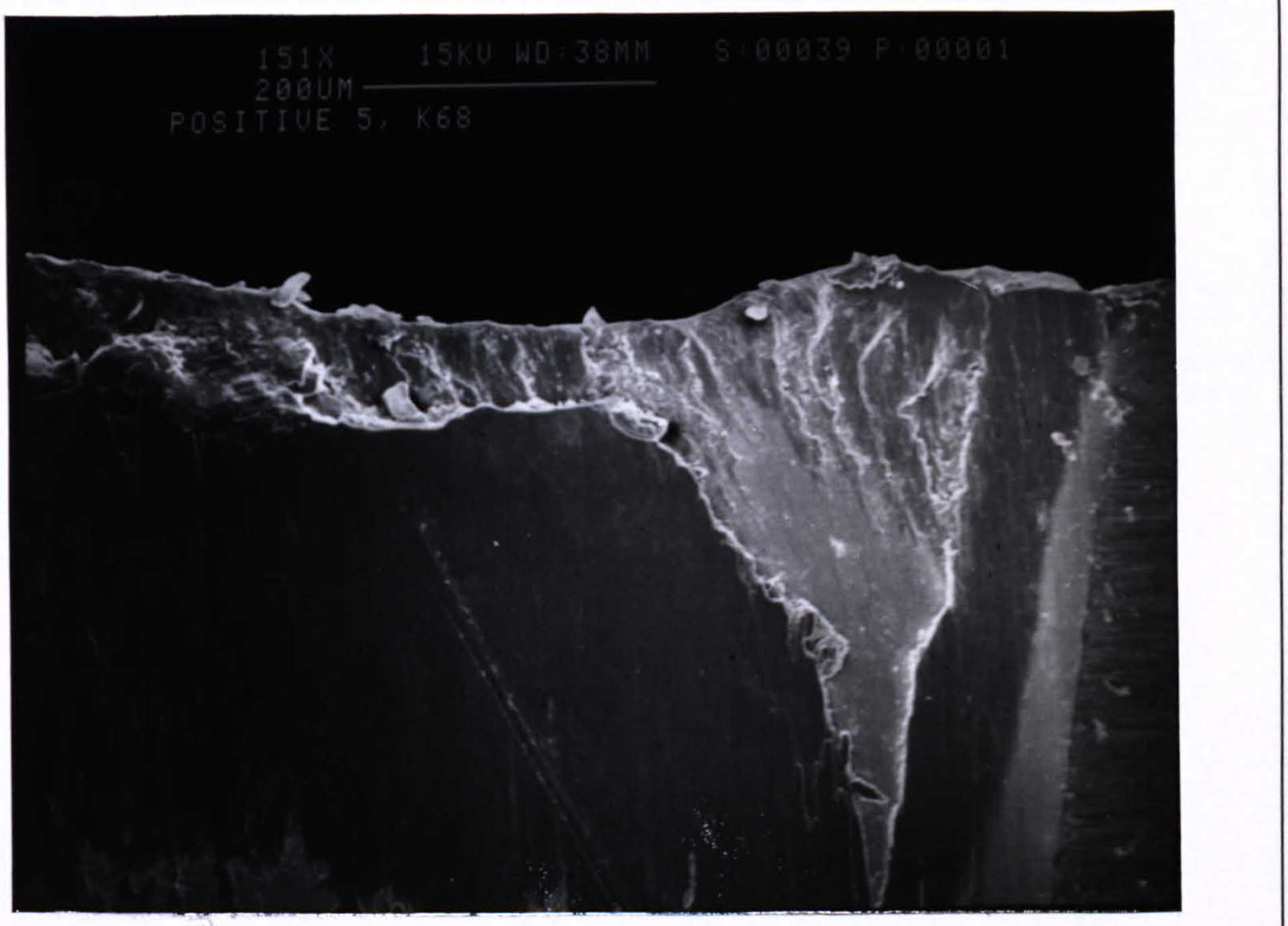

Figure 7.35 Slight Notching On The Depth Of Cut On K68 Insert (V = 15 m/min, Feed = 0.2 mm/rev, DOC = 2 mm)

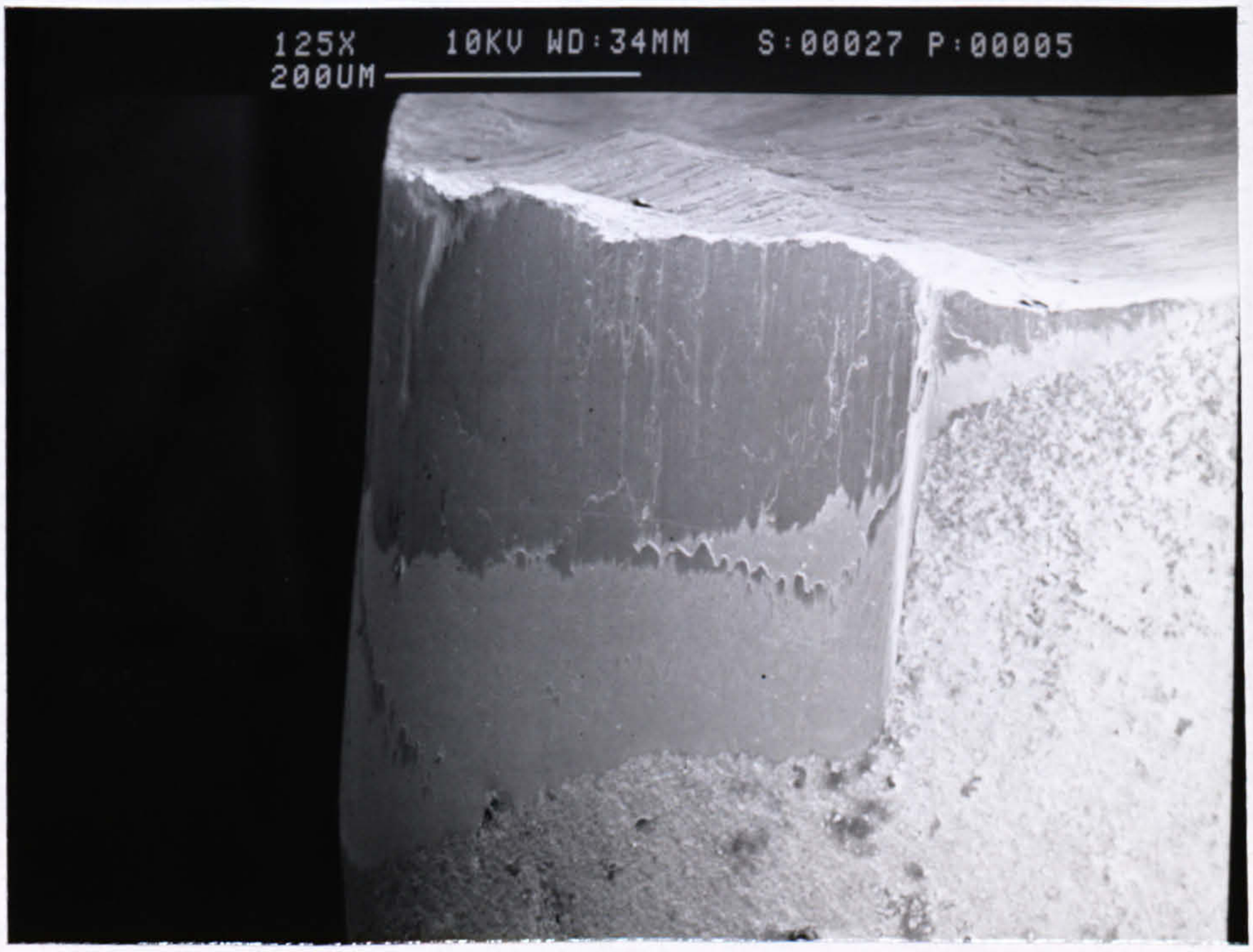

Figure 7.36 Rounding Of Tool Nose On K68 Insert (V = 25 m/min, Feed = 0.2 mm/rev, DOC = 2 mm)

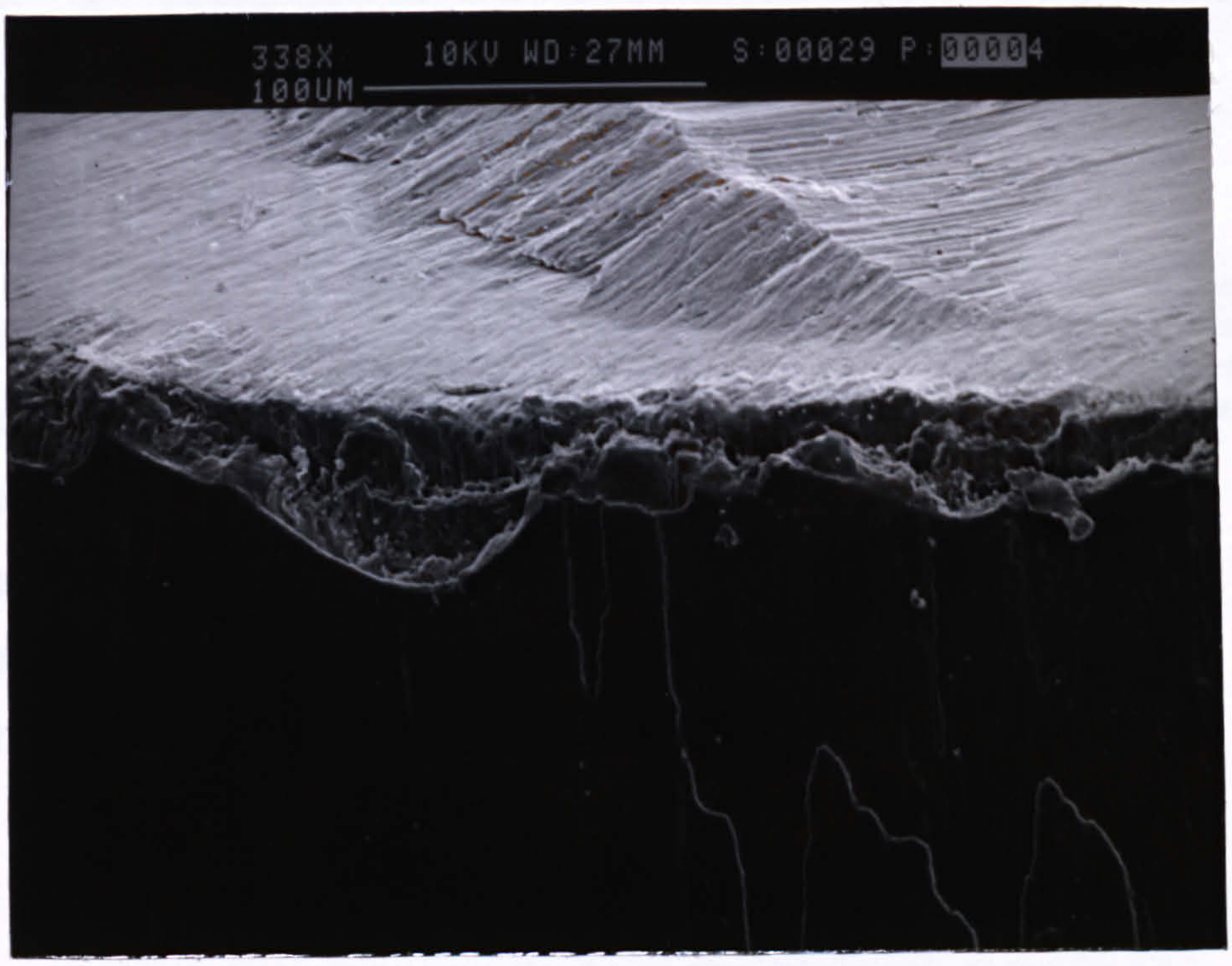

(a)

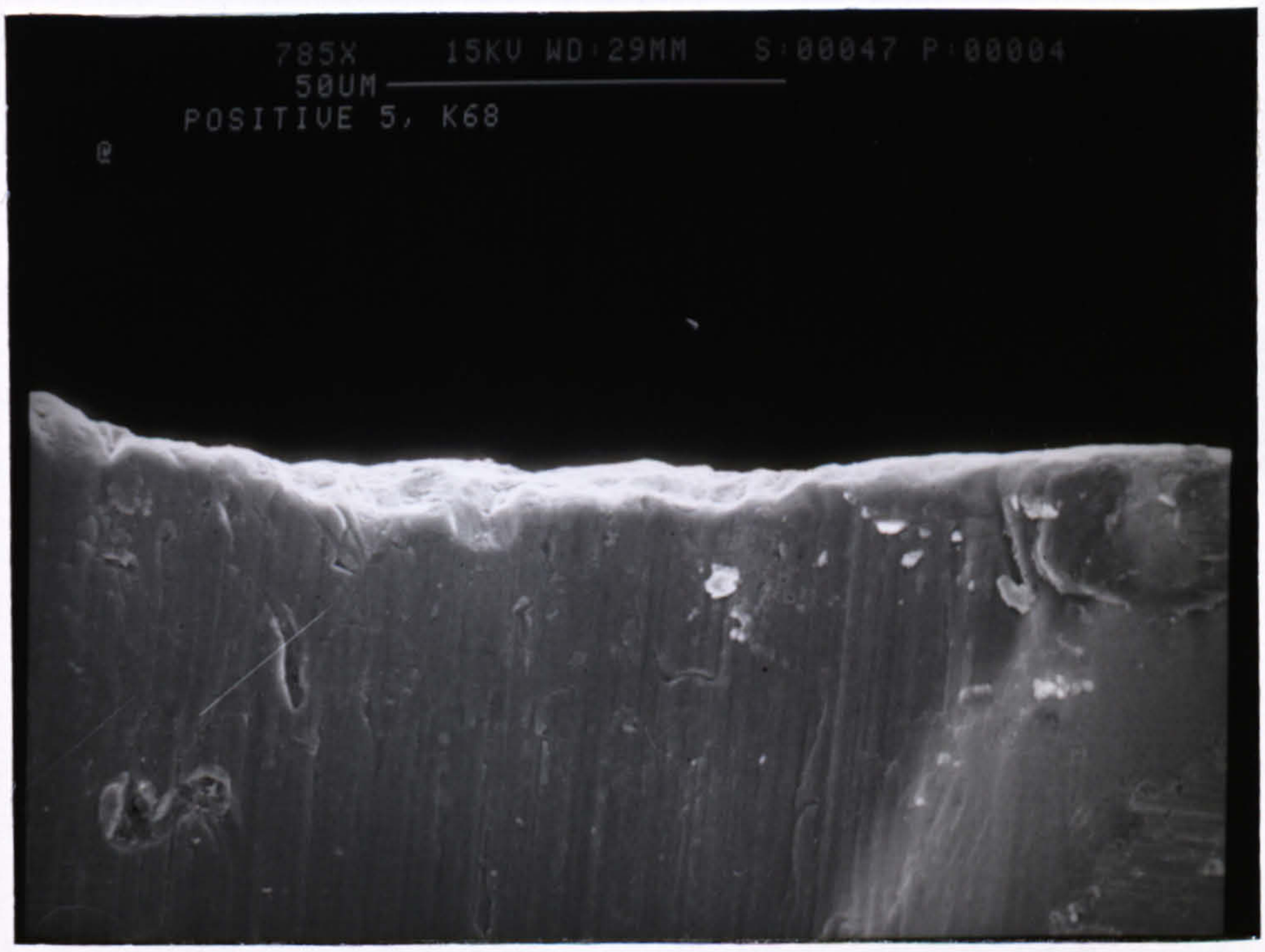

(b)

Figure 7.37 Micro-Chipping On The Cutting Edge Of K68 Insert
(a) V = 20 m/min, Feed = 0.2 mm/rev, DOC = 2 mm
(b) V = 15 m/min, Feed = 0.4 mm/rev, DOC = 4 mm

Figure 7.38 Cutting and Feed Forces Versus Cutting Speed For K68 Inserts At 0.2 and 0.4 Feed Rates (Negative Geometry, DOC = 2 mm)

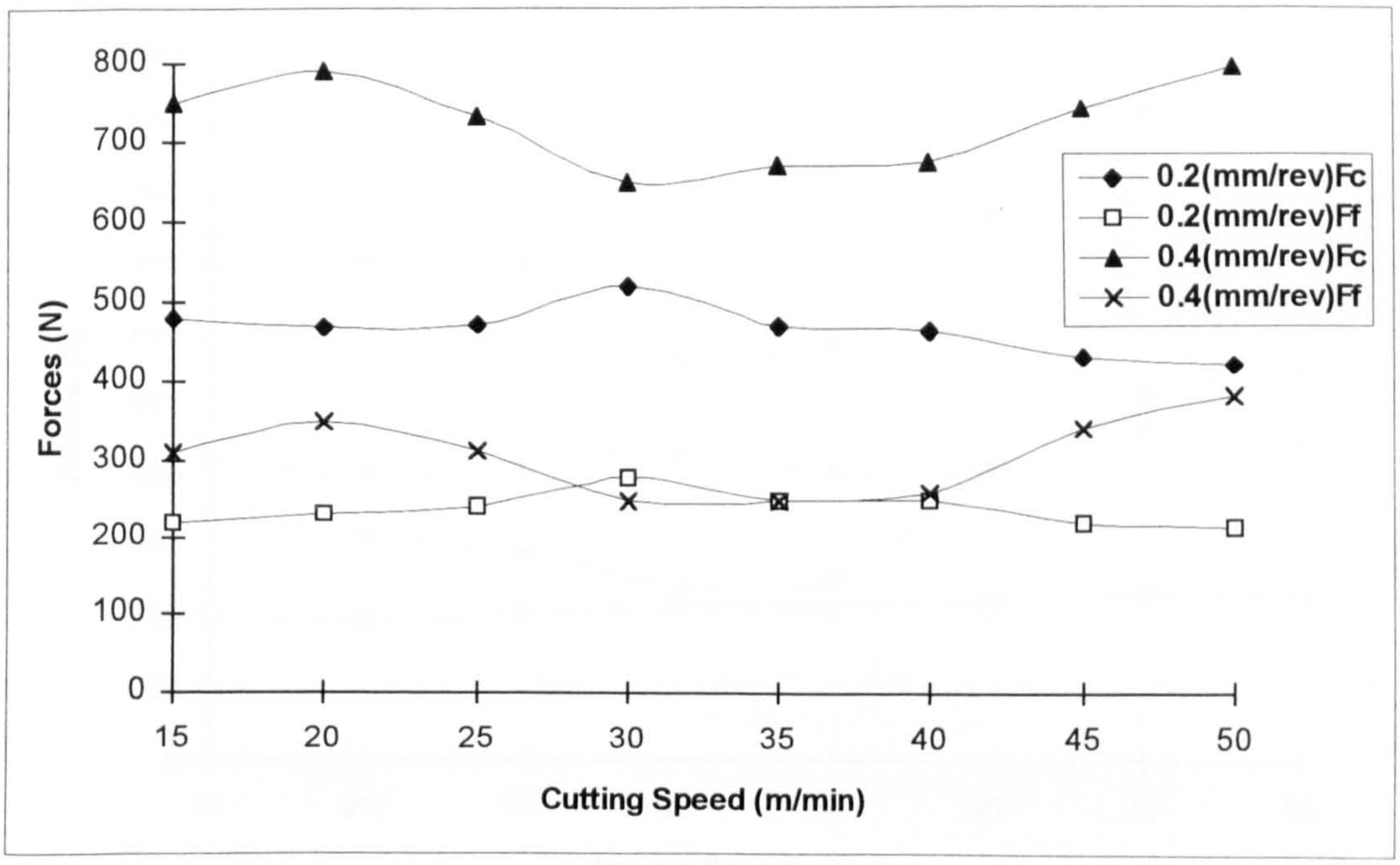

Figure 7.39 Cutting and Feed Forces Versus Cutting Speed For K68 Inserts At 0.2 and 0.4 Feed Rates (Positive Geometry, DOC = 2 mm)

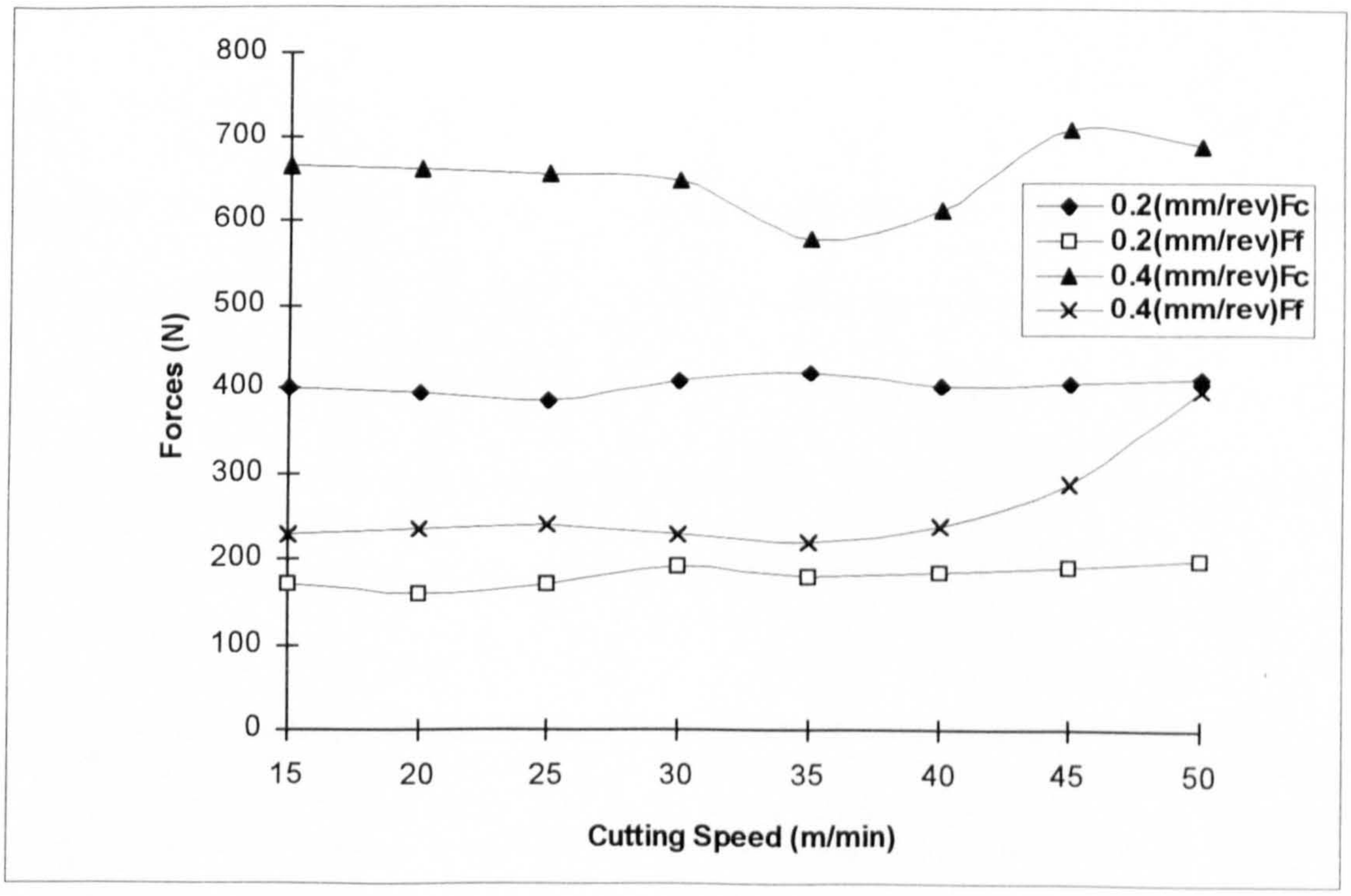

Figure 7.40 Cutting and Feed Forces Versus Cutting Speed For K68 Inserts At 0.2 and 0.4 Feed Rates (Negative Geometry, WITH Chip Breaker, DOC = 2 mm)

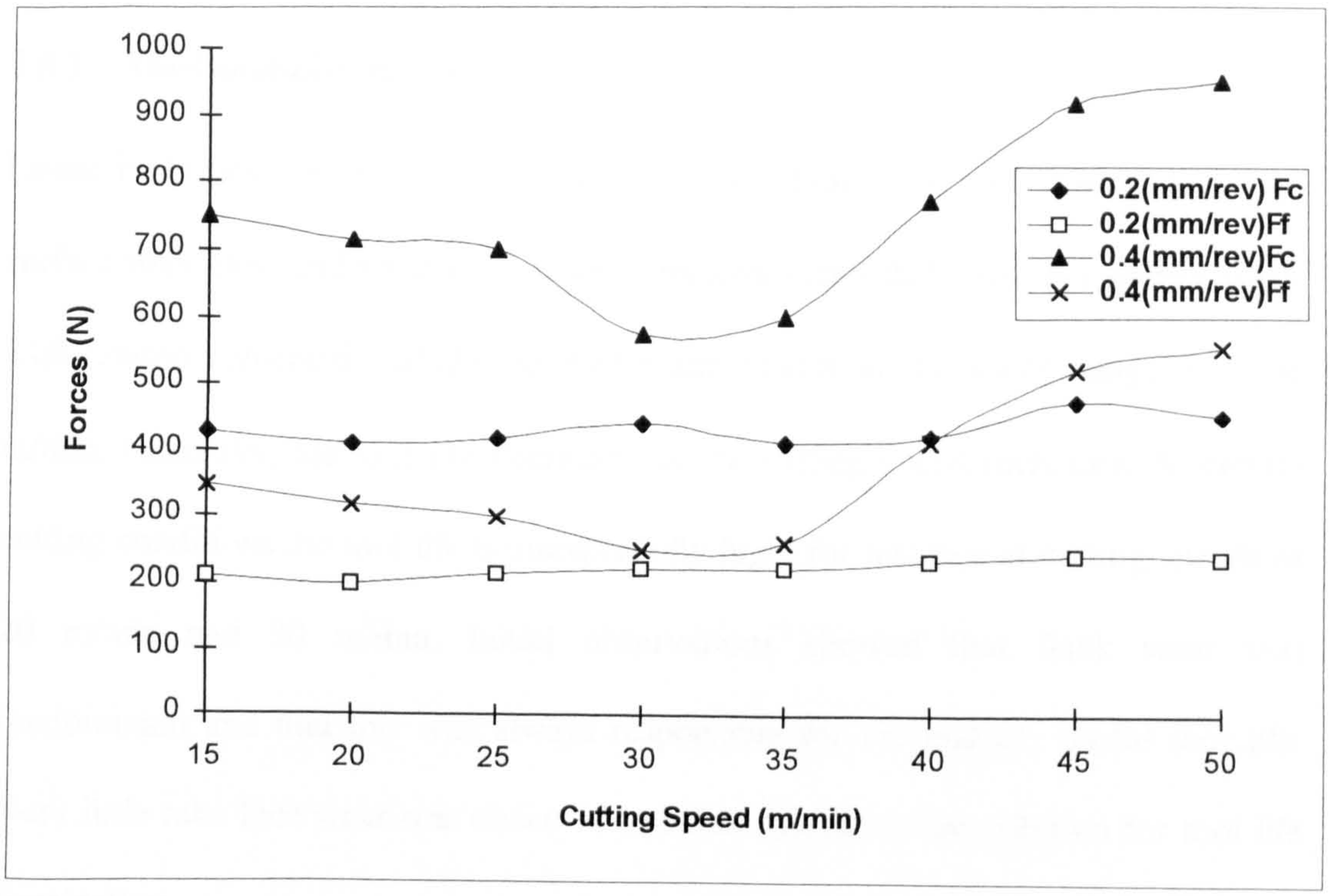

7.5 Machining With Coated Cemented Carbide Tools (KC910 Grade)

7.5.1 Machinability Results

Listed in Tables 7.9 and 7.10 in Appendix 1 are tool lives, tool failure mode, the surface roughness and volume of material removed recorded when machining MMC with coated cemented carbide, KC910 grade inserts in the speed range 15 - 50 m/min. Generally, the tool life decreases as the cutting speed increases. At certain cutting conditions the tool life is unexpectedly high, for instance at cutting speeds of 20 m/min and 30 m/min. Initial observations showed that flank wear was predominant and that this was always responsible for the end of useful tool life. Very little rake face wear was observed and this was never the criterion for tool life termination.

7.5.2 Tool Wear And Tool Life

The development of flank wear against cutting time at various cutting conditions and tool geometries in the speed range 15 to 50 m/min is represented in Figures 7.41 - 7.50. It was observed that the flank wear was rapid at the initial stage of machining. In most cases, the flank wear increase progressively with time. As the cutting speed is increased, the time to reach the defined tool life criteria decreases.

The tool life of KC910 inserts at each specified set of conditions is determined when the flank wear measurement has reached the specified value. Figures 7.51 to 7.55 show the tool life achieved at various cutting conditions with different tool geometry

in the speed range of 15 to 50 m/min when machining the MMC with KC910 inserts. The general trend is for the tool life to decrease as the cutting speed increases.

7.5.2.1 Effect of Tool Geometry on Tool Wear

(a) <u>Negative Rake Geometry</u>

Generally, there is a progressive increase in flank wear with increased material removal rate, as characterised by increases in the cutting speed, at all conditions. Figures 7.41 to 7.44 show the changes in tool flank wear for KC910 with a negative rake geometry with cutting time for feed rates of 0.2 mm/rev to 0.4 mm/rev and depths of cut of 2 mm and 4 mm. It was observed that the tool wear was rapid at the beginning but became uniform with time.

When machining at a low feed with negative rake geometry, Figure 7.41, the flank wear rate increased as the cutting speed increased up to 35 m/min. The wear rate decreased slightly at a cutting speed of 40 m/min. Further increases in speed to 45 m/min and 50 m/min resulted in rapid increases in the flank wear rate. A similar pattern of flank wear rate was observed when machining with negative rake geometry at 0.4 mm/rev, Figure 7.42. A slow flank wear rate were observed at speeds of 25 m/min and 30 m/min. Increasing the depth of cut from 2 mm to 4 mm, Figures 7.43 - 7.44, had no influence on the cutting time especially at 0.2 mm/rev but there is some influence on the cutting time at the feed rate 0.4 mm/rev, especially in the lower speed range between 15 m/min and 20 m/min. The tool reached the

maximum flank wear criterion (0.7 mm) when machining at 15 m/min for feeds of 0.4 mm/rev and 0.6 mm/rev.

(b) Positive Rake Geometry

Figures 7.45 to 7.48 show the average tool wear against cutting time for KC910 with a positive rake angle at various cutting conditions. Positive rake geometry KC910 inserts show less variation in the cutting time. Rapid flank wear was experienced at the lower feed rate of 0.2 mm/rev., and at cutting speeds over 25 m/min the wear reached the flank wear limit in less than 9 minutes. Increasing the feed rate from 0.2 mm/rev to 0.4 mm/rev has no significant effect on cutting time. Increasing the depth from 2 mm to 4 mm did not significantly influence the cutting time and rate of flank wear, Figures 7.47 and 7.48.

(c) Chip Breaker

Figures 7.49 and 7.50 show the average flank wear against cutting time for KC910 negative rake geometry with chip breaker. Gradual and constant wear was observed at 0.2 mm/rev. feed rate in the speed range 15 m/min to 30 m/min. Again, rapid flank wear rate was experienced when speed was increased from 35 m/min to 50 m/min. However, at 0.4 mm/rev feed, the slowest rate of flank wear is recorded at 25 m/min and the tool failed by the maximum flank wear criterion (i.e. Vb_{max} = 0.7 mm) instead of average flank wear. There was no significant influence of the chip breaker on the cutting time at 0.2 mm/rev feed rate, but there was some significant increases in tool life at 0.4 mm/rev feed rate.

7.5.2.2 Effect of Cutting Conditions on Tool Life

(a) <u>Effect of Cutting Speed</u>

The tool lives of negative and positive rake geometry inserts at various cutting condition in the cutting speed range 15 to 50 m/min is graphically represented in Figures 7.51 to 7.55. At most conditions, the tool life decreases steadily as the cutting speed increases. It was observed that there are unexpected increases in tool life at 2 mm DOC in the cutting speed range 20 to 30 m/min for negative rake geometry (Figure 7.51).

(b) <u>Effect of Feed Rate And DOC</u>

The effect of feed rates on tool life at various cutting speeds for KC910 inserts with negative and positive rake geometry at 2 mm and 4 mm depths of cut can be seen in Figures 7.51 to 7.55. The highest tool life recorded is at 20 m/min with a feed rate of 0.6 mm/rev. Further increases in cutting speed have shortened the tool life of the inserts at all feed rates. Positive rake geometry insert showed no significant difference in terms of tool life compared to negative rake geometry tools. Increased feed rates have extended the tool life, with the longest tool life of 35.5 minutes recorded at a speed of 20 m/min with 0.6 mm/rev feed. Increases in the depth of cut from 2 mm to 4 mm has less effect in terms of tool life than increasing the speed, Figures 7.54 - 7.55.

7.5.2.3 Taylor Tool Life Curve

Figures 7.56 - 7.58 show the relationship between the tool lives achieved against cutting speed when plotting on a log-log plot, as suggested by Taylor, according to the expression $VT^n = C$ (where V = cutting speed in metres per minute, T is the tool life in minutes, n is the Taylor exponent and C is constant). Best fit straight lines were calculated using standard regression techniques as described previously. Values for Taylor exponent (n) and constant (C) for KC910 at different cutting conditions are recorded Table 7.11, as are regression coefficients (r).

7.5.3 Volume of Material Removed

Tool performance between different tools at a given speed can be assessed by the volume of material removed during the life of the tool. The effect of feed rate and depth of cut upon tool wear were investigated for KC910 inserts. Bar charts in Figures 7.59 - 7.62 show the appropriate values recorded.

At a feed rate of 0.2 mm/rev. with 2 mm and 4 mm depth of cut, the volume of material removed for negative and positive rake tools is about constant in the speed range tested. As the tool life remains the same when the feed rate is increased to 0.4 mm/rev. the volume of material removed is almost doubled. This would suggest that increasing the feed rate could be an effective way of increasing both tool life and the material removal rate. This proved so in tests with negative rake geometry KC910 insert at 30 m/min at feed rates of 0.2 mm/rev and 0.4 mm/rev. These conditions can be employed in roughing cuts without experiencing additional wear problems. It has

been observed that positive rake geometry KC910 inserts are less sensitive to changing cutting conditions in the same way as negative geometry ones are with respect to tool life and hence material removal rate.

However, another way of representing tool lives can be obtained by plotting flank wear against the distance cut, Figures 7.63 and 7.64, the numerical data from which is recorded in Tables 7.12 - 7.13. This method simply ignores the DOC, i.e. it is a function of speed and feed. This plot allows for the fact that at higher cutting speeds, the tool cuts more material in the same unit of time than a tool used at slower cutting speeds. For KC910 inserts with negative rake geometry, Figures 7.63 and 7.64 indicate that from 35 to 40 m/min and 25 to 40 m/min respectively there is an increase in the distance which could be cut before generating 0.4 mm flank wear, i.e. tool life increases, with a marked increase taking place between 35 and 40 m/min. at a feed of 0.2 mm/rev, and between 25 and 30 m/min at a feed of 0.4 m/min. Increasing the cutting speed beyond 40 m/min was then found to reduce the cut distance with the maximum speed tested (50 m/min) producing the shortest distance.

A similar phenomenon occurred in the case of KC910 inserts with positive rake geometry. The longest distance cut is at a cutting speed of 20 m/min at both feed rates of 0.2 and 0.4 mm/rev., Table 7.14 (Appendix 1).

7.5.4 Tool Failure Modes and Wear Appearance

When machining with KC910 inserts, the tool life was limited by wear on the flank face of the insert. In all cases it was the flank wear which was the main criterion for tool rejection. Even though rake face wear and notching were observed during the tests they were never the tool life limiting factor.

The general tool wear appearance on the flank face, rake face and on the nose for KC910 inserts when machining aluminium 2618 MMC are shown in Figures 7.65(a) and 7.65 (b) respectively. Detailed results on the analysis of tool wear modes and wear mechanisms using SEM techniques and optical microscope are presented in the following section.

7.5.4.1 Flank Wear

Flank wear is the dominant wear when machining with KC910 inserts. Figures 7.66(a) and 7.66(b) show the flank wear modes occurring at the clearance face for both positive and negative rake geometries at different machining conditions. The flank wear area was even and smooth when cutting with negative and positive rake geometries. Further examination of the wear surfaces on the worn flank face at cutting speed of 20 m/min and 30 m/min revealed a smoothly polished wear with scratches parallel to the cutting direction as seen in Figures 7.67(a) (b) and (c). As it is suspected that the SiC particle may be responsible for producing scratches and sharp grooves on the flank face of KC910. In order to confirm this phenomenon, a number of KC910 inserts with work material adhering on the inserts were

metallurgically cross-section and prepared for further examination. The cross-section of KC910 inserts is shown in Figures 7.68(a) and (b) with SiC particle positioning on top of the rake face. These particles are believed to be responsible for producing scratches and grooves found on the worn flank face, Figure 7.67.

7.5.4.1 Rake Face Wear

Slight wear on the rake face of KC910 inserts was observed at most cutting conditions. Normally, the rake face is covered with a smeared layer of work material or built-up edge formation. Figure 7.69 shows slight rake face wear on the rake face of a KC910 insert after cleaning with 10% hydrochloric acid.

7.5.4.2 Notching and Chipping

Small amounts of notching at the depth of cut also was observed when machining at a speed of 15 m/min, as shown in Figure 7.70(a). A lower cutting speeds of 15 m/min and 20 m/min, chipping of the cutting edge was observed on KC910 inserts, as shown in Figure 7.70(b) and (c).

7.5.4.3 Effect of Coating On Tool Performance

It was observed that the coating was 'taken off' during machining with KC910 inserts. Figure 7.71 shows an overall view of KC910 inserts after machining, some of the coating has been lifted. A more detailed SEM photomicrograph of the 'lifting' of the coatings is shown in Figure 7.72(a). Further examination has shown that the

coating has worn through in this region revealing WC beneath the coating layer as seen in Figure 7.72(b). The photomicrograph in Figure 7.73(a) is a backscattered electron image of the flank wear produced when machining with KC910 insert at a speed of 20 m/min. The contrast from the backscattered image makes the progressive wear through the surface coatings to substrate clearly visible, i.e. the three distinct grey levels of the photomicrograph. Further analysis using EDAX of the individual areas seen confirmed that they represented carbide substrate, titanium carbide and alumina respectively, from top to bottom of the image, confirming the gradual progressive wear of both coatings. The X-ray analysis graph showing the composition of aluminium (Al), titanium (Ti) and cobalt (Co) is shown in Figure 7.73(b).

Further evidence of the lifting of the coating can seen from the SEM photomicrograph in Figure 7.74, which shows a cross-section on the flank face of a KC910 insert. The coating of the tool is believed to give some protection on the rake and flank face of the tool during the initial stage of machining but is taken off as machining continues.

7.5.6 Cutting Forces

Both cutting and feed forces were recorded over the speed range 15 - 50 m/min when machining with coated cemented carbide tools. As expected, the cutting force (F_c) was greater than the feed force (F_f). Cutting force and feed force generated during machining were recorded in Tables 7.15 - 7.16 in Appendix 1 and graphically

illustrated in Figures 7.75 and 7.77. In general, the positive geometry insert generated less cutting force and feed force than the negative geometry. At 0.2 mm/rev feed both positive and negative rake geometry experienced a constant cutting force and feed force over the range of cutting speeds tested. However, the opposite situation happened when the feed rate was increased to 0.4 mm/rev. Initially the cutting force was high, but as the speed was increased to 35 m/min, the cutting force dropped. When the cutting speed was increased above 35 m/min, the cutting force increased rapidly. As expected, the cutting force was more than doubled when the depth of cut was doubled, Table 7.16 (Appendix 1). The increased in cutting forces may be explained by the fact that the tool/workpiece interface conditions altered, and hence the effective geometry of the cutting tool changes, leading to a rise in the cutting forces.

The positive and negative rake inserts behaved almost in the same manner at 0.2 mm/rev feed rate where forces are almost constant through the speed range tested. As the feed was increased, negative rake geometry tools generated a higher cutting force than positive rake geometry tools. The presence of a chip breaker has little effect on the cutting force when machining with KC910 cemented carbide inserts.

Figure 7.41 Average Flank Wear Against Cutting Time For KC910 Inserts (Negative Geometry, Feed = 0.2 mm/rev, DOC = 2 mm)

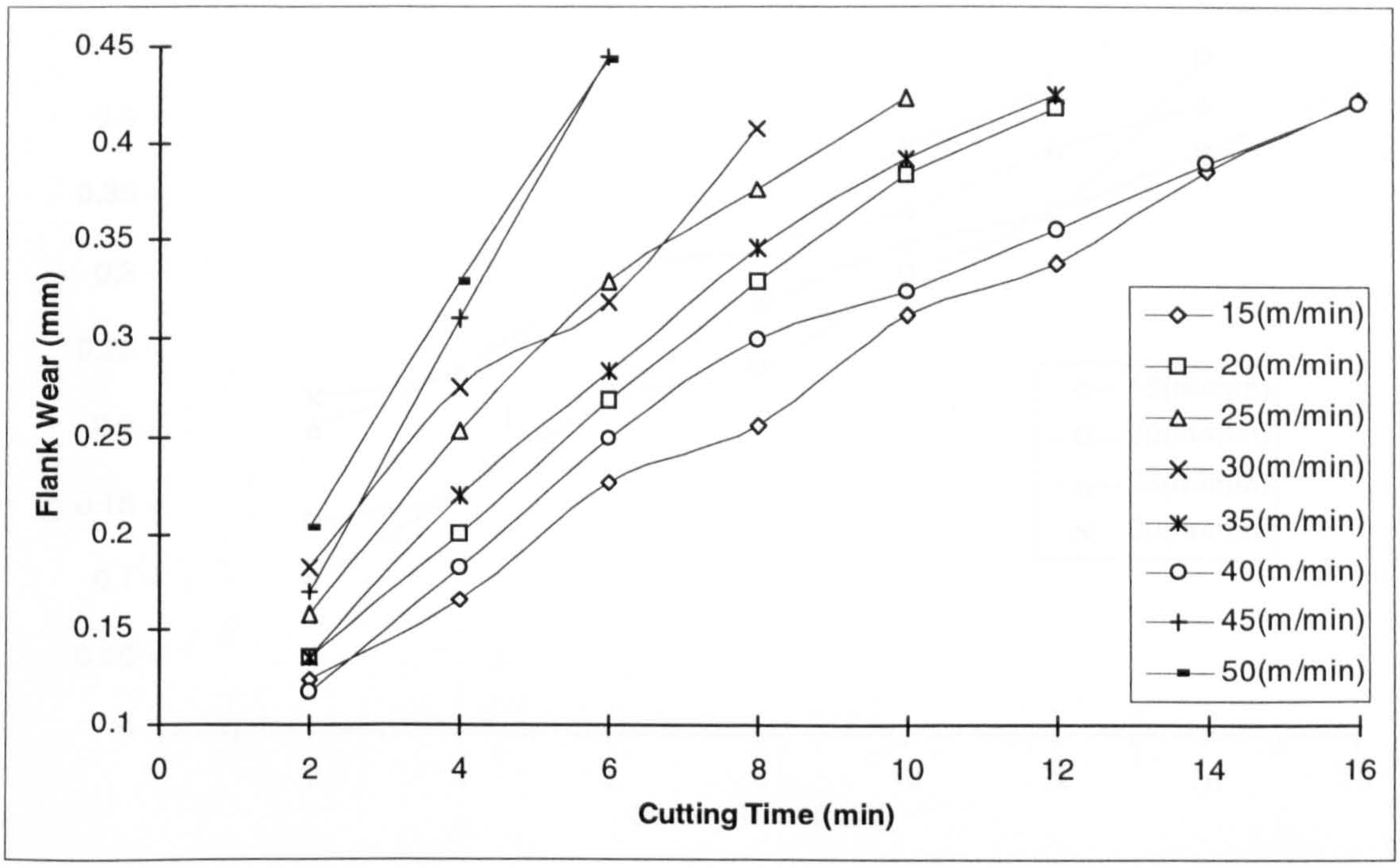

Figure 7.42 Average Flank Wear Against Cutting Time For KC910 Inserts (Negative Geometry, Feed = 0.4 mm/rev, DOC = 2 mm)

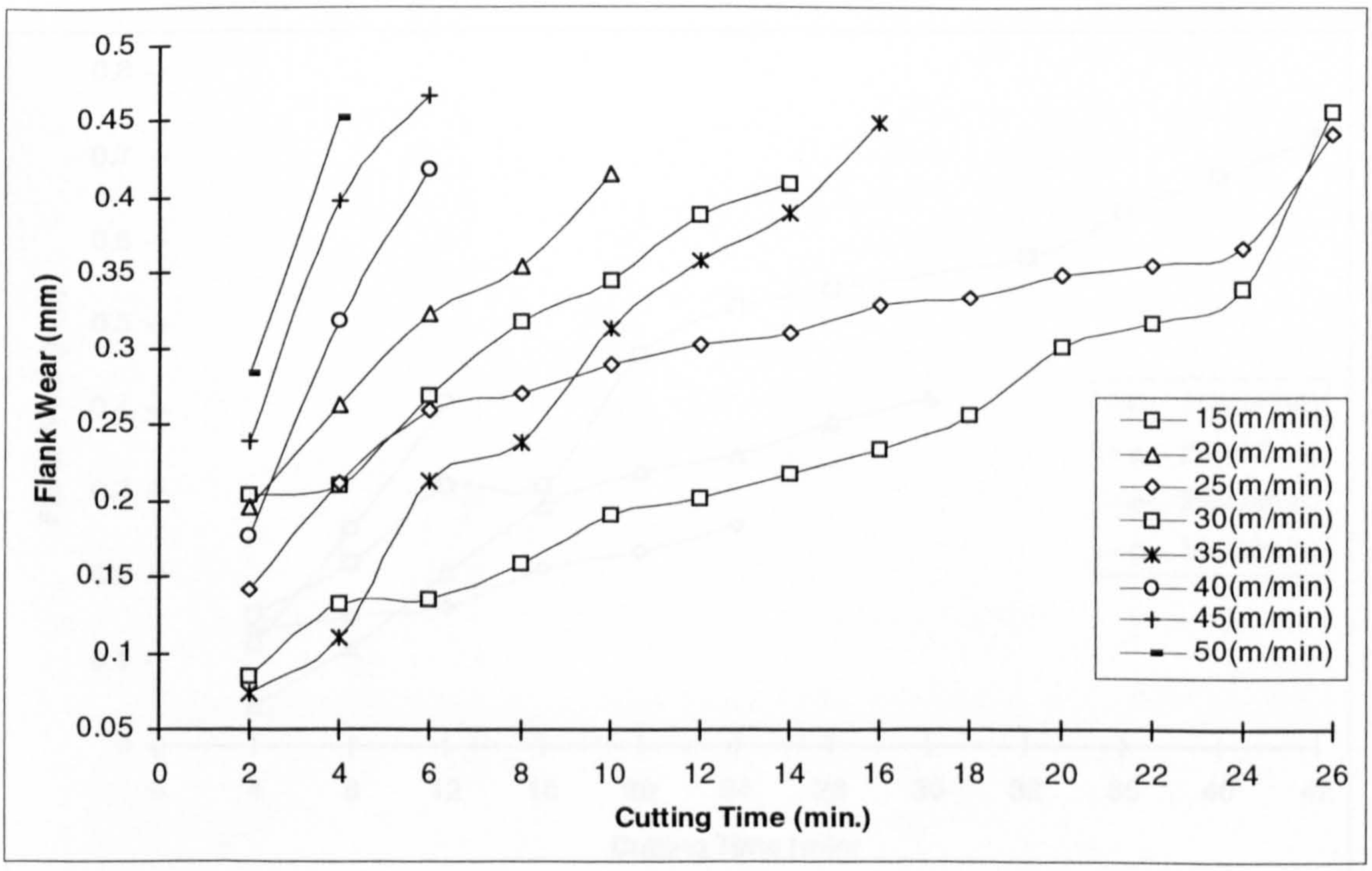

Figure 7.43 Average Flank Wear Against Cutting Time For KC910 Inserts (Negative Geometry, Feed = 0.2 mm/rev, DOC = 4 mm)

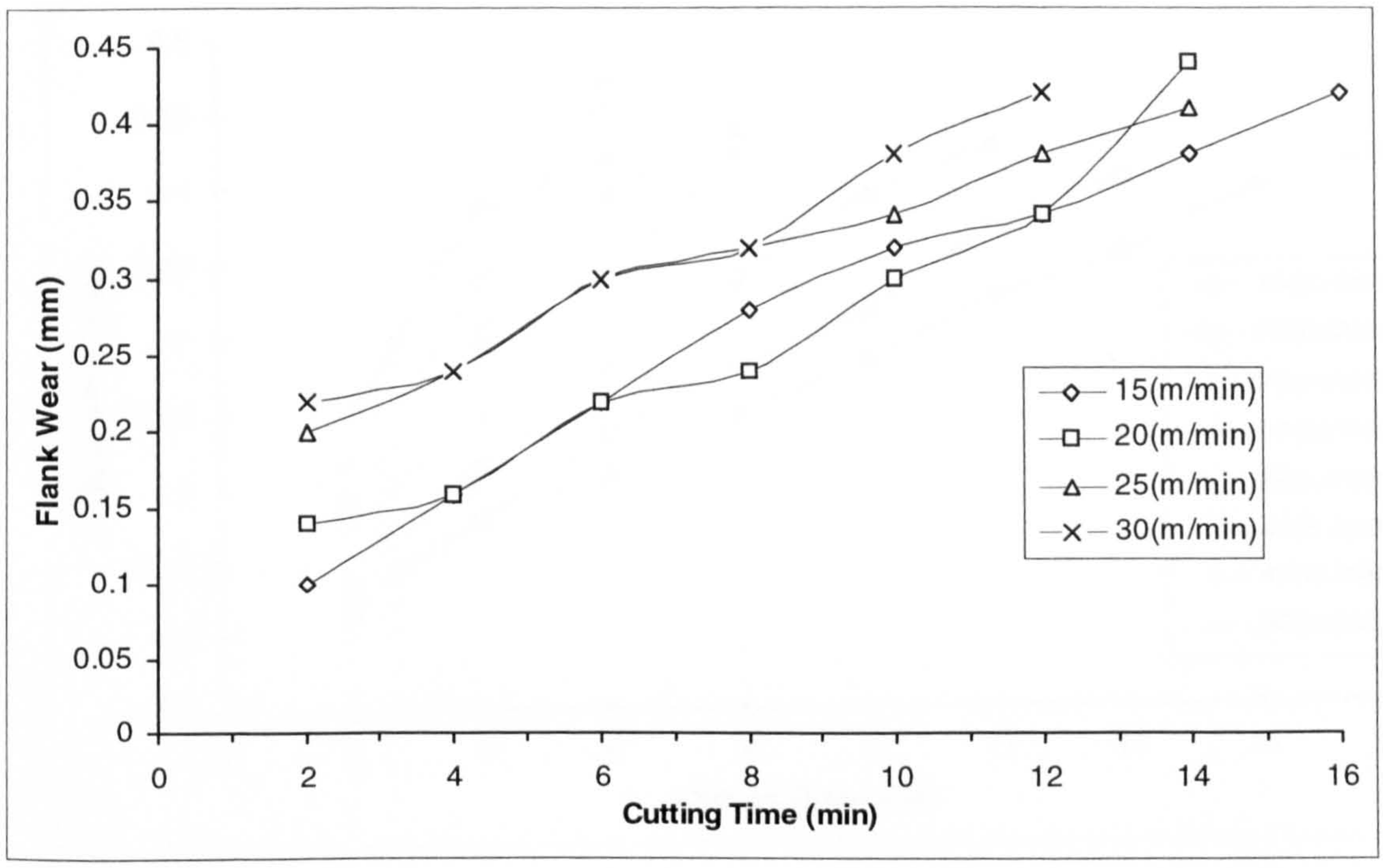

Figure 7.44 Average Flank Wear Against Cutting Time For KC910 Inserts (Negative Geometry, Feed = 0.4 mm/rev, DOC = 4 mm)

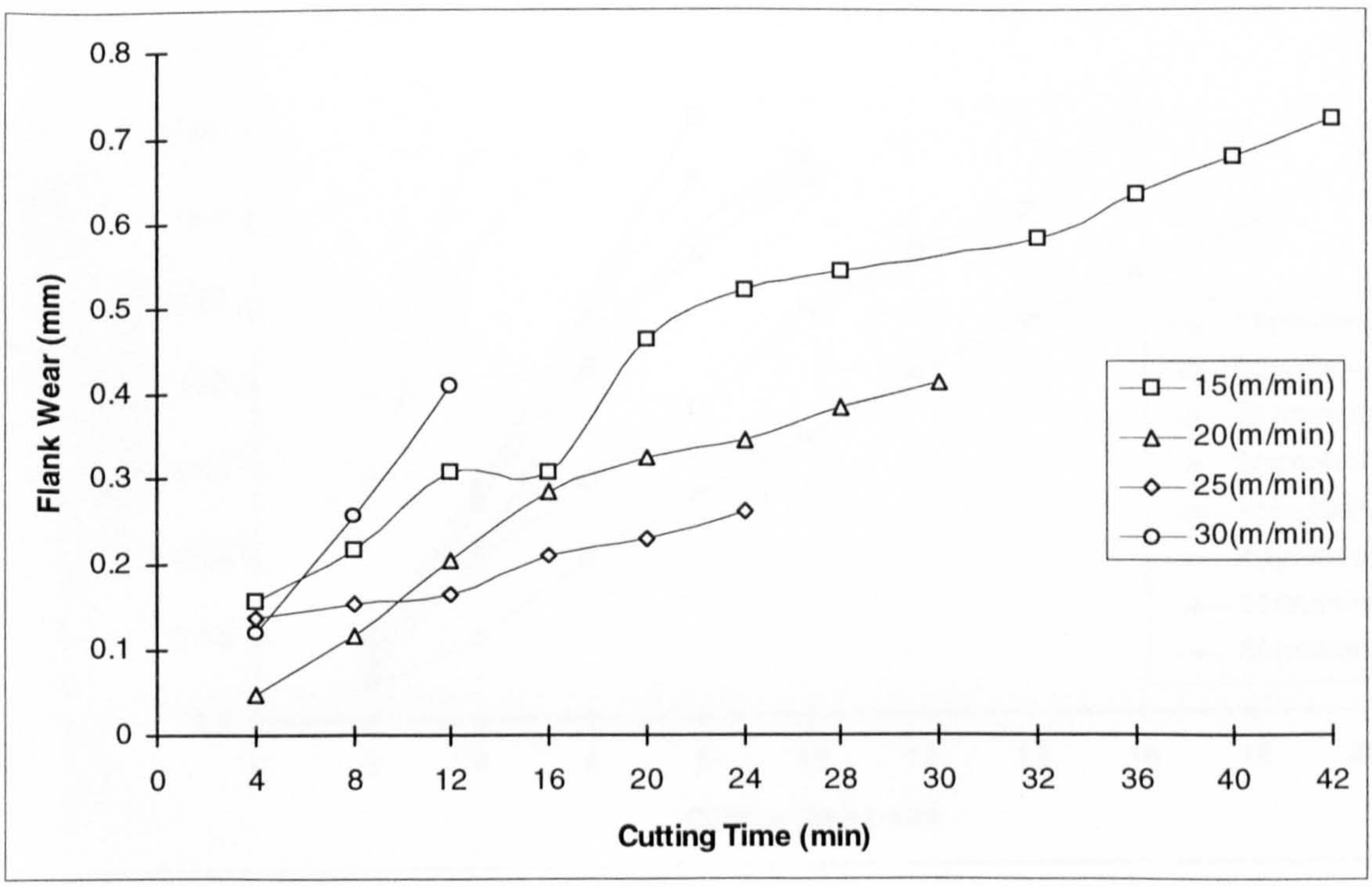

Figure 7.45 Average Flank Wear Against Cutting Time For KC910 Inserts (Positive Geometry, Feed = 0.2 mm/rev, DOC = 2 mm)

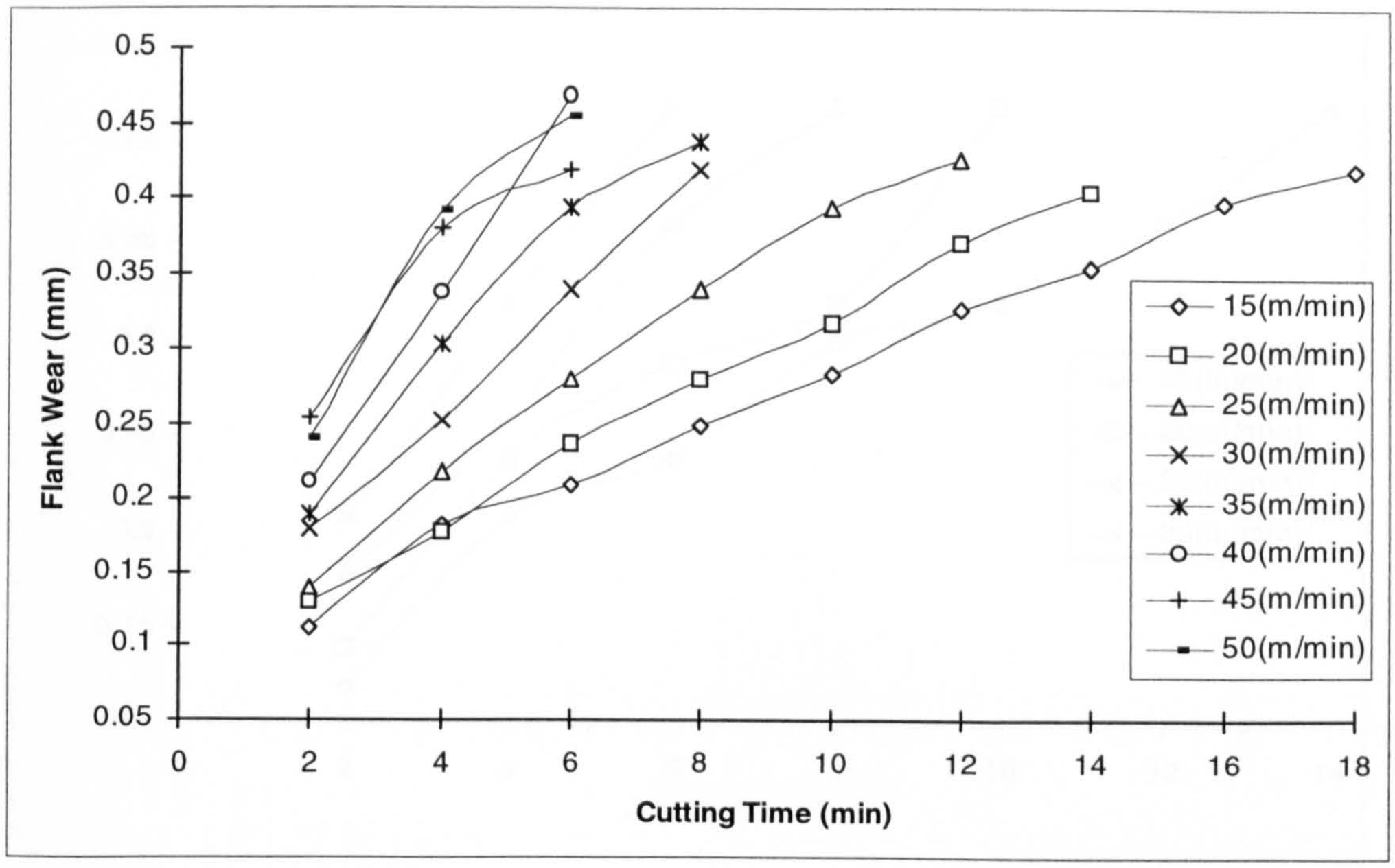

Figure 7.46 Average Flank Wear Against Cutting Time For KC910 Inserts (Positive Geometry, Feed = 0.4 mm/rev, DOC = 2 mm)

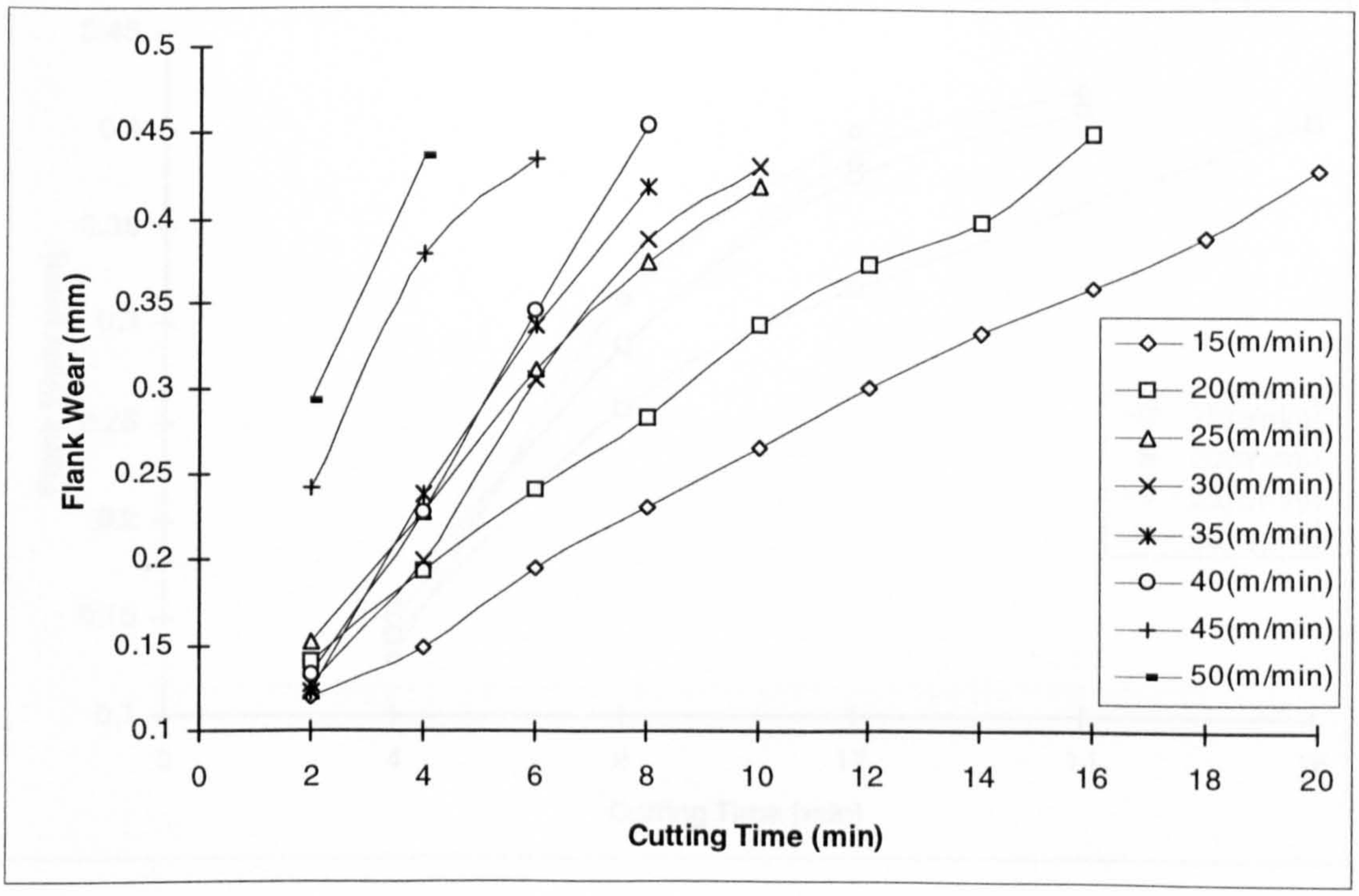

Figure 7.47 Average Flank Wear Against Cutting Time For KC910 Inserts (Positive Geometry, Feed = 0.2 mm/rev, DOC = 4 mm)

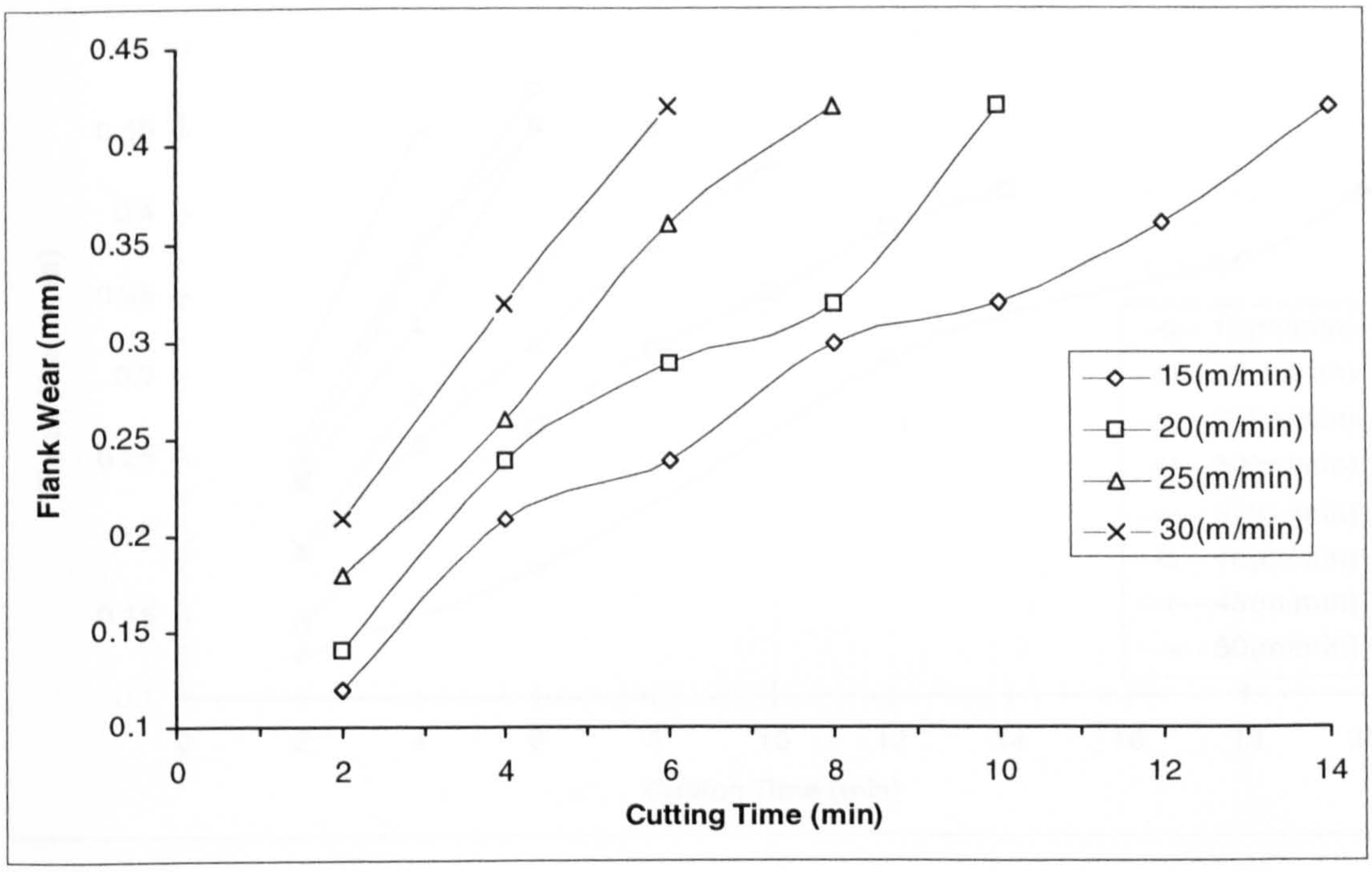

Figure 7.48 Average Flank Wear Against Cutting Time For KC910 Inserts (Positive Geometry, Feed = 0.4 mm/rev, DOC = 4 mm)

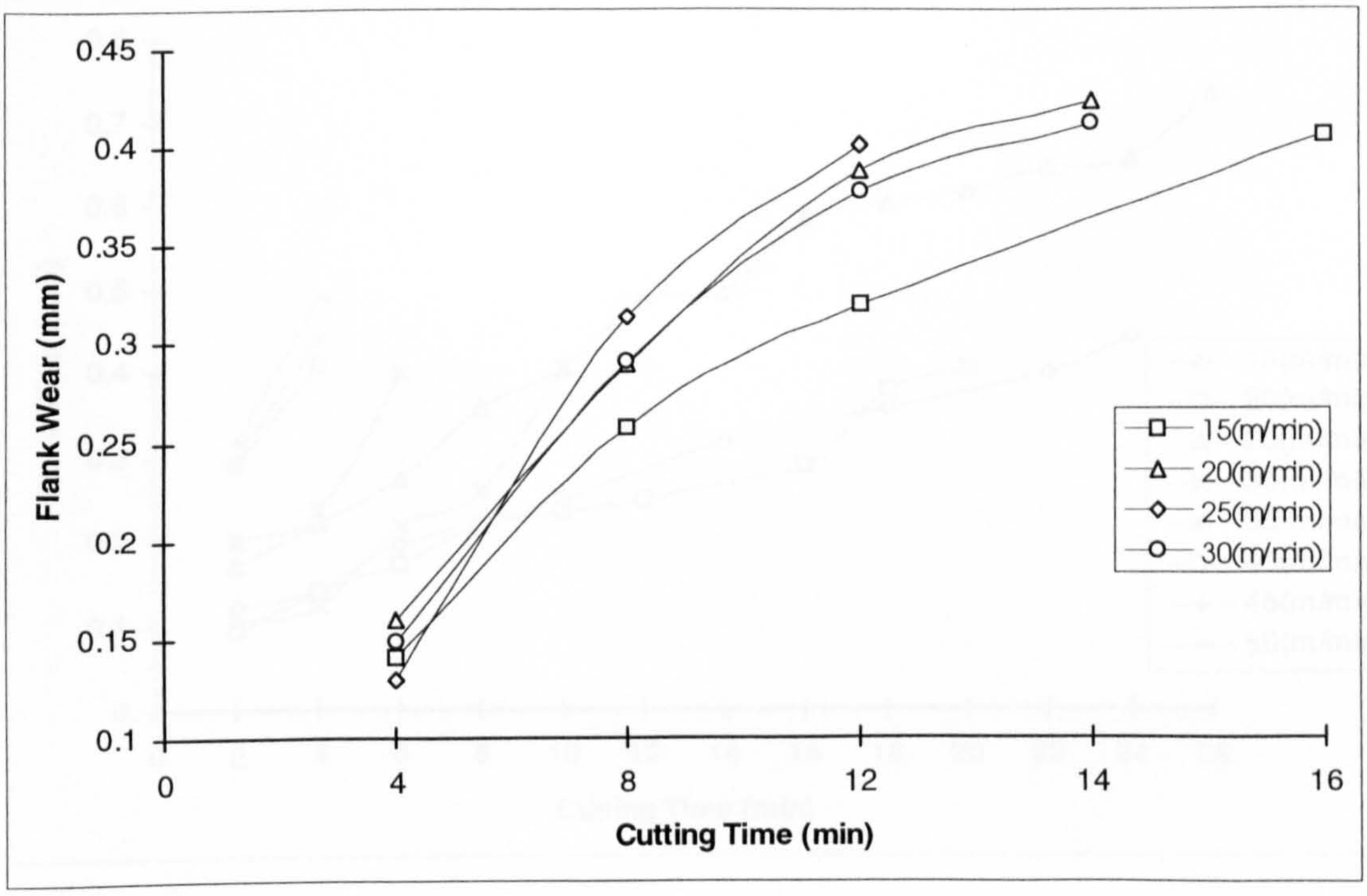

Figure 7.49 Average Flank Wear Against Cutting Time For KC910 Inserts (Negative Geometry,WITH Chip Braker, Feed = 0.2 mm/rev, DOC = 2 mm)

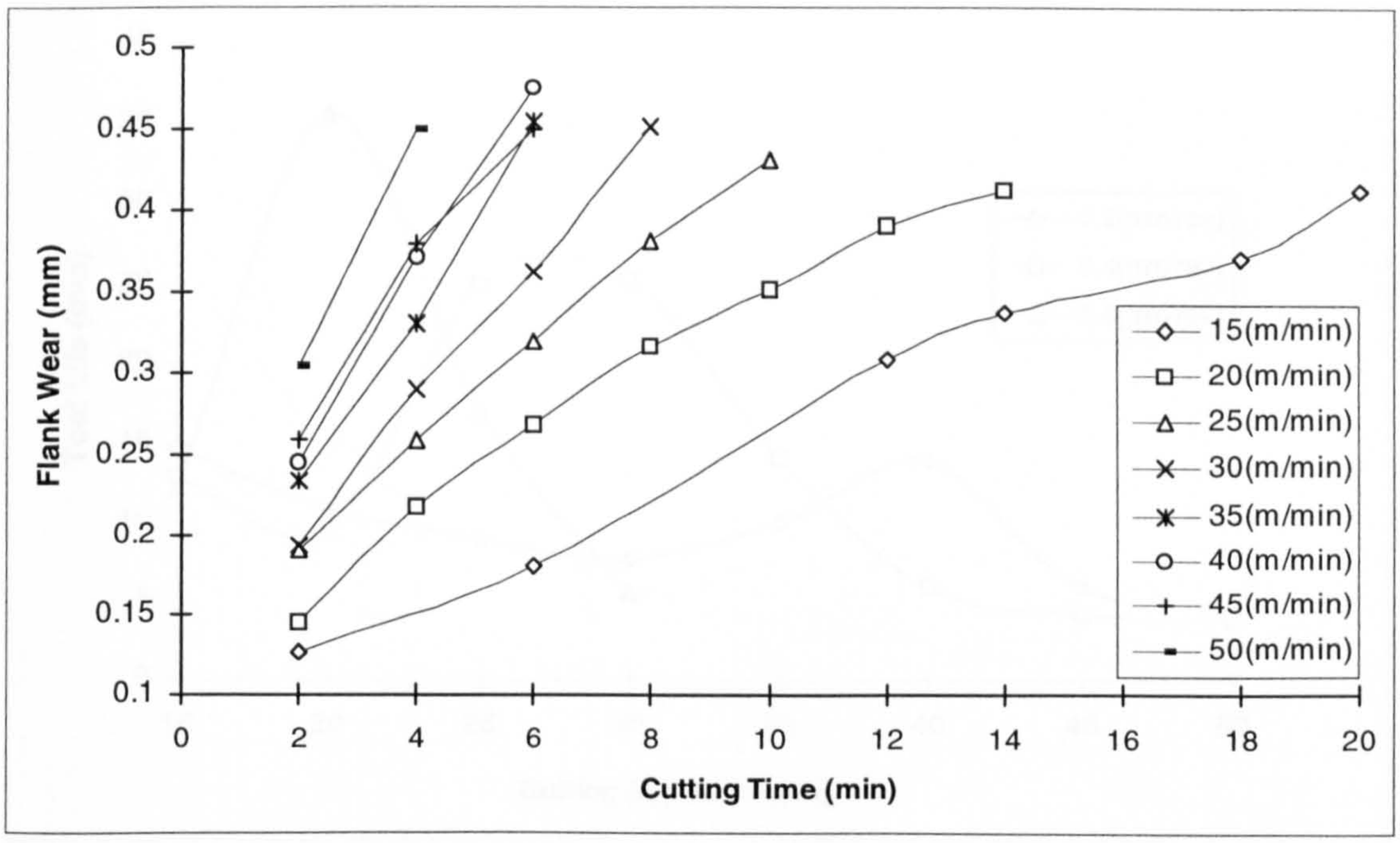

Figure 7.50 Average Flank Wear Against Cutting Time For KC910 Inserts (Negative Geometry,WITH Chip Breaker, Feed = 0.4 mm/rev, DOC = 2 mm)

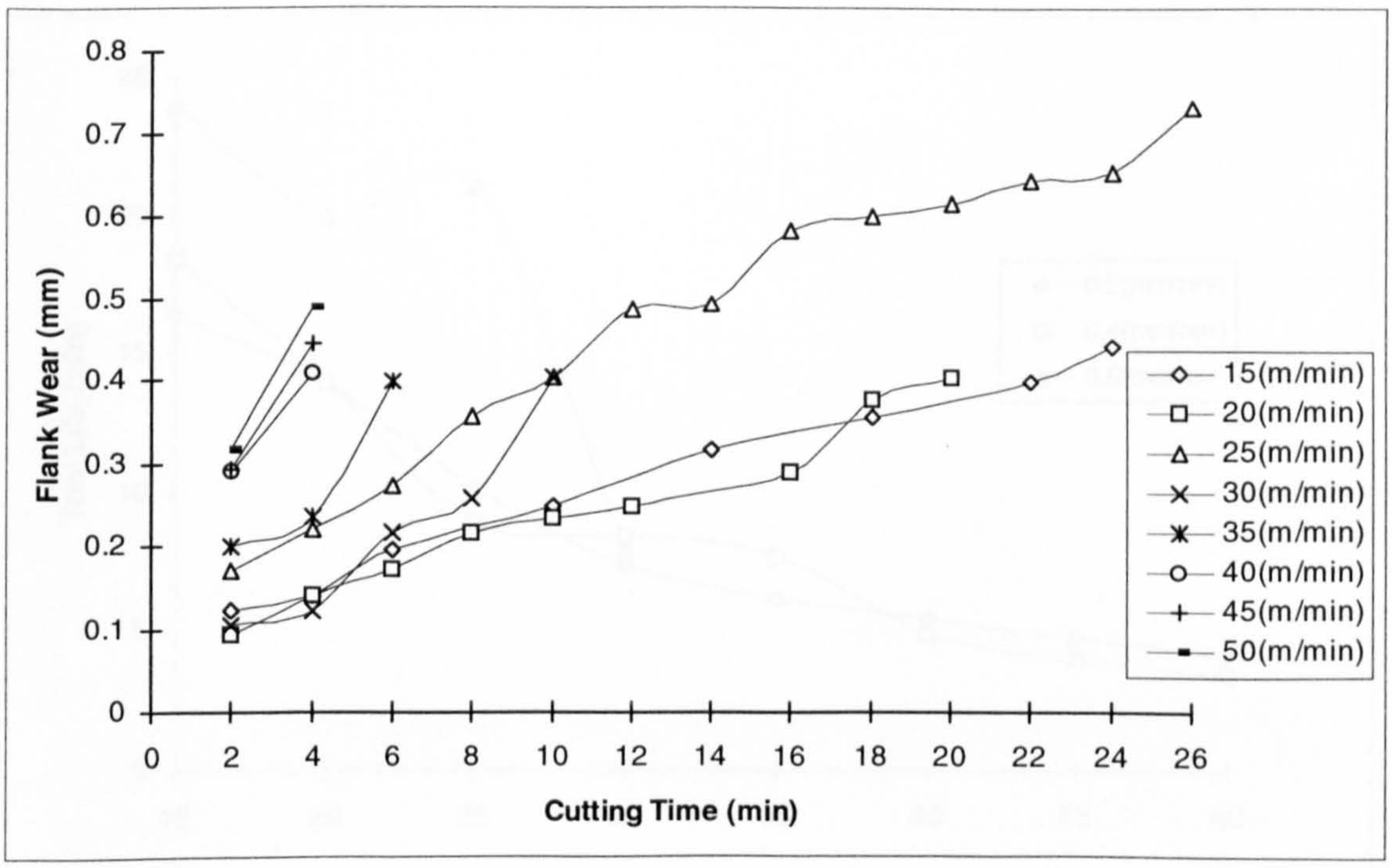

Figure 7.51 Tool Life Versus Cutting Speed For KC910 Inserts At Different Feed Rates (Negative Geometry, DOC = 2 mm)

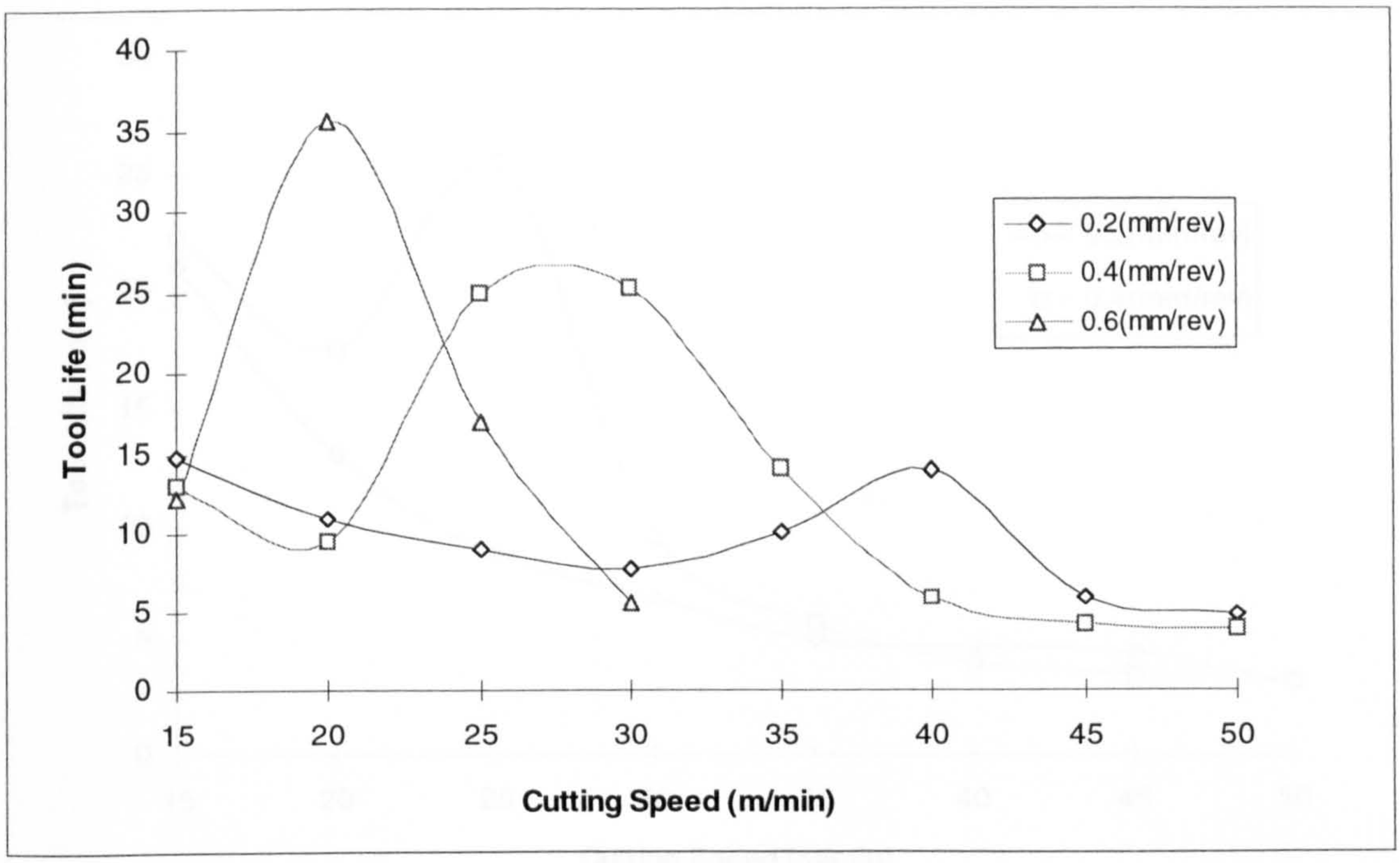

Figure 7.52 Tool Life Versus Cutting Speed For KC910 Inserts At Different Feed Rates (Positive Geometry, DOC = 2 mm)

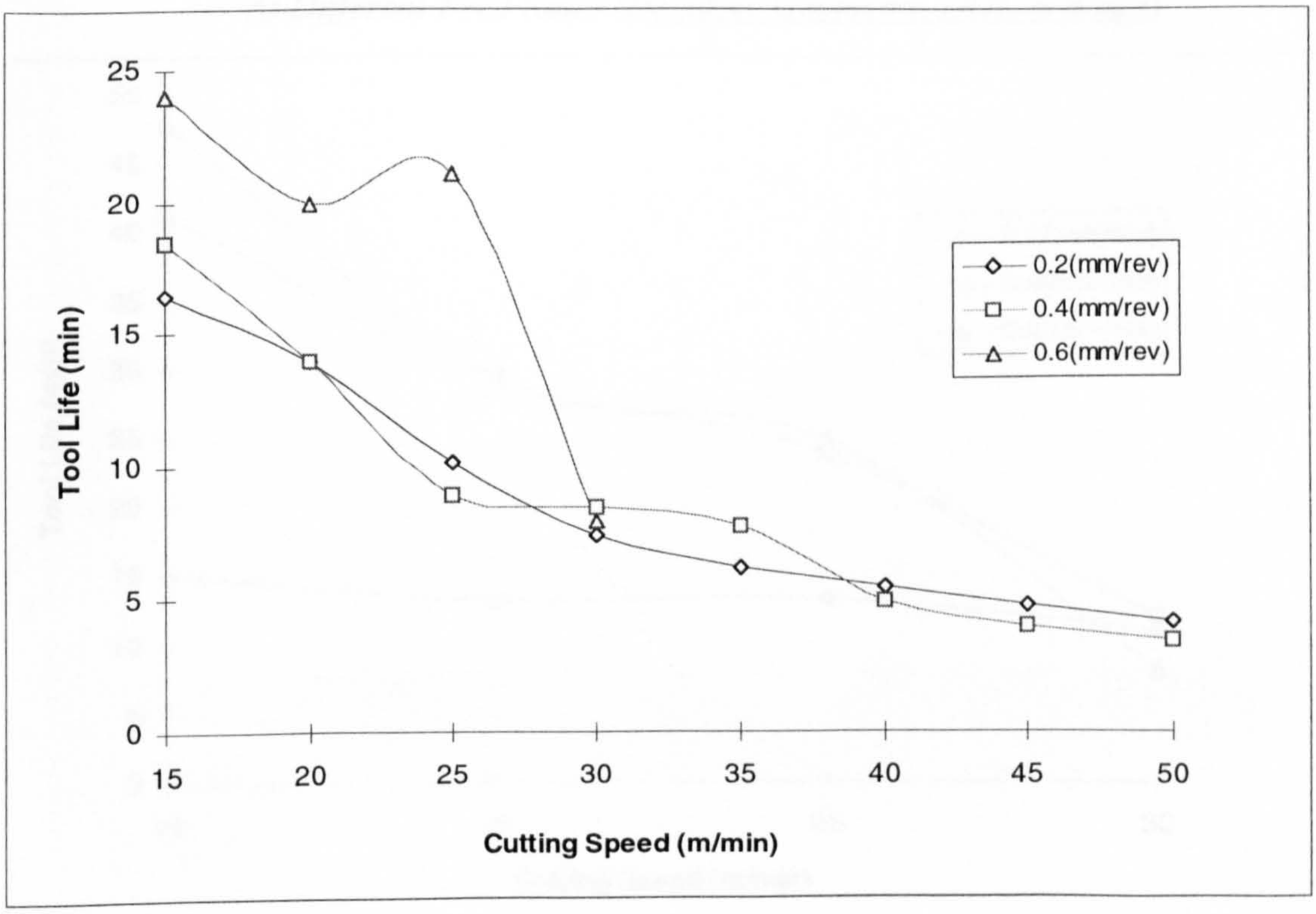

Figure 7.53 Tool Life Versus Cutting Speed For KC910 Inserts At Different Feed Rates (Negative Geometry, WITH CHIP BREAKER, DOC = 2 mm)

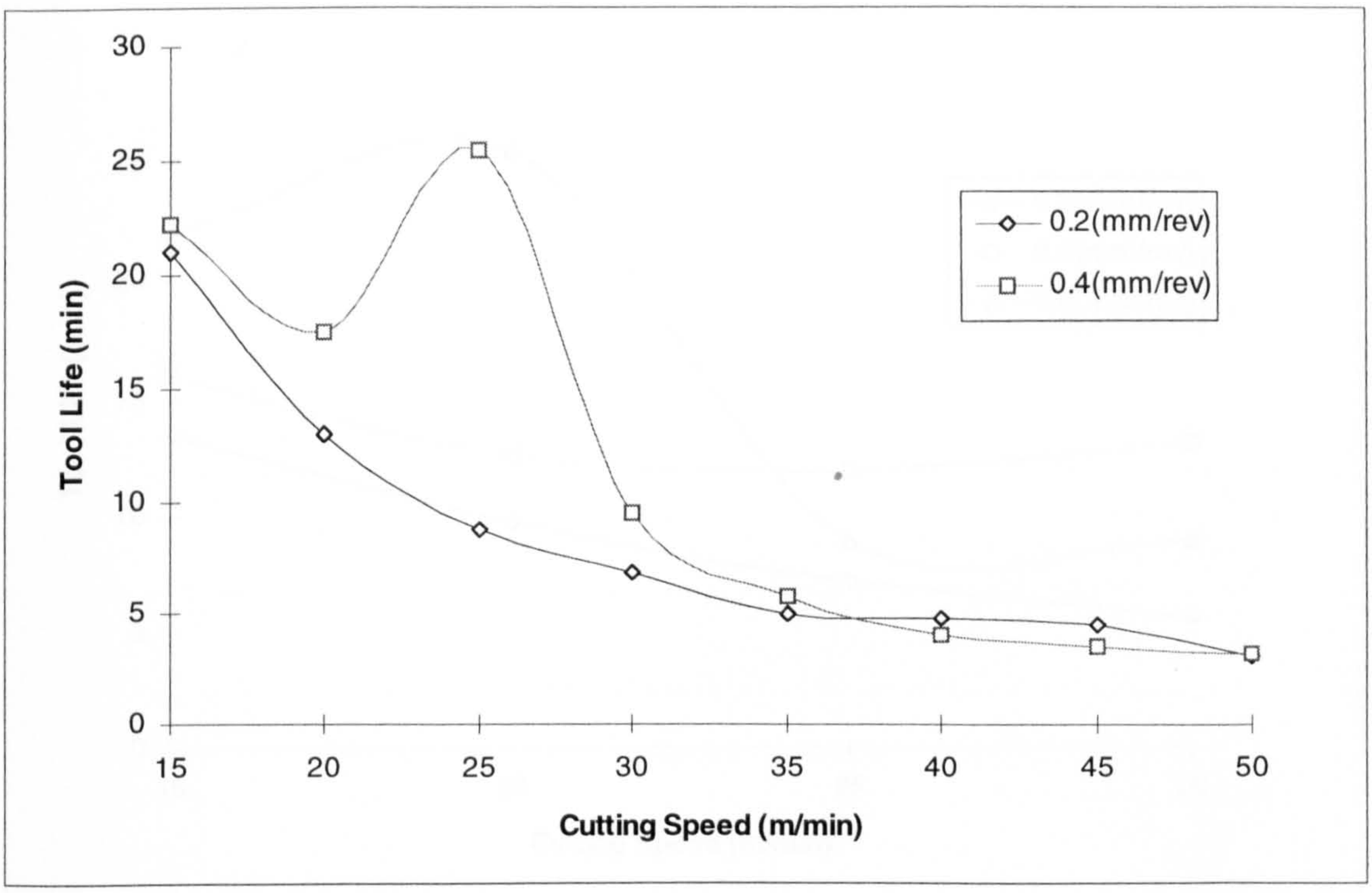

Figure 7.54 Tool Life Versus Cutting Speed For KC910 Inserts At Different Feed Rates (Negative Geometry, DOC = 4 mm)

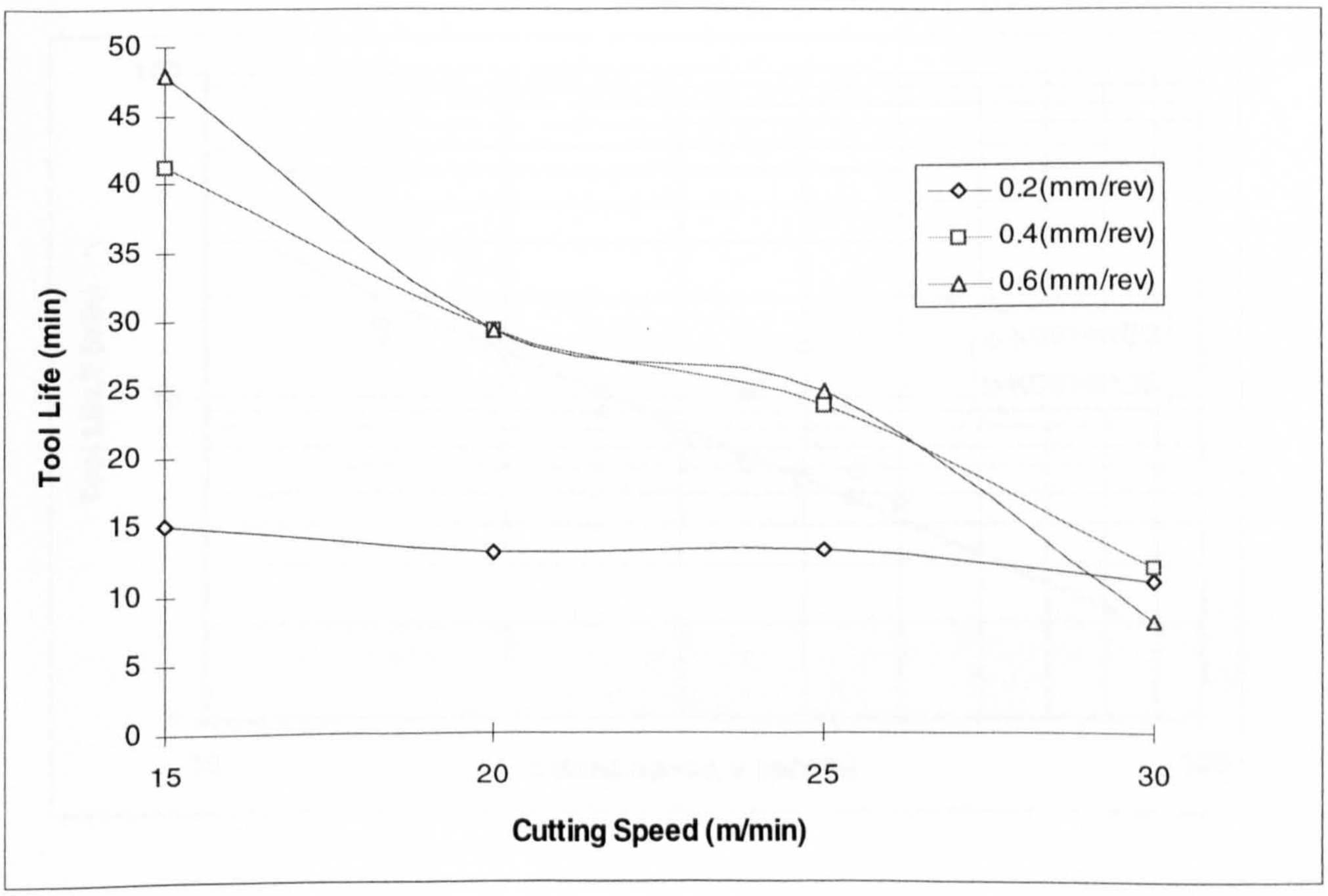

Figure 7.55 Tool Life Versus Cutting Speed For KC910 Inserts At Different Feed Rates (Positive Geometry, DOC =4 mm)

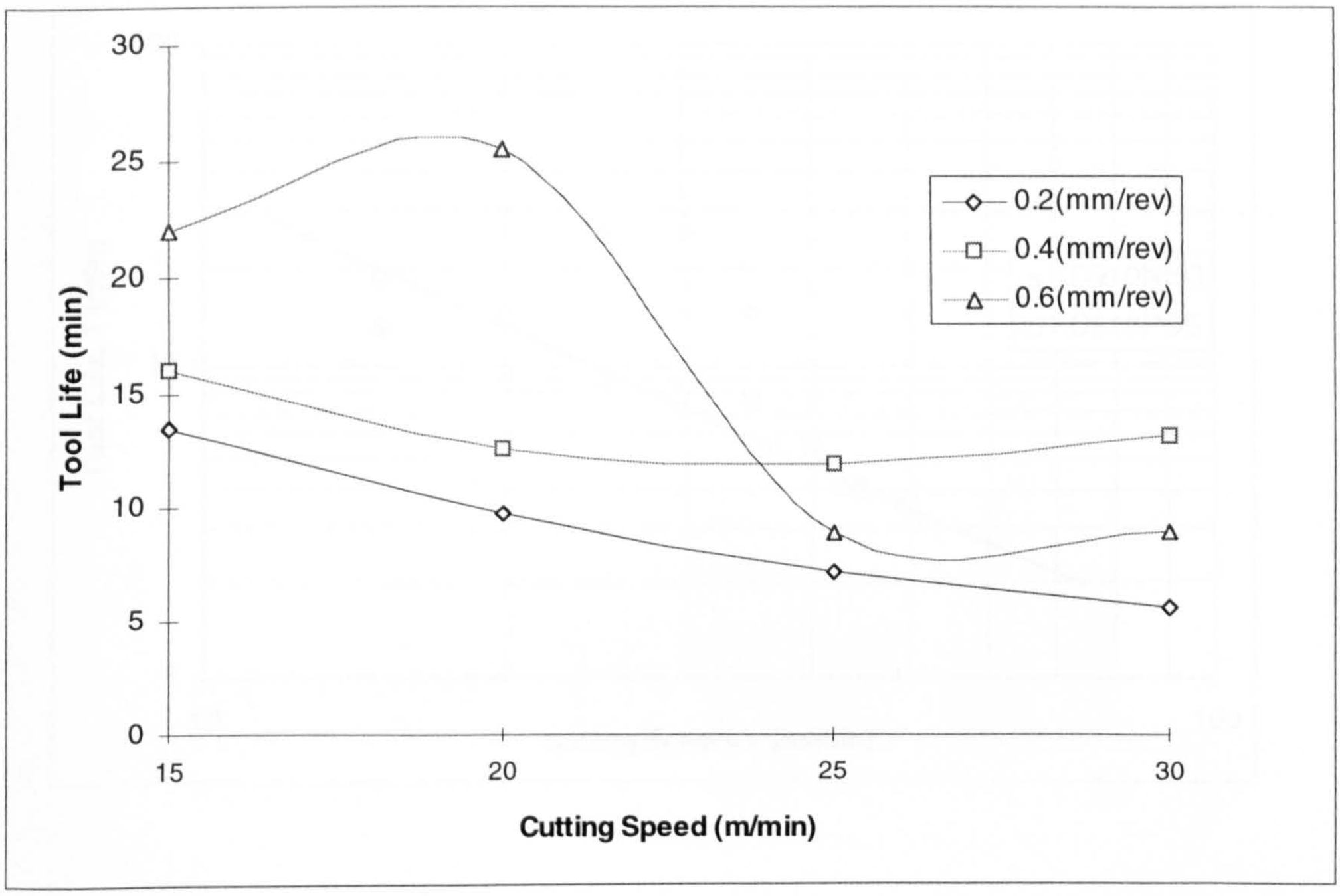

Figure 7.56 Taylor Tool Life Curve For KC910 Inserts (Feed = 0.2 mm/rev, DOC = 2 mm)

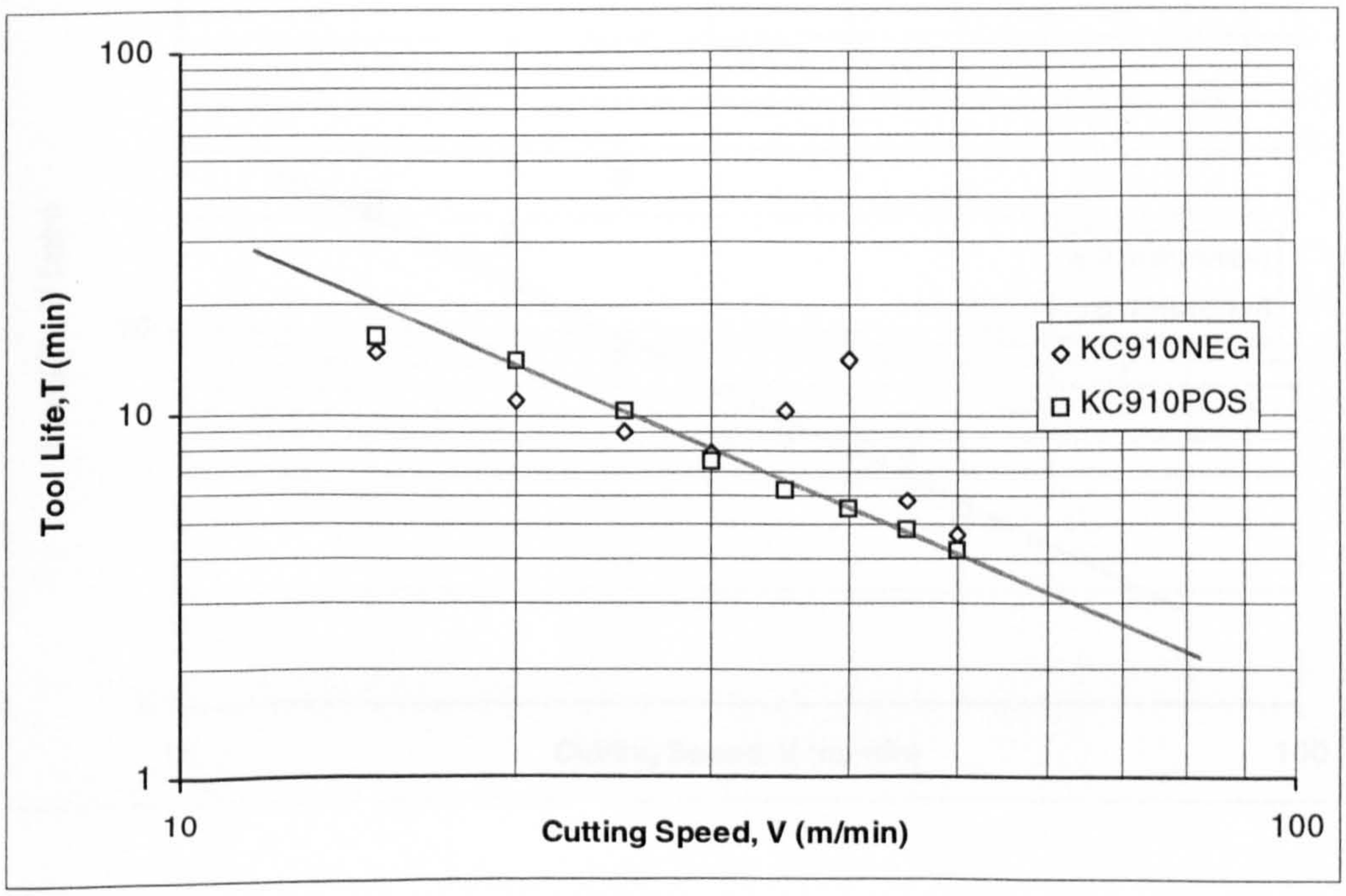

Figure 7.57 Taylor Tool Life Curve For KC910 Inserts (Feed = 0.4 mm/rev, DOC = 2 mm)

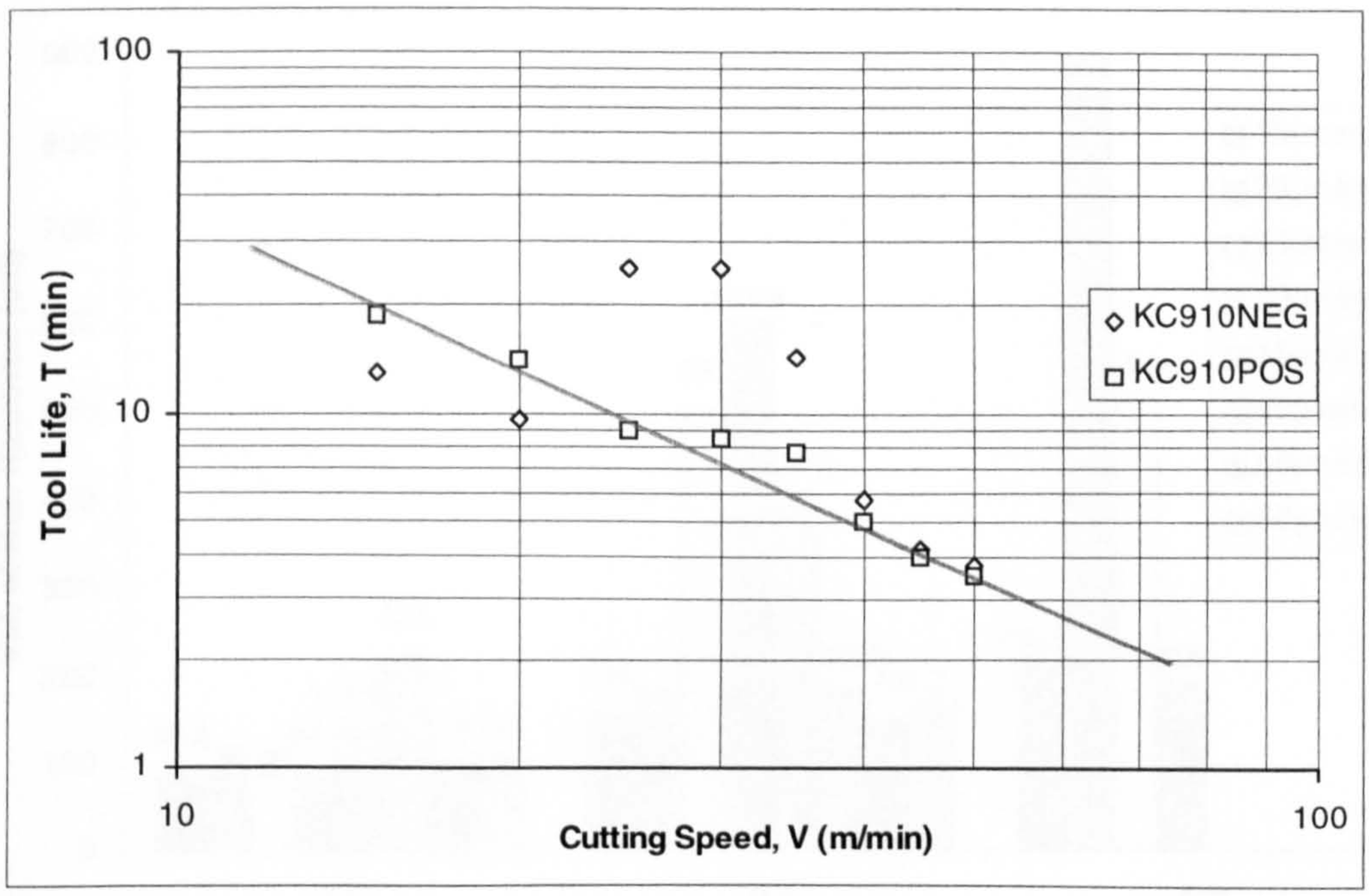

Figure 7.58 Taylor Tool Life Curve For KC910 Inserts With 0.2 (mm/rev) And 0.4 (mm/rev) Feed (WITH Chip Breaker, DOC = 2 mm)

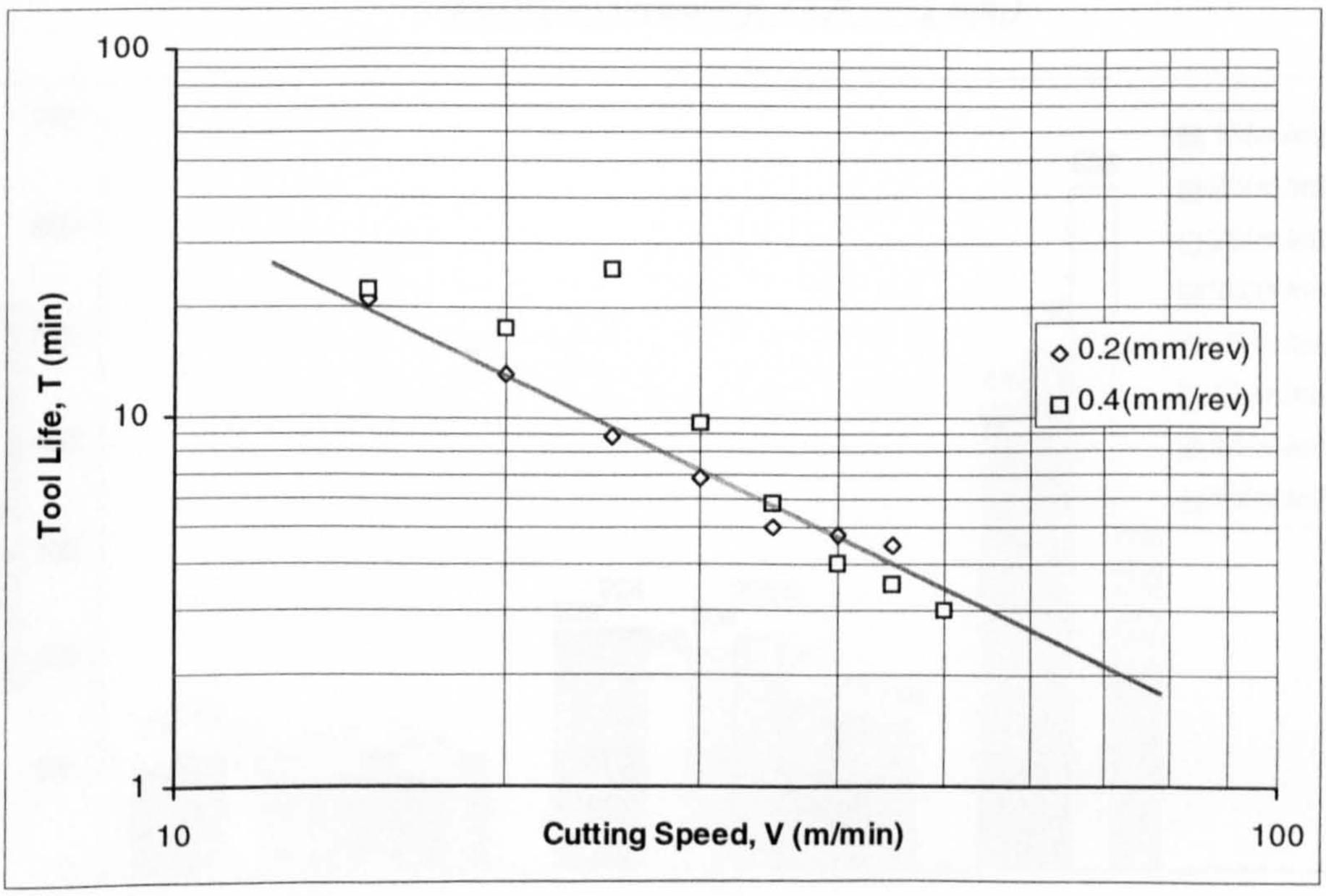

Figure 7.59 Volume Of Material Removed When Machining With KC910 Inserts (Negative Geometry, DOC = 2 mm)

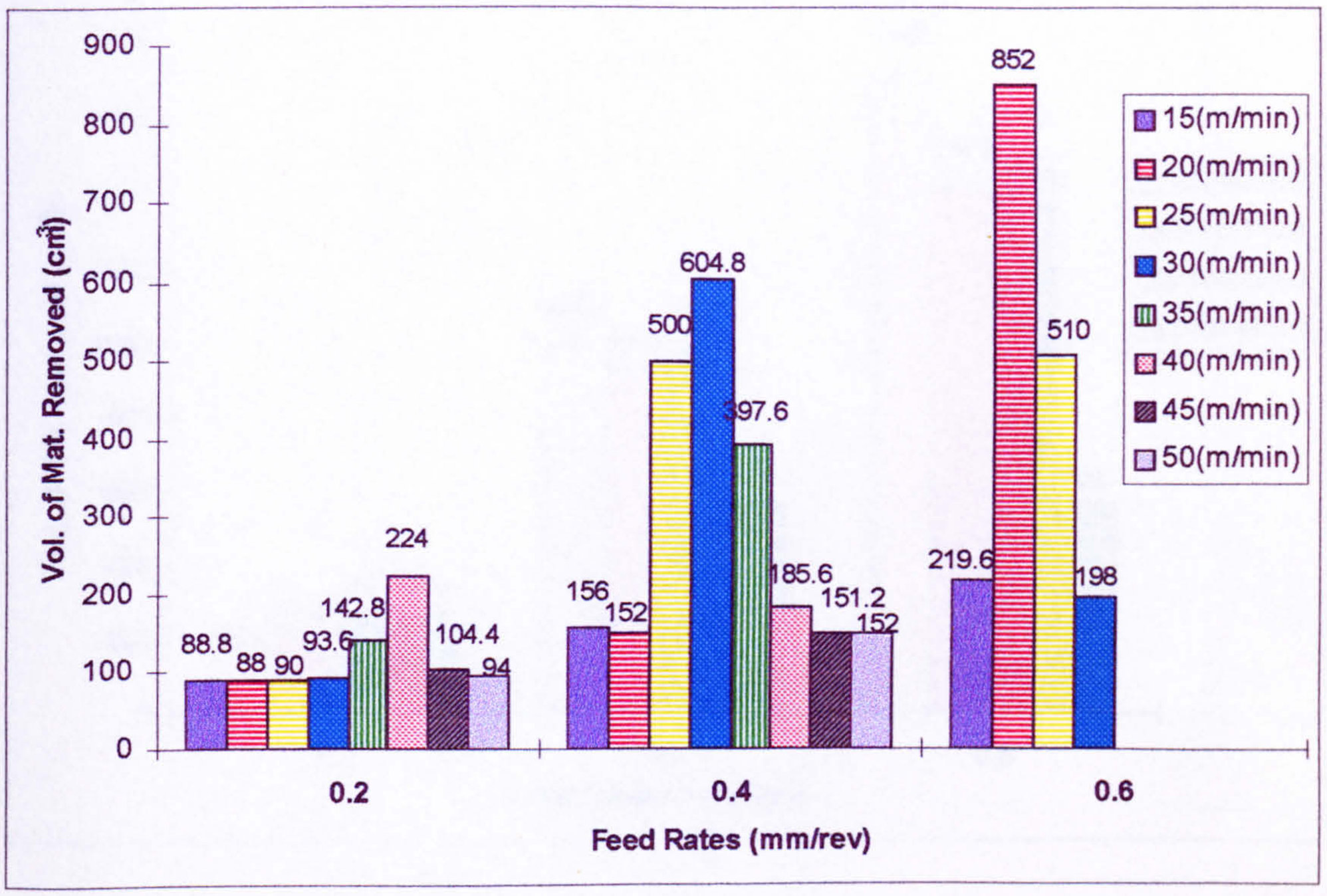

Figure 7.60 Volume Of Material Removed When Machining With KC910 Inserts (Positive Geometry, DOC = 2 mm)

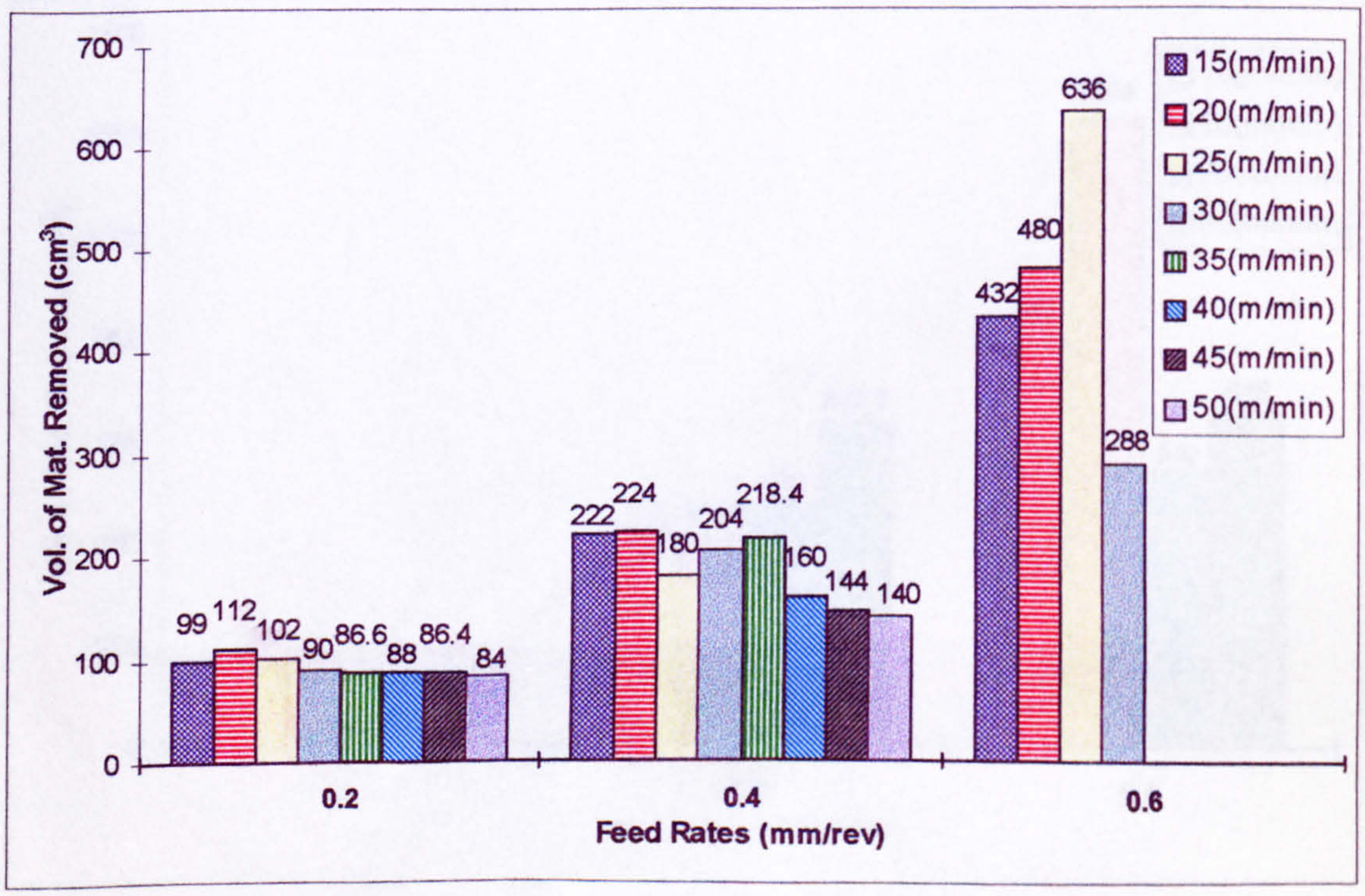

Figure 7.61 Volume Of Material Removed When Machining With KC910 Inserts (Negative Geometry, DOC = 4 mm)

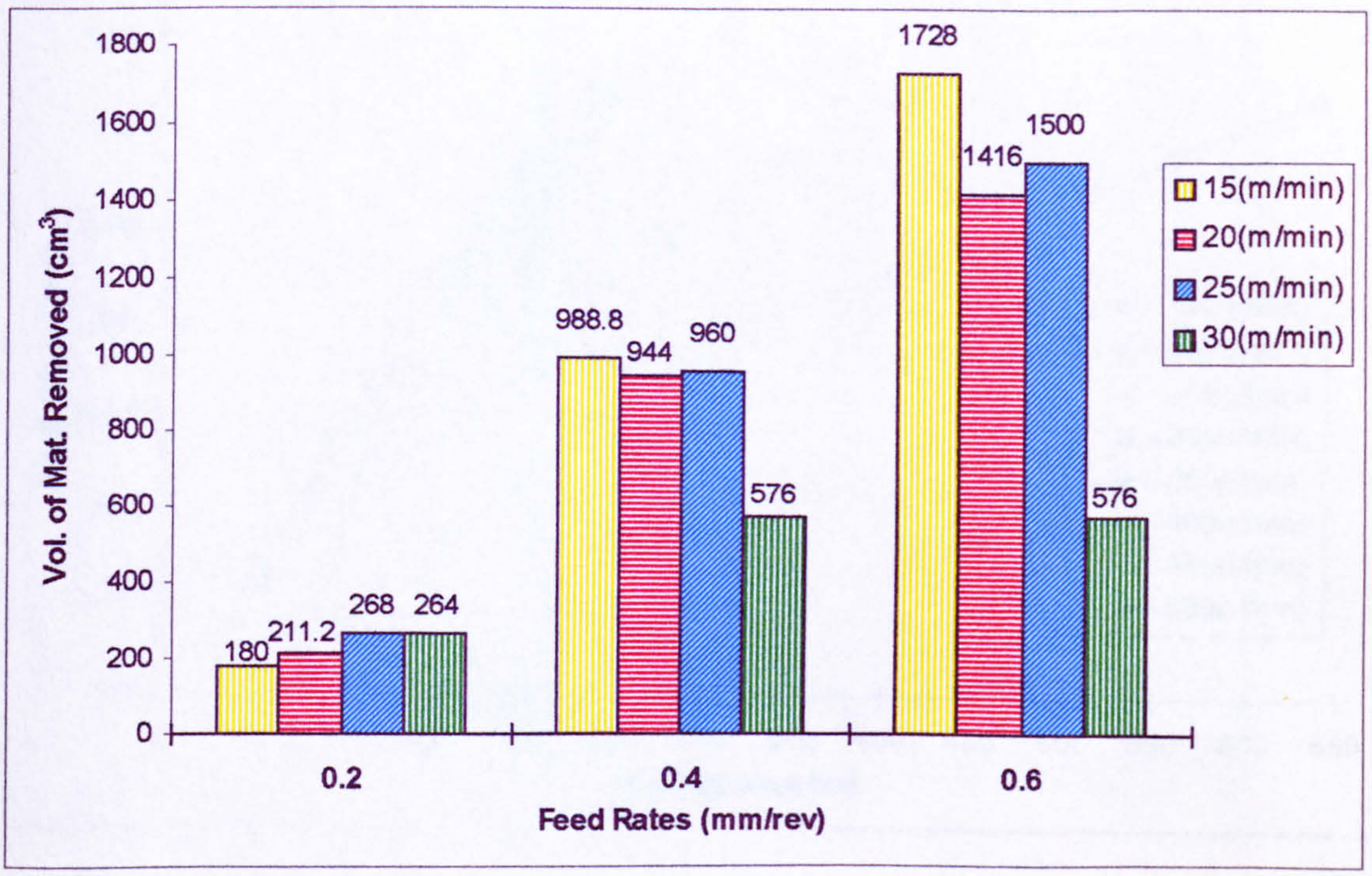

Figure 7.62 Volume Of Material Removed When Machining With KC910 Inserts (Positive Geometry, DOC = 4 mm)

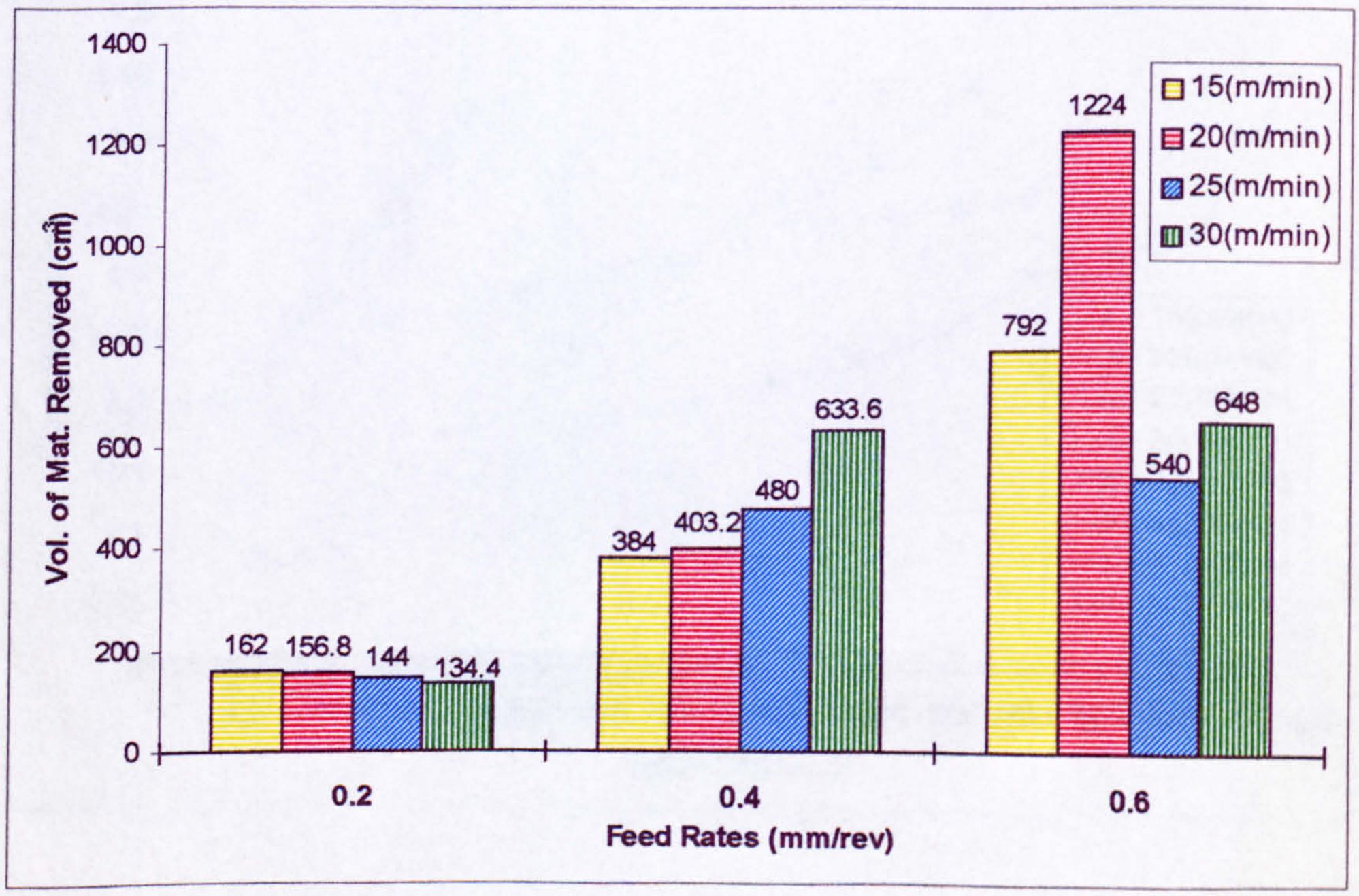

7.63 Variation of Flank Wear With Cut Distance For KC910 Inserts (Negative Geometry, Feed = 0.2 mm/rev, DOC = 2 mm)

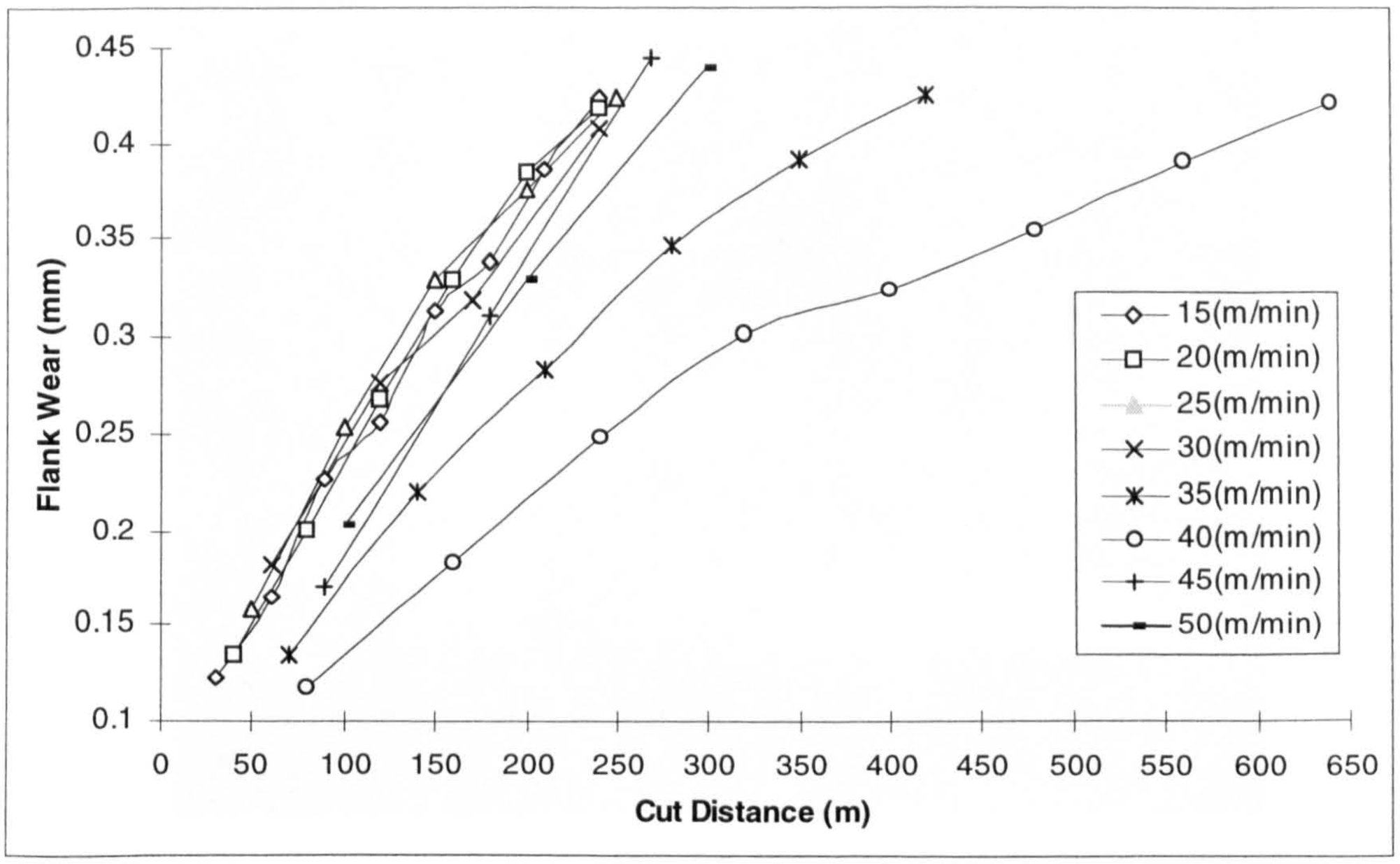

7.64 Variation of Flank Wear With Cut Distance For KC910 Inserts (Negative Geometry, Feed = 0.4 mm/rev, DOC = 2 mm)

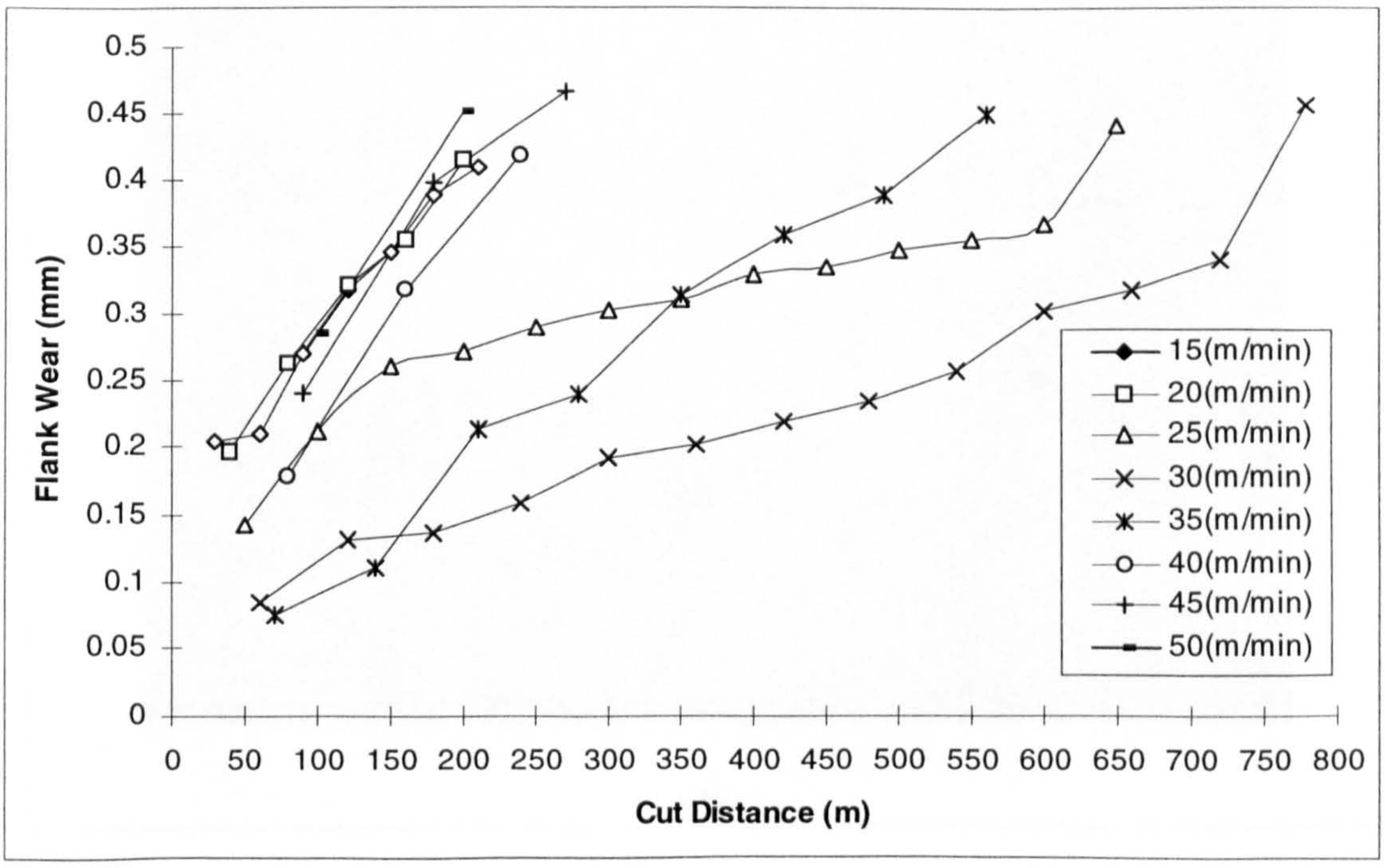

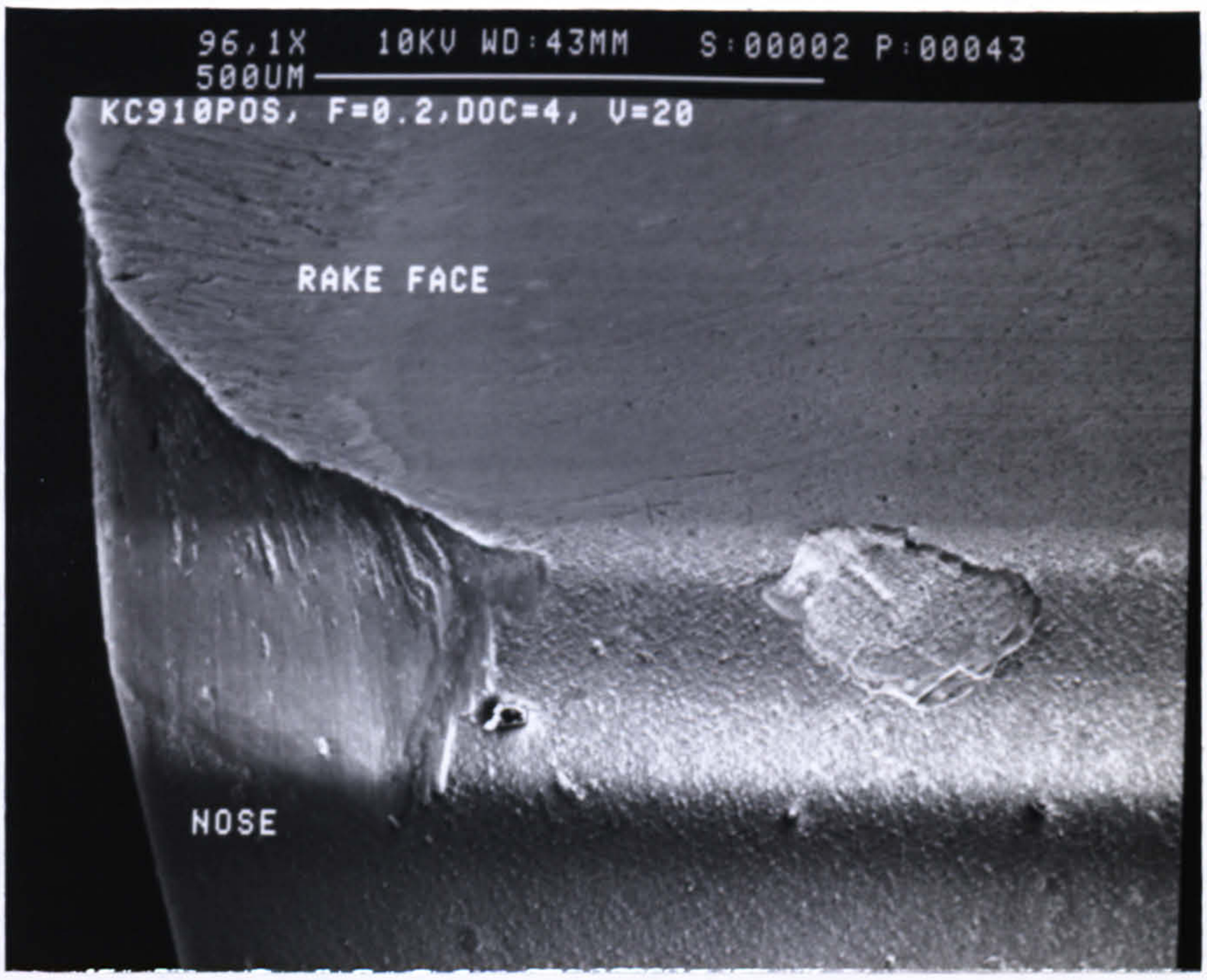

(a)

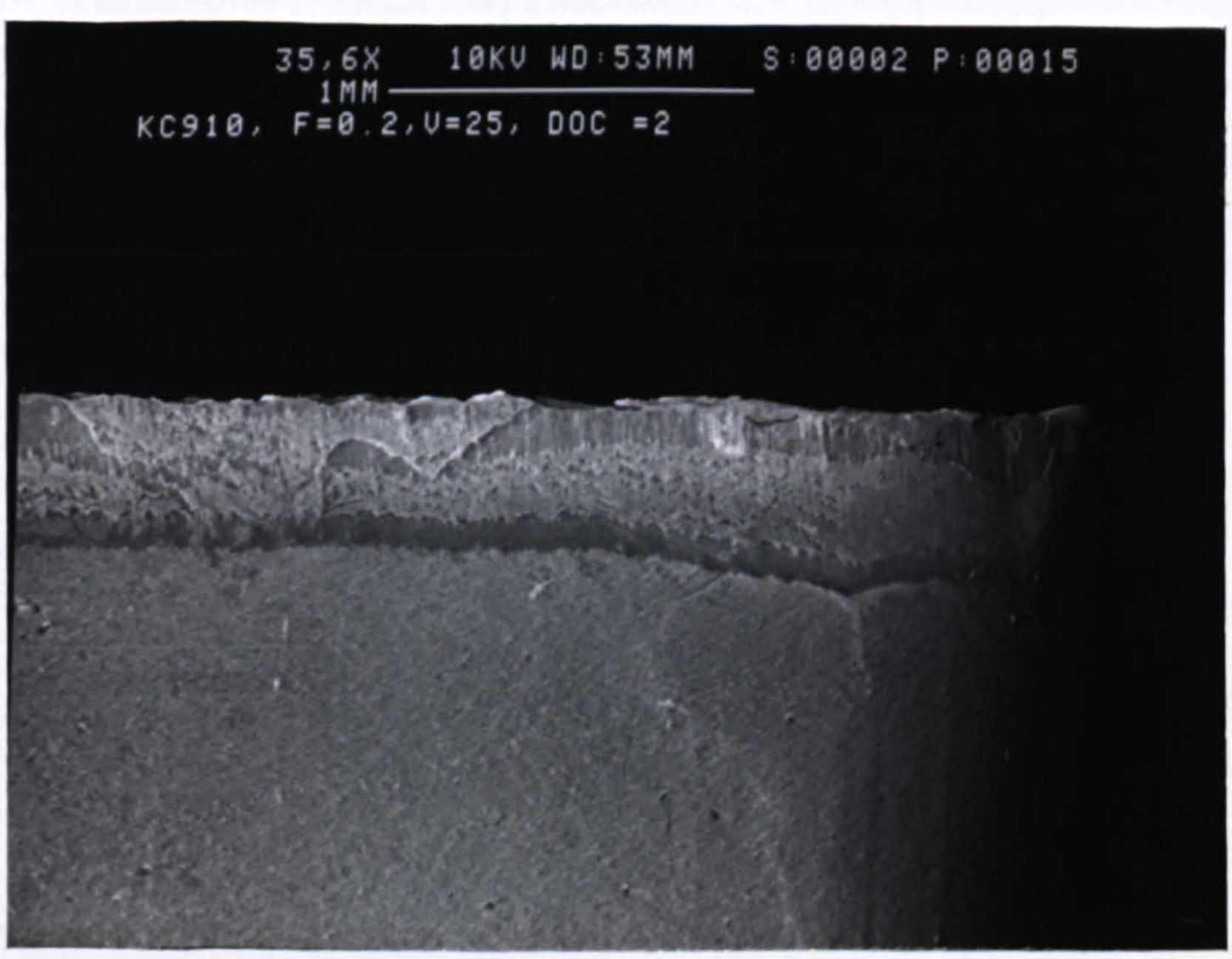

(b)

Figure 7.65 General Wear Appearance For KC910 Insert
(a) Nose and Rake Face, and (b)Flank Face

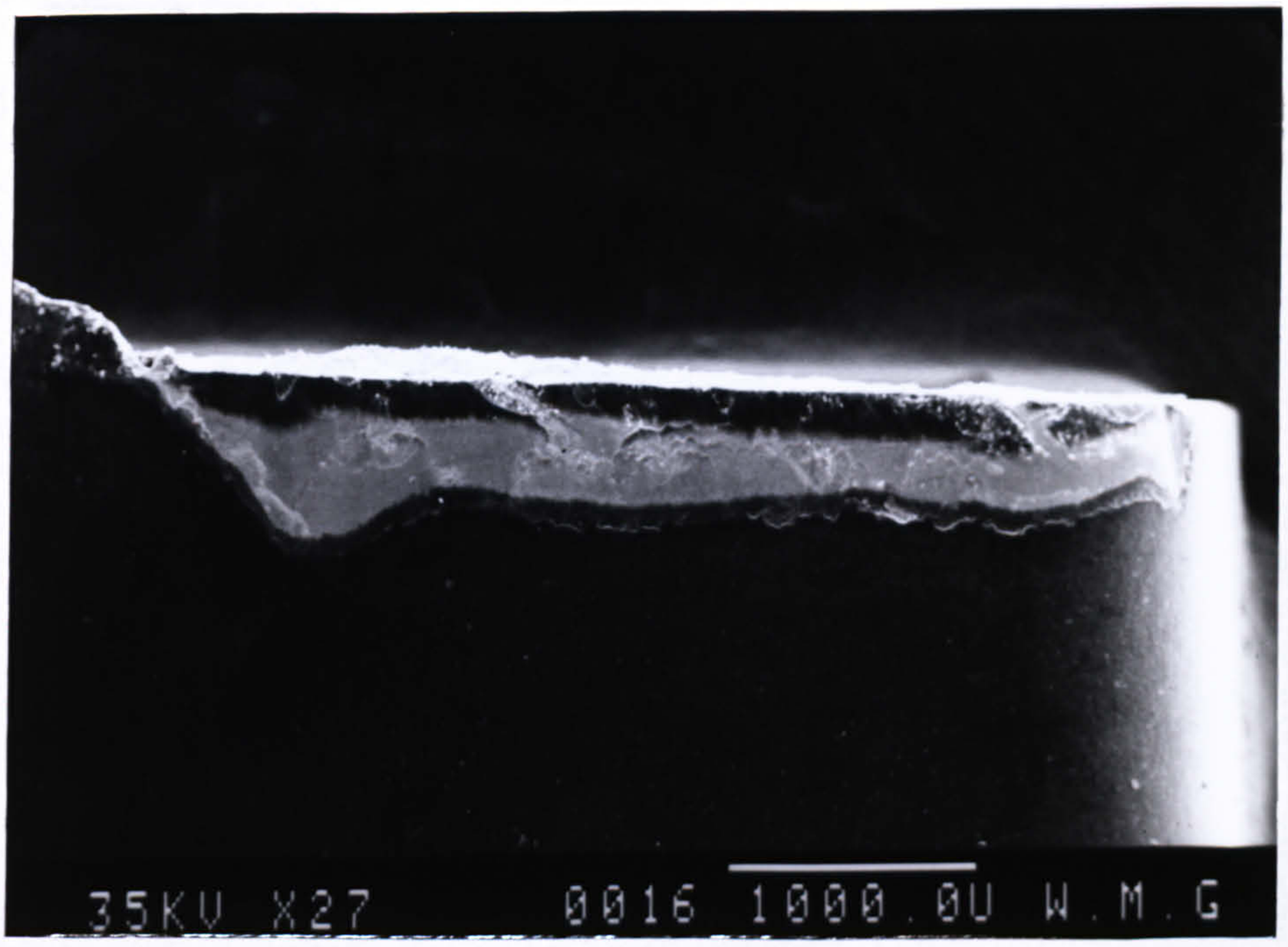

(a)

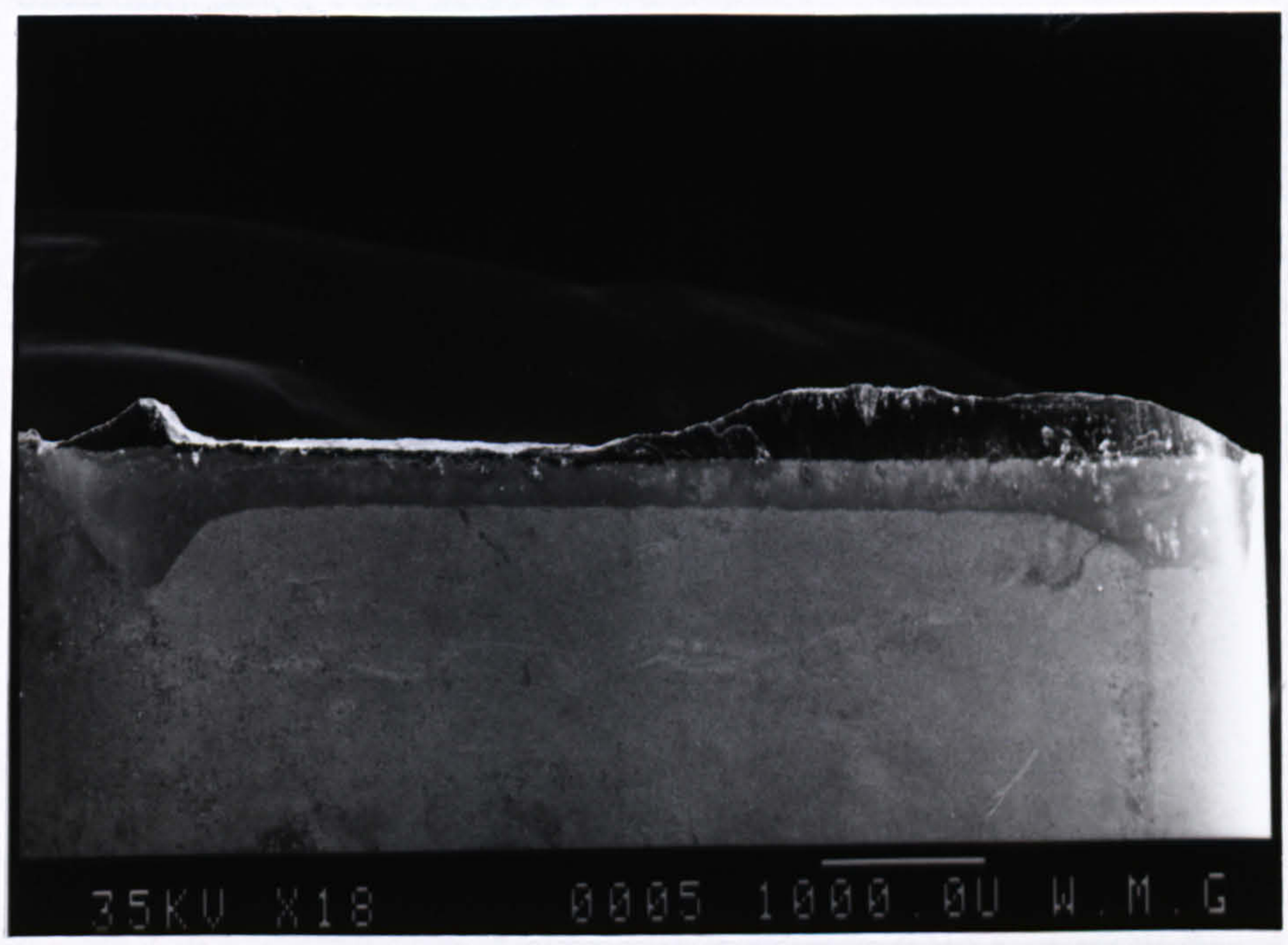

(b)

Figure 7.66 Typical Flank Wear Area On KC910 Insert (a) V = 15 m/min, and (b) V = 30 m/min

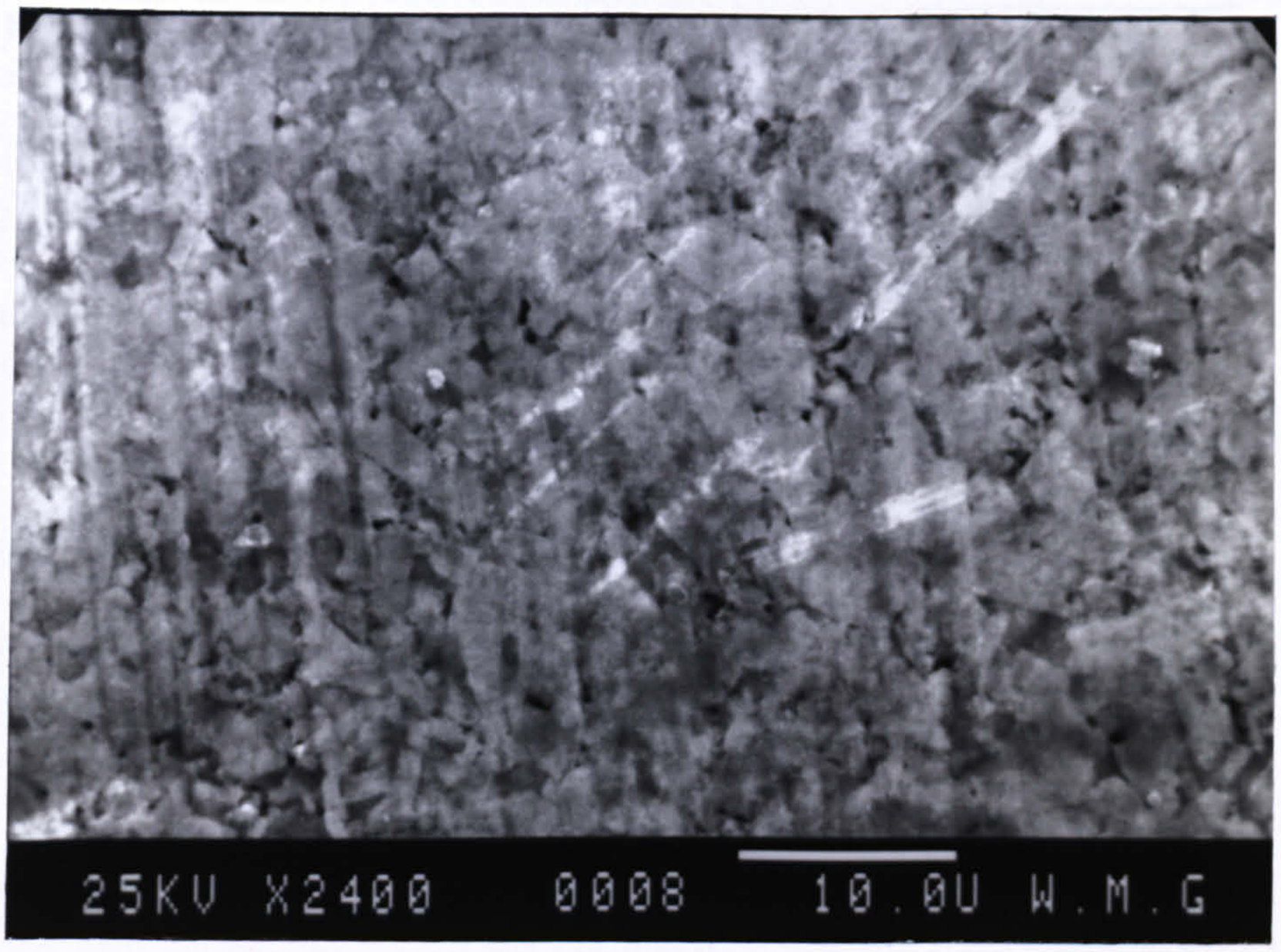

(a)

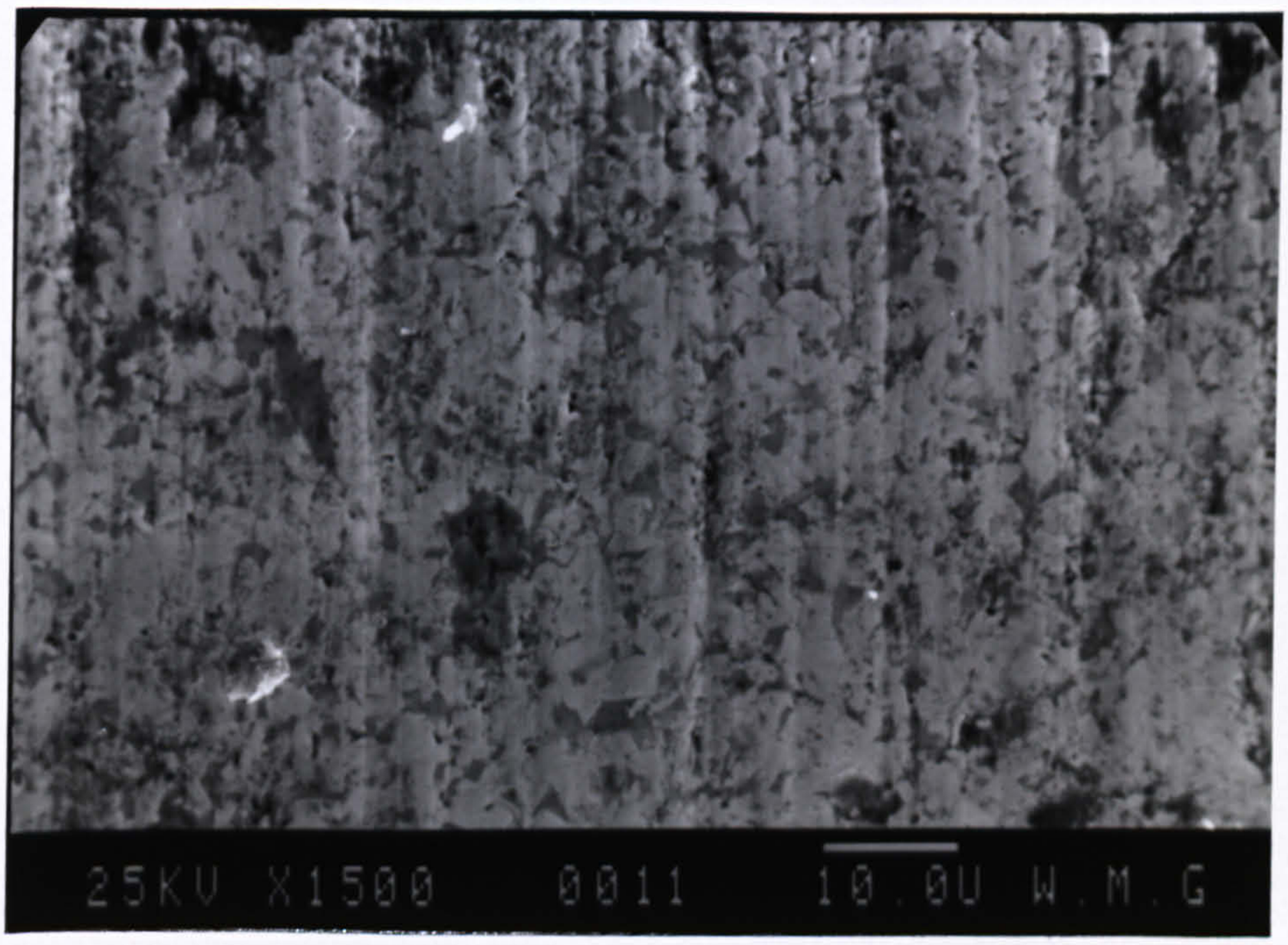

(b)

Figure 7.67 Smooth Flank Surface With Scratches On The Flank Face Of KC910 Insert (a) V = 15 m/min, (b) V = 25 m/min

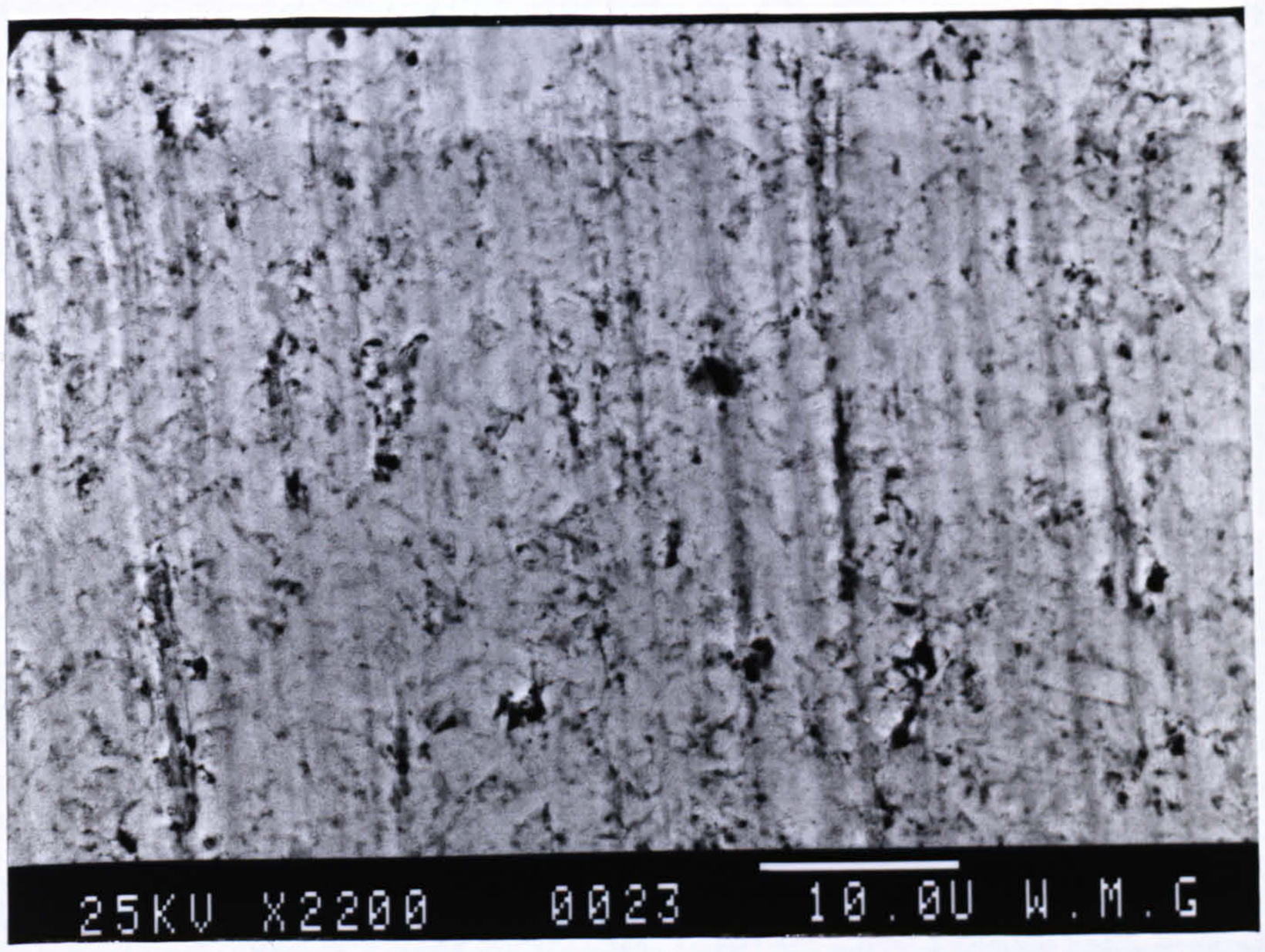

(c)

Figure 7.67 Smooth Flank Surface With Scratches On The Flank Face Of KC910 Insert, (c) 30 m/min

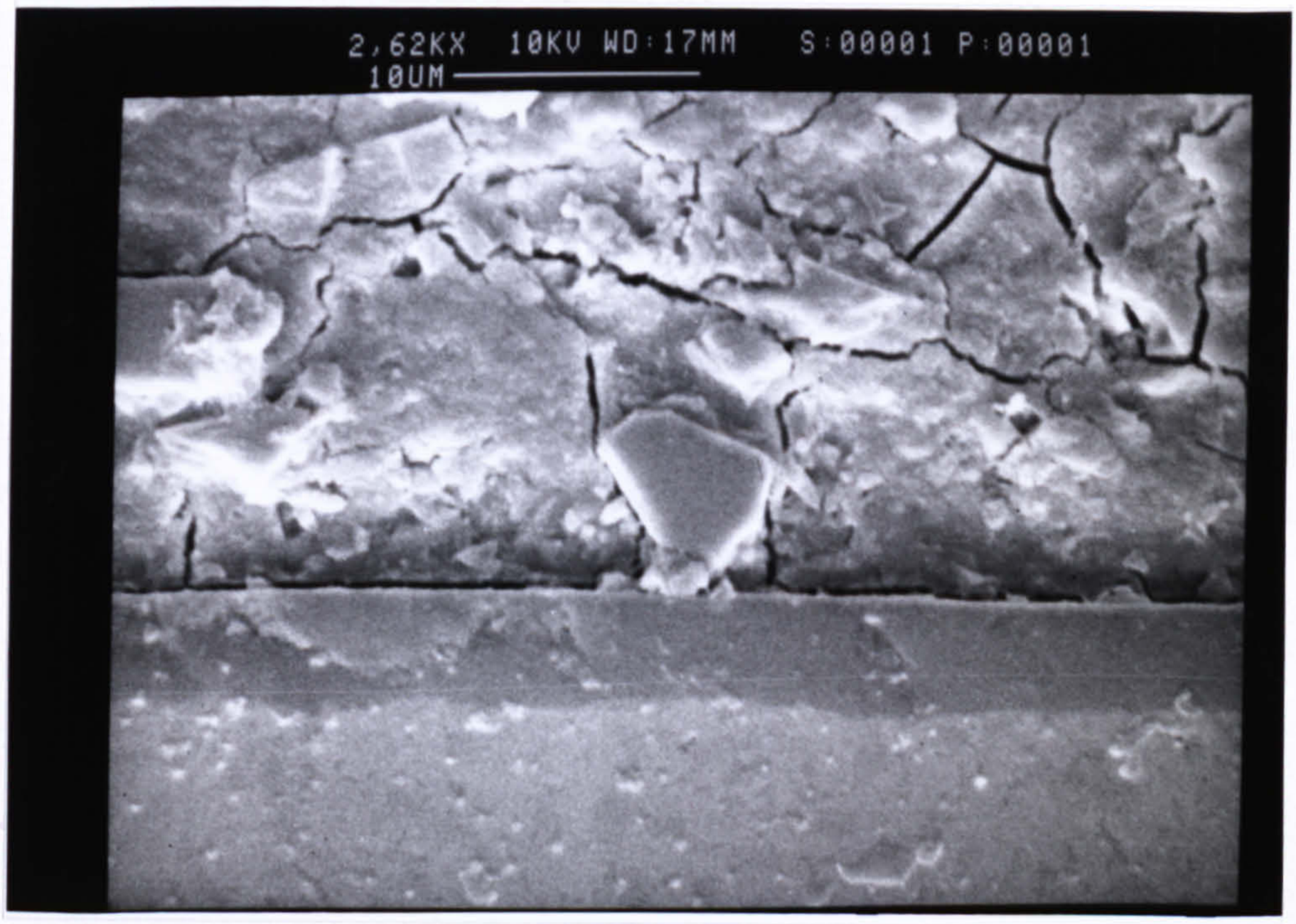

(a)

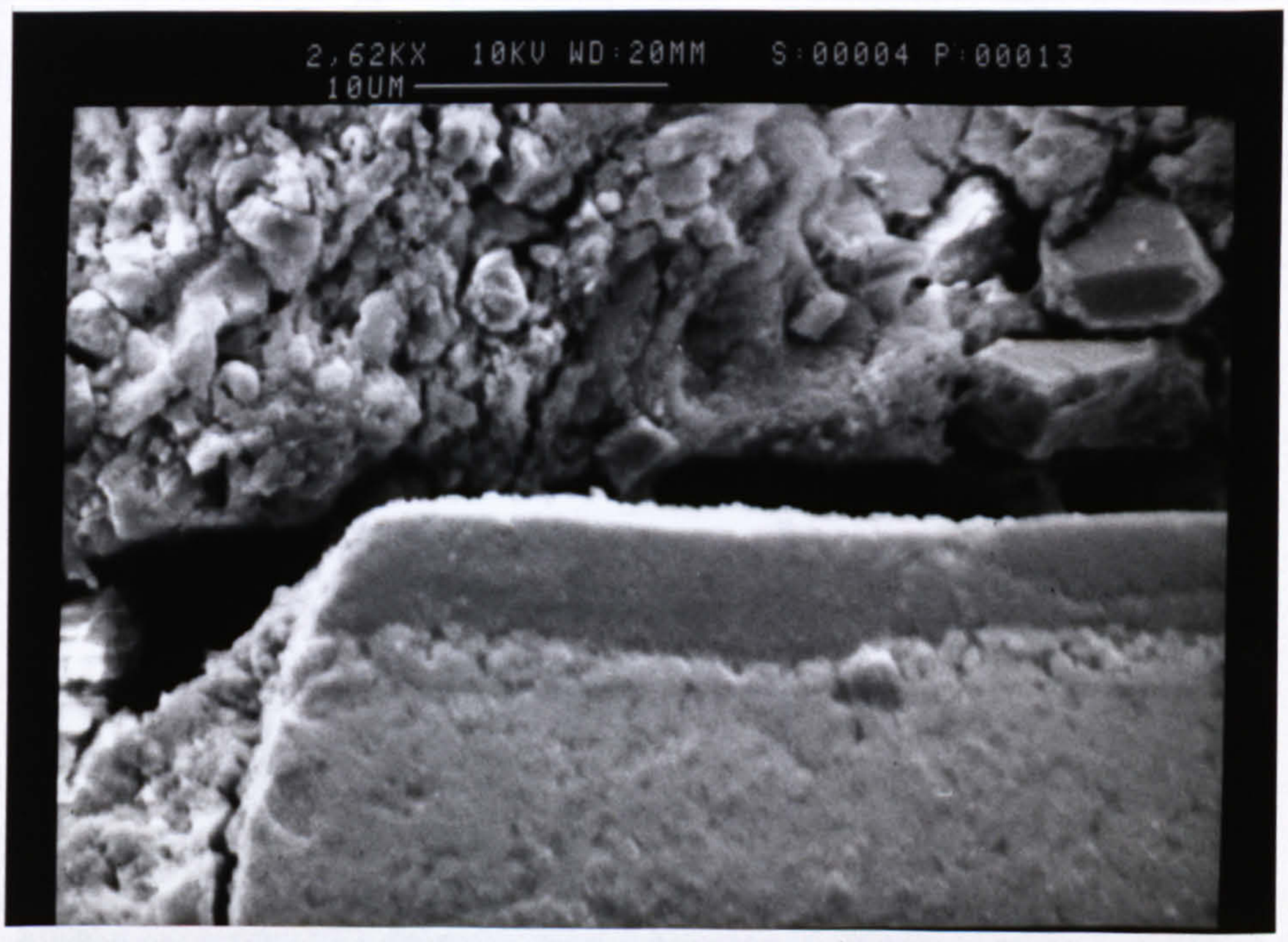

(b)

Figure 7.68 Cross-section of KC910 Inserts Showing The Presence of SiC Particle (a) V = 15 m/min, Feed = 0.2 mm/rev (b) V = 30 m/min , Feed 0.4 mm/rev

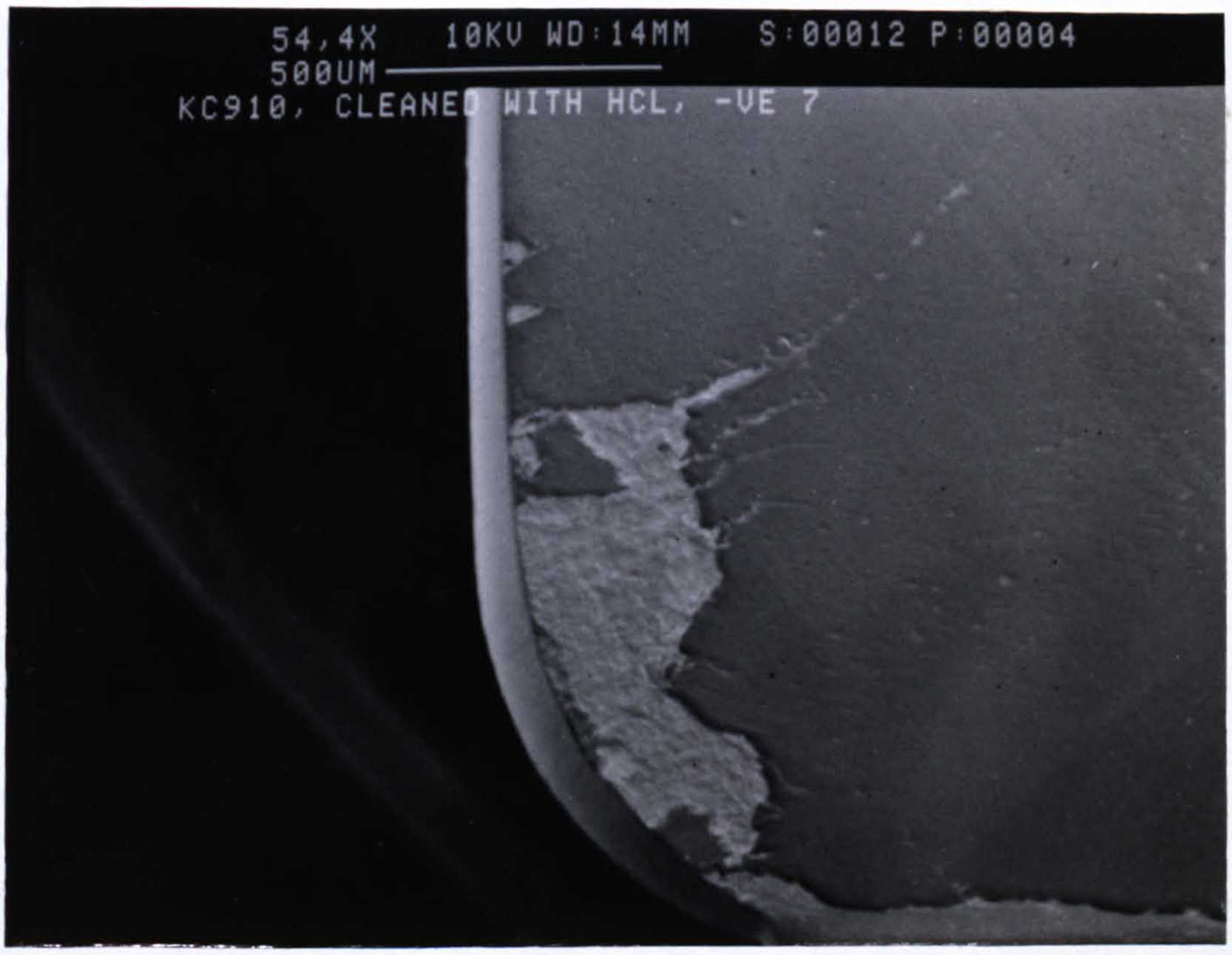

Figure 7.69 Slight Rake Face Wear On The Rake Face Of KC910 Insert (V = 20 m/min, Feed = 0.4 mm/rev, DOC = 2mm)

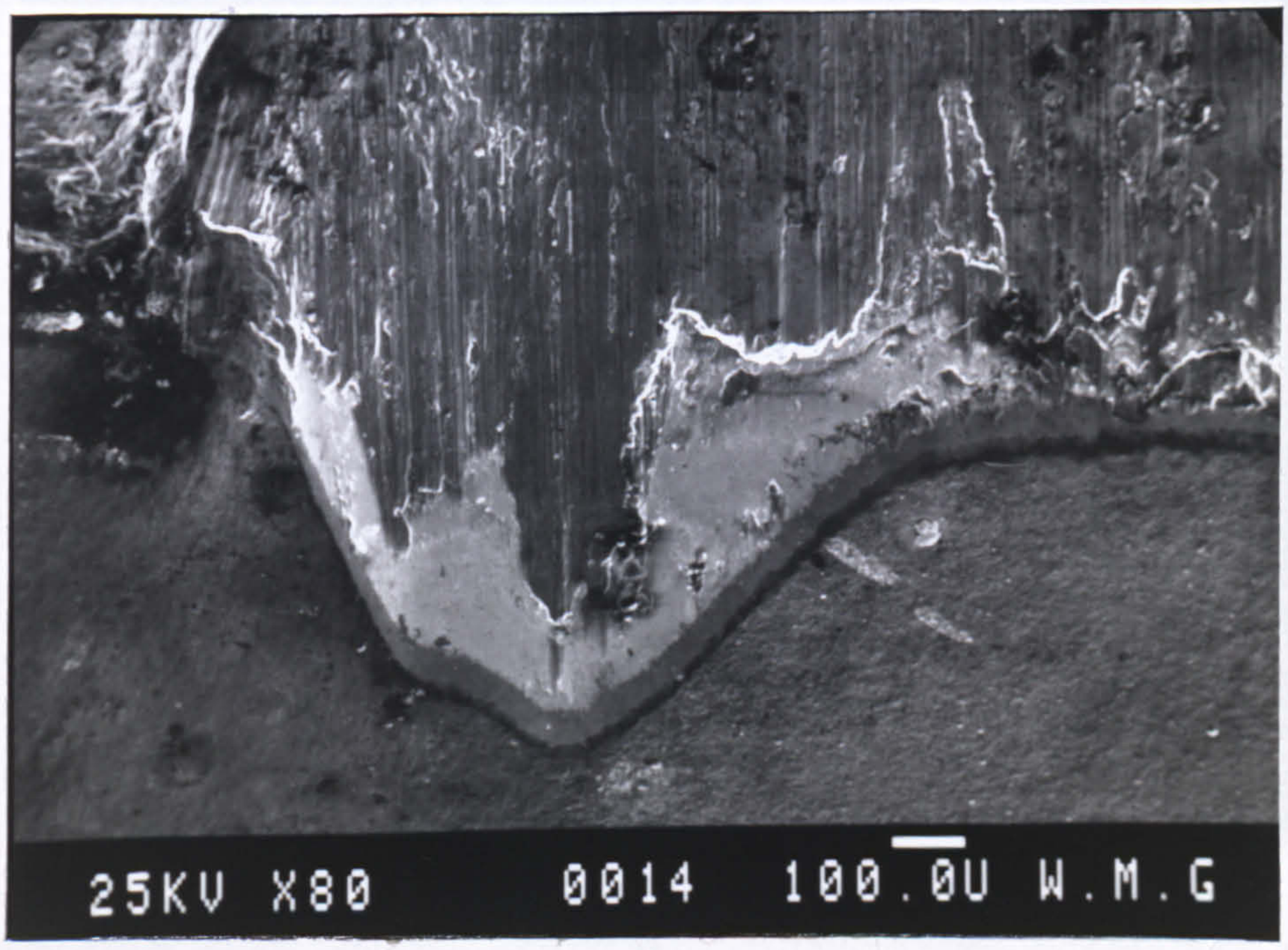

Figure 7.70 (a) Notching At The Depth Of Cut On KC910 Insert (V = 15 m/min, Feed = 0.6 mm/rev, DOC = 4 mm)

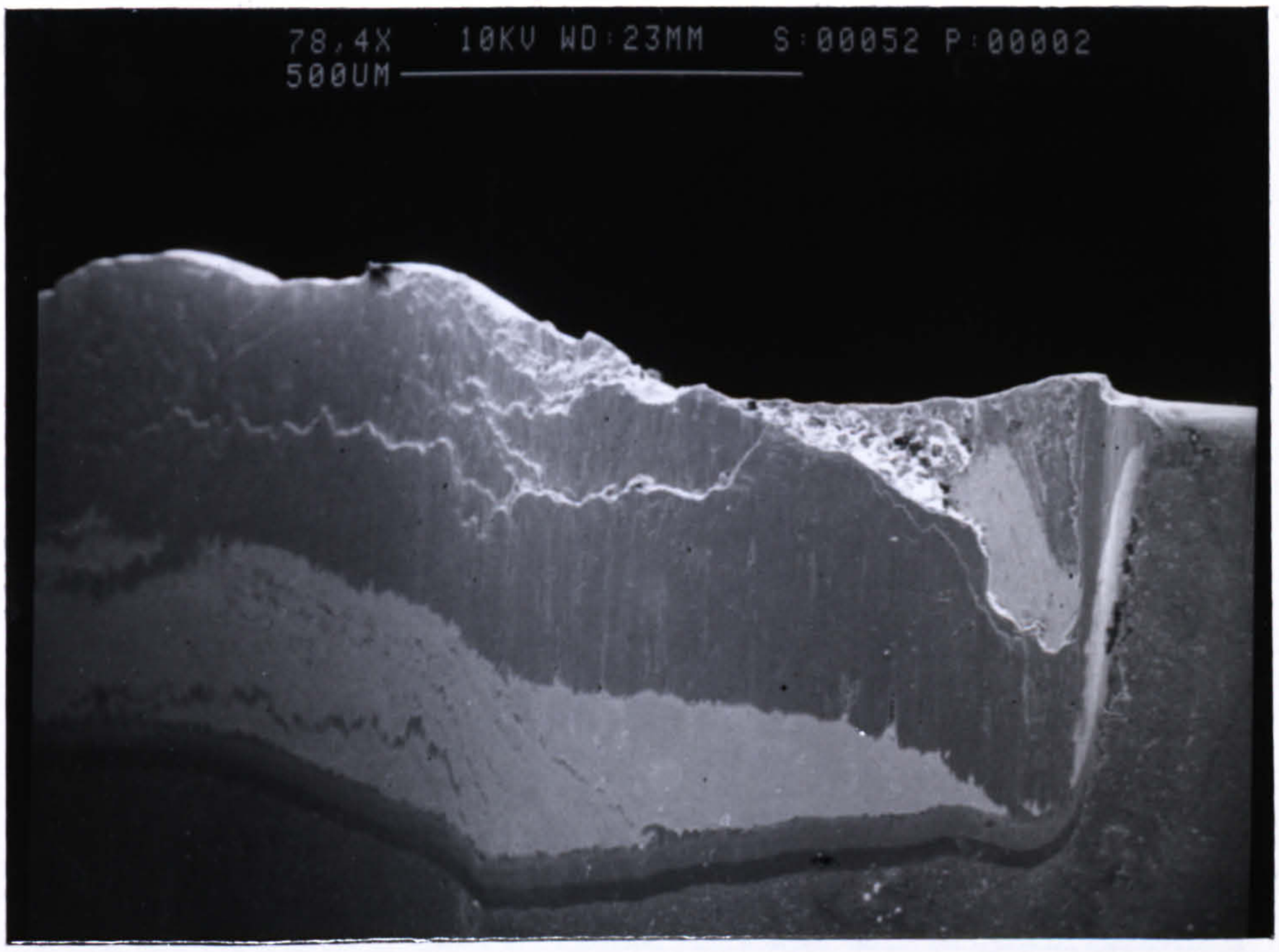

(b)

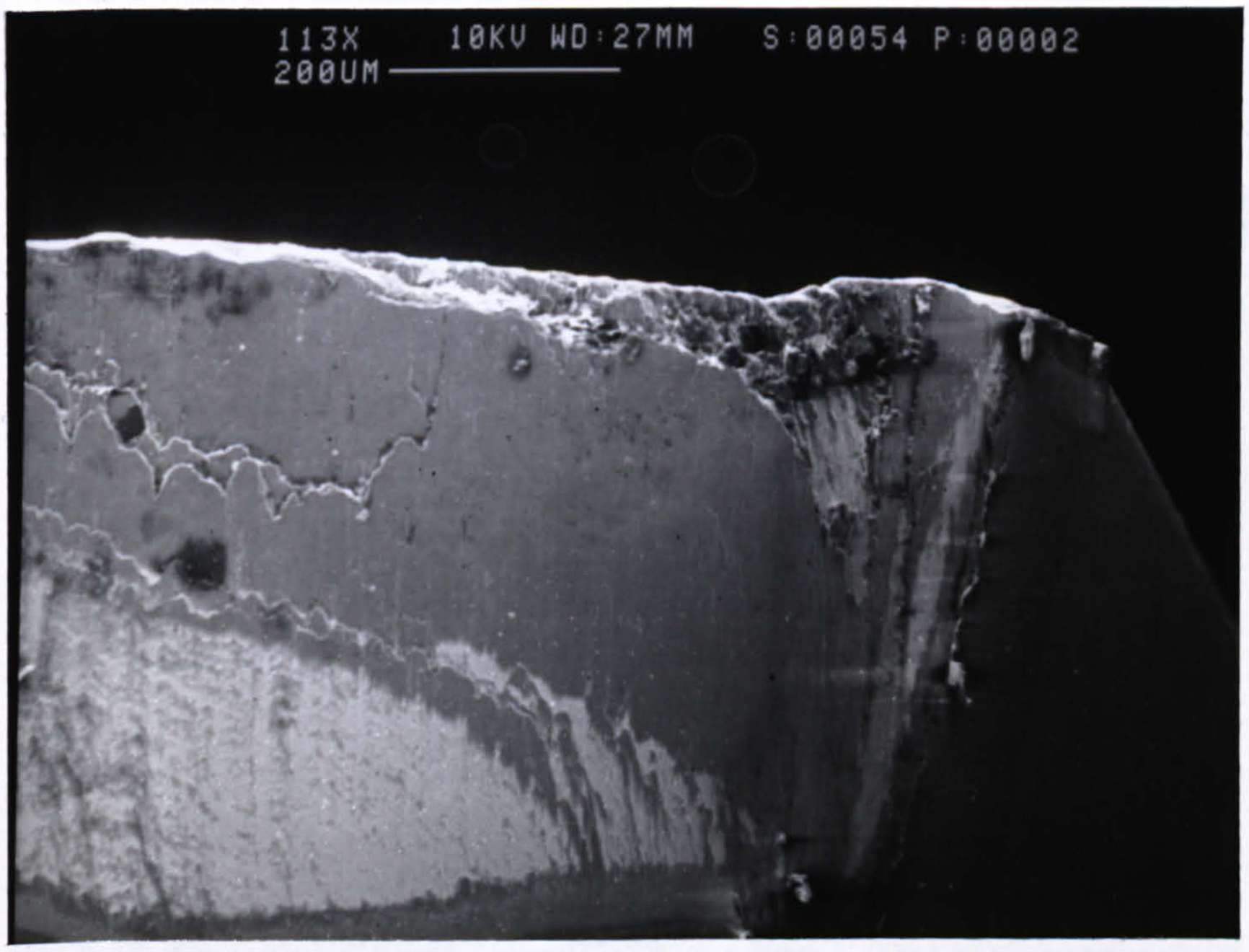

(c)

Figure 7.70 Chipping of KC910 At Cutting Edge
(b) V = 15 m/min, and (c) V=20 m/min

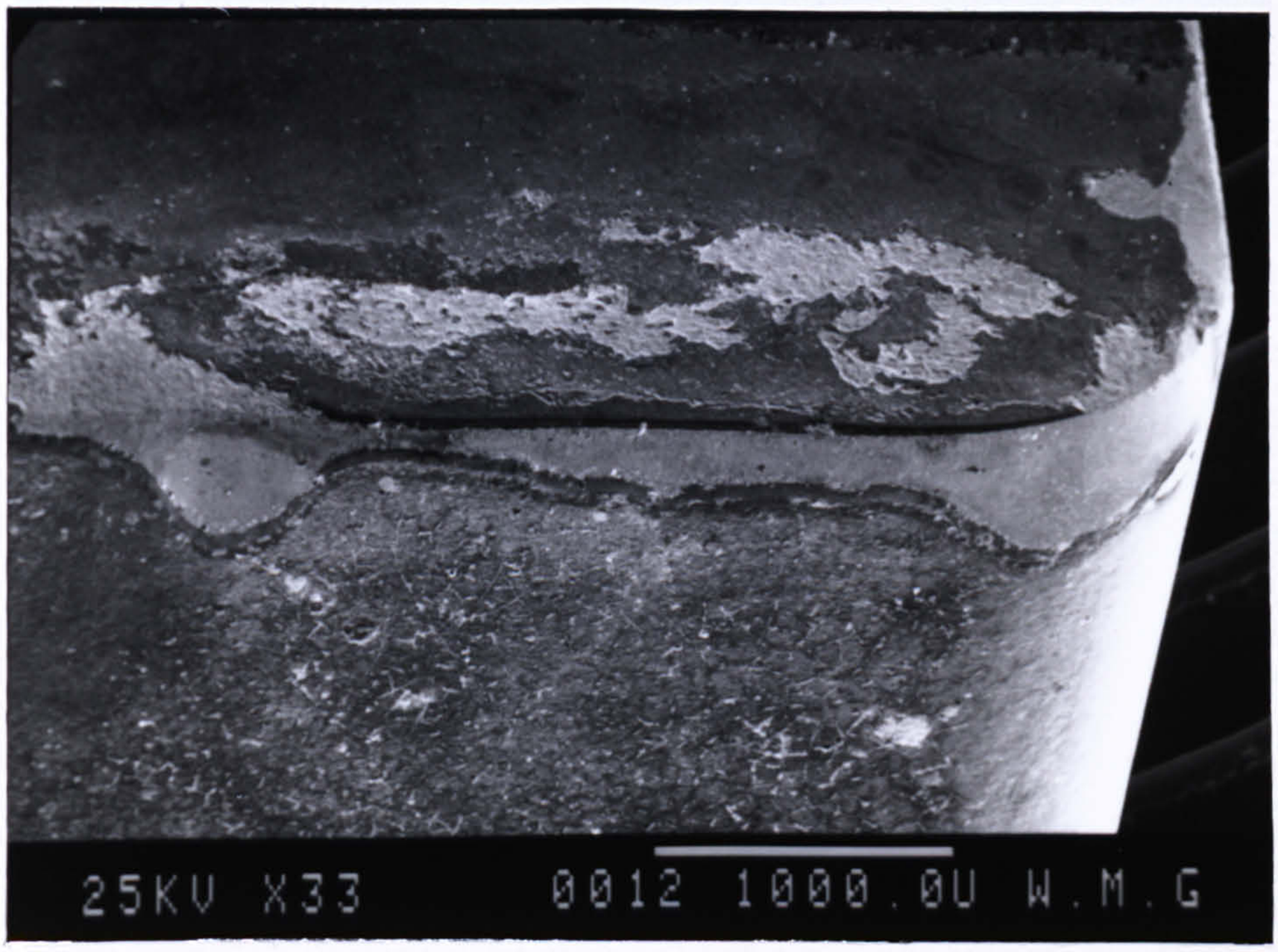

Figure 7.71 Overview Of K910 Insert Showing Lifting Off Coating After Machining (V = 20 m/min, Feed = 0.6 mm/rev, DOC = 2 mm)

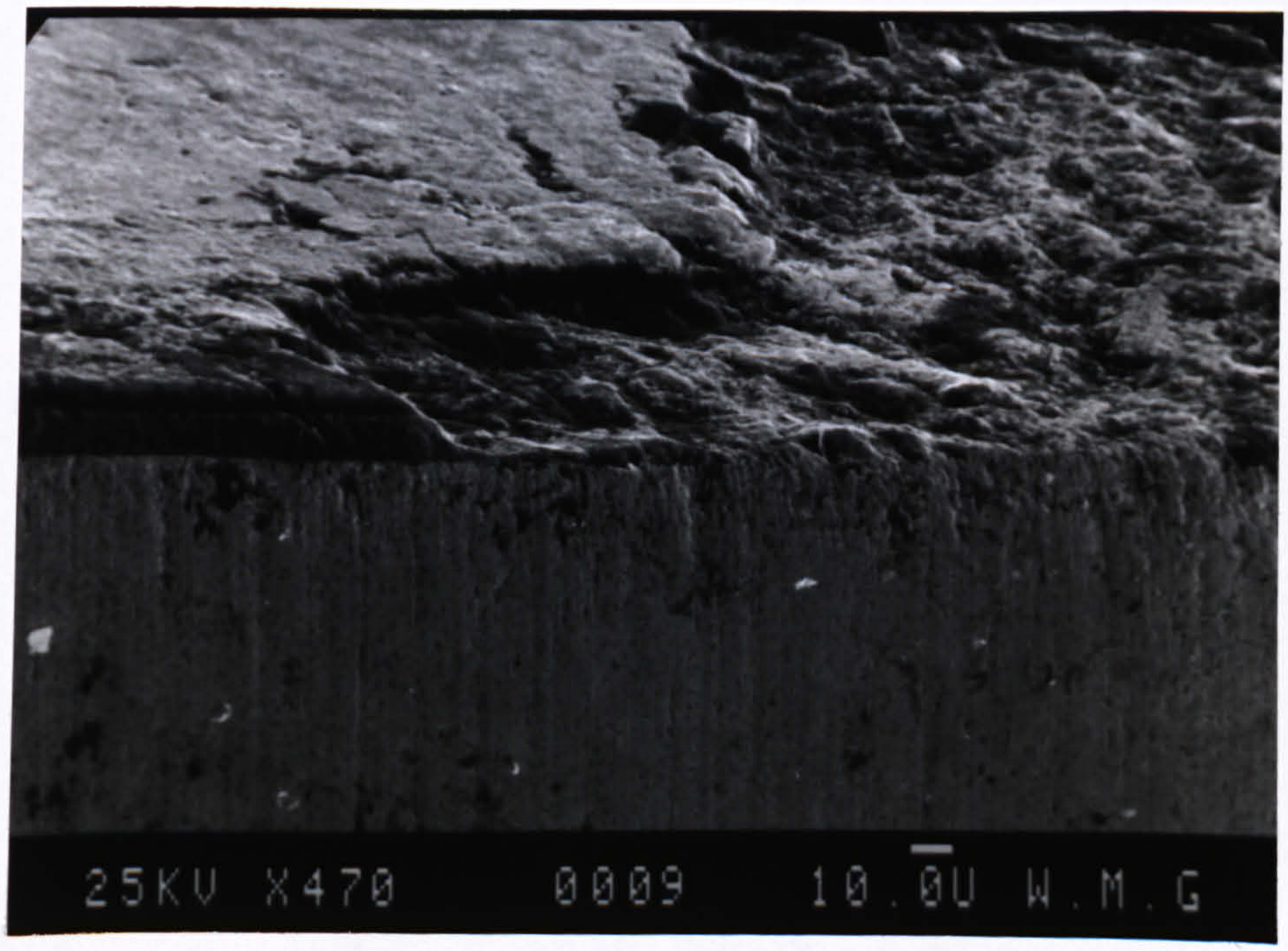

Figure 7.72 (a) Lifting Off Coating On KC910 Insert (V = 20 m/min, Feed = 0.6 mm/rev, DOC = 2 mm)

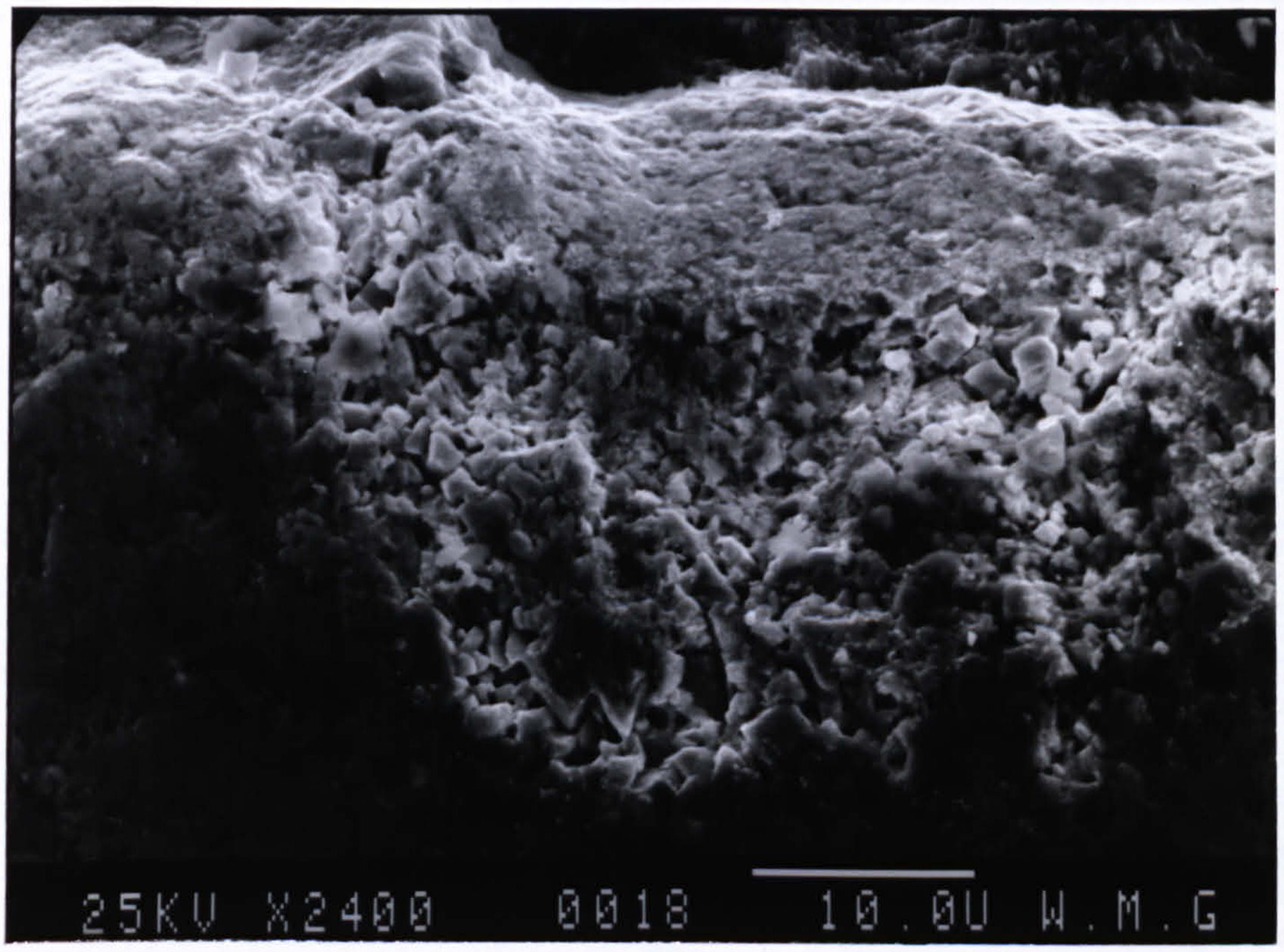

Figure 7.72 (b) Region of Coatings Removed On The Cutting Edge Revealing WC Substrate Material.

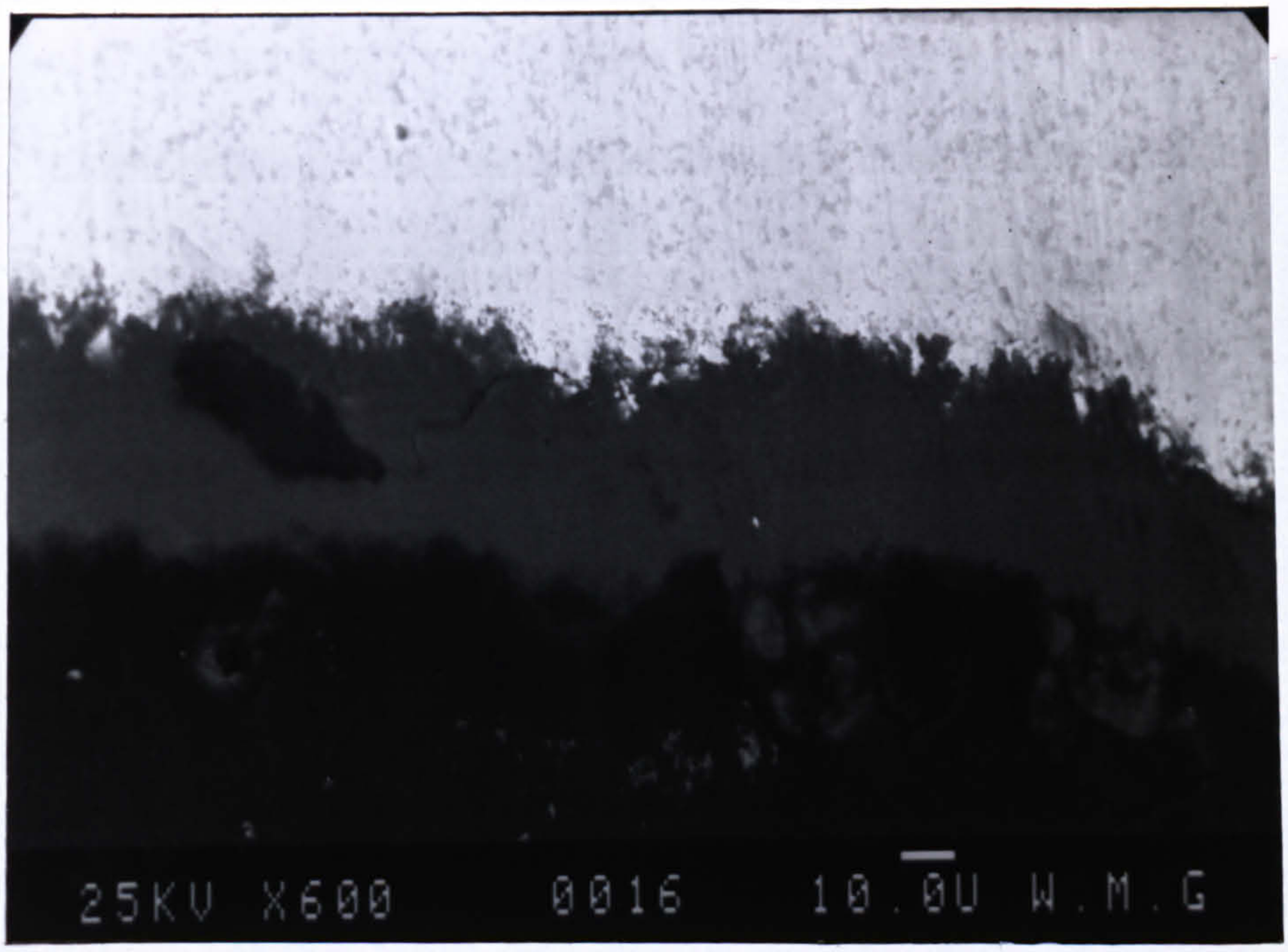

(a)

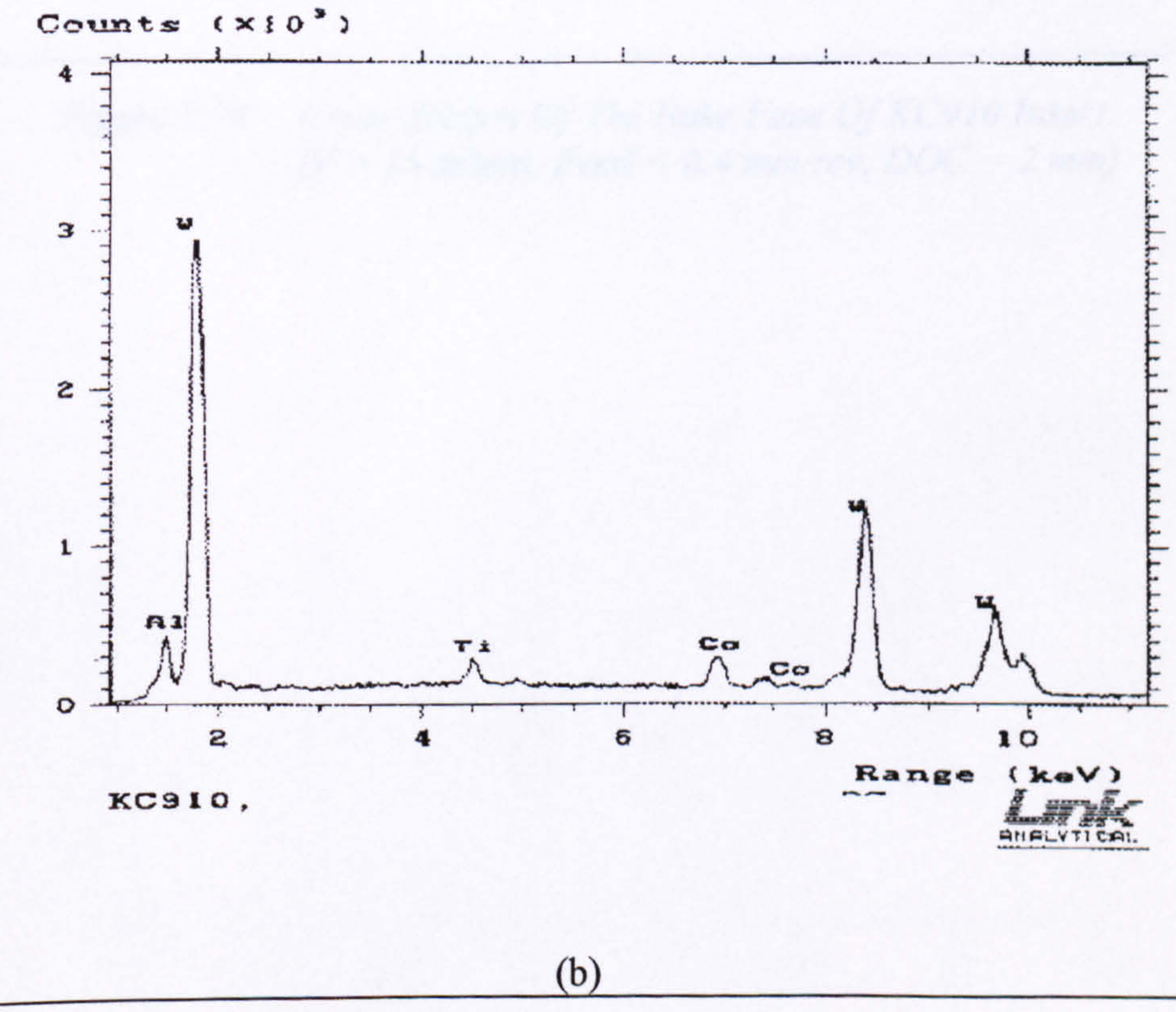

(b)

Figure 7.73 (a)Contrast Of The Backscattered Electron Images On The Flank Wear (b) X-Ray Analysis Graph of Flank Wear of KC910 Insert (V = 15 m/min, Feed = 0.4 mm/rev, DOC = 4 mm)

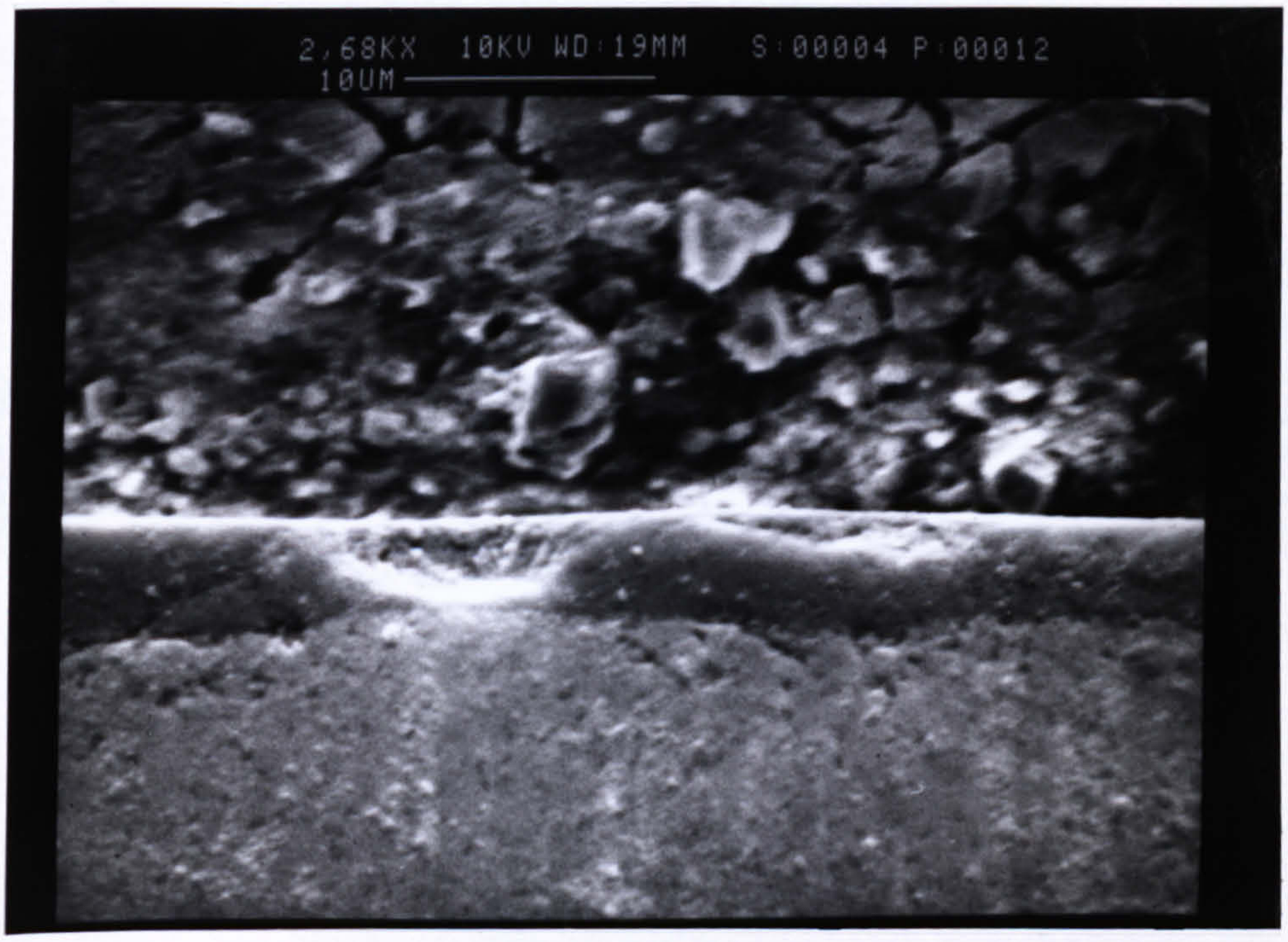

Figure 7.74 Cross Section Of The Rake Face Of KC910 Insert. (V = 15 m/min, Feed = 0.4 mm/rev, DOC = 2 mm)

Figure 7.75 Cutting and Feed Forces Versus Cutting Speed For KC910 Inserts At 0.2 and 0.4 Feed Rates (Neg. Geometry, DOC = 2 mm)

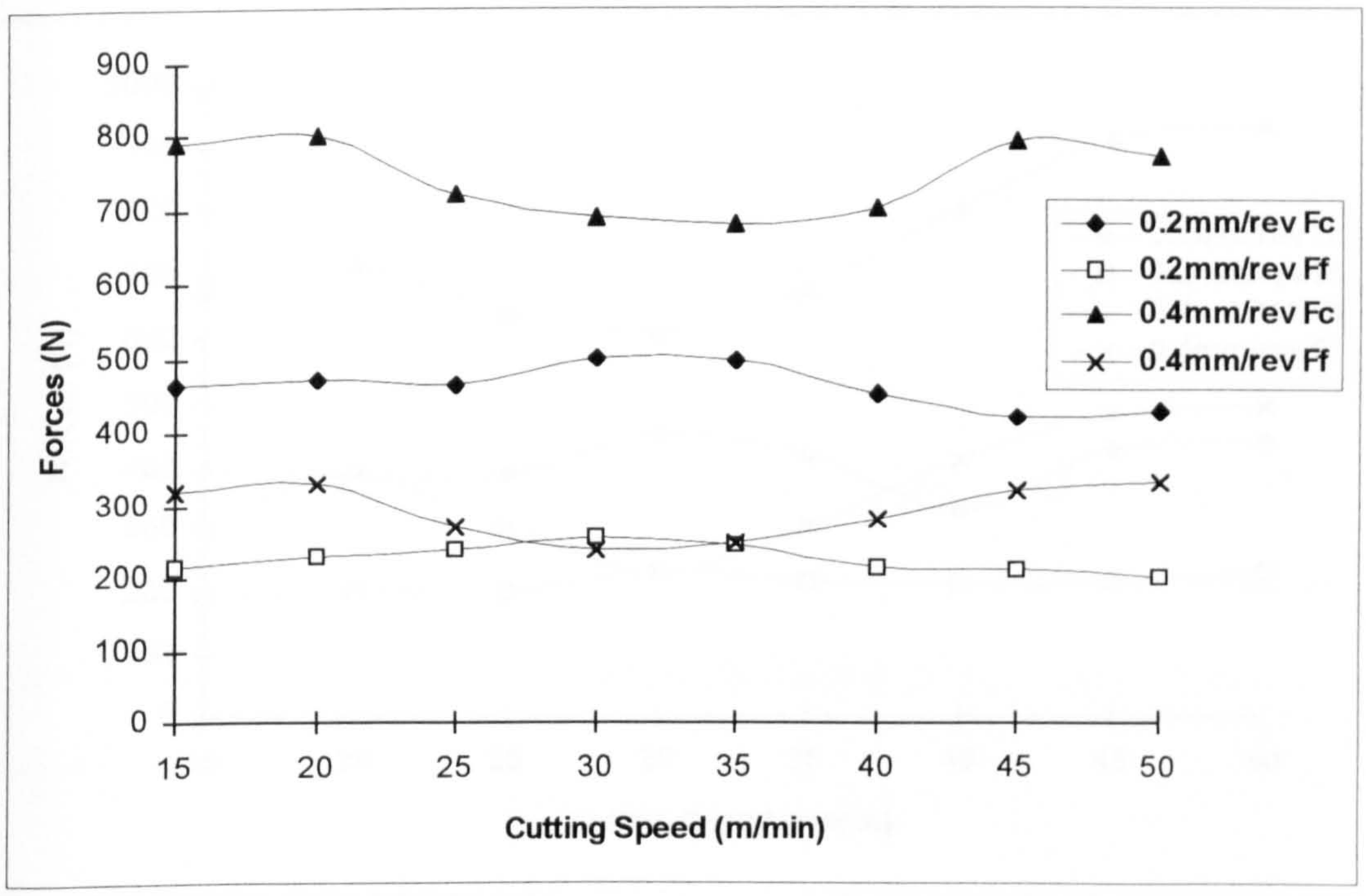

Figure 7.76 Cutting and Feed Forces Versus Cutting Speed For K910 Inserts At 0.2 and 0.4 Feed Rates (Pos. Geometry, 2 mm DOC)

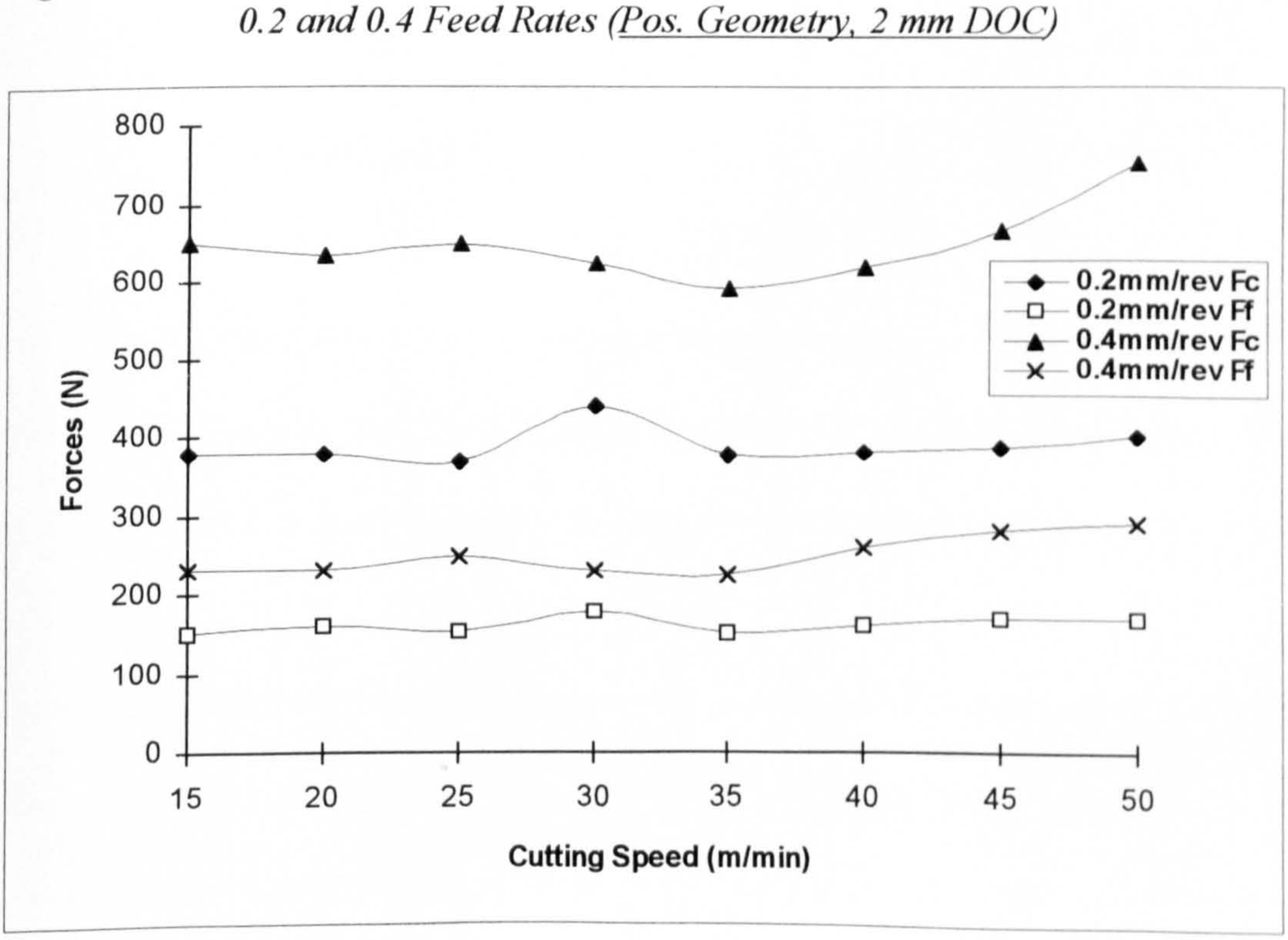

Figure 7.77 Cutting and Feed Forces Versus Cutting Speed For KC910 Inserts At 0.2 and 0.4 Feed Rates At 2mm DOC (Neg. Geometry, WITH Chip Breaker)

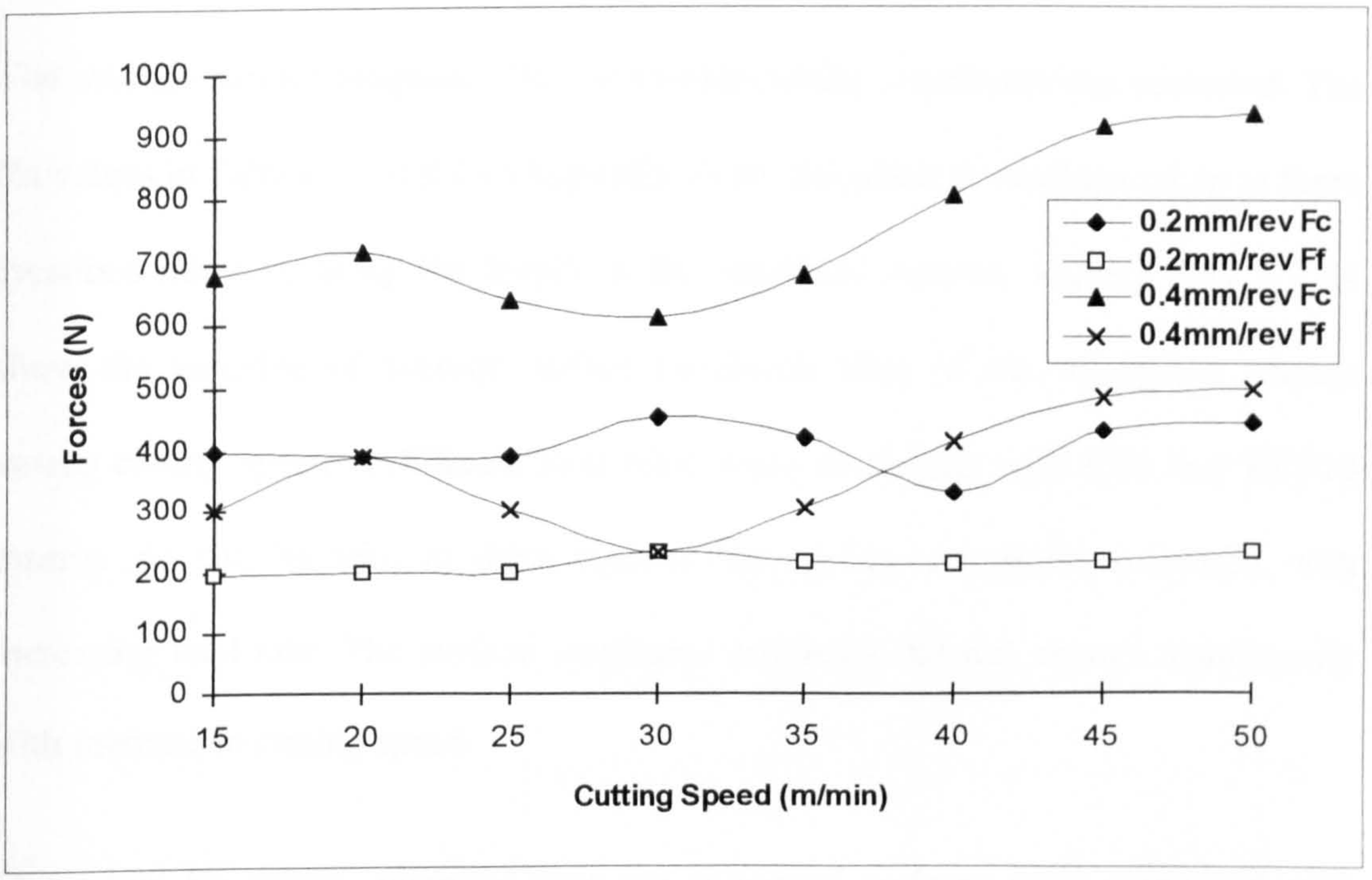

7.6 Surface Roughness

The average surface roughness (Ra) at various cutting conditions was recorded. The Ra values in Tables 7.1 and 7.9 (Appendix 1) are the mean of readings taken at three locations mid-way along the length of the machined surface. Figures 7.81 - 7.84 show the variation of average surface roughness (Ra) of the workpiece surface versus cutting speed at different feed rates when machining with K68 and KC910 inserts. As can be seen in these figures, the surface roughness increased with increasing feed rate. The surface roughness produced did not change significantly with increase in cutting speed.

The actual Ra values obtained from the machined surfaces were compared with those predicted using the following theoretical expression:

$$Ra = 0.0321 \frac{f^2}{r} \quad \text{..... (7.1)}$$

where f is the feed rate and r is the tool nose radius [17]. Consequently, from Equation (7.1), a reduction in the theoretical values of the surface roughness can be obtained if there is an increase in the nose radius or decrease in the feed-rate.

The theoretical values of Ra at 0.2 mm/rev, 0.4 mm/rev and 0.6 mm/rev with 0.8 mm nose radius are 1.61 μm, 6.42 μm and 14.44 μm respectively, as shown by a horizontal dotted lines in Figures 7.81 to 7.84. It can be seen that decreasing the feed rate from 0.6 mm/rev to 0.2 mm/rev brings about a considerable improvement in the

surface finish. It is interesting to note that the difference between the measured values for Ra and those predicted by Equation (7.1) for both inserts are not so great. A differences is obvious between feed rates of 0.2 mm/rev., 0.4 mm/rev. and 0.6 mm/rev.

For K68 negative rake geometry tools at 0.2 mm/rev feed rate the surface roughness is almost constant when cutting in the speed range 15 to 35 m/min. As the speed is increased, the surface finish generated deteriorates and the Ra value recorded is greater than 3.72 μm. As for the positive rake geometry, the cutting speed has little effect on the machined surface, Figure 7.82. However, increases in feed resulted in very poor surface finish for both negative and positive tool geometries, especially for the negative rake geometry. It was observed that the surface roughness generated was very poor when cutting with negative rake geometry at speeds of 25 m/min and 30 m/min, these proved impossible to measure using the method employed.

At 0.4 mm/rev, the higher values of surface finish were recorded between the speeds of 20 m/min to 30 m/min. There was a reduction in Ra values as the speed increased above 35 m/min. Positive rake angle inserts showed a consistent value of Ra throughout the speed range tested.

A similar situation occurred for KC910 inserts, as presented in Figures 7.80 - 7.81. As expected, at the lower feed rate of 0.2 mm/rev there was a significant

improvement in surface finish. The surface finish has expectedly deteriorated with the increase in feed rate, but at lower feed rates, litle difference exists. Again, the surface finish could not be measured in the speed range 25 - 30 m/min.

Samples of the machined surface were cut from the bar, cleaned, examined and micrographs of the surfaces were obtained at various magnifications using SEM, as shown in Figures 7.82 - 7.84.

Figure 7.78 Variation Of Surface Roughness With Feed Rate For K68 Inserts (Negative Rake Geometry, DOC = 2 mm)

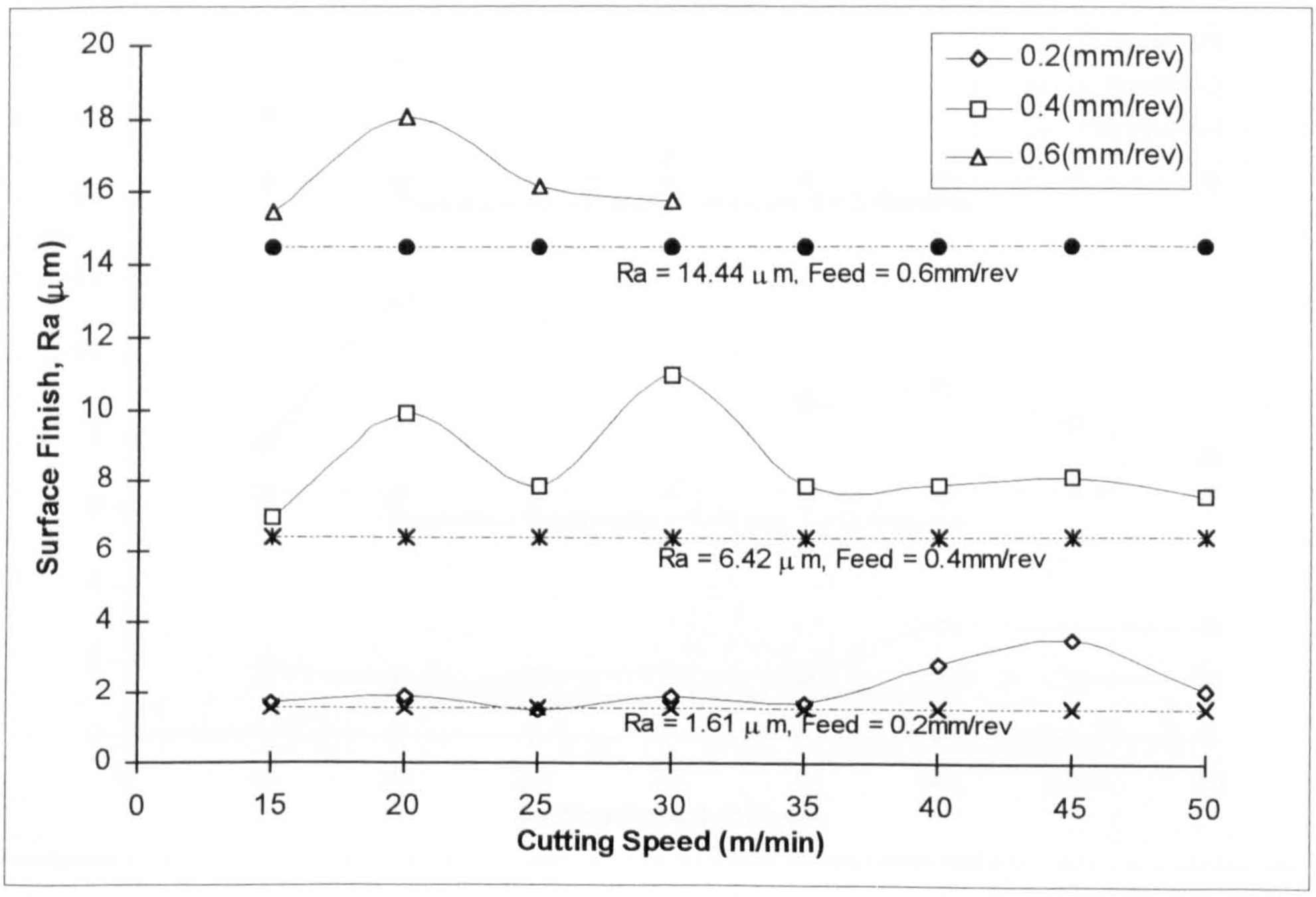

Figure 7.79 Variation Of Surface Roughness With Feed Rate For K68 Inserts (Positive Rake Geometry, DOC = 2 mm)

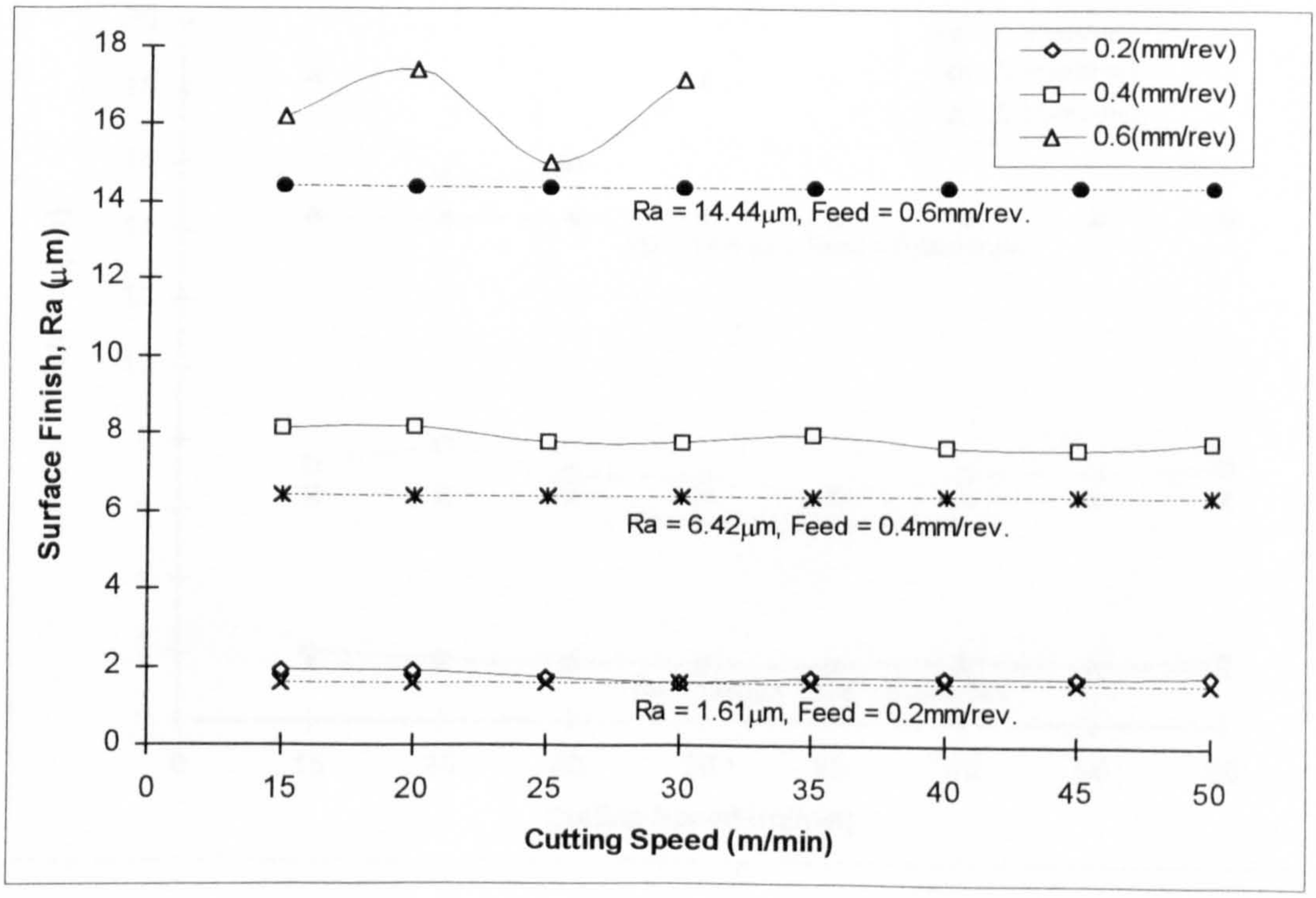

Figure 7.80 Variation Of Surface Roughness With Feed Rate For KC910 Inserts (Negative Rake Geometry, DOC = 2 mm)

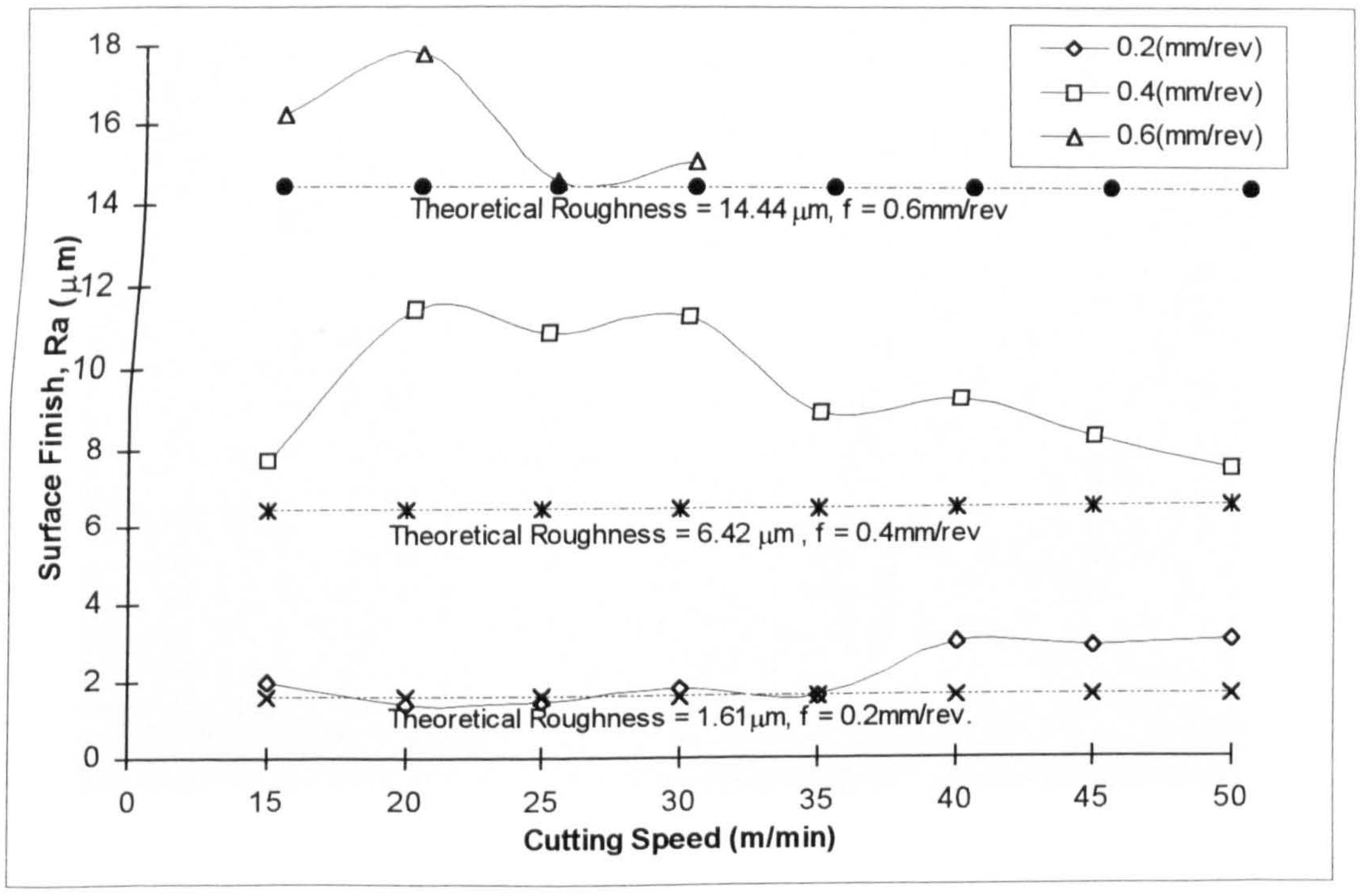

Figure 7.81 Variation Of Surface Roughness With Feed Rate For KC910 Inserts (Positive Rake Geometry, DOC = 2 mm)

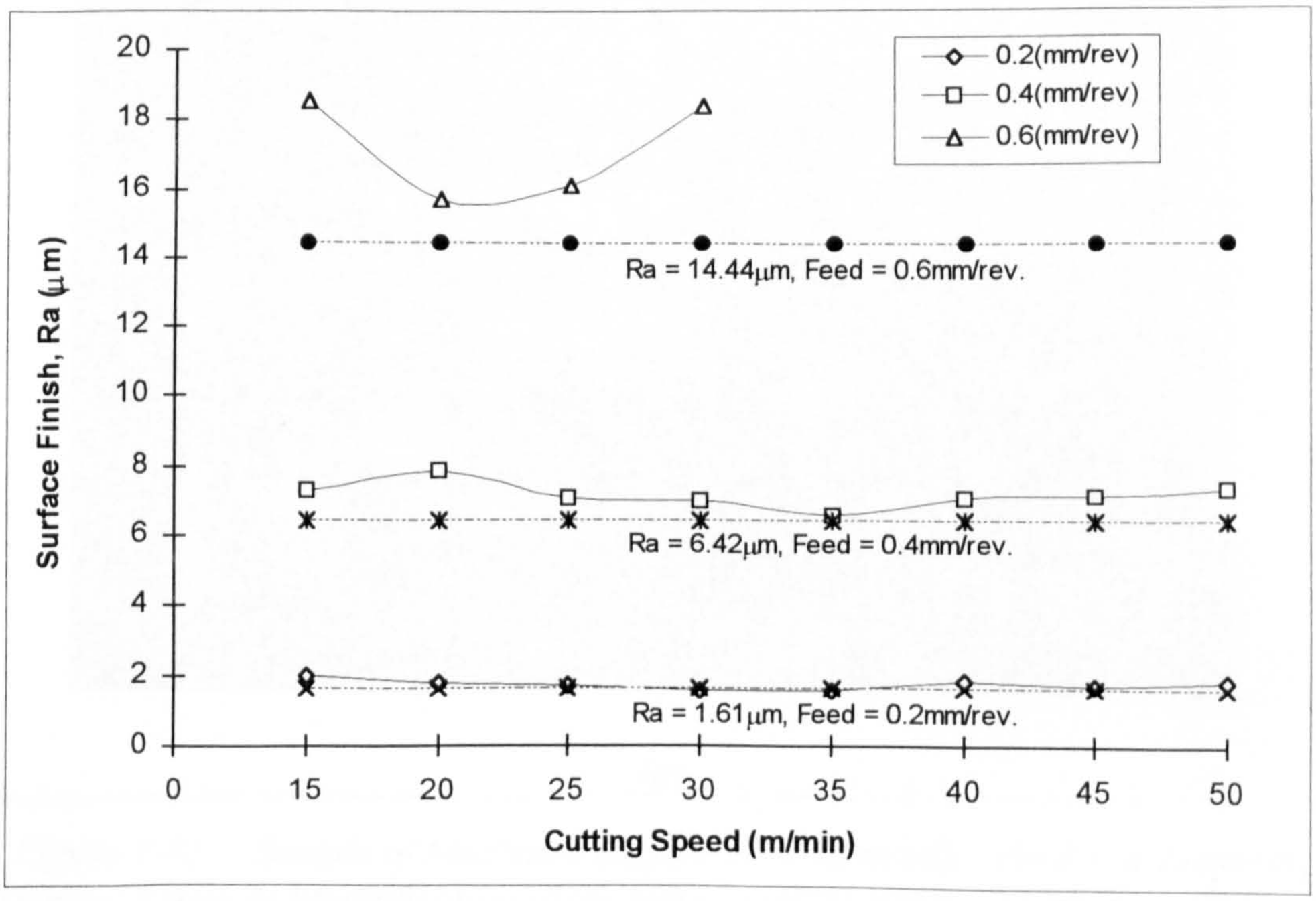

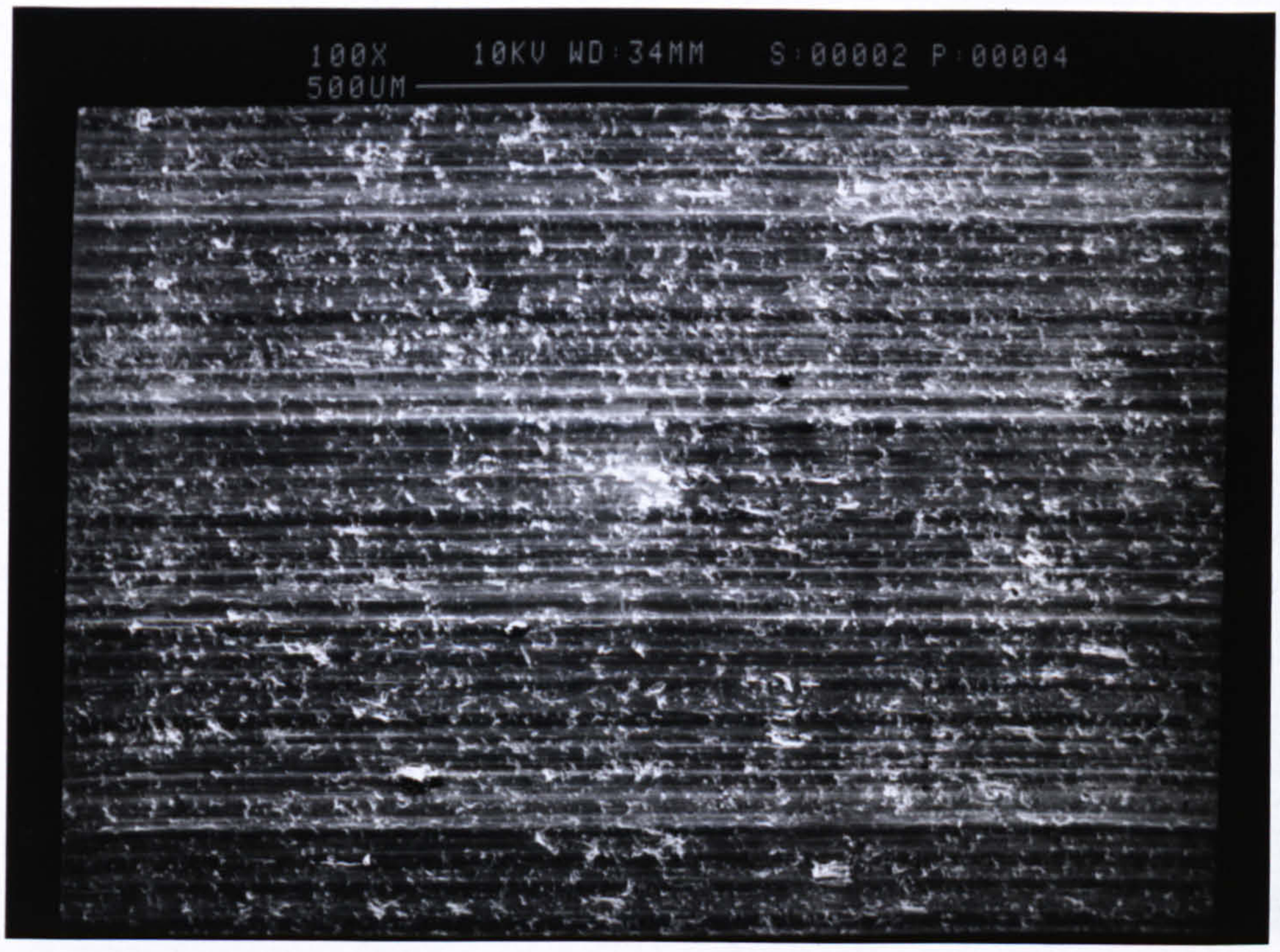

(a)

(b)

Figure 7.82 Sample of Machined Surface (V = 15 m/min , Feed = 0.2 mm/rev, DOC = 2 mm) At Magnification of (a) 100X , and (b) 500X (↑ Direction Of Feed)

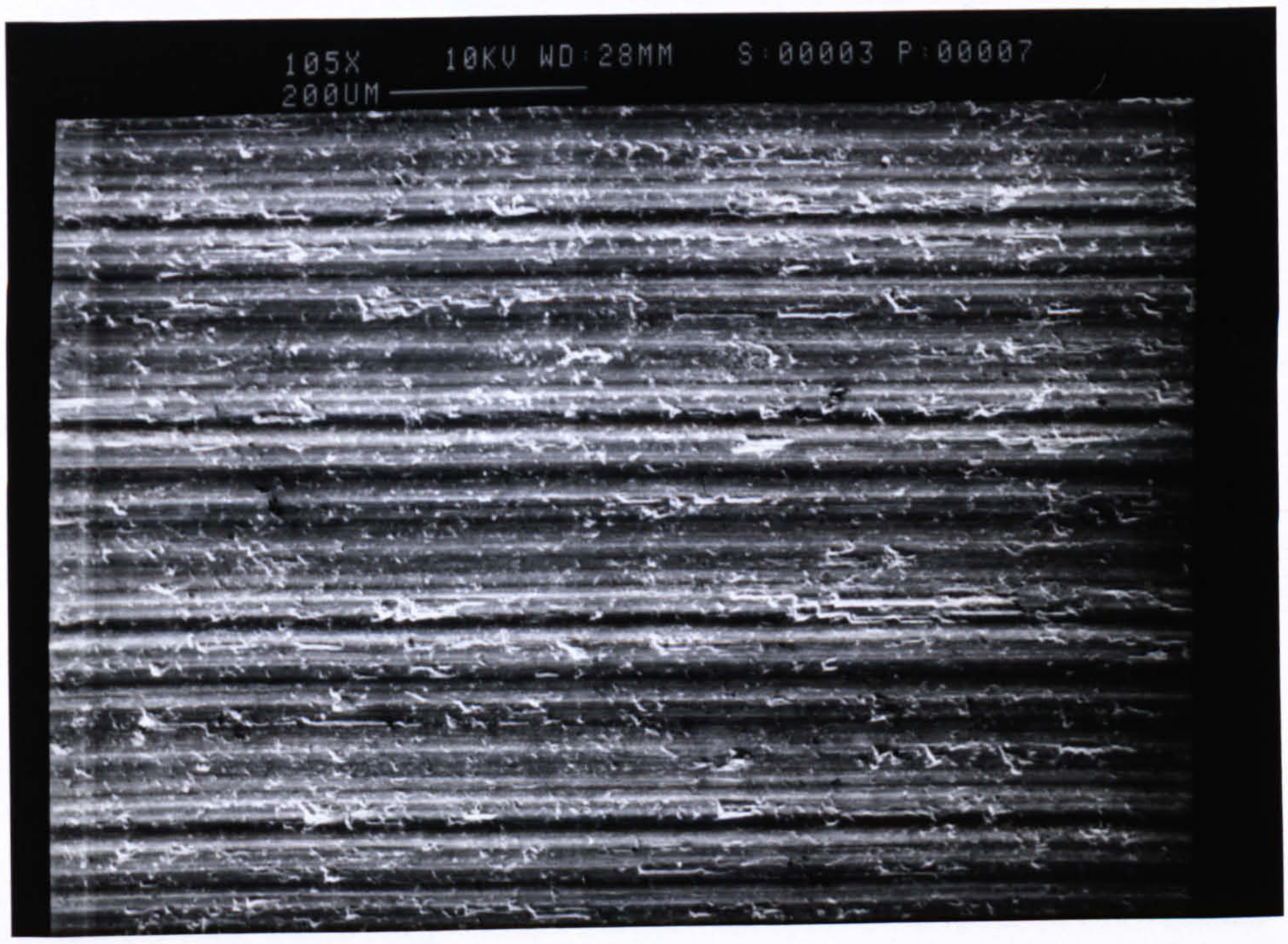

(a)

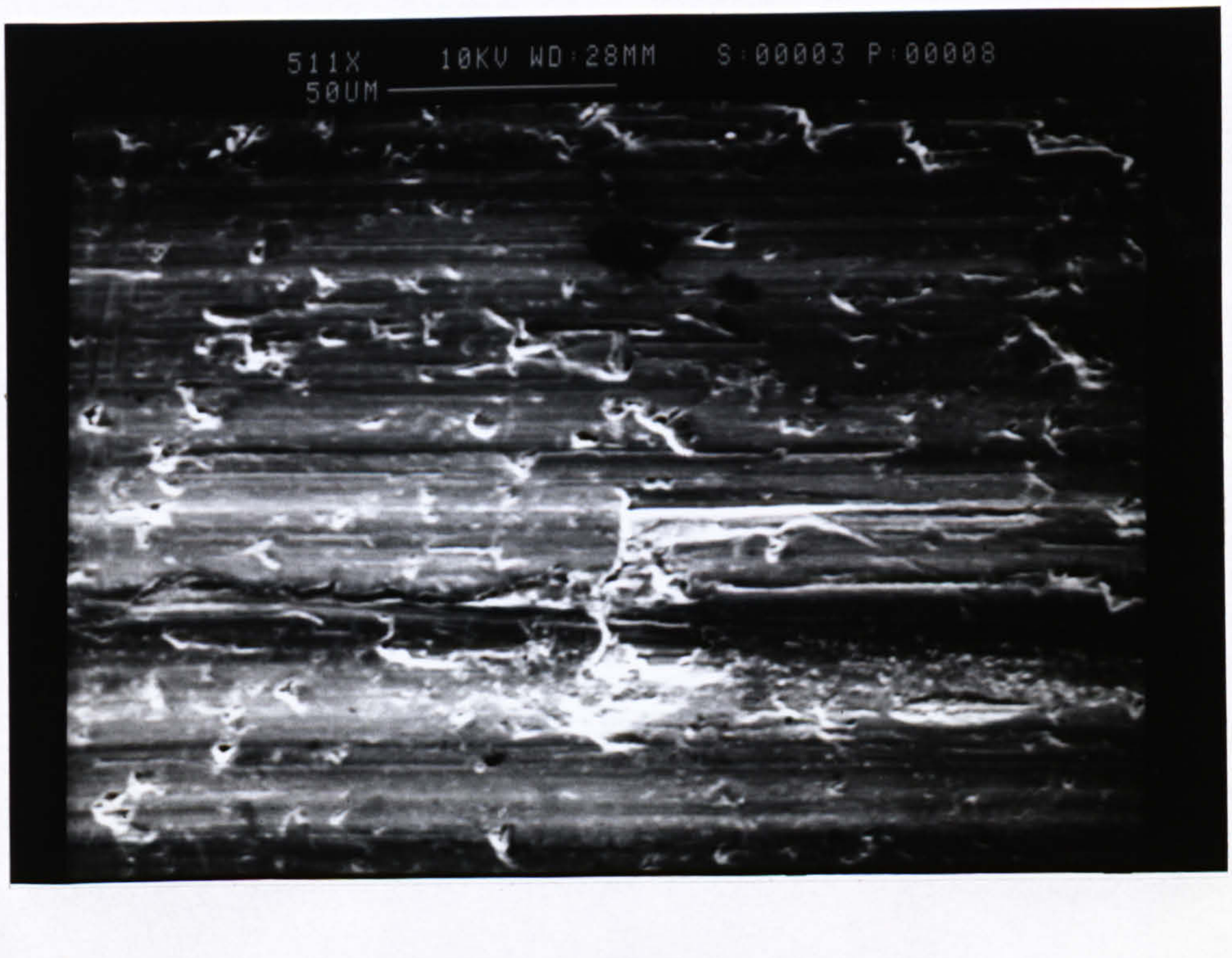

(b)

Figure 7.83 Sample of Machined Surface (V = 20 m/min , Feed = 0.2 mm/rev, DOC = 2 mm) At Magnification of (a) 100X , and (b) 500X (↑ Direction Of Feed)

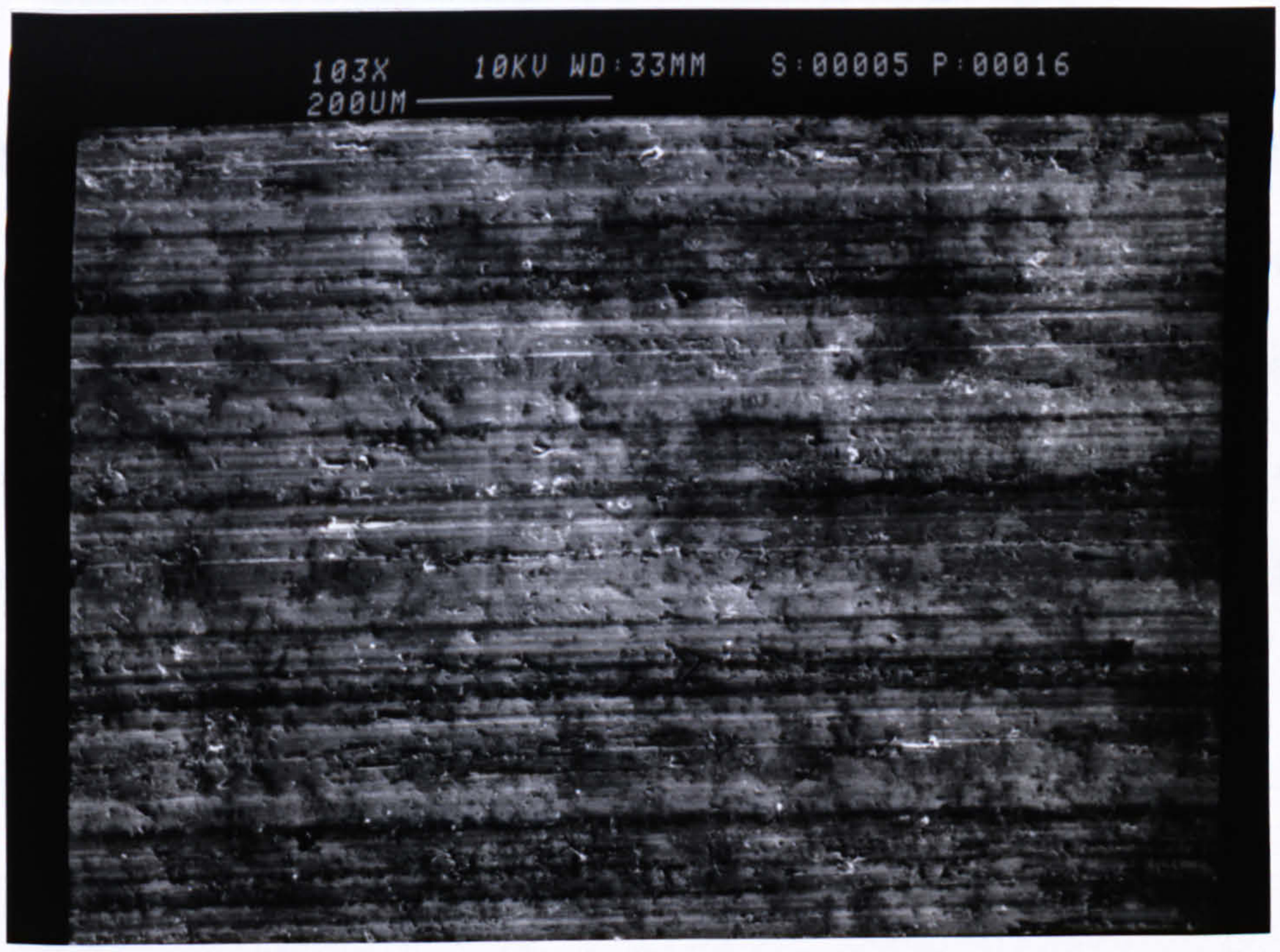

(a)

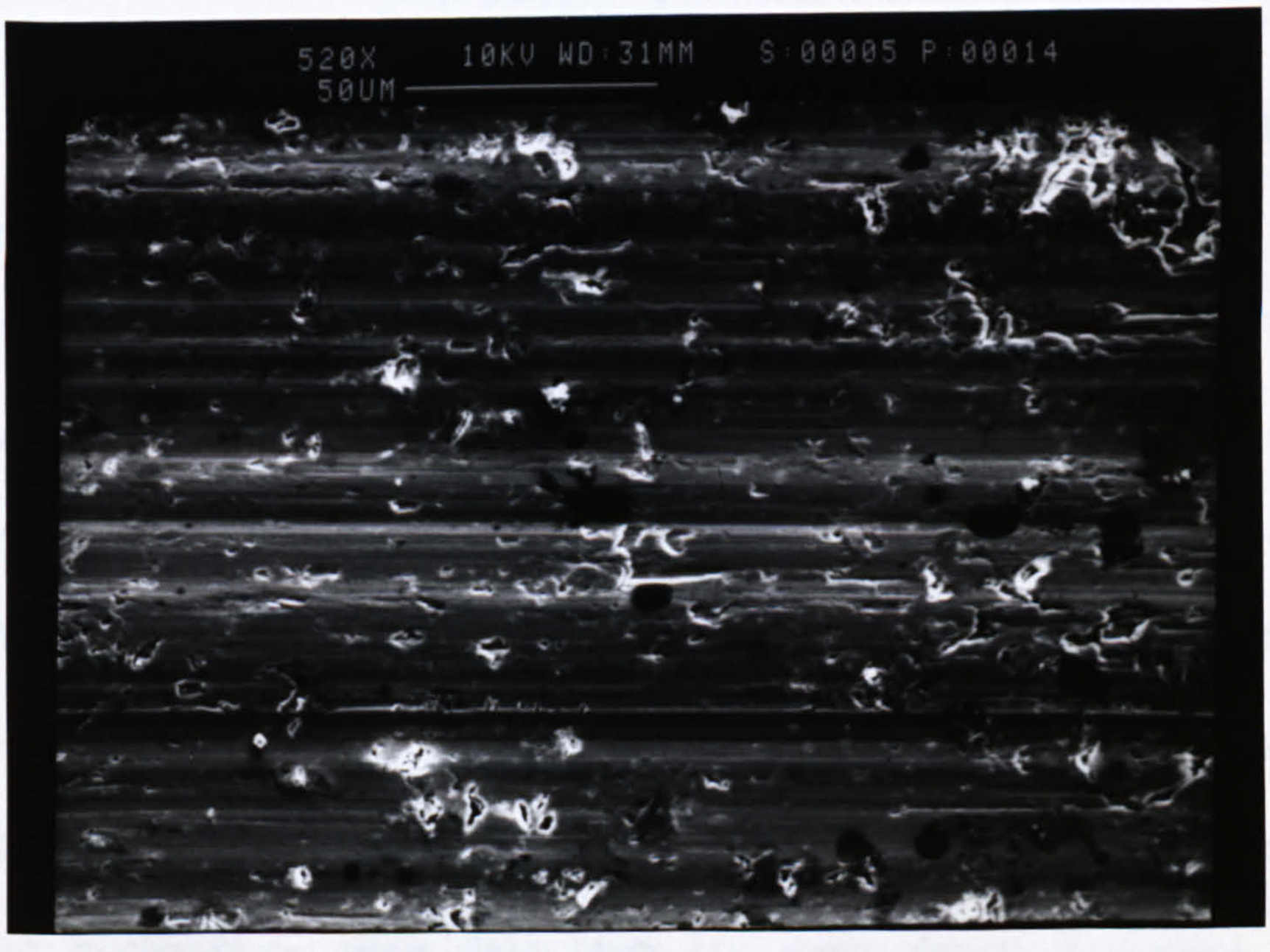

(b)

Figure 7.84 Sample of Machined Surface (V = 20 m/min , Feed = 0.2 mm/rev, DOC = 2 mm) At Magnification of (a) 100X , and (b) 500X (↑ Direction Of Feed)

7.7 Nature Of Chip Formation And Quick-Stop Results

In order to understand the wear mechanism and the surface finish produced, the understanding of both chip and built-up edge (BUE) formation processes when machining aluminium 2618 MMC with cemented carbide tools is very important. A good source of information about chip formation is the quick-stop technique, i.e. to stop the cutting action suddenly. After rapidly removing the tool, a segment of the bar, with chip attached, was cut out, cleaned and examined using SEM.

7.7.1 Chip Formation

It can be said that the nature of chips formed during machining changed with the extent of tool wear. At the start of the cut, when the tool is sharp, long washer type helical chips are mainly formed (type 4.1 ISO: 3685), Figure 7.85, sometimes accompanied by small amounts of snarled washer type helical chips (type 4.3), Figure 7.86. The chip type changed into short washer helical chips (type 4.2), Figure 7.87, with some loose arch, once the tool started to wear. The greater the wear, the more loose arch chips were produced. There might be two reasons for such chips being formed during machining. Firstly, the addition to an aluminium alloy of SiC particle reinforcement reduces ductility and induces fracture in the shear zone. Secondly, any unstable built up edge on the tool tip operates as a chip breaker. In terms of machinability, since short chips can easily detach themselves from workpiece and prevent tool damage by recutting, this type of chip is more desirable - as long as the surface finish generated stays within the allowable limit.

Representations of chip formation obtained from quick stop segment when machining at various cutting conditions are shown in Figures 7.88(a), 7.89(a) and 7.90(a). The chip types obtained from those chip formation processes are presented in Figures 7.88(b), 7.89(b) and 7.90(b) respectively.

7.7.2 Built-up Edge (BUE) Formation

In general, the formation of built-up material was observed under most of the cutting conditions when machining aluminium 2618 MMC with K68 and KC910 inserts. Figures 7.91(a) and 7.91(b) show a typical built up of material formed at cutting speeds of 15 m/min and 20 m/min. Further investigation using the quick-stop technique shows that a built-up edge (BUE) exist under most cutting conditions, as will be shown later. Most BUEs observed were of a stable type, particularly in the lower cutting speed range, with maximum formation in the range 15 m/min to 35 m/min. Figures 7.92(a) (b), (c) and (d) show a section through BUEs produced during machining at cutting speeds of 15 m/min, 25 m/min, 30 m/min and 35 m/min. The shape of the BUE changes as the cutting speed is increased. Figure 7.92(d) (v = 35 m/min) shows some part of a broken BUE, the remainder being left on the rake face. In some instances, the presence of BUE appeared to increase the tool life. The BUE disappeared as the cutting speed was raised.

Figures 7.93(a) and 7.93(b) - 7.96(a) and 7.96(b) show segment of the quick-stop samples with BUE and cross-section of the samples respectively. Figures 7.93(b) -

7.96(b) show distinctively the presence of BUE with different shapes at each particular cutting conditions. At higher magnification, Figures 7.93(c) - 7.96(c), it can be seen that the microstructure of BUE when machining MMC contained heavily compressed layers of work hardened material and a higher concentration of fine SiC particles than the main body of the material. Figure 7.97(a) and 7.97(b) show a segment of a quick-stop sample and a cross-section of the sample which has no BUE.

Alternatively, the presence or absence of BUE can be inferred from a study of the machined surface of the workpiece material, the underside of the chips, the forces generated during cutting and chip thickness measurement. Figures 7.98 - 7.101 show the variation of chip thickness and shear plane angle (ϕ) at various cutting speeds. With reference to Figure 2.17, the shear plane angle (ϕ) determined from experimental values of t_1 (feed rate) and t_2 (chip thickness) using the relationship given in equation (7.2) below [13] [16]:

$$\tan \phi = \frac{r_a \cos \alpha}{1 - r_a \sin \alpha} \quad \text{..... (7.2)}$$

where ϕ = shear angle
r_a = chip thickness ratio (given by t_1/t_2)
α = rake angle

At lower feed rates, chip thickness reduced with increasing cutting speed except at 25 m/min and 30 m/min for both K68 and KC910 tools with negative rake geometry. Increasing the feed rate resulted in increased chip thickness as shown in Figure 7.99.

The same pattern occurred at higher feed rates, except for K68 and KC910 inserts with negative rakes, where the chip thickness was markedly reduced at cutting speeds of 25 m/min and 30 m/min. It then increased constantly as the cutting speed was raised. The effective rake angle is increased when machining in the presence of BUE, the BUE acts as the rake face of the tool and the chip/tool contact area is reduced. The effect between the reduction of chip thickness and the increase in shear plane angle is observed during these machining tests, as seen in Figures 7.98 and 7.101.

Figures 7.102(a) (b) and (c) show the micrographs of the chip undersides produced when machining at 15 m/min, 25 m/min and 30 m/min. Close examination of the chip undersides in the SEM revealed distinct patterns of pile-up structure.

Most of the time, continuous chips were observed when machining in the range 15 to 25 m/min (i.e. smaller shear plane angles) and changed to discontinuous chips in the range 30 to 40 m/min (larger shear plane angle) and the chips became continuous again once the speed is increased to 50 m/min. This phenomenon occurred when machining with K68 and KC910 inserts with both negative and positive rake geometry.

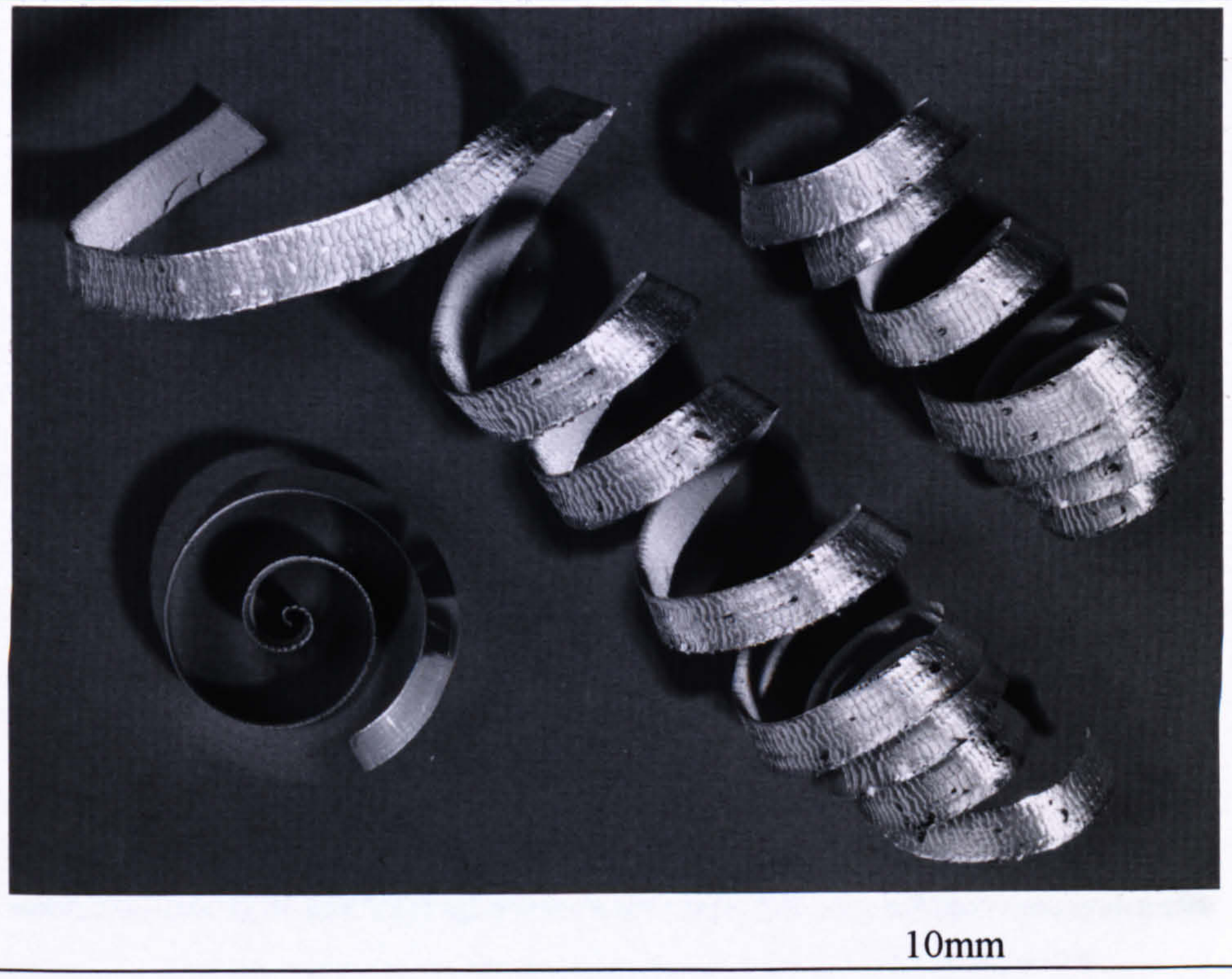

Figure 7.85 Long Washer Helical Chip Type
(V = 25 m/min, Feed = 0.4 mm/rev, DOC = 4 mm)

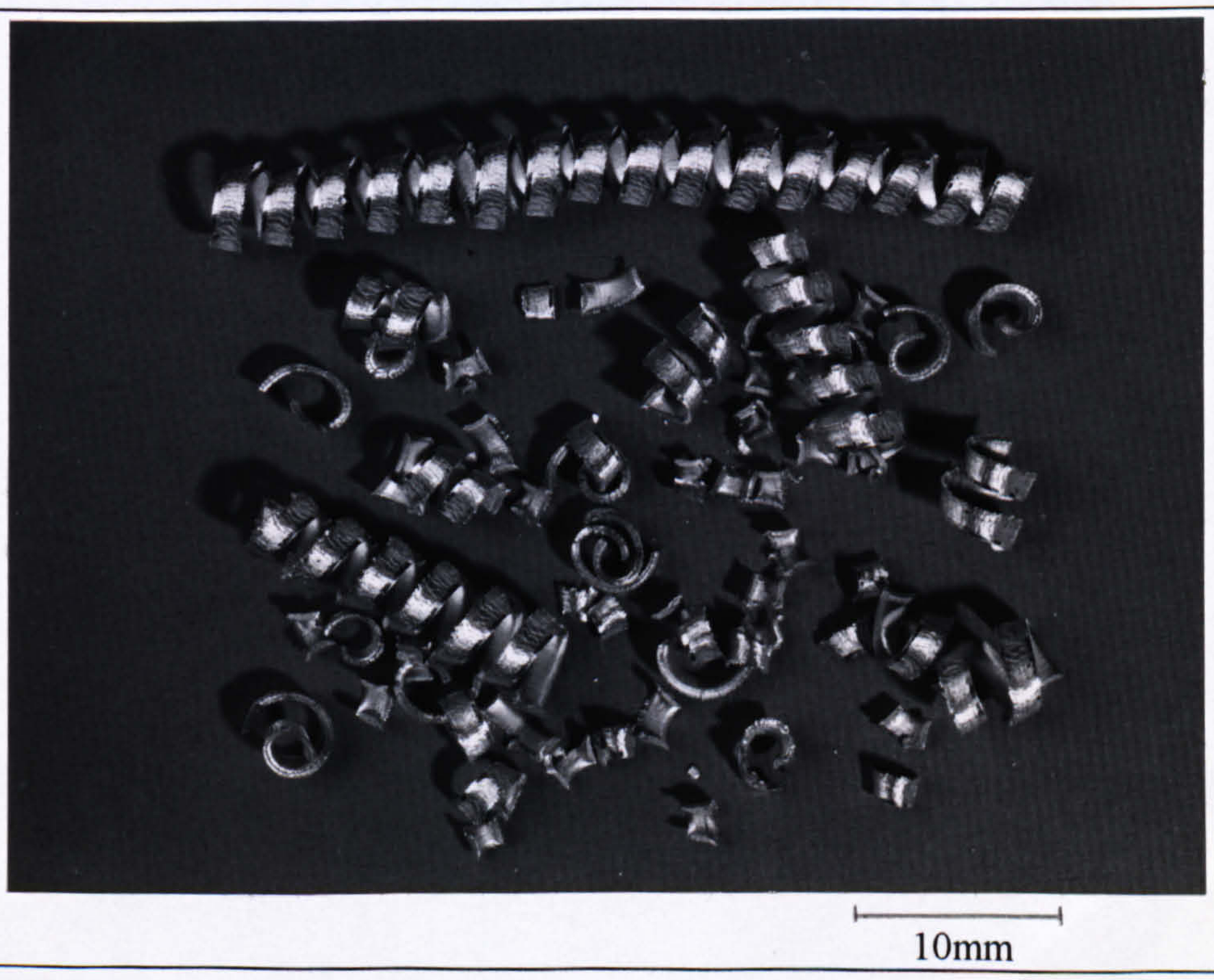

Figure 7.86 Snarled Washer Helical Type Chip
(V = 30 m/min, Feed = 0.6 mm/rev, DOC = 2 mm)

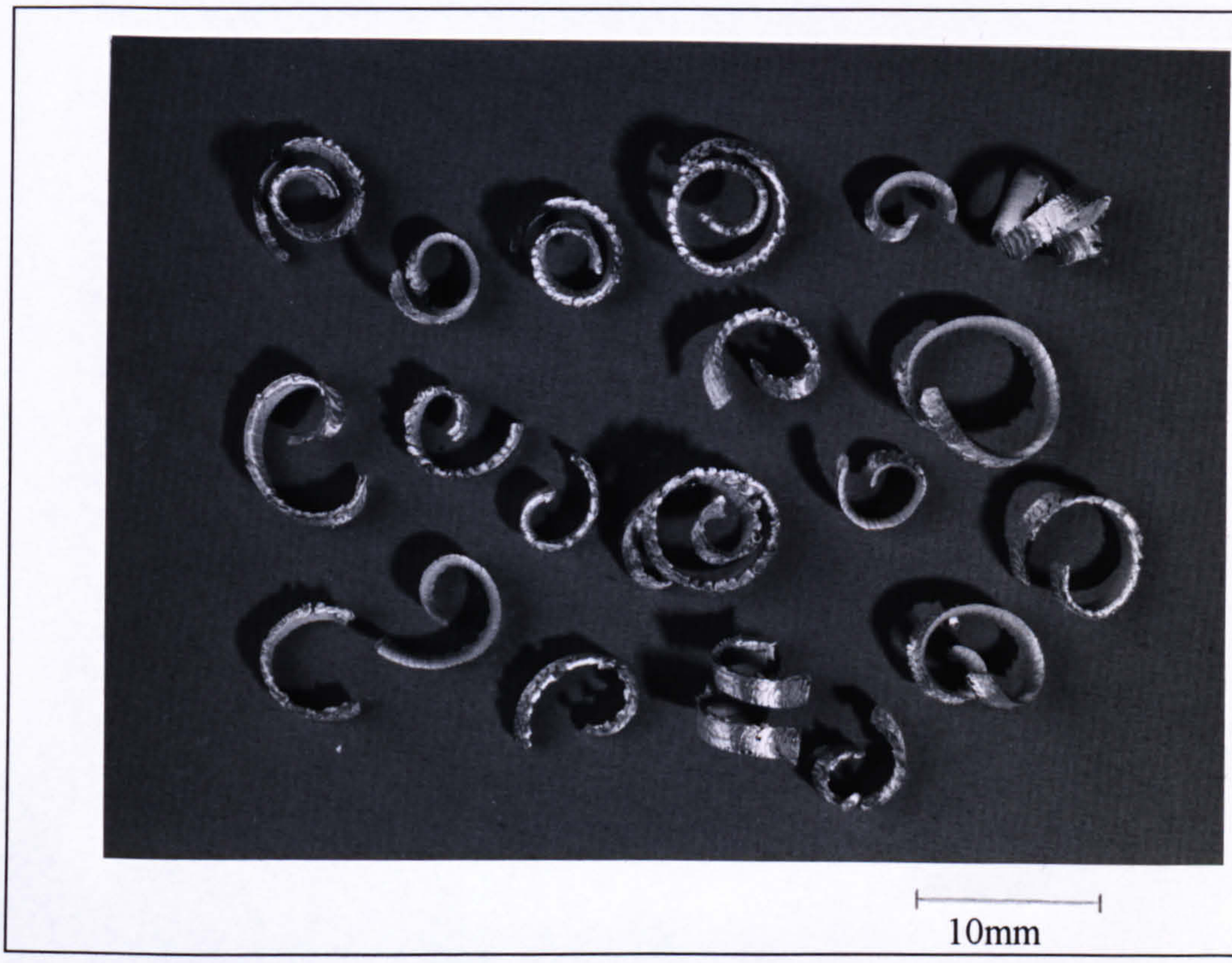

Figure 7.87 Short Washer Helical Type Chip
(V = 25 m/min, Feed = 0.6 mm/rev, DOC = 2 mm)

(a)

(b)

Figure 7.88 (a) Quick Stop Segment With The Chip Attached To The Workpiece (V = 15 m/min, Feed = 0.4 mm/rev., DOC = 4 mm) (b) The Corresponding Chip Produced.

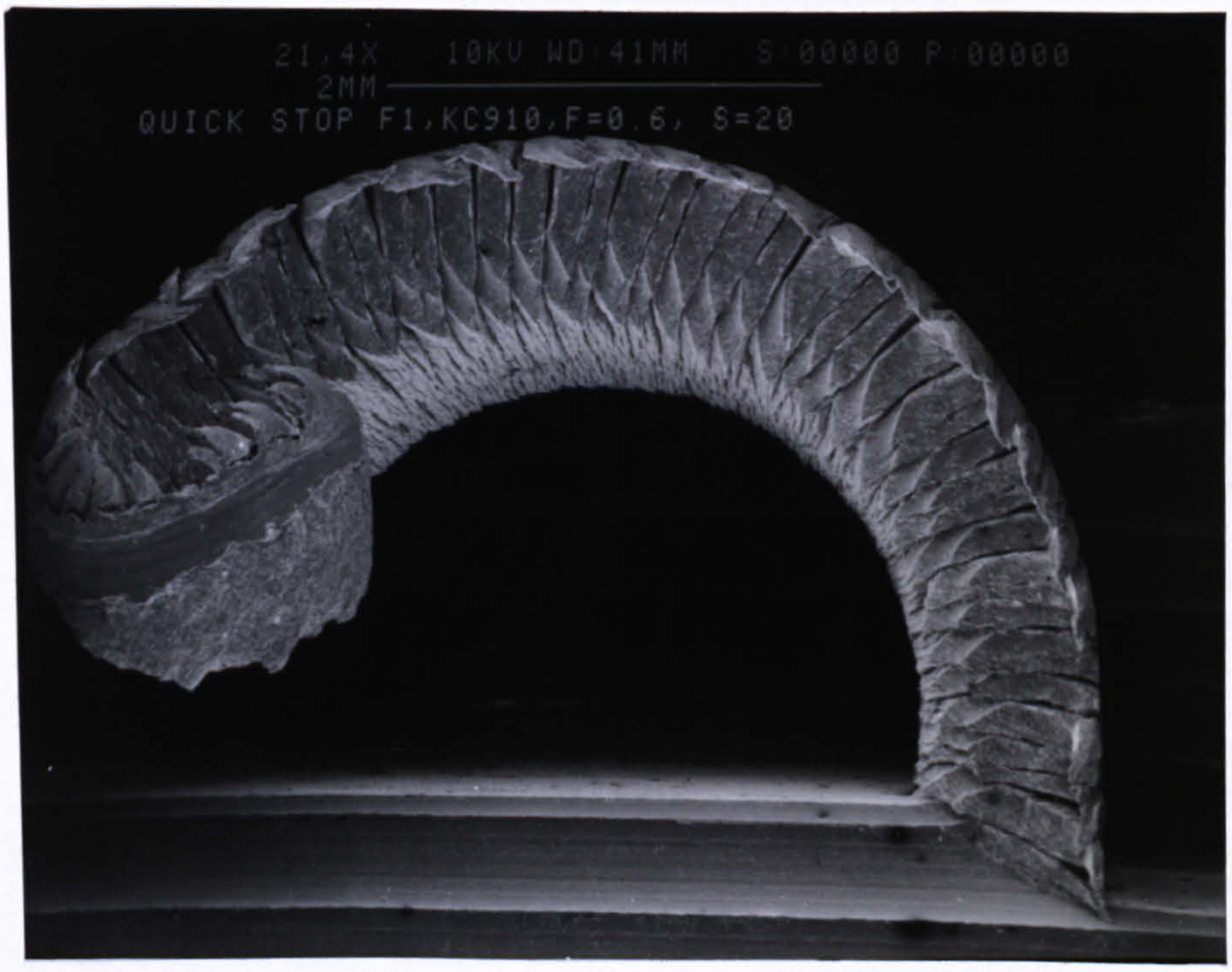

(a)

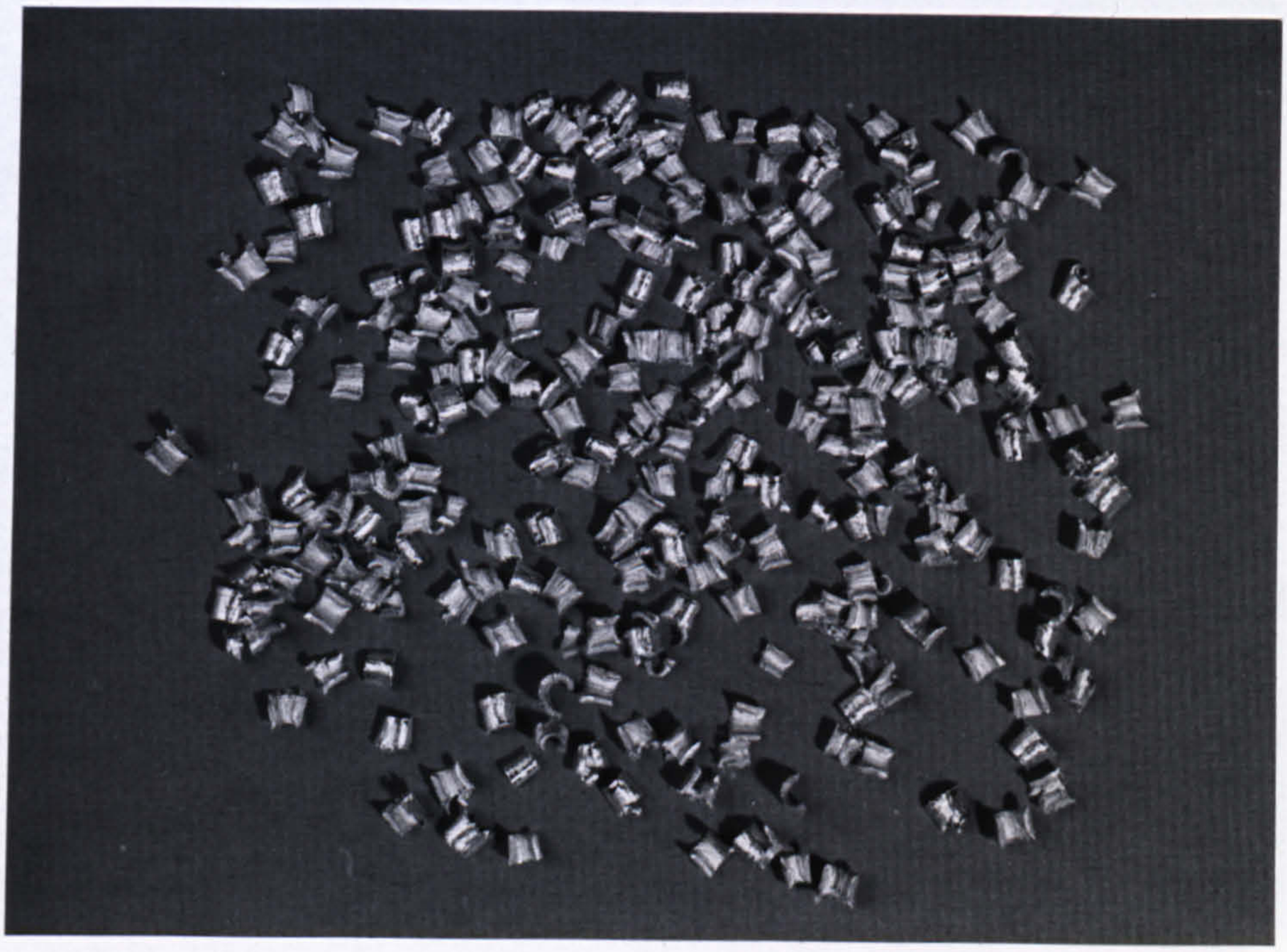

(b)

10mm

Figure 7.89 (a) Quick Stop Segment With The Chip Attached To The Workpiece (V = 20 m/min, Feed =0.6 mm/rev., DOC = 2 mm) (b) The Corresponding Chip Produced

(a)

(b)

10mm

Figure 7.90 (a) Quick Stop Segment With The Chip Attached To The Workpiece (V = 25 m/min, Feed =0.6 mm/rev., DOC = 2 mm) (b) The Corresponding Chip Produced.

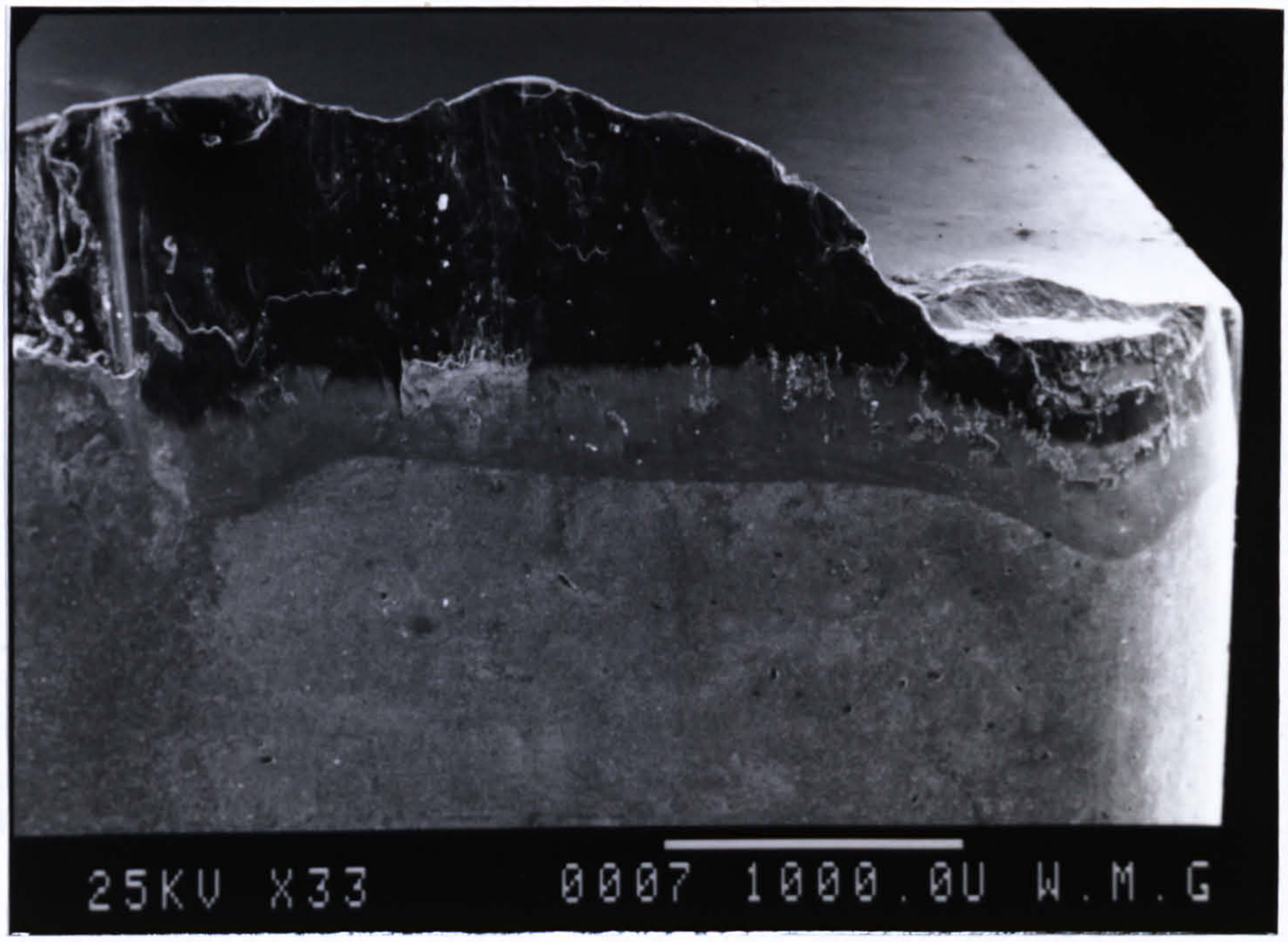

(a)

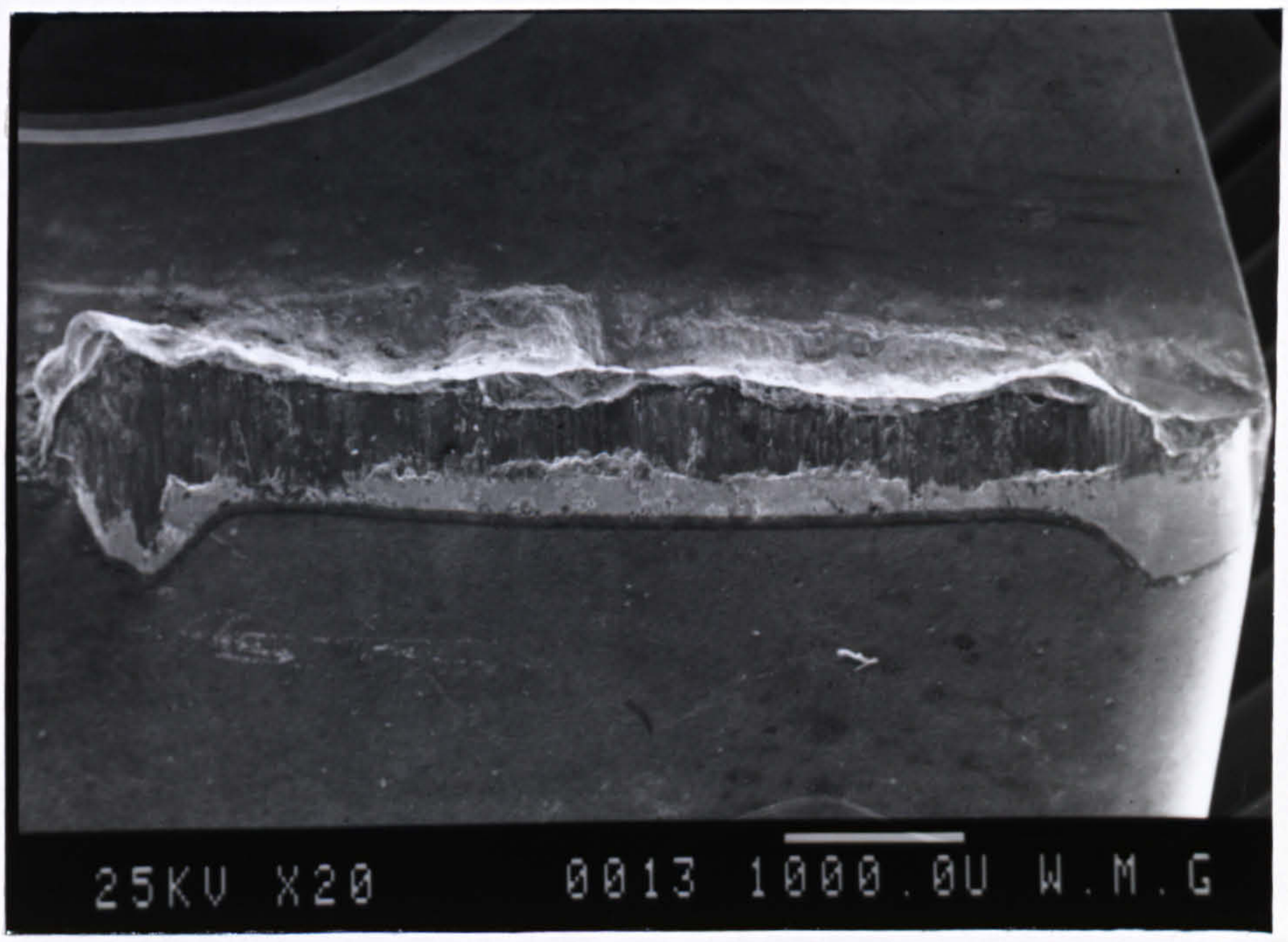

(b)

Figure 7.91 A Typical Built-Up Material Formed On Cemented Carbide Inserts At (a) V = 15 m/min and (b) 30 m/min

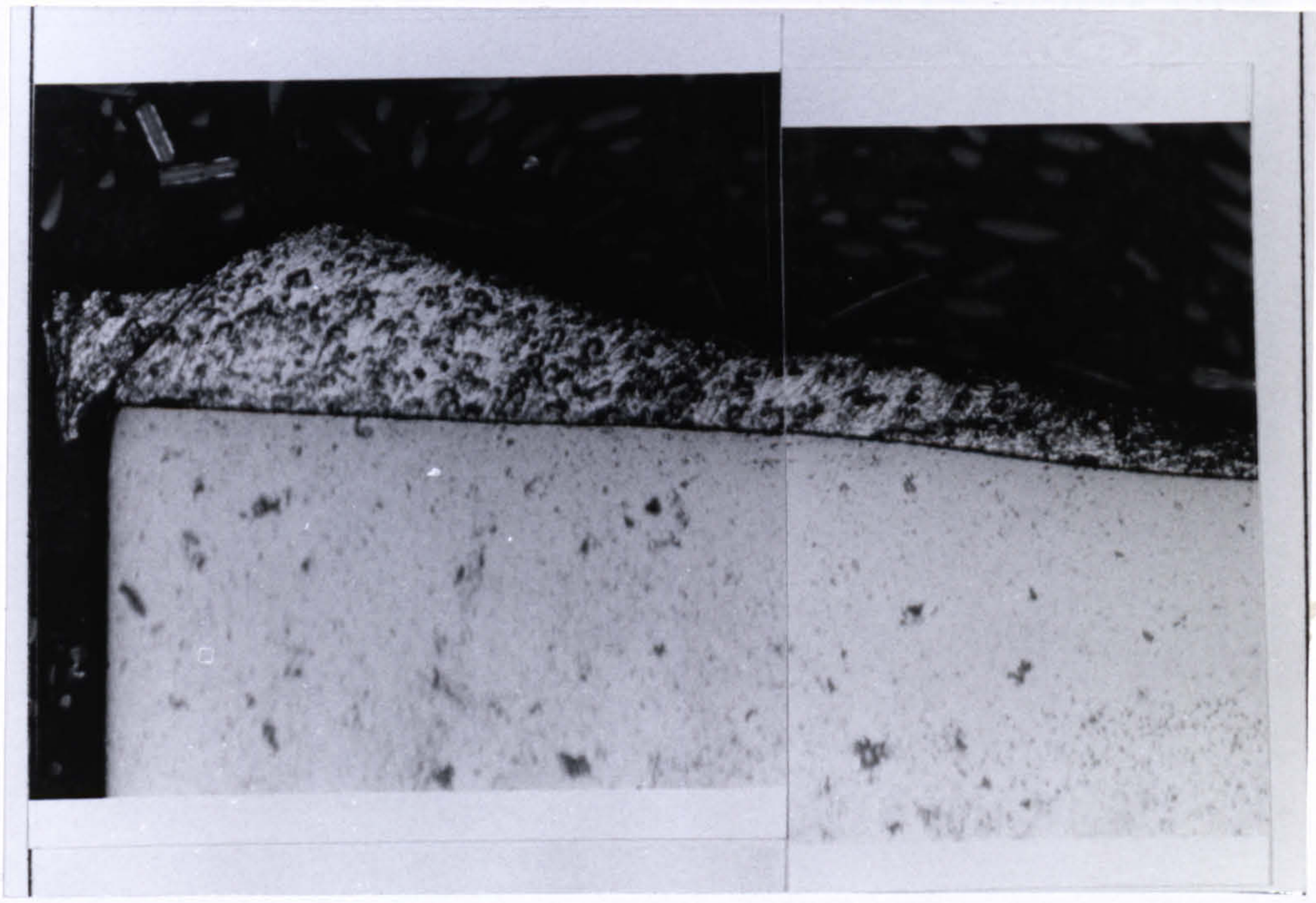

(a)

(b)

Figure 7.92 Cross-section of an Insert Showing A BUE At (a) V= 15 m/min (X185), (b) V = 25 m/min (X185)

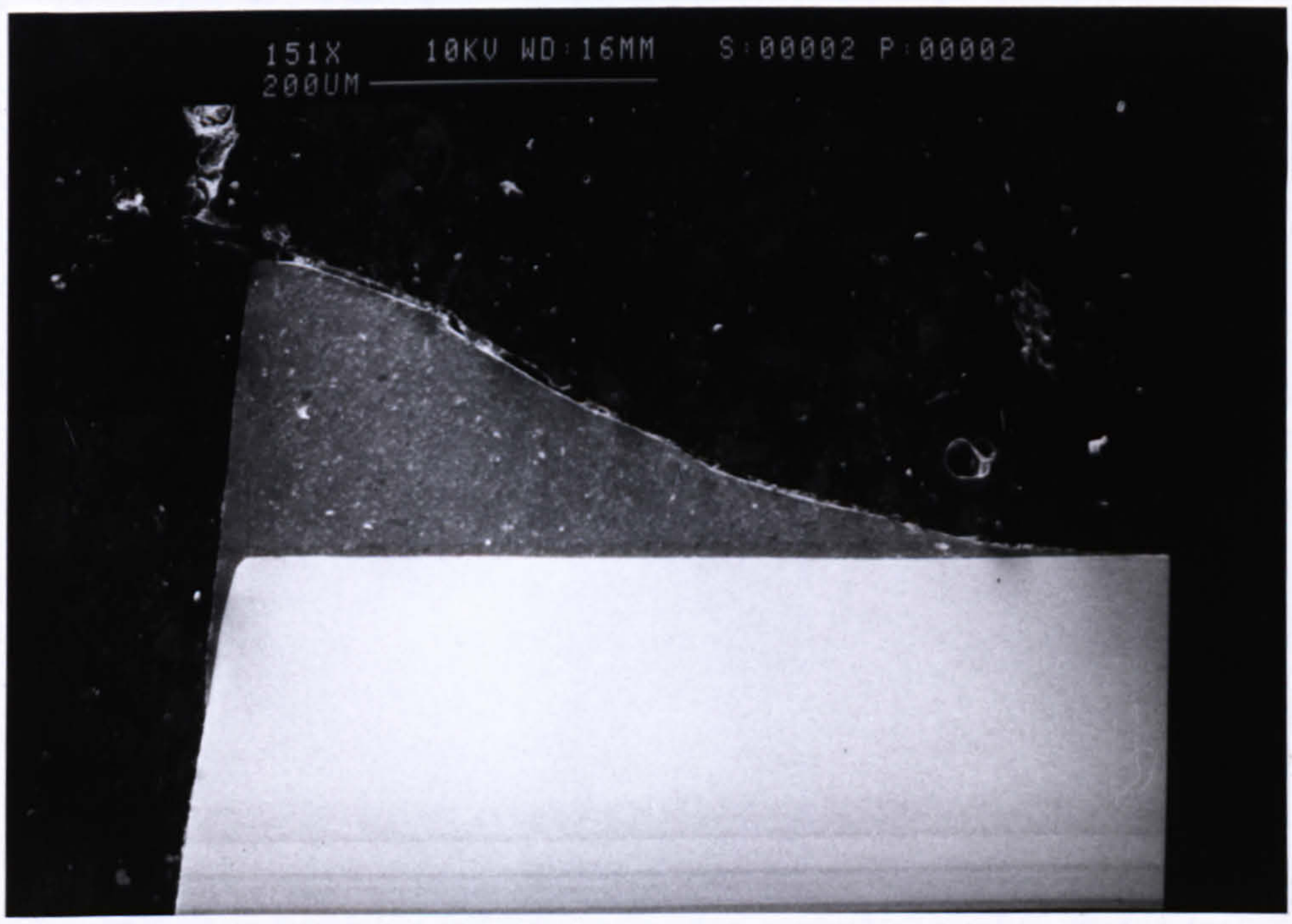

(c)

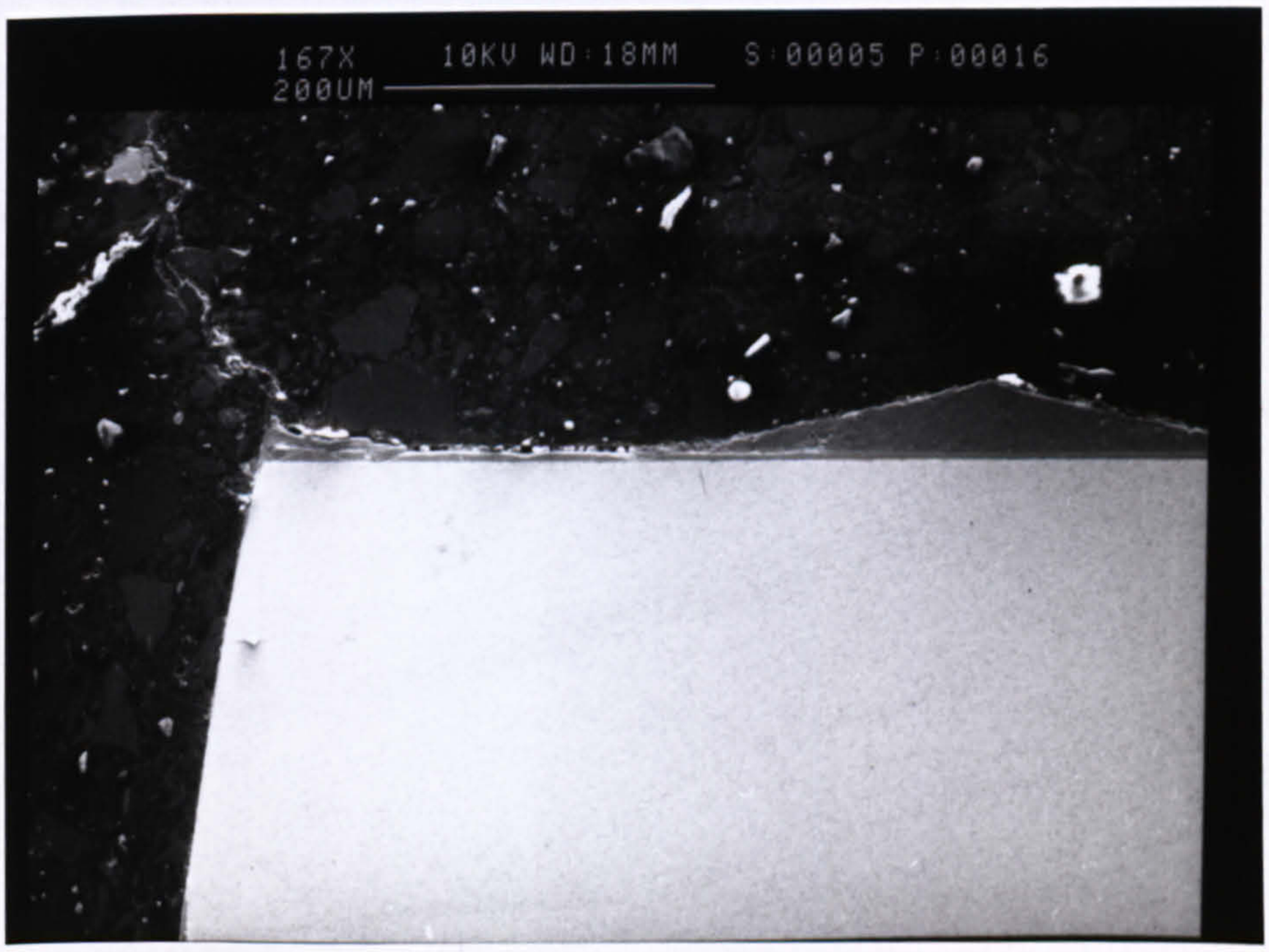

(d)

Figure 7.92 Cross-section of an Insert Showing A BUE At (c) V=30 m/min and (d) V=35 m/min

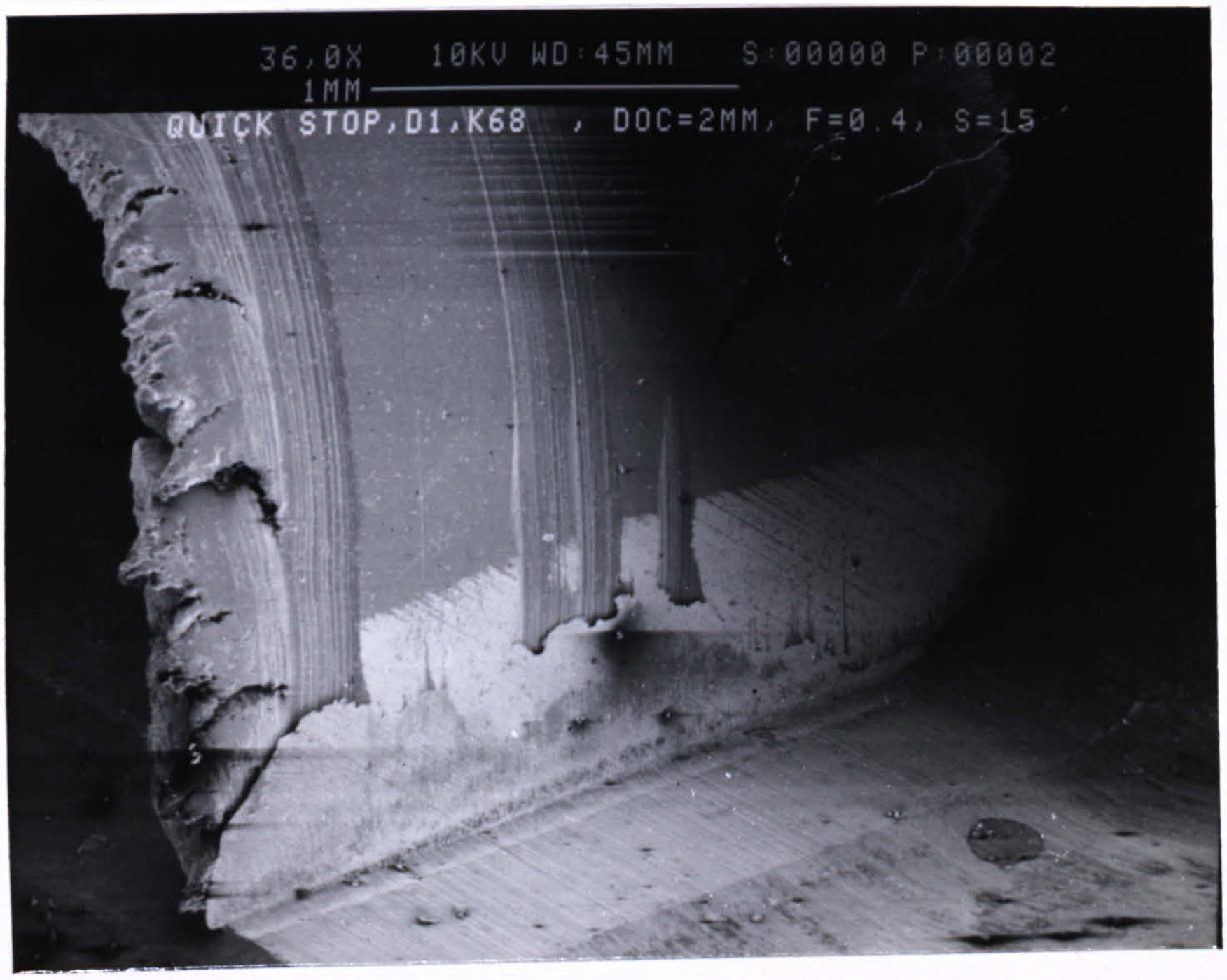

(a)

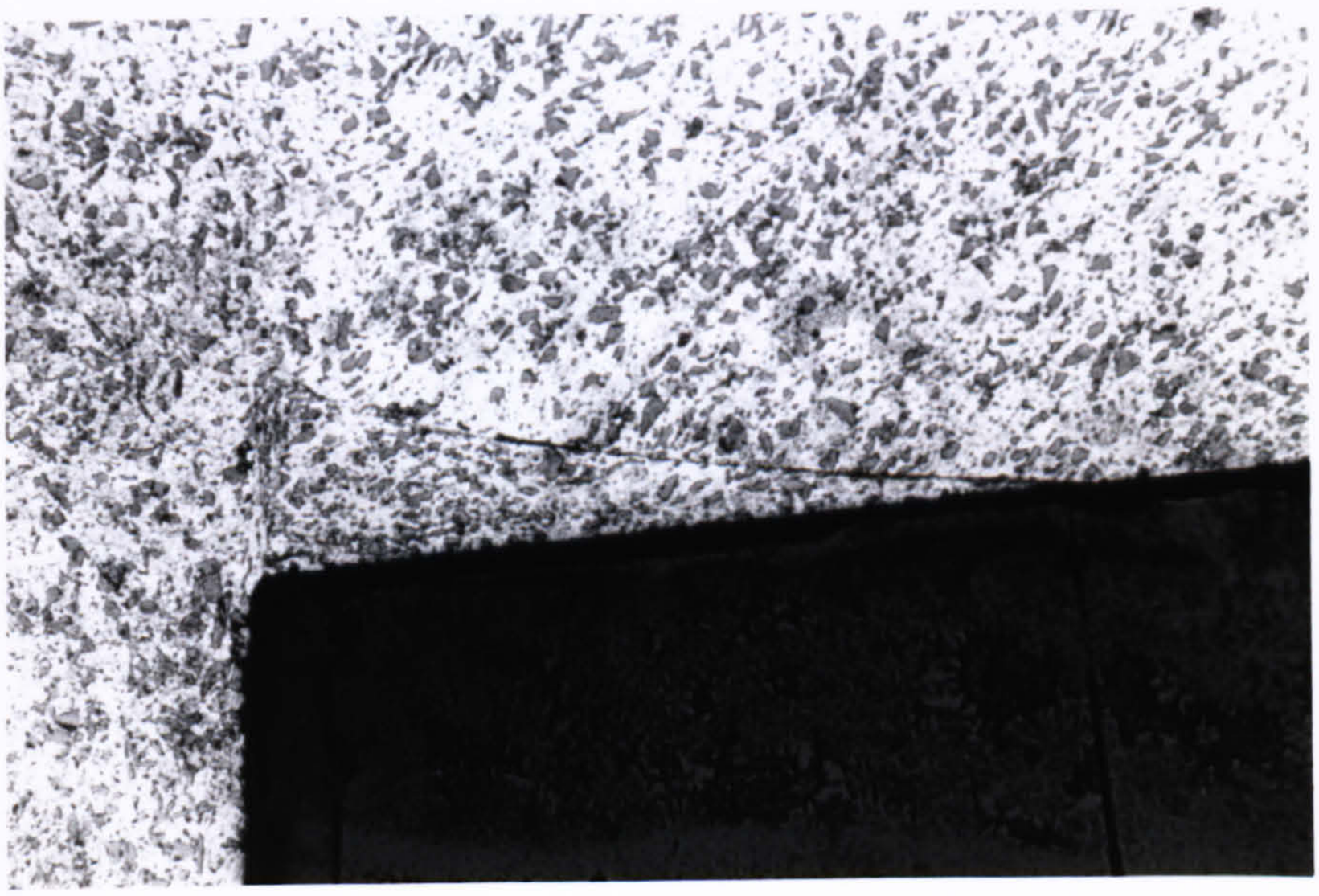

(b)

Figure 7.93 (a) Segment Of Quick Stop With BUE (b) Cross-section Showing The Presence of BUE (V = 15 m/min, Feed = 0.4 mm/rev, DOC = 2mm)(X185)

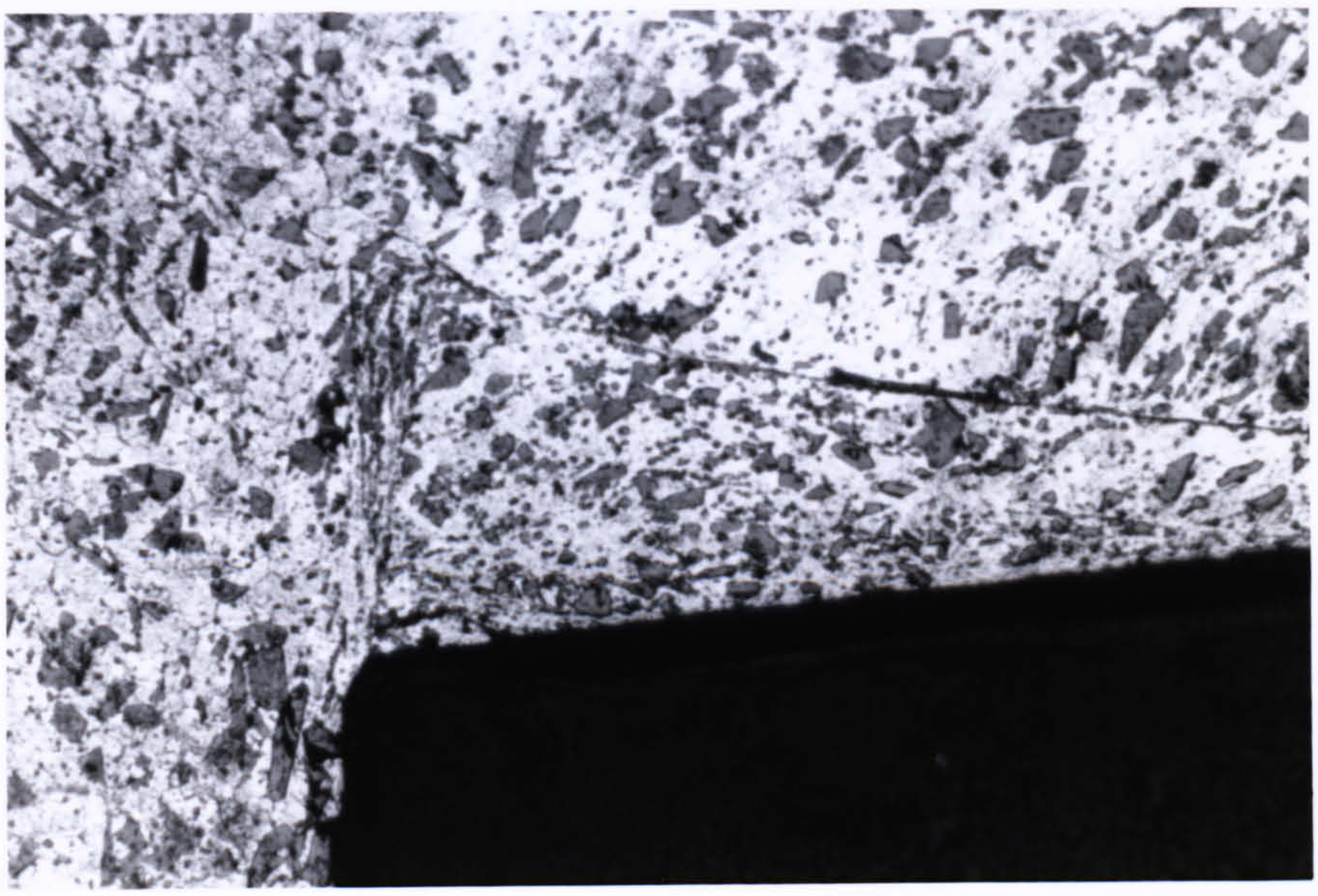

(c)

Figure 7.93 (c) Cross-section Showing The Presence of BUE (V = 15 m/min, Feed = 0.4 mm/rev, DOC = 2 mm)(X400)

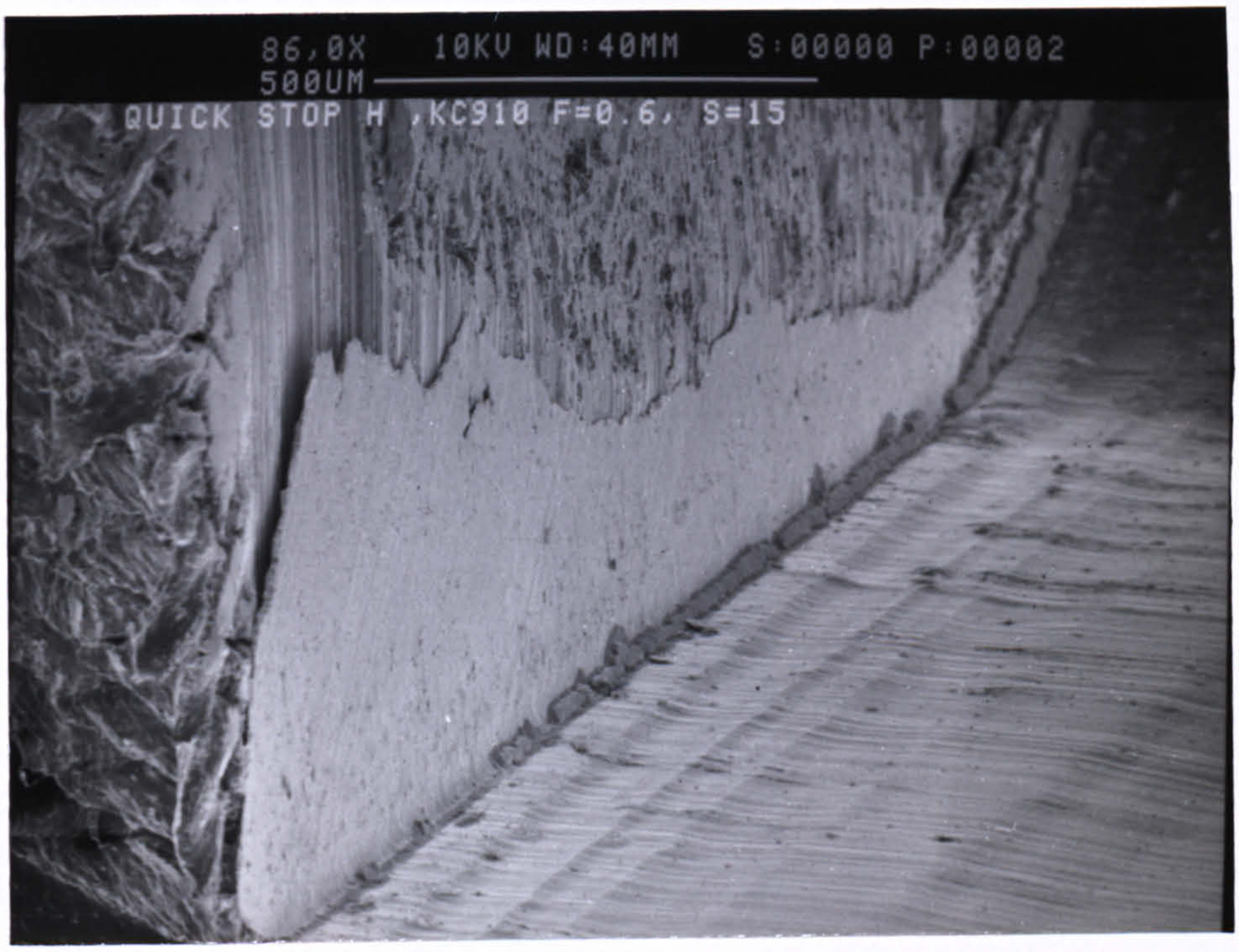

(a)

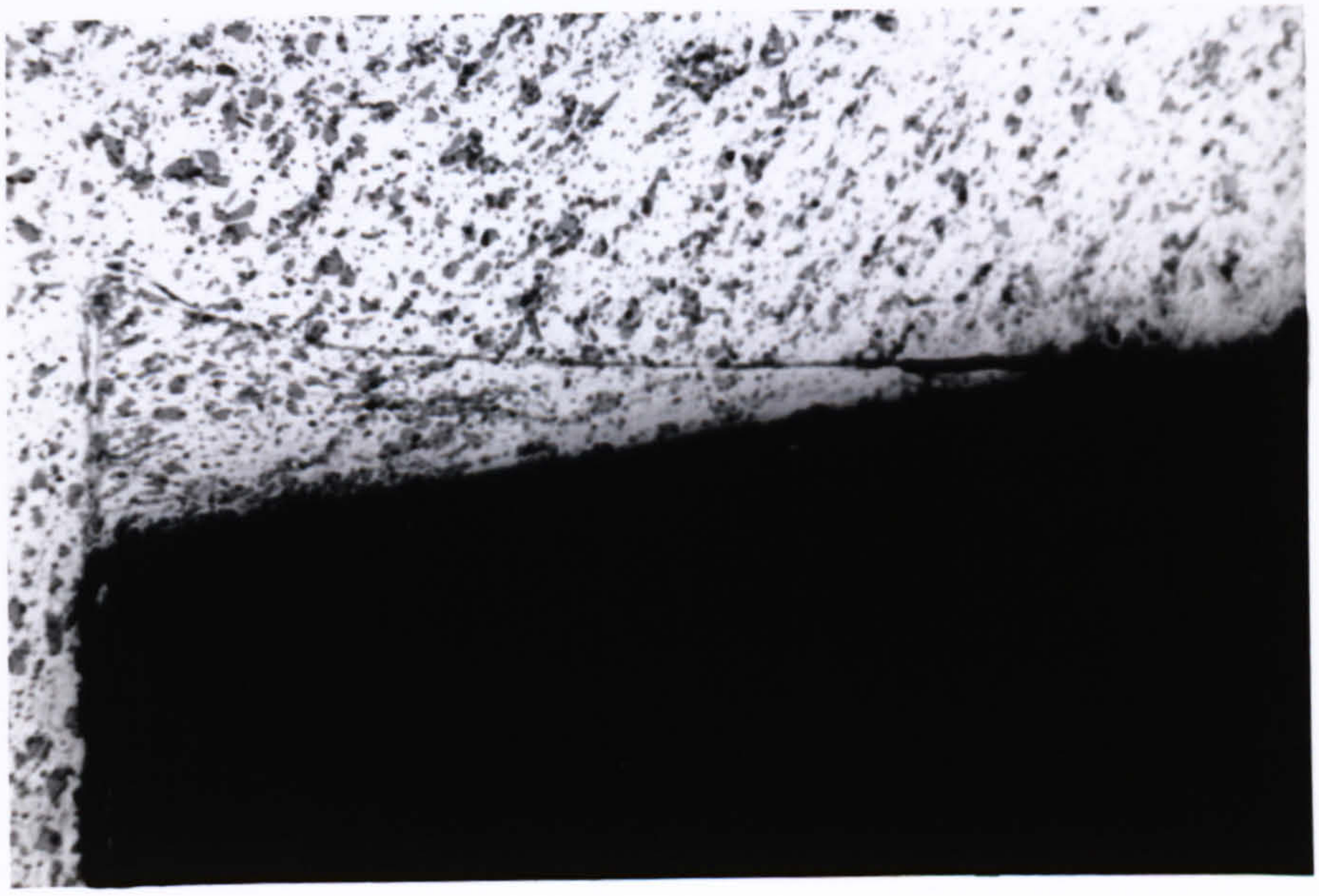

(b)

Figure 7.94 (a) Segment Of Quick Stop With BUE (b) Cross-section Showing The Presence of BUE (V = 15 m/min, Feed = 0.6 mm/rev, DOC = 2 mm)(X185)

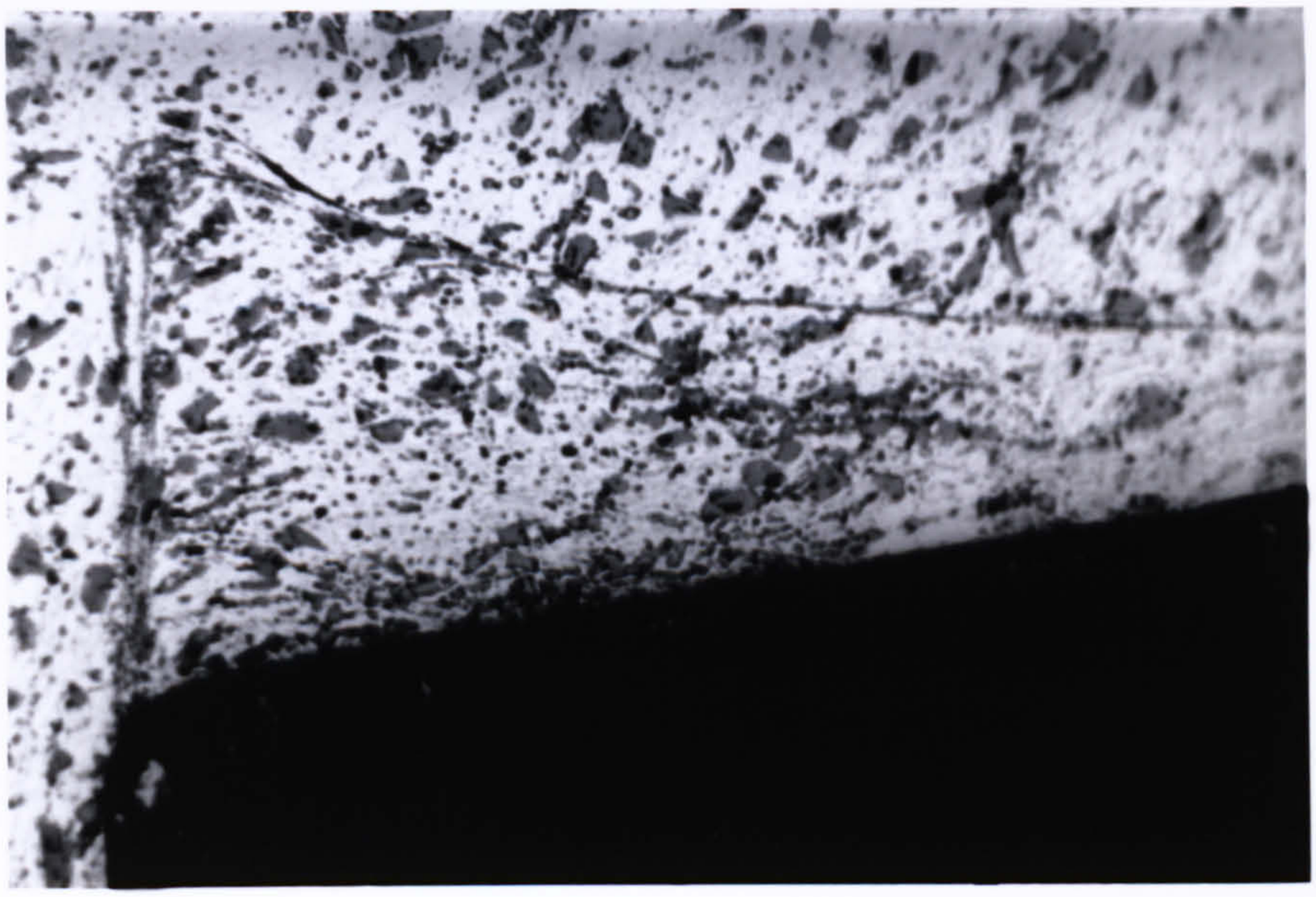

(c)

Figure 7.94 (c) Cross-section Showing The Presence of BUE (V = 15 m/min, Feed = 0.6 mm/rev, DOC = 2 mm)(X400)

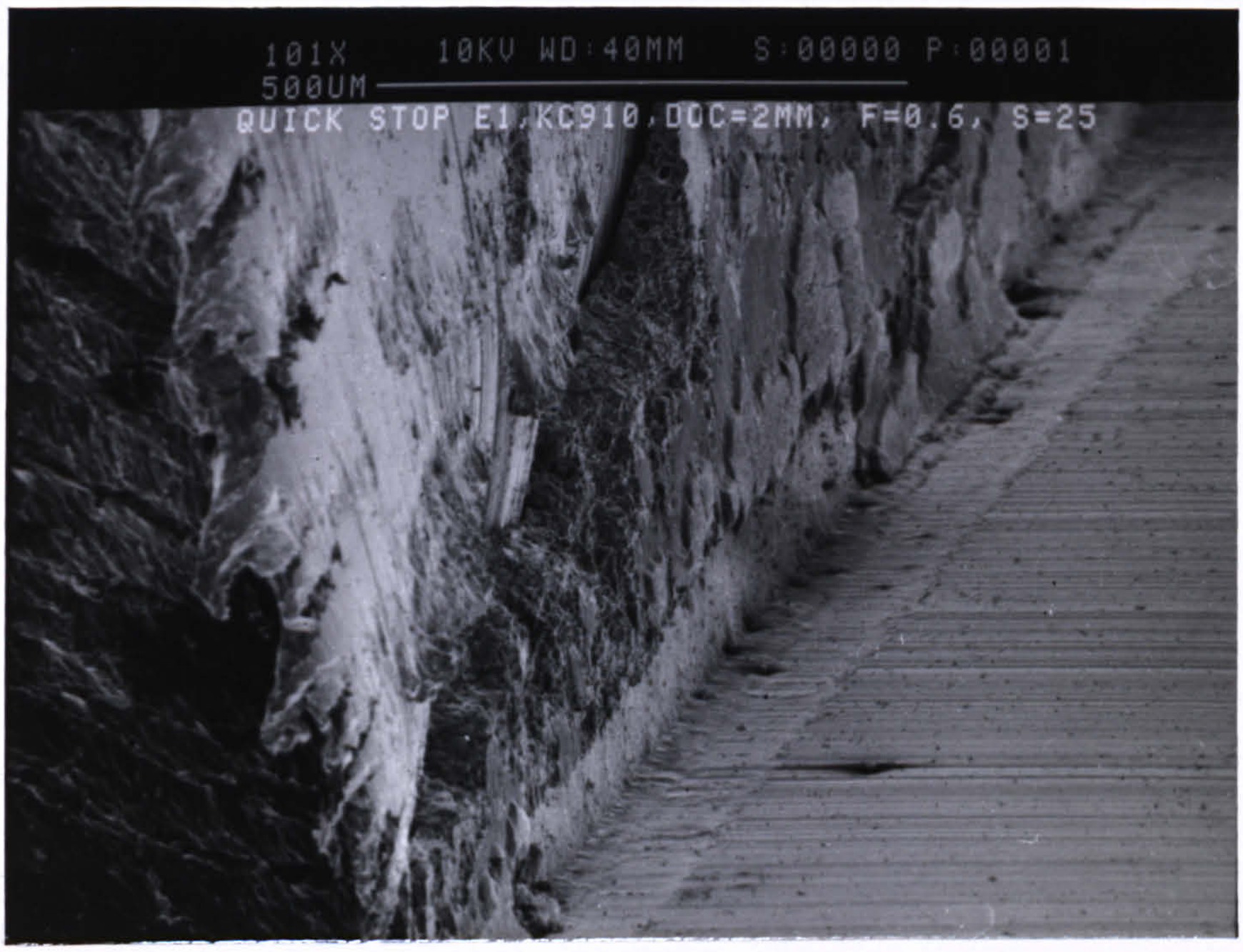

(a)

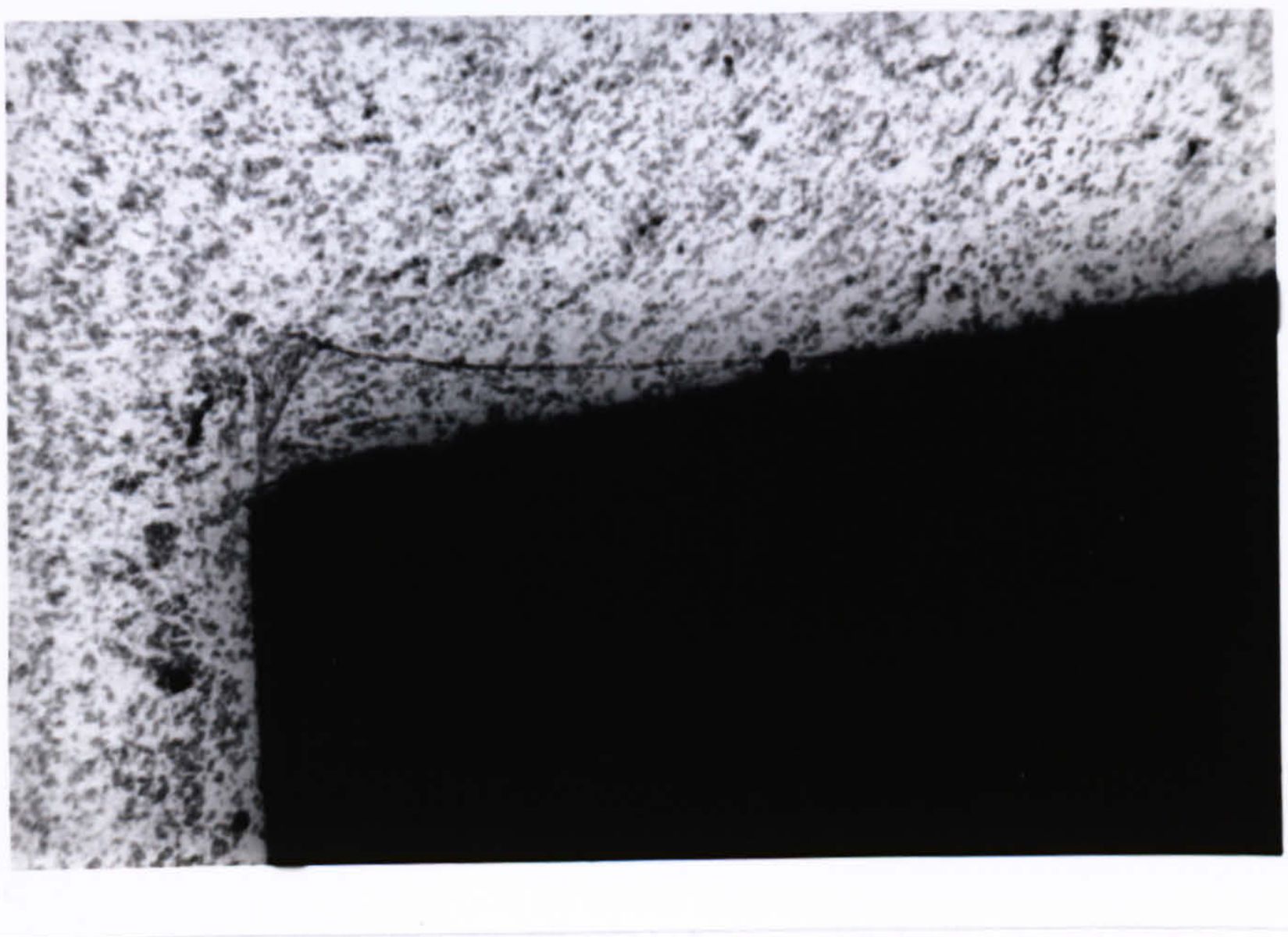

(b)

Figure 7.95 (a) Segment Of Quick Stop With BUE (b) Cross-section Showing The Presence of BUE (V = 25 m/min, Feed = 0.6 mm/rev, DOC = 2 mm)(X185)

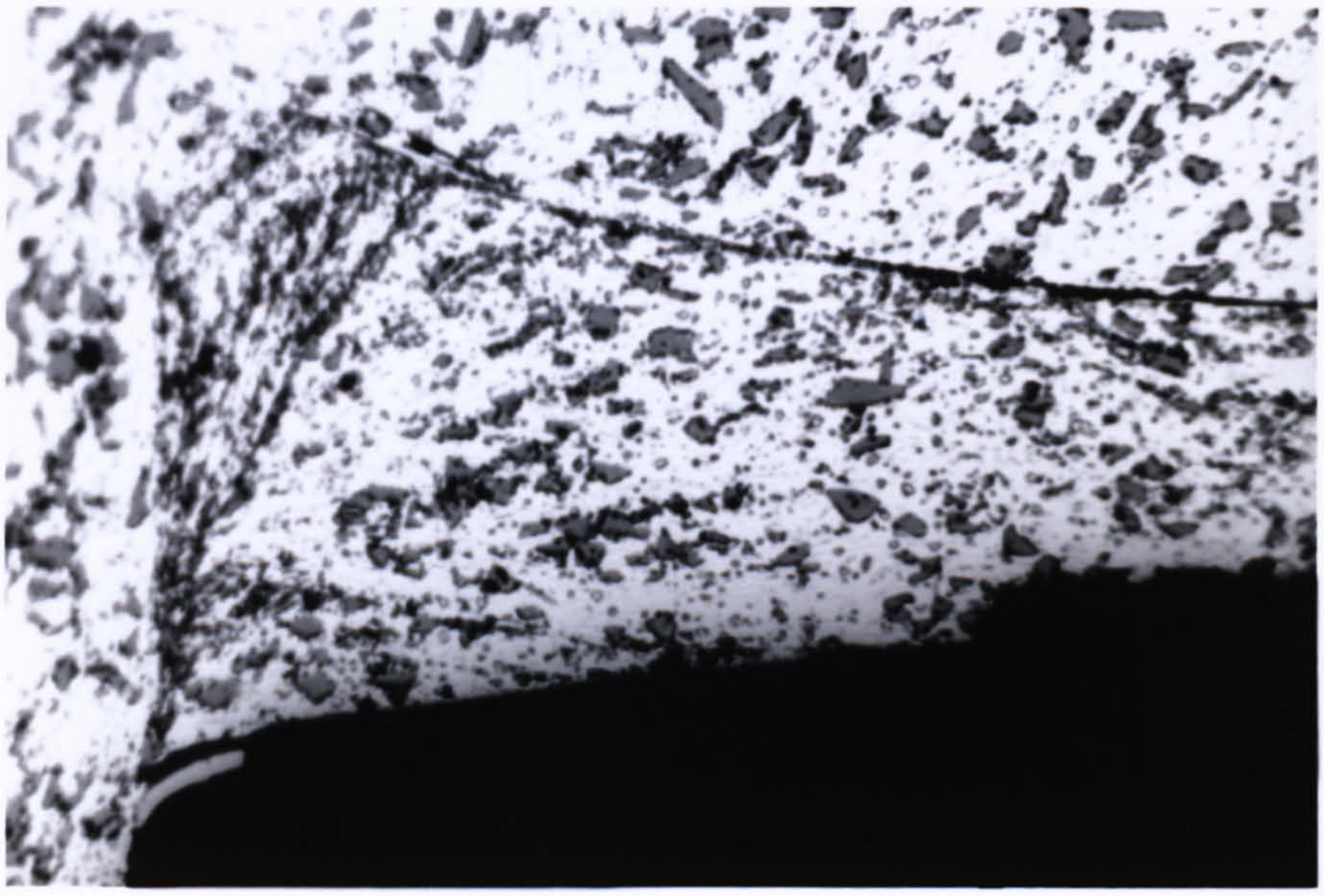

(c)

Figure 7.95 (c) Cross-section Showing The Presence of BUE (V = 25 m/min, Feed = 0.6 mm/rev, DOC = 2 mm)(X400)

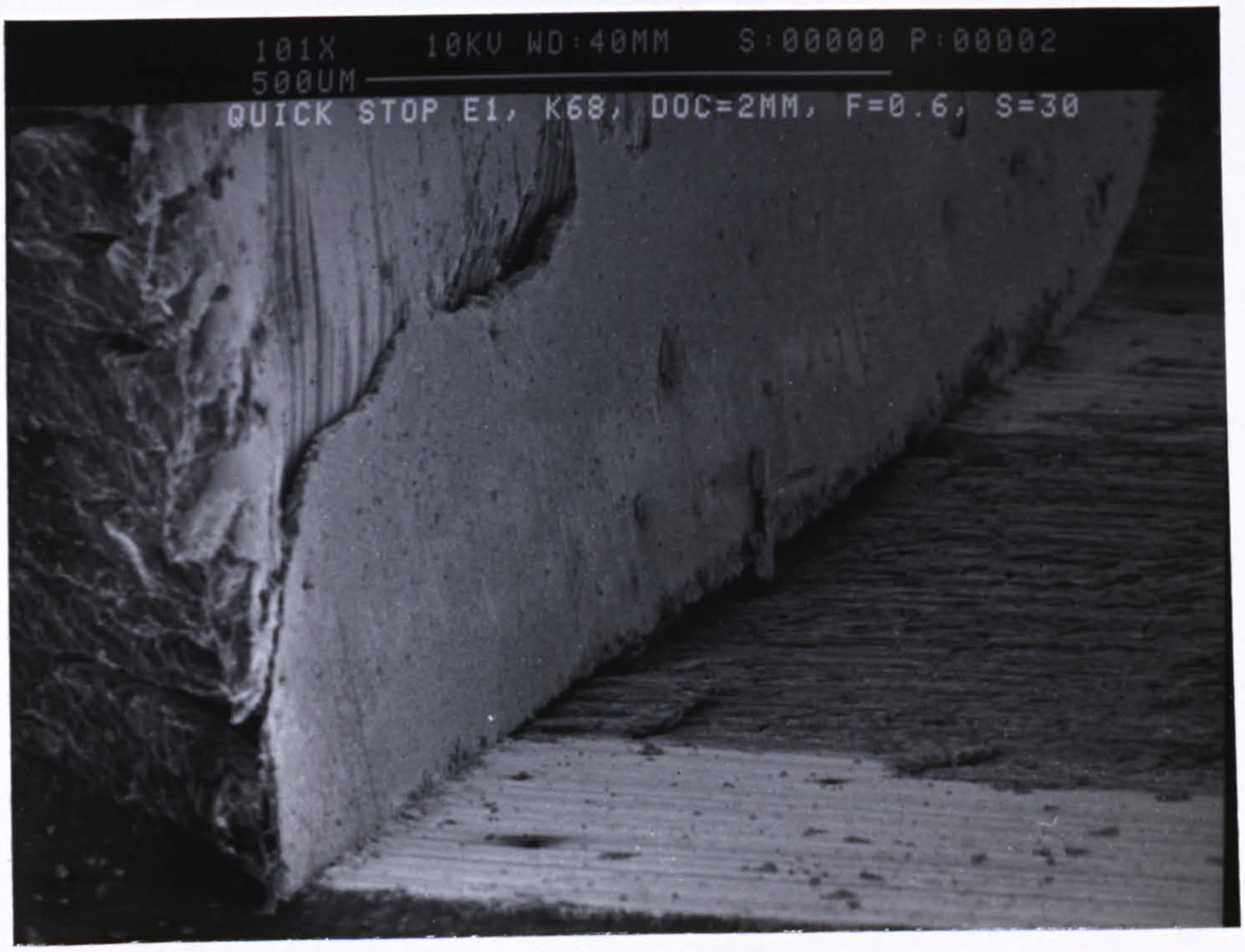

(a)

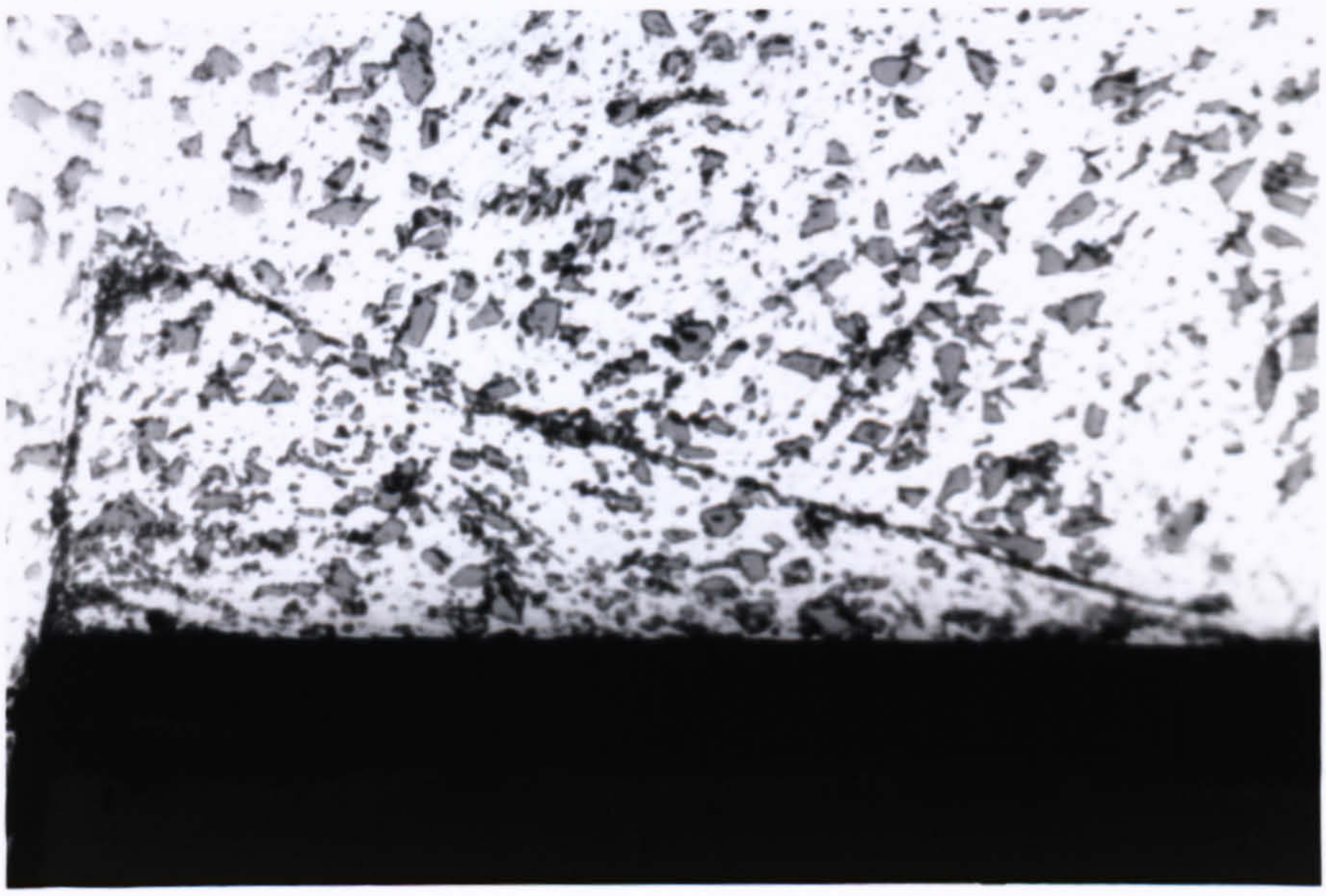

(b)

Figure 7.96 (a) Segment Of Quick Stop With BUE (b) Cross-section Showing The Presence of BUE (V = 30 m/min, Feed = 0.6 mm/rev, DOC = 2 mm)(X185)

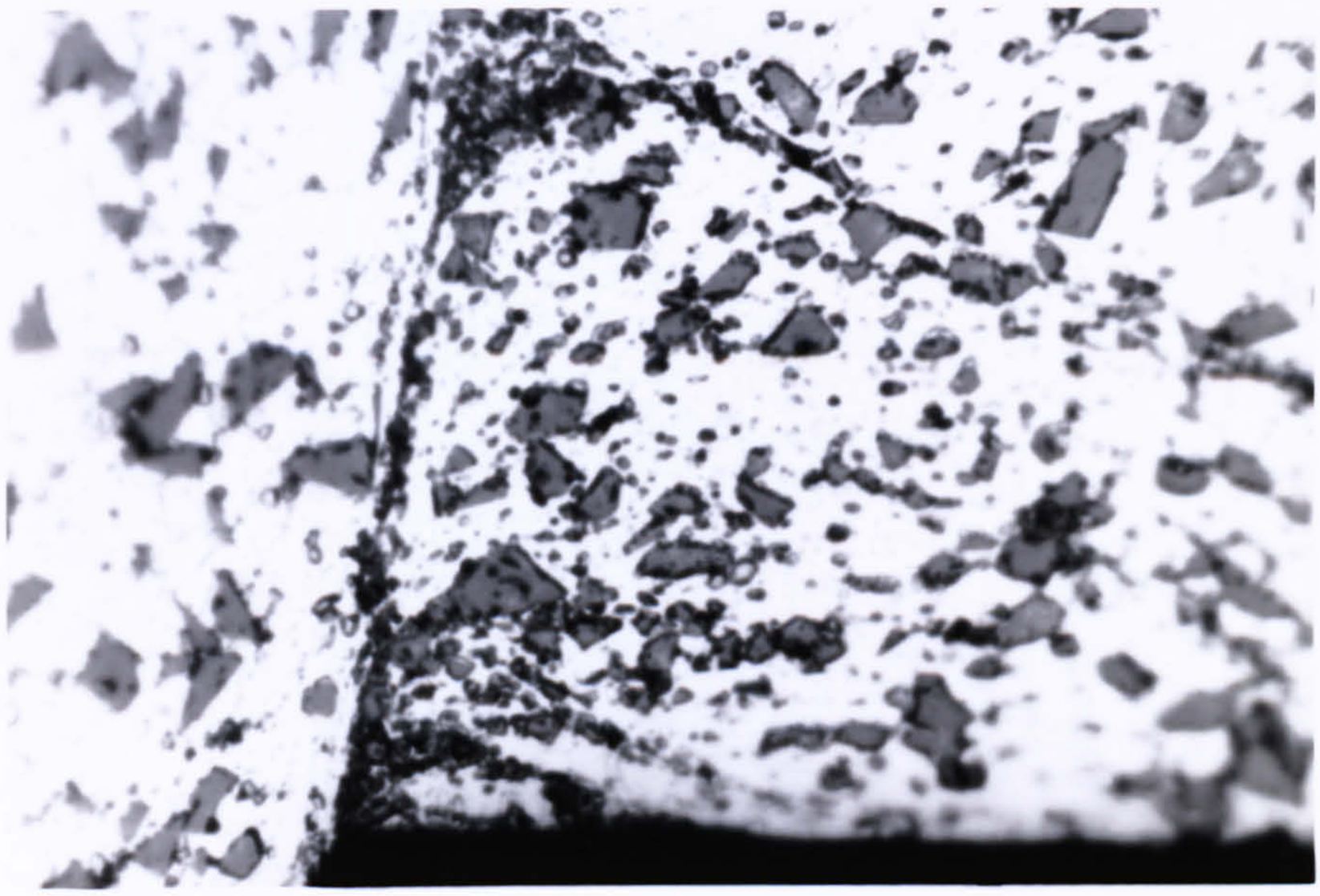

(c)

Figure 7.96 (c) Cross-section Showing The Presence of BUE (V = 30 m/min, Feed = 0.6 mm/rev, DOC = 2 mm)(X750)

(a)

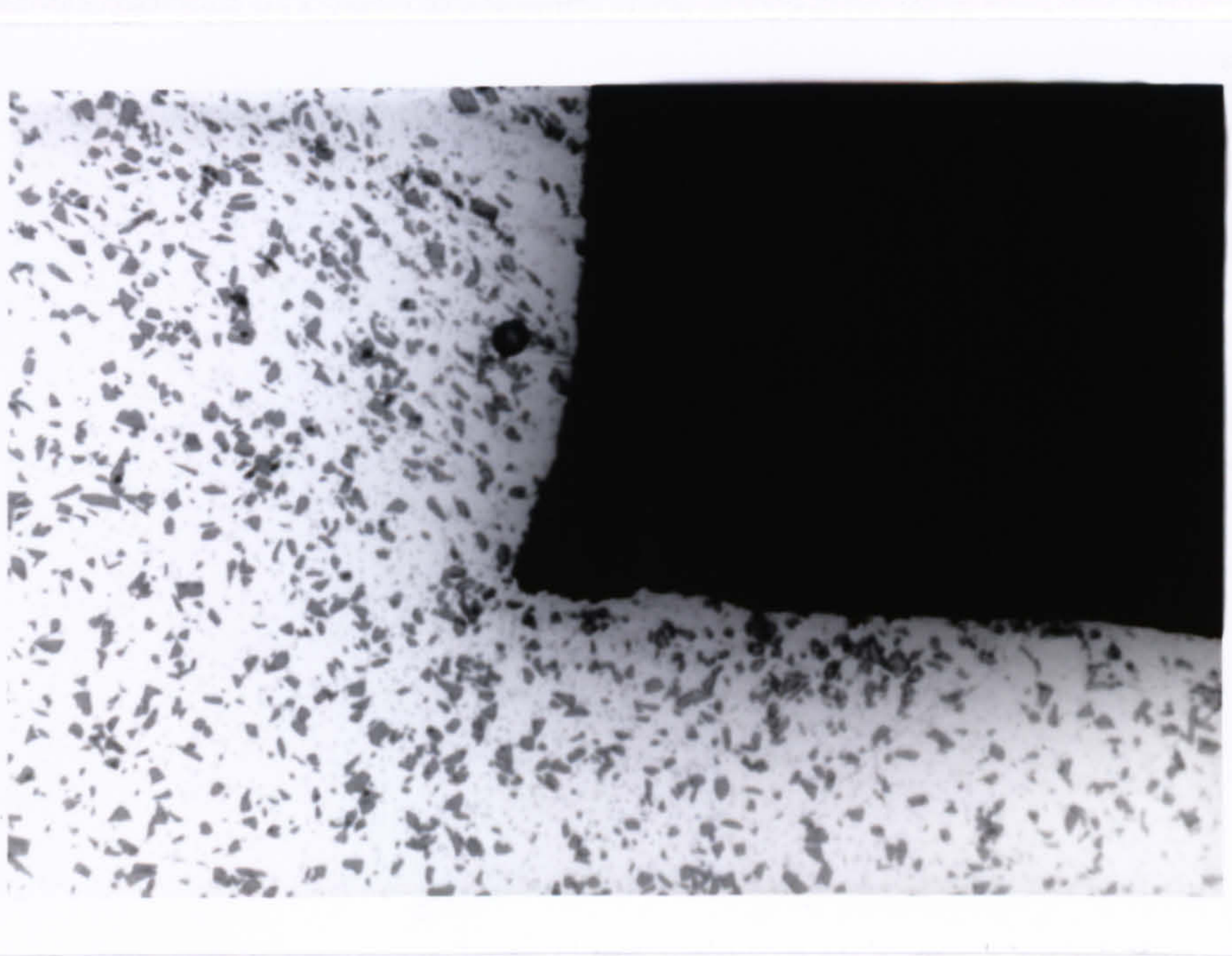

(b)

Figure 7.97 (a) Segment Of Quick Stop Without BUE (b) Cross-section Showing No BUE (V = 30 m/min, Feed = 0.4 mm/rev, DOC = 2 mm)(X185)

Figure 7.98 Variation Of Chip Thickness With Cutting Speed For Cemented Carbide Inserts (Feed = 0.2 mm/rev, DOC = 2 mm)

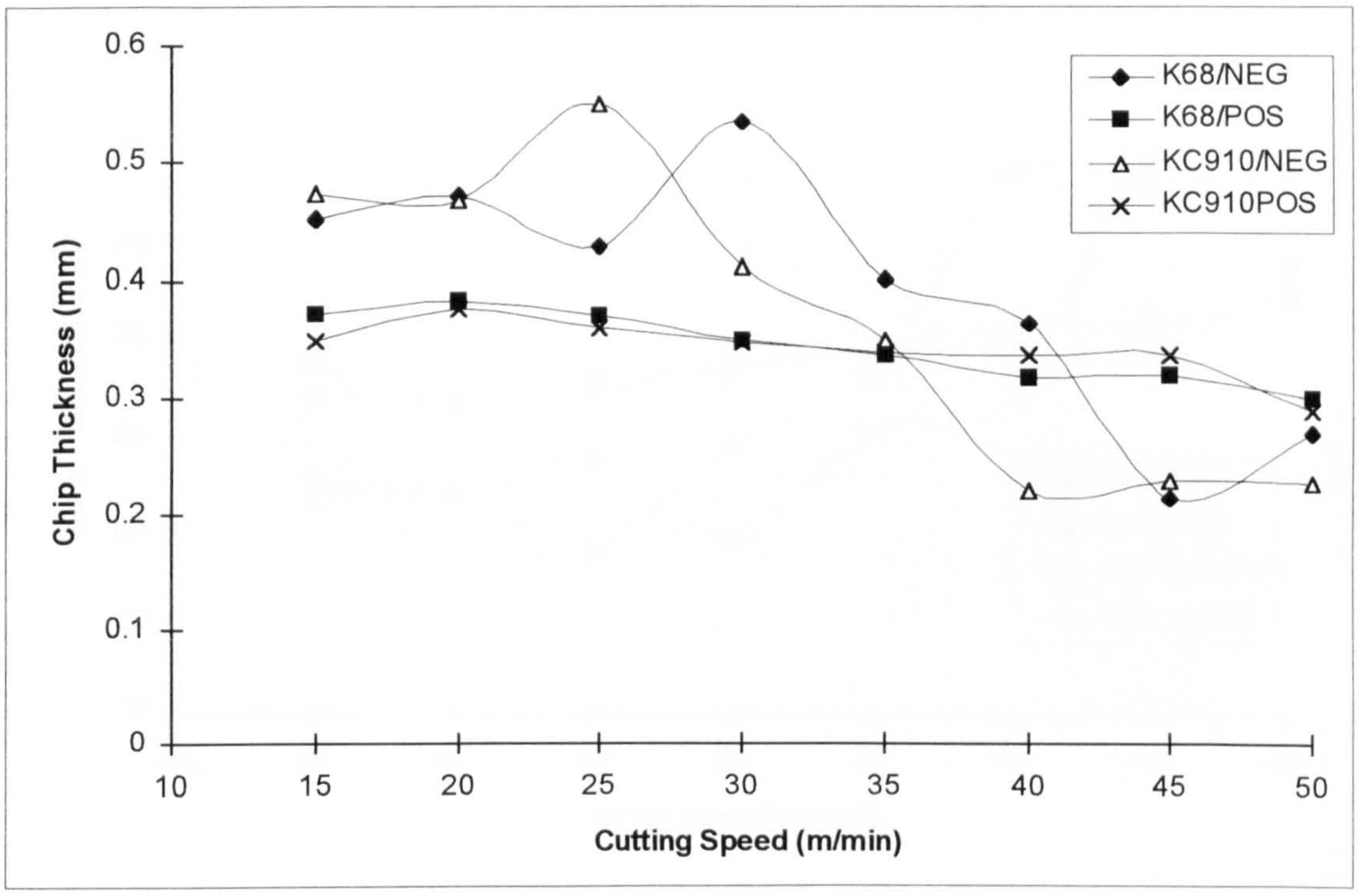

Figure 7.99 Variation Of Chip Thickness With Cutting Speed For Cemented Carbide Inserts (Feed = 0.4 mm/rev, DOC = 2 mm)

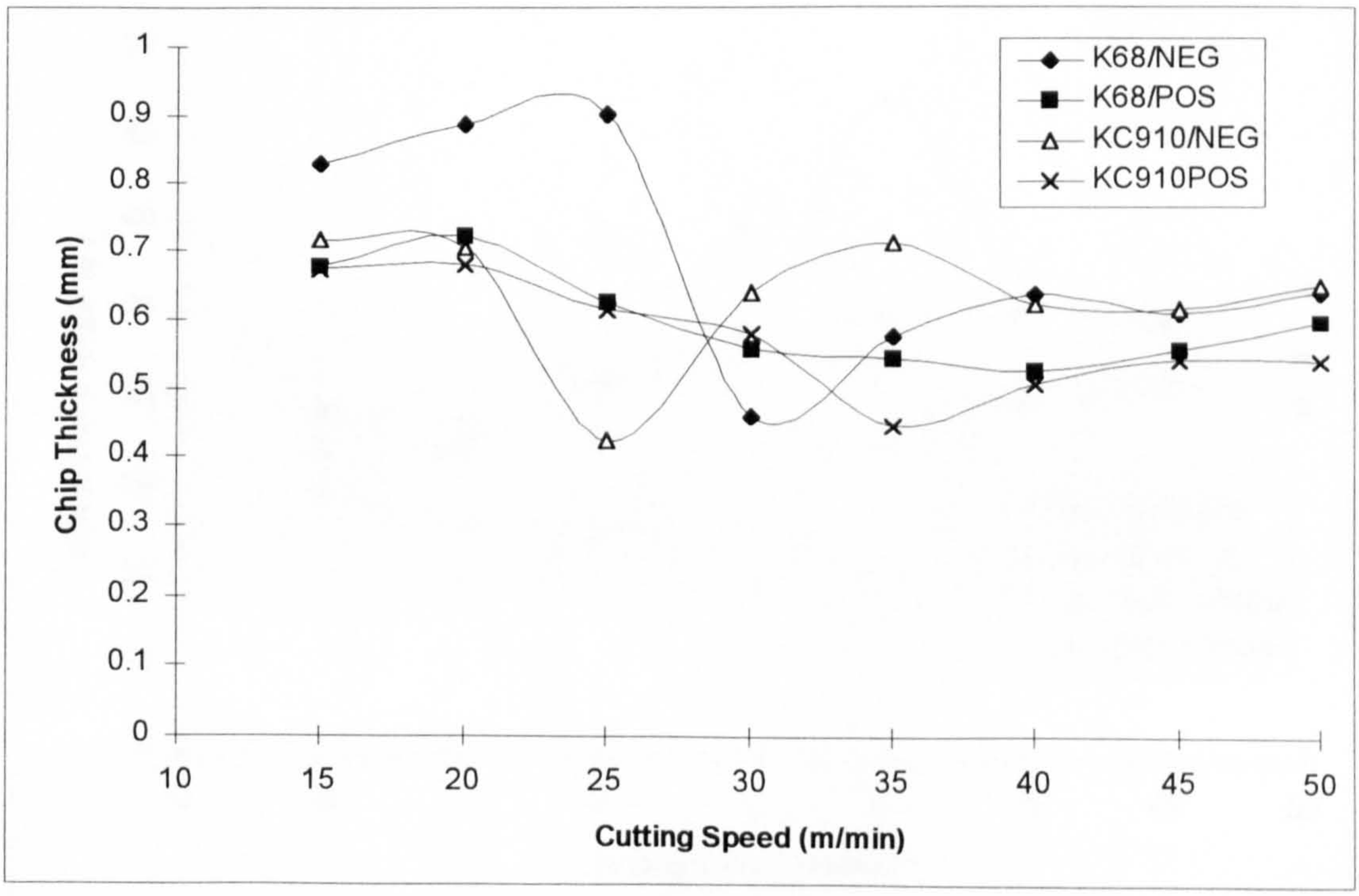

Figure 7.100 Variation Of Shear Plane Angle With Cutting Speed For Cemented Carbide Inserts (Feed = 0.2 mm/rev, DOC = 2 mm)

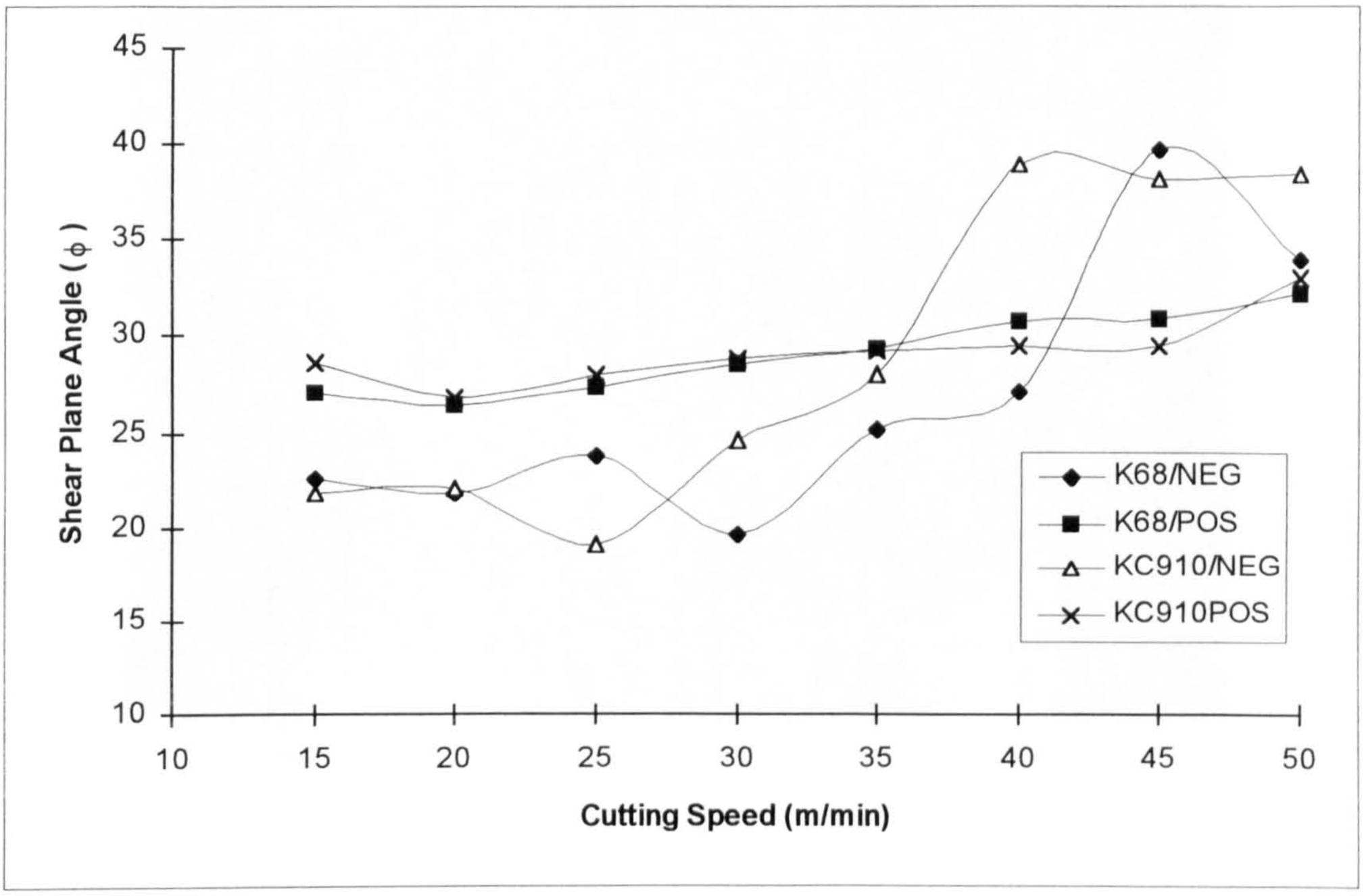

Figure 7.101 Variation Of Shear Plane Angle With Cutting Speed For Cemented Carbide Inserts (Feed = 0.4 mm/rev, DOC = 2 mm)

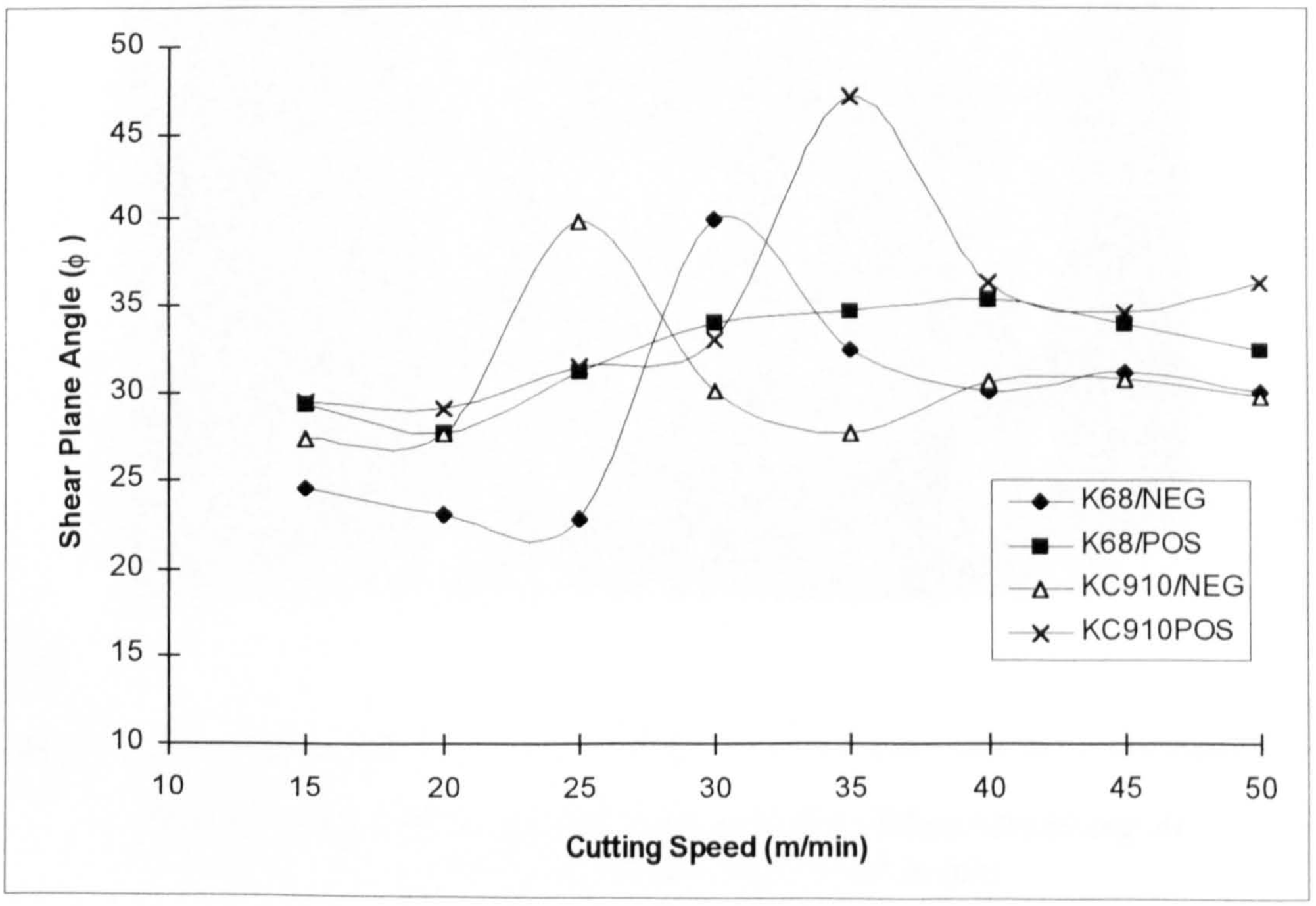

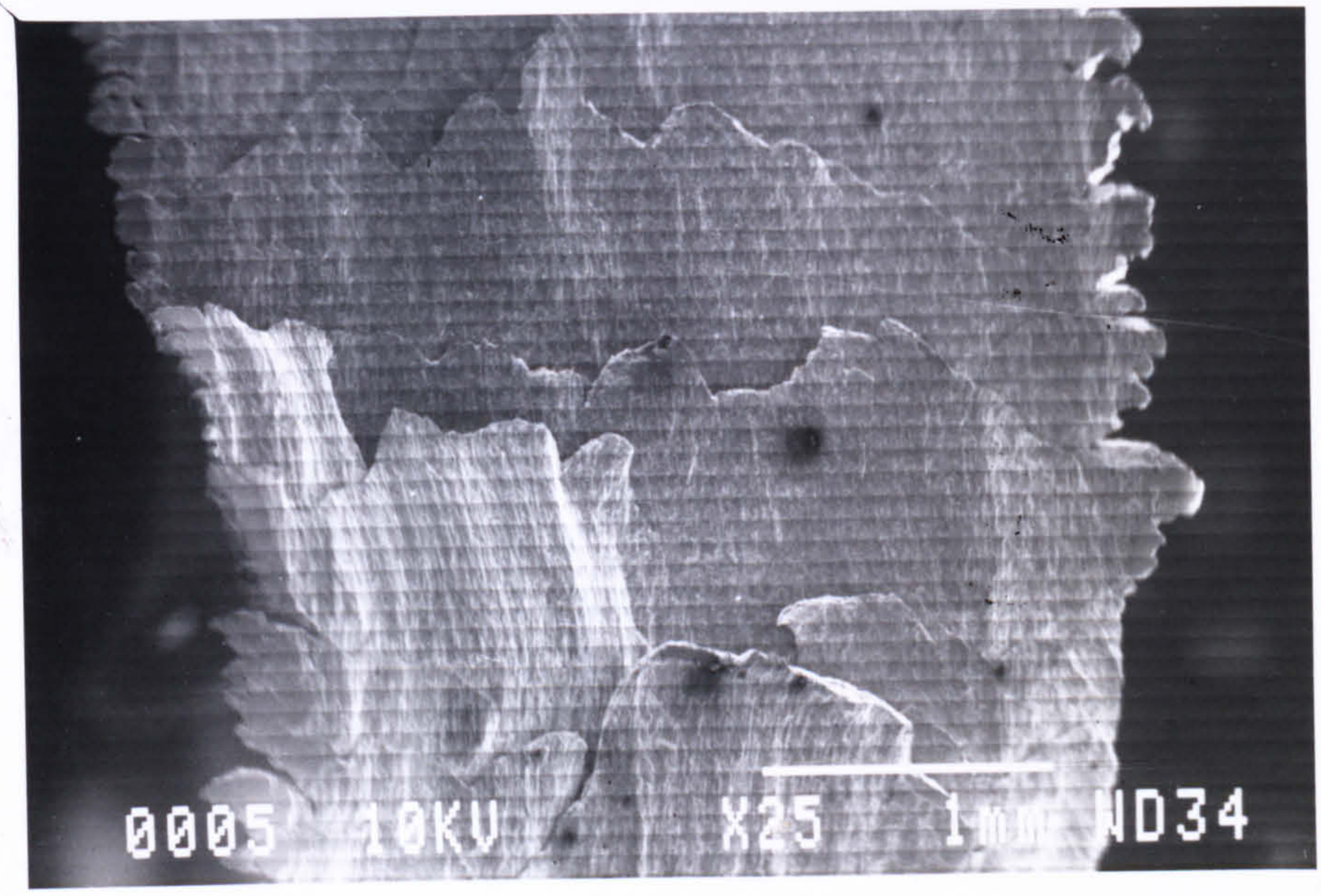

(a)

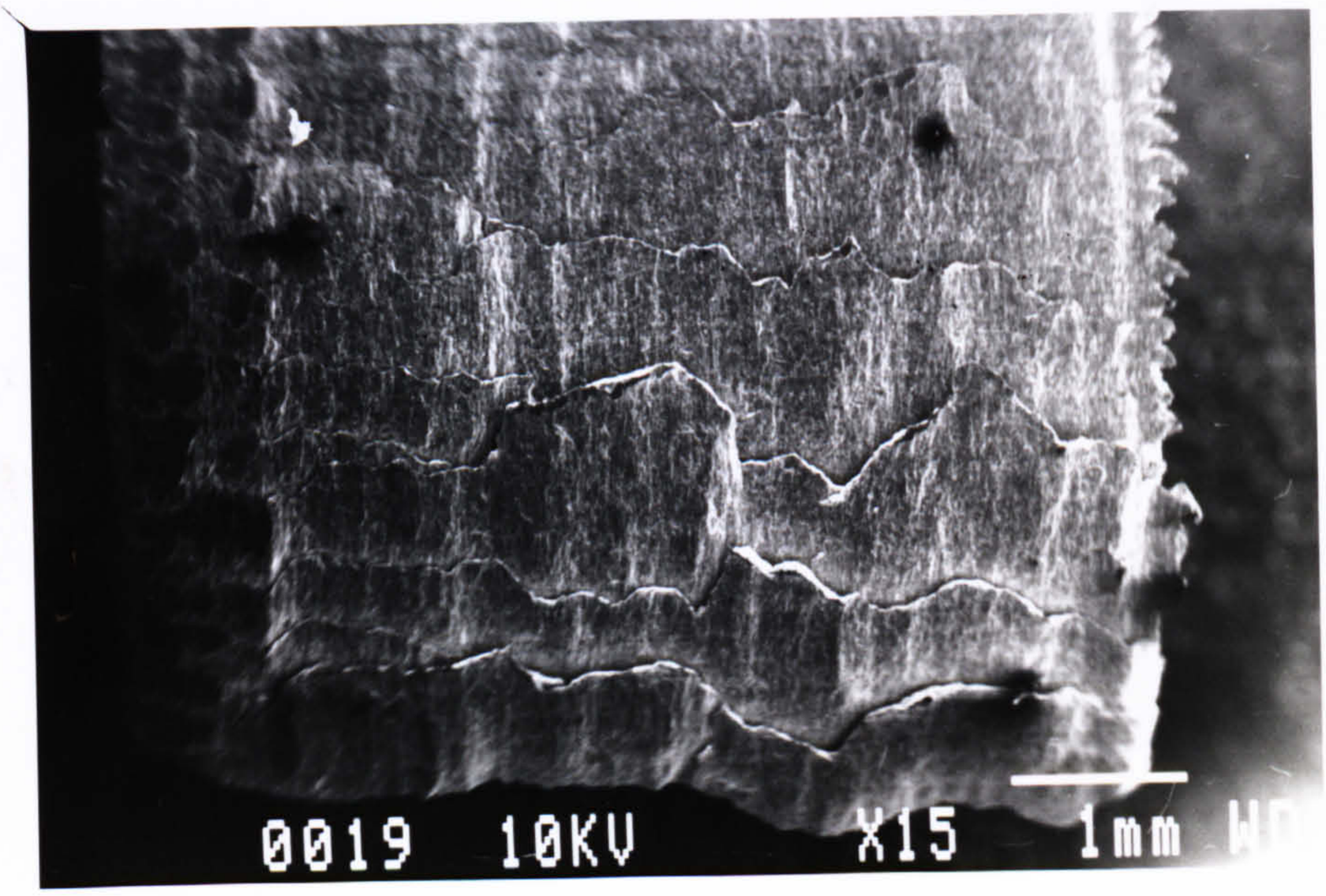

(b)

Figure 7.102 Surface Of The Underside Chip When Machining At (a) V = 15 m/min, (b) V = 25 m/min

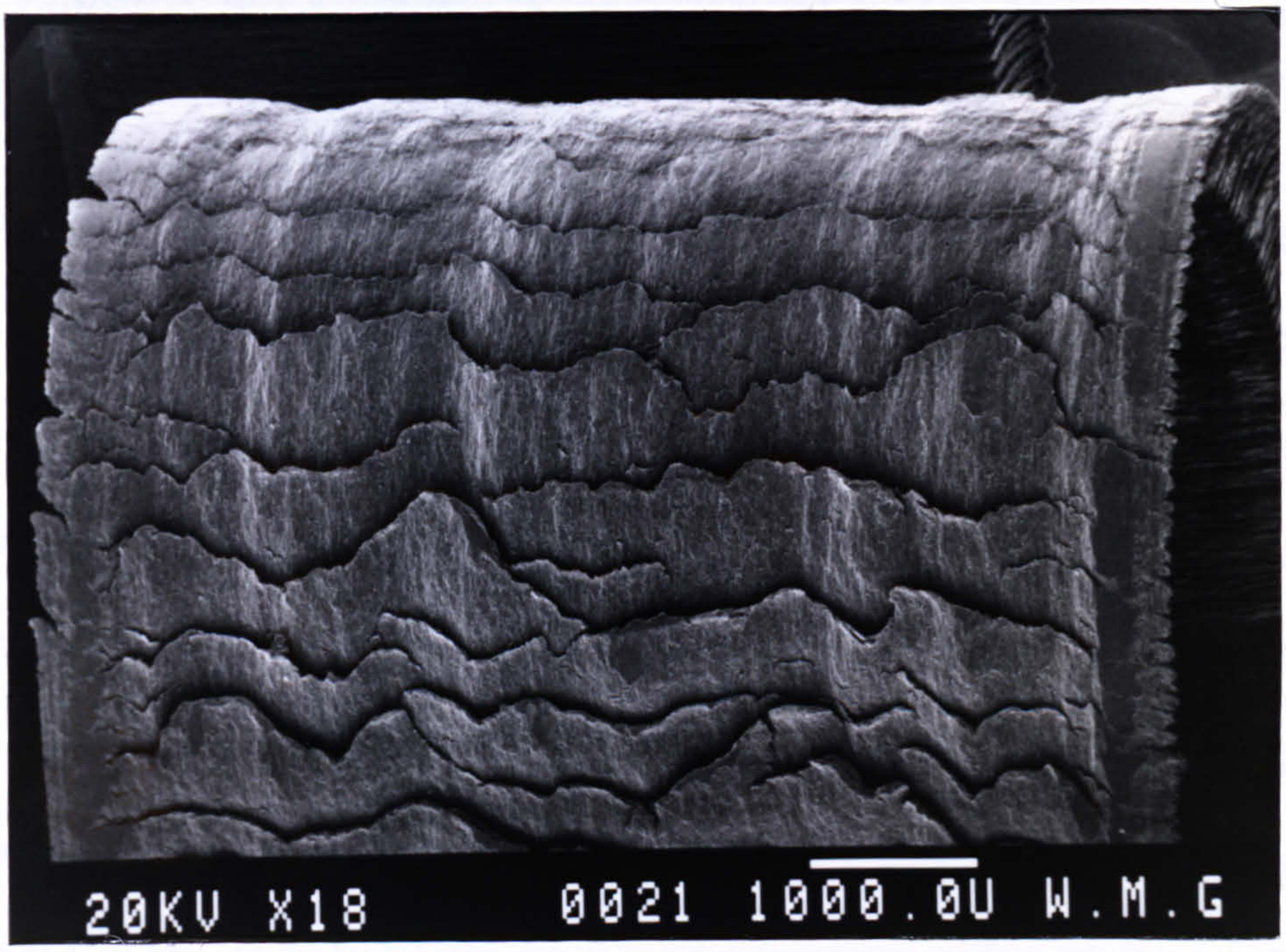

(c)

Figure 7.102 Surface Of The Underside Chip When Machining At (c) V = 30 m/min

7.8 Comparisons Between Uncoated and Coated Cemented Carbide Tools

Figures 7.103 - 7.106 show the comparison between uncoated and coated cemented carbide tools in terms of tool life when machining with K68 and KC910 inserts under various cutting conditions. At the lower feed rate of 0.2 mm/rev and in the cutting speed range from 15 to 25 m/min, KC910 inserts with positive rake geometry gave a longer tool life, followed by KC910 with negative rake geometry. The tool life of KC910 with negative rake geometry increases as the speed increases from 30 m/min to 40 m/min, Figure 7.103. Increasing the feed rate to 0.4 mm/rev shows a marked increase in tool life for KC910 with negative rake geometry in the speed range 20 to 25 m/min, Figure 7.104.

The tool life of K68 inserts with positive rake geometry has not been affected significantly by increases in feed rate, but there is an increase in tool life for K68 inserts with negative rake geometry in the speed range 25 m/min to 30 m/min when the feed is doubled. The life is further increased for both K68 and KC910 inserts when the feed is increased to 0.6 mm/rev. In general, the tool life of K68 and KC910 tools decreases when cutting speed is increased. Increasing the depth of cut from 2 mm to 4 mm has little effect on the tool life of K68 and KC910 inserts (Figure 7.105 - 7.106). Cutting conditions have less effect on the performance of positive rake tools than they do on negative rake ones.

The changes in tool flank wear of cemented carbide tools with cutting speed for feed rates of 0.2 mm/rev and 0.4 mm/rev are shown in Figures 7.107 and 7.108. It can be seen that there is a progressive increase in flank wear for both K68 and KC910 cemented carbide tools. It is interesting to note that the wear rates for KC910 and K68 with negative and positive geometry are almost the same at 0.2 mm/rev feed with KC910 inserts showing a slightly slower wear rate as cutting speed increases. As the feed is increased from 0.2 mm/rev to 0.4 mm/rev, Figure 7.108, the wear rate of K68 is markedly higher than KC910. Tools with positive rake geometry show a slower wear rate than negative rake geometry tools. Figure 7.109 shows the variation of flank wear with feed rate for cemented carbide tools at a speed of 25 m/min and depth of cut of 2 mm. It can be seen that as the feed rate is increased, the tool wear rate decreases. Therefore, increasing the feed rate has significantly increased the tool life of both K68 and KC910 inserts with positive and negative rake geometries.

The volume of material removed is almost constant at the lower feed rate for K68 and KC910 inserts with negative or positive rake geometry. The general pattern is that the volume of material removed is markedly increased when the feed rate is increased, Figure 7.110 - 7.112. There is no significant difference in performance between positive and negative tool geometry inserts at 0.2 mm/rev and 0.4 mm/rev. Hence, from this comparison, coated cemented carbide tools, KC910, gave a better performance in terms of tool life and volume of material removed than uncoated cemented carbide K68 inserts. KC910 with negative rake geometry produced a

longer tool life than positive rake geometry. Inserts with chip breaker has little or no effect in term of tool life or volume of material removed.

Figure 7.103 Tool Life Of Uncoated (K68) and Coated (KC910) Cemented Carbide Inserts At Various Cutting Speed (Feed = 0.2 mm/rev., DOC = 2 mm)

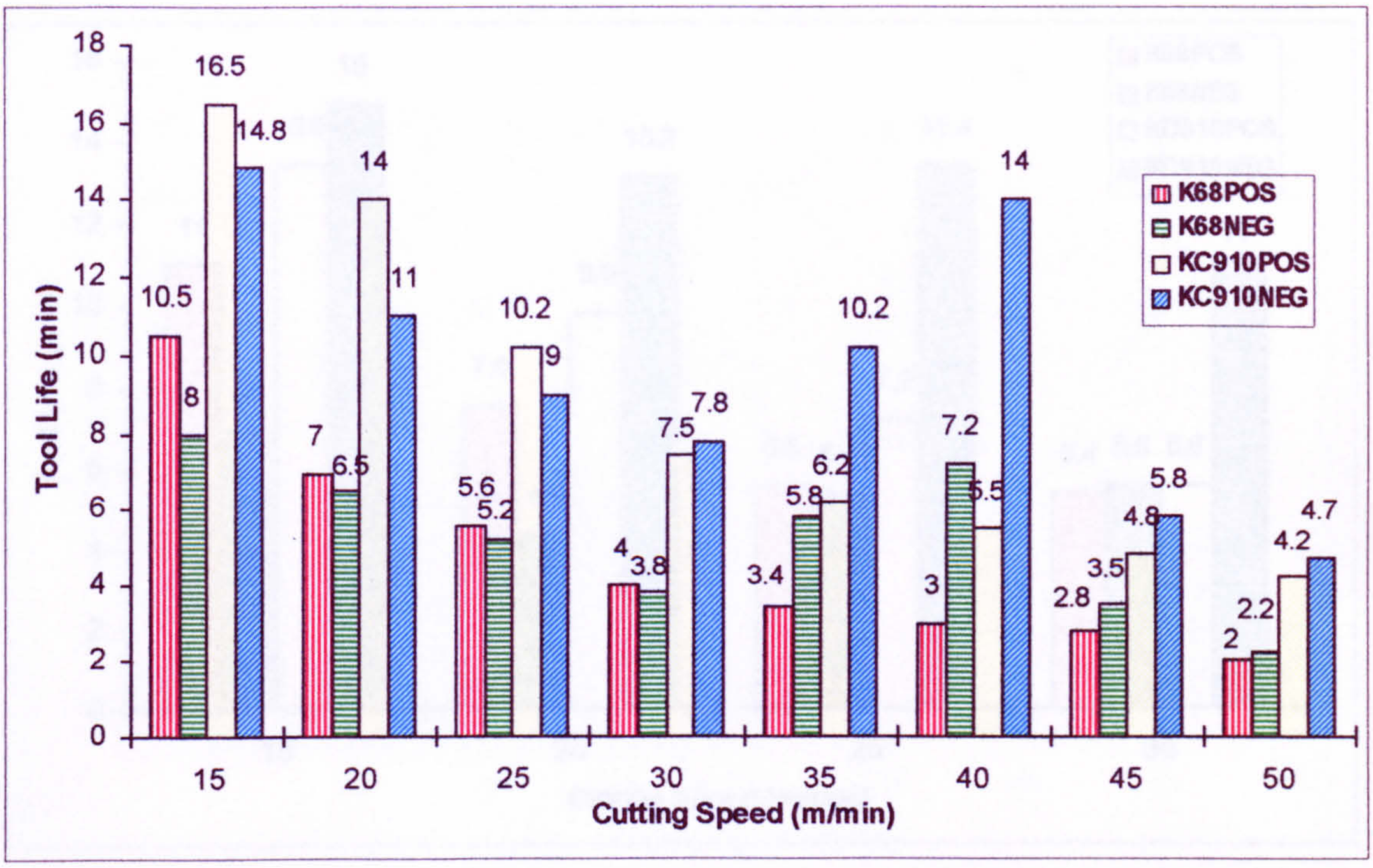

Figure 7.104 Tool Life Of Uncoated (K68) and Coated (KC910) Cemented Carbide Inserts At Various Cutting Speed (Feed = 0.4 mm/rev., DOC = 2 mm)

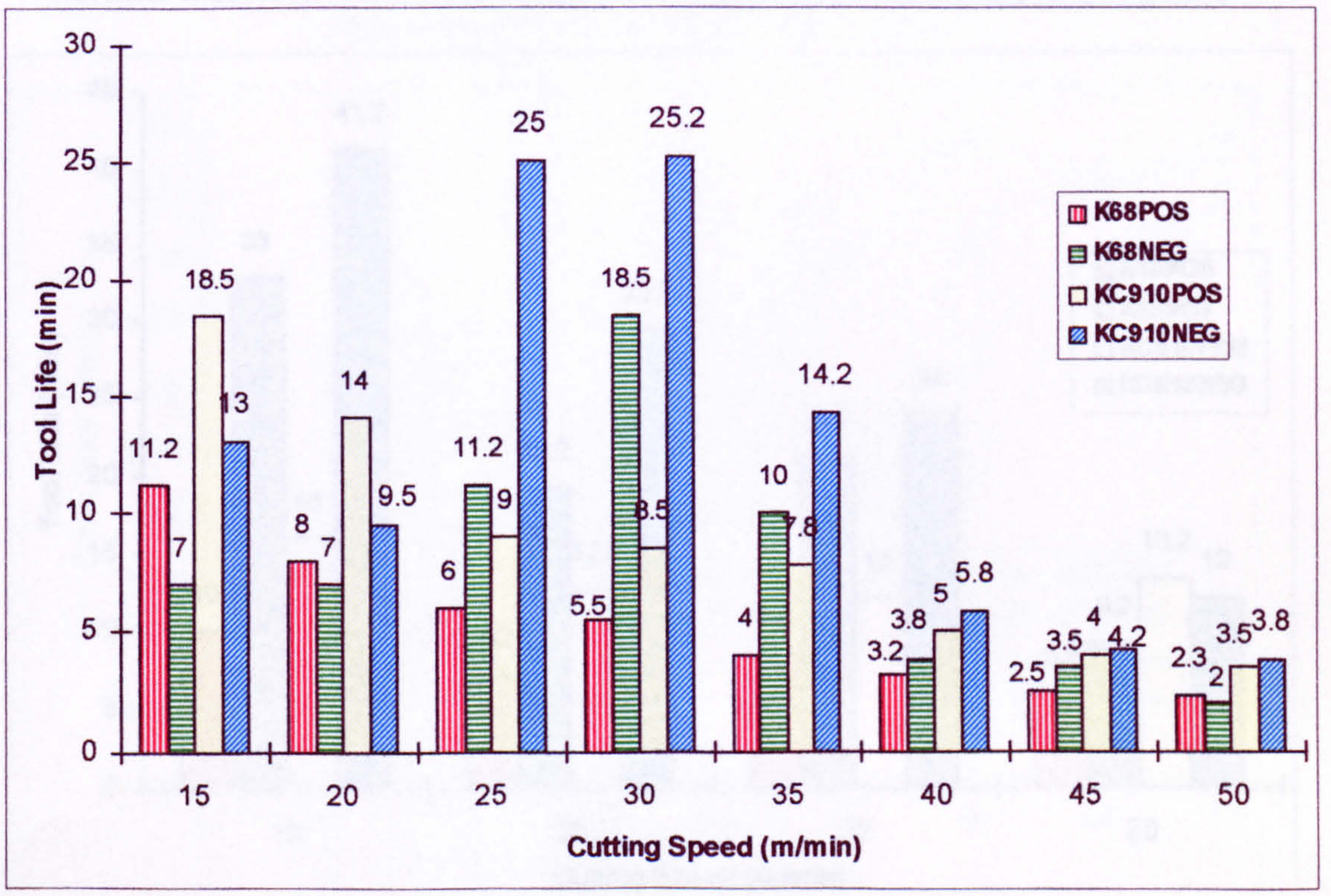

Figure 7.105 Tool Life Of Uncoated (K68) and Coated (KC910) Cemented Carbide Inserts At Various Cutting Speed (Feed = 0.2 mm/rev., DOC = 4 mm)

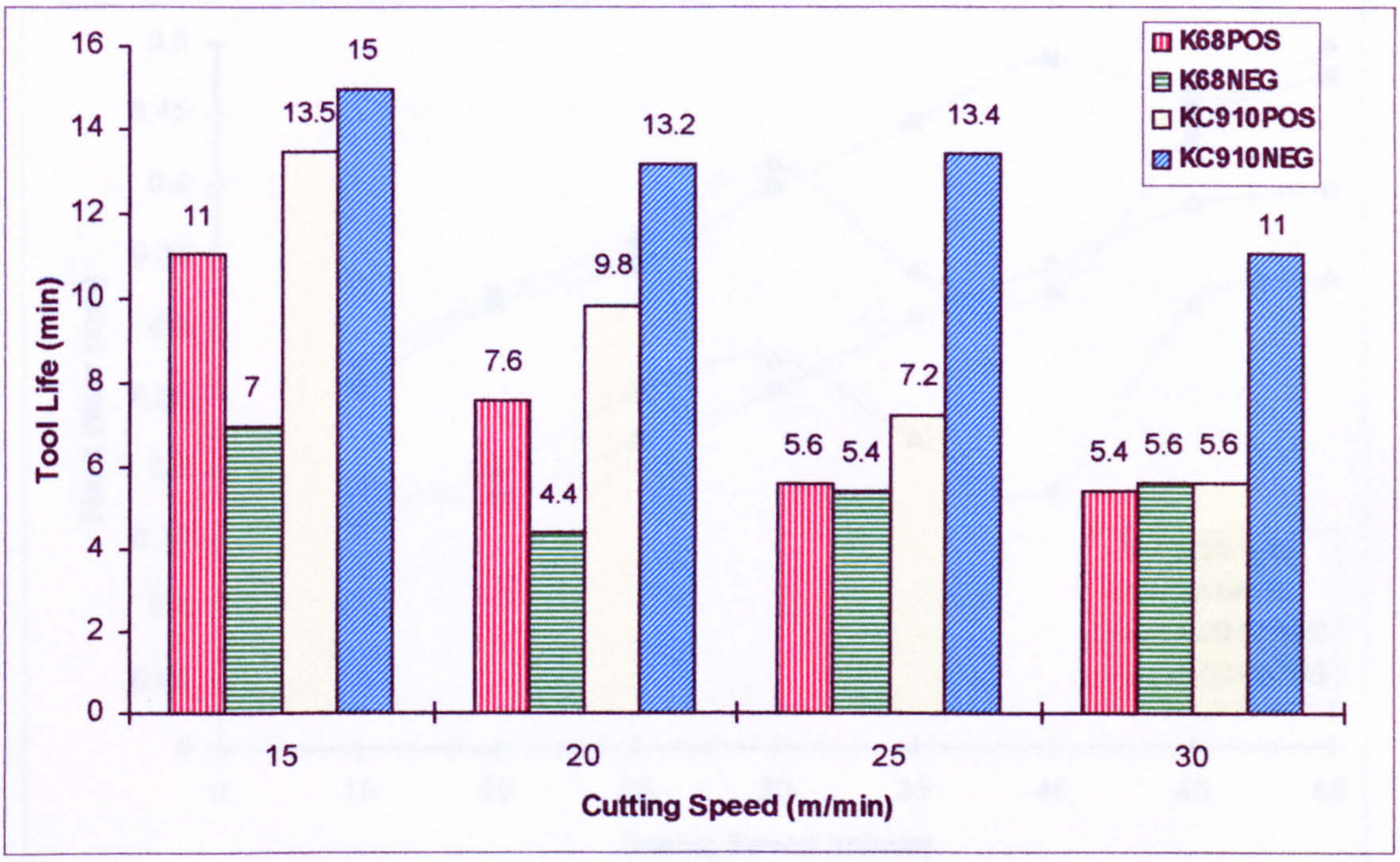

Figure 7.106 Tool Life Of Uncoated (K68) and Coated (KC910) Cemented Carbide Inserts At Various Cutting Speed (Feed = 0.4 mm/rev., DOC = 4 mm)

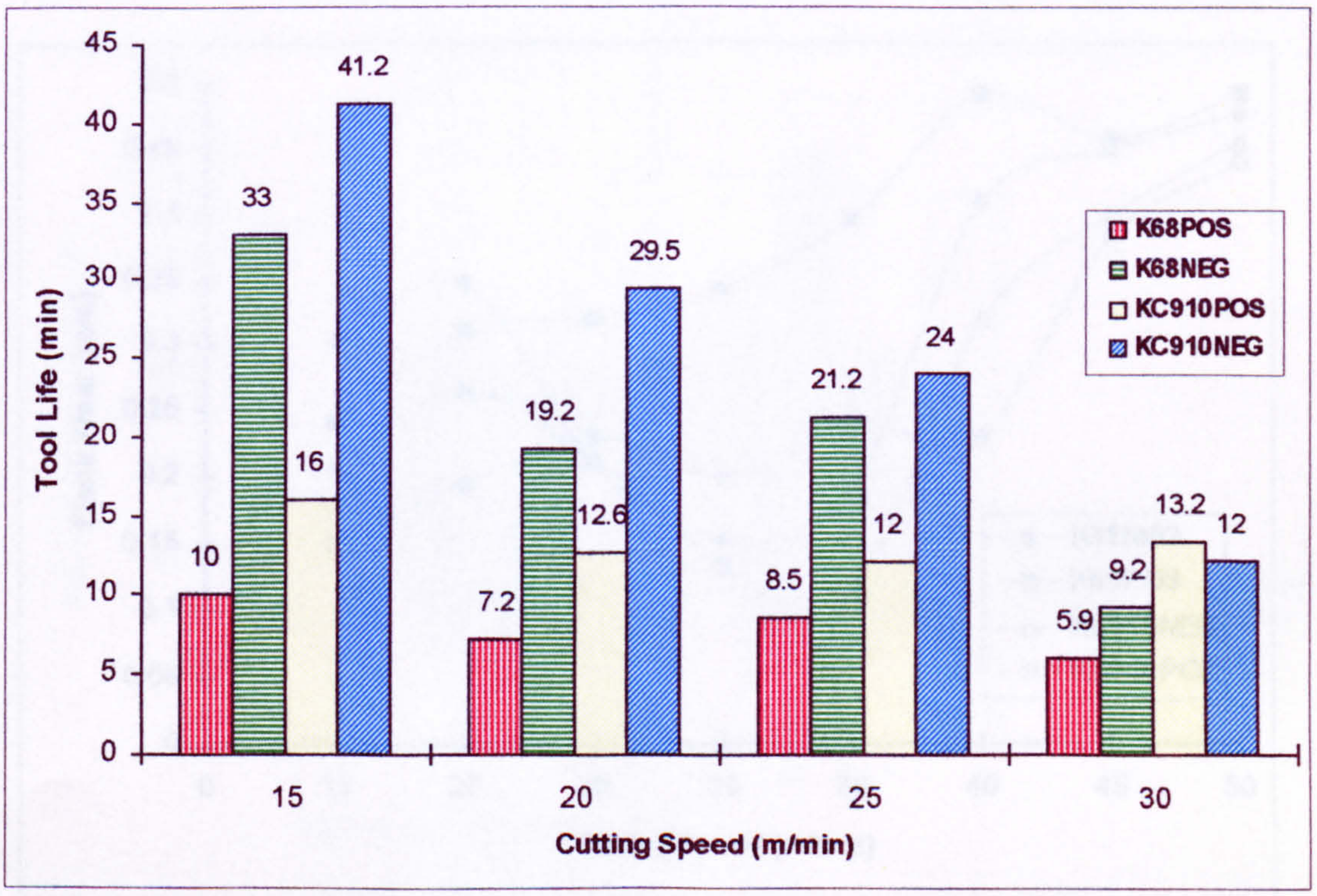

Figure 7.107 Variation Of Flank Wear With Cutting Speed For Cemented Carbide Inserts At 0.2 mm/rev Feed (DOC = 2 mm)

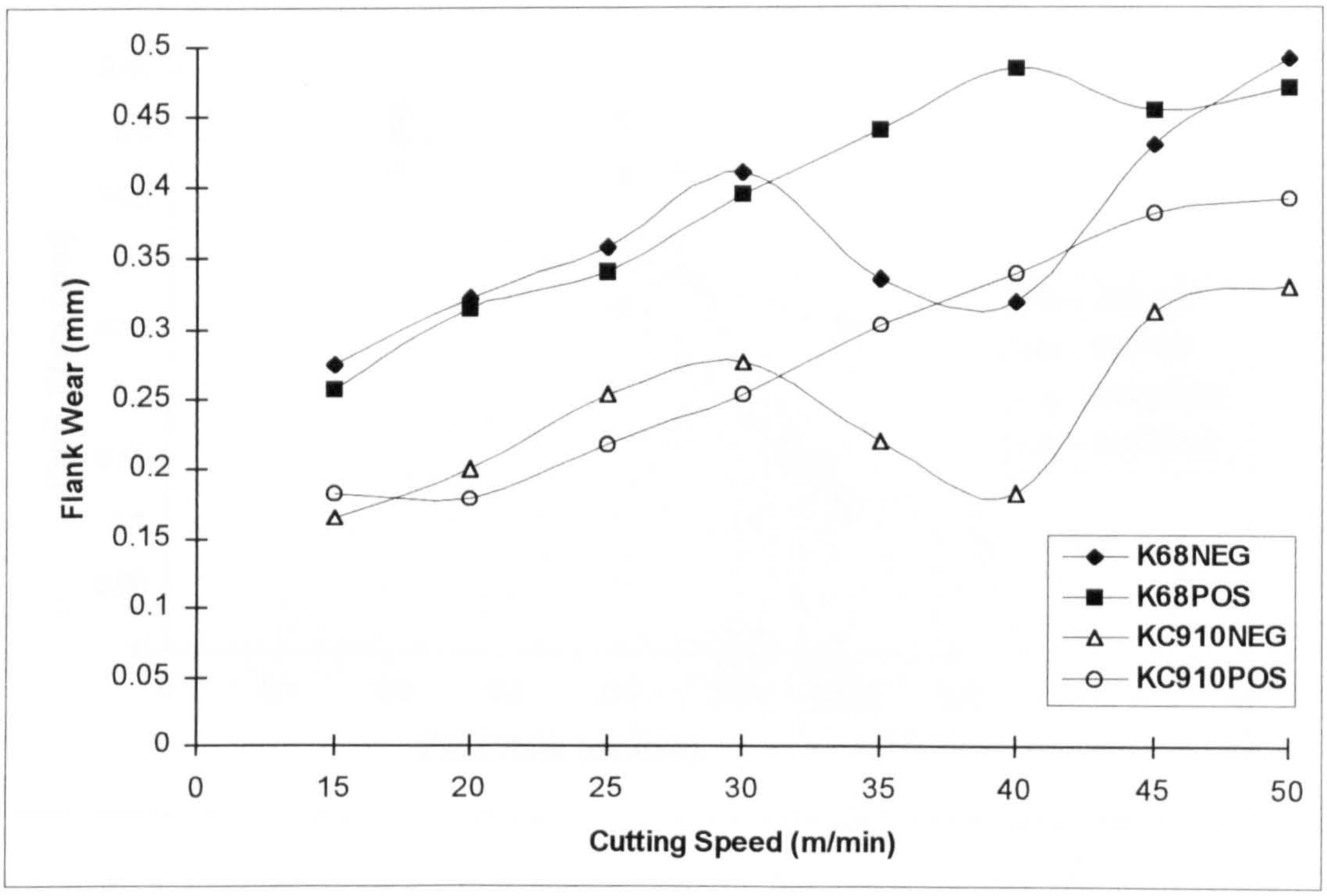

Figure 7.108 Variation Of Flank Wear With Cutting Speed For Cemented Carbide Inserts At 0.4 mm/rev Feed (DOC = 2 mm)

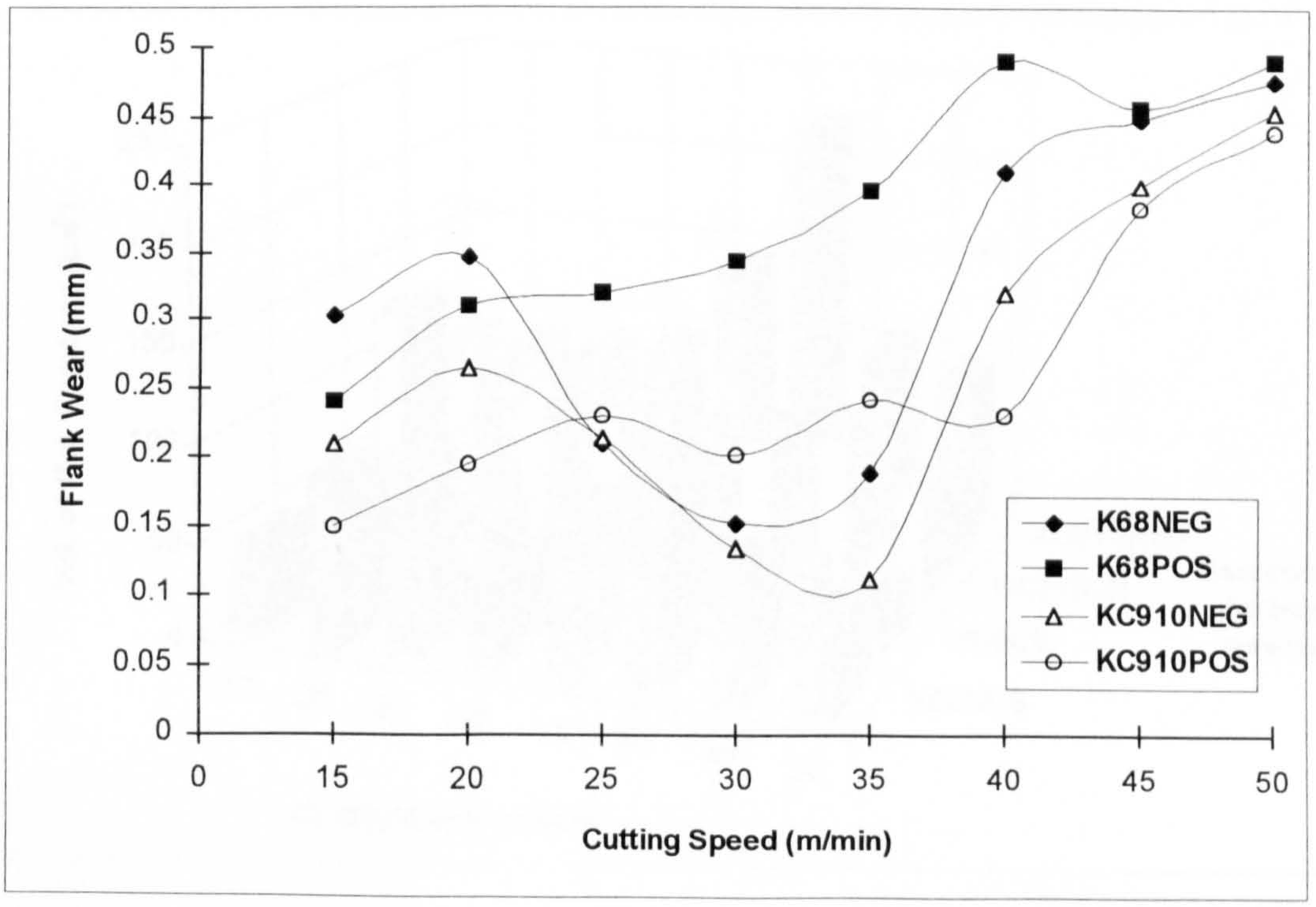

Figure 7.109 Variation Of Flank Wear With Feed Rate For Cemented Carbide Inserts (V = 25 m/min, DOC = 2 mm)

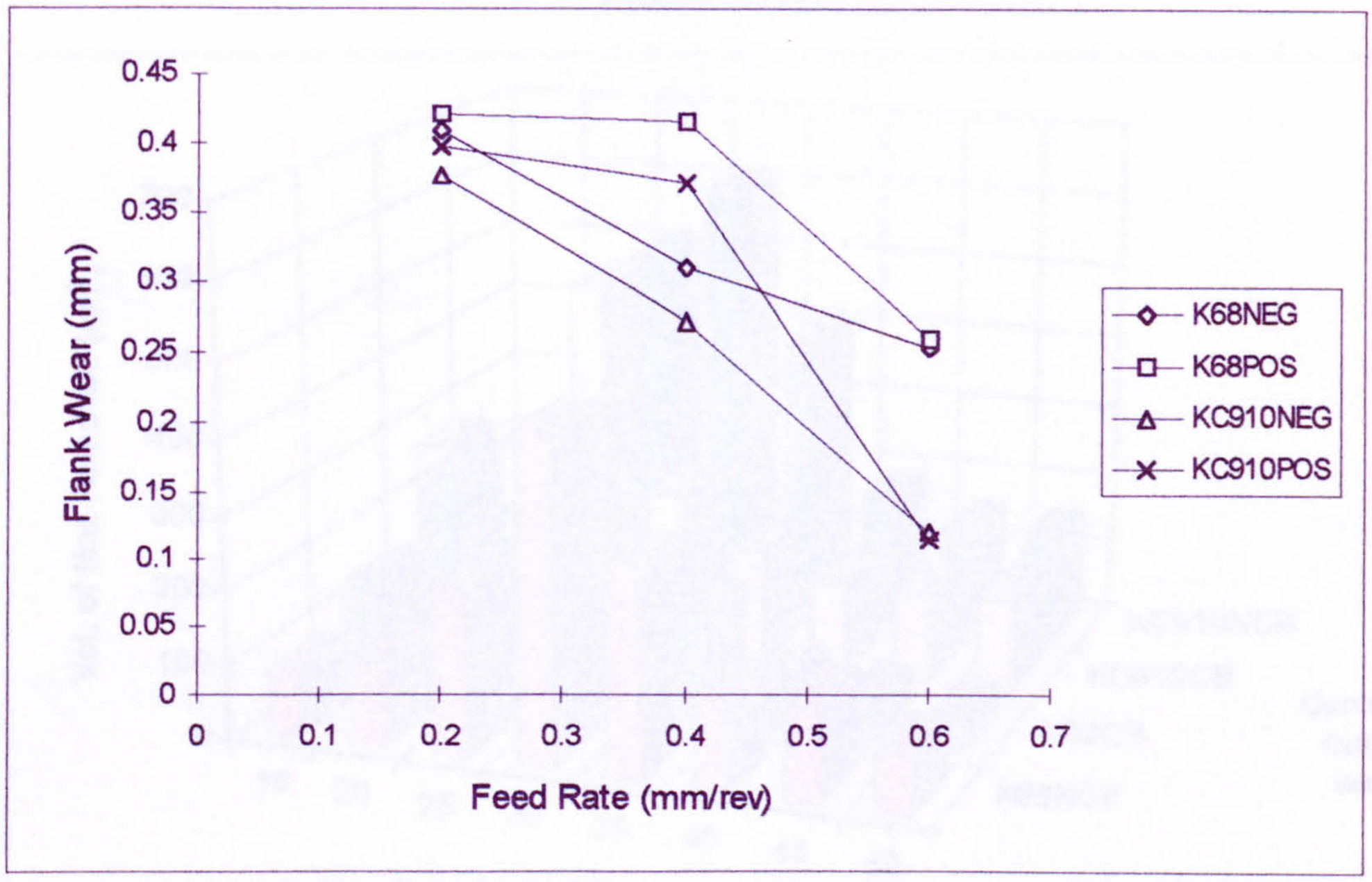

Figure 7.110 Vol. of Material Removed Against Cutting Speed For K68 & KC910 (Neg. Geometry, With & Without Chip Breaker , Feed = 0.2 mm/rev., DOC = 2mm)

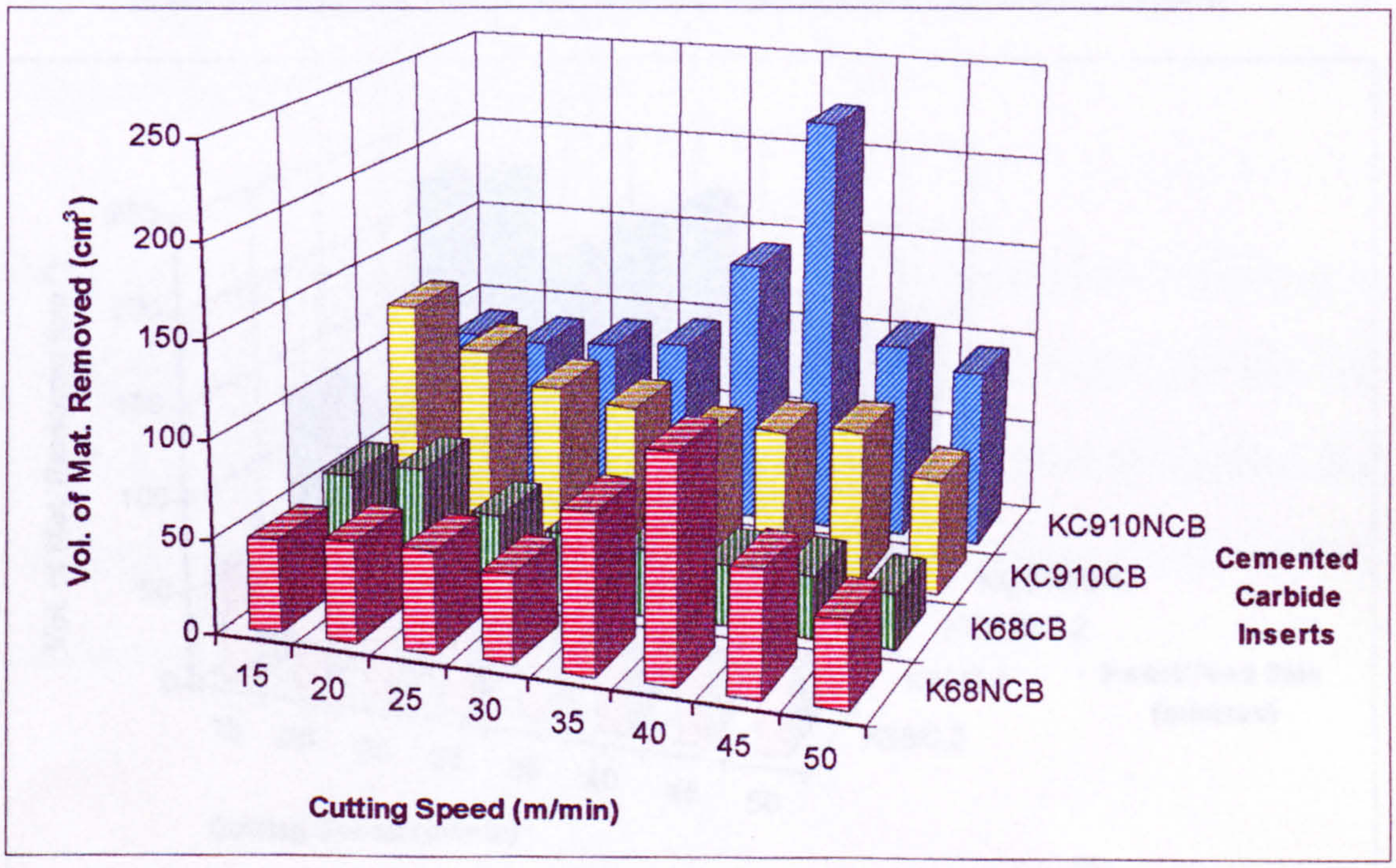

Figure 7.111 Volume of Material Removed Against Cutting Speed For K68 & KC910 (Neg. Geometry, With & Without Chip Breaker, Feed = 0.4 mm/rev., DOC= 2mm)

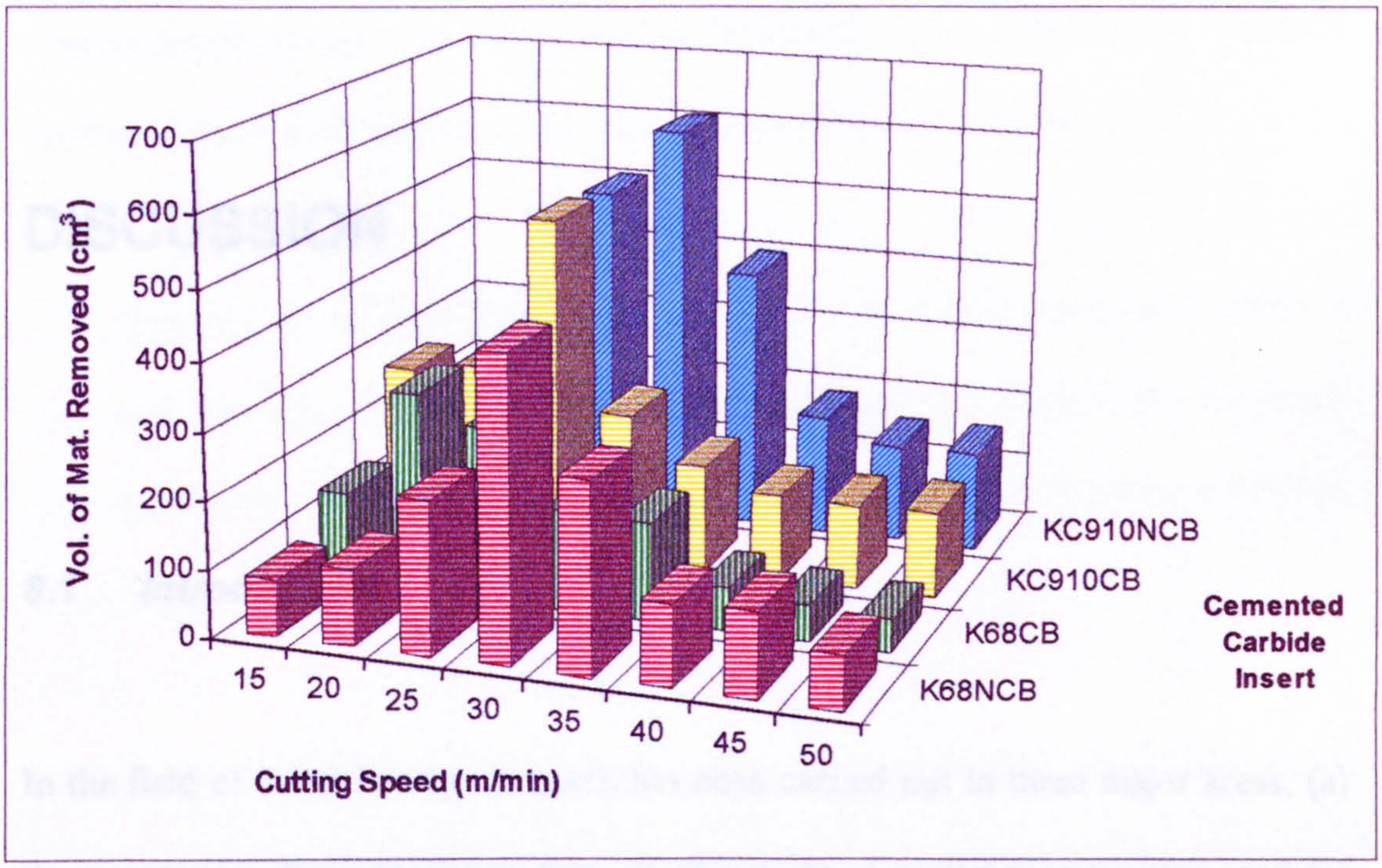

Note: NCB - No Chip Breaker, CB - Chip Breaker

Figure 7.112 Vol. of Material Removed Against Cutting Speed For K68 & KC910 (Pos. Geometry, Feed = 0.2 mm/rev And 0.4 mm/rev, DOC = 2 mm)

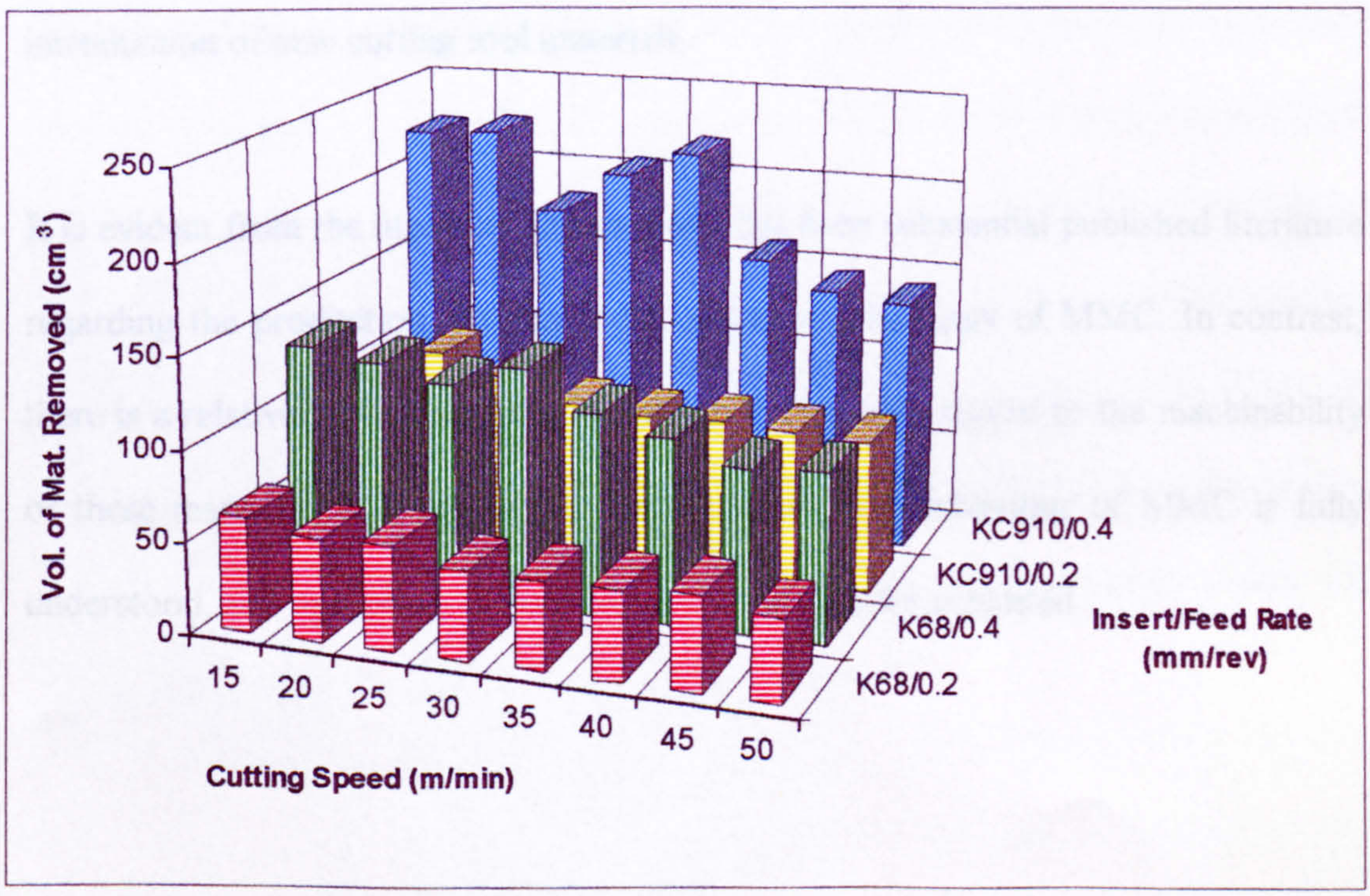

Chapter 8

DISCUSSION

8.1 Introduction

In the field of metal cutting, research has been carried out in three major areas, (a) the generation of machinability data, (b) the study of tool/chip interaction, and (c) the study of tool failure modes and wear mechanisms. The research in this area is continuing with the appearance of more exotic and difficult-to-cut materials and the introduction of new cutting tool materials.

It is evident from the literature review there has been substantial published literature regarding the production, properties and physical metallurgy of MMC. In contrast, there is a relatively small quantity of published data with regard to the machinability of these materials. It is important that the machining behaviour of MMC is fully understood, and optimised, if their potential is to be fully exploited.

The aim of this project is to investigate and develop a fundamental understanding of the machinability of aluminium 2618 MMC reinforced with SiC particles. One of the major types of cutting tool, widely used in the manufacturing industry, i.e. cemented carbide tools, was chosen for the machining experiments in order to:

1) Quantify the effect of cutting conditions (cutting speeds, feed rates, depth of cut), tool geometries, tool materials etc., for machining aluminium 2618 MMC reinforced with SiC particles such that industrially relevant cutting conditions may be specified.

2) Understand the machining process, i.e. tool/chip interaction, tool failure modes and wear mechanism of cemented carbide tools when machining aluminium 2618 MMC reinforced with SiC particles.

The discussion of the experimental results is divided into four main sections. Section 8.2 is concerned with the study of tool wear, tool failure mode and wear mechanism. Section 8.3 deals with the effect of tool geometry and the effects of various cutting conditions on tool life. Section 8.4 deals with the conditions at the tool/chip interface which includes chip formation and built-up edge (BUE), the surface finish and cutting forces. Section 8.5 discusses the relative performance of the two types of cemented carbide tools and the last section deals with some general points with respect to the machining of aluminium 2618 MMC.

8.2 Tool Wear

For many materials, tool wear is linked directly to the influence of temperature within the primary and secondary shear zones. Aluminium and its alloys have low melting points (~600^{0}C), compared to materials such as steel (~1200^{0}C), and the temperature generated during cutting are never high enough to be damaging to cemented carbide tools [155][156]. It is more likely that the rapid tool wear observed is related to the direct contact between the hard abrasive, SiC particles and the cutting edge and their motion relative to the rake and clearance faces. Hence, the hardness of the SiC particles is a dominant factor for tool wear.

In general, the rate of flank wear is quite rapid but the rate and degree of flank wear for K68 and KC910 inserts varied with cutting conditions, as seen in Figures 7.1 - 7.10 and Figures 7.41 - 7.50 respectively. As the feed is increased, the wear rate for both inserts slowed down. But once the speed is increased, rapid wear was experienced. The flank wear rates at the lowest feed rate (0.2 mm/rev) at most cutting speeds inserts are rapid but constant. Increasing the feed rate from 0.2 mm/rev to 0.4 mm/rev slows down the wear rate, especially in the cutting range 20 m/min to 35 m/min. Further increasing the cutting speed increases the wear rate dramatically.

8.2.1 Flank Face Wear

Although various types of wear are operating and can influence the tool life under conditions used in this study, flank wear was the dominant type of wear mode when

machining with K68 and KC910 inserts, as shown in Figures 7.26 and 7.66 respectively. There was a slight complication in examining the worn flank due to the presence of a very thin layer of aluminium which concealed the worn surface below. The thickness of this layer varied with the cutting conditions, the layer being thickest when machining under the presence of BUE on the rake face of the tool. Using a backscattered detector to image the worn surface in the SEM enabled the examination of the worn carbide surface due to the ability of the detector to provide some sub-surface information. On close examination of worn K68 and KC910 inserts, the worn part has a smooth surface containing scratches and sharp grooves in the direction of cutting as seen in Figures 7.28(a)(b)(c) and Figures 767(a)(b)(c) respectively. Further examination of the cutting edge of K68 and KC910 inserts, Figures 7.29(a)(b)(c) and 7.72(a)(b), shows deep grooves parallel to the cutting direction suggesting the action of an abrasion mechanism and there was some erosion of carbide grains on the cutting edge. SiC particles is hard and is consequently abrasive, which means that the MMC which contain SiC particles act as 'dilute' grinding particles during the machining operation and so cause excessive wear and 'blunting' of the cutting tools.

The flank wear mechanisms operating during machining with cemented carbide tools are discussed further in the following section.

8.2.1.1 Flank Wear Mechanism

It is a fundamental factor in the selection of cutting tool materials to determine the extent and type of wear to be expected. There are various types of wear mechanisms which can influence tool life under the machining conditions, these can be classified as abrasion, attrition, chipping, plastic deformation or diffusion wear. The relative importance of these mechanisms for tool wear depends upon many factors, for example the work material, the machining operation, cutting conditions, the tool geometry etc. [160] [163].

In general, abrasion is less likely to be a major wear mechanism in metal cutting because the cutting tools is always harder than workpiece material. However, the majority of workers who have machined MMC with different amounts of SiC particle contents have agreed that abrasion was the major wear mechanism when machining with cemented carbide tools [249 - 254]. This is due to the hardness of the reinforcement material (~ 2700 HV) compared to the tool material (~1800 HV).

The reasons for tool wear are the direct contact between the SiC particles and the cutting edge of the tool and their relative motion to the rake and clearance face. Therefore, the hardness of the SiC particles reinforcement is a dominant factor for tool wear. The hard, rough surface of SiC slides against the softer cemented carbide, digs into it and ploughs a series of grooves as seen in Figures 7.29(a) (b) and (c). Different size and shape of scratches and grooves found on the flank face and rake face was influenced by the size and shape of SiC particles and their orientation.

A number of worn K68 and KC910 inserts were metallurgically sectioned and the mechanical interactions between SiC particles and the tool surface studied. Figures 7.30(a)(b) and Figures 7.68(a)(b) show the cross-section of K68 and KC910 inserts with adhering workpiece material. The particles seen on the rake face immediately behind the cutting edge are identified as SiC particles by using energy dispersive X-ray analysis as seen in Figure 7.31. These particles are believed to be responsible for producing scratches and grooves on the rake face as shown in Figures 7.28(a)(b)(c), Figures 7.29(a)(b)(c) and Figures 767(a)(b)(c). A similar wear process is believed to be responsible for the sharp grooves found on the worn flank face.

It can be seen clearly in Figure 7.30 and 7.68 that a SiC particle is in contact with the surface of the tool, this would produce scratches and grooves, as seen in Figures 7.28(a)(b)(c), and Figures 7.67(a)(b)(c), under any conditions other than complete seizure of the interface. The micro-cutting action on the tool surfaces is done by the SiC particles in the work material or SiC particles on the underside of the chip. A similar process is taking place on the flank face. Figure 8.1 diagramatically represents the manner in which the flank wear land is thought to develop in K68 inserts. At the beginning of the cut the tool is sharp but the SiC particles gradually abrade away the K68 insert by micro-cutting (stage 1-3 in Figure 8.1(a)). As cutting continues, a build up of material is formed and gives some protection on the rake face but not on the flank face (stage 4-6 in Figure 8.1(a)). Hence, the severity of wear on the rake face is somewhat less than on the flank face. Different conditions occur on the flank face where SiC particles have directly impinged on the surface

and caused wear as seen in Figure 7.29. The intimate contact between the flank wear land and the machined surface facilitates this process, Figure 8.1(b). It is therefore suggested that the mechanism of abrasive wear between MMC and K68 inserts is micro-cutting of SiC particles effectively acting as cutting tools.

Figure 8.2 represents the manner in which the flank wear land is thought to develop in KC910 inserts. The substrates of indexable coated KC910 inserts are 'edge honed' before coating, i.e. a small radius ~ 25-50 μm, is formed on the cutting edge to reduce the incidence of edge chipping. Because the cutting edge was radiused, the coating was first worn through some microns below the level of the rake face. Further cutting causes more rapid wear of the substrate in this region (stage 6 in Figure 8.2(a)). At the beginning of the cut the tool is sharp/radiused but the SiC particles gradually abrade away the coatings of KC910 inserts by micro-cutting (stage 1-5 in Figure 8.2(a)). The wear process is similar to that of the uncoated K68 inserts. It is therefore suggested that the mechanism of abrasive wear between MMC and KC910 inserts is micro-cutting by SiC particles.

Further examination of cutting edges of the tools and the extremities of the wear land of KC910 insert show no evidence of spalling or decohesion of either Al_2O_3 or the TiC coatings, Figure 7.72. This suggests that abrasion is largely responsible for coating removal during machining of SiC reinforced MMC with KC910 inserts. The photomicrograph in Figure 7.73 is a backscattered electron image of the flank wear produced during machining at 15 m/min. The contrast in the backscattered image

makes the progressive wear through the surface coatings to the substrate clearly visible, i.e. three distinct grey levels on the photomicrograph. Further analysis using EDAX of the individual areas seen confirmed that they represented carbide substrate, titanium carbide and alumina respectively, from top to bottom of the image, confirming the gradual progressive wear of both coatings. The X-ray analysis graph showing the composition of aluminium (Al), titanium (Ti) and cobalt (Co) is shown in Figure 7.73(b). The coatings are believed to give some protection on the rake and flank face of the tool at the initial stage of machining but were worn away as machining continued.

In terms of tribology, the abrasive wear process on the rake face and clearance face of the tool can be classified as sliding wear [143 - 146]. It is classified as two body wear, where the hard SiC particles fixed in the MMC slides against the softer surface of cemented carbide, digs into it and ploughs a series of grooves, Figures 8.1(b) and 8.2(b). As stated earlier, there exists an intimate contact between the flank wear land and the machined surface which will facilitate this process. This situation is similar to the Archard [147] model which explains the abrasive mechanism of a cutting tool; for example the normal load (N), analogous to the cutting force (Fc), and cutting speed (v), both increase the wear rate. This model is probably correct to describe the wear of a cutting tool. Although rather than all the wear occurring on the softer material (workpiece), wear occurs on the cutting tool, caused by hard particles, but at much lower rate.

To some extent, other tool wear mechanisms besides abrasion undoubtedly play a role in tool wear. Close examination of worn K68 and KC910 inserts as shown in Figures 7.29(a)(b)(c) and Figures 7.72(a)(b) respectively, shows the worn part had a smooth surface containing scratches and sharp grooves in the direction of cutting. A higher magnification view of this region, Figures 7.29(d) and 7.72(b), shows that there was some erosion of carbide grains on the cutting edge. These observations suggest that some attrition has taken place during machining but not as commonly as abrasion. A combined attrition/abrasion mechanism can be proposed although it would appear that abrasion is dominant. The attrition probably resulted from the periodic movement of the part of the chip adhered to the tool rake face.

The abrasion wear process may be summarised as being caused by the following:

1. SiC particles from the workpiece material passing along the rake face and the flank face causing abrasion, and
2. Fragments of BUE and some WC grains eroded from the cutting edge moving down the flank and rake face causing abrasion.

The BUE which was evident under certain cutting conditions during the experimental work also contributes to the wear mechanism process. The BUE formation is further elaborated upon in section 8.4.2.

8.2.1.2 Effect Of Coatings

It is the underlying hardness of the coatings (~ 2000 HV) which controls the wear rate. However, coatings may have an influence over the creation of the BUE. Again, as they are easily removed by the abrasive SiC or WC particles, any influence will be restricted to the early part of the tool life, see Figures 7.41 - 7.46.

The effect of the grain size of the cemented carbide tools on the wear rate is quite interesting. The wear rate of cemented carbide with fine grain (K68 grade) is higher than cemented carbide with medium grain (KC910 grade) when machining aluminium 2618 MMC, see Figures 7.1 - 7.6 and Figures 7.41 - 7.46. This is interesting because fine grained carbide tools generally have higher hardness and better resistance than medium grain against abrasion [83][95]. Also the content of the cobalt phase is about the same for both carbides and cannot be the reason for this unexpected result. Even though KC910 has a medium grain size, the insert is coated with two layers of coating i.e. TiC and Al_2O_3. TiC and Al_2O_3 coatings are said to be very resistant to abrasion [83][100][102]. Therefore, these coatings are responsible for protecting the tool from abrasive wear at the initial stage of machining. A similar phenomenon was encountered by Cronjanger and Biermann [250] when machining B_4C reinforced aluminium with cemented carbide tools.

8.2.2 Rake Face Wear

In machining, generally, rake face wear is mainly observed when the tool is dissolved by the chip or when friction between tool and chip is very large [171][176]. Close

examination of the worn tool from these trials showed that there was no evidence of diffusion wear on the rake face of the tool. This is no surprise since cemented carbide tools have no strong tendency to react with aluminium at the temperatures generated during machining. Slight rake face wear was observed at certain cutting conditions but it was never the tool life determining factor. Only a limited amount of rake face wear was observed on K68 and KC910 inserts, as shown in Figures 7.33 and 7.69. As mentioned earlier, light scratches was found on the rake face as shown in Figure 7.29(a), (b) and (c). These features are probably caused by localised sliding of the chip over the rake face. Wear occurred predominantly on the clearance flank producing a rounded edge as seen in Figure 7.36.

The process of rake face wear for a coated cemented carbide tool is complex and happens due to many phenomena such as friction-adhesion, micro-breakage, diffusion and plastic deformation [185]. Close examination of the worn tool show that there was no evidence of diffusion wear on the rake face of the tool. This is no surprise since the presence of an Al_2O_3 coating would not react with an aluminium based workpiece. Close examination of Figures 7.71 and 7.72(a) and (b) reveal that the coatings of the tool may have been removed along with BUE fragments. The lifting-off mechanism can be seen from the quick stop evidence (Figures 7.95(a) and (b)), it was noticed that some degree of strong bonding exist between the rake face and the BUE. As the chip passed over the rake face of the insert, small pieces of MMC begin to adhere to the coating. Subsequently, these pieces which adhered to the coating bonded to another piece of chip and were ultimately removed with the

chip. As the adhered pieces were removed in the chip, they pulled out small particles of coating which were transported across the face. As machining continued these processes increased because the surface roughness of the coating was increased by the formation of the grooves and holes, thus allowing more MMC to adhere and hence more particles to be removed from the coating. This process of adherence/attrition continued to wear the coating away. Some cracking of the coating was also visible around this region.

8.2.3 Notching and Chipping

A prominent feature observed on the tools was that of notching/micro-chipping on the rake face and along the cutting edge. This feature was observed to varying degrees at different cutting conditions. At lower cutting speeds relatively large sections of the rake face and the cutting edge of K68 were chipped off, Figures 7.34 and 7.37(a)&(b) respectively. Figure 7.35 shows a micrograph of K68 insert with notching. At lower cutting speeds notching at the depth of cut and chipping at the cutting edge of KC910 were observed, Figure 7.70(a) (b) and (c). The appearance of the notching and chipping on the cutting edge suggests that they occurred locally. The chipping-off of the cutting edge at cutting speeds between 15 m/min and 35 m/min may be related to the unstable BUE effect. It is suspected that there might be some degree of bonding between the BUE and tool surface. Chipping will occur when the BUE breaks-off from the insert.

The chipped areas on the cutting edge were rather severe and resembled fractures. The appearance of the chipped section on the cutting edge was a specific observation made under conditions where BUE was thought to exist.

Tlutsty *et. al.* [169] have concluded that chipping of cemented carbide tools is a ductile failure process caused by high shear stresses at the cutting edge. Tabor [150] reports that the BUE might occasionally break away with a small portion of the tool itself.

8.3 Tool Life

8.3.1 Effect Of Geometry On Tool Life

Tool geometries can strongly influence the machining performance of a cutting tool. These geometries include negative versus positive rake (Figure 8.3) and flat top versus chip groove geometry. In the course of this project, negative 7^0 and positive 5^0 rake angle geometries have been used throughout the machining tests. The effect of tool geometry on the tool life of K68 and KC910 inserts will now be discussed.

A positive rake angles are normally recommended when machining aluminium alloys in order to give better surface finish and extended tool life. They allow the chip to flow freely and they produce much lower cutting forces than those which arise with negative rake. Negative rake inserts are not recommended because they can result in built-up edge and lowering of tool life and machining performance [83] [155]. The

highest tool life recorded for negative and positive rake inserts at 0.2 and 0.4 mm/rev are 18.5 minutes and 11.2 minutes respectively. However, the tool life of positive rake insert is slightly higher than negative rake when the feed rate is further increased to 0.6 mm/rev. In general, negative rake geometry inserts give longer tool life than positive rake when machining aluminium 2618 MMC with uncoated K68 grade insert at various cutting conditions. So, this situation contradicts the literature in [83][155]. It is expected that with negative rake (Figure 8.3(b)), the chip flow does not as freely as with positive rake (Figure 8.3(a)) and hence the tendency for BUE formation is high. Moving from positive to a negative rake angle once again influenced the occurrence of BUE, positive rake angle being less likely to produce BUE. Negative geometries have generally longer tool lives because BUEs more likely to form, this protects the tools from abrasive wear and hence extends the tool life.

Chip breaker selection is almost as important as selecting the proper grade. The performance of a cutting tool can be determined not only by the grade properties and coatings type but also by a chip breaker configuration that will allow better utilisation of the machine tool through lower cutting force, better chip handling and control and extended tool life [57][83][103]. Figure 7.12 shows the tool life against cutting speed at various cutting conditions when machining with a chip breaker. Unexpectedly, there is no significant increase in terms of tool life when machining with a chip breaker at 0.2 mm/rev and 0.4 mm/rev. This is due to the contact length on the rake face being small for this particular material. Therefore, when machining

MMC with K68 and KC910 inserts, a chip breaker has no significant affect on tool life.

8.3.2 Effect Of Cutting Conditions On Tool Life

Cutting conditions are the variables that can be changed immediately during the process of machining in order to achieve a satisfactory machining performance for a specific workpiece/tool combination. These variable include cutting speed (v), feed rates (f) and depth of cut (d). Of the three variables, cutting speed is the most important parameter in term of tool life. A study has shows that a 50% increase in cutting speed equals approximately a 80% reduction in tool life, whereas a 50% increase in feed decreased tool life about 60%, and 100% increase in depth of cut showed only a 25% reduction in tool life when machining steel [92][96]. The effects of cutting conditions during machining of MMC with K68 and KC910 inserts are now discussed.

a) Cutting Speed

The effect of cutting speed on various parameters such as flank wear, tool life, cutting forces and surface finish has been monitored throughout the experimental tests as shown graphically in Figures 7.1-7.8, Figures 7.11-7.15, Figures 7.38-7.40 and Figures 7.78-7.79. At most conditions, an increase in speed had a major effect on tool wear and tool life of K68 and KC910 inserts. Rapid wear was experienced at higher speed, this resulted in shorter tool life. The results suggest that at higher speed, abrasion was very active. As speed is increased, more SiC particles pass along

the cutting edge and thus abrade the tool. Therefore, if longer tool life is required, MMC should be machined at lower cutting speeds. Another factor that might be responsible for tool life extension at lower cutting speed is the presence of BUE. The increase in tool life may have been due to the protection offered by BUE formed on the tool surface preventing a direct contact between the tool and the chip.

b) Feed Rate and Depth of Cut

The effect of increasing feed rate when machining at 2 mm DOC has less influence on tool life than speed but there was an improvement in tool life when both feed rate and depth of cut were doubled. A tool life of 18.5 minutes was recorded at a speed of 30 m/min and feed rate of 0.4 mm/rev., while a tool life 3.8 minutes was recorded for the same speed with 0.2 mm/rev (negative rake inserts). The tool life has increased about 5 times when the feed rate is increased from 0.2 to 0.4 mm/rev. It is believed that at higher feed rate and depth of cut the formation of BUE becomes stable during machining and provide protection to the cutting edge and hence increases the tool life. The effect of the presence of BUE can be seen from the reduction of cutting force (Figure 7.39 and 7.76), increased surface roughness, Ra value (Figure 7.78) and decreased chip thickness (Figure 7.99).

Doubling the depth of cut from 2 mm to 4 mm had quite a significant effect, it increases the tool life, especially at high feed rate and low cutting speed. A tool life of 48 minutes was recorded at speed of 15 m/min, 4 mm DOC and 0.6 mm/rev feed (an increase of ~ 48% in tool life). The increase in tool life with the increased feed

rate may be due to the fact that BUE changes its shape with feed rate as it does with speed. Under the above conditions, perhaps the BUE was most stable and hence the tool gave a maximum life.

Therefore, in order to achieve a higher tool life, a combination of high feed rate and depth of cut, as employed during the experiments are suggested.

8.2.3 Taylor Tool Life Equation

A tool life equation is an empirical relationship between the tool life and the cutting conditions such as cutting speed (V), feed (f) and depth of cut (DOC). The famous Taylor tool life equation showed that tool life (T) and cutting speed (V) are related in the following equation [7]:

$$VT^n = C \quad \text{..... (8.1)}$$

where V= cutting speed (m/min)

T = tool life to achieve a specified flank wear (V_b) (in minutes)

n = Taylor exponent

C = Taylor constant

Equation (8.1) can be rewritten as:

$$\log V + n \log T = C \quad \text{..... (8.2)}$$

OR

$$\log T = (1/n) \log C - (1/n) \log V$$

Therefore, on a log-log graph, the Taylor's tool life equation will represents a straight line. In fact, the classical Taylor equation was established with at least two hypotheses:

1) The tool wear mode for example, flank wear , cratering, etc., is constant. If the wear mode varies, the exponent n also varies.
2) The Taylor equation was established for a given tool life criterion.

It is an established practice to use linear regression analysis to obtain the tool-life exponent for the Taylor equation. At most conditions, a near straight-line relationship is obtained as shown by the value of r (near unity) but this is not so for negative rake geometry for K68 and KC910 inserts as seen in Figures 7.6 - 7.8 and 7.56 - 7.58 respectively. By visual inspection, it is not possible to draw a straight line through the plotted points due to the scatter of points obtained during the experiments. It is proposed that the presence of BUE during machining might cause this scatter although multiple mechanisms would have the same effect. Therefore, the Taylor equation cannot be used for predicting tool life for negative rake geometry under these cutting conditions.

A best fit Taylor's tool life equation can be obtained from experimental data for K68 and KC910 inserts with positive geometry at 0.2 mm/rev and 0.4 mm/rev with 2 mm depth of cut, these are $VT^{0.79} = 95.54$, $VT^{0.75} = 95.49$ and $VT^{0.83} = 165.2$, $VT^{0.73} = 131.4$ respectively. There exist a high correlation between the predicted life and the life obtained during the cutting trials (about 95%). The values of the tool life

exponent n with cemented carbide tools are high (0.8 - 1.0) compared to the values of n (0.2 - 0.3) obtained when machining steel [15]. This means that the tool life is much less sensitive to changes in cutting speed. Tomac [252] and Masounave *et. al.* [259] have calculated a Taylor exponent value of 0.6 and 0.5 respectively when machining MMC and suggested that the cutting speed has only a little effect on tool life. When cutting steel, the cutting temperature is high, temperature sensitive wear mechanisms, such as diffusion, operate. These have an exponential relationship with temperature [165][176]. There is no evident to suggest diffusion in case of MMC and if abrasion is dominant a more linear relationship between speed and tool life can be expected.

8.2.4 Volume of Material Removed

It is most interesting to note that if tool life is considered in terms of volume of workpiece material removed, a different picture emerges. For the same cutting speed, the volume removed increases with an increasing feed rate for both K68 and KC910 inserts as seen in Figures 7.19 - 7.22 and 7.59 - 7.62. The increase in volume removed is markedly observed in the speed range 15 to 40 m/min. This shows clearly that the cutting speed has a more dominant influence on the volume of material removed. Consequently, the tool life (i.e. cutting time to reach V_b = 0.4 mm) and material removed show different trends. At a lower feed rate, K68 and KC910 inserts, positive and negative rake geometry, have an almost constant volume of material removed at most cutting speeds.

Further increases of feed rate to 0.4 mm/rev and 0.6 mm/rev markedly increase the volume material removed at all cutting speeds especially for tools with negative rake geometry in the cutting speed range 25 m/min to 35 m/min. As mentioned earlier, longer tool life was obtained at higher feed rate due to the existence of BUE which protects the tool and reduces the wear rate. Therefore, if maximum cutting time between tool changes is needed, a lower feed rate is preferable. On the other hand, if the greatest amount of material removed per insert is desired, then the largest possible feed rate should be chosen - after giving proper consideration towards issues such as surface roughness. This gives an indication that when machining aluminium 2618 MMC, industrially acceptable tool lives are achieved by the combinations of low speed and high feed, which agrees with other published literature [249][254][258].

8.4 Tool/Chip Interface

8.4.1 Nature And Type Of Chip Formation

The information with regards to the chip formation process in machining is important since problems with surface finish, tool-life and workpiece accuracy can be influenced even by minor changes in the chip formation process.

The nature of chips formed during machining changed with the extent of tool wear. At the beginning of cutting, when the tool was sharp, long washer type helical chips are mainly formed (type 4.1 ISO:3685), Figure 7.85, sometimes accompanied by

small amounts of snarled washer type helical chips (type 4.3), Figure 7.86. The chip type changed into short washer helical chips (type 4.2), Figure 7.87, with some loose arch, once the tool started to wear. The greater the wear, the more loose arch chips were produced. There might be two reasons for such chips being formed.

Firstly, the addition to an aluminium alloy of SiC particle reinforcement reduces ductility and induces fracture in the shear zone. Secondly, any unstable built up edge on the tool tip operates as a chip breaker. In terms of machinability, since short chips can easily detach themselves from workpiece and prevent tool damage by recutting, this type of chips is more desirable - as long as the surface finish generated stays within the allowable limit. In term of tool wear, as the cutting edge wear increases, the effective rake angle will increases and thus chip breakability increases. Therefore, the chip type changes to producing more loose arch type of chips as the tools wore.

Representations of chip formation obtained from quick stop segments when machining at various cutting conditions are shown in Figures 7.88(a), 7.89(a) and 7.90(a). The chip types obtained from those chip formation processes are presented in Figures 7.88(b), 7.89(b) and 7.90(b) respectively.

From Figures 7.88(a), 7.89(a) and 7.90(a) we can see clearly that the chip geometry of the aluminium 2618 MMC is irregular and shows evidence that rupture, rather than shear is the controlling mechanisms. As a result, discontinuous and segmented chips were produced.

A discontinuous chip is normally obtained when machining inherently brittle material such as cast iron or when machining ductile materials at low cutting speed where rupture intermittently occurs at the shear plane [26] [27]. This type of chip topography is typical of many two-phase alloys containing a second brittle phase [155 - 157]. With these materials, the spacing between shear zones is small, the frictional contact length on the rake face of the tool is short and the shear plane angle ϕ is high (see Figure 7.101). Furthermore, the presence of SiC particles limits the ductility of the workpiece material.

8.4.2 Built-Up Edge (BUE) Formation

The presence or absence of a build-up edge (BUE) on the rake face of a cutting tool has important implications for all aspects of machining behaviour, including wear of the cutting edge, surface finish and cutting forces. BUE is normally formed when machining aluminium alloys which have structures containing more than one phase, at low cutting speeds [47][50][60][155]. This is readily understandable since, under intense shear, the structural phases align themselves with the direction of flow and encourage further shear to take place along the structural 'faults' initiated by the weaker-phase constituents [49][51]. The presence of BUE have been reported when machining MMC with cemented carbide tools. Unfortunately, direct evidence of the presence of the BUE using quick stop tests was not given in the literature [249 - 254].

It was found that a BUE was present under certain cutting conditions. The presence of BUE is more pronounced at cutting speeds in the range 15 m/min to 40 m/min and at 0.4 mm/rev and 0.6 mm/rev feed rate, as seen in Figures 7.93, 7.94, 7.95 and 7.96. At the lowest cutting speed of 15 m/min, the BUE was very stable and formed a pseudo-cutting edge which changed the effective cutting angles on the tool. A strongly deformed strain hardened material forms a stationary body on the rake and flank surfaces of the tool.

The micrographs presented in Figures 7.92(a - d) represents a cross-section of BUE produced at different cutting speeds. On close examination, there is an overflow of material down the leading edge of the BUE and over the flank face. This overflow material could have been responsible for removing both layers (TiC and Al_2O_3) of the coating and for pulling out WC grains to produce a wear land. This process has taken place during machining and is not simply a smeared layer covering the tool surface during disengagement of the tool from the workpiece. On the rake face, near the cutting edge, where normal stress is maximum, the BUE adhered to the tool, creating a stationary wedge of material, which prevented direct contact between the tool and the chip. Therefore, this particular BUE was responsible for protecting the rake against abrasion during machining. However, as the height of a BUE increases, it becomes unstable and pieces break off, Figure 7.92(d), to slide against the clearance flank so causing the abrasive wear as described previously. There might be some protection on the flank face by the over hang from the workpiece as shown in Figure 7.92. However, this protection was not as stable as that on the rake face due

to the dynamic nature of the movement between the workpiece and the clearance face.

Figures 7.93(a) and 7.93(b) - 7.96(a) and 7.96(b) show segments of the quick-stop samples with BUE and cross-sections of the same samples. From these figures it can been seen that there is a layer of built-up material adhered to the root of the chip and the machined surface behind it is very rough due to the effect of the BUE. Figures 7.93(b) - 7.96(b) show distinctively the presence of BUE with different shapes at each particular cutting conditions. Figures 7.97(a) and 7.97(b) show a segment of a quick-stop sample and a cross-section of the sample which has no BUE. From these micrographs emerge several interesting features.

Firstly, the cross-section of the BUE shows that it consists of a thick stable body resting on a very wide foot. In fact, the toes of this foot are long and thin but remain completely flat when the tool was blown out of action or when the chip plus BUE jump off the tool. This proves that no welding took place, only temporary sticking [53]. This suggest that in most cases the bonding is not so strong, after quick-stopping there was no torn underside of the BUE and nothing remained adherent to the rake face. This is further evidence that there is some interfacial movement and there is not complete seizure at the interface over the majority of the chip/tool length, including the cutting edge. However, by looking at Figure 7.95(b), small parts of the BUE remained adhered further back from the cutting edge suggesting that some degree of bonding exist only at particular cutting conditions. This

particular situation might have been responsible for the chipping-off of some WC grains on the rake face and flank face, and the removal of some coatings, as discussed in section 8.2.2. The BUE formation is dynamic, as the BUE grows bigger, it will break and be swept away on the underside of the chip and slide over the rake face. Some of the fragments may travel down the flank face. Therefore, abrasive flank wear can be caused by hard BUE particles. This is a likely mechanism in this case because the MMC used contain SiC particle inclusions of sufficient hardness, size and shape to abrade the cemented carbide tools.

Secondly, the shapes of BUE resembles the formation and structures of class I (positive wedge) BUE suggested by Heginbotham *et. al.* [47] and Wallbank [54] which occurs by a nucleation process at the lowest cutting speed. The size of the BUE is then regulated by fracture on the workpiece and chip sides of the BUE which do not necessarily occur simultaneously. Close examination of the cutting edge shows that there are several bands containing fine SiC particles, Figure 7.93(b) - 7.95(b). These bands were probably produced by the mechanical disintegration of the larger particles within the workpiece. The fact that these bands follow the general profile of the BUE suggested that they represent evidence of the progressive nature of the BUE formation process. The formation of BUE cannot go on indefinitely and eventually break up of the BUE structure occurs by shearing. According to Heginbotham *et. al.* [47] this breakdown occurs in two regions, one adjacent to the work surface, and the other adjacent to the underside of the chip.

Under particular cutting conditions, the accumulation of SiC particles is found to be higher at the edge than in the body of BUE, as seen in Figure 7.96(b). This group of SiC particles is able to act as several mini cutting edges or as abrasive grains, like those in a low concentration grinding wheel, as the machining process continues. This again suggests that when machining MMC the main wear mechanism is abrasion.

However, the presence or absence of a BUE on the rake face of the tool can be inferred from a study of the surface finish generated on the workpiece, the cutting forces, the chip thickness data and by observation of underside of the chips. During machining, a BUE was believed to exist to some extent at all cutting speeds but was most pronounced between 15 and 40 m/min, especially at higher feed rates. Figure 7.80 shows cutting forces against cutting speed for cemented carbide tools at 0.4 mm/rev feed. The cutting forces are found to be relatively low in the speed range 20 - 40 m/min as a result of the presence of a BUE. The surface finish data presented in Figures 7.78 - 7.81 shows a marked deterioration in the surface finish within the same range, especially at higher feed rates. Indeed, the nature of the surface was such that the surface finish measurement at these conditions was not possible. BUE formation was confirmed by the SEM photomicrographs of the underside of chips generated at these cutting conditions, Figures 7.102(a) (b) and (c).

Machining with the presence of a BUE on the rake face of the cutting tool has the effect of increasing the effective rake angle, and reducing the "chip/tool" contact

area. The combined effect of which results in the reduction of shear plane angle (ϕ) and decrease in chip thickness, this was observed during machining, as shown in Figures 7.98 - 7.101.

8.4.2.1 Effect Of Built-Up Edge On Wear

The BUE can exercise both an accelerating and a retarding function in wear. The effect can be magnified in the intervals in which the built-up edge forms a rounded cutting edge. The degree of plastic deformation of the material increases and results in an increase in cutting temperature. On the other hand, the tool material is protected from heating, at the same time as the effective rake angle increases. Both these factors are capable of reducing the wear rate [58][59]. The presence of a BUE on the rake face of the cutting tool has been shown to protect the flank face, hence eliminating tool wear for long periods of time under certain conditions [13].

On the rake face, near the cutting edge, where the normal stress is maximum, the BUE adhered to the tool creating a stationary wedge of material, which prevented the development of wear by abrasion in this region (see Figure 3.93(b) - 3.96(b)). Unfortunately, the BUE produced protected the rake face of the tool but had no beneficial effect on the rate of flank wear. In fact, the fragments of BUE which detached periodically and smeared against the clearance face, further contributed to flank wear. Since there exists an intimate contact between the workpiece material and the clearance face, flank wear is the most important area of wear because it affects the surface finish and the dimensional accuracy of the workpiece. Therefore,

this work indicated the importance of the nature of the BUE if it is to protect the flank face of the tool during machining. However, from the point of view of preventing flank wear, the presence of a BUE on the rake face of the tool is not always beneficial. Therefore, this work is in agreement with Tomac and Tonnessen [252] who have identified certain cutting conditions which would result in the formation of a protective BUE and thus reduce tool wear.

8.4.3 Surface Finish

The surface roughness values which were recorded were always above the value of the ISO recommended standard of 1.6 μm. In some instances, the value of surface roughness could not be taken due to the very uneven surfaces produced. An interesting feature of the results shown in Figures 7.78 - 7.81 is that the measured values for Ra are not much different from those predicted for a 0.2 mm/rev feed rate and 0.8 mm nose radius combination, especially between cutting speeds of 25 m/min and 35 m/min. The exception to this trend probably occurred owing to the influence of the extensive BUE. The BUE altered the cutting tool geometry and acted as a secondary cutting tool which cut the workpiece material and hence produces a poor surface finish. The reason for the apparent improvement in surface finish at higher cutting speed, especially at a feed rate of 0.4 mm/rev, is a breakdown of the BUE at higher speeds. As a consequence, there is a reduction in the magnitude of the surface roughness.

The surface finish results for the series of tests performed at the lower feed rate of 0.2 mm/rev when using inserts having a nose radius of 0.8 mm are shown in Figure 7.78. As expected, the lower feed rate has resulted in an improvement in the surface roughness. For both insert types, K68 and KC910, the measured Ra values are slightly more than the theoretical 1.61 μm calculated for a feed rate of 0.2 mm/rev and 0.8 mm tool nose radius. It can also be seen from Figure 7.80 and 7.81, measured Ra values are minimum in the speed range 20 m/min - 35 m/min.

Longer tool life was recorded where the BUE was present, but the process of 'building up' on the rake face of the tool cannot go on indefinitely. The resolved stress in the cold-worked material increases until suddenly the position of the shear zone shifts into the BUE and parts of this are carried away on the underside of the swarf, and on the work surface, this results in a poor surface finish. The surface finish generated often has a saw-tooth profile, characteristic of conditions where a BUE exists. The 'tearing off surfaces' were observed under most of the cutting conditions, as seen in Figures 7.82 - 7.84. The BUE on the cutting edge has most likely been responsible for such poor surface finish.

8.4.4 Cutting Forces

One of the fundamental criterion in studying the machining process is the evaluation of cutting forces required to deform the work material in the shear zones. In orthogonal cutting the resultant force, R, is expressed by its two main component, cutting force, F_c, acting in the direction of cut and feed force, F_f, which is in the

opposite direction to the tool travel. It is an accepted view that the forces in orthogonal cutting are influenced by many factors such as cutting speed, feed rate, depth of cut, rake angle, built-up edge, tool and work material characteristics [36]. These factors in effect are controlled and related by conditions at the tool/chip interface, which are identified by shear yield strength of the work material, and on the area and angle of the shear plane and temperature in the region. Higher cutting forces are a result of a large contact area on the rake face of the cutting tool and small shear plane angle [13][63].

8.4.4.1 Effect Of Speed And Feed

Nakayama *et. al.* [58], Shaw [16] and Trent [13], have indicated that no specific relationship exists between the cutting forces at the beginning of a machining process and the cutting speed being used. However, they found that generally, after the initial few seconds of machining, the cutting forces decrease as the cutting speed is raised. It was suggested that this occurred as a result of a rise in temperature and a consequent decrease in the shear resistance of the material within the shear zone adjacent to the chip/workpiece interface. Reference to Figures 7.79 and 7.80 shows that no such reduction in cutting forces with increasing cutting speed occurred during machining. This is because the cutting speed range tested is probably insufficient to raise the temperature between the tool/chip interface in order to destabilise the BUE present at such conditions. Furthermore, the presence of BUE controlled the contact length between the chip and tool, hence the forces produced are low.

The effect of changing the feed rate on the cutting forces can be seen in Figures 7.79 and 7.80. It is interesting to note that the cutting forces are almost constant when cutting at 0.2 mm/rev, but the pattern changes when the feed is raised to 0.4 mm/rev. The cutting forces recorded at 0.2 mm/rev are generally low for cemented carbide tools and this is probably explained by the reinforcement reducing the ductility of the material and short contact length of chip on tool. Increasing the feed rate to 0.4 mm/rev increases the cutting force (Figure 7.75), however, the cutting forces are abnormally low in the cutting range 25 to 35 m/min because the built-up edge acts like a restricted contact tool, effectively reducing contact on the rake face and reducing chip/tool adhesion. As machining takes place in this speed range, the shape of the BUE alters the effective rake angle of the tool and hence reduces the cutting forces [36][47]. One of the findings from the cutting force work was their sensitivity to tool wear. Tool wear certainly explains the increasing tool force with cutting speed experienced by cemented carbide tools when machining MMC. As the speed is being raised, the cutting forces increases progressively due to the disintegration of the BUE resulting from increases in the temperature and the wear of the tool.

At all cutting conditions the positive rake angle of cemented carbide tools generates lower cutting forces when cutting MMC, this is as expected. Higher rake angle will generally produce low forces and vice-versa [47].

8.5 Relative Performance Of Cemented Carbide Tools

Generally, KC910 inserts show longer tool lives than K68, regardless of cutting conditions. The factor that limits tool life for both tools in the speed range tested is identical, i.e. flank wear. At a lower feed rate of 0.2 mm/rev, there was no significant difference in terms of tool life for K68 and KC910 tools with negative or positive rake geometry except at 40 m/min where K68 and KC910 tools with negative rake geometry show a significant difference, Figures 7.103 - 7.106. This is because at lower feed rate little or no BUE exists, and this can be seen by the constant generation of cutting force at this particular conditions. As the feed rate is increased to 0.4 mm/rev, a stable BUE was formed which protects the tools and there is a marked increase in tool life for KC910 with negative rake geometry at speeds of 25 m/min and 30 m/min. The coated KC910 inserts gave longer tool life because the coating (TiC and Al_2O_3) is harder and has higher abrasion resistance than K68 inserts.

Negative rake geometry outperformed positive rake because of its tendency to produce BUE which provide an extra protection to the tool during machining and thus prolong the tool life. Further increase in feed rate to 0.6 mm/rev and depth of cut to 4 mm did not significantly increase the tool life or affect tool wear of either cemented carbide tools at any cutting speed as can be seen in Figure 7.103 and Figures 7.104 - 7.106.

Obviously, the increase in feed rate and depth of cut will increase the volume of material removed, Figures 7.56 - 7.58. This indicates that industrially acceptable tool lives can be achieved with a combination of low cutting speed and high feed rates. Hence, the tool life and volume of material removed can be increased effectively by increasing the feed rate. This proved so in tests with KC910 negative rake geometry at 25 m/min and feed rates of 0.2 and 0.4 mm/rev as shown in Figure 7.109. Cutting times of 9 minutes and 25 minutes were recorded to achieve 0.4 mm flank wear at 0.2 and 0.4 mm/rev feeds respectively. At these conditions the existence of a stable BUE gives some form of protection to the cutting edge and hence reduces tool wear rate.

Figures 7.107 and 7.108 show the variation of flank wear with cutting speed for cemented carbide tools at 0.2 mm/rev and 0.4 mm/rev feed. At almost all cutting conditions the coated cemented carbide tools (KC910) with negative and positive rake geometry have a lower rate of wear compared to uncoated K68 grade inserts. It has been discovered that TiC coatings provide some measure of protection to the flank face of a cutting tool under abrasive wear condition [77][188].

8.6 General Points

The main feature of the machining of aluminium 2618 MMC is that it is extremely abrasive and requires cutting tools of sufficient hardness to resist abrasive wear. It has been shown throughout this work that cemented carbide tools are capable of

machining these material, even though polycrystalline diamond (PCD) tools seem to fit the role admirably there are several situations where it is more economical to use cemented carbide (WC) tooling. A low speed and high feed rate is an ideal combination when machining these material with WC tooling in order to achieve longer tool life and higher volume of material removed. This is the situation where the beneficial BUE exists to prolong the tool life, being able to predict conditions under which this will occur allows tool performance to be maximised. WC tooling is suitable for rough machining which can be followed by polycrystalline diamond (PCD) tools for finishing. Extra care should be exercised in handling expensive tools like polycrystalline diamond (PCD) in a hostile environment, like a factory workshop, cemented carbide tools are more tolerant of abuse.

The SiC particles incorporated into the MMC interfere with the chip formation process and the swarf produced during machining was easily handled. However, the abrasive SiC debris generated during the chip formation interfered with all aspects of the machining process, and if mixed with cutting fluid can cause severe wear to the machine tool, the cutting fluid system and perhaps affect the operators' health unless precautions are taken to contain this debris.

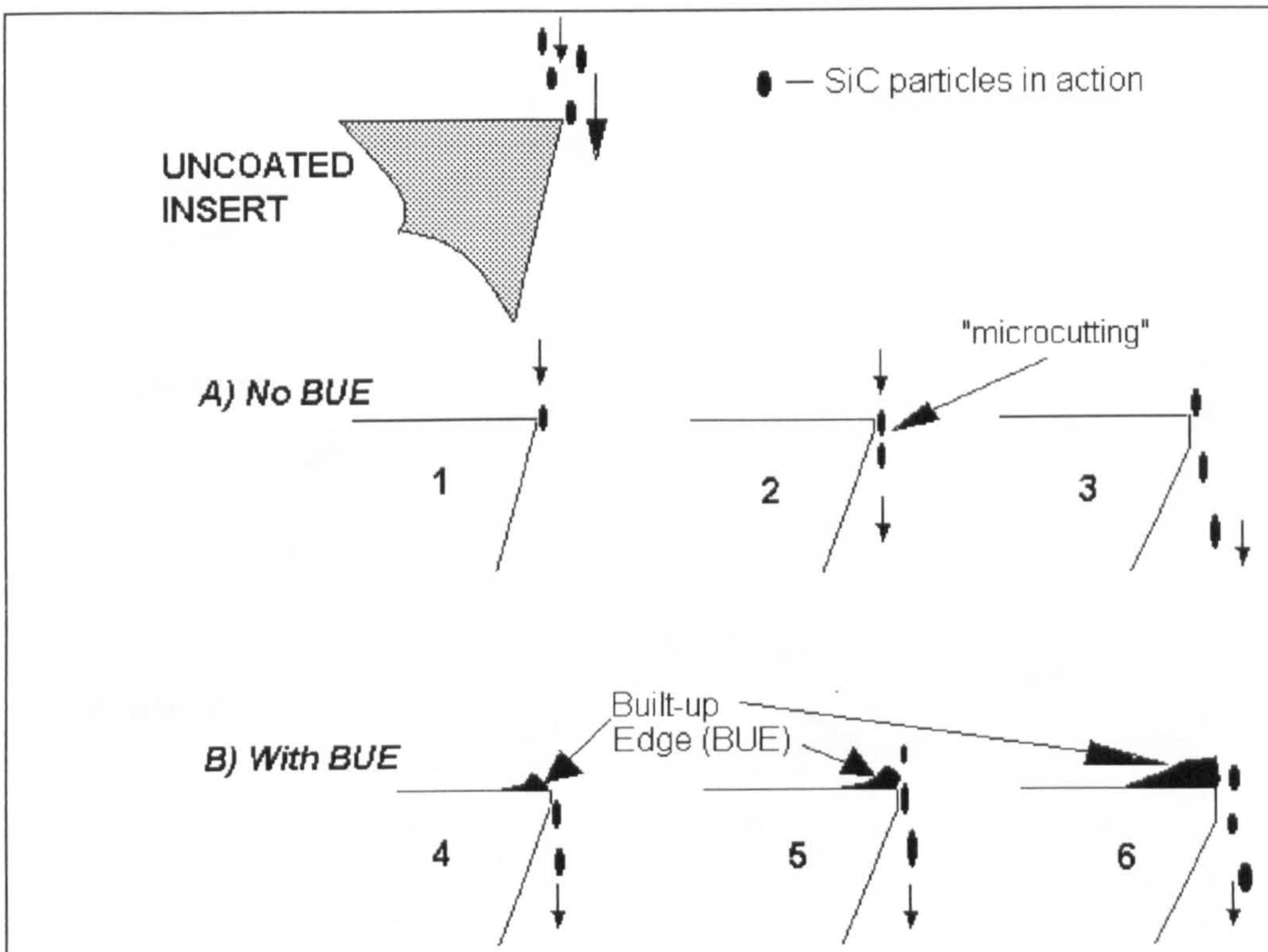

(a)

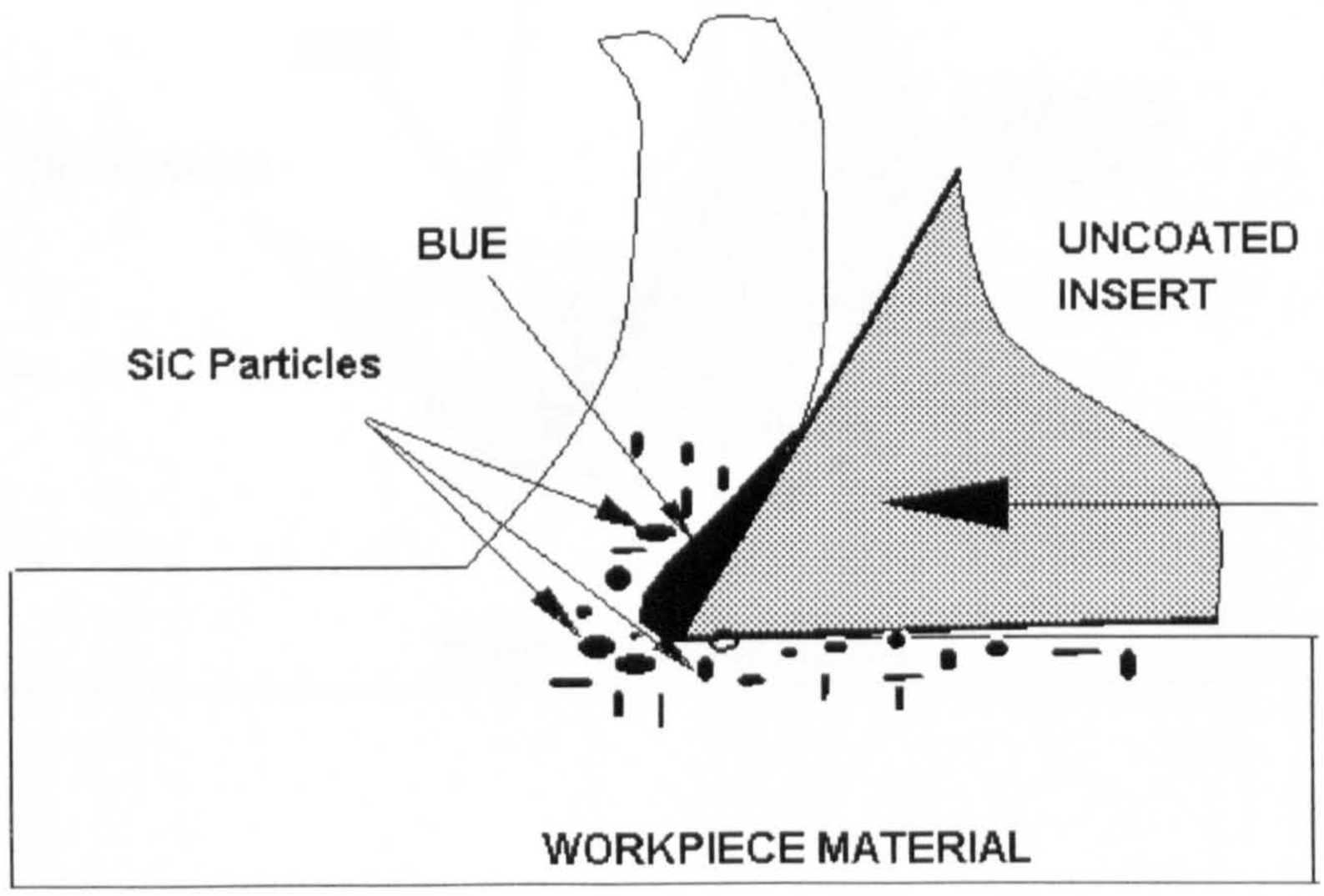

(b)

Figure 8.1 Abrasion Model Proposed For Flank Wear of Uncoated Cemented Carbide K68 Insert

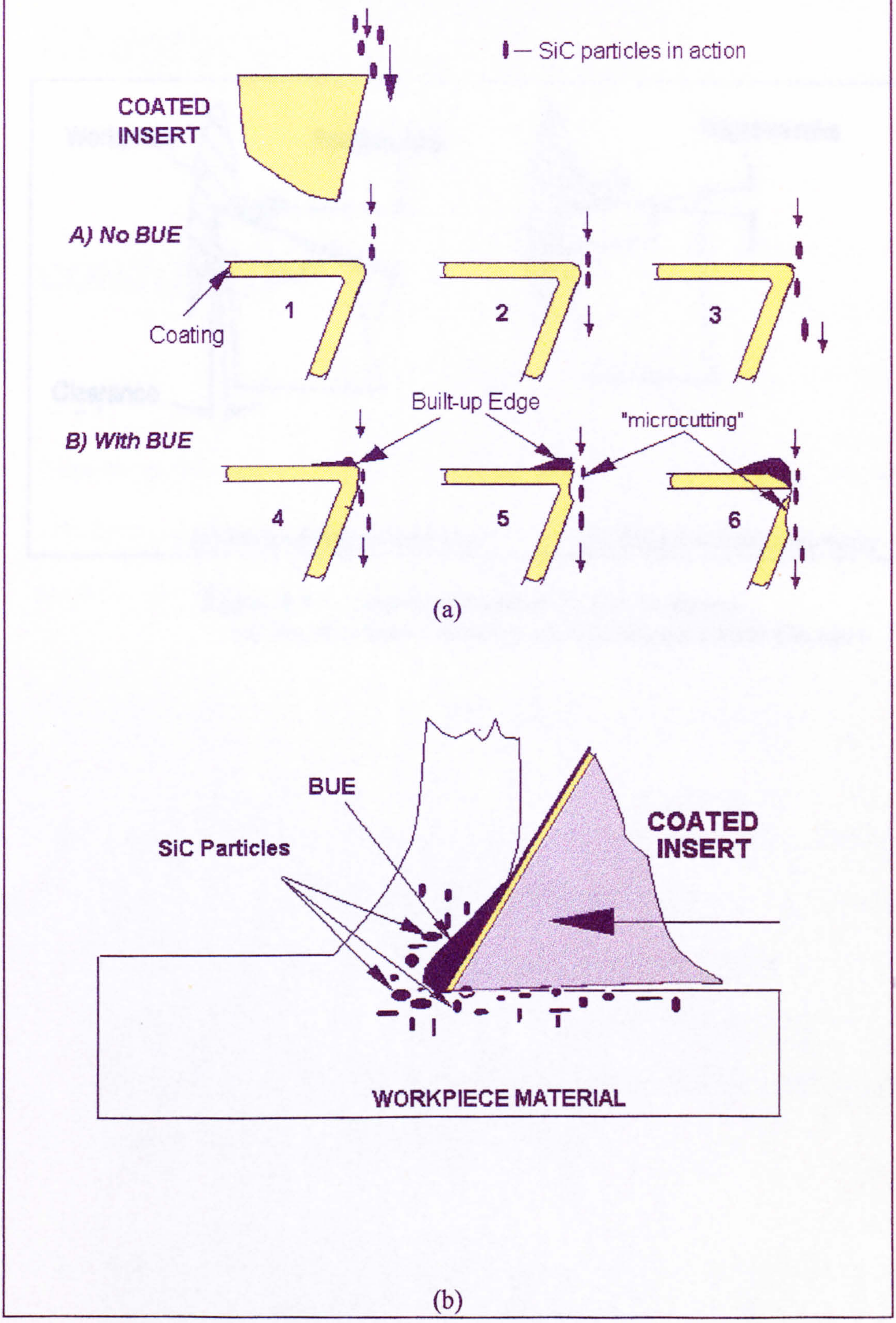

Figure 8.2 Abrasion Model Proposed For Flank Wear of Coated Cemented Carbide KC910 Grade

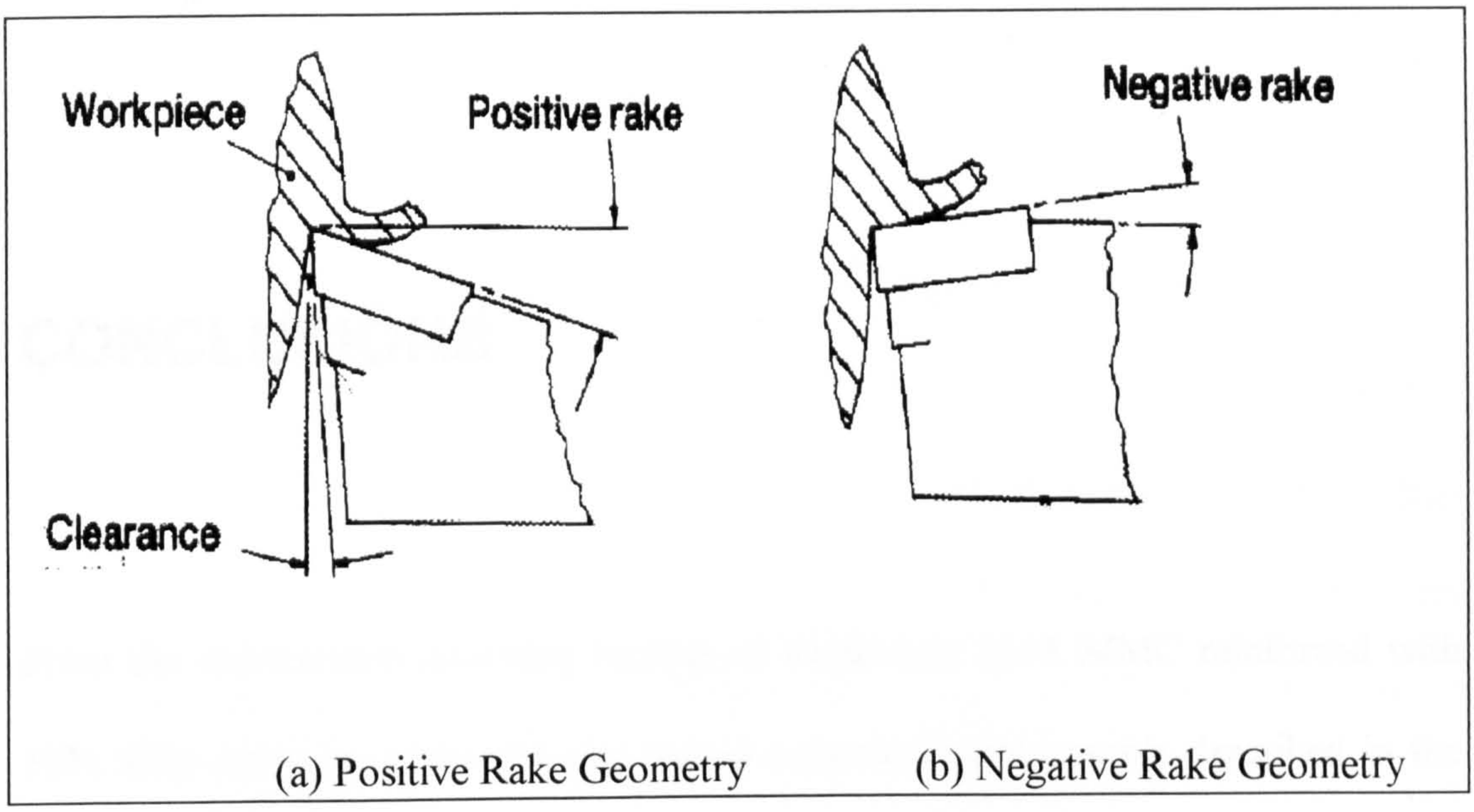

Figure 8.3 Insert Orientation To The Workpiece
(a) Positive Rake Geometry, and (b) Negative Rake Geomery

Chapter 9

CONCLUSIONS

From the experiments involving turning of aluminium 2618 MMC reinforced with 18% SiCp using the uncoated and coated cemented carbide tools described in the present work, the following conclusions can be drawn:

1. Flank wear was the dominant failure mode under all cutting conditions.

2. Abrasion was found to be the main tool wear mechanism when machining MMC with cemented carbide tools. It is believed that abrasion was caused on the flank and rake face by either SiC particles from the workpiece material or the WC particles which were lifted from the tool face because of adhesion. Abrasion mechanism models based upon micro-cutting for uncoated and coated cemented carbide have been suggested.

3. Built-up edge (BUE) having a distinctive shape was present during the process of machining. The presence of BUE is more distinct in the cutting speed range 25 m/min to 40 m/min when using 0.4 mm/rev feed, this applies

to both negative and positive rake angle tools. The presence of BUE has been found to increase tool life and reduce tool wear. However, the surface finish generated during such conditions was poor.

4. The values of the n exponent of the Taylor relation for both uncoated and coated cemented carbide tools are high (0.8-1.0) compared to the value of n (0.2-0.3) when machining steel. This indicates that the tool life is less sensitive to cutting speed for MMC than it is for steel. Hence, less temperature sensitive wear mechanisms in the case of MMC are a more likely explanation.

5. Cemented carbide tools have been found suitable for cutting MMC. Conditions where a combination of a low cutting speed and high feed rate can be employed allow longer tool lives and higher volume of material removed, which is suitable for industrial situation. Negative rake tools gave longest tool life and highest volume of material removed when turning aluminium 2618 MMC. The tendency for BUE formation was high for inserts having negative rake angle and this was perhaps responsible for longer tool life.

6. In terms of performance ranking, KC910 inserts with negative rake geometry generally gave the best performance. TiC and Al_2O_3 coatings which are harder and have higher abrasion resistance than cemented carbide gave

protection on the tools during the initial stages of cutting. As the machining continued the coatings were found to be removed and abraded away by the SiC particles, this resulted in more rapid tool wear.

7. The surface finish of the machined surface deteriorates with increasing feed rates. However, increase in cutting speed did not have any significant effect on surface finish. Under conditions where the BUE was present, the surface roughness generated was unpredictable.

8. The cutting forces generated during the machining of MMC with cemented carbide tools are relatively low, generally remain constant within the range of cutting speeds tested but drop when BUE is present. However, forces increased as the feed rate was increased.

9. Discontinuous chips were produced when turning MMC with both uncoated and coated cemented carbide tools regardless of whether a chip breaker was present. This is due to the low ductility of MMC caused by the presence of SiC particles, which induce fracture in the shear zone, and the presence of BUE which operates as a chip breaker. Segmented chips were the major types of chip produced, this renders the material well-suited for automated machining operations.

10. The presence of a chip breaker did not have a significant effect on the tool performance, tool failure modes and wear mechanism.

Chapter 10

SUGGESTIONS FOR FURTHER WORK

When machining MMC with cemented carbide tools the SiC particle reinforcement plays a major role with respect to tool wear and the machining process. Therefore , it would be appropriate to address the following issues in future work:

1. *Reinforcement Materials*: There are aluminium alloys with different types of reinforcement, these includes SiC, Al_2O_3 and B_4C particle reinforcement with different compositions and particle sizes. Different types of reinforcement have different physical and mechanical properties and thus they may have different effects on the tool and machining process during machining.
2. *Reinforcement Size*: SiC, Al_2O_3 and B_4C particle reinforcement have different average diameter ranges from 2 μm to 130 μm with different shapes. This could cause different effects on aspects of the machining process such as tool wear and surface finish when machining with cemented carbide tools. The orientation and the flow of SiC particles during the chip formation process over the cutting tool edge could influence the amount and rate of wear. Both large and small size

particles have a chance of abrading the surface during machining. The particle size and shape may well influence BUE formation as well as abrasion.

3. *Volume Fraction of The Reinforcement*: The reason for the high tool wear when machining MMC is due to the hard and abrasive reinforcement, therefore changes in percentage can have a dramatic change on the machining process of these material.

4. *Cutting Conditions and Tool Geometry*: The conditions at the tool/work interface will be influenced greatly by changing the cutting conditions and the application of different types of tool geometry. Hence, a wide range of cutting speeds, feed rates and depth of cut, together with different tool geometry, should be investigated in order to predict more precisely the behaviour of MMC during machining.

5. *Machining with Polycrystalline Diamond (PCD) Tools*: Different grain size of polycrystalline diamond (PCD) tools should be used to cut MMC to investigate the machining process, particularly to determine if BUE exists during machining and under what specific cutting conditions.

6. *Different Processing Routes*: Physical and mechanical properties of MMC are closely related to the processing routes. Different processing route can also have a decisive influence on the machinability of MMC and this should be categorised. This also applies to the heat treatment condition of the matrix (and, therefore matrix composition may play a role).

Appendix 1

Machinability Results For K68 And KC910 Inserts

Table 7.1 Tool Life, Failure Mode, Surface Finish And Volume Of Material Removed For K68 Inserts With 2mm Depth Of Cut

TOOL GEOMETRY / CUTTING CONDITIONS		NEGATIVE RAKE ANGLE				POSITIVE RAKE ANGLE				NEGATIVE RAKE ANGLE WITH CHIP BREAKER			
Cutting Speed (m/min)	Feed Rate (mm/rev)	Tool Life (min)	Failure Mode	Surface Finish (μm)	Vol. Mat. Removed (cm^3)	Tool Life (min)	Failure Mode	Surface Finish (μm)	Vol. Mat. Removed (cm^3)	Tool Life (min)	Failure Mode	Surface Finish (μm)	Vol. Mat. Removed (cm^3)
15	0.2	8.0	FW	1.72	48.0	10.5	FW	1.91	63.0	9.5	FW	1.72	57.0
20	0.2	6.5	FW	1.92	52.0	7.0	FW	1.88	56.0	8.0	FW	1.82	64.0
25	0.2	5.2	FW	1.51	52.0	5.6	FW	1.71	56.6	4.4	FW	1.72	44.0
30	0.2	3.8	FW	1.94	45.6	4.0	FW	1.60	48.0	3.2	FW	1.76	38.4
35	0.2	5.8	FW	1.71	81.2	3.4	FW	1.74	47.6	2.5	FW	1.74	35.0
40	0.2	7.2	FW	2.82	115.2	3.0	FW	1.72	48.0	2.0	FW	1.50	32.0
45	0.2	3.5	FW	3.50	63	2.8	FW	1.70	50.4	1.8	FW	1.35	32.4
50	0.2	2.2	FW	2.09	44.0	2.2	FW	1.78	44.0	1.4	FW	1.82	28.0
15	0.4	7.0	FW	7.0	84.0	11.2	FW	8.15	134.4	11.5	FW	6.50	138.0
20	0.4	7.0	FW	9.9	112.0	8.0	FW	8.23	128.0	18.8	FW	NM	300.8
25	0.4	11.2	FW	7.9	224.0	6.0	FW	7.81	120.0	13.2	FW	NM	264.0
30	0.4	18.5	FW	10.9	444.0	5.5	FW	7.82	132.0	6.2	FW	6.77	148.8
35	0.4	10.0	FW	7.9	280.0	4.0	FW	8.02	112.0	5.2	FW	7.23	145.6
40	0.4	3.8	FW	7.86	121.6	3.2	FW	7.67	102.4	2.0	FW	8.03	64.0
45	0.4	3.5	FW	8.1	126.0	2.5	FW	7.65	90.0	1.5	FW	7.00	54.0
50	0.4	2.0	FW	7.54	80.0	2.3	FW	7.81	92.0	1.2	FW	7.8	48.0
15	0.6	8.0	FW	NM	144.0	22.0	FW	16.2	396.0				
20	0.6	15.4	FW	18.05	369.6	12.0	FW	17.4	288.0				
25	0.6	15.4	FW	16.1	462.0	15.5	FW	15.1	465.0				
30	0.6	3.8	FW	15.7	136.8	5.0	FW	17.2	180.0				

NOTE : FW - Flank Wear NM - Non Measurable

Table 7.2 Tool Life, Failure Mode, Surface Finish And Volume Of Material Removed For K68 Inserts With 4mm Depth Of Cut

TOOL GEOMETRY / CUTTING CONDITIONS		**NEGATIVE RAKE ANGLE**				**POSITIVE RAKE ANGLE**			
Cutting Speed (m/min)	Feed Rate (mm/rev)	Tool Life (min)	Failure Mode	Surface Finish (μm)	Vol. Mat. Removed (cm^3)	Tool Life (min)	Failure Mode	Surface Finish (μm)	Vol. Mat. Removed (cm^3)
15	0.2	7.0	FW	1.99	84.0	11.0	FW	1.78	132.0
20	0.2	4.4	FW	2.14	70.4	7.6	FW	1.73	121.6
25	0.2	5.4	FW	2.73	108.0	5.6	FW	1.86	112.0
30	0.2	5.5	FW	4.58	132.0	5.4	FW	1.60	129.6
15	0.4	33.0	FW	NM	792.0	10.0	FW	6.71	240.0
20	0.4	19.2	FW	NM	614.4	7.2	FW	6.75	230.4
25	0.4	21.2	FW	NM	848.0	8.5	FW	6.85	340.0
30	0.4	9.2	FW	10.86	441.6	5.9	FW	6.87	283.2
15	0.6	46.0	FW	NM	1654.0	18.0	FW	17.5	648.0
20	0.6	15.5	FW	15.9	744.0	24.0	FW	15.8	1152.0
25	0.6	7.5	FW	16.17	450.0	6.0	FW	17.2	360.0
30	0.6	4.0	FW	NM	288	5.0	FW	17.1	360.0

NOTE : FW - Flank Wear NM - Non Measurable

Table 7.3 Values of n and C for Taylor Tool Life Curve For K68 Inserts At 0.2 and 0.4 (mm/rev) Feed Rates With 2 mm And 4 mm Depth of Cut

TOOL GEOMETRY	NEGATIVE RAKE ANGLE		POSITIVE RAKE ANGLE		NEGATIVE RAKE ANGLE WITH CHIP BREAKER	
DOC = 2 mm	0.2 (mm/rev)	0.4 (mm/rev)	0.2 (mm/rev)	0.4 (mm/rev)	0.2 (mm/rev)	0.4 (mm/rev)
Value of n	1.38	1.07	0.79	0.75	0.60	0.44
Value of C	272.8	223.45	95.54	95.49	61.8	60.77
Regression Coefficient (r)	0.6919	0.5336	0.9958	0.9911	0.9912	0.9029
TOOL GEOMETRY	**NEGATIVE RAKE ANGLE**		**POSITIVE RAKE ANGLE**			
DOC = 4 mm	0.2 (mm/rev)	0.4 (mm/rev)	0.2 (mm/rev)	0.4 (mm/rev)		
Value of n	3.65	0.65	0.92	1.64		
Value of C	$10.7X10^3$	138.5	133.5	625.2		
Regression Coefficient (r)	0.4312	0.8994	0.9771	0.8062		

Table 7.4 Tool Life And Distance Cut For 0.4 mm Flank Wear For K68 Inserts At 0.2 and 0.4 mm/rev Feed Rates (Negative Rake Angle, DOC = 2 mm)

Cutting Speed (m/min)	Tool Life (min)		Distance Cut (m)	
	0.2 (mm/rev)	0.4 (mm/rev)	0.2 (mm/rev)	0.4 (mm/rev)
15	8.0	7.0	120	105
20	6.5	7.0	130	140
25	5.2	11.2	130	280
30	3.8	18.5	114	555
35	5.8	10.0	203	350
40	7.2	3.8	288	152
45	3.5	3.5	157.5	157.5
50	2.2	2.0	110	100

Table 7.5 Tool Life and Distance Cut For 0.4 mm Flank Wear For K68 Inserts At 0.2 and 0.4 mm/rev Feed Rates (Negative Rake Geometry, DOC = 2 mm, WITH Chip Breaker)

Cutting Speed (m/min)	Tool Life (min)		Distance Cut (m)	
	0.2 (mm/rev)	0.4 (mm/rev)	0.2 (mm/rev)	0.4 (mm/rev)
15	9.5	11.5	142.5	172.5
20	8.0	18.8	160	376
25	4.4	13.2	110	330
30	3.2	6.2	96	186
35	2.5	5.2	87.5	182
40	2.0	2.0	80	80
45	1.8	1.5	81	67.5
50	1.4	1.2	70	60

Table 7.6 Tool Life and Distance Cut For 0.4 mm Flank Wear For K68 Inserts At 0.2 and 0.4 mm/rev Feed Rates (Positive Rake Geometry, DOC = 2 mm)

Cutting Speed (m/min)	Tool Life (min)		Distance Cut (m)	
	0.2 (mm/rev)	0.4 (mm/rev)	0.2 (mm/rev)	0.4 (mm/rev)
15	10.5	11.2	157.5	168
20	7.0	8.0	140	160
25	5.6	6.0	140	150
30	4.0	5.5	120	165
35	3.4	4.0	119	140
40	3.0	3.2	120	128
45	2.8	2.5	126	112.5
50	2.2	2.3	110	115

Table 7.7 Cutting Force (F_c) and Feed Force (F_f) For K68 Inserts At 0.2 mm/rev Feed Rate and 2 mm DOC

CUTTING SPEED (m/min)	K68 (NEG.Geometry) NO Chip Breaker		K68 (NEG.Geometry) WITH Chip Breaker		K68 (POS.Geometry) NO Chip Breaker	
	F_c (N)	F_f (N)	F_c (N)	F_f (N)	F_c (N)	F_f (N)
15	480	220	430	210	400	170
20	470	235	410	200	395	160
25	475	245	420	215	385	170
30	520	280	440	220	410	190
35	470	250	410	220	420	180
40	465	250	420	230	405	185
45	430	220	470	240	410	190
50	420	215	450	235	415	200

Table 7.8 Cutting Force (F_c) and Feed Force (F_f) For K68 Inserts At 0.4 mm/rev Feed Rate and 2 mm DOC

CUTTING SPEED (m/min)	K68 (NEG.Geometry) NO Chip Breaker		K68 (NEG.Geometry) WITH Chip Breaker		K68 (POS.Geometry) NO Chip Breaker	
	F_c (N)	F_f (N)	F_c (N)	F_f (N)	F_c (N)	F_f (N)
15	750	310	750	350	665	230
20	790	350	715	320	660	235
25	735	315	700	300	655	240
30	650	250	575	250	645	230
35	670	250	600	260	580	220
40	675	260	770	410	615	240
45	740	340	916	520	710	290
50	795	380	950	550	690	400

Table 7.9 Tool Life, Failure Mode, Surface Finish And Volume Of Material Removed For KC910 Inserts With 2mm Depth Of Cut

TOOL GEOMETRY / CUTTING CONDITIONS		NEGATIVE RAKE ANGLE				POSITIVE RAKE ANGLE				NEGATIVE RAKE ANGLE WITH CHIP BREAKER			
Cutting Speed (m/min)	Feed Rate (mm/rev)	Tool Life (min)	Failure Mode	Surface Finish (μm)	Vol. Mat. Removed (cm^3)	Tool Life (min)	Failure Mode	Surface Finish (μm)	Vol. Mat. Removed (cm^3)	Tool Life (min)	Failure Mode	Surface Finish (μm)	Vol. Mat. Removed (cm^3)
15	0.2	14.8	FW	1.97	88.8	16.5	FW	1.98	99.0	21.0	FW	1.71	126.0
20	0.2	11.0	FW	1.42	88.0	14.0	FW	1.80	112.0	13.0	FW	1.65	104.0
25	0.2	9.0	FW	1.50	90.0	10.2	FW	1.73	102.0	8.8	FW	1.86	88.0
30	0.2	7.8	FW	1.79	93.6	7.5	FW	1.54	90.0	6.8	FW	1.73	81.6
35	0.2	10.2	FW	1.63	142.8	6.2	FW	1.54	86.8	5.0	FW	1.75	70.0
40	0.2	14.0	FW	2.95	224.0	5.5	FW	1.82	88.0	4.8	FW	2.02	76.8
45	0.2	5.8	FW	2.84	104.4	4.8	FW	1.70	86.4	4.5	FW	1.75	81.0
50	0.2	4.7	FW	2.95	94.0	4.2	FW	1.85	84.0	3.0	FW	1.85	60.0
15	0.4	13.0	FW	NM	156.0	18.5	FW	7.27	222.0	22.2	FW	6.80	266.4
20	0.4	9.5	FW	11.4	152.0	14.0	FW	7.86	224.0	17.5	FW	NM	280.0
25	0.4	25.0	FW	10.86	500.0	9.0	FW	7.08	180.0	25.4	FW	NM	508.0
30	0.4	25.2	FW	11.25	604.8	8.5	FW	6.98	204.0	9.6	FW	7.03	230.4
35	0.4	14.2	FW	8.84	397.6	7.8	FW	6.54	218.4	5.8	FW	7.4	162.4
40	0.4	5.8	FW	9.13	185.6	5.0	FW	7.08	160.0	4.0	FW	6.8	128.0
45	0.4	4.2	FW	8.17	151.2	4.0	FW	7.16	144.0	3.5	FW	7.3	126.0
50	0.4	3.8	FW	7.38	152.0	3.5	FW	7.32	140.0	3.2	FW	7.5	128.0
15	0.6	12.2	FW	16.25	219.6	24.0	FW	18.5	432.0				
20	0.6	35.5	FW	17.80	852.0	20.0	FW	15.7	480.0				
25	0.6	17.0	FW	14.60	510.0	21.2	FW	16.1	636.0				
30	0.6	5.5	FW	15.10	198.0	8.0	FW	18.4	288.0				

NOTE : FW - Flank Wear NM - Non Measurable

Table 7.10 Tool Life, Failure Mode, Surface Finish And Volume Of Material Removed For KC910 Inserts With 4mm Depth Of Cut

TOOL GEOMETRY / CUTTING CONDITIONS		**NEGATIVE RAKE ANGLE**				**POSITIVE RAKE ANGLE**			
Cutting Speed (m/min)	Feed Rate (mm/rev)	Tool Life (min)	Failure Mode	Surface Finish (μm)	Vol. Mat. Removed (cm^3)	Tool Life (min)	Failure Mode	Surface Finish (μm)	Vol. Mat. Removed (cm^3)
15	0.2	15.0	FW	4.12	180.0	13.5	FW	1.79	162.0
20	0.2	13.2	FW	3.56	211.2	9.8	FW	1.66	156.8
25	0.2	13.4	FW	3.02	268.0	7.2	FW	2.14	144.0
30	0.2	11.0	FW	3.73	264.0	5.6	FW	3.13	134.4
15	0.4	41.2	FW	NM	988.8	16.0	FW	6.9	384.0
20	0.4	29.5	FW	NM	944.0	12.6	FW	7.2	403.2
25	0.4	24.0	FW	NM	960.0	12.0	FW	7.9	480.0
30	0.4	12.0	FW	11.16	576.0	13.2	FW	6.2	633.6
15	0.6	48.0	FW	NM	1728.0	22.0	FW	16.9	792.0
20	0.6	29.5	FW	NM	1416.0	25.5	FW	17.6	1224.0
25	0.6	25.0	FW	16.17	1500.0	9.0	FW	17.4	540.0
30	0.6	8.0	FW	15.90	576.0	9.0	FW	18.6	648.0

NOTE : FW - Flank Wear NM - Non Measurable

Table 7.11 Values of n and C for Taylor Tool Life Curve For KC910 Inserts At 0.2 and 0.4 mm/rev Feed Rates With 2 mm And 4 mm Depth of Cut

TOOL GEOMETRY	NEGATIVE RAKE ANGLE		POSITIVE RAKE ANGLE		NEGATIVE RAKE ANGLE WITH CHIP BREAKER	
DOC = 2 mm	0.2 (mm/rev)	0.4 (mm/rev)	0.2 (mm/rev)	0.4 (mm/rev)	0.2 (mm/rev)	0.4 (mm/rev)
Value of n	1.53	0.95	0.83	0.73	0.66	0.52
Value of C	877	268.78	165.2	131.4	109	91.22
Regression Coefficient (r)	0.6747	0.5900	0.9936	0.9799	0.9903	0.9232

TOOL GEOMETRY	NEGATIVE RAKE ANGLE		POSITIVE RAKE ANGLE	
DOC = 4 mm	0.2 (mm/rev)	0.4 (mm/rev)	0.2 (mm/rev)	0.4 (mm/rev)
Value of n	12.57	0.61	0.78	3.31
Value of C	$16.2X10^3$	151.32	114.8	$11.5X10^5$
Regression Coefficient (r)	0.9265	0.9443	0.9984	0.7164

Table 7.12 Tool Life And Distance Cut For 0.4 mm Flank Wear For KC910 Inserts At 0.2 and 0.4 mm/rev Feed Rates (Negative Rake Angle, DOC = 2 mm)

Cutting Speed (m/min)	Tool Life (min)		Distance Cut (m)	
	0.2 (mm/rev)	0.4 (mm/rev)	0.2 (mm/rev)	0.4 (mm/rev)
15	14.8	13.0	222	195
20	11.0	9.5	220	190
25	9.0	25.0	225	625
30	7.8	25.2	234	756
35	10.2	14.2	357	497
40	14.0	5.8	560	232
45	5.8	4.2	261	189
50	4.7	3.8	235	190

Table 7.13 Tool Life and Distance Cut For 0.4 mm Flank Wear For KC910 Inserts At 0.2 and 0.4 mm/rev Feed Rates (Negative Rake Geometry, DOC = 2 mm, WITH Chip Breaker)

Cutting Speed (m/min)	Tool Life (min)		Distance Cut (m)	
	0.2 (mm/rev)	0.4 (mm/rev)	0.2 (mm/rev)	0.4 (mm/rev)
15	21.0	22.2	315	333
20	13.0	17.5	260	350
25	8.8	25.4	220	635
30	6.8	9.6	204	288
35	5.0	5.8	175	203
40	4.8	4.0	192	160
45	4.5	3.5	202.5	157.5
50	3.0	3.2	150	160

Table 7.14 Tool Life and Distance Cut For 0.4 mm Flank Wear For KC910 Inserts At 0.2 and 0.4 mm/rev Feed Rates (Positive Rake Geometry, DOC = 2 mm)

Cutting Speed (m/min)	Tool Life (min)		Distance Cut (m)	
	0.2 (mm/rev)	0.4 (mm/rev)	0.2 (mm/rev)	0.4 (mm/rev)
15	16.5	18.5	247.5	277.5
20	14.0	14.0	280	280
25	10.2	9.0	255	225
30	7.5	8.5	225	255
35	6.2	7.8	217	273
40	5.5	5.0	220	200
45	4.8	4.0	216	180
50	4.2	3.5	210	175

Table 7.15 Cutting Force (F_c) and Feed Force (F_f) For KC910 Inserts At 0.2 mm/rev Feed Rate and 2 mm DOC

CUTTING SPEED (m/min)	KC910 (NEG.Geometry) NO Chip Breaker		KC910 (NEG.Geometry) WITH Chip Breaker		KC910 (POS.Geometry) NO Chip Breaker	
	F_c (N)	F_f (N)	F_c (N)	F_f (N)	F_c (N)	F_f (N)
15	465	215	400	195	380	150
20	470	230	390	200	380	160
25	465	240	390	200	370	155
30	500	255	450	230	440	180
35	495	245	420	215	375	150
40	450	215	330	210	380	160
45	420	210	425	215	385	170
50	425	200	440	230	400	170

Table 7.16 Cutting Force (F_c) and Feed Force (F_f) For KC910 Inserts At 0.4 mm/rev Feed Rate and 2 mm DOC

CUTTING SPEED (m/min)	KC910 (NEG.Geometry) NO Chip Breaker		KC910 (NEG.Geometry) WITH Chip Breaker		KC910 (POS.Geometry) NO Chip Breaker	
	F_c (N)	F_f (N)	F_c (N)	F_f (N)	F_c (N)	F_f (N)
15	790	320	680	300	650	230
20	800	330	715	390	635	230
25	720	270	640	300	650	250
30	690	240	610	230	625	230
35	680	250	675	305	590	225
40	700	280	800	410	620	260
45	790	320	910	480	665	280
50	770	330	930	490	750	290

Appendix 2

Sample Calculation For Value n and C Of Taylor Equation

Sample calculation of regression line for $y = a + k(x - x)$ as described in ISO publication [33]. The following example is for K68 insert with negative geometry at feed rate of 0.2 mm/rev and 2 mm depth of cut.

The values in this example has been calculated using Microsoft Excel 5.0 package.

Observation	V(m/min)	T(min)	x=log V	y=log T	xy	x^2	y^2
1	15	8	1.176091	0.90309	1.062116	1.383191	0.815572
2	20	6.5	1.30103	0.812913	1.057625	1.692679	0.660828
3	25	5.2	1.39794	0.716003	1.00093	1.954236	0.512661
4	30	3.8	1.477121	0.579784	0.856411	2.181887	0.336149
5	35	5.8	1.544068	0.763428	1.178785	2.384146	0.582822
6	40	7.2	1.60206	0.857332	1.373498	2.566596	0.735019
7	45	3.5	1.653213	0.544068	0.89946	2.733112	0.29601
8	50	2.2	1.69897	0.342423	0.581766	2.886499	0.117253
Sum			$\Sigma x =$	$\Sigma y =$	$\Sigma xy =$	$\Sigma x^2 =$	$\Sigma y^2 =$
			11.85049	5.519041	8.01059	17.78235	4.056314
			$(\Sigma x)^2$	$\Sigma x.\Sigma y$			
			140.4342	65.40336			
			$(\Sigma x)^2/n$	$\Sigma x.\Sigma y/n$			
			17.55427	8.17542			

Criterion V_B = 0.4 mm
No. of observations, n = 8

$x = \Sigma x/n = 1.481312$

$a = y = \Sigma y/n = 0.68988$

$$k = \frac{\Sigma xy - \Sigma x.\Sigma y/n}{\Sigma x^2 - (\Sigma x)^2/n} = \frac{-0.16483}{0.228073}$$

$k = -0.72271$

$-1/k = 1.38$ (Taylor exponent)

$\log C = x - y/k = 2.435888$

$C = 272.82$ (constant)

Regression Coefficient, $r = 0.6919$

Appendix 3

Published Papers

During the present work, the following papers have been published for publication:

1. ***"Milling of Aluminium 2618 Metal Matrix Composite (MMC)"***
A Abdullah, I R Pashby, S K Bhattacharyya and S Barnes
International Conference On Advanced Manufacturing Technology (ICAMT '94), University Technology Malaysia (UTM), Johor Bharu, MALAYSIA, 29 - 30 August 1994, pp. 585 - 598
Edited by V C Venkatesh

2. ***"Machining of Particulate 2618 Aluminium Metal Matrix Composite (MMC) With Cemented Carbides Tools"***
A Jawaid and A Abdullah
Seventh International Conference On Production/Precision Engineering ($7^{th.}$ ICPE), The Japan Society of Precision Engineering, Chiba, JAPAN, 15 -17 September 1994, pp. 419 - 425
Edited by Eiji Usui

3. ***"Tool Life When Turning SiC Particulate Reinforced 2618 Aluminium Metal Matrix Composite (MMC) With Polycrystalline Diamond (PCD) and Cemented Carbide Cutting Tools"***
A Abdullah, I R Pashby and S Barnes
Third International Conference On The Behaviour of Machining "Solutions To Your Machining Problems", University of Warwick, UNITED KINGDOM, 15-17 November 1994, pp. 168 - 179

REFERENCES

[1] Richter D, *"Commercial Alternatives In Metal Matrix Composites"*, Advanced Material Technology International, Vol. 60, 1992 , pp. 57 - 60

[2] Suresh S, Mortensen A and Needleman A, *"Fundamentals of Metal Matrix Composites"*, Butterworth-Heinemann , 1993. ISBN 0-7506-9321-5

[3] Flemings M C, *"Materials Engineering 2000 and Beyond: Strategies for Competitiveness"*, Advanced Materials & Processes, Vol. 1, 1994, pp. 22 - 35

[4] Klimowicz T F, *"The Large-Scale Commercialization of Aluminium-Matrix Composites"*, Journal of Material (JOM), November 1994, pp. 49 - 53.

[5] Hoover W R , *"Recent Advances in Castable MMCs"*, Proc. Of the Fabrication of Particulate Reinforced Metal Composites, Montreal, Quebec, Canada, Edited by J Masouhave and F G Hamel, 17 - 22 Sept 1990, pp. 115 - 123

[6] Finnie I., *"Review Of The Metal Cutting Analyses Of The Past Hundred Years"*, Mech. Eng., 1956, Vol. 78, No. 8, pp. 715 - 721.

[7] Taylor F. W., *"On The Art of Cutting Metals"* , Trans. ASME, Vol. 28, 1906.

[8] Shaw MC, *"Historical Aspects Concerning Removal Operations On Metals"*, In Metal Transformation, 1968, Gordon and Breach, New York, pp. 211 - 260

[9] Shaw MC *"The Assessment of Machinability"*, Proceeding of the Conference on Machinability, Iron and Steel Institute, London, 4-6 October 1965, pp. 1 - 9

[10] Ernst, H., and M. E. Merchant, *"Chip Formation, Friction And High Quality Machined Surfaces"* , Surface Treatment of Metals, 1941, Vol. 29, American Society of Metals, New York, p.299.

[11] Peel C, Robertson J and Tarrant J, *"Have Metal Matrix Composites Proved Their Worth?"*, Materials World, January 1995, pp. 8 - 9.

[12] Vaccari J and Lane C, *"Machining a New Breed of Aluminium"*, American Machinist, November 1993, pp. 56 - 60.

[13] Trent E.M., *"Metal Cutting"*, 3rd. Edition, Butterworth-Heinemann, 1991. ISBN 0-7506- 1068-9

[14] Zorev N N , *"Metal Cutting Mechanics"*, 1966, Pergamon, Oxford.

[15] Shaw M C , *"Resume and Critique of Papers in Part One"*, Proceeding of the International Research in Production Engineering Conference, ASME, Sept. 9 - 12, 1963, pp. 3 - 17

[16] Shaw M C , *" Metal Cutting Principles"*, Oxford University Press, 1991. ISBN 0-19-859020-2

[17] Boothroyd G. and Knight W A, *"Fundamentals of Machining and Machine Tools"*, 2nd. Edition, Marcel Dekker Inc., 1989. ISBN 0-8247-7852-9

[18] Mills B., *"Machinability of Engineering Materials"*, Applied Science Pub. Ltd., 1983. ISBN 0-85333-183-4

[19] BS 1296 Part 2:1972, *"Specification For Single Point Cutting Tools"*.

[20] BS5623:1979, *"Specification For Tool Life Testing With Single Point Turning Tools"*. (Withdrawn)

[21] Piispanen V, *"Eripaines Teknillisesläa Aikakauslehdesläa"*, 1937, Vol. 27, pp. 315 - 322

[22] Merchant M E , *"Mechanics of Metal Cutting and Type 2 Chip"*, Journal of Applied Physics, 1945, Vol. 16, No.5, pp. 267

[23] Lee E H & Shaffer B W, *"The Theory Of Plasticity Applied To A Problem Of Machining"*, Journal of Applied Mechanics, Trans. ASME, 1951, Vol. 18, Issue No. 4, pp. 405 - 413

[24] Ernst H, *"Physics of Metal Cutting"*, American Society for Metals, Metals Park, Ohio, 1938, pp. 1-34

[25] Merchant M E , *"Basic Mechanics Of The Metal Cutting Process"*, Journal Applied Mechanics, Vol. 11, 1944, pp. 168 - 175

[26] Field M and Merchant M E, *"Mechanics Of Formation Of The Discontinuous Chip In Metal Cutting"*, Trans. ASME, Vol. 71, 1949, pp. 421 - 430

[27] Cook N H, Finnie I, and Shaw M, *"Discontinuous Chip Formation"*, Trans. ASME, 1954, pp. 153 - 162

[28] Iwata K, *"The Significance of Dynamic Crack Behaviour in Chip Formation"*, Annal of the CIRP, Vol. 25, No.1, 1976, pp. 65-70

[29] Pashby, I R, *"The Effect of Heat Treatment On The Machinability of Austempered Ductile Iron"*, PhD Thesis, University of Warwick, 1992.

[30] DeVries W R , *"Analysis of Material Removal Processes"*, Springer-Verlag, New York, Inc., 1992.
ISBN 0-387-97728-7

[31] Oxley P L B., *"The Mechanics of Machining : An Analytical Approach to Assessing Machinability"*, Ellis Horwood Ltd., 1989.
ISBN 0-7458-0007-6

[32] Okushima K and Hitome K, *"An Analysis of The Mechanism of Orthogonal Cutting and its Application to Discontinuous Chip Formation"*, Trans. ASME, J of Eng. For Industry, Vol. 83, 1961, pp. 214 - 218

[33] ISO 3685:1977 - *"Tool-Life Testing With Single-Point Turning Tools"*

[34] Nakayama K and Arai M, *"Comprehensive Chip Form Classification Based On The Cutting Mechanism"*, Annals of the CIRP, Vol. 41(1), 1992, pp. 71 - 74

[35] Shaw M C, Ber A and Mamin P A, *"Friction Characteristics of Sliding Surfaces Undergoing Subsurface Plastic Flow"*, Trans ASME, J. Of Basic Eng. Vol. 82, June 1960, pp. 342-346

[36] Wallace P W and Boothroyd G, *"Tool Forces and Tool-Chip Friction in Orthogonal Machining"*, J. of Mech. Eng. Sci., Vol. 6, No.1, 1964, pp. 74 - 87

[37] Zorev N N , *"Interrelationship Between Shear Processes Occurring Along Tool Face And On Shear Plane In Metal Cutting"*, Proc of Int. Prod Eng Res Conf., Pittsburgh, Pennsylvania, USA, Sept. 9-12, 1963, pp. 42- 49

[38] Trent E M, *"Conditions of Seizure At The Tool/ Work Interface"*, Proceeding of the Conference on Machinability, Iron and Steel Institute, London, 4-6 October 1965, pp. 11-18

[39] Trent E M , *"Metal Cutting And The Tribology of Seizure: 1 - Seizure in Metal Cutting"*, Wear, Vol.28, 1988, pp. 29-45

[40] Trent E M , *"Metal Cutting And The Tribology of Seizure: I1 - Movement of Work Material over the Tool in Metal Cutting"*, Wear, Vol.28, 1988, pp. 47-64

[41] Trent E M , *"Metal Cutting And The Tribology of Seizure: III - Temperature in Metal Cutting"*, Wear, Vol.28, 1988, pp. 65-81

[42] Wright P K, *"Frictional Interactions In Machining: Comparisons Between Transparent Sapphire And Steel Cutting Tools"*, Metals Technology, April 1981, pp. 150-160

[43] Doyle E D, Horne J G and Tabor D, *"Frictional Interactions Between Chip and Rake Face in Continuous Chip Formation"*, Proc. R Soc., London, A-366, 1979, pp. 173-183

[44] Wright P K, Horne J G, and Tabor D, *"Boundary Conditions at the Chip-Tool Interface in Machining: Comparisons Between Seizure and Sliding Friction"*, Wear, Vol.54, 1979, pp. 371-390

[45] Wright P K and Trent E M, *"Metallurgical Appraisal of Wear Mechanisms and Processes on High Speed Steel Cutting Tools"*, Metals Technology, January 1974, pp. 13 - 23

[46] Yaguchi H, *"Built-Up Edge In Low-Carbon Resulfurized Free-Machining Steels"*, 1st. Int. Conf. On the Behaviour of Materials in Machining, 8 - 10 Nov. 1988, Stratford-upon-Avon, Paper 24.

[47] Heginbotham W B and Gogia S L, *"Metal Cutting and Built-Up Nose"*, Proc. Inst. Mech Engrs, Vol.175, No.18, 1961, pp. 892-903

[48] Hoshi K, *"On the Metal Cutting Mechanism with the Built-up Edge"*, Advances in Machine Tool Res, 9th. MTDR Conf., Sept.1968, pp. 1099 - 1111

[49] Nakajima K, Ohgo K and Awano T, *"Formation of a Built-Up Edge During Cutting"*, Wear, 11(1968), pp. 369-377

[50] Takeyama H and Ono T, *"Basic Investigation of Built-Up-Edge"*, Transaction of the ASME, Journal of Engineering For Industry, May 1968, pp. 335 - 342

[51] Williams J E and Rollason E C, *"Metallurgical and Practical Machining Parameters Affecting Built-up Edge Formation in Metal Cutting"*, J Inst. Metals, Vol. 98, 1970, pp. 144-153

[52] Ramaswami R, *"The Effects of the Built-up Edge (BUE) on the Wear of Cutting Tools"*, Wear, 18(1971), pp. 1-10

[53] Pekelharing A J, *"Built-Up Edge (BUE): Is The Mechanism Understand?"*, Annals of the CIRP, Vol. 23/2 1974, pp. 207 - 212

[54] Wallbank J, *"Structure of Built-Up Edge Formed in Metal Cutting"*, Metals Technology, April 1979, pp. 145-153

[55] Wallbank J and Milovic R, *"The Machining of Low Carbon Free Cutting Steels with High Speed Steel Tools"*, The Machinability of Engineering Materials, ASM, 1983, pp. 23-44

[56] Bandyopadhyay B P, *"Mechanism of Formation of Built-up Edge"*, Precision Engineering, Vol.6, No.3, July 1984, pp. 148-151

[57] Smith G T, *"Advanced Machining : The Handbook of Cutting Technology"*, IFS Publ. Ltd., 1989.
ISBN 1-85423-022-0

[58] Nakayama K, Shaw M C and Brewer R C, *"Relationship Between Cutting Forces, Temperatures, Built-up Edge and Surface Finish"*, Annal of the CIRP Vol.16, 1966, pp. 211-223

[59] Svahn O, *"Wear of Cutting Tools and Tool Life"*, Proc. On the Int. Prod. Eng. Res. Conf. Sept. 9-12, 1963, pp. 120-129

[60] Yaguchi H, *"Scanning Electron Microscopy and Electron Microprobe Analysis Of Built-Up Edges In Low Carbon Resulfurized Free-Machining Steel"*, Materials Science and Engineering, Vol. 80, 1986, pp. L27 - L30.

[61] Oishi K, *"Built-up Edge Elimination in Mirror Cutting of Hardened Steel"*, Trans. Of ASME, Jnl. Of Engineering for Industry, February 1995, Vol. 117, pp. 62 - 66

[62] Williams J E, Smart E F and Milner D R, *"The Metallurgy of Machining"*, Metallurgia, February 1970, pp.51-59

[63] Rowe G W and Spick P T, *"A New Approach to Determination of the Shear-Plane Angle in Machining"*, Trans. Of the ASME, J. For Ind. Eng., August 1967, pp. 530-538

[64] Kobayashi S and Thomsen E G, *"Metal Cutting Analysis II: New Parameters"* Trans. Of the ASME, J For Ind. Eng., February 1962, pp. 71-80

[65] Amini E, *"Photoelastic Analysis of Stress and Forces in Steady Cutting"*, Journal of Strain Analysis, Vol.3, No.3, 1968, pp. 206-213

[66] Usui E and Takeyama H, *"A Photoelastic Analysis of Machining Stresses"*, Trans. Of the ASME, J of Eng. For Industry, November 1960, pp. 303-308

[67] Chandrasekaran H and Kapoor D V, *"Photoelastic Analysis of Tool-Chip Interface Stresses"*, Trans of the ASME, J of Eng. For Industry, November 1965, pp. 495-502

[68] Barrow G, Graham W, Kurimoto T and Leong Y F, *"Determination of Rake Face Stress Distribution in Orthogonal Machining"*, Int. J Mach Tool Des Res., Vol.22, No.1, 1982, pp. 75-85

[69] Childs T H C and Mahdi M I, *"On the Stress Distribution Between the Chip and Tool During Metal Turning"*, Annals of the CIRP, Vol. 38/1/1989, pp. 55-58

[70] Kato S, Yamaguchi K and Yamada M, *"Stress Distribution at the Interface Between Tool and Chip in Machining"*, Trans of the ASME, J of Eng. For Industry, May 1972, pp. 683-689

[71] Boothroyd G, *"Effect of Tool Flank Wear on the Temperature Generated During Metal Cutting"*, Advances in MTDR, 1967, pp. 667-671

[72] Lenz E, Katz Z and Ber A, *"Investigation of the Flank Wear of Cemented Carbide Tools"*, Trans. Of the ASME, J of Eng. For Industry, Feb. 1976, pp. 246-251

[73] Juneja B L and Sekhon G S, *"Fundamentals of Metal Cutting and Machine Tools"*, Publ. John Wiley & Sons, 1987.
ISBN 0-85226-519-0

[74] Smart E F and Trent E M, *"Temperature Distribution in Tools Used For Cutting Iron, Titanium and Nickel"*, Int. J. Prod. Res., Vol. 13, No. 3, 1975, pp. 265-290

[75] Bickel E, *"The Temperature on a Turning Tool"*, Proc. Int. Prod. Eng Res Conf, Pittsburgh, Pennsylvania, USA, Sept. 9-12, 1963, pp. 89-94

[76] Arndt G and Brown R H, *"On the Temperature Distribution in Orthogonal Machining"*, Int J Mech Tool Des Res , Vol.7, 1967, pp. 39-53

[77] Dearnley P A and Trent E M, *"Wear Mechanisms of Coated Carbides Tools"*, Metals Technology, Feb.1982, pp. 60-75

[78] Colson B, *"Developing and Implementing Cutting Tool Technology"*, Cutting Tool Engineering, August 1986, pp. 81-84

[79] Wallbank J, *"Development in Tool Materials"*, Advanced Machining for Quality and Productivity: Second Int. Conf. On the Behaviour of Materials in Machining , 14-15 November 1991, York

[80] Pastor H, *"Present Status and Development of Tool Material: Part 1 - Cutting Tools"*, Int. Jrnl of Refractory and Hard Metals, Vol. 6, Issue No. 4, Dec. 1987, pp. 196-209

[81] Trent E M, *"Cutting Tool Materials"*, Metallurgical Review, No. 127, 1968, pp. 129-144

[82] Smart R F, *"Performance of Tool Materials : The User's View"*, Towards Improved Performance of Tool Materials, National Physical Lab., Teddington, 8-29 April 1981, Pre-print, Paper 1

[83] Edwards R, *"Cutting Tools"*, The Institute of Materials, 1993.
ISBN 0-901716-48-0

[84] Almond E A, *""Performance of Tool Materials : The User's View"*, Towards Improved Performance of Tool Materials, National Physical Lab., Teddington, *28-29 April 1981, Pre-print, Paper 29*

[85] Hoyle G, *"High Speed Steels"*, Butterworths, 1988, ISBN 0-408-11032- 5

[86] Komanduri R, *"Cutting Tool Materials"*, Encyclopaedia of Material Science and Engineering (Ed. Bever M B), Pergamon Press, 1982, pp. 1003-1012

[87] Kirk F A, *"Towards Improved Performance of Tool Materials"*, Metals Society Book No. 278, 1981, pp. 45 - 60

[88] Komanduri R and Desai J D, *"Tools Materials For Machining - Part One"*, The Carbide and Tool Journal, September-October 1983, pp. 3-10

[89] Edenhofer B, *"Heat Treatment of Metals"*, Vol. 1, 1974, pp.23 - 30

[90] Dearnaly G, *"Materials in Engineering Appliances"*, Metals and Materials, Vol. 1, 1978, pp.28-34

[91] Staines A B, *"Thermochemical Treatments In A Glow Discharge Environment"*, Metals and Materials, Vol. 1, 1985, pp. 739-744

[92] Metals Handbook, *"Machining"*, 9th Edition, Vol. 7, ASM, pp. 773-783

[93] Shaw M C, *"Carbide Cutting Tools : Past, Present and Future"*, Proc. Of Int. Conf. On Hard Material Tool Technology, Carnegie-Mellon University, Pittsburgh, Pennsylvania, USA, 22-24 June, 1976, pp. 3-27

[94] Kalish H S and August J S, *"How Composition Affects The Properties and Performance of Cemented Carbide Cutting Tools"*, Metal Progress, June 1979, pp. 64 -70

[95] Brookes K J A, *"World Directory and Handbook of Hardmetals and Hard Materials"*, 5th. Edition, January 1992

[96] Kalish H S, *"Selecting The Optimum Cutting Tool Material"*, Proc. Of Int. Conf. On Hard Material Tool Technology, Carnegie-Mellon University, Pittsburgh, Pennsylvania, USA, 22-24 June, 1976, pp. 28-53

[97] Kalish H S, *"Some Plain Talks About Carbides"*, American Machinist, 1978, pp.95

[98] Schwarzkopf P and Kieffer R, *"Cemented Carbides"*, The MacMillan Co., 1960.

[99] Komanduri R and Desai J D, *"Tools Materials For Machining - Part Two"*, The Carbide and Tool Journal, November-December 1983, pp. 2-10

[100] Schintlmeister W, Pacher O and Raine T, *"Wear Characteristics of Hard Material Coatings Produced by Chemical Vapour Deposition with Particular Reference to Machining "*, Wear, 48(1978), pp. 251-266

[101] Lee M and Richman M H, *"Some Properties of TiC Coated Cemented Tungsten Carbides"*, Metals technology, Dec. 1974, pp. 538-546

[102] Hunt J L and Santhanam A T, *"Coated Carbide Metal Cutting Tools: Development and Applications"*, Fundamental Issues in Machining : PED-Vol. 43, Ed. Klamecki B E and Weinmann K J, 1990, pp. 139-155

[103] Metals Handbook, *"Machining"*, 9th Edition, Vol. 16, ASM International, March 1989

[104] Schintlmeister W, Wallgram W, Kanz J and Gigl K, *"Cutting Tool Materials Coated By Chemical Vapour Deposition"*, Wear, 100(1984), pp. 153-169

[105] Jackson D, *"Coatings: Key Factor in Cutting Tool Performance"*, Machine and Tool Blue Book, January 1986, pp. 62-64

[106] Porat R, *"Multilayer CVD Coatings of TiC + TiN and Their Effect on Cutting Tool Life"*, Surface Engineering, Vol. 8, No., 1992, pp. 292-294

[107] Konig W, *"Advances In The Coating Of Tools"*, Powder Metallurgy International, Vol. 24, pt. 5, 1992, pp. 297-302

[108] Chatterjee S, Chandrashekhar s and Sudarshan T S, *"Review Deposition Processes and Metal Cutting Applications of TiN Coatings"*, Journal of Materials Science, Vol. 27, 1992, pp. 3409-3423

[109] Pierson H O, *"A Review of the Chemical Vapour Deposition (CVD) of the Refractory Compounds of Titanium - A Unique Family of Coatings"*, Materials & Manufacturing Processes, Vol. 8(4&5), 1993, pp. 519-534

[110] Koelsch J R, *"Beyond TiN: New Tool Coatings Pick Up Where TiN Left Off"*, Manufacturing Engineering, Oct. 1992, pp. 27-32.

[111] North B, *"Indexable Metal Cutting Inserts: A Review Of Recent Developments"*, Proc. Of the 1st. International Conference On The Behaviour Of Materials In Machining , Stratford-upon-Avon, September 1980, Paper 35

[112] Wick C, *"Coated Carbide Tools Enhance Performance"*, Manufacturing Engineering, March 1987, pp. 45-50

[113] Jawaid A and Ezugwu E O, *"Cutting Tools in Manufacturing - A Review"*, International Manufacturing Conference with China, IMCC, 1993, 10 -12 March 1993, Hong Kong, pp. A371-A379

[114] King A G and Wheildon W M, *"Ceramics in Machining Processes"*, 1966, Academic Press, London

[115] Jack D H, *"Hard Materials For Metal Cutting"*, Metals and Materials, September 1987, pp. 516-520

[116] Ezugwu E O and Wallbank J, *"Manufacture And Properties Of Ceramic Cutting Tools: A review"*, Materials Science and Technology, Vol. 3, November 1987, pp. 881-887

[117] Whitney E D, *"Modern Ceramic Cutting Tool Materials"*, Powder Metallurgy International, April 1983, pp. 201-205

[118] Komanduri R and Desai J D, *"Tools Materials For Machining - Part Three"*, The Carbide and Tool Journal, January-February 1984, pp. 3-11

[119] Schaible J, *"Inserts Turn To The Future"*, Cutting Tool Engineering, August 1991, pp. 93-97

[120] Smith K H, *"Making The More to Whisker-Reinforced Ceramic Tools"*, Cutting Tool Engineering, Dec. 1987, pp. 381-387

[121] Bhattacharyya S K and Jawaid A, *"Syalon Ceramics in Metal Cutting"*, Int. J. Prod. Res., Vol. 19, No. 5, 1981, pp. 589-594

[122] Bhattacharyya S K, Ezugwu E O and Wallbank J, *"Machining of Cast Iron With Available Ceramic Tools"*, Proceeding of the 6th. International Conference on Production Engineering, Osaka, 1987, pp. 176

[123] Bhattacharyya S K, Ezugwu E O and Jawaid A, *"The Performance of Ceramic Tool Materials For The Machining of Cast Iron"*, Wear, Vol. 135(1989), pp. 147-159

[124] Baldoni J G and Buljan S T, *"Ceramics for Machining "*, Ceramic Bulletin, Vol. 67, No. 2, 1988, pp. 381-387

[125] Jennings M, *"The Production and Uses of Industrial Diamond"*, Metals and Materials, September 1987, pp. 525-531

[126] Wilks J and Wilks E, *"Properties and Applications of Diamond"*, Butterworth-Heinemann Ltd., 1991.
ISBN 0-7506-1067-0

[127] Krar S Fand Ratterman E, *"Superabrasives: Grinding and Machining With CBN and Diamond"*, Glencoe/Mc Graw Hill Educational Division, 1990.
ISBN 0-07-035587-8

[128] Lammer A, *"Mechanical Properties of Polycrystalline diamond (PCD)"*, Materials Science and Technology, Vol. 4, Nov. 1988, pp. 949-955

[129] Takatsu S, *"Recent Development in Hard Cutting Tool Materials"*, High Temperature Materials and Processes, Vol. 9, Nos. 2-4, 1990, pp. 175 -193

[130] Wolf M and Dreher R, *"Machining of Aluminium Engine Parts For The Porsche 928"*, Industrial Diamond Review, No. 5/81, 1981, pp. 254-257

[131] Herbert S, *"Jaguar's Long Distance Runner"*, Industrial Diamond Review, No. 3/87, 1987, pp. 100-102

[132] Herbert S, *"Austin Rover's PCD Switch Pays Dividends"*, Industrial Diamond Review, No. 6/85, 1985, pp. 278-281

[133] Worsley, R, *"Superhard Tooling - Has The Edge"*, Metalworking Production, April 1984, pp. 88-92

[134] Oboloer M, *"Machining Of Hard Ferrous Materials And Grey Cast Iron With Polycrystalline CBN Cutting Tools"*, Advances in metal production, Conference Proceeding, MPR Publishing Ltd. 1984

[135] Stephen P M, Hay R A and Dean C D, *"The New Diamond Technology And Its Application In Cutting Tools"*, Diamond and Related Materials, Vol. 1, 1992, pp. 710-716

[136] Krauskopf B, *"Diamond Turning: Reflecting Demands for Precision"*, Manufacturing Engineering, May 1984, pp. 90-94

[137] Bhattacharyya S K and Aspinwall D, *"The Application of Polycrystalline Tooling"*, Machining Hard Materials, Ed. Dr. Roy Williams, Society of Manufacturing Engineers, 1982, pp. 95-103

[138] Bhattacharyya S K and Aspinwall D K, *"Aspects of Machinability Using Polycrystalline diamond and CBN Compact Tooling"*, Cutting Tool Materials, Proc. Of International Conference, ASM, 1980, pp. 249-264

[139] Ingle S S, Subramanian S V and Kay D A R, *"Micromechanisms of Crater Wear"*, 2nd. Int. Conf. On the Behaviour of Materials in Machining , 14 -15 November 1991, York, pp. 112 - 124

[140] Floyd T, *"Diagnose Insert Failure"*, Manufacturing Engineering, Oct. 1992, pp. 37-38

[141] Heydari F, Wallbank J and Pashby I R, *"Evaluation of Wear Mechanisms and Tool Lives When Machining 0.3% Mn-Mo Steel With Coated Carbide and Ceramic Tools"*, The Int. Conf. On Wear of Materials, Houston, Texas, 1987, ASME, pp. 313 - 324

[142] Niebel B W, Draper A B and Wysk R A, *"Modern Manufacturing Process Engineering"*, Mc Graw Hill International Editions, 1989. ISBN 0-07-100381-9

[143] Burwell J T, *"Survey of Possbile Wear Mechanisms"*, Wear, Vol. 1 (1957/58), pp. 119 - 141

[144] Misra A and Finnie I, *"A Review of the Abrasive Wear of Metals"*, Journal of Engineering Material and Technology, Transactions of the ASME, Vol. 104, April 1982, pp. 94 -104

[145] Gahr Z K H , *"Microstructure and Wear of Materials"*, Tribology Series, Vol. 10, Elsevier Amsterdam, 1987, pp. 80 - 130

[146] Kato K, *"Abrasive Wear"*, Characterisation of Tribological Materials, Ed. William A Glaeser, Butterworth-Heinemann, 1993. pp. 80 - 97 ISBN - 0-7506-9297-9

[147] Archard J F, *"Contact and Rubbing of Flant Surfaces"*, Journal of Applied Physics, Vol. 24, 1953, pp. 981 - 988

[148] Larsen-Badse J, *"Influence of Grit Size On The Groove Formation During Sliding Abrasion"*, Wear, Vol. 11, 1968, pp. 213 - 223

[149] Aghan R L and Samuels L E, *"Mechanisms of Abrasive Polishing"*, Wear, Vol. 16, 1970, pp. 293 - 301

[150] Tabor D, *"Some Basic Mechanisms Of Wear That May Be Relevant To Tool Wear And Tool Failure"*, Proc. BISRA-ISI Conference On Materials For Metal Cutting, London, 1970, pp. 21- 24

[151] Suh N P, *"New Theories Of Wear And Their Implications For Tool Material"*, Wear, Vol. 62, 1980, pp. 1-20

[152] Lardner E, *"Material For Metal Cutting"*, Iron and Steel Institute, Preprint 126, 1965

[153] Focke A A, Westerman F E, Kemhaus J, Shih W T and Hoch M, *"Wear of Superhard Materials When Cutting Superalloys"*, Wear, 46 (1978), pp. 65 - 79

[154] Ramalingam S and Wright P K, *"Abrasive Wear in machining: Experiments With Materials of Controlled Microstructure"*, Journal of Engineering

Materials and Technology, Transtions of the ASME, Vol. 103, April 1981, pp. 151-156

[155] Metals Handbook, *"Machining of Aluminium and Aluminium Alloys"*, 9th. Edition, Vol. 16, ASM, pp. 761 - 804

[156] Sully W J, *"The Machinability of Cast Aluminium Alloys"*, Proceedings of the Conference on Machinability, Iron and Steel Institute, 4 - 6 Oct. 1965, London, pp. 127 - 133

[157] Konig W and Erinsk D, *"Machining and Machinability of Aluminium Cast Alloys"*, Annals of the CIRP, Vol. 32, No. 2, 1983, pp. 535 - 540

[158] Konig W and Erinski D, *"Machinability of Aluminium-Silicon Pressure Die Cast Alloys"*, Proceeding of the 20th. MTDR-Conference, University of Birmingham, Birmingham, UK, 10-14 Sept. 1979, pp. 337 - 344

[159] Burant R O and Skingle T J, *"Machining the Silicon-Containing Aluminium Alloys"*, SAE Technical Paper No. 800489, Society of Automotive Engineering Congress, 25/29 Feb. 1980, pp. 1 - 13

[160] Trent, E M, *"Wear of Metal Cutting Tools"*, Treatise on Material Science and Technology, Vol. 13, 1979, pp. 443-488

[161] Ohgo K, *"A Study of Peeling of Built-up Edge From a Cutting Tool and Its Effect on Tool Life"*, Wear, 47(1978), pp. 155-161

[162] Bhattacharyya A and Ghosh A, *"Diffusion Wear of Cutting Tools"*, 5th. Int. MTDR Conf., Birmingham, September 1964, pp. 225 - 242

[163] Opitz H and Konig W, *"On The Wear of Cutting Tool"*, Proc. 8th. Int. MTDR Conf., Manchester 1967, pp. 173-186

[164] Trent E M, *"Cutting Steels and Iron With Cemented Carbide Tools"*, J. Iron and Steel Inst., Vol. 201, 1963, pp. 847, 923, 1001

[165] Colding B and Konig W, *"Validity of the Taylor Equation in Metal Cutting"*, Annals of the CIRP, Vol. 19(1971), pp. 793 - 812

[166] Trent E M, *"Metallurgical Changes at The Tool/Work Interface"*, Proceedings of the Conference on Machinability, Iron and Steel Institute, 4 - 6 Oct. 1965, London, pp. 77 - 87

[167] Trent E M, *"Tool Wear and Machinability"*, Production Engineering, Vol. 38, No.3, 1959, pp. 105-130

[168] Loladze T N, *"Nature of Brittle Failure of Cutting Tool"*, Annal of the CIRP Vol. 24/1/1975, pp. 13 - 16

[169] Tlusty J and Masood Z, *"Chipping and Breakage of Carbide Tools"*, Trans. Of the ASME, Journal of Engineering for Industry, Vol. 100, November 1978, pp. 403 - 412

[170] Brownsword R, Hague A G, Panton R F and Pyle T, *"Studies of Wear in High-Speed Steel Tools"*, Proc. BISRA-ISI Conf. On Materials For Metal Cutting, Scarborough-London, 1970, pp. 39 - 42

[171] Venkatesh V C, *"Diffusion Wear of High-Speed Steel Tools"*, 7th. Int. MTDR Conf., University of Birmingham, 1966, pp. 401 - 413

[172] Shabaik A H, *"Wear of cutting tools"*, Int. Proc. Of Machine Tool Design and Research (MTDR), 1979, pp. 421- 430

[173] Opitz H and Gappisch M, *"Some Research On The Wear Behaviour of Carbide Cutting Tools"*, Int. J. Mach. Tool. Des. Res., Vol. 2, 1962, pp. 43 - 73

[174] Ber A, *"The Effect of Abrasion Resistance and Thermal Properties of the Cemented Carbide Tool Grade on the Flank Wear Characteristics"*, Transactions of the ASME, Journal of Engineering for Industry, August 1973, pp. 794 - 796

[175] Optiz H and Konig W, *"Basic Research On Wear Of Carbide Cutting Tools"*, Proceedings of the conference on Machinability, Iron and Steel Institute, 4 - 6 Oct. 1965, London, pp. 35 - 41

[176] Naerheim Y and Trent E M, *"Diffusion Wear Of Cemented Carbide Tools When Cutting Steel At High Speeds"*, Metals Technology, Dec. 1977, pp. 548 -556

[177] Dawihl W, *A Handbook of Hard Metals* , HMSO, London, 1948

[178] Venkatesh V C, *"A Discussion on Tool Life and Total Failure Causes"*, Annals of the CIRP, Vol. 29/1/1980, pp. 19 - 22

[179] Cook N H, *"Tool Wear and Tool Life"*, Trans. of ASME, Journal of Engineering for Industry, November 1973, pp. 931 - 938

[180] Chambers A R, *"Wear of Cemented Carbides Cutting Tools"*, PhD Thesis, University of Birmingham, 1976

[181] Mari D and Gonseth D R, *"A New Look At Carbide Tool Life"*, Wear, Vol. 165, 1993, pp. 9 - 17

[182] Suh N P, *"Coated Carbides - Past, Present and Future"*, Carbide Journal, Vol. 9, 1977, pp. 3 - 9

[183] Schintlmeister W, Pacher O, Krall T, Wallgram W and Raine T, *"Wear Characteristics of CVD-Coated Hard Metal Cutting Tools"*, Powder Metallurgy International, Vol. 13, No. 1, Feb. 1981, pp. 26 - 30

[184] Venkatesh V C, Raju A S and Srinivasan K, *"On Some Aspects of Wear Mechanisms in Coated Carbide Tools"*, Annal of the CIRP, Vol. 25/1/1977, pp. 5 - 9

[185] Chubb J P and Billingham J, *"Coated Cutting Tools - A Study of Wear Mechanisms in High Speed Machining"*, Wear, Vol. 61, 1980, pp. 283-293

[186] Peterson J R, *"Partial Pressure of TiCl4 in CVD of TiN"*, Journal Vac. Sci. Technology, Vol. 11, No. 4, July/August 1974, pp. 715 - 718

[187] Hale T and Graham D, *"How Effective are the Carbide Coatings"*, Modern Machine Shop, April 1981, pp. 98 - 105

[188] Dearnley P A, *"Rake and Flank Face Wear Mechanisms of Coated and Uncoated Cemented Carbides"*, Trans. Of the ASME, Journal of Engineering Materials and Technology, Vol. 107, January 1985, pp. 68 - 82

[189] Lee M and Richman M H, *"Some Properties of TiC Coated Cemented Tungsten Carbides"*, Metals Technology, December 1974, pp. 538 - 546

[190] Venkatesh V C, *"Wear Studies on TiC Coated Cemented Titanium Carbide Tools"*, Trans. Of The ASME, Journal of Engineering Materials and Technology, Vol. 108, Jan. 1984, pp. 84 - 87

[191] Konig W , Fritsh R and Kammermeier D, *"New Approaches to Characterising the Performance of Coated Cutting Tools"*, Annals of the CIRP, Vol. 41/1/1992, pp. 49 - 54

[192] Minevich A A, *"Wear of Cemented Carbide Cutting Inserts With Multilayer Ti-based PVD coatings"*, Surface and Coatings Technology, Vol. 53, 1992, pp. 161 - 170

[193] King A G, *"Behaviour of Ceramic Cutting Tool Materials"*, Materials for Metal Cutting, April 1970, pp. 162 -165

[194] Ham I and Narutaki N, *"Wear Characteristics of Ceramic Tools"*, Trans. of the ASME, Journal of Engineering for Industry, November 1973, pp. 951 - 959

[195] Brandt G, *"Flank and Crater Wear Mechanisms of Alumina-Based Cutting Tools When Machining"*, Wear, Vol. 112, 1986, pp. 39 -56

[196] Kim, S and Durham D R, *"Microscopic Studies of Flank Wear on Alumina Tools"*, Transaction of the ASME, Journal of Tribology, January 1991, Vol. 113, pp. 205 - 209

[197] Pashby I R, Wallbank J and Boud F, *"Ceramic Tool Wear When Machining Austempered Ductile Iron"*, Wear, Vol. 162 -164 , 1993, pp. 22 - 33

[198] Masuda M, Sato T, Kori T and Chujo Y, *"Cutting Performance And Wear Mechanism of Alumina-Based Ceramic Tools When Machining Austempered Ductile Iron"*, Wear, Vol. 174, 1994, pp. 147 -153

[199] Wallbank J and Ezugwu E, *"Wear of Ceramic Tools When Machining Cast Iron"*, Adv. Materials and Manufacturing Processes, Vol. (3), 1988, pp. 447 - 468

[200] Jawaid A, *"Syalon Ceramic In Metal Cutting"*, PhD Thesis, University of Warwick, 1982

[201] Bajalan M R, *"Machining of Steels With Ceramic Tools"*, PhD Thesis, University of Warwick, 1992

[202] Keen D and Grogan A F, *"Wear of Single Point Diamond Tools In The Machining Of Aluminium/Silicon Alloy Pistons - A Final Report"*, Industrail Diamond Review, June 1971, pp. 229 -235

[203] Keen D, *"Some Observation on the Wear of Diamond Tools used in Piston Machining"*, Wear, Vol. 17, 1971, pp. 195 - 208

[204] Oomen J M and Eisses J, *"Wear of Monocrystalline Diamond Tools During Ultraprecision Machining of Nonferrous Metals"*, Precision Engineering, Vol. 14, No. 4, October 1992, pp. 206 - 218

[205] Konig W and Neises A, *"Wear Mechanisms of Ultrahard, Non-Metallic Cutting Materials"*, Wear, Vol. 162 - 164, 1993, pp. 12 - 21

[206] Takatsu S, Shimoda H and Otani K, *"Effects of CBN Content on the Cutting Performace of Polycrystalline CBN Tools"*. Int. J. Of Refractory and Hard Metals, Vol. 2, No. 4, December 1983, pp. 175 - 178

[207] Snooks,"*Metal Matrix Composite In UK*", Materials and Design, 1993, Vol. 14, Issue No. 2, pp. 133-135

[208] Taya M and Arsenault R J, *"Metal Matrix Composites: Thermomechanical Behaviour"*, Pergamon Press 1989. ISBN 0-08-036983-9

[209] Dieter G E, "*Mechanical Metallurgy*", Mc Graw Hill, 1988 ISBN 0-07-100406-8

[210] Huda D, El Baradie M A, Hashmi M S J, "*Metal Matrix Composites: Material Aspects. Part II*", Journal of Material Processing Technology, Vol. 37, 1993, pp. 529-541

[211] Terry B and Jones G, *"Metal Matrix Composites: Current Development and Future Trends In Industrial Research and Applications"*, Elsevier Science Publishers, 1990.
ISBN 1-85617-021-7

[212] Trumper R L, "*MMC - Applications and Prospects*", Metal and Materials, Vol. 3 ,1987, pp. 662-667

[213] Brown A, *"Metal Matrix Composites On The Road*", Materials World, Jan. 1993, pp. 20-21

[214] White J and Willis T C, *"The Production of Metal Matrix Composites by Spray Deposition"*, Materials & Design, Vol. 10, No.3, May/June 1989, pp. 121 - 127

[215] Feest E E, *"Exploitation of the metal matrix composites concept*", Metals and Materials, May 1988, pp. 273-278

[216] Bader M G, *"Reinforced Fibres: The Strength Behind Composites"*, Composite Materials, January 1993, pp. 22 - 26

[217] Yue Wu and Lavernia E J, "*Spray-Atomised and Codeposited 6061 Al/SiCp Composites*", Journal of Metals (JOM), Aug. 1991, pp. 16-23

[218] Geiger A L and Jakson M, *"Low Expansion MMCs Boosts Avionics"*, Advanced Material Processing, Vol. 136(1), July 1989, pp. 23-30

[219] Dhingra A K, *"Metals Replacement By Composites"*, Journal of Metals (JOM), 38, March 1986, pp. 17

[220] Higgins R A, *"Properties of Engineering Materials"*, Hodder & Stoughton, 1986

[221] Everett R K and Arsenault R J, *"Metal Matrix Composites: Processing and Interface"*, Academic Press, 1991.
ISBN 0-12-341832-1

[222] Ibrahim I A, Mohamed F A and Lavernia E J, *"Particulate Reinforced Metal Matrix Composite - A Review"*, Journal of Materials Science, Vol. 26, 1991, pp. 1137 - 1156

[223] Bacon M, "*Metal Matrix Composites: Engineering Materials Solutions*", Material Edge, July/Aug. 1989, pp. 33-48

[224] Baker C, "*Production, Properties and Applications of Particulate Reinforced Aluminium Alloy Composites*", BNF 7th. International Conference, 1990, Paper 9.

[225] Trumper R L, Sherwood P J and Clifford A W, "*Metal Matrix Composites*", Royal Aeronautical Soc. London, 1986, Vol. 2, pp. 249-278

[226] Allison J E and Cole G S, "*MMC in the Automotive Industry: Opportunities and Challenges*", Journal Of Metals (JOM), Jan. 1993, pp. 19-24

[227] Lovell B, "*Metal Matrix Composites: A Relevant Technology*", Racecar Engineering, Vol. 2, No. 6, 1993, pp. 37-42

[228] Dibble A M, "*Metals On The Aerospace Frontier*", Machine Design, June 1991, pp. 44 - 48

[229] Charles D, "*Unlocking the Potential of Metal Matrix Composites for Civil Aircraft*", Materials Science and Engineering, Vol. 135A, 1991, pp. 295 - 297

[230] McGuire P F, "*Aluminium Composites Come In For A Landing*", Machine Design, April 1992, pp. 71 - 74

[231] Nath D, Asthana R, and Rothatgi P K, "*Particle Distribution Control in Cast Aluminium Alloy-Mica Composites*", Journal of Materials Science, Vol. 22, 1987, pp. 170 -176

[232] Jaha A K, Dan T K, Prasad S V, and Rohatgi P K, "*Aluminium Alloy-Solid Lubricant Talc Particle Composite*", Journal of Materials Science, Vol. 21, 1986, pp. 3681 - 3685

[233] Driver D, "*Introduction to Metal Matrix Composites And Review of Their Potential Uses*", IOP Short Meeting Series No. 28, Institute of Physics, November 1990, London.

[234] Friend C M, Young R J and Horsfall I, "*Development in the Science and Technology of Composite Materials*", Proc. Of European Conf. On Composite Materials, ECCM3, Bordeaux, March 1989, pp. 227 - 232

[235] Dermarkar S, "*Metal Matrix Composites*", Metal and Material, March 1986, pp. 144 - 146

[236] McKimpson M G and Scott T E, "*Processing and Properties of Metal Matrix Composites Containing Discontinuous Reinforcement*", Materials Science and Engineering, Vol. A107, 1989, pp. 93 - 106

[237] Lloyd D J, "*Particle Reinforced Aluminium and Magnesium Matrix Composites*", International Materials Review, Vol. 39, No. 1, 1994, pp. 1-23

[238] Matthews F L and Rawlings R D, *"Composite Materials: Engineering and Science"*, Chapman and Hall, 1994.
ISBN 0- 412-55960-9

[239] Huda D, El Baradie M A, Hashmi M S J, "*Metal Matrix Composites: Manufacturing Aspects. Part I*", Journal of Material Processing Technology, 37 (1993), pp. 513-528

[240] El Baradie M A, "*Manufacturing Aspects Of Metal Matrix Composites*", Journal of Materials Processing Technology, Vol. 24 , 1990, pp. 261-272

[241] Chadwick G A, *"Progress in Metal Matrix Composites"*, Cast Metals, Vol. 4, No. 3, 1991, pp. 165-167

[242] Ponzi C, "*Metal Matrix Composite Fabrication Processes For High Performance Aerospace Structure*", Composite Manufacturing Vol. 3, No. 1, 1992, pp. 33-41

[243] Foltz J V and Harrigan W C, "*Powder Metallurgy Metal Matrix Composites Overview*", Proc. of P/M in Aerospace and Defence Tech., Tampa, Florida, 1991, pp. 123-129

[244] Chadwick G A and Yue T M, "*Principles And Applications Of Squeeze Casting*", Metals and Materials, Jan. 1989, pp. 6-12

[245] Driver D, "*Metal Matrix Composites and Powder Processing for Aero-Engine Applications*", BNF 7th. Int. Conf., 1990, Paper No. 2

[246] Clyne T W and Withers P J, "*An Introduction To Metal Matrix Composites*", Cambridge Univ. Press 1993.
ISBN 0-521-41808-9

[247] Hunt M, *"Form and Function in Metal Matrix Composites"*, Materials Engineering, June 1990, pp. 27 - 32

[248] Chadwick G A and Heath P J, "*Machining of Metal Matrix Composites*", Metals and Materials, Feb. 1990, pp.73-76.

[249] Chambers A R and Stephens S E, *"Machining of Al-5Mg Reinforced with 5 vol.% Saffil and 15 vol.% SiC'*, Material Science and Engineering, Vol. A135(1991), pp. 287-290.

[250] Crojanger L and Biermann D, *"B2a-4Turning of Metal Matrix Composites'*, Proc. 2nd. European Conf. on Advanced Material and Processes, Cambridge, 1991, Vol. 2, pp.73-80.

[251] Gindy N N Z and Clegg A J, "*Machining of Metal Matrix Composites*", BNF 7th. Int. Conf., The Materials Revolution Through the 90's, Oxford, 1989

[252] Tomac N and Tonnessen K, "*Machinability of Particulate Aluminium Matrix Composites*", Annals of the CIRP, Vol. 41/1/1992, pp. 55-59

[253] Waldrop P S, *"Metal Matrix Composites: Manufacturing Challenges"*, Composites in Manufacturing 4, Anaheim, California, January 7 - 10, 1985, SME Technical Publication Paper EM85-106

[254] Chambers A R, *"The Machinability of Light Alloy Matrix MMC"*, Tribology in Metal Cutting and Grinding, August 1992, The Inst. Of Mechanical Engineers, London, pp. 73 - 81

[255] McGinty M J and Preuss C F, *"Machining of Ceramic Fiber Metal Matrix Composites"*, Proc. Of Int. Conf. On High Productivity Machining, Materials and Processing, New Orleans, Louisiana, 7 - 9 May 1985, pp. 132 - 243, Ed. by Sarin V K

[256] Lane C, *"The Effect of Different Reinforcements on PCD Tool Life for Aluminium Composites"*, Proc. Of the Machining of Composite Materials Symposium, Chicago, Illinois, Nov. 1992, pp. 17-27

[257] Brun M K and Lee M, *"Wear Characteristics of Various Hard Materials for Machining SiC Reinforced Aluminium Alloy"*, Wear, 104(1985), pp. 21-29

[258] Weinert K, *"A Consideration of Tool Wear Mechanism When Machining Metal Matrix Composites (MMC)"*, Annals of the CIRP, Vol. 42/1/1993, pp. 95-98

[259] Masounave J, Litwin J and Hamelin D, *"Prediction of Tool Life in Turning Aluminium Matrix Composite"*, Materials & Design, Vol. 15, No. 5, 1994, pp. 287 - 293

[260] Weinert K and Bierman D, *"Turning of Fiber and Particle Reinforced Aluminium"*, Proc. Of the International on Machining of Advanced Materials, Gaithersburg, Maryland, USA, July 20-22, 1993, pp. 437 - 445

[261] Chen P and Miyake Y, *"Machining Characteristics of SiC Whiskers Reinforced Aluminium"*, Proceedings of the International Conference on Factors Influencing Machining and Their Control, Cincinnati, Ohio, USA, 12-14 Sept. 1989, pp. 65 - 75

[262] Monaghan J M, *"The Use of a Quick-Stop Test To Study The Chip Formation of A SiC/Al Metal Matrix Composite Material And Its Matrix Alloy"*, Processing of Advanced Materials, Vol. 9 (1994), pp. 170 - 179

[263] Lane C T, *"Machining Characteristics Of Particulate -Reinforced Aluminium "*, Fabrication of Particles Reinforced Metal Composites, Int. Conf., Montreal, Sept. 1990, Ed. Massounave J and Hamel F G, ASM International, pp. 195-201

[264] Pashby I R, Bhattacharyya S K, Barnes S and Abdullah A, *"The Milling of SiC Reinforced Aluminium Metal Matrix Composite With Coated And Uncoated Carbides"*, Proc. Of the Int. Conf. On Advanced Manufacturing Technology, 29 - 30 August 1994, Johor, Malaysia, Ed. Venkatesh V C, pp. 585 - 598

[265] Chambers A R and Jarmakier, *"The Effect of Volume Fraction Reinforcement on the Machinability of an Al-5%Mg Metal Matrix Composite (MMC) "*, Proc. Conf. CIMTEC VII, June 1990, Montecatinis, pp. 2803-2809

[266] Cronjager L and Meister D, *"Machining of Fibre and Particulate Reinforced Aluminium "*, Annals of the CIRP, Vol. 41/1/1992, pp. 63-66

[267] Lane C, *"Machinability of Aluminium Composites as a Function of Matrix Alloy And Heat Treatment"*, Proc. Of the Machining of Composite Materials Symposium, Chicago, Illinois, Nov. 1992, pp. 3-15

[268] Coelho R T, Yamada S, Aspinwall D K and Wise M L H, *"Conventional Machining of an Aluminium Based SiC Reinforced Metal Matrix Composite (MMC) Alloy"*, Proc. Of the 30th. MATADOR Conference, Manchester, 31 March - 1 April, 1993, pp. 125 - 133

[269] Jawaid A, Barnes S and Ghadimzadeh S R, *"Drilling of Particulate Aluminium Silicon Carbide Metal Matrix Composites"*, Proc. of the Machining of Composite Materials Symposium, Chicago, Illinois, 1 - 5 November 1992, pp. 35 - 47, Edited by Srivatsan T S and Bowden D M

[270] Cronjager L and Meister, *"Drilling of Fibre and Particle Reinforced Aluminium "*,Composite Material Technology, ASME 1991, PD-Vol. 37, pp. 185-189

[271] Coelho R T, Yamada S, Aspinwall D K and Wise M L H, *"The Application of PCD Tool Material When Drilling and Reaming Aluminium-Based Alloys Including MMC"*, Int. Journal of Machine Tools and Manufacture, Vol. 35, No. 5 March 1995, pp. 761 - 770

[272] Abrate S and Walton D, *"Machining of Composite Materials. Part II: Non-Traditional Methods"*, Composite Manufacturing, No. 2, 1992, pp. 85-94

[273] Ramulu M and Taya MI, *"EDM Machinability of SiCw/Al Composites"*, Journal Materials Science, Vol. 24, No. 3 ,1989, pp. 1103-1108

[274] Neailey K and Bacon B A, *"Electrodischarge Machining Of Metal Matrix Composites"* 3rd. Int. Conf. On The Behaviour of Materials in Machining, 15 - 17 November 1994, Univeristy of Warwick, UK

[275] Hashish M, "*Machining of Advanced Composites With Abrasive Waterjets*", Manufacturing Review 2, No. 2, 1989, pp. 142-150

[276] Hashish M, "*Turning with Abrasive Waterjets - A First Investigation*", Journal of Engineering for Industry, Trans. Of ASME, Vol. 109, No. 4 , 1987, pp. 281-290

[277] Komanduri R, "*Machining Fibre-Reinforced Composites*", Mechanical Engineering, April 1993, pp. 58-62

[278] Tuersley I P, Jawaid A and Pashby I R, *"Review: Various Methods of Machining Advanced Ceramic Materials"*, Journal Materials Processes Technology, Vol. 42, 1994, pp. 377 - 390